

University of Alberta

Systematics, evolution, and biogeography of the ankylosaurid dinosaurs.

by

Victoria Megan Arbour

A thesis submitted to the Faculty of Graduate Studies and Research
in partial fulfillment of the requirements for the degree of

Doctor of Philosophy

in

Systematics and Evolution

Department of Biological Sciences

©Victoria Megan Arbour
Spring 2014
Edmonton, Alberta

Permission is hereby granted to the University of Alberta Libraries to reproduce single copies of this thesis and to lend or sell such copies for private, scholarly or scientific research purposes only. Where the thesis is converted to, or otherwise made available in digital form, the University of Alberta will advise potential users of the thesis of these terms.

The author reserves all other publication and other rights in association with the copyright in the thesis and, except as herein before provided, neither the thesis nor any substantial portion thereof may be printed or otherwise reproduced in any material form whatsoever without the author's prior written permission.

ABSTRACT

The Ankylosauria is a group of herbivorous, quadrupedal, armoured dinosaurs subdivided into at least two major clades, the Ankylosauridae and the Nodosauridae. The most derived members of the Ankylosauridae had a unique tail club formed from modified, tightly interlocking distal caudal vertebrae and enlarged osteoderms that envelop the terminus of the tail. A review of all known ankylosaurid species, as well as ankylosaurs of uncertain affinities, was undertaken in order to conduct a revised phylogenetic analysis of the clade. Sources of morphological variability were investigated using the relatively large number of specimens referred to *Euoplocephalus tutus*. Taphonomic distortion can influence the morphology of certain features which were thought to be taxonomically significant. However, the cranial ornamentation of ankylosaurs can be useful for distinguishing species and genera and should not be discounted as being too intraspecifically variable. The overall shape, size, and pattern of the frontonasal caputegulae, the number and shapes of the caputegulae that rim the skull in dorsal view (the nuchal, supraorbital, lacrimal, loreal, and supranarial caputegulae), and the general shapes of the squamosal and quadratojugal horns are all taxonomically important features. Information from the review of *Euoplocephalus* allows for the recognition of new ankylosaurid species, synonymization of other species, and resurrection of some previously synonymized species. The revised phylogenetic analysis resulted in a

monophyletic Ankylosauridae consisting of *Aletopelta*, *Gastonia*, *Gobisaurus*, *Liaoningosaurus*, *Shamosaurus*, and a suite of derived ankylosaurids (Ankylosaurinae). There is convincing evidence for the presence of nodosaurids in Asia during the Early Cretaceous. In the mid Cretaceous, Asian nodosaurids were replaced by ankylosaurine ankylosaurids. Modifications to the tail of ankylosaurines occurred at this time, with distinct handle vertebrae appearing potentially as early as the Albian, with *Liaoningosaurus*. The large osteodermal knob did not appear until the Late Cretaceous. Ankylosaurines migrated into North America from Asia between the Albian and Turonian, where they diversified into a clade of ankylosaurines characterized by arched snouts and numerous flat caputegulae. There is no evidence for any ankylosaurids in Gondwana; the Ankylosauridae appears to be completely restricted to Asia and North America.

ACKNOWLEDGEMENTS

A lot of people help make a PhD. First and foremost, thanks go to my family, friends, and mentors who have supported me all the way to this point. My parents, Edith and Joseph Arbour, and my sister Jessica Arbour, have been unendingly encouraging, and I can never really say thanks enough for everything. I owe a debt of gratitude to M. Graves, A-M. Ryan, D. Scott, G. Wach, and M. Zentilli at Dalhousie University, for giving me my first research opportunities. At the University of Alberta, thanks are due to J. Acorn, M. Burns, M. Caldwell, C. Coy, P. Currie, E. Koppelhus, A. Murray, S. Persons, R. Sissons, and A. Torices, for excellent advice and fruitful discussions. Conversations with all of these people have been influential on the development of this research project. (And a big thanks to everyone who has passed through the UALVP while I have been here.) Extra special thanks go to my husband Peter Maguire, who says he knows what he signed up for, but who actually goes above and beyond in his support of my work, and who is also an awfully good fellow. Thank you for hanging in there with me.

I was very fortunate to be able to travel extensively to see many specimens in person, and many thanks go to the following people who provided access to collections and assistance at their respective institutions: M. Norell and C. Mehling (AMNH), K. Shepherd (CMN), J. Bartlett and R. Barrick (CEUM), K. Carpenter and L. Ivy (DMNH), Xu X. and Zheng F. (IVPP), M. Reguero (MLP), J. Horner and the MOR grad students (MOR), K. Tsogtbaatar and Chinzorig Tsogtbaatar (MPC), C. Muñoz (MPCA), J. Foster (MWC), S. Chapman (NHMUK), S. Lucas (NMMNH), T. Tumanova (PIN), D. Evans and B. Iwama (ROM), T. Deméré and K. Randall (SDNHM), R. Sullivan (SMP), B. Strilisky (TMP), M. Carrano (USNM), and M. Borsuk-Białynicka (ZPAL). Thanks also to Y.-N. Lee and the Korea-Mongolia International Dinosaur Project 2010 field crew, D. Badamgarav

(MPC), the organizers of the Flugsaurier 2010 Third International Symposium on Pterosaurs, and R. Coria and his field crew, for facilitating fieldwork and museum travel in Mongolia, China, and Argentina, respectively. Thanks also to the staff at the BXGM for donating a cast of the *Crichtonsaurus benxiensis* holotype skull to the UALVP collections.

K. Barclay, M. Burns, C. Chornell, C. Coy, I. Macdonald, I. Riemer, and R. Sissons assisted with preparation of UALVP 31. MPC D100/1338 was discovered by R. Gabbard (Clifton, Colorado) and excavated by R. Gabbard, P. Currie, M. Marsovsky (Calgary, Alberta) and A. Miniaci (Fort Lauderdale, Florida). C. Coy (UALVP) prepared MPC D100/1338, and J. Tansey prepared the illustrations used in Figures 6.8, 6.9, and 6.10. Photographs of Canada Fossils Ltd. specimens prior to reconstruction were provided by A. Dzindic. Specimen locality data used in Chapter 3 was provided by M. Currie (CMN), A. Dzindic (Canada Fossils Ltd.), D. Evans (ROM), and B. Strilisky (TMP). H. Street (UALVP) provided help with the identification of marine reptile elements associated with the holotype of *Antarctopelta*. I am very grateful to R. Sullivan for inviting me to help describe a new ankylosaurid from New Mexico.

CT scanning of UALVP 31 was facilitated by G. Schaffler (University of Alberta Hospital) and A. Locock (University of Alberta, Department of Earth and Atmospheric Sciences). CT scans of AMNH 5405 were provided by L. Witmer (Ohio University Heritage College of Osteopathic Medicine), and CT scans of INBR 21004 were provided by V. Ramachandran (University of California San Diego). Many thanks to B. Dumont and I. Grosse for their excellent “Finite Element Modeling in Biology” workshop at the University of Massachusetts Amherst in August 2009.

Funding for various museum visits, fieldwork, and other research activities was provided by an NSERC CGS-D, NSERC Michael Smith Foreign Study Supplement, Izaak Walton Killam Memorial Scholarship, Alberta Ingenuity Studentship, the Dinosaur Research Institute, the Korea-Mongolia International Dinosaur Project, the University of Alberta China Institute, the University of Alberta Graduate Students Association, and the Society of Vertebrate Paleontology. The University of Alberta Women in Scholarship, Engineering, Science and Technology Summer Research Program provided salaries for two research assistants (C. Chornell and I. Riemer) in 2009.

TABLE OF CONTENTS

PART 1. INTRODUCTION	1
1. Introduction and overview	2
1.1 Introduction	2
1.2 A brief overview of the ankylosaur fossil record	3
1.3 Aims and scope	7
1.4 Section overview	8
PART 2. TAPHONOMIC DEFORMATION AND RETRODEFORMATION	16
2. Analyzing taphonomic deformation of ankylosaur skulls using retrodeformation and finite element analysis.	17
2.1 Introduction	17
2.2 Methods	21
2.2.1 The orbit as a strain ellipse	21
2.2.2 3D model creation	22
2.2.3 3D retrodeformation in Geomagic	23
2.2.4 Finite element analysis of taphonomic deformation	23
2.3 Results	25
2.3.1 Results of orbit shape measurements	25
2.3.2 Retrodeforming ankylosaur skulls	30
2.3.3 Finite element analysis of taphonomic deformation	32
2.4 Discussion	35
PART 3. TAXONOMIC ASSESSMENTS	40
3. <i>Euoplocephalus tutus</i> and the diversity of ankylosaurid dinosaurs in the Late Cretaceous of Alberta, Canada, and Montana, USA	41
3.1 Introduction	41

3.2 Materials and methods	52
3.2.1 Material examined	52
3.2.2 Terminology	53
3.2.3 Stratigraphic and geographic positions of specimens	55
3.2.4 Phylogenetic analyses	57
3.3 Results	58
3.3.1 Morphological variation in specimens referred to <i>Euoplocephalus tutus</i>	58
3.3.1.1 Cranium	59
3.3.1.2 Mandible	67
3.3.1.3 Vertebral Column	68
3.3.1.4 Pectoral girdle and forelimb	76
3.3.1.5 Pelvic girdle and hindlimb	79
3.3.1.6 Osteoderms and integument	81
3.3.2 Stratigraphic distribution of ankylosaurid specimens from Alberta and Montana	90
3.4 Discussion	94
3.4.1 Taxonomic implications of variation in specimens previously referred to <i>Euoplocephalus tutus</i>	94
3.4.1.1 Status of <i>Anodontosaurus lambei</i>	94
3.4.1.2 Status of <i>Scolosaurus cutleri</i>	100
3.4.1.3 Status of <i>Oohkotokia horneri</i>	104
3.4.1.4 Status of other specimens previously referred to <i>Euoplocephalus tutus</i>	108
3.4.2 Systematic Paleontology	113
3.4.2.1 <i>Anodontosaurus lambei</i> Sternberg, 1929	113
3.4.2.2 <i>Dyoplosaurus acutosquameus</i> Parks, 1924	114
3.4.2.3 <i>Euoplocephalus tutus</i> Lambe, 1910	115
3.4.2.4 <i>Scolosaurus cutleri</i> Nopcsa, 1928	116

3.4.2.5 Indeterminate Ankylosauridae	117
3.4.3 Phylogenetic relationships of Campanian-Maastrichtian ankylosaurids from Alberta and Montana	119
3.4.4 Biogeographic and biostratigraphic implications	123
3.5 Conclusions	127
4. Other ankylosaurs from North America	162
4.1 Introduction	162
4.2 The "Stegopeltinae": <i>Aletopelta</i> , <i>Glyptodontopelta</i> , and <i>Stegopelta</i>	162
4.2.1 <i>Aletopelta coombsi</i> Ford and Kirkland, 2001	164
4.2.2 <i>Glyptodontopelta mimus</i> Ford, 2000	167
4.2.3 <i>Stegopelta landerensis</i> Williston, 1905	169
4.3 Other ankylosaurids or putative ankylosaurids from North America	171
4.3.1 <i>Ahshislepelta minor</i> Burns and Sullivan, 2011	171
4.3.2 <i>Ankylosaurus magniventris</i> Brown, 1908	172
4.3.3 <i>Nodocephalosaurus kirtlandensis</i> Sullivan, 1999	178
4.3.4 <i>Tatankacephalus cooneyorum</i> Parsons and Parsons, 2009	182
4.3.5 <i>Ziapelta sanjuanensis</i> Arbour, Burns, Sullivan, and Lucas in preparation	182
4.4 Other North American specimens	185
4.5 Discussion and conclusions	185
5. The taxonomic identity of a nearly complete ankylosaurid dinosaur skeleton from the Gobi Desert of Mongolia	188
5.1 Introduction	188
5.2 Materials and methods	189
5.3 Stratigraphic provenance of MPC 100/1305	189

5.4 MPC 100/1305 compared to <i>Saichania chulsanensis</i>	192
5.5 Comparison with <i>Pinacosaurus</i>	197
5.6 What is MPC 100/1305?	201
6. The ankylosaurid dinosaurs of the Upper Cretaceous	
Baruungoyot and Nemegt formations of Mongolia	203
6.1 Introduction	203
6.2 Materials and methods	204
6.3 Systematic Palaeontology	205
6.3.1 <i>Dyoplosaurus giganteus</i> Maleev, 1956	205
6.3.2 <i>Tarchia kielanae</i> Maryańska, 1977	208
6.3.3 <i>Zaraapelta nomadis</i> gen. et sp. Nov.	215
6.3.4 <i>Saichania chulsanensis</i> Maryańska, 1977	227
6.3.5 Ankylosauridae gen. et sp. indet., from the Baruungoyot and Nemegt formations of Mongolia	234
6.4 Discussion	235
6.5 Conclusions	240
7. Other ankylosaurs from Mongolia and Uzbekistan	254
7.1 The "Shamosaurinae": <i>Cedarpelta</i> , <i>Gobisaurus</i> , and <i>Shamosaurus</i>	254
7.1.1 <i>Cedarpelta bilbeyhallorum</i> Carpenter, Kirkland, Burge, and Bird, 2001	254
7.1.2 <i>Gobisaurus domoculus</i> Vickaryous, Russell, Currie, and Zhao, 2001	256
7.1.3 <i>Shamosaurus scutatus</i> Tumanova, 1983	262
7.2 Other ankylosaurids from Mongolia	264
7.2.1 <i>Amtosaurus magnus</i> Kurzanov and Tumanova, 1978	264
7.2.2 <i>Maleevus disparoserratus</i> (Maleev, 1952)	264

7.2.3 <i>Talarurus plicatospineus</i> Maleev, 1952	265
7.2.4 <i>Tsagantegia longicranialis</i> Tumanova, 1993	279
7.3 Other Ankylosaurids from Central Asia	271
7.3.1 <i>Bissektipelta archibaldi</i> (Averianov, 2002)	271
8. Ankylosaurs from China	273
8.1 Introduction	273
8.2 Systematic Palaeontology	273
8.2.1 <i>Bienosaurus lufengensis</i> Dong, 2001	273
8.2.2 <i>Crichtonsaurus bohlini</i> Dong, 2002	275
8.2.3 <i>Crichtonpelta</i> gen. nov.	276
8.2.4 <i>Dongyangopelta yangyanensis</i> Chen, Zheng, Azuma, Shibata, Lou, Jin, and Jin, 2013	284
8.2.5 <i>Heishansaurus pachycephalus</i> Bohlin, 1953	286
8.2.6 <i>Liaoningosaurus paradoxus</i> Xu, Wang, and You, 2001	286
8.2.7 <i>Peishansaurus philemys</i> Bohlin, 1953	291
8.2.8 <i>Pinacosaurus</i> Gilmore, 1930	291
8.2.9 <i>Saichania chulsanensis</i> Maryańska, 1977	300
8.2.10 <i>Sauroplices scutiger</i> Bohlin, 1953	307
8.2.11 <i>Taohelong jinchengensis</i> Yang, You, Li, and Hong, 2013	308
8.2.12 <i>Tianchisaurus nedegoapeferima</i> Dong, 1993	309
8.2.13 <i>Zhejiangosaurus lishuiensis</i> Lü, Jin, Sheng, Li, Wang, and Azuma, 2007	310
8.2.14 Other ankylosaurian remains from China	313
8.2.15 Japanese ankylosaur	313
8.3 Discussion and conclusions	314
9. Ankylosaurian dinosaurs from Gondwana	315
9.1 Introduction	315

9.2 Systematic Palaeontology	316
9.2.1 <i>Minmi paravertebra</i> Molnar, 1980	316
9.2.2 <i>Antarctopelta oliveroi</i> Salgado and Gasparini, 2006	318
9.2.3 Argentinian ankylosaur	322
9.2.4 Other Gondwanan ankylosaurs	325
9.3 Discussion and conclusions	326
PART 4. PHYLOGENETIC ANALYSIS	328
10. Revised phylogenetic analysis of the Ankylosauridae	329
10.1 Introduction	329
10.1.1 Previous phylogenetic analyses	332
10.1.2 Carpenter (2001) and compartmentalization	335
10.2 Methods	337
10.2.1 Taxon Selection	337
10.2.2 Character revision and new characters	340
10.2.2.1 Characters removed from the character list in Thompson et al. (2012)	344
10.2.3 Characters	351
10.2.4 Analytical methods and software	377
10.3 Results	378
10.3.1 First iteration: All taxa included	378
10.3.2 Second iteration: Safe taxonomic reduction	381
10.3.3 Third iteration: Additional taxonomic reduction	382
10.3.4 Results of the biogeographic analysis	393
10.4 Discussion	394
10.4.1 Nodosaurid ankylosaurs were present in Asia	395
10.4.2 Shamosaurinae is monophyletic but unnecessary	395
10.4.3 Stegopeltinae is not monophyletic	396
10.4.4 <i>Ahshislepelta</i> , <i>Tatankacephalus</i> , and most 'polacanthids' are	397

nodosaurids	
10.4.5 Gondwanan ankylosaurs are not monophyletic	398
10.4.6 Cranial caputegulae evolved independently in ankylosaurids and nodosaurids	398
10.4.7 The tail club handle appears before the knob in the fossil record	399
10.4.8 Ankylosaurines replace nodosaurids in Asia during the late Early Cretaceous, and migrate into North America during the mid Late Cretaceous	402
PART 5. CONCLUSIONS	414
5. Conclusions and Future Work	415
6. Literature Cited	418

LIST OF TABLES

Table 2.1. Summary of force and constraint parameters in five finite element tests simulating taphonomic deformation of AMNH 5405 and INBR 21004.

Table 2.2. Orbit rostrocaudal length:dorsoventral height ratios of extant taxa.

Table 2.3: Orbit rostrocaudal length:dorsoventral height ratios of ankylosaurid specimens.

Table 5.1. Comparative measurements of MPC 100/151 (holotype of *Saichania chulsanensis*), PIN 614 (*Pinacosaurus grangeri*), and MPC 100/1305, in millimeters.

Table 10.1: Status of ankylosaur taxa discussed in this thesis.

Table 10.2: Summary of character revisions and additions.

LIST OF FIGURES

Figure 1.1. Time-calibrated phylogeny of *Lesothosaurus* and the Thyreophora.

Figure 2.1 Comparison of AMNH 5405 (*Euoplocephalus*) and INBR 21004 (*Minotaurasaurus*) in ventral view.

Figure 2.2: Measuring orbit shape, and deforming digital models in Geomagic.

Figure 2.3. Results of orbit shape measurements for extant taxa.

Figure 2.4. Results of orbit shape measurements for ankylosaurs.

Figure 2.5. Results of deformation and retrodeformation of models using Geomagic.

Figure 2.6. Results of the finite element analyses simulating taphonomic deformation in *Euoplocephalus*.

Figure 2.7. Results of the finite element analyses simulating taphonomic deformation in *Minotaurasaurus*.

Figure 3.1. Geographic distribution of Albertan ankylosaurids.

Figure 3.2: CMN 0210, holotype of *Euoplocephalus tutus* skull.

Figure 3.3. UALVP 31, referred *Euoplocephalus tutus* skull.

Figure 3.4. ROM 784, holotype of *Dyoplosaurus acutosquameus* skull.

Figure 3.5. CMN 8530, holotype of *Anodontosaurus lambei* skull.

Figure 3.6. USNM 11892 and MOR 433, referred *Scolosaurus cutleri* skulls.

Figure 3.7. TMP 1991.127.1, referred *Euoplocephalus tutus* skull.

Figure 3.8. TMP 1997.132.1, referred *Anodontosaurus lambei*.

Figure 3.9. Cranial anatomy of ankylosaurids, including terminology for ornamentation patterns.

Figure 3.10. Skulls in dorsal view.

Figure 3.11. Cranial ornamentation patterns compared.

Figure 3.12. Skulls in lateral view.

Figure 3.13. Cranial and mandibular anatomy.

Figure 3.14. Cervical and dorsal vertebrae.

Figure 3.15. Dorsal vertebrae of AMNH 5337.

Figure 3.16. Dorsosacral, sacral, caudosacral, and caudal vertebrae.

Figure 3.17. Pectoral and pelvic girdles.

Figure 3.18. Forelimb elements.

Figure 3.19. Hindlimb elements.

Figure 3.20. Cervical half rings.

Figure 3.21. Tail clubs.

Figure 3.22. Stratigraphic distribution of ankylosaurid specimens in the Dinosaur Park and Horseshoe Canyon formations of Alberta.

Figure 3.23. Results of phylogenetic analysis 1, retaining character state codings from Thompson et al. (2012).

Figure 3.24. Results of phylogenetic analysis 2, modifying character state codings from Thompson et al. (2012).

Figure 3.25. Results of phylogenetic analysis 3, with new characters added to modified character state codings from analysis 2.

Figure 3.26. Stratigraphic distribution of Campanian-Maastrichtian ankylosaurid species in Alberta and northwest Montana.

Figure 4.1. Map of Canada and the United States (excluding Alaska and the Canadian Arctic Archipelago)

Figure 4.2. SDNHM 33909, holotype of *Aletopelta coombsi*.

Figure 4.3. Preserved elements of SDNHM 33909.

Figure 4.4. Pelvic shield osteoderms of USNM 8611.

Figure 4.5. SMP VP-1930, holotype of *Ahshislepelta minor*.

Figure 4.6. Skulls of *Ankylosaurus* and *Anodontosaurus* compared.

Figure 4.7. Narial regions of *Ankylosaurus* and *Euoplocephalus* compared.

Figure 4.8. Tail clubs of *Ankylosaurus* and *Anodontosaurus* compared.

Figure 4.9. SMP VP-900, holotype of *Nodocephalosaurus kirtlandensis*.

Figure 4.10. NMMNH P-64484, *Ziapelta sanjuanensis* compared to other North American Campanian-Maastrichtian ankylosaurids.

Figure 4.11. Stratigraphic distribution of Campanian-Maastrichtian ankylosaurids from North America.

Figure 5.1. MPC 100/151 (holotype of *Saichania chulsanensis*) and MPC 100/1305 compared.

Figure 5.2. Maps of Mongolia and Omnogovi showing locations of Alag Teeg, Bayan Zag, Khulsan, Ukhaa Tolgod, and Zamyn Khond.

Figure 5.3. Maximum humeral width plotted against maximum humeral length.

Figure 6.1. Maps of Mongolia and Omnogovi showing locations of specimen localities.

Figure 6.2. Ankylosaurid postcranial elements from the Nemegt Formation.

Figure 6.3. Comparison of the supraorbital, postorbital, and squamosal region of three Mongolian ankylosaurid specimens.

Figure 6.4. Ankylosaurid skulls in dorsal view.

Figure 6.5. Mongolian ankylosaurid skulls in left lateral view.

Figure 6.6. Crania of MPC 100/151, holotype of *Saichania chulsanensis* and INBR21004, *Tarchia kielanae* in anterior view.

Figure 6.7. Mandibles of Mongolian ankylosaurids in lateral view.

Figure 6.8. MPC D100/1338, *Zaraapelta nomadis* in lateral view.

Figure 6.9. MPC D100/1338, *Zaraapelta nomadis* in dorsal view.

Figure 6.10. MPC D100/1338, *Zaraapelta nomadis* in ventral view.

Figure 6.11. MPC D100/1338, *Zaraapelta nomadis*, anterior and posterior views and detail of the braincase.

Figure 6.12. Strict consensus trees recovered from the cladistic analyses using the traditional search option in TNT.

Figure 7.1. Skulls of shamosaurine ankylosaurids compared.

Figure 7.2. HGM 41HIII-0002, the holotype of *Zhongyuansaurus luoyangensis*, includes a tail club handle.

Figure 7.3. First and second cervical half rings of PIN 3779/2, holotype of *Shamosaurus scutatus*.

Figure 7.4. Mounted skeleton of PIN 557, *Talarurus plicatospineus*.

Figure 7.5. PIN 557-3, holotype skull of *Talarurus plicatospineus*.

Figure 7.6. MPC 700/17, holotype of *Tsagantegia longicranialis*.

Figure 8.1. Geographic locations of Chinese ankylosaurs discussed in this chapter.

Figure 8.2. Holotype specimen of *Crichtonpelta benxiensis*, BXGMV0012, and possible referable specimen on display in Liaoning.

Figure 8.3. Pelvic shields of ankylosaurs from China and Europe.

Figure 8.4. IVPP V12560, holotype of *Liaoningosaurus paradoxus*, overview of specimen.

Figure 8.5. Closeup of preserved integument in IVPP V12560, *Liaoningosaurus paradoxus*.

Figure 8.6. Sternal elements of ankylosaurids from Asia.

Figure 8.7. Narial anatomy of the Mongolian ankylosaurids *Pinacosaurus grangeri*, *Pinacosaurus mephistocephalus*, and *Tarchia kielanae*.

Figure 9.1. Non-ankylosaurian elements of MLP 86-X-28-1, holotype of *Antarctopelta oliveroi*.

Figure 9.2. Femur and osteoderms of an Argentinian ankylosaur.

Figure 10.1. Three hypotheses for the evolution of the ankylosaurid tail club.

Figure 10.2. Previous phylogenetic analyses of the Ankylosauria and Ankylosauridae.

Figure 10.3. Summary of new cranial characters presented in this dissertation.

Figure 10.4. Results of the phylogenetic analysis, first iteration, with all taxa included.

Figure 10.5. Results of the phylogenetic analysis, second iteration, with *Bissektipelta* and *Minmi paravertebra* removed.

Figure 10.6. Results of the phylogenetic analysis, third iteration, with *Ahshislepelta*, "*Antarctopelta*", *Dyoplosaurus*, "*Tianchisaurus*", and "*Zhejiangosaurus*" removed.

Figure 10.7. Results of the biogeographic analysis.

Figure 10.8. Time-calibrated phylogeny of the Ankylosauridae and selected nodosaurids and other thyreophorans, based on the strict consensus tree of the third iteration of the character matrix.

Figure 10.9. Distal caudal vertebrae of *Liaoningosaurus* and *Mymoorapelta* compared.

Figure 10.10. Stratigraphic distributions of ankylosaurs and early thyreophorans discussed in this dissertation.

LIST OF APPENDICES

Appendix 1.1 Material examined.

Appendix 3.1. Locality information for specimens referred to *Anodontosaurus lambei*, *Dyoplosaurus acutosquameus*, *Euoplocephalus tutus*, and *Scolosaurus cutleri*.

Appendix 3.2. Character statements and remarks. All character statements are the same as those in Thompson et al. (2012), but some character state codings have been altered for the 'updated codings' analysis (Matrix 2, Analysis 2). New characters for Matrix 3 and Analysis 3 appear last.

Appendix 3.3. Phylogenetic data matrix 1, original codings plus *Anodontosaurus lambei* and *Scolosaurus cutleri*.

Appendix 3.4. Phylogenetic data matrix 2, updated codings.

Appendix 3.5 Phylogenetic data matrix 3, updated codings with new characters.

Appendix 6.1. Character statements.

Appendix 6.2. Character matrix.

Appendix 10.1 Character matrix for all three iterations of the analysis presented in this chapter. The percentage of missing data as calculated by TAXEQ3 is indicated for each specimen.

LIST OF INSTITUTIONAL ABBREVIATIONS

AMNH – American Museum of Natural History, New York, New York, USA

BXGM – Benxi Geological Museum, Liaoning, China

CCM – Carter County Museum, Ekalaka, Montana

CD – New Zealand Geological Survey Collection, Lower Hutt, New Zealand

CEUM – College of Eastern Utah Prehistoric Museum, Price, Utah, USA

CMN – Canadian Museum of Nature, Ottawa, Ontario, Canada

CYGYB – Chaoyang Bird Fossil National Geopark, Chaoyang, Liaoning, China

DMNH – Denver Museum of Nature and Science, Denver, Colorado, USA

DYM – Dongyang Museum, Dongyang City, Zhejiang, China

FMNH – Field Museum of Natural History, Chicago, Illinois, USA

FPDM-V – Fukui Prefectural Dinosaur Museum (Vertebrate Collection),
Katsuyama, Fukui Prefecture, Japan

GSDM – Gansu Dinosaur Museum, Yangouxia, Yongjing County, Gansu, China

HBV – Geoscience Museum, Shijiazhuang University of Economics (previously
Hebei College of Geology), Shijiazhuang, Hebei, China

HGM – Henan Geological Museum, Zhengzhou, Henan, China

IMM – Inner Mongolia Museum, Hohhot, Nei Mongol, China

INBR – Victor Valley Museum, Apple Valley, California, USA

IVPP – Institute for Vertebrate Paleontology and Paleoanthropology, Beijing,
China

LPM – Paleontology Museum of Liaoning, China (possibly equivalent to Sihetun
Fossil Museum/Sihetun Visitor Facility)

MACN Pv – Colección nacional de Paleontología de Vertebrados del Museo
Argentino de Ciencias Naturales “Bernardino Rivadavia”, Buenos Aires,
Argentina

MCM – Mikasa City Museum (Municipal Museum of Mikasa), Hokkaido, Japan

MLP – Museo de La Plata, La Plata, Argentina

MPC – Paleontological Center, Mongolian Academy of Sciences, Ulaanbaatar, Mongolia (MPC KID refers to Korea-Mongolia Dinosaur Project field numbers)

MPCA – Museo Provincial Carlos Ameghino, Cipolletti, Argentina

MOR – Museum of the Rockies, Bozeman, Montana, USA

MWC – Museum of Western Colorado Dinosaur Journey, Fruita, Colorado, USA

NHMUK – Natural History Museum, London, United Kingdom

NMMNH – New Mexico Museum of Natural History and Science, Albuquerque, New Mexico, USA

NMV – Museum Victoria, Melbourne, Australia; NSM PV, National Museum of Nature and Science, Tokyo, Japan

PIN – Palaeontological Institute, Russian Academy of Sciences, Moscow, Russia

QM – Queensland Museum, Brisbane, Australia

ROM – Royal Ontario Museum, Toronto, Ontario, Canada

RSM – Royal Saskatchewan Museum, Regina, Saskatchewan, Canada

SDNHM – San Diego Natural History Museum, San Diego, California, USA

SMP – State Museum of Pennsylvania, Harrisburg, Pennsylvania, USA

TMP – Royal Tyrrell Museum of Paleontology, Drumheller, Alberta, Canada

UALVP – University of Alberta Laboratory for Vertebrate Paleontology, Edmonton, Alberta, Canada

UAMZ – University of Alberta Museum of Zoology, Edmonton, Alberta, Canada

USNM – Smithsonian Museum of Natural History, Washington, DC, USA

YPM – Yale Peabody Museum, New Haven, Connecticut, USA

ZIN PH – Paleoherpetological Collection, Zoological Institute, Russian Academy of Sciences, St. Petersburg, Russia

ZMNH – Zhejiang Natural History Museum, Hangzhou, Zhejiang, China

ZPAL – Zakład Paleobiologii, Polish Academy of Sciences, Warsaw, Poland

Part 1: Introduction

1. INTRODUCTION AND OVERVIEW

1.1 Introduction

The armoured ornithischian dinosaurs known as the Ankylosauria are generally subdivided into two major clades, the Nodosauridae and Ankylosauridae (Vickaryous et al. 2004); a third clade, the Polacanthidae or Polacanthinae, has been proposed (Kirkland 1998, Carpenter 2001) but is weakly supported. The most derived members of the Ankylosauridae had a unique tail club formed from modified, tightly interlocking distal caudal vertebrae (the handle, *sensu* Coombs 1995a) and enlarged osteoderms that envelop the terminus of the tail (the knob, *sensu* Coombs 1995a). Derived ankylosaurids also have a proportionately shorter rostrum compared to nodosaurids and basal ankylosaurs, and cranial ornamentation subdivided into distinct polygons (caputegulae, *sensu* Blows 2001).

The interrelationships of the ankylosaurid dinosaurs have been investigated (Vickaryous et al. 2004, Thompson et al. 2012), but these have not included detailed taxonomic assessments for the species under study. Additionally, the goal of these studies has typically been to determine whether or not a given ankylosaur is a nodosaurid or ankylosaurid ankylosaur, and the evolutionary and biogeographic trends within the Ankylosauridae have been less important. In this study, the diversity and interrelationships of the Ankylosauridae will be examined by reviewing and revising all known taxa and conducting a revised phylogenetic analysis. Previous phylogenetic studies of ankylosaurs have focused extensively on cranial morphology (e.g., Vickaryous et al. 2004). The revised phylogenetic analysis will incorporate additional characters representing the postcrania and osteoderms.

Apart from *Lesothosaurus*, *Scutellosaurus* is the most basal known thyreophoran (Butler et al. 2008). *Scutellosaurus* is known from a nearly complete skeleton and several referred specimens, all from the Lower Jurassic Kayenta Formation of Arizona (Rosenbaum and Padian 2000). Unlike *Lesothosaurus*, *Scutellosaurus* possessed osteoderms as in more derived thyreophorans, but based on limb proportions it would have been bipedal, not secondarily quadrupedal as in later thyreophorans (Rosenbaum and Padian 2000).

Scelidosaurus is known from the Early Jurassic (Sinemurian) of England (Norman 2001). Although the original description included non-thyreophoran material in the holotype, subsequent revisions stabilized the nomenclature by erecting a lectotype consisting of a skull and articulated skeleton with *in situ* osteoderms (Norman 2001). Several excellent, nearly complete skeletons including *in situ* osteoderms are on display at the Bristol City Museum, but remain the private property of the collector and so cannot yet be described in the scientific literature. *Emausaurus*, from the lowest Toarcian (Lower Jurassic) of Germany, is represented by a nearly complete skull, caudal vertebrae, ribs, phalanges, and osteoderms (Haubold 1990). A few other fragmentary taxa may represent 'scelidosaurian-grade' thyreophorans. *Tatisaurus oehleri* Simmons, 1965, from the Lower Lufeng Formation of China (?Hettangian, Luo and Wu 1994), is known only from a partial left dentary and poorly preserved angular, quadrate, and surangular. Norman et al. (2007) considered it a basal thyreophoran and a *nomen dubium*, but distinct from *Scelidosaurus* (contra Lucas (1996), who had synonymized *Tatisaurus* with *Scelidosaurus* to form *S. oehleri*). *Bienosaurus lufengensis* Dong, 2001, also from the Lower Lufeng Formation of China, is discussed in greater detail later. *Lusitanosaurus liasicus* Lapparent and Zbyszewski, 1957, is based on a fragment of maxilla from the

Lower Jurassic of Portugal, and Lapparent and Zbyszewski (1957) considered it to be similar in form to *Scelidosaurus*.

The earliest records of both stegosaurs (Maidment et al. 2008) and ankylosaurs indicate that the Thyreophora had diverged into its major clades by the Middle Jurassic. *Sarcolestes leedsi* Lydekker, 1893, from the Callovian of the United Kingdom has sculpturing along the lateral edge of the mandible, a feature that is only present in ankylosaurs and not present in stegosaurs or more basal thyreophorans. *Tianchisaurus nedegoapeferima* Dong, 1993 from the Middle Jurassic of China, was described as possessing sculpturing and ornamentation on the skull roof and on the mandible. These features would suggest *Tianchisaurus* is an ankylosaur rather than a more basal thyreophoran, but they are difficult to confirm in the figures and the specimen could not be located at the IVPP in 2010. At present, the holotype of *Sarcolestes* is the earliest specimen that is definitely an ankylosaur.

More complete Jurassic ankylosaurs occur in the Upper Jurassic of North America. *Gargoyleosaurus parkpinorum* Carpenter, Miles, and Cloward, 1998, is known from a nearly complete skeleton including a skull, and *Mymoorapelta maysi* Kirkland and Carpenter, 1994 is also represented by abundant material, although most of the cranium is missing. Together, these species exhibit many of the features found in later and more derived ankylosaurs: extensive cranial ornamentation, a wide and low-slung body, horizontally-oriented ilia, and at least partial closure of the acetabulum. "*Dracopelta zbyszewskii*" Galton, 1980 from the Tithonian of Portugal is represented by a single partial, articulated skeleton consisting of the thoracic region, with *in situ* osteoderms, and an autopodium (Galton 1980; Pereda Suberbiola et al. 2005). "*Cryptosaurus eumerus*" Lydekker, 1889 (= *Cryptodraco*; Naish and Martill 2008) is represented by an isolated femur from the Oxfordian of England. It is similar to the femora of many other ankylosaurs, except that the greater trochanter and anterior trochanter are unfused, a condition also present in *Scelidosaurus* (Romer 1927)

and the North American Barremian-aged *Hoplitosaurus marshi* Lucas, 1901 (USNM 4752; Gilmore 1914). The trochanters are not fused in the North American Barremian-aged *Gastonia burgei* Kirkland, 1998 or the European Barremian- to Aptian-aged *Polacanthus foxii* Fox, 1866 (NHMUK R175).

Ankylosaurs continued to diversify during the Early Cretaceous, and became more abundant locally as well. The higher-level classification of some of the Early Cretaceous ankylosaurs has been contentious and remains unresolved. In his landmark revision of the ankylosaurs, Coombs (1978a) classified almost all valid species as belonging either to the Nodosauridae or the Ankylosauridae, a division that has been well supported by numerous subsequent studies. A third clade of primarily pre-Albian species has also been proposed, as either the Polacanthidae (of equal rank with Ankylosauridae and Nodosauridae) or the Polacanthinae (as a nested clade within the Ankylosauridae or within the Nodosauridae). Kirkland (1998) defined the Polacanthinae as ankylosaurs with an ankylosaurid-like skull, straight and parallel tooth rows, long basiptyergoid processes, scapulae with prominent acromion flanges, ventrally-flexed ischia, fused pelvic osteoderms forming a continuous shield, long, posteriorly grooved pectoral osteoderms, and long, hollow-based, triangular caudal osteoderms. In a phylogenetic analysis, Kirkland (1998) recovered a Polacanthinae consisting of *Gastonia*, *Mymoorapelta*, and *Polacanthus*, and also referred *Hoplitosaurus* and *Hylaeosaurus* to this clade. Carpenter (2001) *a priori* assigned taxa to three 'compartments' – Ankylosauridae, Nodosauridae, and Polacanthidae – before conducting phylogenetic analyses on each compartment. The resulting phylogenetic tree cannot be considered support for the Polacanthidae, because taxa were assigned to clades before analysis of the character matrix. A subsequent larger phylogenetic analysis using only cranial characters (Vickaryous et al. 2004) was unable to test the validity of the Polacanthidae/Polacanthinae, because *Mymoorapelta* and *Polacanthus* lack cranial material. The most recent revised comprehensive analysis of the Ankylosauria did not recover a

polacanthid or polacanthine clade, but instead found that 'polacanthid' ankylosaurs were basal members of the Nodosauridae (Thompson et al. 2012).

Crichtonsaurus bohlini Dong, 2002 (late Albian, China) and *Shamosaurus scutatus* Tumanova, 1983 (Aptian-Albian, Mongolia) are among the earliest ankylosaurid ankylosaurs. The phylogenetic relationships of other potential Early Cretaceous ankylosaurids will be tested in the revised phylogenetic analysis, in order to further refine the origin of the Ankylosauridae. The diversity of Late Cretaceous ankylosaurids was greatest during the Campanian-Maastrichtian, and ankylosaurids seem to have been present primarily in North America and Asia.

1.3 Aims and scope

All known ankylosaurids were examined through first-hand examination or literature review for this project, as were ankylosaurs with more ambiguous phylogenetic affiliations. A complete list of specimens and taxa can be found in Appendix 1.1. Using the revised taxonomic descriptions and assessments, a new phylogenetic analysis is performed in order to provide new information on the phylogenetic relationships within the Ankylosauridae. The following questions will be addressed using the results of the revised phylogenetic tree:

1. Is there any evidence for nodosaurid ankylosaurs in Asia? Several recently described Chinese and Japanese ankylosaurs have been referred to the Nodosauridae, but only two of these descriptions include phylogenetic analyses to support this referral (Chen et al. 2013, Yang et al. 2013).
2. Is the Shamosaurinae a valid clade? *Shamosaurus* and *Gobisaurus domoculus* Vickaryous, Russell, Currie, and Zhao, 2001 are sometimes recovered as sister-taxa in phylogenetic analyses (Vickaryous et al. 2004), whereas Thompson et al. (2012) found them to be successive outgroups to more derived ankylosaurids. Carpenter (2001) and Carpenter et al. (2008) have suggested that *Cedarpetta bilbeyhallorum* Carpenter,

Kirkland, Bird, and Burge, 2001 may be a shamosaurine ankylosaur;
Thompson et al. (2012) recovered *Cedarpelta* as a basal ankylosaurid.

3. Is the Stegopeltinae a valid clade? Ford (2000) hypothesized that *Aletopelta coombsi* Ford and Kirkland, 2001, *Glyptodontopelta mimus* Ford, 2000, and *Stegopelta landerensis* Williston, 1905 may form a clade within the Ankylosauridae based on the presence of a pelvic shield composed of coossified hexagonal osteoderms. Only *Stegopelta* has been included in previous phylogenetic analyses.
4. At what point does the tail club first appear? Carpenter et al. (2008) considered the tail club a synapomorphy of adult ankylosaurids, although their definition of tail club was most likely restricted to the tail club knob. These authors also considered the tail club to be absent in shamosaurine ankylosaurids (including *Cedarpelta*), based on the putative absence of a tail club in *Zhongyuansaurus luoyangensis* Li, Lü, Zhang, Jia, Hu, Zhang, Wu, and Ji, 2007.
5. Are there any trends in tail club evolution? Does the size of the knob change through time? Is the tail club ever secondarily lost in ankylosaurid evolution?
6. Are there any biogeographic patterns within the Ankylosauridae? Do ankylosaurids originate in Asia or North America? Is *Nodocephalosaurus kirtlandensis* Sullivan, 1999, from the Late Cretaceous of North America, more closely related to Mongolian ankylosaurids than other North American ankylosaurids, as proposed by Sullivan (1999)? Are any ankylosaurids present in Gondwana?

1.4 Section overview

In addition to the introduction and conclusion, chapters in this dissertation are grouped into three main sections. Part 2 examines the effects of taphonomy on the interpretation of ankylosaur cranial characters. Part 3, the

largest section, includes taxonomic assessments and revisions for all known ankylosaurids, as well as more ambiguous taxa that may or may not be ankylosaurids. A revised phylogenetic analysis is presented in Part 4, along with discussions of ankylosaurid evolution and biogeography.

Appendix 1.1. Material examined.

Taxon	Material
<i>Acanthopholis horrida</i>	NHMUK R44581 (anterior caudal)
<i>Ahshislepelta minor</i>	SMP VP-1930 (holotype: associated incomplete postcranial skeleton, including both scapulocoracoids, left humerus, proximal portion of left radius, vertebral fragments, osteoderms, and unidentifiable fragments).
<i>Aletopelta coombsi</i>	SDNHM 33909 (holotype: eight teeth, fragmentary scapulae, partial humerus, partial ulna, possible fragment of right ?radius, ulna, partial left and possibly right ischium, femora, tibiae, fibulae, four-five partial vertebrae, dorsal neural arch, neural arches of the sacrum, fragmentary ribs, osteoderms including pelvic shield and cervical half ring)
<i>Amtoosaurus magnus</i>	PIN 3780/2 (holotype: isolated braincase)
<i>Animantarx ramaljonesi</i>	CEUM 6268 (parietals), CEUM 8070 (left quadrate), CEUM 8277 (braincase), CEUM 8281 (left orbit), CEUM 9173 (right dentary)
<i>Ankylosaurus magniventris</i>	AMNH 5895 (holotype: three caudal vertebrae, portions of both cervical half rings). AMNH 5214, complete skull, both mandibles, seven caudal vertebrae including tail club, on display; cast of skull UALVP 54722.
<i>Anodontosaurus lambei</i>	CMN 8530 (holotype: skull, lower jaws, caudal vertebra, ischium, pedal phalanx, and osteoderms including first cervical half ring). AMNH 5216 (tail club), AMNH 5223 (skull), AMNH 5245 (caudosacral and caudal vertebra, pelvis, tail club). NHMUK R4947 (skull). ROM 832 (fragmentary skull). TMP 1982.9.3 (two posterior dorsals with coossified ribs, partial pelvis, right femur, osteoderms including cervical half ring fragments), TMP 1994.168.1 (tail club), TMP 1996.75.01 (partial skull, cervical vertebra, partial ?first cervical half ring, ?second cervical half ring), TMP 1997.59.1 (skull), TMP 1997.132.01 (skull, three dorsal vertebrae, ribs, ?scapula, left humerus, ulna, radius, tibia, first and possibly second cervical half rings). USNM 10753 (tail club).
<i>Antarctopelta oliveroi</i>	MLP 86-X-28-1 (holotype: cranial fragments, left dentary fragment with <i>in situ</i> tooth, three isolated teeth, two cervical vertebrae and latex cast prepared from natural mould of three articulated vertebrae, fragments of dorsal ribs, two dorsosacral centra, three coossified sacral centra, eight caudals, glenoid portion of left scapula, fragment of right ilium, distal portion of left femur, five metapodials, two phalanges, osteoderms)
<i>Bienosaurus lufengensis</i>	IVPP V15311 (holotype: partial right lower mandible, fragmentary frontal, other cranial fragments)
<i>Cedarpetta bilbeyhallorum</i>	CEUM 1026 (ischium), CEUM 10258 (caudal), CEUM 10261 (braincase), CEUM 10372 (juvenile parietals), CEUM 10405 (left premaxillary), CEUM 10412 (caudal), CEUM 10417 (left quadrate), CEUM 10425 (prefrontal), CEUM 10525 (dentary), CEUM 10560 (lacrimal), CEUM 10574 (jugal), CEUM 12360 (holotype skull), CEUM reconstructed cast skull
<i>Crichtonsaurus benxiensis</i>	BXGMV0012 cast UALVP 52015 (holotype: skull). Mounted skeleton on display at Sihetun Fossil Centre.
<i>Cryptosaurus eumerus</i>	NHMUK R1609 (cast of right femur); NHMUK R1617 (dorsal vertebra)

<i>Dyoplosaurus acutosquameus</i>	ROM 784 (holotype: fragmentary skull, complete caudal series of vertebrae including tail club, ribs, pelvis, hindlimb including pes, osteoderms <i>in situ</i>). UALVP 47273 (partial tail club).
<i>Dyoplosaurus giganteus</i>	PIN 551/29 (holotype: caudal vertebrae, metatarsals, phalanges, osteoderms including tail club knob)
<i>Edmontonia longiceps</i>	CMN 8521 (holotype: caudals)
<i>Euoplocephalus tutus</i>	CMN 210 (holotype, fragmentary skull roof and partial first cervical half ring). AMNH 5337 (skull, left mandible, one cervical vertebra, eleven dorsal vertebrae, humeri, scapulocoracoid, pelvis, osteoderms including first cervical half ring), AMNH 5403 (skull, both mandibles including prementary, four cervicals including axis, scapula, forelimbs, first and second cervical half rings, partial tail club knob), AMNH 5404 (skull, five caudals, ribs, right humerus, ischium, right femur, tibia, fibula, osteoderms, first cervical half ring), AMNH 5405 (skull, right mandible including prementary, handle vertebrae, humerus, ulna, osteoderms, first cervical half ring, tail club knob), AMNH 5406 (three dorsal vertebrae, ribs, scapulae, right humerus, ulna, radius, phalanges, osteoderms including first and second cervical half rings). CMN 842 (first cervical half ring), CMN 8876 (skull). ROM 1930 (skull, three dorsal vertebrae, two ?sacral vertebrae, twelve free caudals, transitional caudal, fragmentary right scapula, right humerus, osteoderms including <i>in situ</i> osteoderms and skin impressions on caudal vertebrae). TMP 1979.14.74 (partial skull). UALVP 31 (skull, right mandible, ribs, sacrum, scapula, humeri, right ilium, right ischium, right femur, tibia, pedal elements, osteoderms including first and second cervical half rings), UALVP 47977 (partial skull roof).
<i>Gargoyleosaurus parkpinorum</i>	DMNH 27726 (holotype; pubis, axis, atlas, 3 rd cervical, caudals)
<i>Gastonia burgei</i>	CEUM 10293 (skull), CEUM cast pelvic shield, CEUM (holotype skull), cast of holotype skull UALVP 54755. Bonebed material, mostly caudals, at DMNH
<i>Glyptodontopelta mimus</i>	USNM 8611 (several osteoderm fragments)
<i>Gobisaurus domoculus</i>	TMP 1990.000.4 (cast of holotype skull)
<i>Hoplitosaurus marshi</i>	USNM 4752 (femur, osteoderms, vertebrae)
<i>Heishansaurus pachycephalus</i>	Casts (AMNH 2062) of some of the vertebrae.
<i>Hylaeosaurus armatus</i>	NHMUK R28936 (middle of sacrum), NHMUK R3773 (cervicals and osteoderms), R3789 (caudal vertebrae and haemal arches), NHMUK R3782 (osteoderm)
<i>Liaoningosaurus paradoxus</i>	IVPP V12560 (holotype: nearly complete, articulated skeleton preserved with the ventral surface exposed on a limestone). CYGYB 208 (nearly complete skeleton preserved on slab with dorsal surface exposed), CYGYB 237 (nearly complete skeleton preserved on slab with ventral surface exposed)

<i>Minmi</i> sp.	QM F1801, USNM cast 508490 (nearly complete skeleton including skull, axial skeleton to proximal part of tail, left shoulder girdle, left humerus, radius, and ulna, left ilium, both ischia, both pubes, both femora, <i>in situ</i> dorsal osteoderms)
<i>Mymoorapelta maysi</i>	MWC holotype ilium. MWC 5819 (two caudal vertebrae with fused haemal arches), MWC 1806 (anterior caudal), MWC 5820 (two partial caudal vertebrae), MWC 5643 (left ulna), MWC 876 (preacetabular portion of right ilium), MWC 4027 (ischium), MWC 3763 (rib), MWC no number (radius), MWC 2610 block A4 (two paramedian osteoderms with ossified tendons preserved ventrally), MWC 5641 (posterior cervical or anterior dorsal), MWC 1801 (dorsal), MWC 1907 (middle caudal with fused haemal arch), MWC 3744 (possible piece of cervical half ring), MWC 5320 (possible cervical osteoderm), MWC 5435 (partial braincase), MWC 5438 (radius),
<i>Nodocephalosaurus kirtlandensis</i>	SMP VP-900 (holotype: partial skull)
<i>Panoplosaurus mirus</i>	CMN 2769 (holotype: skull, sacrum, pes)
<i>Pawpawsaurus campbelli</i>	Cast of holotype UALVP 54698.
<i>Pinacosaurus grangeri</i>	AMNH 6523 (holotype: skull and mandibles) MPC 100/1305 (complete skeleton with <i>in situ</i> osteoderms but lacking skull and cervical half rings, on display at MPC) PIN 614 (complete skeleton with osteoderms but lacking skull, on display at the Orlov Museum of Paleontology (Russian Academy of Sciences). PIN 3780/3 (skull). ZPAL MgD II/1 (skull, mandibles, preentary, cervicals, dorsal, caudals, ribs, scapula, coracoids, humerus, radius, ulna, ilium, both femora, tibia, fibula, cervical half ring fragments). ZPAL MgD II/9 (caudals, tail club handle, pelvis, manus, femur, tibia, pes), ZPAL MgD II/31 (tail club handle); <u>From the Alag Teeg Bonebed:</u> MPC 100/1307, pedal elements; MPC 100/1308 tibiae, pedal elements; MPC 100/1309, pedal elements; MPC 100/1310, left forelimb; MPC 100/1311, hindlimb and pedal elements; MPC 100/1312, pedal elements; MPC 100/1313, pedal elements; MPC 100/1315, manual elements from two individuals; MPC 100/1316, tibiae, fibulae, pedal elements; MPC 100/1317, manual elements; MPC 100/1318, manual elements; MPC 100/1319, left pes; MPC 100/1320, tibia, fibula, right pes; MPC 100/1321, skull and postcranial elements; MPC 100/1322, quadrates, coracoid, ulna, ischium, three femora of two individuals; MPC 100/1323, right ulna, manus, both pedes; MPC 100/1324, vertebrae, coracoid, osteoderms; MPC 100/1325, right manus; MPC 100/1326, forelimb, manus, associated caudal vertebrae; MPC 100/1327, left tibia and pes; MPC 100/1328, left pes; MPC 100/1329, vertebrae, manual and pedal elements; MPC 100/1330, cervical half ring fragments, vertebrae, manus; MPC 100/1331, complete right pes; MPC 100/1332, scapula, coracoid, ribs; MPC 100/1333, ilia, humeri, radius, ulna, both manus, pes (large individual); MPC 100/1334, tibia, fibula, pedal elements; MPC 100/1335, skull, forelimbs, hindlimb; MPC 100/1335, osteoderms; MPC 100/1337, right manus; MPC 100/1338, manual elements; MPC 100/1339, right ulna, radius, manus, tibiae, fibulae, both pedes; MPC 100/1340, radius, ulna, manus; MPC 100/1341, radius, ulna, manus; MPC 100/1342, tibia, fibula, pes; MPC 100/1343, hindlimb, both pedes; MPC 100/1344, skull,

	cervical vertebrae, cervical half ring, articulated dorsal vertebrae, scapula, humerus, both femora, tail; MPC 100/1345, cervical half ring, rib; MPC 100/1346, coracoid, humerus; MPC 100/1347, frontal. Additional undescribed Alag Teeg material in the Hayashibara Museum collections, and at the PIN. <u>From Bayan Mandahu:</u> IVPP V16853, skull and cervical half rings (Bayan Mandahu, locality 100); IVPP V16283, partial skull (Bayan Mandahu, locality 100), IVPP V16854, nearly complete skeleton with skull (Bayan Mandahu, locality 101); IVPP V16346, partial skull (Bayan Mandahu, locality 106); IVPP V16855, skull and skeleton (Bayan Mandahu, unknown locality).
<i>Polacanthus foxii</i>	NHMUK R1926 (portion of ilium and sacrum), NHMUK R9293 (dorsal vertebra, cervical, two caudals, portions of pelvic shield), NHMUK R4952 (caudal vertebra), NHMUK R9950 (sacrum in matrix), NHMUK R175 (proximal caudal, distal caudals in series, tibia, femur), cast of putative 'tail club' cast at CEUM
<i>Priconodon crassus</i>	USNM 437985 (teeth)
<i>Regnosaurus northamptoni</i>	NHMUK R2422 (fragmentary jaw)
<i>Saichania chulsanensis</i>	Cast of holotype skull mounted with MPC 100/1305. Cast of <i>in situ</i> holotype skeleton at ZPAL Museum of Evolution. PIN 3142/250 (complete skull, both mandibles, and predentary; some osteoderms on display)
<i>Sarcolestes leedsi</i>	NHMUK R2682 (holotype; partial mandible)
<i>Sauropelta edwardsorum</i>	AMNH 3036 (skeleton, on display)
<i>Scelidosaurus harrisonii</i>	NHMUK R1111 (cast of complete skeleton, axis, dorsal, two caudals with osteoderms); specimens on display at the Bristol City Museum
<i>Scolosaurus cutleri</i>	NHMUK R5161 (holotype: nearly complete skeleton with <i>in situ</i> osteoderms and skin impressions, lacking skull, distal half of tail, right forelimb, and right hindlimb). MOR 433 (partial skull, both humeri, free caudal vertebra, and osteoderms). TMP 2001.42.19 (skull, partial first cervical half ring, dorsals, sacrals, caudals including complete tail club, left humerus, left scapula, right femur, right and left tibiae, osteoderms) USNM 7943 (partial first cervical half ring), USNM 11892 (skull).
<i>Shamosaurus scutatus</i>	PIN 3779/2 (holotype: skull and cervical half rings)
<i>Struthiosaurus transylvanicus</i>	NHMUK R4966 (skull, scapula, cervical, caudal)
<i>Talarurus plicatospineus</i>	PIN 557 (holotype: partial skull (PIN 557-3) and postcranial skeleton; mounted composite specimen on display at PIN). Undescribed material collected by the Korea-Mongolia Joint International Dinosaur Project, from Bayn Shiree, includes: MPC KID 154 (dorsal vertebra neural arch), MPC KID 167 (dorsal vertebra, partial cervical half ring), MPC KID 185 (partial coracoid), MPC KID 186 (quadrate, quadratojugal horn), MPC KID 187 (free caudal centrum with fused haemal arch, cervical half ring fragments, possible tail club knob fragments), MPC KID 166 (skull). Undescribed material collected by the Korea-Mongolia Joint International Dinosaur Project, from Shine Us Khudag, includes: MPC KID 151 (braincase), KID MPC 155 (seven dorsals, three caudal vertebrae, ribs, ilia and sacrum, both ischia, osteoderms,

ossified tendons), MPC KID 162 (bonebed collection - skull roof fragments, quadrate, unidentified cranial fragments, dentary fragment, two caudal vertebrae, pathological rib, tibia with coossified astragalus, distal fibula with coossified calcaneum and distal tarsal, phalanges, cervical ring fragments, osteoderm, indeterminate fragments; some non-ankylosaurian material as well).

<i>Tarchia kielanae</i>	UALVP 49402, cast of INBR 21004 (holotype of <i>Minotaurasaurus</i>)
<i>Tsagantegia longicranialis</i>	MPC 700/17 (holotype: skull)
<i>Zaraapelta nomadis</i>	MPC D100/1388 (skull)
<i>Ziapelta sanjuanensis</i>	NMMNH P-64484 (nearly complete skull, left side of first cervical half ring, partial second cervical half ring, post-cervical osteoderms).
Ankylosauridae indet. Alberta	<p>AMNH 5211 (tail club), AMNH 5266 (juvenile individual with vertebrae, ischium, right hindlimb with pes).</p> <p>CMN 125 (skull roof fragment), CMN 135 (tail club knob), CMN 268 (fragmentary first cervical ring), CMN 349 (tail club), CMN 2251 (partial tail club knob), CMN 2252 (partial tail club knob), CMN 2253 (partial tail club knob).</p> <p>MACN Pv 12554 (tail club).</p> <p>NHMUK R8265 (left quadratojugal horn), NHMUK R36629 (?posterior supraorbital), NHMUK R36630 (quadratojugal horn), NHMUK R36631 (?squamosal horn).</p> <p>ROM 788 (tail club), ROM 813 (partial skeleton with <i>in situ</i> osteoderms, skin impressions), ROM 7761 (tail club knob).</p> <p>TMP 1967.13.2 (tail club knob fragment), TMP 1967.19.4 (left squamosal horn), TMP 1967.20.20 (right quadratojugal horn), TMP 1979.14.164 (partial skull), TMP 1980.8.284 (supraorbital), TMP 1980.16.1685 (fragmentary right mandible), TMP 1983.36.120 (tail club), TMP 1984.121.33 (partial tail club knob), TMP 1985.36.70 (free caudal vertebra), TMP 1985.36.330 (highly fragmentary skull in numerous pieces), TMP 1988.106.5 (left supraorbital), TMP 1991.36.321 (fragmentary first cervical ring), TMP 1991.36.743 (portion of frontonasal region), TMP 1992.36.334 (free caudal vertebra), TMP 1992.36.421 (right mandible), TMP 1993.36.79 (left squamosal), TMP 1993.36.421 (tail club), TMP 1998.83.1 (skull, cervical half ring: indeterminate because unprepared as of 2012), TMP 1993.66.13 (quadratojugal horn), TMP 1996.12.15 (portion of supraorbital region), TMP 1997.36.313 (right mandible), TMP 1998.93.55 (free caudal vertebra), TMP 1998.93.65 (free caudal vertebra), TMP 2000.57.3 (phalanges, tail club), TMP 2000.57.30 (portion of lacrimal/frontonasal region), TMP 2003.12.166 (fragmentary ?second cervical ring), TMP 2003.12.169 (first cervical ring distal osteoderm), TMP 2003.12.311 (skull, cervical half ring: indeterminate because unprepared as of 2012), TMP 2004.98.06 (mandible), TMP 2005.09.75 (free caudal), TMP 2005.12.43 (free caudal vertebra), TMP 2005.49.178 (portion of frontonasal region), TMP 2007.020.0063 (small quadratojugal horn), TMP 2007.20.80 (free caudal vertebra), TMP 2007.12.52 (second cervical half ring), TMP 2007.20.100 (free caudal vertebra), TMP 2012.005.2 (portion of lacrimal/frontonasal region).</p> <p>UALVP 16247 (tail club), UALVP 45931 (partial first and second cervical half rings), UALVP 47273 (tail club), UALVP 49314 (anterior supraorbital), UALVP 52875 (partial tail club knob), UALVP 54685</p>

	(posterior supraorbital). Additionally, many isolated osteoderms and teeth from the Dinosaur Park Formation are in the TMP and UALVP collections.
Ankylosauridae indet. Montana	AMNH 5470 (partial sacrum), AMNH 20870 (handle vertebrae). MOR 363 (braincase, both quadratojugal horns, and skull roof fragments). USNM 16747 (handle vertebrae).
Ankylosauridae indet. Baruungoyot Formation	PIN 3142/251 (tail club on display at PIN, cast at DMNH)
Ankylosauridae indet. Nemegt Formation	PIN 5011/87 (first cervical half ring, on display at PIN as <i>Tarchia</i>); MPC KID 373 (partial dentary); MPC KID 515 (dorsal vertebrae, pedal phalanx, and osteoderms); MPC KID 538 (partial tail club handle); KID 586 (humerus); MPC KID 589 (cervical half ring fragment); MPC KID 591 (free caudal vertebra and osteoderms); MPC KID 630 (humerus); MPC KID 636 (free caudals, handle caudal, osteoderms); MPC KID 637 (free caudal, osteoderms); numerous isolated osteoderms or clusters of osteoderms from MPC KID expeditions; ZPAL MgD I/42 (tail club); ZPAL MgD I/43 (tail club, housed at MPC)
Ankylosauria indet., Argentina	MPCA-Pv 77 (tooth), MPCA-Pv 68/69/70 (three posterior dorsal vertebrae); MPCA-Pv 71, (caudal vertebrae); MPCA-Pv 72/73 (two caudal centra); MPCA-SM 1 (right femur); MPCA-Pv 78 (partial cervical half ring); MPCA-Pv 41-43, 74-76 (osteoderms).

Part 2: Taphonomic deformation and retrodeformation

2. ANALYZING TAPHONOMIC DEFORMATION OF ANKYLOSAUR SKULLS USING RETRODEFORMATION AND FINITE ELEMENT ANALYSIS¹

2.1 Introduction

Variation among specimens referred to a single fossil taxon can originate from several biological sources, such as ontogeny, sexual dimorphism, and individual variation, but taphonomy can also be a source of morphological variation in fossils. During fossilization and diagenesis, bones can become deformed, and this deformation can lead to difficulties in understanding taxonomic variation, phylogenetic relationships, and functional morphology (Motani 1997, Retallack 2007, White 2003, Zollikofer et al. 2005). Understanding the effects of taphonomic deformation on bones is therefore important for interpreting morphological variation.

Fossils can become distorted from the effects of brittle or plastic deformation (or both). In geological terms, brittle deformation results in fractures, joints, and faults, and plastic deformation results in folds. Whether or not a fossil undergoes brittle or plastic deformation is dependent on the temperature, confining pressure, and strain rate it experiences. Brittle deformation occurs at low temperatures, low confining pressures, and high strain rates; plastic deformation occurs at high temperatures, high confining pressures, and low strain rates. Many fossils undergo brittle deformation prior to burial, cracking and fracturing during transport, and brittle deformation can occur during diagenesis as well, such as if a fossil is faulted. Plastic deformation of a fossil is more likely to occur during fossilization and diagenesis, during which time bone can act like a ductile material. Fossils rarely survive more than a single phase of plastic deformation, and as such, identifiable but plastically distorted

¹ A version of this chapter has been published. Arbour and Currie 2012. PLOS ONE 7:e39323. P. Currie supervised the project and edited the manuscript.

fossils typically have a simple deformation history (Hughes 1999). Not all fossils in a single bedding plane may deform homogeneously, and not all elements within a single specimen will necessarily deform homogeneously (Hughes 1999). The orientation of a specimen within the sediment will also affect how the specimen deforms (Ponce de León 2002).

The goal of this study is to introduce some techniques for understanding three-dimensional (3D) plastic deformation in ankylosaurid dinosaur skulls. First, skulls of extant vertebrates were examined to determine if the shape of the orbit can be used as an indicator for whether or not plastic deformation has occurred. If the periorbital rims of a variety of extant vertebrates are generally circular, then fossil skulls with elliptical orbits have probably undergone some amount of plastic deformation. Retrodeformation and finite element analysis were then used as tools for understanding what parts of an ankylosaur skull are most likely to undergo deformation and therefore least likely to be phylogenetically useful. This information can then be used to enhance the quality of cranial characters used in phylogenetic analyses. No attempt was made to undistort taphonomically distorted skulls into their original shape, as there are few features on the skull to act as constraints guiding the decisions in retrodeforming ankylosaur skulls. Retrodeforming an ankylosaur skull with the goal of restoring its true shape would be highly subjective. Instead, the focus of this study is on understanding which morphological features on an ankylosaur skull are most likely to become taphonomically deformed.

The software program Geomagic is used to investigate potential effects of deformation by modifying digital models of ankylosaur skulls. It can be used to restore symmetry to a skull, and to measure the amount of shape change in various models of the same structure. Finite element analysis (FEA) can be used to investigate the way in which we might expect a fossil to have deformed under a variety of geological forces. FEA has been used to investigate the effects of biologically-induced forces in extant and extinct vertebrates (Degrange et al.

2010, Porro et al. 2011, Tseng and Binder 2010). However, FEA has not been used to investigate the effects of geological forces on vertebrate fossils, such as sediment compaction and diagenesis. In this paper, the retrodeformation analyses represent the subtraction of deformation from a skull, and the finite element analyses represent the addition of deformation to a skull. If the same parts of the skull undergo shape change during both retrodeformation and FEA, then these parts of the skull are most likely to experience deformation during fossilization and diagenesis.

This study examines two cases where understanding deformation can be used to better interpret ankylosaur cranial morphology: 1) intraspecific variation in *Euoplocephalus tutus* (Lambe, 1902), and 2) the taxonomic validity of *Minotaurasaurus ramachandrani* Miles and Miles, 2009. *Euoplocephalus* (Fig. 2.1) is the best represented ankylosaurid from the Late Cretaceous of North America, and more than 15 skulls have been referred to this genus. Coombs (1978) synonymized four taxa within *Euoplocephalus tutus*: *Dyoplosaurus acutosquameus* Parks, 1924, *Scolosaurus cutleri* Nopcsa, 1928, and *Anodontosaurus lambei* Sternberg, 1929. Arbour et al. (2009) recognized *Dyoplosaurus* as a distinct taxon, a result supported by an ankylosaur phylogenetic analysis by Thompson et al. (2012). Penkalski (2001) noted a great deal of variation among skulls referred to *Euoplocephalus*, and identified sexual dimorphism, ontogeny, and individual differences as the sources for much of this variation, in addition to potential taxonomic differences. Many of the distinctive features of individual specimens noted by Penkalski (2001) are unlikely to change during deformation, because they represent quantities or surface texture (e.g. surface texture of cranial sculpturing, number of osteoderms in the nuchal crest). However, some, such as the erectness of the squamosal horns, may be affected by dorsoventral compaction. Retrodeformation of two *Euoplocephalus* skulls (AMNH 5405 and UALVP 31) will highlight the changes that can occur during crushing, and can be used to identify areas of the skull that are most likely to

change and therefore be less taxonomically informative. For example, if the erectness of the squamosal horns changes with retrodeformation, or if there is high strain in this area after FEA, then the erectness of the squamosal horn may be affected by dorsoventral compaction.

The second case study examines the taxonomic validity of *Minotaurasaurus* (Fig. 2.1), known from a single specimen of unknown provenance, but likely from the Gobi Desert of Mongolia or China (Miles and Miles 2009). This taxon bears a strong overall resemblance to *Saichania chulsanensis* Maryańska, 1977, *Tarchia gigantea* Maryańska, 1977, and *Tianzhenosaurus youngi* Pang and Cheng, 1998, although the most recent phylogenetic analysis of the Ankylosauria (Thompson et al. 2012) found a close relationship between *Minotaurasaurus ramachandrani* and *Pinacosaurus grangeri* Gilmore, 1933 (but not *Pinacosaurus mephistocephalus* Godefroit, Pereda Suberbiola, Li, and Dong, 1999). Although the holotype of *Minotaurasaurus* does not appear obviously taphonomically distorted, it has a much lower, flatter profile compared to ankylosaurs such as *Euoplocephalus*. Additionally, several features are described by Miles and Miles (2009) as being flatter or more dorsoventrally compressed compared to other taxa, such as the orientation of the pterygoid, the articular surface of the quadrate, the pterygoid-quadrate contact, and the angle of projection of the quadratojugal horn. If the pterygoid, quadrate, and quadratojugal horn undergo more shape change than other portions of the skull during retrodeformation and FEA, then these features are most likely the result of dorsoventral compaction and the diagnosis of *Minotaurasaurus* should be revised.

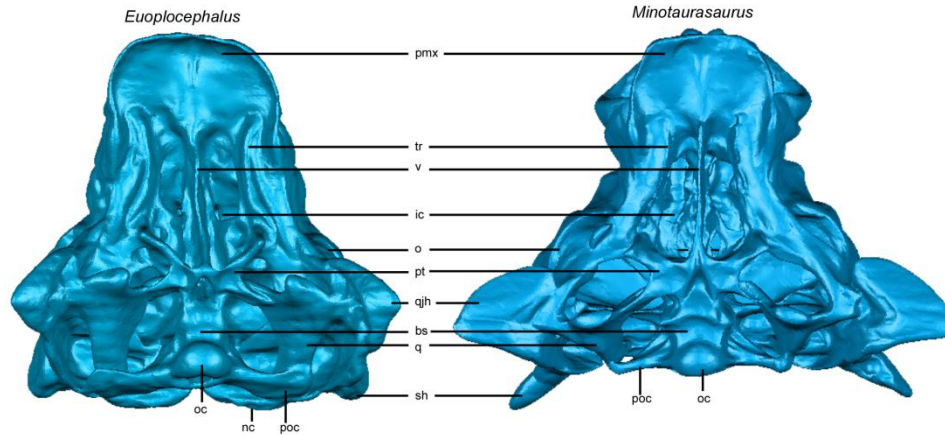


Figure 2.1. Comparison of AMNH 5405 (*Euoplocephalus*) and INBR 21004 (*Minotaurasaurus*) in ventral view. Specimens scaled to same premaxilla-occipital condyle length. Abbreviations: bs, basisphenoid; ic, internal choana; nc, nuchal crest; o, orbit; oc, occipital condyle; pmx, premaxilla; poc, paroccipital process; pt, pterygoid; q, quadrate; qjh, quadratojugal horn; sh, squamosal horn; tr, tooth row; v, vomer.

2.2 Methods

2.2.1 The orbit as a strain ellipse

In order to identify crushed ankylosaur skulls, it is necessary to identify a feature on the skull that has a particular shape or symmetry in the undeformed state. The change in size and shape that a body undergoes during deformation is known as strain (Twiss and Moores 1992). Strain can be represented by a strain ellipsoid (or strain ellipse, for plane strain). The shape of a strain ellipse is described by determining the ratio of the principal axes, the ellipticity (R). The strain ellipse is useful for studies of retrodeformation because it indicates the magnitude and orientation of deformation. Srivastava and Shah (2006) noted that circular objects such as crinoid stems deform into ellipses. A possible strain ellipse in vertebrate skulls could be the orbit, but the shape of a normal, undeformed orbit needs to be determined. Orbits of extant vertebrate skulls in the TMP, UALVP, and UAMZ collections were measured to determine the range of shape variation within and among taxa. The greatest dimension of the

periorbital rim (approximately the anteroposterior length of the orbit), and the perpendicular dimension (which together are the major and minor axes of the ellipse) were measured using digital calipers placed flush with the bone surface (Fig. 2.2). The sample includes mammals, turtles, squamates, crocodylians, and birds. Birds and squamates are poorly represented in this sample because most do not have continuous periorbital rims, making it difficult to accurately measure the maximum anteroposterior lengths of the orbits. The sample is also biased towards large mammals because these were easier to measure accurately and more were available for study. The same measurements were collected for a variety of ankylosaurid taxa. Measurements for two ankylosaur skulls (AMNH 5214 and AMNH 5404) were obtained using photographs and the software program ImageJ because these two specimens are mounted behind glass; all other specimens were measured directly from real or cast specimens.

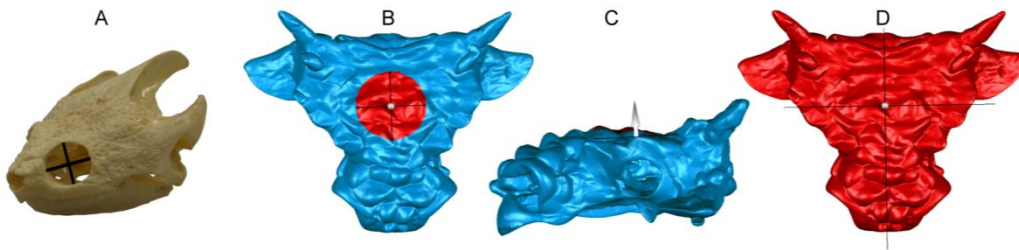


Figure 2.2. Measuring orbit shape, and deforming digital models in Geomagic. A) Two dimensions were measured for each orbit, the maximum anteroposterior length, and the perpendicular height, shown here on TMP 1999.58.79, *Chelydra serpentina*. B) To retrodeform digital skull models in Geomagic, the “Deform Region” tool is selected and placed at the midline of the skull, between the orbits. C) The arrow is adjusted into the desired position, in this case, pointing dorsally. D) The tool is then expanded to encompass the entire skull.

2.2.2 3D model creation

Three ankylosaur skulls were converted into 3D digital models from computed tomography (CT) scans. UALVP 31 (*Euoplocephalus*) was CT scanned at the University of Alberta Hospital ABACUS Facility. CT scans of the holotype of *Minotaurasaurus* (INBR 21004) were provided by V.S. Ramachandran (University

of California San Diego). L. Witmer (Ohio University Heritage College of Osteopathic Medicine) provided CT scans of AMNH 5405, (*Euoplocephalus*), which were originally published in Witmer and Ridgely (2008). New 3D models of AMNH 5405, INBR 21004, and UALVP 31 were created from the CT data using the segmentation tools in the software program Mimics. Rock matrix was digitally removed from the nasal cavities and endocranial spaces, and cracks in the bones were filled. These models were then exported as surface stereolithography (.stl) files for importing into Geomagic.

2.2.3 3D retrodeformation in Geomagic

To investigate the effects of dorsoventral compaction, the models of *Minotaurasaurus* and two *Euoplocephalus* specimens (AMNH 5405 and UALVP 31) were imported into the software program Geomagic and retrodeformed using the Deform Region tool (Fig. 2.2). The tool was placed at the midline on the dorsal surface of each skull, at the midlength of the orbits. The skull was then ‘pulled’ and ‘pushed’ in the dorsoventral plane using the distance criterion tool.

2.2.4 Finite element analysis of taphonomic deformation

The AMNH 5405 and INBR21004 stereolithography files were reimported into Mimics in order to create volume meshes for finite element analyses, in order to test the effects of potential geological forces on ankylosaur skulls. These volume meshes were exported as Nastran (.nas) files and imported into the software program Strand7. The models were given the material properties of compact bone (Poisson’s ratio = 0.4, and Young’s modulus = 8×10^9 GPa; see Arbour and Snively 2009). Deformation could also occur after permineralization, but the material properties of the average fossil bone from the Dinosaur Park Formation (from which both specimens of *Euoplocephalus* were recovered) are unknown, and the provenance of the holotype of *Minotaurasaurus* is unknown. Finally, each of the models were put through five different analyses (Table 2.1)

approximating dorsoventral compaction, and analyzed using the linear static solver in Strand7, solving for stress, strain, and displacement. Each analysis models the effects of dorsoventral compaction on an ankylosaur skull that is resting on a horizontal surface with the dorsal side up, with forces acting downwards in the vertical direction. These conditions are meant to approximate the forces acting on a skull during burial and sediment compaction: ankylosaur skulls are wider than tall and more likely to come to rest on a flat surface either right-side-up or upside-down. As the skull becomes buried, the weight of sediment will exert downwards, vertical forces on the skull. The number of nodes with constraints and/or forces applied is increased in each analysis, to create a number of potential scenarios mimicking dorsoventral compaction. It should be noted that the absolute values of force used are irrelevant for this test, because it is only the distribution of strain, and not the value of absolute strain, that is of interest.

Table 2.1. Summary of force and constraint parameters in five finite element tests simulating taphonomic deformation of AMNH 5405 and INBR 21004.

	Constraint Location	Force Location and Direction
Test 1	On the anterolateral edges of the premaxilla, and on the medial end of each quadrate head.	On the dorsal surface at the midline between the orbits, ventrally directed.
Test 2	On the anterolateral edges of the premaxilla, on the medial end of each quadrate head, and on the ventrolateral tip of the quadratojugal horns.	On the dorsal surface at the midline between the orbits, ventrally directed.
Test 3	As for Test 2.	On the dorsal surface at the midline between the orbits, ventrolaterally directed.
Test 4	As for Test 2.	On the dorsal surface at the midline between the orbits, and at the midline near the rostral end of the maxilla, ventrally directed.
Test 5	As for Test 2.	On the dorsal surface at the midline between the orbits, at the midline near the rostral end of the maxilla, and at the distal tip of each squamosal horn, ventrally directed.

2.3 Results

2.3.1 Results of orbit shape measurements

Orbit shape measurements of extant taxa (Table 2.2, Fig. 2.3) have a mean anteroposterior length:dorsoventral height ratio of 1.14 ± 0.14 ; archosaurs have higher orbit ratios compared to mammals. Few specimens of ankylosaurs (Table 2.3, Fig. 2.4) have an orbit ratio below 1.28. Several ankylosaur specimens (AMNH 5403, MOR 433) have noticeably different orbit ratios for the left and right orbits.

Table 2.2. Orbit anteroposterior length:dorsoventral height ratios of extant taxa.

Family	Species	Mean \pm SD	Number of Specimens
Ornithorhynchidae	<i>Ornithorhynchus anatinus</i>	1.10	1
Tachyglossidae	<i>Tachyglossus aculeatus</i>	1.09	1
Cebidae	<i>Saimiri</i> sp.	1.05	1
Leporidae		1.24 \pm 0.10	2
	<i>Lepus americanus</i>	1.17	1
	<i>Oryctolagus cuniculus</i>	1.31	1
Camelidae	<i>Lama glama</i>	1.10 \pm 0.04	2
Suidae		1.26 \pm 0.21	5
	<i>Babyrousa babyrussa</i>	1.54	1
	<i>Pecari tajacu</i>	1.05 \pm 0.06	2
	<i>Phacochoerus aethiopicus</i>	1.13	1
	<i>Potamochoerus porcus</i>	1.16	1
Cervidae		1.16 \pm 0.05	25
	<i>Alces alces</i>	1.08 \pm 0.05	10
	<i>Cervus canadensis</i>	1.10	1
	<i>Muntiacus</i> sp.	1.07	1
	<i>Odocoileus hemionus</i>	1.05 \pm 0.04	2
	<i>Odocoileus virgianus</i>	1.07 \pm 0.02	4
	<i>Rangifer tarandus</i>	1.09 \pm 0.06	7
Antilocapridae	<i>Antilocapra americana</i>	1.09 \pm 0.03	4
Bovidae		1.20 \pm 0.12	20
	<i>Bison bison</i>	1.02	1
	<i>Bos taurus</i>	1.07 \pm 0.16	4
	<i>Damaliscus hunteri</i>	1.17	1
	<i>Kobus ellipsiprymnus defassa</i>	1.02	1
	<i>Oreamnos americanus</i>	1.13 \pm 0.03	8
	<i>Ovibos moschatus</i>	1.04 \pm 0.01	3
	<i>Ovis canadensis</i>	1.46	1
	<i>Syncerus caffer</i>	1.01	1
Equidae		1.01	1
	<i>Equus caballus</i>		

Family	Species	Mean ± SD	Number of Specimens
Felidae		1.28 ± 0.13	8
	<i>Felis concolor</i>	1.25 ± 0.10	6
	<i>Felis pardus</i>	1.18	1
	<i>Panthera tigris</i>	1.51	1
Hyaenadae	<i>Proteles cristata</i>	1.03	1
Herpestidae		1.10 ± 0.04	4
	<i>Cynictis penicillata</i>	1.09 ± 0.02	2
	<i>Galerella pulverulenta</i>	1.11 ± 0.06	2
Phocidae		1.09 ± 0.06	5
	<i>Erignathus barbatus</i>	1.11 ± 0.06	2
	<i>Halichoerus grypus</i>	1.16	1
	<i>Pusa hispida</i>	1.04 ± 0.01	2
Mustelidae	<i>Taxidea taxus</i>	1.16	1
Chelydridae		1.11 ± 0.02	4
	<i>Chelydra serpentina</i>	1.11 ± 0.02	3
	<i>Macrochelys temminckii</i>	1.13	1
Emydidae	<i>Terrapene carolina</i>	1.30	1
Helodermatidae	<i>Heloderma suspectum</i>	1.09	1
Varanidae	<i>Varanus</i> spp.	1.56 ± 0.09	4
Gavialidae	<i>Tomistoma schlegelii</i>	1.10	1
Alligatoridae		1.32 ± 0.34	2
	<i>Melanosuchus niger</i>	1.56	1
	<i>Paleosuchus trigonatus</i>	1.08	1
Crocodylidae	<i>Crocodylus niloticus</i>	1.13	1
Anatidae	<i>Branta canadensis</i>	1.32	1
Total		1.15 ± 0.14	96

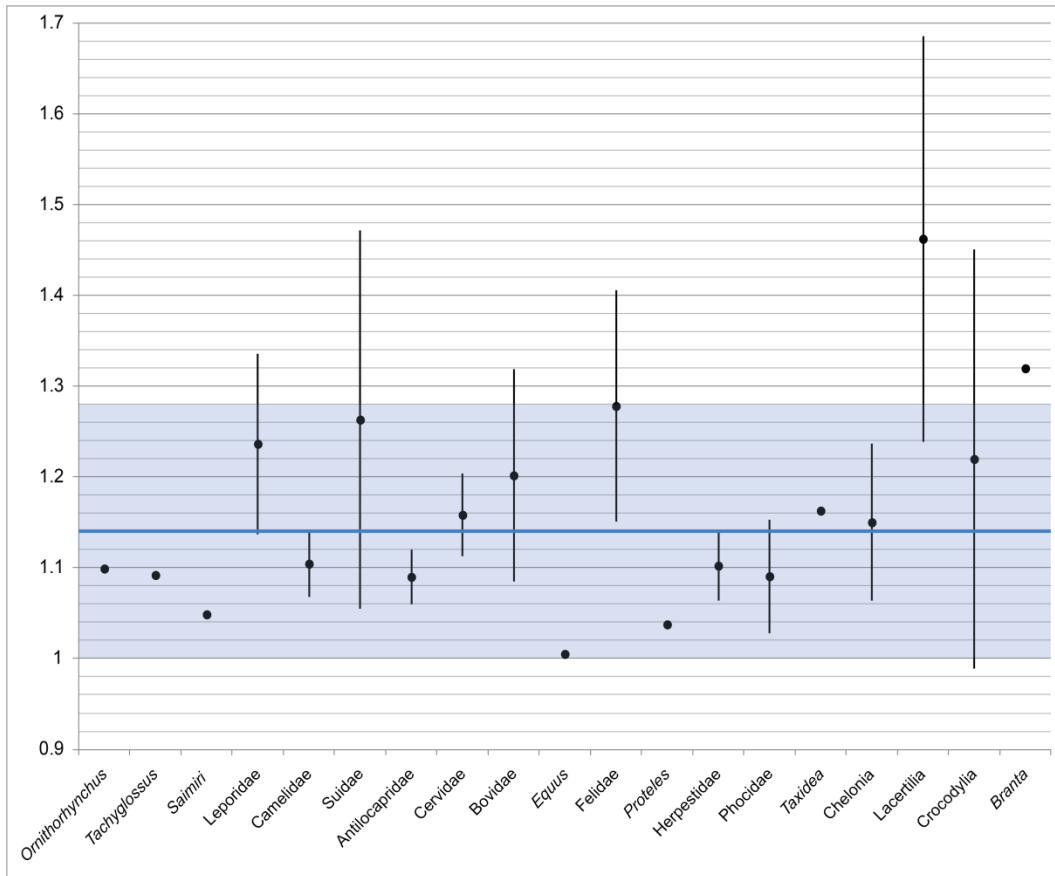


Figure 2.3. Results of orbit shape measurements for extant taxa. The mean ratio for each taxon is represented by the black circle, and the standard deviation by the vertical line. The blue horizontal line shows the mean ratio for all taxa except crocodilians and lizards, and the light blue box represents the standard deviation. The mean orbit ratio is 1.14 ± 0.14 ($n = 96$).

Table 2.3. Orbit anteroposterior length:dorsoventral height ratios of ankylosaurid specimens.

Taxon	Specimen Number	Right Orbit Width: Height	Left Orbit Width: Height
<i>Ankylosauridae indet.</i>	MPC-D100/1338		1.03
<i>Ankylosaurus magniventris</i>	AMNH 5214		^A 1.53
<i>Crichtonsaurus benxiensis</i>	BXGMV0012 R	^B 1.23	
<i>Euoplocephalus tutus</i>	AMNH 5337	1.44	1.59
	AMNH 5403	1.663	2.69
	AMNH 5404		^C 1.38
	AMNH 5405	1.90	1.18
	BMNH R4947	1.50	
	MOR 433	4.15	2.85
	ROM 1930	1.35	1.49
	TMP 1997.132.01	1.59	1.42
	TMP 1997.59.1		1.05
	UALVP 31	1.89	2.13
	USNM 11892	2.42	
<i>Pinacosaurus grangeri</i>	AMNH 6523		2.84
	IVPP V16346	1.43	
	IVPP V16853	1.24	1.20
	IVPP V16854	1.42	
	PIN 3780/3		1.10
	ZPAL MgD II/1	1.13	
<i>Gobisaurus domoculus</i>	IVPP V12563	^D 1.57	1.41
<i>Minotaurasaurus ramachandrani</i>	INBR 21004	^E 1.72	1.43
<i>Saichania chulsanensis</i>	MPC 100/151		^F 1.25
<i>Shamosaurus scutatus</i>	PIN 3779/2	1.09	1.05
<i>Tarchia gigantea</i>	PIN 551/29	1.14	1.02

^{A,C}AMNH 5214 and AMNH 5404 are mounted behind glass, but because the ratio does not require absolute values, the ratio can be determined using a photograph orthogonal to the orbit and the software program ImageJ. ^BMeasured from cast UALVP 52015. ^DMeasured from cast TMP 1990.000.0004. ^EMeasured from cast UALVP 49402. ^FMeasured from cast mounted with MPC 100/1305. MPC-D100/1338 is an indeterminate ankylosaurid from the Nemegt Formation of Mongolia.

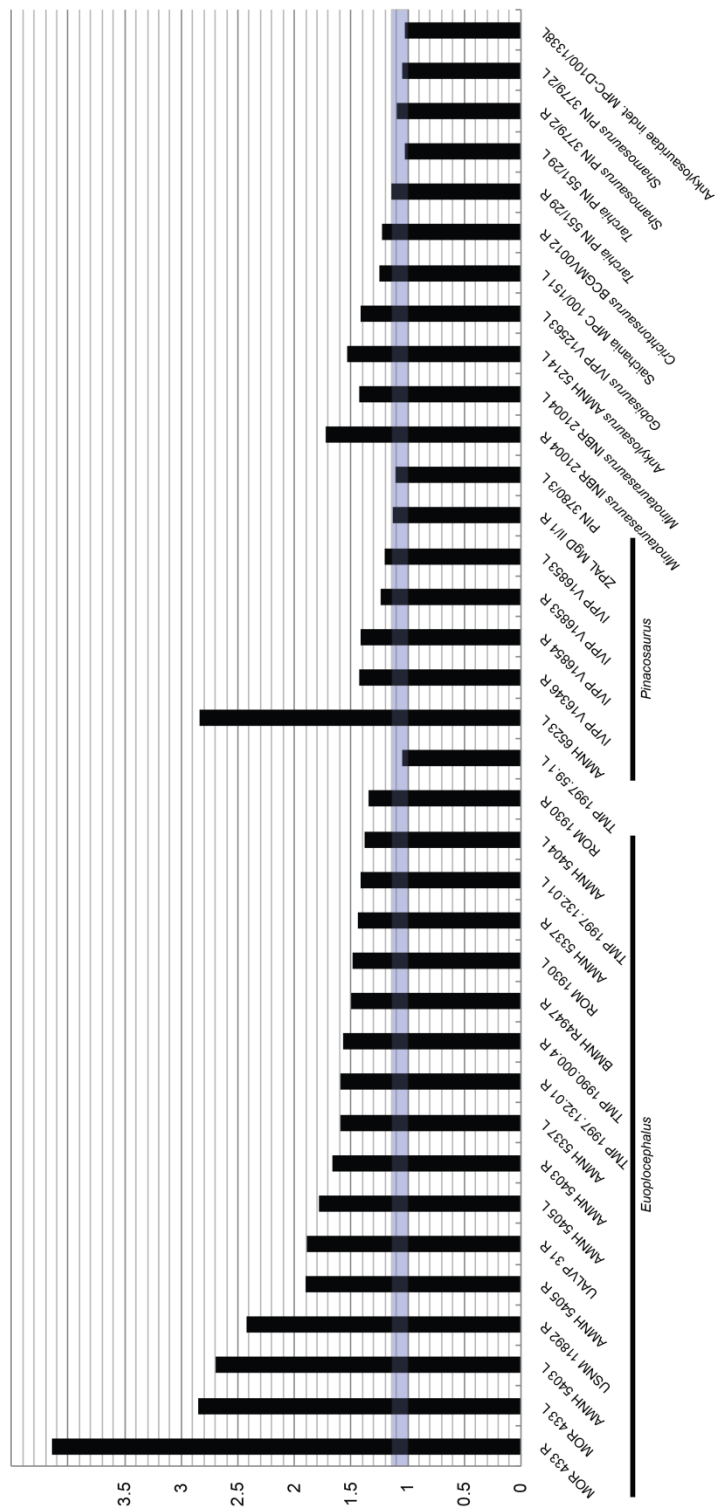


Figure 2.4. Results of orbit shape measurements for ankylosaurs. An R or L after the specimen number denotes the right or left orbit, respectively. The light blue box represents the mean orbit ratio \pm one standard deviation for extant taxa (1.14 ± 0.14).

2.3.2 Retrodeforming ankylosaur skulls

The original AMNH 5405 *Euoplocephalus* skull is bilaterally asymmetrical, but the arched profile in lateral view suggests that the skull has not been dorsoventrally compacted. Surprisingly, the orbit ratios (left 1.78, right 1.9) are higher than what would be expected if the skull was not crushed at all (Fig. 2.4), and are similar to that for UALVP 31 (1.89). Deforming the digital skull in Geomagic resulted in less dorsoventral height, more upright squamosal horns relative to the rest of the skull, and more laterally projecting quadratojugal horns (Fig. 2.5). The nuchal crest became more dorsally prominent in rostral view. The ventral edge of the paroccipital process became more horizontally oriented. Changes were minimal on the ventral surface of the skull. Dorsoventrally compressing AMNH 5405 by 8 cm in Geomagic resulted in a shape similar to that seen in UALVP 31, suggesting that the differences between these two specimens may be due to taphonomic changes.

The *Minotaurasaurus* skull (INBR21004) is low and flat in lateral view and is nearly symmetrical. The orbit ratios are 1.72 (right) and 1.43 (left), which is slightly higher than what would be expected based on the survey of extant skulls. The orbits are also teardrop-shaped, which suggests that the skull may have been dorsoventrally compressed. Retrodeforming the skull in Geomagic resulted in an arched rostrum similar to that of AMNH 5405, more horizontally projecting squamosal horns, and more ventrally projecting quadratojugal horns (Fig. 2.5). The dorsal margins of the paroccipital processes and the supraoccipital became curved. There were few changes to the ventral surface of the skull.

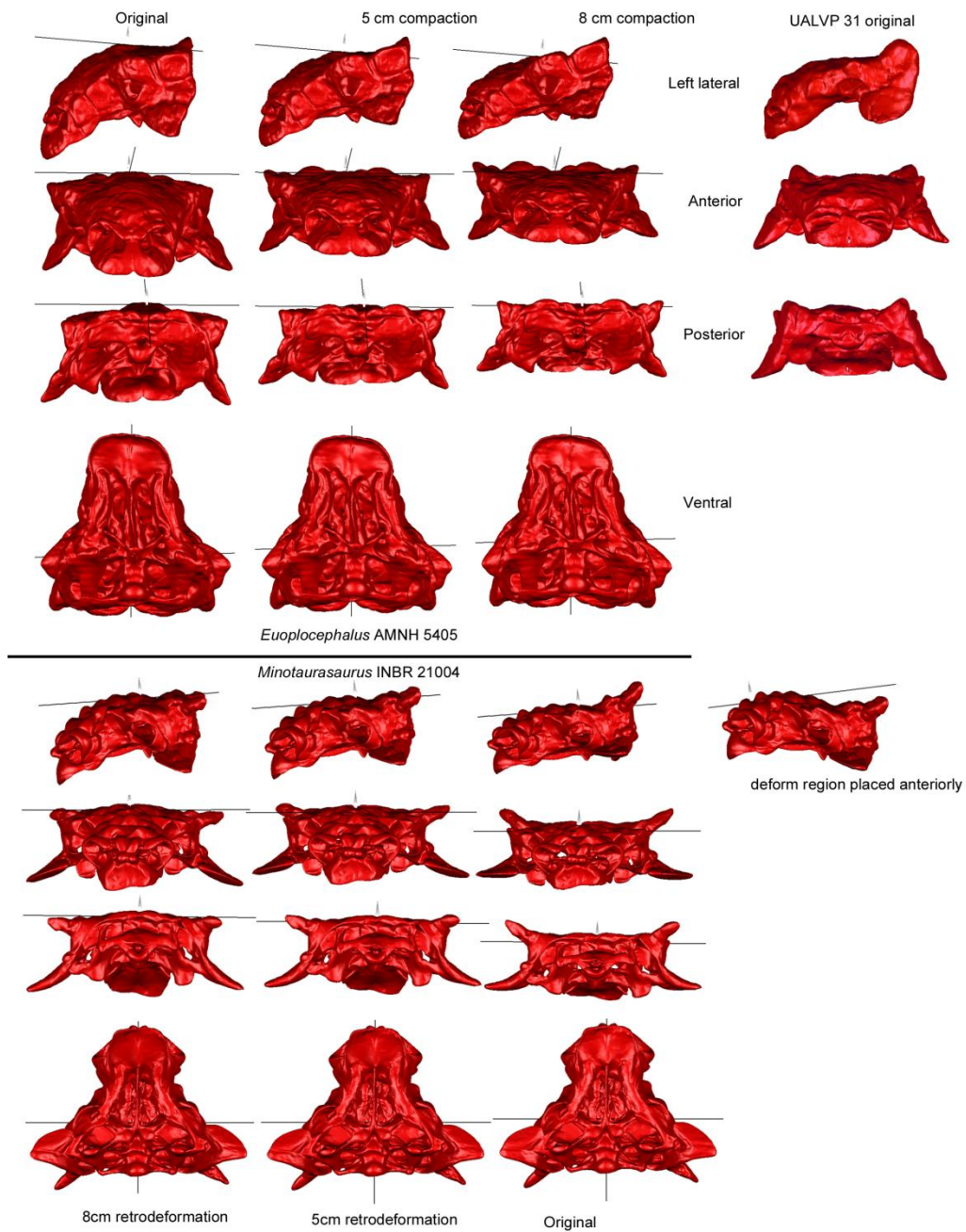


Figure 2.5. Results of deformation and retrodeformation of models using Geomagic. The top half of the image shows AMNH 5405 with (from left to right) no compression, 5 cm compression, and 8 cm compression; the rightmost column shows the original UALVP 31 skull for comparison. The bottom half of the image shows INBR 21004 with (from left to right) 8 cm retrodeformation, 5 cm retrodeformation, and no retrodeformation.

2.3.3 Finite element analysis of taphonomic deformation

The five FEA tests progressively increase the number of constraints and force locations (Table 2.2), which results in progressively greater overall strain in the model. In Test 1 for AMNH 5405, strain is greatest at the premaxillae, jugals (and possibly lacrimals), vomers, palatines, pterygoids, paroccipital processes, and at the forces and constraints (Fig. 2.6). The addition of constraints at the quadratojugal horns in Test 2 decreased the strain at the premaxillae and the quadrate heads relative to Test 1, but increased the strain on the quadratojugal horns. The shearing force modeled in Test 3 resulted in an asymmetric strain distribution on the skull. Test 4 added a force on the nasal, and resulted in increased strain on the premaxilla and maxilla. The addition of forces at the squamosal horns in Test 5 resulted in increased strain on the frontals, prefrontals, parietals, squamosals, quadratojugals, and much of the ventral surface of the skull except for the occipital condyle.

The FEA tests on INBR21004 were generally similar to that of AMNH 5405 (Fig. 2.7). In Test 1, strain was greatest on the jugals, quadrates, vomers, and palatines, and at the forces and constraints. In Test 2, where constraints were added to the quadratojugals, strain increased along the quadratojugals. Strain was asymmetrically distributed in Test 3. The addition of a force on the nasals in Test 4 resulted in increased strain on the premaxillae. Test 5 added forces to the squamosal horns, and resulted in increased strain on the premaxillae, jugals, lacrimals, quadratojugals, squamosals, quadrates, pterygoids, and paroccipital processes.

In both models, strain was high within and below the nares, but low on the narial osteoderms (Figs. 2.6, 2.7). The paroccipital processes experienced more strain in AMNH 5405 than in INBR21004. The distribution of strain around the orbit also differed between the two skulls: in AMNH 5405, strain was high in all of the bones surrounding the orbit, whereas in INBR21004 strain was high only on the bones forming the ventral border of the orbit.

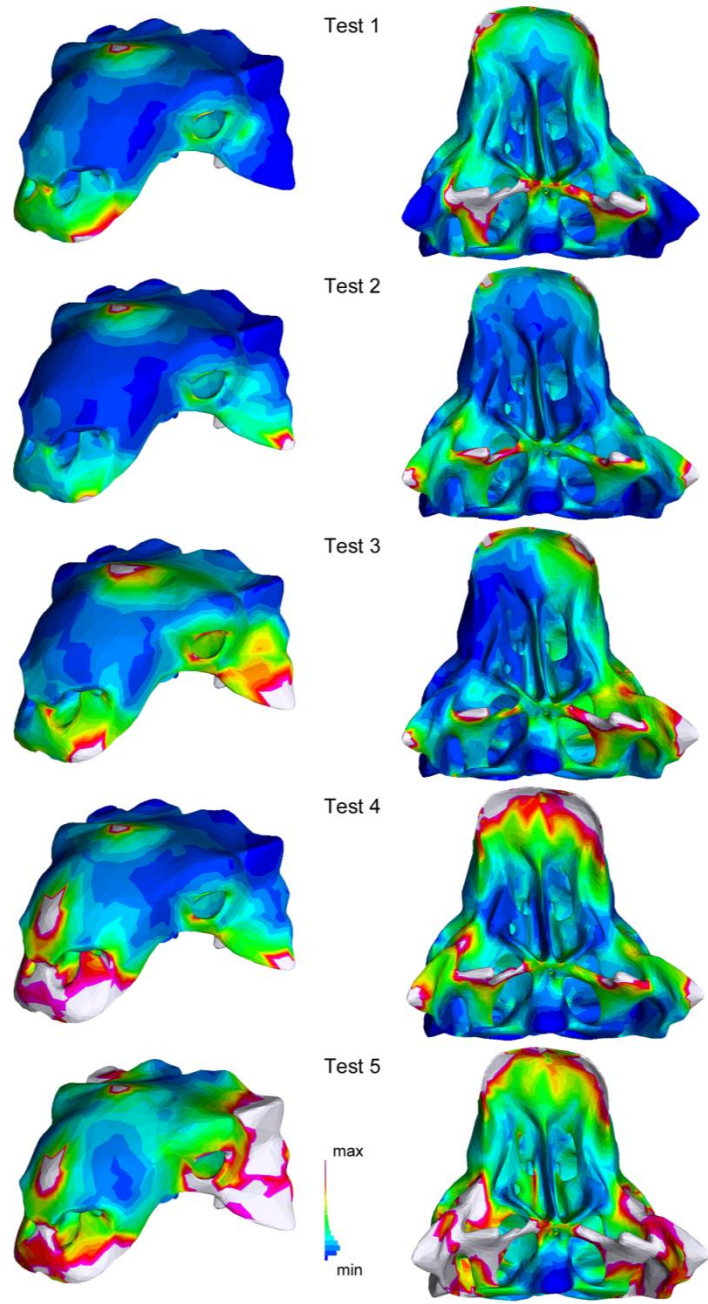


Figure 2.6. Results of the finite element analyses simulating taphonomic deformation in *Euoplocephalus*. AMNH 5405 in oblique anterolateral view (left column) and ventral view (right column).

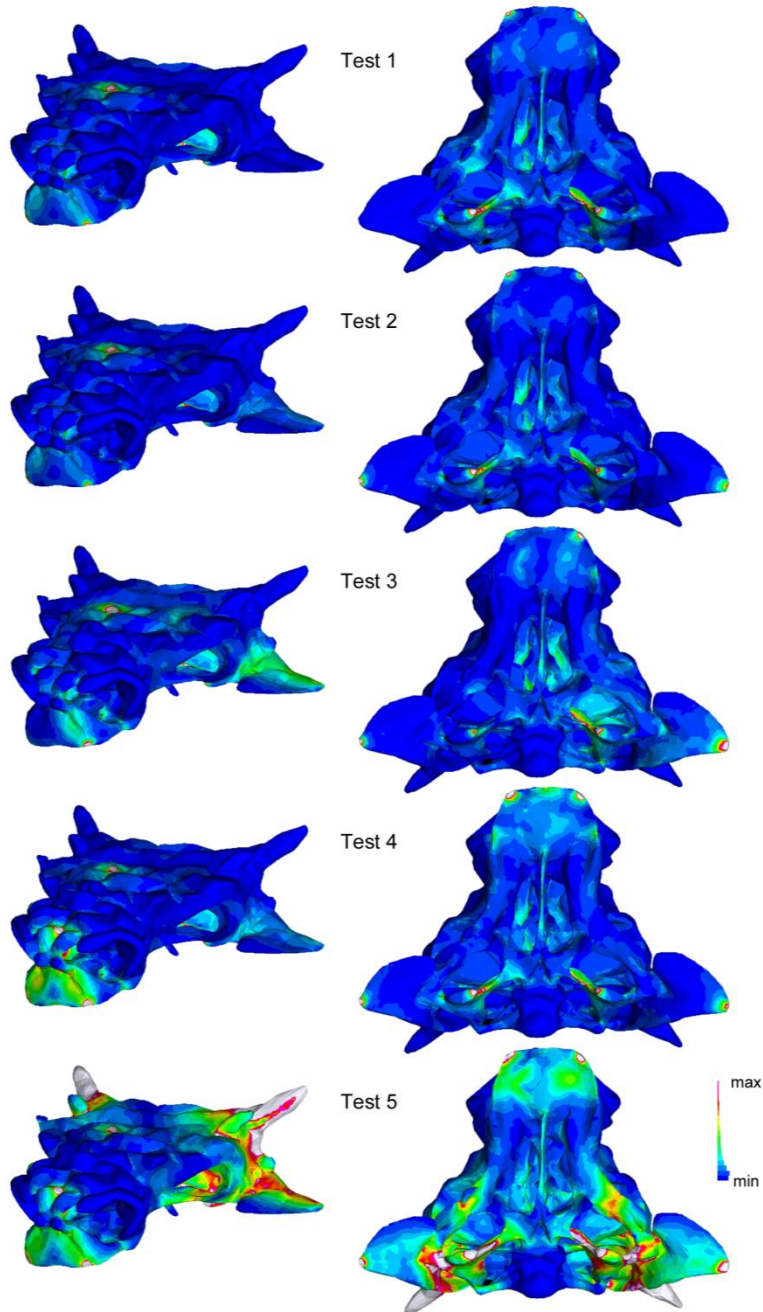


Figure 2.7. Results of the finite element analyses simulating taphonomic deformation in *Minotaurasaurus*. INBR 21004 in oblique anterolateral view (left column) and ventral view (right column).

Strain is artificially high at the constraints and nodes, and it is important to remember that in reality a skull experiencing taphonomic deformation would be crushed along more surfaces than are represented in the tests presented

here. However, these tests indicate which areas of the skull were most likely to experience strain, and as a result were more likely to deform, relative to other areas of the skull.

2.4 Discussion

Taphonomic distortion of some ankylosaur skulls is immediately easy to identify if there are obvious and extreme asymmetries, such as those seen in the holotypes of *Crichtonsaurus benxiensis* Lü, Ji, Gao, and Li, 2007 (BXGM V0012) and *Nodocephalosaurus kirtlandensis* Sullivan, 1999 (SMP VP900). Prieto-Márquez (2010) noted that bending ridges and unusual bulges can also be signs of dorsoventral crushing in fossil skulls. However, Boyd and Motani (2008) have shown that a symmetrical model does not indicate that plastic deformation from overburden compaction has been removed, and it can be easy to reconstruct a skull into an incorrect shape if there is no knowledge of accurate skull morphology. As such, symmetry alone may be insufficient for identifying deformation.

Measurements of the ellipticity of extant, undeformed vertebrate orbits suggest that orbits are not perfectly circular, but that the length:height ratio is generally between 1.00 and 1.28. As such, elliptical orbits in fossil specimens may not necessarily indicate that dorsoventral compaction has occurred. However, an orbit shape ratio greater than 1.28 in fossil skulls may indicate that some amount of dorsoventral crushing has occurred.

The higher orbit ratios in the few crocodylian and avian taxa in this study (representing the extant phylogenetic bracket for ankylosaurs) may suggest that archosaurian orbits are less circular than those of mammals, and that undeformed orbit ratios from 1.3 – 1.7 could be expected for dinosaurs. However, many of the ankylosaurid skulls had orbit ratios well above the maximum undeformed ratio recorded in this study (1.66 for *Varanus* sp.), and the range of orbit ratios was much greater for ankylosaurs than for all extant

taxa combined. A plot of ankylosaur orbit ratios (Fig. 2.3) shows that few specimens have a ratio below 1.28. This suggests that either ankylosaurid orbits were not generally circular, or that many skulls have undergone some dorsoventral crushing during fossilization and diagenesis. AMNH 5405 has surprisingly high orbit ratios, given that the arched profile of the skull suggests little crushing took place. In contrast, *Crichtonsaurus benxiensis* has a relatively low orbit ratio, despite the fact that this skull is highly asymmetrical and has certainly been flattened and distorted. Several specimens (AMNH 5403, MOR 433) have noticeably different orbit ratios for the left and right orbits, which suggests that the skulls underwent shearing or uneven dorsoventral compaction. Orbit ratios may be most useful when compared across multiple specimens of the same taxon, and very high ratios above 2 (in specimens where the orbit is completely encircled by the periorbital rim) are likely to indicate that dorsoventral crushing has occurred. The orbit ratio can serve as a general indicator if an ankylosaurid skull has been dorsoventrally compacted, but cannot be used to definitely indicate how much compaction has occurred. The true orbit ratio may not be known for a given fossil taxon, but high orbit ratios relative to the mean for a given sample of fossil specimens could also be used to identify if dorsoventral compaction has occurred. The orbit ratio could be a useful indicator of compaction for skulls that are symmetrical and which may not be obviously deformed.

Geomagic is a useful tool for investigating potential shape changes resulting from dorsoventral compression. The results of these tests can be independently assessed using finite element analysis to investigate which areas of the skull are most likely to experience strain (and therefore shape change). The FEA tests (Figs. 2.6, 2.7) showed high strain on the jugals, quadratojugals, and squamosals, which correspond to areas of change in the Geomagic models (Fig. 2.5). Strain was also present on the quadrates, pterygoids, and vomers, which did not change much in the Geomagic models. This indicates that

retrodeforming a flattened skull in Geomagic will provide a good approximation for which features have been most affected, but may not reveal changes in all regions of the skull. Finite element analysis of several taphonomic scenarios is useful for determining which forces a skull may have been subjected to during deformation.

Taphonomic distortion may be responsible for some of the variation in skulls referred to *Euoplocephalus*. For example, Penkalski (2001) suggested that the more upright squamosal horns of MOR 433 (in comparison to USNM 11892) may have been a result of crushing. This is supported by results from this study, where dorsoventrally compressing AMNH 5405 in Geomagic resulted in more upright squamosal horns similar to those of UALVP 31 (Fig. 2.5). The most noticeable change to AMNH 5405 was the flattening of the skull in lateral view. Skulls referred to *Euoplocephalus* have a range of morphologies in lateral view, from arched (AMNH 5405, ROM 1930), to flat (CMN 8530, USNM 11892). It is possible that the arching of the skull may be related to ontogeny, in which case a correlation between flatness and size would be expected. It is also possible that the relative flatness may be a true taxonomic difference. However, many of the skulls that are flat also have subcircular orbits, which suggests that the skulls have undergone crushing and in life were more arched.

Miles and Miles (2009) identify several features of *Minotaurasaurus* as being flatter or more horizontal than their equivalents in other ankylosaurids: the angle of projection of the jugal horns, the articular surface of the quadrate, the pterygoid-quadrate contact, and the orientation of the pterygoid body. Additionally, the 'flaring' narial osteoderms may be a product of dorsoventral crushing. Retrodeformation of INBR21004 in Geomagic resulted in more ventrally projecting quadratojugal horns, but did not affect the quadrates or pterygoids (Fig. 2.5). However, finite element analyses simulating crushing in INBR21004 showed increased strain (and therefore shape change) in the quadrates and the caudal portion of the pterygoids (Fig. 2.7). This suggests that

the retrodeformation techniques outlined in this study do not necessarily capture all of the shape changes on the ventral side of the skull, and emphasizes the need for multiple approaches when attempting to understand deformation in fossils. The dorsoventral angle of projection of the quadratojugal horn can be easily affected by taphonomic distortion, and should not be used as a diagnostic character for ankylosaur taxa. It is less clear if the articular surface of the quadrate, pterygoid-quadrate contact and horizontal pterygoid body in *Minotaurasaurus* are a result of deformation or represent true taxonomic differences. The flaring appearance of the narial osteoderms did not change during retrodeformation (Fig. 2.5), and dorsoventral compaction of AMNH 5405 did not result in more flaring narial osteoderms. UALVP 31, which is probably dorsoventrally compacted, also lacks flaring narial osteoderms (Fig. 2.5). In the finite element analyses of INBR21004, the narial osteoderms never experienced increased strain under any of the load regimes (Fig. 2.7). This suggests that the wide, flaring nares of *Minotaurasaurus* are real, and not an artifact of preservation.

Although Geomagic contains tools that could be used to correct plastic deformation in a fossil, there are many challenges associated with reconstructing a distorted fossil into its true, original shape. It is difficult to determine the accuracy of the retrodeformed skull in which there is no extant, undeformed analog. Simply restoring symmetry is insufficient to determine if a retrodeformed skull represents an accurate shape. Boyd and Motani (2008) demonstrated that a digitally fragmented and distorted skull could be pieced back together into a symmetrical, but incorrect shape. As such, the results presented in this paper should not be taken to indicate that dorsoventrally compacted ankylosaur skulls can be retrodeformed into their true shape, but that retrodeformation tools can be used to understand which parts of the skull were most likely to be deformed. Three-dimensional retrodeformation techniques are useful for understanding potential sources of morphological variation in ankylosaur skulls, but it is not

possible to confidently retrodeform an ankylosaur skull to its original shape.

Retrodeformation of a specimen may result in new taxonomic interpretations because of changes in shape. The accuracy of 3D retrodeformation techniques is still being investigated; retrodeformation is more likely to be successful when morphological constraints, based on features of extant taxa, can be used (Zollikofer et al. 2005). Although the FEA results differed somewhat from the retrodeformation results, some morphological features consistently changed (or did not change), and this provides information on which ankylosaur cranial characters may or may not be taxonomically informative. Overall skull morphology was easily changed with minimal retrodeformation, but features of the palate and braincase were less likely to be affected. The dorsoventral angle of projection of the quadratojugal horn is easily altered by dorsoventral compaction and should not be used to support taxonomic distinctions among ankylosaurs. Many of the diagnostic features of *Minotaurasaurus* did not change during retrodeformation, which suggests that these features are either unique to this genus or represent intraspecific or ontogenetic variation within a different taxon. Much of the variation in skull morphology in specimens referred to *Euoplocephalus* may also be a result of taphonomic distortion, although again intraspecific and ontogenetic variation cannot be ruled out.

Part 3. Taxonomic Revisions

3. EUOPLOCEPHALUS TUTUS AND THE DIVERSITY OF ANKYLOSAURID DINOSAURS IN THE LATE CRETACEOUS OF ALBERTA, CANADA, AND MONTANA, USA²

3.1 Introduction

More fossil material has been referred to *Euoplocephalus tutus* (= *Stereocephalus tutus* Lambe, 1902) than to any other North American ankylosaurid to date. As such, this taxon features prominently in discussions of ankylosaurid anatomy, systematics, and paleobiology (Carpenter 1982; Coombs 1971, 1978a-c, 1978b, 1978c, 1979, 1986, 1995a; Haas 1969; Miyashita et al. 2011; Penkalski 2001; Rybczynski and Vickaryous 2001; Vickaryous et al. 2001; Vickaryous and Russell 2003; Witmer and Ridgely 2008). *Euoplocephalus tutus* is identified primarily from Alberta (Fig. 3.1), but a few referred specimens have been recovered from the Two Medicine and Judith River formations of Montana. Compared to most other dinosaurs from the Late Cretaceous of Alberta, specimens identified as *Euoplocephalus tutus* have an unusually long stratigraphic range, spanning both the Dinosaur Park and Horseshoe Canyon formations, from about 76 to 67 Ma. In contrast, species of nodosaurid ankylosaurs, ceratopsians, hadrosaurs, and tyrannosaurs all have relatively restricted stratigraphic ranges within the Dinosaur Park Formation (Mallon et al. 2012).

² A version of this chapter has been published. Arbour and Currie 2013a. PLOS ONE 8:e62421. P. Currie supervised the project and edited the manuscript.

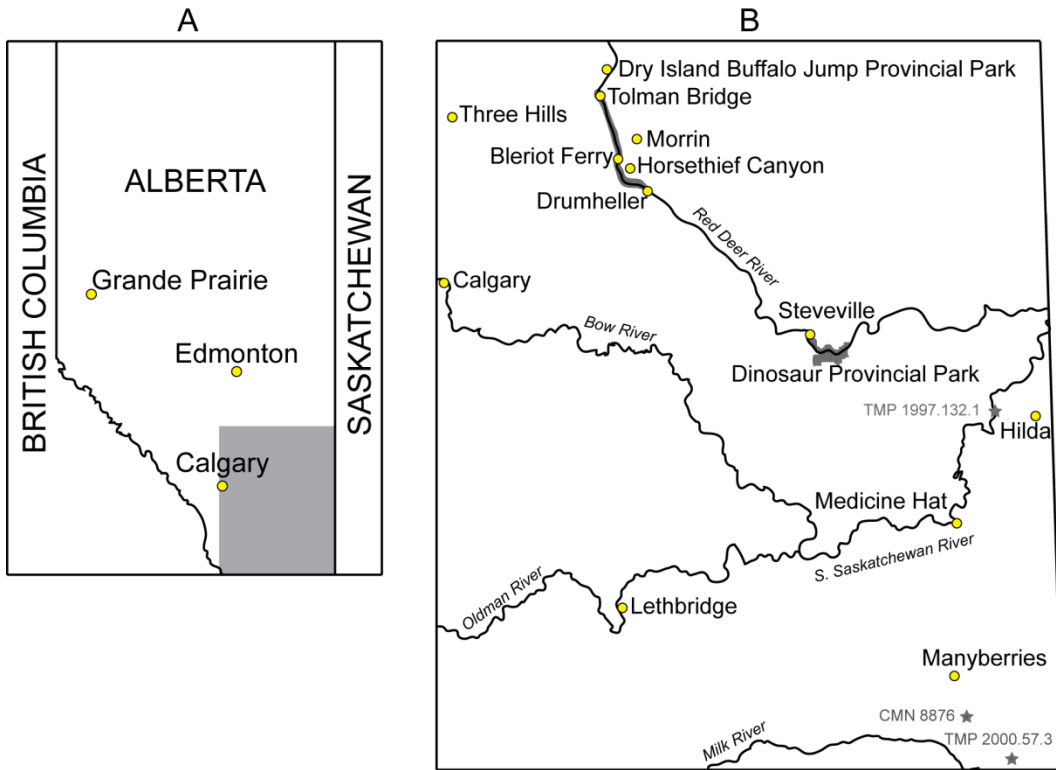


Figure 3.1. Geographic distribution of Albertan ankylosaurids. A) Map of the Canadian province of Alberta. B) Area represented by grey square in (A), showing locations of localities discussed in this paper. Specimens referred to *Euoplocephalus tutus* have been collected from sediments between Tolman Bridge and Drumheller, within Dinosaur Provincial Park, west of Hilda, and south of Manyberries.

Understanding variation in *Euoplocephalus tutus* is important for two reasons. First, the number of taxa represented by specimens referred to *Euoplocephalus tutus* has important implications for understanding biogeographic and biostratigraphic patterns of dinosaur diversity in the Upper Cretaceous of North America; either *Euoplocephalus tutus* differs from other Albertan ornithischian genera in having an unusually long stratigraphic range, or ankylosaurid diversity in Alberta is greater than generally thought. Second, variation in *Euoplocephalus tutus* (one of only a few ankylosaurid taxa represented by a reasonably large sample size) could provide support for (or against) morphological features used to diagnose other ankylosaurid taxa by clarifying which features are most likely to result from intraspecific variation.

Coombs (1978a) synonymized several taxa with *Euoplocephalus tutus*: *Anodontosaurus lambei* Sternberg, 1929, *Dyoplosaurus acutosquameus* Parks, 1924, and *Scolosaurus cutleri* Nopcsa, 1928. Lambe (1902) named *Euoplocephalus tutus* (as *Stereocephalus tutus*) on the basis of CMN 0210, a fragmentary skull roof (Fig. 3.2), partial first cervical half ring, and rib (Vickaryous and Russell (2003) note that an unprepared right mandible is associated with this specimen). Lambe (1902) also referred a tooth and two large osteoderm spikes to *Euoplocephalus tutus*, but provided no specimen numbers. Vickaryous and Russell (2003) provided specimen numbers for the rib fragment (CMN 1463), tooth (CMN 1772), and large spiked osteoderms (CMN 0317, CMN 0608), and suggested that the tooth belonged to a nodosaurid ankylosaur. The figured osteoderm spike (CMN 0317) appears to belong to a nodosaurid ankylosaur such as *Edmontonia* (e.g., AMNH 5665, USNM 11868); no ankylosaurid is known to possess a solid, narrow, conical spike such as CMN 0317. Lambe (1902) referred *Euoplocephalus tutus* to the Stegosauridae on the basis of T-shaped rib cross-sections and noted that the skull was unlike any dinosaur described up to that time. Although Lambe (1902) did not explicitly state any diagnostic characters, the cranial ornamentation pattern and first cervical half ring would have been unknown in any other dinosaur at the time. In fact, Lambe (1902) interpreted the cervical half ring as perhaps belonging to the posterior border of a cranial crest. A second, better preserved skull (UALVP 31; Fig. 3.3) was referred to *Euoplocephalus tutus* (although incorrectly called "*Europlocephalus*" *tutus* throughout) by Gilmore (1923), based on the shape and arrangement of the cranial ornamentation.

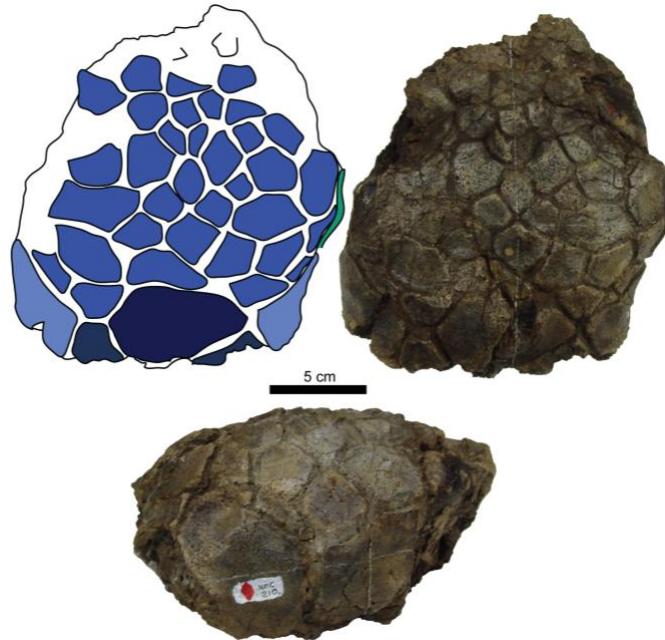


Figure 3.2. CMN 0210, holotype of *Euoplocephalus tutus*, skull in dorsal and left lateral views with interpretive dorsal view diagram.

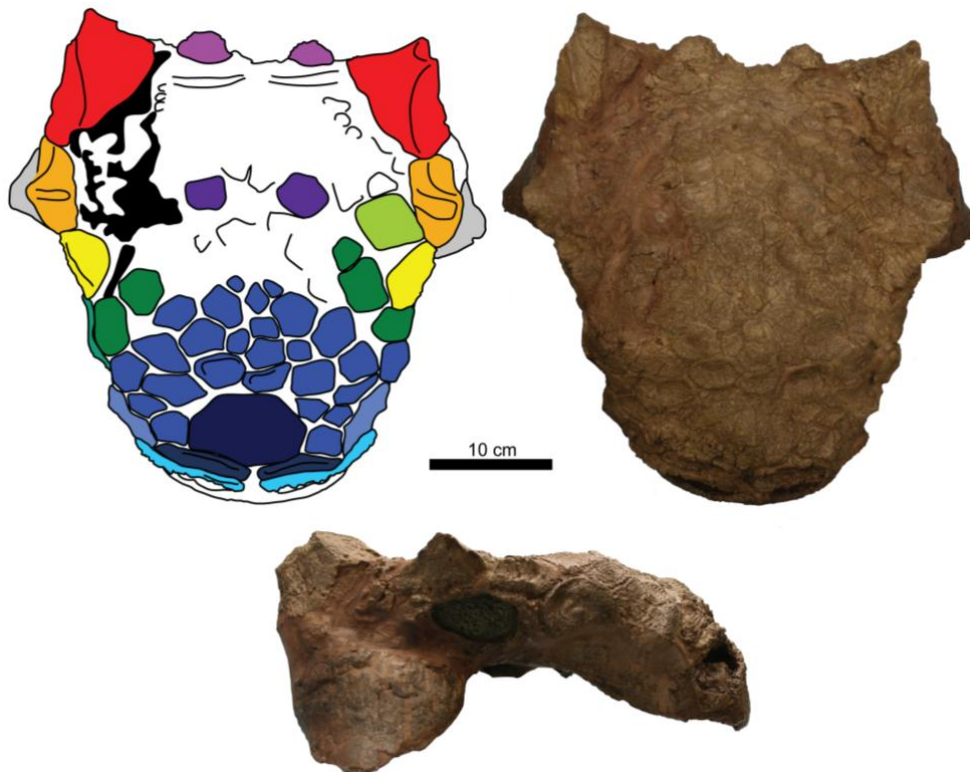


Figure 3.3. UALVP 31, referred *Euoplocephalus tutus* skull in dorsal and right lateral views with interpretive dorsal view diagram.

The holotype of *Dyoplosaurus acutosquameus* (Parks 1924) (ROM 784), includes a fragmentary skull (Fig. 3.4), a partial pelvis, a well preserved caudal series including the tail club and ossified tendons, and forelimb and hindlimb elements. This was the first description of the unique ankylosaurid tail club in the scientific literature. Parks (1924) noted that the fragmentary skull was unsatisfactory for comparison with *Euoplocephalus tutus*, but observed that the cranial ornamentation in ROM 784 differed from that of *Euoplocephalus tutus*.

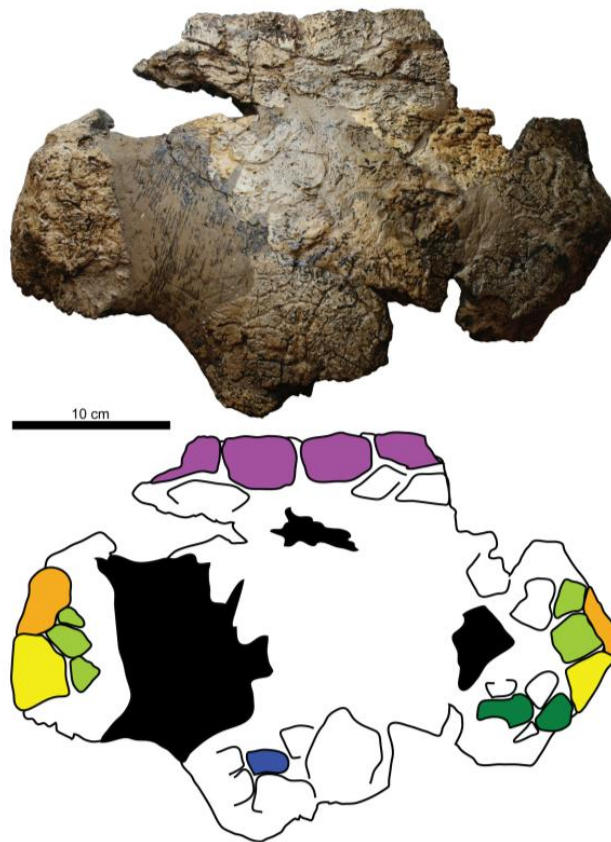


Figure 3.4. ROM 784, holotype of *Dyoplosaurus acutosquameus*, skull in dorsal view with interpretive diagram.

The holotype of *Scolosaurus cutleri* (Nopcsa 1928) is a remarkable specimen that preserves nearly the entire skeleton as well as *in situ* osteoderms and skin impressions, but lacks the skull and distal half of the tail. Nopcsa (1928) made numerous comparisons with *Dyoplosaurus acutosquameus* in his description of *Scolosaurus cutleri*, but because at the time only the skull and first

cervical ring of *Euoplocephalus tutus* were known, and because *Scolosaurus cutleri* lacks a skull, no comparisons were made with *Euoplocephalus tutus*.

Anodontosaurus lambei (Sternberg 1929) includes a skull and left mandible (Fig. 3.5), caudal vertebra, phalanx, and osteoderms. Sternberg (1929) listed several diagnostic features of *Anodontosaurus lambei*, including the absence of teeth (and the development of 'bony plates' on the maxilla and dentary instead), a reduced mandible, dorsoventrally flattened skull, and thin-walled osteoderms. Sternberg (1929) acknowledged that the skull of *Anodontosaurus lambei* was similar to that of UALVP 31 (*Euoplocephalus tutus*), but noted that *Anodontosaurus lambei* lacked the large central nasal ornamentation present in *Euoplocephalus tutus*.

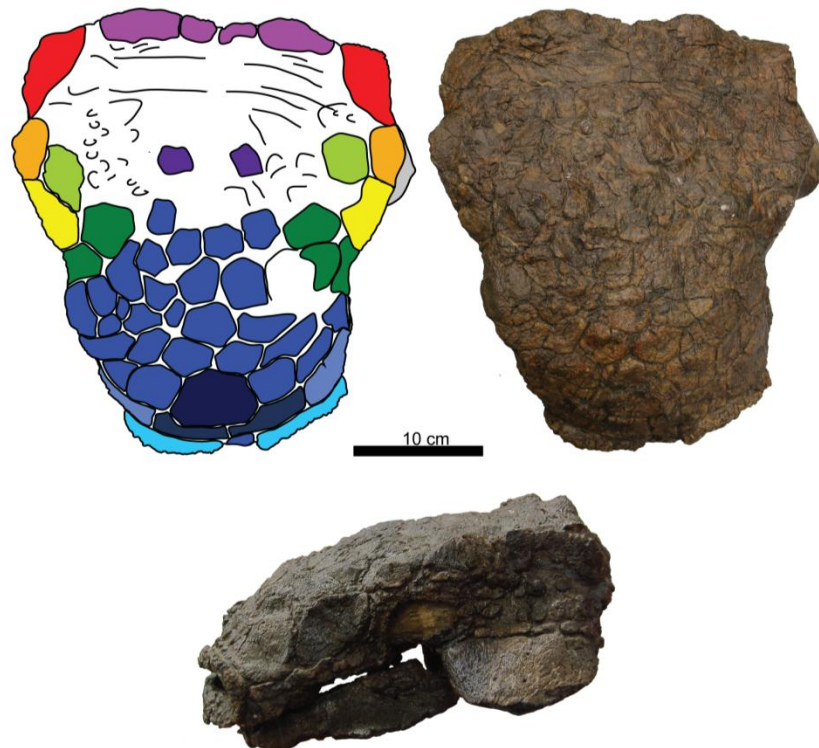


Figure 3.5. CMN 8530, holotype of *Anodontosaurus lambei*, skull in dorsal and left lateral views with interpretive dorsal view diagram.

Several ankylosaurid specimens from the Two Medicine Formation of Montana have also been referred to *Euoplocephalus* and its synonyms. Gilmore (1930) described USNM 11892, a partial, crushed skull (Fig. 3.6), and referred it to *Dyoplosaurus* on the basis of similar tooth morphology. This specimen was later referred to *Euoplocephalus* by Coombs (1978a), who considered *Dyoplosaurus* as a junior synonym. Arbour et al. (2009) did not reclassify USNM 11892 as *Dyoplosaurus* in their revision of that genus. Penkalski (2001) described MOR 433, which includes a skull (Fig. 3.6) and partial postcranium, in a review of variation in *Euoplocephalus*; differences between MOR 433 and other *Euoplocephalus* specimens prompted Penkalski (2001) to consider MOR 433 a distinct taxon, but no new name was erected at that time. Most recently, MOR 433 has been assigned as the holotype specimen of *Oohkotokia horneri* Penkalski, 2013. *Oohkotokia* includes all diagnostic ankylosaurid material from the Two Medicine Formation of Montana.

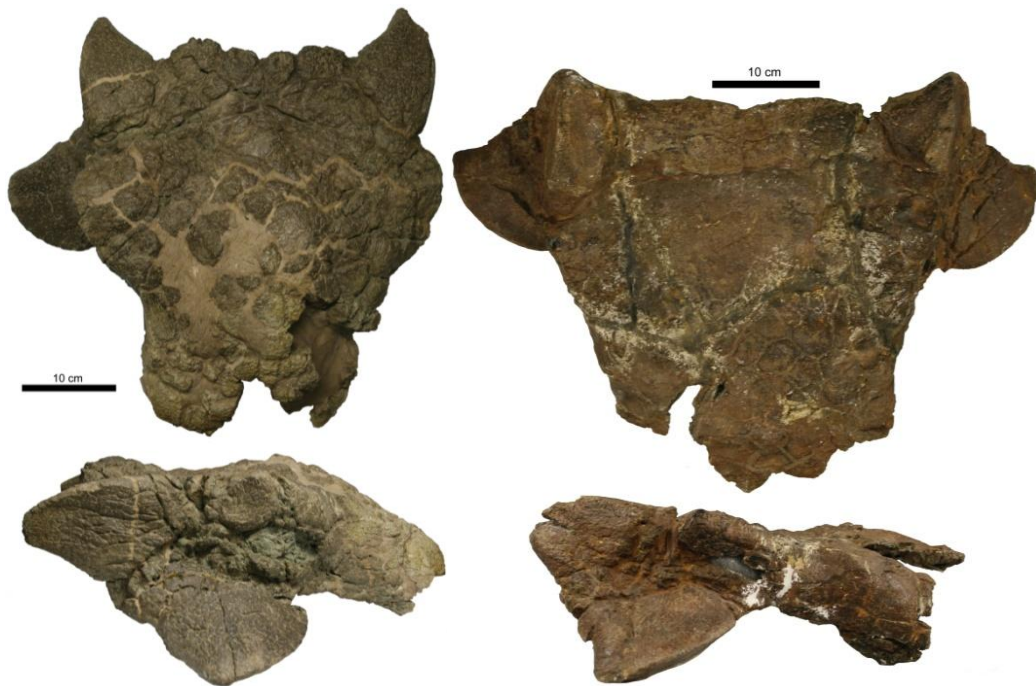


Figure 3.6. Left: USNM 11892, referred *Scolosaurus cutleri* skull in dorsal and right lateral views. Right: MOR 433, holotype of *Oohkotokia horneri* (= *Scolosaurus cutleri*), in dorsal and right lateral views.

Anodontosaurus lambei, *Dyoplosaurus acutosquameus*, and *Scolosaurus cutleri* were synonymized with *Euoplocephalus tutus* by Coombs (1978a), but he did not formally rediagnose *Euoplocephalus tutus* or provide any justification for these synonymies. In his Ph.D. thesis, Coombs (1971) explained his reasoning for these synonymies, and provided a diagnosis for *Euoplocephalus*. *Euoplocephalus tutus*, however, was not diagnosed, because Coombs (1971) could find no characters separating it from the Mongolian species *Euoplocephalus giganteus* (previously *Dyoplosaurus giganteus* Maleev, 1956, and currently accepted as *Tarchia gigantea* by Maryńska (1977)). Coombs (1978a) noted that variation in skull size and overall shape, squamosal and quadratojugal horn sizes and shapes, and cranial ornamentation pattern could not split Judithian/Edmontonian ankylosaurids into subgroups, so either each skull must represent a distinct species, or all of the skulls must represent one species (*Euoplocephalus tutus*). Although no skull was known for *Dyoplosaurus acutosquameus* or *Scolosaurus cutleri*, Coombs (1978a) reasoned that if only one ankylosaurid species was valid in the Campanian of North America, then these two species must be junior synonyms of *Euoplocephalus tutus*. Coombs maintained the synonymy of *Anodontosaurus lambei*, *Dyoplosaurus acutosquameus*, and *Scolosaurus cutleri* with *Euoplocephalus tutus* throughout his publications on ankylosaurid anatomy (Coombs 1978a-c, 1979, 1986, 1995a). Features considered diagnostic of *Euoplocephalus tutus* by Coombs (1978a) included premaxillae that are not covered by expanded nasals, long and slit-like nostrils, a premaxillary width that is equal or greater than the width between the most posterior maxillary teeth, a palate that does not taper anteriorly, and squamosal horns that are less prominent than those in *Ankylosaurus magniventris* Brown, 1908.

Although Parks (1924) presented skeletal and life restorations of the preserved material of *Dyoplosaurus acutosquameus*, the first attempt to restore the skeleton and life appearance of *Euoplocephalus tutus* was by Carpenter (1982). Carpenter (1982) accepted the synonymy of *Anodontosaurus lambei*,

Dyoplosaurus acutosquameus, and *Scolosaurus cutleri* with *Euoplocephalus tutus*. In particular, he noted the similarity between the skulls of *Anodontosaurus lambei* and *Euoplocephalus tutus*, but also noted that the cervical half ring of *Anodontosaurus lambei* was more similar to that of *Scolosaurus cutleri* than to that of *Euoplocephalus tutus*.

Penkalski (2001) documented variation among the skulls and postcranial elements of *Euoplocephalus tutus*. A morphometric analysis of skull proportions did not yield discrete clusters of skulls, but did suggest that certain features (squamosal horn height, supraorbital ornamentation, location of apex of quadratojugal horn, and textures of cranial ornamentation) may be associated with overall skull size. Cervical half ring morphology was divided into two categories based on the number of osteoderms fused to the underlying band of bone (Penkalski 2001). Other features were more difficult to cluster, partly because of the lack of overlapping material among many specimens referred to *Euoplocephalus*. Although Penkalski (2001) did not formally resurrect any of the synonymized taxa, he did strongly suggest that *Scolosaurus cutleri* was distinct from *Euoplocephalus tutus*.

Vickaryous and Russell (2003) described and figured two new skulls (TMP 1991.127.1, Fig. 3.7, and TMP 1997.132.1, Fig. 3.8) from the Dinosaur Park Formation, and provided a revised diagnosis of the cranium for *Euoplocephalus tutus*. New diagnostic features included the presence of a ciliary osteoderm (referred to as a modified palpebral by Vickaryous and Russell (2003), but see Maidment and Porro (2010)), a shallow nasal vestibule, a vertical process of the premaxilla forming an intranarial septum (also present in *Tsagantegia longicranialis* Tumanova, 1993), and medially convergent, anteriorly and posteriorly divergent maxillary tooth rows. Vickaryous and Russell (2003) supported the synonymy of *Anodontosaurus lambei* with *Euoplocephalus tutus*, finding no significant morphological differences between the holotype of *Anodontosaurus lambei*, the holotype of *Euoplocephalus tutus*, and referred

Euoplocephalus tutus specimens. They suggested that many of the differences among *Euoplocephalus tutus* specimens can be attributed to taphonomic deformation, a hypothesis largely supported by the analysis in Chapter 2.

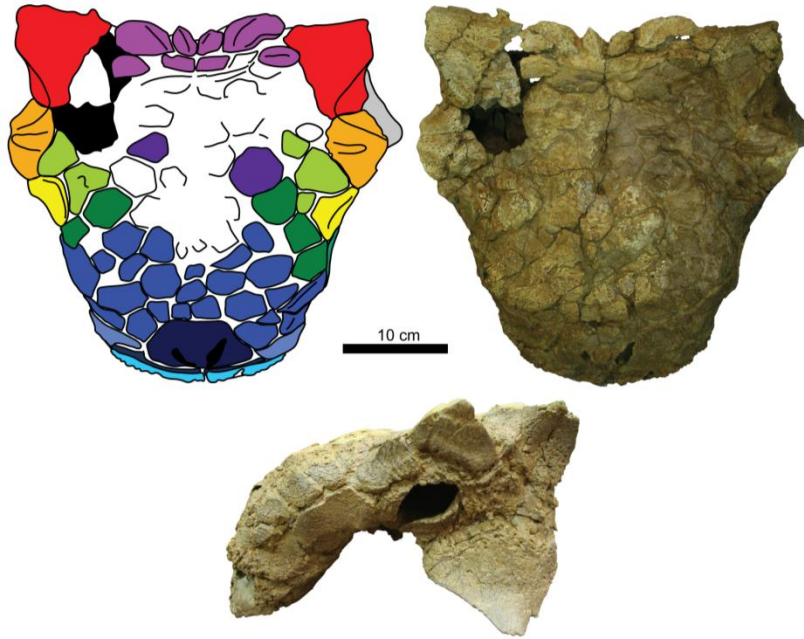


Figure 3.7. TMP 1991.127.1, referred *Euoplocephalus tutus* skull in dorsal and left lateral views, with interpretive dorsal view diagram.

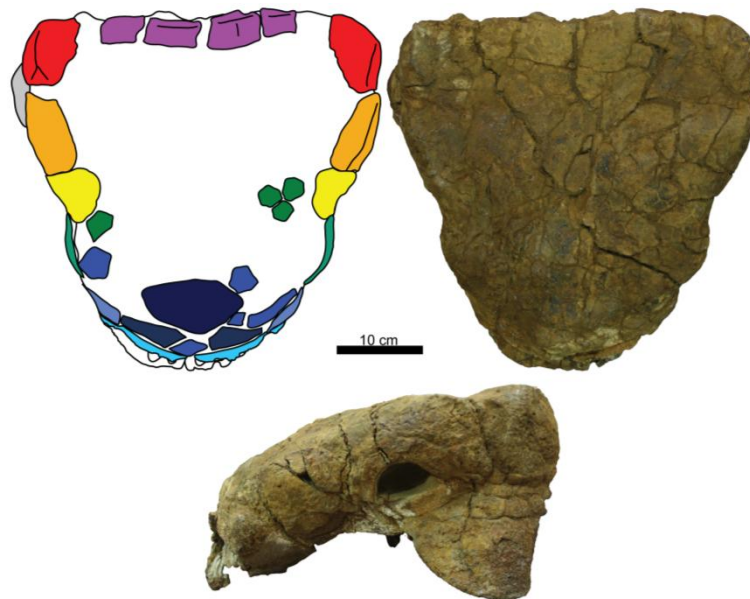


Figure 3.8. TMP 1997.132.1, referred *Anodontosaurus lambei* skull in dorsal and left lateral views, with interpretive dorsal view diagram.

Arbour et al. (2009) reassessed the holotype specimen of *Dyoplosaurus acutosquameus* (ROM 784) and concluded that this represented a distinct species from *Euoplocephalus tutus sensu lato*, based on features of the pelvis and pes. The separation of *Dyoplosaurus acutosquameus* from *Euoplocephalus tutus* was supported by a phylogenetic analysis by Thompson et al. (2012); *Dyoplosaurus acutosquameus* was recovered as the sister taxon of *Pinacosaurus mephistocephalus* Godefroit et al., 1999, and is well removed from *Euoplocephalus tutus*.

Penkalski and Blows (2013) reassessed the holotype of *Scolosaurus cutleri* and found it to be distinct from *Euoplocephalus tutus* and *Dyoplosaurus acutosquameus* as well. These authors also noted that *Scolosaurus* differed from *Euoplocephalus* in the morphology of the cervical half rings, osteoderms, humerus, and radius, in the texture of the osteoderms, and in overall size. *Scolosaurus* differed from *Dyoplosaurus* in the morphology of the osteoderms, pelvis, and pedal unguals.

Vickaryous and Russell (2003:161), like Coombs (1978a), found that variable morphological features in specimens referred to *Euoplocephalus* did not co-occur exclusively in some specimens and not others; in other words, variable features occur randomly among *Euoplocephalus* specimens. This constitutes a testable hypothesis for the variation in *Euoplocephalus tutus*; if the same combination of variable features is present in some specimens but not others, then there may be justification for the segregation of *Euoplocephalus tutus* into multiple species. Furthermore, if these combinations of variable features are stratigraphically separated, this would provide additional support for the hypothesis that more than one species is currently included in *Euoplocephalus tutus*. Continued collecting in western Canada and the USA has produced additional ankylosaurid specimens, which may provide new information about variation in *Euoplocephalus tutus*. Now, there is also a better understanding of the stratigraphic distribution of dinosaur faunas in Alberta (Currie and Russell

2005; Mallon et al. 2012; Ryan and Evans 2005) as well as the stratigraphic placement of ankylosaur specimens with which to assess stratigraphic variation in *Euoplocephalus tutus*. In this paper, the apparent stratigraphic longevity of *Euoplocephalus tutus* is investigated by conducting a detailed review of all specimens referred to *Euoplocephalus tutus*, as well as specimens that were previously referred to *Euoplocephalus* but that are now identified as *Dyoplosaurus* and *Scolosaurus*. Variation in *Euoplocephalus tutus* is assessed by looking for morphological groupings among specimens referred to *Euoplocephalus tutus*, and looking for stratigraphic patterns that correspond to any of these morphological groupings. The taxonomic statuses of the junior synonyms of *Euoplocephalus tutus* are then reassessed. Finally, the phylogenetic relationships of *Euoplocephalus tutus* are investigated with any resurrected or new species within the Ankylosauridae.

3.2 Materials and methods

3.2.1 Material examined

Evaluating morphological variation in *Euoplocephalus tutus* is confounded by the fragmentary nature of the holotype specimen, CMN 210, which consists of only the skull roof of the antorbital region, and a partial first cervical half ring. Cervical half ring morphology has been considered taxonomically useful (Arbour et al. 2009; Penkalski 2001; Penkalski and Blows 2013). Based on the forms of the first cervical half rings, two additional specimens have recently been referred to *Euoplocephalus tutus*: AMNH 5406 (Penkalski 2001), and UALVP 31 (Arbour et al. 2009). AMNH 5406 consists of the shoulder girdle and forelimbs, and UALVP 31 includes a skull, right scapula, partial pelvis, both humeri, femur, tibia, metatarsal, and osteoderms. Together these specimens increase the amount of definitive *Euoplocephalus tutus* skeletal material, which can then be compared to other referred specimens. When Arbour et al. (2009) was published, UALVP 31

was still undergoing preparation; this specimen is now fully prepared and described herein.

All of the specimens collected by Canada Fossils Ltd. were prepared as display specimens and have been heavily reconstructed; it is difficult to determine the extent of real bone in FPDM V-31, NSM PV 20381, and TMP 2001.42.19. In this paper, only elements of these specimens that are obviously original fossils are described. Photographs of these specimens prior to reconstruction were provided by A. Dzindic.

The holotype of *Dyoplosaurus acutosquameus* (ROM 784) was redescribed in detail by Arbour et al. (2009). However, since that paper was published the skull has been removed from display, and the ventral surface has been revealed for the first time. Discussion of ROM 784 in this paper is limited to comparisons with other specimens referred to *Euoplocephalus*.

3.2.2 Terminology

Cranial ornamentation is useful for identifying differences and similarities among ankylosaur taxa, but a brief review of relevant terminology is required before reviewing variation in specimens referred to *Euoplocephalus* (Fig. 3.9) Ankylosaur cranial ornamentation may arise either through coossification of osteoderms to the underlying skull bones, through elaboration of the skull elements themselves, or through a combination of both processes (Hill et al. 2003; Vickaryous et al. 2001). Many ankylosaurs have flat cranial ornamentation subdivided by shallow furrows (e.g., *Ankylosaurus*, *Edmontonia*), and in some ankylosaurs these discrete areas are bulbous (e.g., *Saichania chulsanensis* Maryańska, 1977). Blows (2001) created the term caputegulum (Latin, “skull tile”; plural caputegulae) for the flat bones covering the skulls of ankylosaurs. This term is useful because it does not matter whether or not the discrete polygons of cranial ornamentation are formed by coossified osteoderms or

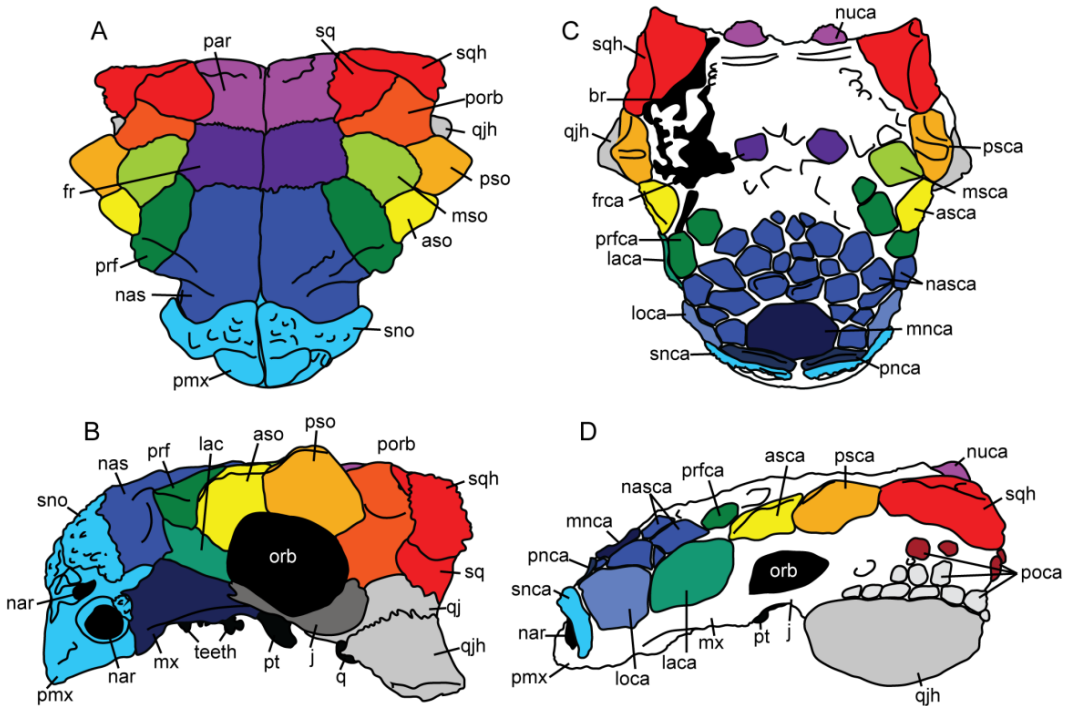


Figure 3.9. Cranial anatomy of ankylosaurids, including terminology for ornamentation patterns. ZPAL MgD II/1, juvenile *Pinacosaurus grangeri* in **A)** dorsal and **B)** left lateral views, showing boundaries of cranial bones. Boundaries between cranial bones are not visible in most adult ankylosaurids. **C)** UALVP 31, *Euoplocephalus tutus*, in dorsal view. **D)** CMN 8530, *Anodontosaurus lambei* (holotype), in left lateral view. Cranial ornamentation that is subdivided into discrete polygons (rather than generalized rugosity) are referred to as caputegulae. Abbreviations: asca, anterior supraorbital caputegulum; aso, anterior supraorbital; br, break or plaster; fr, frontal; frca, frontal caputegulum; j, jugal; lac, lacrimal; laca, lacrimal caputegulum; loca, loreal caputegulum; mnca, median nasal caputegulum; msca, middle supraorbital caputegulum; mso, middle supraorbital; mx, maxilla; nar, naris; nas, nasal; nasca, nasal caputegulum; nuca, nuchal caputegulum; orb, orbit; par, parietal; pmx, premaxilla; pnca, postnarial caputegulum; poca, postocular caputegulum; porb, postorbital; prf, prefrontal; prfca, prefrontal caputegulum; psca, posterior supraorbital caputegulum; pso, posterior supraorbital; pt, pterygoid; q, quadrate; qj, quadratojugal; qjh, quadratojugal horn; snca, supranarial caputegulum; sno, supranarial ornamentation; sq, squamosal; sqh, squamosal horn.

cranial sculpturing (or both). The ability to identify and describe ornamentation patterns by naming discrete caputegulae facilitates the comparison of individual specimens and species. The term is here used with modifiers indicating the location (e.g. prefrontal caputegulum, supraorbital caputegulae), to compare

cranial ornamentation patterns across ankylosaur taxa (Fig. 3.9). The pyramidal ornamentations of the squamosals and quadratojugals have been variously referred to as scutes (Coombs 1978a; Gilmore 1923), bosses (Vickaryous and Russell 2003), horns (Carpenter 2004; Maryańska 1977), and coronuces (Blows 2001). The term “horn” is used in this paper to refer either to the squamosal or quadratojugal ornamentation.

3.2.3 Stratigraphic and geographic positions of specimens

Evans (2007) outlined methods for resolving the biostratigraphic distribution of lambeosaurine dinosaurs in Dinosaur Provincial Park, using high-precision differential GPS coordinates of known quarries and Oldman-Dinosaur Park Formation contacts that were published on a supplemental CD-ROM by Currie and Russell (2005). (This method in turn was derived from similar methods used by Ryan (2003) to evaluate the stratigraphic position of centrosaurine dinosaurs in Dinosaur Provincial Park). In this way, the elevation above the Oldman-Dinosaur Park contact (and thus the stratigraphic position within the Dinosaur Park Formation) could be calculated for each specimen. Software updates to ArcGIS have unfortunately made the data on the CD-ROM unreadable, and so a modified version of the method proposed by Evans (2007) using Google Earth is used here. Several *Euoplocephalus* specimens have also been collected from the Horseshoe Canyon Formation, but their quarries have not been relocated. Many *Euoplocephalus* quarries within Dinosaur Provincial Park have not been relocated, and so some specimen locality data are less precise. Specimen locality data (Appendix 3.1) were collected from online collections databases (American Museum of Natural History, Division of Paleontology Collections Database; Government of Alberta Heritage Resources Management Information System, Royal Tyrrell Museum), institutional catalogues (UALVP), specimen cards (AMNH, CMN, NHMUK, ROM, TMP, UALVP, USNM), field notes (CMN, also as the Geological Survey of Canada, GSC, or

National Museum of Canada, NMC; ROM), from previously published coordinates in Currie and Russell (2005: supplementary CD-ROM), from Steeveville Map 969A (Sternberg 1950), and from discussions with other researchers. Latitude and longitude coordinates (or UTM coordinates) were entered into Google Earth. Some specimen data are in the form of Township and Range coordinates, and these were converted to UTM coordinates using the Alberta Geological Survey's online conversion tool. Finally, the positions of specimens without township and range or GPS coordinates (largely those collected prior to 1980) were estimated from field notes and Google Earth measurement tools. For example, field notes by B. Brown and P. Kaisen for AMNH 5409 (available via the AMNH online Vertebrate Paleontology Archives) indicate that this specimen was collected 20 feet above the left bank of the Red Deer River, 1.5 miles below the town of Steeveville. Steeveville was located in the northwest corner of Dinosaur Provincial Park, and the location 1.5 miles downstream can be estimated using the ruler tool in Google Earth. Then the appropriate elevation above river level can be determined. The position of AMNH 5409 has also been measured using differential GPS (Currie and Russell 2005), and these coordinates correspond to estimates made based on Brown and Kaisen's notes and Google Earth tools.

Elevation above the Oldman-Dinosaur Park formational contact was estimated for each specimen. Eberth (2005) created a map showing the elevations of the contact throughout Dinosaur Park, and this was digitally overlaid in Google Earth. For each specimen, the plotted elevation was noted, as was the Oldman-Dinosaur Park contact elevation segment from Eberth (2005). Using Microsoft Excel, estimates for elevation above the contact were calculated for each specimen, and plotted to show the distribution of specimens in the Dinosaur Park Formation. For specimens that had both field note estimates and accurate GPS data, both elevations were plotted to demonstrate the potential range of error for specimens with only field note estimates.

3.2.4 Phylogenetic analyses

The phylogenetic relationships of *Euoplocephalus tutus*, as well as the resurrected ankylosaurid species *Anodontosaurus lambei*, *Dyoplosaurus acutosquameus*, and *Scolosaurus cutleri*, were investigated using T.N.T. v1.1 (Goloboff et al. 2008). Three data matrices (Appendices 3.3-3.5) were prepared using the character matrix in Thompson et al. (2012):

1) the 'original' matrix in which all previous character codings were retained, except for moving data to *Anodontosaurus lambei* and *Scolosaurus cutleri* from *Euoplocephalus tutus*, in order to understand the effects of the addition of new taxa to the matrix;

2) an 'updated codings' matrix in which numerous character codings were revised (changes are explained in Appendix 3.2), with many changes in particular to the codings for *Dyoplosaurus acutosquameus*, *Minotaurasaurus ramachandrani* Miles and Miles, 2009, *Nodocephalosaurus kirtlandensis* Sullivan, 1999, and *Tianzhenosaurus youngi* Pang and Cheng, 1998, in order to correct incorrectly coded characters in the original matrix, and;

3) a 'new characters' matrix in which new characters identified in this paper were added to the 'updated codings' matrix.

The dataset was assembled in Mesquite version 2.72 (Maddison and Maddison 2011), and a maximum of 177 characters (in analysis 3) and 18 taxa were used in the analysis. The analyses include 14 ingroup taxa consisting only of unequivocal ankylosaurine ankylosaurids, and the outgroup taxa *Lesothosaurus* (a basal ornithischian), *Scelidosaurus* (a basal thyreophoran), *Stegosaurus* (a stegosaur) and *Edmontonia* (a nodosaurid ankylosaur). Characters were treated as unordered and of equal weight. A parsimony analysis was conducted in T.N.T. using the Traditional Search option with one random seed and 1000 replicates of Wagner trees and the tree bisection reconnection (TBR) swapping algorithm. A strict consensus and a 50% majority rule consensus tree was created where more than one tree was recovered; for Analysis 3, a reduced consensus tree was

also created using Mesquite. Because of the poor resolution of the strict consensus trees in Analysis 3, Matrix 3 was analyzed using the software program TAXEQ (Wilkinson 2001) to search for taxonomic equivalents that could be safely deleted and thereby reduce the amount of missing data in the analysis ("Safe Taxonomic Reduction" (Wilkinson 2001, 2003)). The data were then subjected to a bootstrap analysis that was resampled with 1000 replicates to create a bootstrap tree using a heuristic search with the TBR swapping algorithm. Bremer supports were calculated in T.N.T., and the consistency and retention indices were calculated in Mesquite. Character state changes were investigated in Mesquite using the "Parsimony Ancestral States" analysis.

3.3 Results

3.3.1 Morphological variation in specimens referred to *Euoplocephalus tutus*

The skull of *Euoplocephalus tutus* has been described and illustrated by several authors (Coombs 1971, 1978a; Haas 1969; Miyashita et al. 2011; Penkalski 2001; Rybczynski and Vickaryous 2001; Vickaryous et al. 2001; Vickaryous and Russell 2003; Witmer and Ridgely 2008), and so only new observations of variable features are provided here. Descriptions of the postcrania of *Euoplocephalus tutus* by Coombs (1978b-c, 1979, 1986, 1995a), Carpenter (1982), Penkalski (2001), and Arbour et al. (2009) include information on most, but not all, aspects of the postcranial skeleton; in particular, the pre-caudal vertebral series has received relatively little attention. As such, more detailed descriptions and comparisons of the postcrania of specimens referred to *Euoplocephalus tutus* are presented. These descriptions include newly collected or newly prepared specimens in the TMP and UALVP collections, as well as a review of previously published specimens.

3.3.1.1 Cranium

Skulls referred to *Euoplocephalus tutus* (Figs. 3.2-3.8, 3.10-3.13) have received a great deal of attention in the literature, but less attention has been paid to the shapes and patterns of the cranial caputegulae. Examination of 22 complete or partial skulls, and numerous cranial fragments (such as isolated quadratojugal horns or small skull fragments), shows that some caputegulae are consistent in form and location, and homologies can be proposed for these elements (Figs. 3.9-3.12). These include the supranarial (*sensu* Vickaryous and Russell 2003), postnarial, median nasal, loreal (anterior to the orbit, e.g. Dixon 2000), prefrontal, supraorbital, and nuchal caputegulae, and the squamosal and quadratojugal horns. The arched supranarial caputegulae form the rim of the external nares, and are usually more rugose than the other caputegulae. The postnarial caputegulae are paired, subrectangular, flat caputegulae posterior to the supranarial caputegulae. Posterior to the postnarial caputegulae, and centered on the midline of the skull, is the large, hexagonal, median nasal caputegulum. A large, keeled caputegulum posterior to the postnarial caputegulae (loreal caputegulum) forms the lateral edge of the snout and extends onto the dorsal surface of the skull. A similar caputegulum is found posterior to the loreal caputegulum, on the lacrimal, but this does not extend as far onto the dorsum. There are two supraorbital caputegulae, an anterior one and a posterior one, each of which is triangular in dorsal view and has a keel approximately in line with the keel of the squamosal horn. The supraorbital caputegulae do not have distinct peaks, but instead the lateral keel of each forms a continuous edge with the adjacent supraorbital. The posterior supraorbitals of TMP 1991.127.1 (Figs. 3.7, 3.10) and UALVP 31 (Figs. 3.3, 3.10) each have a prominent transversely-oriented sulcus, which is not visible on any other specimens. In lateral view, the posterior supraorbitals of TMP 1991.127.1 (Figs. 3.7, 3.12) and UALVP 31 (Figs. 3.3, 3.12) are prominent and triangular. In each specimen, the posterior supraorbital is lower and more rounded.

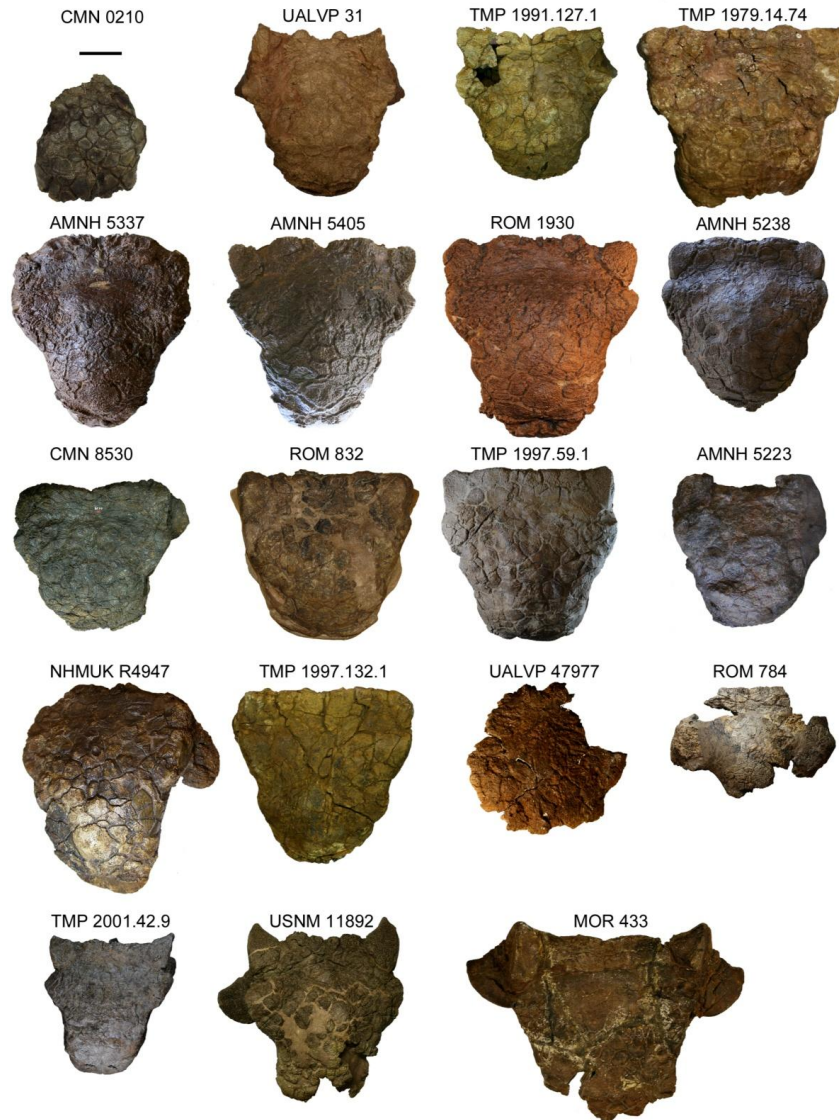


Figure 3.10. Skulls in dorsal view. CMN 0210 is the holotype of *Euoplocephalus tutus*, CMN 8530 is the holotype of *Anodontosaurus lambei*, MOR 433 is the holotype of *Oohkotokia horneri*, and ROM 784 is the holotype of *Dyoplosaurus acutosquameus*. AMNH 5337, AMNH 5405, CMN 0210, ROM 784, ROM 1930, TMP 1979.14.74, TMP 1991.127.1, TMP 1997.132.1, and UALVP 31 are from the Dinosaur Park Formation. AMNH 5238 and UALVP 47977 are of uncertain stratigraphic position within Dinosaur Provincial Park. AMNH 5223, CMN 8530, ROM 832, and TMP 1997.59.1 are from the Horseshoe Canyon Formation. NHMUK R4947 is from an unknown stratigraphic position in Alberta. MOR 433, TMP 2001.42.9 (much of the anterior rostrum in heavily reconstructed), and USNM 11892 are from the Upper Two Medicine Formation in Montana. Scale equals 10 cm. Photograph of ROM 832 by C. Brown, and of ROM 1930 by J. Arbour, and used with permission.

The frontals and nasals are completely obscured by the frontonasal caputegulae (Figs. 3.10-3.12). Each skull referred to *Euoplocephalus* has a unique pattern of frontonasal caputegulae, which are generally subcircular, hexagonal, or subrectangular. The posterior extents of distinct caputegulae vary between individual specimens, but in most specimens individual caputegulae are not visible in the parietal regions posterior to the supraorbitals. The nuchal caputegulae can also vary in size and shape; usually, there are four square-to-rectangular caputegulae, and the median pair is smaller than the lateral pair (Figs. 3.10, 3.11).

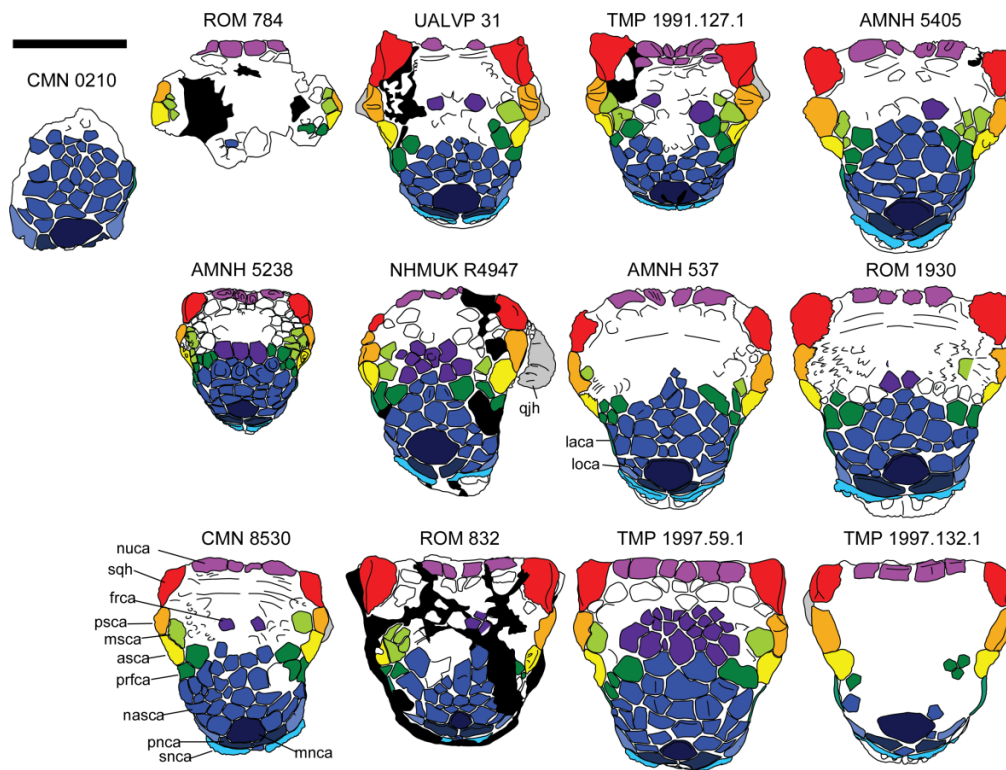
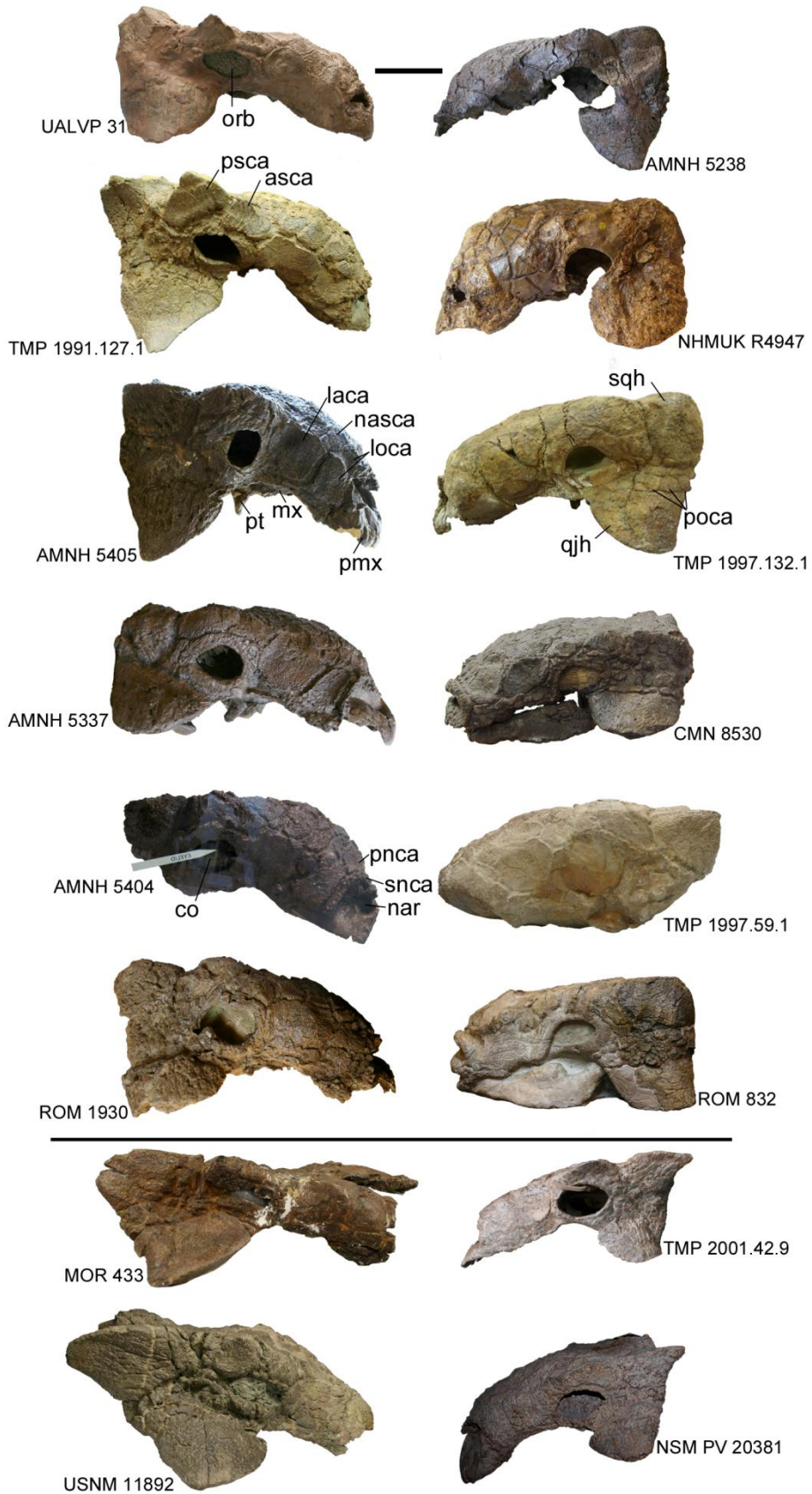


Figure 3.11. Cranial ornamentation patterns compared. CMN 0210 is the holotype of *Euoplocephalus tutus*, CMN 8530 is the holotype of *Anodontosaurus lambei*, and ROM 784 is the holotype of *Dyoplosaurus acutosquameus*. **Abbreviations:** asca, anterior supraorbital caputegulum; frca, frontal caputegulum; laca, lacrimal caputegulum; loca, loreal caputegulum; mnca, median nasal caputegulum; msca, middle supraorbital caputegulum; nas apt, nasal aperture; nasca, nasal caputegulum; nuca, nuchal caputegulum; orb, orbit; pnca, postnarial caputegulum; prfca, prefrontal caputegulum; psca, posterior supraorbital caputegulum; qjh, quadratojugal horn; snca, supranarial caputegulum; sqh, squamosal horn.

The squamosal horn is one of the most variable features on the skull in specimens referred to *Euoplocephalus tutus*, but is generally triangular in dorsal and lateral views (Figs. 3.10, 3.11). The length and sharpness of the squamosal horn varies, as does the angle at which the squamosal horn projects from the skull. The longest, most pointed squamosal horns are found in FPDM V-31, MOR 433, NSM PV 20381, TMP 2001.42.19, and USNM 11892 (Fig. 3.10). TMP 1991.127.1 and UALVP 31 have pointed squamosal horns that are relatively shorter, whereas the shortest, bluntest squamosal horns are found in AMNH 5337 and AMNH 5403 (Fig. 3.10). In dorsal view, the posterior edge of the squamosal horn is nearly continuous with the nuchal crest in some specimens (ROM 832, TMP 1997.59.1, TMP 1997.132.1; Figs. 3.10, 3.11). In other skulls (AMNH 5337, AMNH 5405, ROM 1930; Figs. 3.10, 3.11), the squamosal horn is distinct from the nuchal crest in dorsal view. The squamosal horns of FPDM V-31, MOR 433, NSM PV 20381, TMP 2001.42.19, and USNM 11892 (Figs. 3.10-3.12) are back-swept, i.e., a line drawn from the center of the base of the squamosal horn through the apex of the horn in lateral view is more horizontal in these specimens compared to other referred *Euoplocephalus* specimens like ROM 1930 or UALVP 31 (Fig. 3.12). The squamosal horns extend well past the nuchal caputegulae in FPDM V-31, MOR 433, NSM PV 20381, TMP 2001.42.19, and USNM 11892 (Fig. 3.10), a condition more similar to that observed in *Ankylosaurus* than in other specimens referred to *Euoplocephalus*.



The quadratojugal horn also varies considerably in terms of size, sharpness, and angle of projection from the skull. In dorsal and lateral views, the apex of the quadratojugal horn may be sharp (AMNH 5405, TMP 1991.127.1, UALVP 31) or round (CMN 8530, NHMUK R4947; Figs. 3.10-3.12). The apex may be centrally positioned, so that the quadratojugal horn is an equilateral triangle in dorsal or lateral view (AMNH 5405, TMP 1991.127.1, UALVP 31; Figs. 3.10-3.12), or posteriorly offset, so that the horn is a right-angle triangle (ROM 832, TMP 1997.132.1, USNM 11892; Figs. 3.10-3.12). The orientations of the squamosal and quadratojugal horns are likely controlled by the taphonomic deformation of the skulls (Arbour and Currie 2012). Some specimens referred to *Euoplocephalus tutus* have small circular caputegulae at the bases of the squamosal and quadratojugal horns postocular caputegulae (CMN 8530, TMP 1997.132.1), and other specimens lack these caputegulae (AMNH 5405, UALVP 31; Fig. 3.12).

Figure 3.12 [previous page]. Skulls in lateral view. Skulls from Alberta appear above the horizontal line, and skulls from Montana below the line. The left column of skulls from Alberta includes skulls without postocular caputegulae around the base of the squamosal and quadratojugal horns, in right lateral view (AMNH 5337, AMNH 5404, AMNH 5405, ROM 1930, TMP 1991.127.1, and UALVP 31). The right column of skulls from Alberta includes skulls with postocular caputegulae around the base of the squamosal and quadratojugal horns, in left lateral view (AMNH 5238, CMN 8530 (*Anodontosaurus lambei* holotype), NHMUK R4947, ROM 832, TMP 1997.59.1, TMP 1997.132.1. Below the horizontal line are skulls from Montana (MOR 433 (*Oohkotokia horneri* holotype), NSM PV 20381, TMP 2001.42.9, and USNM 11892). The anterior rostrum of TMP 2001.42.9 and NSM PV 20381 are heavily reconstructed. AMNH 5404, AMNH 5405, and TMP 1991.127.1 are mirrored left lateral views, and AMNH 5238 is a mirrored right lateral view. Photograph of NSM PV 20381 by T. Miyashita and used with permission. Scale equals 10 cm. **Abbreviations:** asca, anterior supraorbital caputegulum; co, ciliary osteoderm; laca, lacrimal caputegulum; loca, loreal caputegulum; mx, maxilla; nar, naris; nasca, nasal caputegulum; orb, orbit; pmx, premaxilla; pnca, postnarial caputegulum; poca, postocular caputegulum; psca, posterior supraorbital caputegulum; pt, pterygoid; qjh, quadratojugal horn; snca, supranarial caputegulum; sqh, squamosal horn.

The shape of the posterior edge of the nuchal crest in dorsal view varies among specimens referred to *Euoplocephalus* (Figs. 3.10, 3.11). In most specimens, shallow notches separate the medial pairs of nuchal caputegulae (AMNH 5238, AMNH 5405, TMP 1991.127.1). In other specimens, the posterior edges of the nuchal crests are straight (ROM 832, TMP 1997.59.1, TMP 1997.132.1), as they are in *Dyoplosaurus* (ROM 784).

AMNH 5405 and TMP 1991.127.1 have arched skulls in lateral view (Fig. 3.12), but in other specimens (AMNH 5403, CMN 8530, MOR 433; Fig. 3.12) the anterodorsal profiles of the skulls are nearly flat. It is likely, but not certain, that these differences are the results of taphonomic deformation (Arbour and Currie 2012). Posterior to the orbits, the parietal region varies from flat to concave in lateral profile.

Cranial sutures are generally undetectable in adult ankylosaurids (Hill et al. 2003). Although cranial sutures on the dorsum are obliterated by ornamentation in all referred *Euoplocephalus* skulls, sutures are occasionally visible on the ventral surfaces of some specimens. For example, the contacts between the premaxilla and maxilla, pterygoid and palatine, pterygoid and quadrate, and quadrate and quadratojugal are visible in AMNH 5405 (Fig. 3.13B). In the palatal region (Fig. 3.13A, B, D, E), a longitudinal furrow at the midline between the paired premaxillae may be present or absent. Some specimens have depressions lateral to the palatal apertures.

3.3.1.2 Mandible

The mandible of *Euoplocephalus* is described in detail by Vickaryous and Russell (2003). Much of the variation in mandibular morphology in specimens referred to *Euoplocephalus* (Fig. 3.13I-L) results from taphonomic distortion. The mandible of AMNH 5403 is much lower and flatter than those of AMNH 5337, AMNH 5405, and UALVP 31, but the cranium of AMNH 5403 has clearly been taphonomically crushed. The coronoid projects markedly from the dorsal border of the mandible in UALVP 31 (Fig. 3.13I, J), but not in AMNH 5337, AMNH 5403 (Fig. 3.13L), or AMNH 5405 (Fig. 3.13K). The significance of this difference is unclear, but does not appear to be taphonomically related, as the coronoid is not abraded in AMNH 5337, AMNH 5403, or AMNH 5405, and AMNH 5405 does not appear taphonomically distorted.

Figure 3.13 [previous page]. Cranial and mandibular anatomy. **A)** AMNH 5337 in ventral view. AMNH 5405 in **B)** ventral and **C)** anterior views. **D)** TMP 1997.132.1 in ventral view. ROM 1930 in **E)** ventral and **F)** posterior views. **G)** ROM 784 (holotype of *Dyoplosaurus acutosquameus*) in ventral view. **H)** AMNH 5238 skull in ventral view. Right mandible of UALVP 31 in **I)** lateral view and **J)** medial view. Right mandible in lateral view of **K)** AMNH 5405 and **L)** AMNH 5403. Scale bars equal 10 cm. **Abbreviations:** alv, tooth alveolus; art, articular; bas, basioccipital; bpt, basipterygoid process; bs, basisphenoid; ch, choana; co, ciliary osteoderm; cor, coronoid; d, dentary; dpf, descending process of frontal; ee, ectethmoid; endo, endocranial cavity; fm, foramen magnum; inb, internarial bar; ls, laterosphenoid; ltf, laterotemporal fenestra; maca, mandibular caputegulum; meck, Meckelian groove; mnca, median nasal caputegulum; mx, maxilla; mx tom, maxillary tomium; nas apt, nasal aperture; nc, nasal canal; ns, nasal septum; nuc, nuchal crest; oc, occipital condyle; of, olfactory region of nasal canal; orb, orbit; orbs, orbitosphenoid; pal, palatine; pal apt, palatal aperture; para apt, paranasal aperture; parocc, paroccipital process; pmx, premaxilla; pmx n, premaxillary notch; pmx tom, premaxillary tomium; pnca, postnarial caputegulum; preart, prearticular; pro nas pmx, intranasal process of premaxilla; ps, parasphenoid (cultriform process); pt, pterygoid body; ptq, quadrate ramus of pterygoid; ptv, interpterygoid vacuity; ptw, pterygoid wing; q, quadrate; qh, quadrate head; qjh, quadratojugal horn; snca, supranarial caputegulum; socc, supraoccipital; spd, sulcus for prementary; spl, splenial; sqh, squamosal horn; sur, surangular; v, vomer.

3.3.1.3 Vertebral Column

Associated cervical vertebrae (Fig. 3.14) are only preserved in AMNH 5337, AMNH 5403, and NHMUK R5161. The cervicals of AMNH 5403 are taphonomically distorted and asymmetrical. The cervicals are only partly visible in dorsal view in NHMUK R5161 as this specimen is displayed as a panel mount.

The atlas is unknown for *Euoplocephalus tutus*, but an axis is preserved in AMNH 5403 (Fig. 3.14). The axial centrum is anteroposteriorly longer than those of other cervical centra in AMNH 5403. The odontoid is wide and massive, with a shallow U-shaped trough on the dorsal surface. Cervical ribs are fused to the centrum; because of extensive plaster reconstruction it is unclear if the ribs are dichcephalic or holocephalic. In dorsal view, the neural spine is V-shaped, with the arms of the V directed posteriorly. The neural spine slopes dorsoposteriorly. Prezygapophyses are not preserved. The large postzygapophyses are located on the posterolateral ends of the V-shaped neural spine, and overhang the posterior end of the centrum. The articular faces of the postzygapophyses are oval and anteroposteriorly long.

One posterior cervical is preserved in AMNH 5337 (Fig. 3.14), and three postaxial cervicals are preserved in AMNH 5403 (Fig. 3.14). The cervical centra are wider than long or approximately as long as wide, with subcircular to elliptical amphicoelus articular faces. The position of the anterior face relative to the posterior face (dorsal or ventral to, or in line with) varies among the three vertebrae. The neural spine is transversely oriented and is U-shaped in dorsal view. In anterior view, the neural spine is an inverted triangle. Although partly damaged in all specimens, a thin horizontal sheet of bone, of unknown anterior extent, occurred between the widely-separated prezygapophyses. The prezygapophyses overhang the anterior edge of the centrum (unlike the postzygapophyses, which do not overhang the posterior edge of the centrum). There are no epipophyses. The neural canal is square in cross-section. The transverse process is low on the neural arch and projects ventrolaterally. The

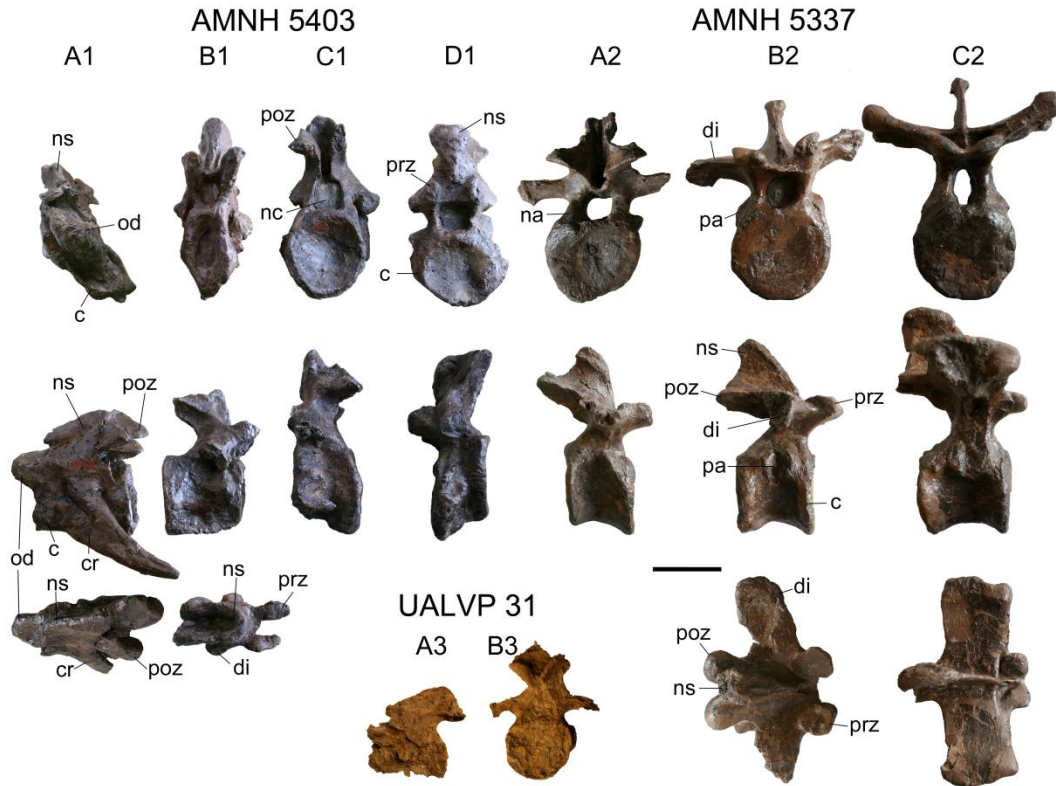


Figure 3.14. Cervical and dorsal vertebrae. AMNH 5403 axis (**A1**) in anterior, left lateral, and dorsal views; cervical (**B1**) in anterior, right lateral, and dorsal views; cervical (**C1**) in posterior, left lateral, views; cervical (**D1**) in anterior, left lateral views. AMNH 5337 cervical (**A2**) in posterior, right lateral views; dorsals (**B2,C2**) in anterior, right lateral, and dorsal views. UALVP 31 axis (**A3**) in left lateral view, and cervical (**B3**) in posterior view. **Abbreviations:** c, centrum; cr, cervical rib; di, diapophysis; ns, neural spine; na, neural arch; nc, neural canal; od, odontoid; pa, parapophysis; poz, postzygapophysis; prz, prezygapophysis;

parapophysis is a subcircular protuberance positioned anteriorly on the centrum, although the dorsoventral position varies. Variation in the position of the articular faces relative to each other, the positions and sizes of the transverse processes (diapophyses), and the proportions of the centra in AMNH 5403 reflect positional differences along the vertebral column.

AMNH 5337 preserves the most complete presacral vertebral series of any specimen referred to *Euoplocephalus tutus*, and includes the final cervical vertebra (Fig. 3.14B1), eleven free dorsals (Figs. 3.14B2-3, 8), four dorsosacrals

(dorsals incorporated into the sacral rod of the pelvis, with fused centra and neural spines), three sacrals, and one caudosacral. The parapophysis is located at the junction between the neural arch and centrum on one of the vertebrae (Fig. 3.14B2), and is transitional between the cervical and dorsal vertebrae; it is here considered as a dorsal vertebra because the morphology of the neural spine is more similar to those of the dorsals than cervicals. In addition to the location of the parapophysis, the dorsal vertebrae (Fig. 3.15) can be differentiated from the cervicals based on morphological differences of the neural spines, which are anteroposteriorly-oriented and blade-like in the dorsals (rather than transversely-oriented and U-shaped, as in the cervicals). The shapes of the dorsal neural spines vary along the vertebral column; each is a mediolaterally thin and rectangular (in lateral view) plate that overhangs the posterior edge of the centrum. A rugose, mediolateral swelling occurs towards the distal end of the neural spine. The dorsal centrum is spool-shaped, with concave lateral sides and circular articular faces. The neural canal is tall and elliptical. The transverse processes are mediolaterally wide and anteroposteriorly long. The orientation at which they project from the neural arch varies from horizontal to dorsolateral. In some vertebrae, paired fossae occur at the junctions of the transverse processes, neural spines, and prezygapophyses (Fig. 3.15C2). The diapophysis is an inverted triangle on the end of the transverse process. The parapophysis is a subcircular to teardrop-shape articular surface in the anterior dorsals and sutural surface in the posterior dorsals. Posteriorly in the vertebral series, the dorsal ribs fuse to the dorsal vertebrae. The prezygapophyses are closely set and steeply angled, forming a U-shaped trough. The postzygapophyses are fused together along their lengths to form a peg-like, midline structure.



Figure 3.15. Dorsal vertebrae of AMNH 5337. AMNH 5337, **D** in anterior and left lateral views; **E** in posterior and right lateral views; **F** in anterior and right lateral views; **G** in anterior and right lateral views; **H** in posterior and left lateral views; **I** to **L** in anterior and left lateral views.

Abbreviations: c, centrum; di, diapophysis; na, neural arch; nc, neural canal; ns, neural spine; pa, parapophysis; poz, postzygapophysis; prz, prezygapophysis; r, rib; tp, transverse process.

Features that vary among the dorsal vertebrae include the angles of projection of the transverse processes (more steeply inclined posteriorly in the series), the extents that the neural spines and postzygapophyses overhang the posterior ends of the centra (more overhanging posteriorly in the series), and whether or not the ribs are coossified to the transverse processes (unfused anteriorly, and fused posteriorly in the series). Because only one specimen preserves a relatively complete dorsal series (AMNH 5337), it is impossible to compare vertebrae in the same positions in different specimens; the dorsals of AMNH 5337 are similar in most respects, other than size, to those of *Ankylosaurus* (Carpenter 2004). Coombs (1986), in describing the juvenile specimen AMNH 5266, noted that the dorsal centra were not as constricted midlength relative to the articular faces as in other *Euoplocephalus tutus* specimens, a difference he attributed to ontogenetic change. It is unknown at present how vertebral morphology may change throughout ontogeny in ankylosaurids. Additionally, Coombs (1986) noted that the diapophyses of the preserved dorsal neural arch were less blade-like compared to *Ankylosaurus magniventris* and other *Euoplocephalus tutus* specimens.

The synsacrum (Figs. 3.16, 3.17) includes coossified dorsal, sacral, and caudal vertebrae. Currently, only the sacra of AMNH 5245, NHMUK R5161, and ROM 1930 can be observed in ventral view, as all of the other pelvises are mounted for display with only the dorsal surface accessible. A full description of the pelvis of specimens referred to *Euoplocephalus tutus* is provided by Coombs (1979). Vickaryous et al. (2004) and Thompson et al. (2012), only noted the presence or absence of the synsacrum, but did not fully describe it. Where sacral vertebrae are preserved, they are always coossified, except for AMNH 5266, a juvenile specimen (Coombs 1986). The number of dorsosacrals and caudosacrals is variable. True sacrals are identified here as those that immediately bracket the acetabulum, and in all referred specimens there appear to have been no more than three. AMNH 5337 and AMNH 5409 each have four dorsosacrals, three

sacrals, and one caudosacral. AMNH 5245 has two dorsosacrals, three sacrals, and one caudosacral, but the anterior end of the sacrum is broken and there were almost certainly additional dorsosacrals. The sacrum of ROM 1930 is in several pieces, but includes a block of five coossified vertebrae (with a sixth broken off), which appear to be dorsosacrals based on the flattened, T-shaped ribs (Fig. 3.16A, B). The most anterior vertebra in this section has free, unfused prezygapophyses, which indicates that this is the first vertebra in the fused sacral rod. The most posterior vertebra preserved in this section may be a sacral vertebra. A second section of fused vertebrae consists of two vertebrae that are most likely sacral vertebrae, based on the morphology of the centra and the large broken area representing the attachments of the sacral ribs. These two sections do not fit back together, so it is unclear if an additional vertebra is missing between them. In total, at least seven dorsosacral and sacral vertebrae formed the sacral rod of ROM 1930. There are an additional three unfused caudosacral vertebrae in ROM 1930 (Fig. 3.16G-J). The distal ends of the transverse processes are large, not tapering, which suggests they contacted or fused with the ilia. This specimen also has three loose vertebrae, one of which is probably a true sacral, and two of which are probably caudosacrals. ROM 1930 may have had up to eleven vertebrae in the pelvis. NHMUK R5161 includes at least three dorsosacrals, three sacrals and three caudosacrals (see Nopcsa 1928:Pl. VI, Fig. 2). TMP 1982.9.3 preserves four dorsosacrals and two sacrals, with the posterior portion of the sacral rod broken (Fig. 3.17P).

The intervertebral facets of centra of all of the dorsosacral and sacral vertebrae are coossified in adult specimens (unfused sacral vertebrae are known in the juvenile specimen AMNH 5266), but the centra of the caudosacral vertebrae may not be coossified. The neural spines of all of the vertebrae of the sacrum fuse into a single continuous sheet of bone, such that the prezygapophyses and postzygapophyses become indistinct. In TMP 1982.9.3, the distal ends of the neural spines are laterally expanded, forming a

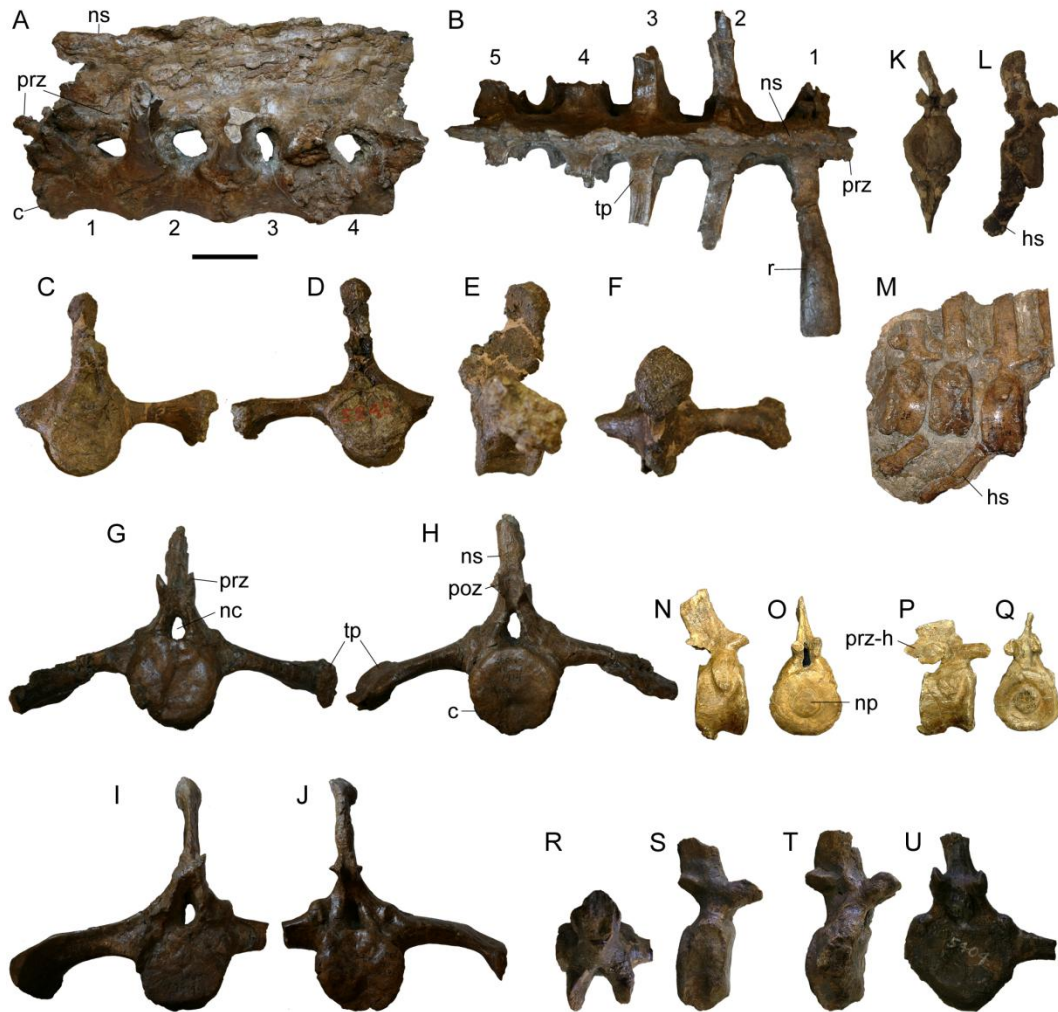


Figure 3.16. Dorsosacral, sacral, caudosacral, and caudal vertebrae. Partial sacrum of ROM 1930 in **A**) left lateral and **B**) dorsal (with anterior to the right) views. Sacrocaudal of AMNH 5245 in **C**) anterior, **D**) posterior, **E**) left lateral, and **F**) dorsal views. Sacrocaudal of ROM 1930 in **G**) anterior and **H**) posterior views. Sacrocaudal of ROM 1930 in **I**) anterior and **J**) posterior views; distal end of transverse process is partially reconstructed. Anterior free caudal vertebra of CMN 8530 (holotype of *Anodontosaurus lambei*) in **K**) anterior and **L**) right lateral views. **M**) Block of articulated anterior free caudal vertebrae of ROM 1930, in right lateral view. Penultimate free caudal vertebra of ROM 1930 in **N**) right lateral and **O**) anterior views. Transitional caudal vertebra (last free caudal vertebra before first handle vertebra of the tail club) of ROM 1930 in **P**) right lateral and **Q**) anterior views. AMNH 5404 free caudal vertebra in **R**) dorsal and **S**) right lateral views. Next most posterior AMNH 5404 free caudal vertebra in **T**) right lateral and **U**) anterior views. Scale equals 10 cm. **Abbreviations:** c, centrum; hs, haemal spine; nc, neural canal; np, notochordal prominence; ns, neural spine; poz, postzygapophysis; prz, prezygapophysis; prz-h, prezygapophysis of the first handle vertebra; r, rib; tp, transverse process.

flat to slightly concave dorsal surface (Fig. 3.17P). Although the neural spines are completely coossified in ROM 1930, in dorsal view the individual neural spines form a repeating teardrop pattern (Fig. 3.16B). This region is unprepared in AMNH 5245, somewhat reconstructed with plaster in both AMNH 5337 and AMNH 5409, and obscured by skin impressions in NHMUK R5161. The centra of the dorsosacrals have lateral surfaces that are slightly more concave compared to the centra of the sacrals. Ventrally, the sacral vertebrae lack a midline groove (AMNH 5245) or have a shallow, discontinuous midline groove (ROM 1930). The transverse processes of the dorsosacrals are T-shaped in cross section, whereas those of the sacrals are more rectangular, and proportionately thicker in cross-section.

Arbour et al. (2009) noted differences in the shapes of centra among caudal vertebrae referred to *Euoplocephalus tutus*, with most specimens having circular to subcircular cross-sections, and CMN 8530 being octagonal (Fig. 3.16K). Features of the caudal vertebrae (Fig. 3.16) that do not appear to vary among specimens include the orientations of the neural and haemal spines, and the shapes of the neural and haemal spines (in all instances, the spines taper distally and are blade-like). The presence or absence of a notochordal prominence on the centrum varies among vertebrae within a single individual. The number of vertebrae incorporated into the tail club handle (terminology *sensu* Coombs 1995a) may be a useful character, but few tail clubs are complete and this character cannot be coded in most specimens.

Penkalski (2001) observed differences in the orientations of the articular faces of the zygapophyses in the caudal vertebrae, with ROM 784 (*Dyoplosaurus acutosquameus*) having more horizontal articular faces than those of AMNH 5404. However, the orientations of the articular faces vary along the caudal series in ROM 784, and the posterior caudals have more vertically oriented zygapophyseal articular faces.

3.3.1.4 Pectoral girdle and forelimb

All scapulae referred to *Euoplocephalus tutus* are dorsoventrally broad and paddle-shaped (Fig. 3.17A-G). The posterior (distal) end of the scapular blade is weakly expanded, and the posteroventral edge of the blade is weakly concave. The distal end of the scapula is broader and rounder in AMNH 5406 (Fig. 3.17A-D) when compared to AMNH 5424 (Coombs 1978c: Fig. 3). The acromion occurs on the dorsal border of each scapula, laterally overhangs the main body of the scapula, and is most prominent over the glenoid. The infraspinous fossa is approximately triangular and ventral to the acromion. The acromion gradually decreases in size along the posterior edge of the infraspinous fossa. A prominent entheses probably marks the insertion of the M. triceps longus caudalis (as in *Ankylosaurus*, see Carpenter 2004: Fig. 15) in AMNH 5406 (Fig. 3.17A-D), TMP 2001.42.19 (Fig. 3.17E), and UALVP 31 (Fig. 3.17G). On the medial side, a prominent horizontal ridge, the scapulocoracoid buttress, occurs at the junction of the scapula and coracoid. The scapula and coracoid are unfused in AMNH 5406 (Fig. 3.17H) but fused in the larger specimens AMNH 5337 and AMNH 5424 (Coombs 1978c: Fig. 3) and in the smaller specimen TMP 2001.42.9 (Fig. 3.17E,F); the sutural edge of the scapula in ROM 1930 is broken, possibly indicating that it was fused to the coracoid. The right coracoid of ROM 813 (Fig. 3.17I) has been heavily reconstructed with plaster so that it is unclear if fusion with the scapula had occurred. In lateral view, the scapula has a triangular ventral projection at the glenoid. The scapula and the coracoid contribute about equally to the glenoid, and the coracoid sutural surface in AMNH 5406 is flat (Fig. 3.17H). The coracoid is approximately square in lateral view, with a straight anterior margin and a prominent, hooked ventral (sternal) process. The coracoid foramen is circular.

All humeri referred to *Euoplocephalus tutus* (Fig. 3.18) are stout and hourglass-shaped. The deltopectoral crest extends for more than 42% the length of the humerus. Penkalski (2001) noted that the deltopectoral crest in MOR 433



does not appear to extend as far down the shaft of the humerus compared to other *Euoplocephalus* specimens. This is difficult to quantify because the proximal and distal ends of both humeri are badly damaged in MOR 433, making the total length of each humerus impossible to determine. In all specimens

where this feature is preserved, distally the lateral margin of the deltopectoral crest is rotated slightly anteriorly, and merges with the shaft of the humerus as a prominent, thick knob (e.g. AMNH 5337, Fig. 3.18E). Prominent striations on the deltopectoral crest represent the attachments for the *M. supracoracoideus* and *M. pectoralis* (Coombs 1978c). Humeri referred to *Euoplocephalus tutus* differ in the relative sizes of the deltopectoral crests (both in terms of length and width) and the lateral supracondylar crests. These crests are largest in AMNH 5337 (Fig. 3.18D, E) and smallest in AMNH 5406 (Fig. 3.18A) and UALVP 31 (Fig. 3.18B). The humerus of AMNH 5337 is longer than the humeri of AMNH 5406 or UALVP 31, and so the larger crests of AMNH 5337 may be size-related. The humeral head in proximal view is semicircular (Fig. 3.18F), and subcircular to slightly triangular in medial view. Anteriorly the broad, shallow, bicipital fossa is bounded by the deltopectoral crest and humeral head. The medial (internal) tuberosity is prominent, and the proximal margin posterior to the humeral head is flat. The radial (lateral) condyle is slightly larger than the ulnar (medial) condyle, although

Figure 3.17 [previous page]. Pectoral and pelvic girdles. AMNH 5406 right scapula in **A)** medial and **B)** lateral views, left scapula in **C)** lateral and **D)** medial views. TMP 2001.42.19 left scapulocoracoid in **E)** lateral and **F)** ventral views. **G)** UALVP 31 right scapula in medial view. **H)** AMNH 5406 left scapula in anteroventral view. **I)** ROM 813 right coracoid in lateral view. **J)** AMNH 5404 left coracoid in lateral view. **K)** AMNH 5245 right ilium in ventral view, anterior is up. TMP 2001.42.19, **L)** right ischium and **M)** left ischium in medial views. **N)** CMN 8530 (*Anodontosaurus lambei* holotype) right ischium in medial view. **O)** UALVP 31 associated right ilium, sacrum, right femur and right tibia, with ilium in ventral view (anterior is up), and femur in medial view. **P)** TMP 1982.9.3 pelvis in dorsal view (the right half of the pelvis is reconstructed), anterior is up. Photograph of AMNH 5404 coracoid by R. Sissons and used with permission. Scale bar for A-H and J is 5cm, scale bar for I is 10 cm. **Abbreviations:** ace, acetabulum; acr, acromion; cf, coracoid foramen; ds, dorsosacral; fem, femur; gl, glenoid; glf, glenoid fossa; il, ilium; ip, iliac peduncle; is, ischium; ost, osteoderm; medr, medial ridge; mt, metatarsal; mtlc, entheses of *M. triceps longus caudalis*; ns, neural spine; posta, postacetabular process; pp, pubic peduncle; prea, preacetabular process; r, rib; s1-3, sacrals 1-3; scb, scapulocoracoid buttress; scor, surface for coracoid; stp, sternal process; sscap, surface for scapula; tib, tibia.

both are large and transversely expanded. The olecranon fossa is shallow and triangular, and the intercondylar notch is shallow and rounded. The radial and ulnar condyles and the humeral heads in the humeri of AMNH 5337, AMNH 5404, and ROM 1930 have networks of deep furrows covering the articular surfaces similar to those of large individuals of hadrosaurids, iguanodontids, ceratopsids, sauropods, and some theropods (Fig. 3.18F, G).

The radius is only known from a few specimens (Fig. 3.18L, M). It is a stout bone with a flared, concave proximal articular surface, and a rugose, bluntly pointed distal end in anterior view (Fig. 3.18L, M). The proximal and distal ends of the radius of AMNH 5337 (Fig. 3.18L) are proportionately wider transversely than those of AMNH 5406 (Fig. 3.18M), ROM 784, and TMP 1997.132.1. In specimens where the ulnae are preserved, the proximal end has a prominent, rugose olecranon process (Fig. 3.18N). A complete manus is not preserved in any specimen referred to *Euoplocephalus tutus*.

3.3.1.5 Pelvic girdle and hindlimb

The pelves of specimens referred to *Euoplocephalus* are mediolaterally broad, anteroposteriorly long, and have strongly divergent ilia (Fig. 3.17K, O, P). Complete pelves are preserved in AMNH 5337, AMNH 5409 (Coombs 1979:Figs. 12, 13), and NHMUK R5161 (Nopcsa 1928:Pl VI, Fig.2, Pl. VII, Fig. 1), and partial pelves are also known for AMNH 5245 (Fig. 3.17K), TMP 1982.9.3 (Fig. 3.17P) and UALVP 31 (Fig. 3.17O), as well as ROM 784 (*Dyoplosaurus*, Arbour et al. 2009:Fig. 1). The postacetabular process of the ilium is proportionately longer in NHMUK R5161 compared to other referred specimens, and the process is longer than the maximum diameter of the acetabulum. The pubis is unknown. The ischium is wide proximally, and a sulcus on the lateral side contributes to the closed acetabulum (Fig. 3.17L, M). In medial view, the dorsal margin is rounded, and the

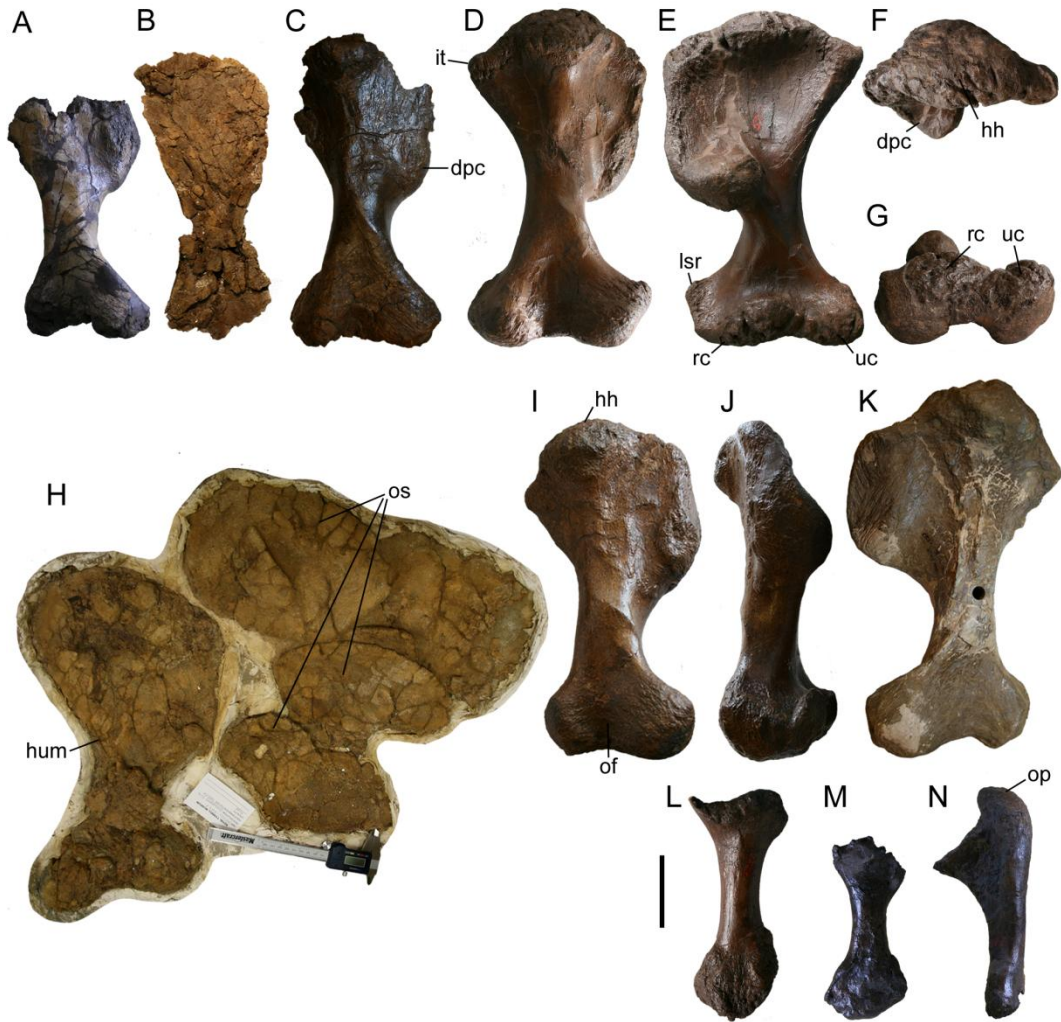


Figure 3.18. Forelimb elements. AMNH 5406 right humerus in **A)** posterior view. UALVP 31 right humerus in **B)** anterior view. ROM 1930 right humerus in **C)** posterior view. AMNH 5337 right humerus in **D)** posterior, **E)** anterior, and **F)** proximal and **G)** distal views. **H)** TMP 1997.132.1 left humerus and associated osteoderms with humerus in anterior view and osteoderms mostly in interior view. AMNH 5404 right humerus in **I)** posterior and **J)** anterior views. **K)** ROM 47655 left humerus in posterior view. AMNH 5337 right radius in **L)** medial view. AMNH 5406 **M)** right radius in medial view and **N)** right ulna in medial view. Scale bar equals 10 cm. **Abbreviations:** dpc, deltopectoral crest; hh, humeral head; hum, humerus; it, internal tuberosity; lsc, lateral supracondylar ridge; of, olecranon fossa; op, olecranon process; os, osteoderm; rc, radial condyle; uc, ulnar condyle.

iliac and pubic peduncles are not distinct from each other (Fig. 3.17N). The wide proximal end tapers abruptly into the ischial shaft. The ischial shaft is laterally compressed, and slightly sigmoidal in anterior and posterior views. The anterior and posterior margins are parallel for the length of the shaft, and the distal terminus is squared-off.

The femur (Figs. 3.19A-D, I-K, N, O) is stout and has a straight shaft with an oval cross-section. The femoral head is round, and the greater trochanter is neither prominent nor distinctly separated from the head. The fourth trochanter is a low and indistinct rugosity distal to the midlength of the femur. The distal condyles are posteriorly expanded, and the medial condyle is slightly larger than the lateral condyle. Posteriorly, the intercondylar groove is shallow. The lateral epicondyles are proportionately larger in AMNH 5266 (Fig. 3.19D) and TMP 1982.9.3 (Fig. 3.19C) than in AMNH 5404 (Fig. 3.19K).

The proximal and distal ends of the tibia (Figs. 3.19E-H, L, M, P) are greatly expanded relative to the shaft. In anterior view (Fig. 3.19H), the maximum dimension of the proximal end is slightly less than that of the distal end, whereas in lateral view (Fig. 3.19G), the proximal end is more than twice as wide as the distal end. In AMNH 5404 the astragalus is fused to the distal end of the tibia (Fig. 3.19L, M), but it is unfused in AMNH 5266 (Fig. 3.19E). Complete pedes are present in AMNH 5266 (Coombs 1979: Fig. 4) and ROM 1930; in each the pes is tridactyl, with U-shaped unguals (rather than triangular, as in ROM 784, *Dyoplosaurus acutosquameus*; Arbour et al. 2009: Fig. 5) in dorsal view.

3.3.1.6 Osteoderms and integument

The cervical half rings of ankylosaurids (Fig. 3.20) are composed of two separate layers of ossification: a superficial (upper) layer of primary osteoderms similar to those found on the rest of the body (sometimes ringed by smaller interstitial osteoderms), and a deep (lower) layer of bone of unknown origin, referred to here as the band. The band is formed of several dorsoventrally



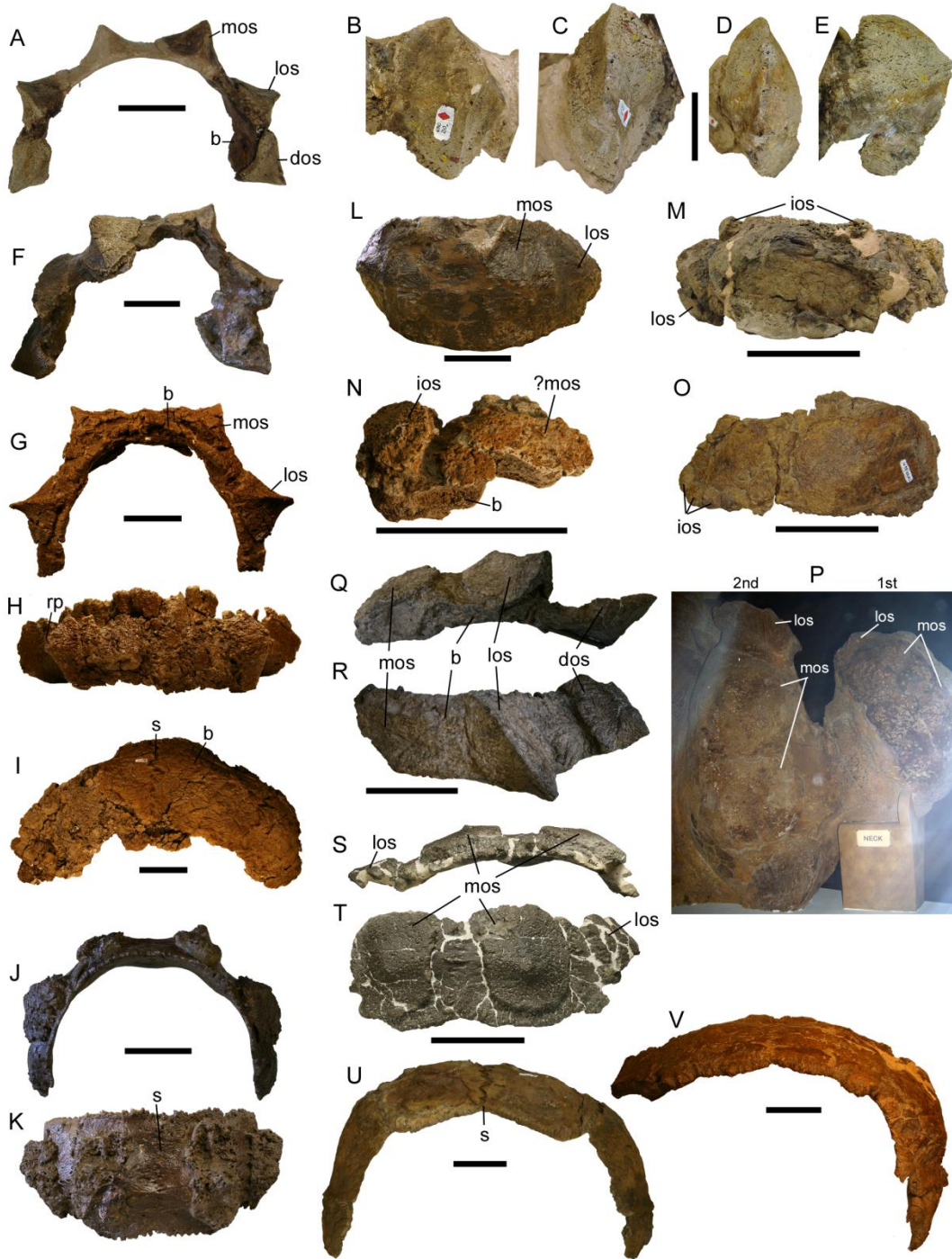
Figure 3.19. Hindlimb elements. TMP 1982.9.3 left femur in **A)** anterior, **B)** medial, and **C)** posterior views. **D)** AMNH 5266 right femur in posterior view. **E)** AMNH 5266 right tibia in anterior view. **F)** AMNH 5266 right fibula. ROM 813 left tibia in **G)** lateral and **H)** posterior views. AMNH 5404 right femur in **I)** anterior, **J)** medial, and **K)** posterior views, and right tibia in **L)** lateral and **M)** anterior views. **N)** AMNH 5404 right femur in distal view. **O)** TMP 1982.9.1 left femur in distal view. **P)** AMNH 5404 right tibia in distal view. **Abbreviations:** 4th, fourth trochanter; as, astragalus; ca, calcaneum; cn, cnemial crest; fh, femoral head; im, inner malleolus; lc, lateral condyle; le, lateral epicondyle; mc, medial condyle; om, outer malleolus.

arched, approximately rectangular segments joined by serrated sutures; most cervical rings have six segments. Each band segment may have zero (Fig. 3.20V), one (Fig. 3.20B), or more than one (Fig. 3.20N) osteoderm superficial to the band; most commonly a single large osteoderm is present and centered on the segment. In some specimens (AMNH 5337, AMNH 5404; Fig. 3.20J-L), the

overlying osteoderm is fused to the underlying band, but in others (UALVP 31; Fig. 3.20G, H) the osteoderm is only partially fused or not fused at all to the band. Band segments are always smooth-textured and are more similar in appearance to endochondral bone than to osteodermal bone, which is typically pitted or rugose in ankylosaurids. Weathered band segments can have a fibrous, interwoven texture. In most ankylosaurids (*Ankylosaurus magniventris*, *Pinacosaurus mephistocephalus*, and *Saichania chulsanensis*), the morphologies of the first and second cervical half rings are similar, with the second half ring being larger and broader than the first.

Paired osteoderms on the cervical half ring share unique shapes, but the medial, lateral, and distal pairs differ from each other. In AMNH 5406, CMN 210 and UALVP 31 (Fig. 3.20A-H), the primary medial osteoderms have wide oval bases with anteroposteriorly-aligned keels, and the primary lateral osteoderms have narrower bases with sigmoidal keels (Arbour et al. 2009). The distal osteoderms (*sensu* Penkalski 2001) are missing in UALVP 31 (Fig. 3.20G), but in CMN 210 (Fig. 3.20A) they are deeply excavated and compressed (Arbour et al. 2009). AMNH 5406, CMN 210, and UALVP 31 have the smallest known half rings referable to *Euoplocephalus tutus*. The half rings in AMNH 5337, AMNH 5403, AMNH 5404, and AMNH 5405 all have lower, more rounded and rugose osteoderms on the first half ring (Fig. 3.20J-L). The distal osteoderms are missing in all of these specimens, but because the distal osteoderms do not seem to be as strongly fused in AMNH 5406 and CMN 210, they may not have been preserved.

Several first cervical half rings referred to *Euoplocephalus tutus*, including CMN 8530, TMP 1982.9.3, TMP 1996.75.1, and TMP 1997.132.1, have small subcircular osteoderms present around the bases of the larger half ring osteoderms (Fig. 3.20M-O). These interstitial osteoderms are present even on small fragments of half rings (TMP 1982.9.3, TMP 1996.75.1; Fig. 3.20N). In CMN 8530 (Fig. 3.20M), only three of the interstitial osteoderms are preserved, but



much of the dorsal surface of the half ring is broken. In TMP 1997.132.1 (Fig. 3.200), the interstitial osteoderms ring the border of the preserved ?medial osteoderm, and are smaller and more irregularly distributed around the preserved ?lateral osteoderm. Unusually, AMNH 5404 has two knob-like

projections on the ventral surface of the first cervical half ring, but these do not appear to be the same structures as the interstitial osteoderms found on other half rings.

The cervical rings in NHMUK R5161 (Fig. 3.20P) may have only four band segments rather than the six found in most other cervical rings referred to *Euoplocephalus tutus*. However, it is difficult to determine if the terminal edges of the half rings are broken or complete. No medial osteoderms are visible on the first cervical half ring, and if they are present, they are low and indistinct from the deep band. The lateral osteoderms have tall, laterally-directed keels and narrow bases, and are shaped like right-angle triangles in dorsal view. The second cervical ring also appears to have only four segments. The medial osteoderms are circular with posteriorly-directed apices. The lateral osteoderms are similar to those of the first cervical ring, but are somewhat more rectangular in dorsal view.

A partial first cervical half ring was found with TMP 2001.42.19 (Fig. 3.20Q, R), and preserves the right medial, lateral, and distal osteoderms.

Figure 3.20 [previous page]. Cervical half rings. CMN 0210 (*Euoplocephalus tutus* holotype) first cervical half ring in **A)** anterior view; **B)** left medial osteoderm in superficial view; **C)** right lateral osteoderm in superficial view; **D)** right distal osteoderm in superficial view and **E)** dorsal view. **F)** First cervical half rings of AMNH 5406 in anterior view. UALVP 31, first cervical half ring in **G)** anterior and **H)** dorsal views, and second cervical half ring in **I)** dorsal view. AMNH 5337 first cervical half ring in **J)** anterior and **K)** dorsal views. **L)** AMNH 5404 first cervical half ring in dorsal view. **M)** CMN 8530 (holotype of *Anodontosaurus lambei*) first cervical half ring in dorsal view. **N)** Fragment of first cervical half ring of TMP 1982.9.3 in superficial view. **O)** Partial first cervical half ring of TMP 1997.132.1 in ?dorsolateral view. **P)** NHMUK R5161 *in situ* cervical rings in dorsal view, anterior is to the right. TMP 2001.49.2 partial first cervical half ring in **Q)** posterior and **R)** left lateral views. USNM 7943 partial first cervical half ring in **S)** ?anterior and **T)** dorsal views. **U)** TMP 2007.12.52 second cervical half ring in anterior view. **V)** UALVP 45931 partial second cervical half ring in anterior view. Scales in A, G-R equal 10 cm, scales in B-F equal 5 cm. **Abbreviations:** b, band; dos, distal osteoderm; ios, interstitial osteoderm; los, lateral osteoderm; mos, medial osteoderm; rp, resorption pit on medial osteoderm; s, suture between band segments.

(Osteoderms associated with TMP 2001.42.19 have been mounted onto a curved armature for display over the skeleton, which also includes two fragments of either the first and/or second cervical ring.) The medial osteoderm is nearly flat. Although the keel on the lateral osteoderm is broken, it appears to have been tall and straight rather than sigmoidal, and the distal tip of the osteoderm overhangs the underlying band. The distal osteoderm has a tall keel, and envelopes the distal end of the band. The flat medial osteoderm is unlike the keeled, subconical medial osteoderms of AMNH 5406, UALVP 31, and many other referred *Euoplocephalus* specimens, but similar to that of NHMUK R5161. The apices of the osteoderm keels are usually more centrally positioned in specimens referred to *Euoplocephalus* (AMNH 5406, UALVP 31), and never overhang the band. An isolated first cervical half ring, USNM 7943 (Fig. 3.20S, T) also preserves nearly flat medial osteoderms with low, centrally positioned prominences.

Osteoderms along the body may also provide useful information, although few specimens preserve osteoderms in the original arrangements. Specimens that do retain *in situ* osteoderms include NHMUK R5161, ROM 813, ROM 1930, and TMP 1997.132.01. The *in situ* osteoderms of NHMUK R5161 were described in detail by Nopcsa (1928) and Penkalski and Blows (2013). NHMUK R5161 has large, circular-based osteoderms covering most of the dorsal surface of the body, as well as paired, taller, conical osteoderms at the midline in the pectoral region.

ROM 813 is an exceptional specimen preserving abundant osteoderms, ossicles (<5mm), and epidermal (soft-tissue) scale impressions (Arbour et al. 2013). Although it was referred to *Euoplocephalus tutus* by Penkalski (2001), it preserves few diagnostic features of the Ankylosauridae, and none for the genus *Euoplocephalus tutus*. The straight shaft of the broken ischium, and the rugose, thin-walled osteoderms, suggest that ROM 813 is an ankylosaurid rather than a nodosaurid. The skeleton is disarticulated, but large portions of the integument

remain intact. There are nine large blocks with *in situ* osteoderms. Two adjoining blocks contain a cluster of seven closely-packed large (length >25 cm) keeled osteoderms with rectangular bases. Each of these is surrounded by ossicles, and at the anterior edge of the cluster is a distinct crease similar to that found in NHMUK R5161. Another cluster of osteoderms surrounded by epidermal impressions and ossicles includes mostly osteoderms with subcircular bases, similar to those on the tail of NHMUK R5161. Unfortunately, it is difficult to determine the original positions on the body of many of the integument pieces, because the endochondral elements are disarticulated.

ROM 1930 includes abundant osteoderms that have been completely prepared from the surrounding matrix, as well as *in situ* osteoderms on a block containing several caudal vertebrae. Three large (width >15 cm) keeled osteoderms with oval bases are preserved, as well as hundreds of small (<5 mm) irregularly-shaped ossicles.

Two additional specimens (TMP 1997.132.01 and UALVP 31) include some osteoderms that may be close to their *in situ* positions. TMP 1997.132.01 preserves large (>20 cm diameter) osteoderms near the humerus, articulated radius and ulna, and tibia, as well as a second cervical half ring band with *in situ* (but not coossified) osteoderms. Osteoderms near the humerus are large, keeled, and have subcircular bases (Fig. 3.18H). Osteoderms near the radius and ulna are smaller, with peaked keels overhanging one end of the base, and with narrower bases compared to osteoderms near the humerus. The cervical ring osteoderms also have oval bases and low keels, and the peaks of the keels do not overhang the bases of the osteoderms.

The tail club (Fig. 3.21) is one of the most recognizable features of derived ankylosaurids, but has been represented by only a few characters that essentially code for the presence or absence of the tail club. Tail club absent/present (character 173 in Thompson et al. (2012) and this paper) refers to the presence or absence of terminal osteoderms that envelop the end of the tail (knob

osteoderms *sensu* Coombs 1995a). Two additional characters define the handle vertebrae (*sensu* Coombs 1995a): shape of distal caudal postzygapophyses (character 115) and extent of pre- and postzygapophyses over their adjacent centra in posterior vertebrae (character 116). However, morphological variation in the handle vertebrae and knob osteoderms may have taxonomic and phylogenetic significance. There is always a pair of large osteoderms (major osteoderms *sensu* Coombs 1995a), and a variable number of smaller osteoderms that envelop the end of the tail (minor osteoderms *sensu* Coombs 1995a). Variations in tail club knob morphology have been noted by Coombs (1995a), Arbour (2009), and Arbour et al. (2009). AMNH 5216, AMNH 5245, and TMP 1994.168.1 are all wider than long, and have relatively pointed, triangular (in dorsal view) major knob osteoderms (Fig. 3.21A-D). UALVP 47273 is longer than wide and one of the smallest tail club knobs from Alberta; it is similar to the tail club of ROM 784, *Dyoplosaurus acutosquameus* (Fig. 3.21N-P). The tail club knob of TMP 2001.42.19 (Fig. 3.21M) is also relatively small, but the length and width are nearly equal, unlike the condition in *Dyoplosaurus*. The major osteoderms of the knob are hemispherical in dorsal view. The distal part of the knob is somewhat damaged, making it difficult to determine how many minor osteoderms were present. The remaining tail clubs are usually equally as wide as long, or slightly longer than wide, and have major knob osteoderms that are semicircular in dorsal view. The number of minor osteoderms forming the terminus of the tail varies among specimens. Keels may be present at the mid-height of each major osteoderm (giving the knob a lenticular cross-section as in CMN 135 and ROM 7761), or near the dorsal surface of each osteoderm (giving the knob a semicircular cross-section as in AMNH 5245 and UALVP 16247).

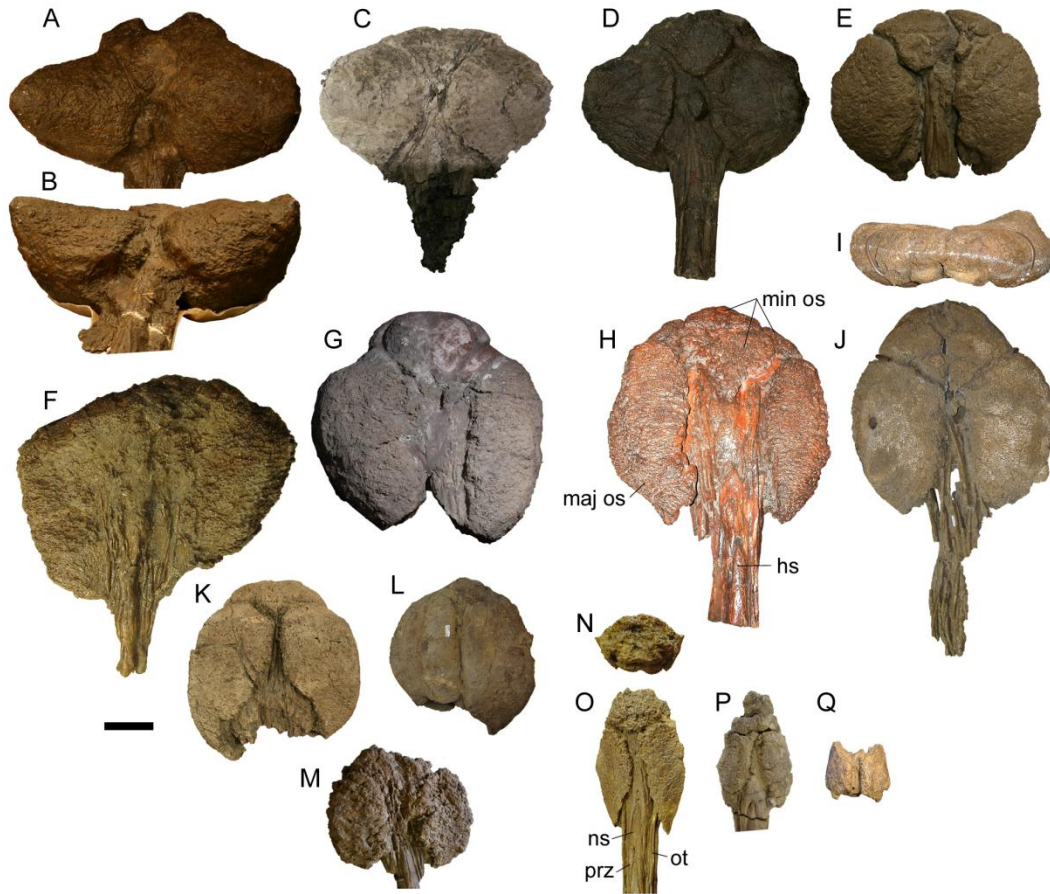


Figure 3.21. Tail clubs. Tail club knobs from the Horseshoe Canyon Formation in **A-E**: AMNH 5245 in **A**) dorsal and **B**) anterior views; **C**) TMP 1994.168.1 in dorsal view; **D**) AMNH 5216 in dorsal view; **E**) USNM 10753 in dorsal view. Tail club knobs from the Dinosaur Park Formation in **F-Q**: **F**) ROM 788 in ventral view; **G**) MACN Pv 12554 in ventral view; **H**) CMN 349 in ventral view; TMP 1983.36.120 in **I**) posterior and **J**) dorsal views; **K**) UALVP 16247 in dorsal view; **L**) CMN 135 in dorsal view; **M**) TMP 2001.42.9 in dorsal view; ROM 784 (holotype of *Dyoplosaurus acutosquameus*) in **N**) posterior and **O**) dorsal views; **P**) UALVP 47273 in dorsal view; **Q**) ROM 7761 in dorsal view. Scale bar equals 10 cm. Photograph of MACN Pv 12554 taken by E. Snively, photograph of CMN 349 taken by M. Burns, used with permission. Photograph of AMNH 5216 courtesy of the American Museum of Natural History. **Abbreviations:** hs, haemal spine; maj os, major osteoderm of the tail club knob; min os, minor osteoderm of the tail club knob; ns, neural spine; ot, ossified tendon; prz, prezygapophysis.

3.3.2 Stratigraphic distribution of ankylosaurid specimens from Alberta and Montana

Ankylosaurid remains have been recovered from several localities in southern Alberta, including the badlands along the Red Deer River from Tolman Bridge to Drumheller, and from the older strata within Dinosaur Provincial Park, to the east near Hilda, and to the south near Manyberries and Onefour (Fig. 3.1, Appendix 3.1). Ankylosaurids are represented primarily by isolated teeth in the Milk River (Baszio 1997, Larson 2010), Foremost, and Oldman formations, and by more complete material in the Dinosaur Park, Horseshoe Canyon, and Scollard formations (Ryan and Russell 2001).

The exact locality for the holotype of *Euoplocephalus tutus* (CMN 0210) is unknown. Field notes by L. Lambe (18 August 1897; CMN) state that it was collected from the east side of the Red Deer River near the mouth of Berry Creek, a region of Dinosaur Provincial Park that is today referred to as the Steveville area. The holotype of *Dyoplosaurus acutosquameus* (ROM 784) was found within a region of Dinosaur Provincial Park known today as the core area, and the location of the quarry is figured in Arbour et al. (2009: Fig. 2). Good locality data are known for CMN 8530, the holotype of *Anodontosaurus lambei*, which was collected from the Horseshoe Canyon Formation along the Red Deer River, southwest of the town of Morrin.

There is uncertainty regarding the location of the quarry for NHMUK R5161, the holotype of *Scolosaurus cutleri*. Nopcsa (1928) gave the location for NHMUK R5161 as one half mile below Happy Jack ferry on the Red Deer River, about halfway up a 400-foot-deep canyon; this information was passed on to Nopcsa from F. A. Bather (NHMUK), who had received this information from W. Parks (ROM), who in turn had received this information from L. Sternberg. W. E. Cutler, who had originally discovered NHMUK R5161, was badly injured during its excavation (Tanke 2010), and so either one or several members of the Sternberg family finished the excavation. The quarry location was marked on the Steveville

topographic map (Sternberg 1950), but frequent attempts to find the quarry between 1967 and 2007 failed to find a quarry stake. When this locality was visited in 2007, the quarry stake was found downstream and down-section from where it had been marked on the map. Furthermore, it was posted at an angle at the top of a vertical wall, which makes it unlikely that this represents the quarry for NHMUK R5161 (Tanke pers. comm. 2013). GPS coordinates for this quarry stake provided by Currie and Russell (2005) were taken from the map position. No photographs of the quarry are known in either museum collections or archives. However, a potential quarry has been located a short distance away from where the original quarry stake was found in 2007, and the skyline matches that in a poor photograph of the quarry that was published in a magazine (Tanke pers. comm. 2013). Unfortunately, no definitive evidence such as newspaper scraps with dates, used to identify 'lost' quarries (Tanke 2005), or ankylosaurid elements, have been recovered, and there is some ambiguity regarding whether or not this quarry lies within the lowest Dinosaur Park Formation or the Oldman Formation (Tanke pers. comm. 2013). Additional fieldwork and research is required to verify the geographic and stratigraphic position of NHMUK R5161. The stratigraphic position for NHMUK R5161 reported in this paper is from Currie and Russell (2005), but it should be noted that this specimen may instead have come from the Oldman Formation.

In the Dinosaur Park Formation, nearly all ankylosaurid specimens that include more than a single isolated element (such as a tooth, isolated caudal vertebra, or osteoderm) have been recovered from within the lowest 30 meters of the formation (Fig. 3.22A). This is consistent with previous findings (Brinkman et al. 1998) that the proportion of ankylosaur teeth in microsite samples decreases in the upper part of the Dinosaur Park Formation. Exceptions to this are ROM 1930 (a skull with partial postcrania), and TMP 1997.132.01 (a skull with partial postcranium). TMP 1997.132.1 was not collected from Dinosaur Provincial Park, but from the area around Hilda, close to the Saskatchewan

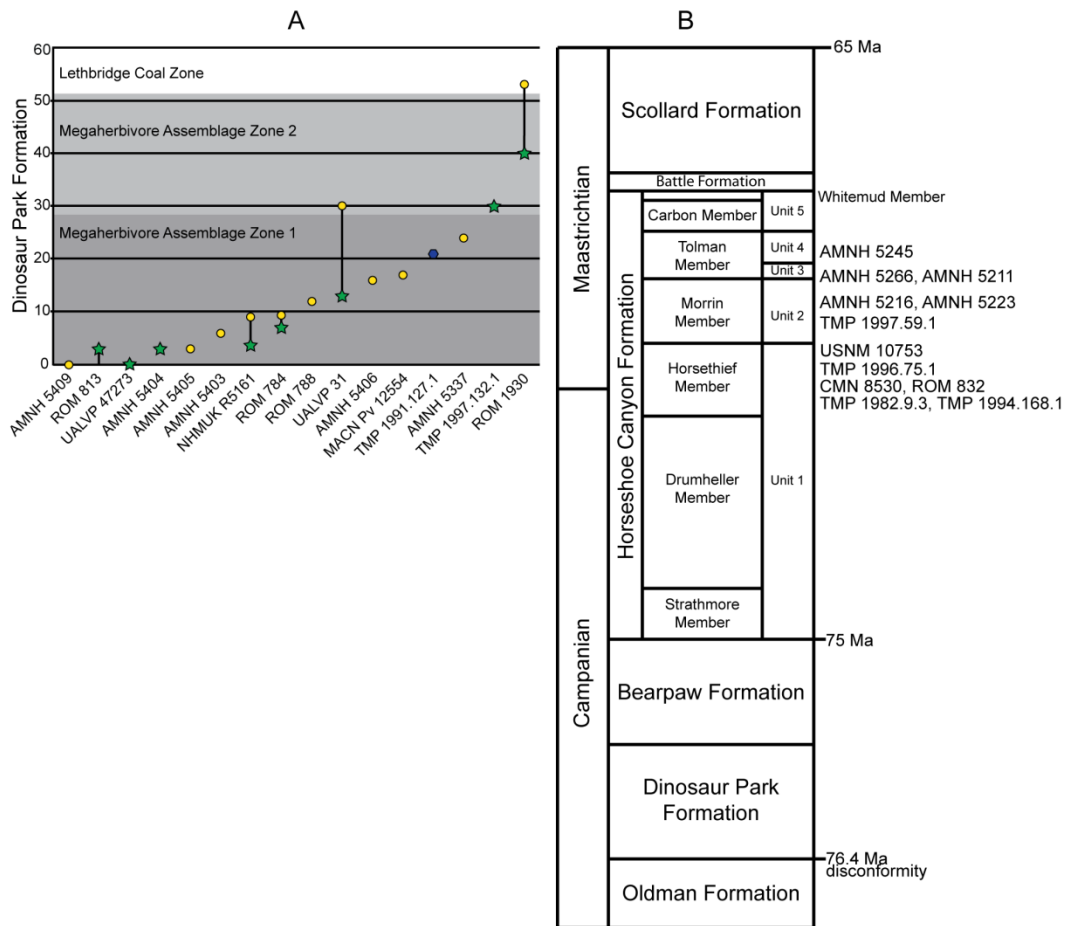


Figure 3.22. Stratigraphic distribution of ankylosaurid specimens in the Dinosaur Park and Horseshoe Canyon formations of Alberta. **A)** Distribution of ankylosaurid specimens within the Dinosaur Park Formation. Megaherbivore Assemblage Zones after Mallon et al. (2012). Specimens marked with green stars have GPS coordinates and accurate elevation data, specimens marked with yellow dots have elevations estimated from field notes, and the location of TMP 1991.127.1 (marked by a blue hexagon) was estimated from Alberta Township System coordinates. The elevation of some specimens with GPS coordinates was also estimated using field notes and Google Earth; the vertical lines associated with these illustrate the maximum elevation from using field note data only. Specimens marked by yellow dots, as such, could vary in elevation anywhere from three to seventeen meters. ROM 784 is the holotype of *Dyoplosaurus acutosquameus* and NHMLUK R5161 is the holotype of *Scolosaurus cutleri*. Although the exact locality and elevation for the holotype of *Euoplocephalus tutus* (CMN 0210) is unknown, AMNH 5406 and UALVP 31 can be confidently referred to that taxon. **B)** Stratigraphic column showing Upper Cretaceous formations in southern Alberta. Nomenclature for the Horseshoe Canyon Formation follows Eberth and Braman (2012). CMN 8530, the holotype of *Anodontosaurus lambei*, occurs in the Horsethief Member.

border. Within Dinosaur Provincial Park, numerous specimens are known from the western and central areas of the park, and fewer are known from the eastern end of the park and from the northern side of the Red Deer River.

Two specimens, CMN 8876 and TMP 2000.57.30, were collected between Manyberries and Onefour, near the Alberta-Montana border (Fig. 3.1). The Dinosaur Park Formation thins in this region, and the Oldman Formation is well exposed. The exact locality is unknown for CMN 8876, so it is not clear if this specimen derives from the Oldman or Dinosaur Park Formation.

Specimens from the Horseshoe Canyon Formation were collected from exposures along the Red Deer River between Tolman Bridge and the Royal Tyrrell Museum of Palaeontology in Drumheller, from Rosebud Creek, and from west of the Red Deer River at the Three Hills Creek Locality (Fig. 3.1). CMN 8530 and TMP 1994.168.1 were collected between Morrin and the Bleriot Ferry (Fig. 3.1). In their review of *Anchiceratops*, Mallon et al. (2011) noted that specimens collected in this region occur within a large sediment package that includes Coal Seams 8 and 9, in the upper part of Unit 1 of the Horseshoe Canyon Formation, now defined as the Horsethief Member (Eberth and Braman 2012). TMP 1982.9.3 was collected from Fox Coulee, between Coal Seams 7 and 8 (Eberth pers. comm.), placing this specimen within the Horsethief Member. AMNH 5266 and USNM 10753 were collected north of Morrin, and the original field notes do not include any distinctive lithostratigraphic or palaeontological features. However, these ankylosaur specimens occur south of *Anchiceratops* specimens that had good stratigraphic data constraining them to Unit 2 (Morrin Member *sensu* Eberth and Braman 2012) of the Horseshoe Canyon Formation (Mallon et al. 2011), and north of *Anchiceratops* and ankylosaur specimens that are likely in the upper part of Unit 1 (Horsethief Member *sensu* Eberth and Braman 2012). AMNH 5266 and USNM 10753 were thus probably collected in the Horsethief or Morrin members of the Horseshoe Canyon Formation. AMNH 5211, 5216, 5223, and 5245 were collected between 2.4 km (1.5 mi) upstream and 5.6 km (3.5 mi)

downstream of the Tolman Bridge (previously the Tolman Ferry). Unfortunately, the exact localities for these specimens are unknown, but the Morrin, Tolman and Carbon members (*sensu* Eberth and Braman 2012) of the Horseshoe Canyon Formation crop out in this region of the Red Deer River (Mallon et al. 2011). Two specimens were collected from localities other than those along the Red Deer River. TMP 1996.75.1 was collected from Three Hills Creek, from the Horsethief Member (Eberth pers. comm.), and TMP 1997.59.1 was collected from Rosebud Creek, from the Morrin Member (Eberth pers. comm.).

Only one species, *Ankylosaurus magniventris*, is found in the Scollard Formation in Alberta and no other ankylosaurids appear to have been contemporaneous with this taxon. At present, no definitive ankylosaurid fossils have been recovered from Judithian sediments in Alberta anywhere north of Dry Island Buffalo Jump Provincial Park, including the fossiliferous localities in the city of Edmonton, or around Grande Prairie in northwestern Alberta.

Trexler (2001) noted the presence of cf. *Euoplocephalus* at two localities (Landslide Butte and Two Medicine River) in the Two Medicine Formation and fragmentary ankylosaurid remains from the Choteau/Bynum locality. At all three localities, ankylosaurids were only recovered from the upper part of the Two Medicine Formation. MOR 433 was collected from approximately 55 m below the contact with the Bearpaw Shale (Penkalski, in press).

3.4 Discussion

3.4.1 Taxonomic implications of variation in specimens previously referred to *Euoplocephalus tutus*

3.4.1.1 Status of *Anodontosaurus lambei*

Variation within a population can result from ontogenetic differences, individual differences (both heritable and acquired), sexual dimorphism, and

pathologies (and, additionally for fossil organisms, from taphonomic changes). If *Euoplocephalus tutus* is monotypic, there should be no clusters of shared, distinctive morphological features, (unless there is sexual dimorphism) and there should be no stratigraphic separation of groupings of morphological features. A review of morphological variation in specimens previously referred to *Euoplocephalus tutus* shows that certain features previously considered to result from individual variation are associated with each other, and are stratigraphically separated. These features include the presence or absence of small circular caputegulae at the base of the squamosal and quadratojugal horns (postocular caputegulae, Fig. 3.12), the presence or absence of similar small circular osteoderms (interstitial osteoderms) around the primary osteoderms of the first cervical half ring (Fig. 3.20), the width:length ratio of the tail club knob, and the shape (semicircular vs. triangular) of the tail club knob osteoderms in dorsal view (Fig. 3.21).

Specimens previously referred to *Euoplocephalus tutus* that lack postocular caputegulae never have interstitial osteoderms on the first cervical half ring. Specimens referred to *Euoplocephalus tutus* that have postocular caputegulae may or may not have interstitial osteoderms on the first cervical half ring. This is a subtle difference and could be attributed to intraspecific variation; however, the presence or absence of small caputegulae near the squamosal and quadratojugal horns and on the cervical half rings correlates with the stratigraphic position of the specimen. All specimens from the Horseshoe Canyon Formation have small caputegulae at the bases of the squamosal and quadratojugal horns and interstitial osteoderms on the cervical half rings (these are visible even on highly fragmentary cervical half rings such as the one preserved with TMP 1982.9.3). Only two specimens from the Dinosaur Park Formation have these small caputegulae: AMNH 5238, from Dinosaur Provincial Park, and TMP 1997.132.1, from the area around Hilda, Alberta (near the Alberta-Saskatchewan border). TMP 1997.132.1 is from the upper 30 m of the

Dinosaur Park Formation, but the stratigraphic position of AMNH 5238 is unknown. No specimens from the lower 30 m of the Dinosaur Park Formation have small caputegulae at the bases of the squamosal and quadratojugal horns or secondary osteoderms on the cervical half rings. The stratigraphic separation of the presence or absence of these caputegulae and osteoderms suggests that specimens from the Horseshoe Canyon Formation are not the same species as those from the lower part of the Dinosaur Park Formation. TMP 2001.49.2, from the Two Medicine Formation of Montana, has postocular osteoderms on the skull, but does not have interstitial osteoderms on the first cervical half ring; an isolated half ring (USNM 7943) from the Two Medicine Formation also lacks interstitial osteoderms.

The size and shape of the tail club knob (Fig. 3.21) varies significantly among specimens referred to *Euoplocephalus tutus*, as reviewed by Coombs (1995a). However, tail club knobs that are wider than long (AMNH 5216, AMNH 5245; Figs. 3.21A, D) also tend to have major knob osteoderms that are triangular (“bluntly pointed” *sensu* Coombs 1995a) in dorsal view. Tail club knobs that are longer than wide (UALVP 47273; Fig. 3.21P) or approximately as wide as long (TMP 1983.36.120, TMP 2001.49.2; Figs. 3.21J, M) have major knob osteoderms that are semicircular in dorsal view. Again, these differences are stratigraphically separated, with wide, pointed tail club knobs found in the Horseshoe Canyon Formation, and round or elongate, semicircular tail club knobs found in the Dinosaur Park and Two Medicine formations. Differences in proportions are not entirely related to absolute size, as both ROM 788 (from the Dinosaur Park Formation) and AMNH 5245 (from the Horseshoe Canyon Formation) are almost the same width, but AMNH 5245 is not as long as ROM 788. Unfortunately, no tail club knobs from the Horseshoe Canyon Formation are associated with cranial material. Only a few tail club knobs from the Dinosaur Park Formation have associated cranial material: AMNH 5403, AMNH 5405, and the holotype of *Dyoplosaurus acutosquameus*, ROM 784.

The morphology of osteoderms, and their distribution on the body, is known to vary in several extant animals. The number of moveable thoracic carapace segments in several species of armadillos can vary by one to three bands; in the nine-banded armadillo (*Dasybus novemcinctus*), variation in number of segments is associated with geographic occurrence (Nowak 1999). The number of osteoderms in the cervical region of crocodylians differs between species, but also varies among individuals of each species (Ross and Mayer 1983). Ornamentation on the osteoderms of the broad-headed skink *Eumeces laticeps* increases with an increase in body size (Oliver 1951). Given the documented variation in extant taxa, caution should be used when identifying potential taxonomically useful features in the osteoderms and cranial ornamentation of ankylosaurs. Some caputegulae positions and shapes are consistent in all known skulls previously referred to *Euoplocephalus*: all skulls have rugose, arched supranarial caputegulae, all have a roughly hexagonal median nasal plate that is larger than all of the other frontonasal caputegulae, and all have rectangular lacrimal and loreal caputegulae. Variation in cranial ornamentation also exists within specimens previously referred to *Euoplocephalus*, most notably in the number, shapes, and sizes of the caputegulae of the frontals, parietals, and nasals. However, discontinuous, stratigraphically-separated variation in the presence or absence of postocular caputegulae, the presence or absence of interstitial osteoderms on the first cervical half ring, and tail club knob osteoderm shape, is more likely the result of taxonomic variation rather than intraspecific or ontogenetic variation in *Euoplocephalus*.

The stratigraphic separation of unique sets of morphological features in specimens referred to *Euoplocephalus tutus* indicates that more than one species is currently represented by material referred to *Euoplocephalus tutus*. Although the exact type locality for *Euoplocephalus tutus* (CMN 210) is unknown, the localities for AMNH 5406 and UALVP 31 (which can be confidently referred to

Euoplocephalus tutus based on cervical half ring morphology) are known, and both are from the lower Dinosaur Park Formation. The skull of UALVP 31 does not have postocular caputegulae (Fig. 3.12), and the cervical half rings of AMNH 5406, CMN 0210, and UALVP 31 do not have interstitial osteoderms (Fig. 3.20). As such, the Horseshoe Canyon Formation morphotype, which has these caputegulae and osteoderms, should not be referred to *Euoplocephalus tutus*. The holotype of *Anodontosaurus lambei* (CMN 8530) was collected from section 3, township 21, range 31, W 4th Meridian, placing this specimen within the Horseshoe Canyon Formation. CMN 8530 has postocular caputegulae at the base of the squamosal and quadratojugal horns (Fig. 3.12) and interstitial osteoderms on the first cervical half ring (Fig. 3.20). The presence of these caputegulae and osteoderms on the skull and cervical half ring suggest that *Anodontosaurus lambei* is distinct from *Euoplocephalus tutus*, and specimens from the Horseshoe Canyon Formation should be referred to *Anodontosaurus lambei* rather than *Euoplocephalus tutus*. It could be argued that these differences are insufficient for resurrecting the genus *Anodontosaurus*, and instead the Horseshoe Canyon Formation specimens should be referred to as a second species of *Euoplocephalus*, *E. lambei*. Given that the phylogenetic resolution of derived ankylosaurids is poor at present (Parsons and Parsons 2009, Thompson et al. 2012, this paper), it is here considered best to simply resurrect *Anodontosaurus lambei* rather than create additional taxonomic confusion by creating a new combination.

Although no tail club knobs are associated with diagnostic cranial material, the consistent morphology of tail club knobs from the Horseshoe Canyon Formation suggests that a single taxon is represented, and so it is best to refer them to *Anodontosaurus lambei* as well. As such, *Anodontosaurus lambei* also differs from *Euoplocephalus tutus* in the morphology of the tail club knob. In *Anodontosaurus lambei*, the tail club knob is wider than long, and the major knob osteoderms are bluntly pointed and triangular in dorsal view (Fig. 3.21).

Another potential difference between *Anodontosaurus lambei* and specimens referred to *Euoplocephalus tutus* is the shape of the free caudal vertebrae. CMN 8530 includes a free caudal vertebra that differs from ankylosaurid free caudal vertebrae from the Dinosaur Park Formation, as the centrum has octagonal anterior and posterior faces, rather than circular (Fig. 3.16K). The only other specimen from the Horseshoe Canyon Formation that preserves free caudal vertebrae is AMNH 5245, and in this specimen the vertebrae are pathological and their original shapes are obscured. It is therefore not possible to determine if the centrum shape in CMN 8530 represents a taxonomic difference or individual variation, although it should be noted that centrum shape does not appear to vary among specimens from the Dinosaur Park Formation.

Although the sample size is small, femoral morphology appears to differ between specimens from the Horseshoe Canyon Formation and Dinosaur Park Formation (Fig. 3.19). In the femora of AMNH 5266 and TMP 1982.9.3 from the Horseshoe Canyon Formation (Figs. 3.19C, D), the lateral epicondyles are more prominent than that of AMNH 5404, from the Dinosaur Park Formation (Fig. 3.19K). This does not appear to be size-related, as the lateral epicondyle is proportionately larger in AMNH 5266 even though this femur is less than half the length of AMNH 5404.

Within the Dinosaur Park Formation, most specimens that include more than just teeth or isolated osteoderms have been collected from the lowest 30 m of the formation. Two notable exceptions to this are ROM 1930 and TMP 1997.132.1, which were collected from the upper 30 m of the formation. TMP 1997.132.1 has postocular caputegulae, but ROM 1930 does not (Fig. 3.12), and, TMP 1997.132.1 has interstitial osteoderms on the first cervical half ring (Fig. 3.200). Based on the presence of these osteoderms, TMP 1997.132.1 is referred to *Anodontosaurus lambei*, which extends the stratigraphic range of this species into the upper Dinosaur Park Formation. This makes TMP 1997.132.01 by far the

most complete specimen of *Anodontosaurus lambei*, as this specimen includes a complete skull, right mandible, three dorsal vertebrae, ribs, ?scapula, left humerus, ulna, radius, and tibia.

AMNH 5266, a partial juvenile skeleton, was referred to *Euoplocephalus tutus* by Coombs (1986); because Coombs had previously synonymized *Anodontosaurus lambei* with *Euoplocephalus tutus*, his comparison focused on differences between *Ankylosaurus magniventris* and *Euoplocephalus tutus* only. This specimen derives from either the Morrin or Tolman member of the Horseshoe Canyon Formation, and thus is most likely referable to *Anodontosaurus lambei*. AMNH 5266 lacks a skull, first cervical half ring, and tail club, and so it preserves no diagnostic features of *Anodontosaurus lambei*. However, the femur has a prominent lateral epicondyle, similar to that of TMP 1982.9.3 but different from that of AMNH 5404 (Fig. 3.19). Because this feature is subtle and the sample size is limited, the relative prominence of the lateral epicondyle is not here considered a diagnostic feature. However, the similarity of the femora of AMNH 5266 and TMP 1982.9.3 suggests that AMNH 5266 can be referred to *Anodontosaurus*.

3.4.1.2 Status of *Scolosaurus cutleri*

With the recognition of *Dyoplosaurus acutosquameus* (Arbour et al. 2009), and now *Anodontosaurus lambei* as species distinct from *Euoplocephalus tutus*, only *Scolosaurus cutleri* remains from the list of taxa synonymized by Coombs (1978a). Penkalski and Blows (2013) have argued for the separation of *Scolosaurus* from *Dyoplosaurus* and *Euoplocephalus* based on several morphological features. The holotype of *Scolosaurus cutleri* (NHMUK R5161) is one of the most complete ankylosaurs ever collected, preserving nearly the entire skeleton as well as *in situ* osteoderms and skin impressions. However, it is challenging to compare this specimen with other specimens for several reasons. First, it lacks a skull and tail club, which contain important taxonomic

information. Second, although the *in situ* osteoderms and skin impressions provide important information on the integument of ankylosaurs, they also obscure certain skeletal elements such as the scapula and pelvis. Third, the specimen is currently on display tipped onto its right side, in a relatively dark area, in a glass cabinet that cannot be easily opened, which makes detailed examination of the specimen difficult, especially the anterior and left side of the animal. Nevertheless, it is possible to assess the taxonomic status of NHMUK R5161 as it preserves the first cervical half ring, and thus can be compared to both *Anodontosaurus lambei* and *Euoplocephalus tutus*.

The first cervical half ring of NHMUK R5161 (Fig. 3.20P) lacks interstitial osteoderms ringing the larger primary osteoderms, which indicates that NHMUK R5161 is not referable to *Anodontosaurus lambei*. Although these may appear to be present on the second cervical half ring, these are epidermal scales and not osteoderms (see Penkalski and Blows 2013). NHMUK R5161 differs subtly from *Euoplocephalus tutus* (AMNH 5406, CMN 0210, and UALVP 31) in the shape of the first cervical ring osteoderms, as it has low medial osteoderms, each of which lacks a distinct keel but has a low, somewhat posteriorly placed prominence (Fig. 3.20P). The lateral osteoderms appear to have a prominent, laterally-directed keel. In contrast, AMNH 5406, CMN 0210, and UALVP 31 have tall medial osteoderms with prominent keels (Fig. 3.20A, B, F, G). Some referred *Euoplocephalus tutus* first cervical half rings (AMNH 5337, AMNH 5404) also have low medial osteoderms (Fig. 3.20J-L), but in these specimens the medial osteoderms still have a keel, and the lateral osteoderms are also low, which differs from the condition in NHMUK R5161 where the lateral osteoderms are tall.

Penkalski and Blows (2013) also note differences in shape between the medial osteoderms of NHMUK R5161 and other referred *Euoplocephalus* specimens. They point out that the anteroposterior length of the cervical half ring band was larger in NHMUK R5161 than in *Euoplocephalus* specimens AMNH

5406 and UALVP 31. However, the humerus of NHMUK R5161 is also larger than those of AMNH 5406 and UALVP 31, and so the greater anteroposterior band length in NHMUK R5161 may simply be a result of NHMUK R5161 being a larger individual than either AMNH 5406 or UALVP 31.

The first cervical half ring in NHMUK R5161 is not as well preserved as that of the second half ring, which at first seems to differ greatly from second cervical half rings referred to *Euoplocephalus tutus* (AMNH 5403, TMP 2007.12.52). No other second cervical half rings referred to *Euoplocephalus tutus* preserve the superficial primary osteoderms (Fig. 3.20U, V), but these are present on NHMUK R5161 (Fig. 3.20P). However, it appears that the cervical half ring osteoderms do not always fuse to the band; matrix separates the osteoderms from the band in the first cervical half ring of UALVP 31 (Fig. 3.20G). As such, the presence or absence of osteoderms on the second cervical half ring is not taxonomically informative. The morphology of the osteoderms on the second cervical half ring in NHMUK R5161 can, however, be used to corroborate the morphology of the more poorly preserved first cervical half ring. In the ankylosaurids *Pinacosaurus mephistocephalus* (Godefroit et al. 1999), *Saichania chulsanensis* (MPC 100/151), and *Shamosaurus scutatus* Tumanova, 1983 (PIN 3779/2), the first and second cervical half rings are nearly identical except in terms of overall size. In the second cervical half ring of NHMUK R5161, the medial osteoderms are nearly flat with low posterior prominences and circular bases, and the lateral osteoderms are tall and sharply keeled, a morphology unknown in any other referred *Euoplocephalus tutus* half ring from Alberta. The morphology of the cervical half rings in NHMUK R5161 supports the interpretation by Penkalski and Blows (2013) of *Scolosaurus cutleri* as a species distinct from *Euoplocephalus tutus*, and also separates it from *Anodontosaurus lambei*. As discussed for *Anodontosaurus lambei*, it is preferred to maintain separation at the generic level rather than creating the new combination *E. cutleri*.

Scolosaurus cutleri can also be differentiated from *Dyoplosaurus acutosquameus* by the orientation of the anterior sacral ribs, which are anteroventrally directed in *Dyoplosaurus* but laterally directed in *Scolosaurus*. NHMUK R5161 also has a proportionally longer postacetabular process of the ilium. *Scolosaurus cutleri* may also have incorporated more caudals into the sacrum (but not necessarily sacral rod – caudosacrals may not fuse at the centra, but their transverse processes fuse to the ilium) compared to *Anodontosaurus lambei*, *Dyoplosaurus acutosquameus*, and specimens referred to *Euoplocephalus tutus*. NHMUK R5161 has three caudosacrals, whereas *Dyoplosaurus* ROM 784 preserves two, and AMNH5337 and AMNH5409 each preserve one (the sacra for AMNH 5245 and TMP 1982.9.3 are incomplete). However, it is unclear if the number of caudosacrals is associated with absolute size or ontogeny. The pelves of AMNH 5409 and NHMUK R5161 are nearly the same length (length of ilium in NHMUK R5161 = 96 cm, from Nopcsa (1928); length along midline of pelvis in AMNH 5409 = 92 cm). ROM 1930 may have had three caudosacrals, but these are not preserved in association with a complete pelvis, so it is not possible to determine for certain if these vertebrae were fused to the ilia. It is possible that fewer sacral vertebrae are present in specimens other than NHMUK R5161 because of post-depositional damage, although this seems unlikely for ROM 784 (*Dyoplosaurus acutosquameus*), which has a complete, articulated caudal series. At present, the number of dorsosacral, sacral, and caudosacral vertebrae cannot be used to support taxonomic distinctions among Albertan and Montanan ankylosaurids.

Penkalski and Blows (2013) observed differences in the humeri and radii of AMNH 5406 and NHMUK R5161: AMNH 5406 is smaller, the deltopectoral crest does not extend as far down the shaft as that in NHMUK R5161, and the radial condyle extends farther distally than in other specimens (although these other specimens are not specified in Penkalski and Blows (2013)). The deltopectoral crest of AMNH 5406 (Fig. 3.18A) does not extend as far down the

shaft as in AMNH 5337, a larger specimen, but seems to extend proportionately as far in ROM 47655 (Fig. 3.18K), the largest humerus encountered in this study. The radial condyle does extend somewhat further distally compared to AMNH 5404 (Fig. 3.18I), but is again similar to ROM 47655. It should be stressed that variations in the extent of the deltopectoral crest and radial condyle are both subtle, and size should not be used as a diagnostic character in the absence of ontogenetic data. For this reason, there is no reason to consider the morphology of the humerus in NHMUK R5161 significantly different than that of other referred *Euoplocephalus* specimens. As such, humeral morphology is not diagnostic for *Scolosaurus*. Penkalski and Blows (2013) considered the radius of NHMUK R5161 to be more sigmoidal than those of any other referred *Euoplocephalus* specimens, or than that in *Dyoplosaurus*. The radius as figured by Nopcsa (1928: plate VI) does have a weakly sigmoidal appearance that differs from the radii of AMNH 5337 (Fig. 3.18L) and AMNH 5406 (Fig. 3.18M), and so this may be a diagnostic character of NHMUK R5161.

NHMUK R5161 differs from ROM 784 (*Dyoplosaurus*) in the morphology of the pedal unguals, which are U-shaped in ventral view in NHMUK R5161 and triangular in ROM 784. *Scolosaurus* may also differ from *Dyoplosaurus* in the morphology and pattern of post-cervical osteoderms (Penkalski and Blows 2013). ROM 784 has triangular osteoderms on the lateral sides of the posterior region of the pelvis and anterior part of the tail, which are not present in NHMUK R5161. Although the integument is fairly complete dorsally in NHMUK R5161, osteoderms are not preserved lateral to the caudal vertebrae, and so it is possible that compressed, triangular osteoderms were present in NHMUK R5161 but not preserved.

3.4.1.3 Status of *Oohkotokia horneri*

Penkalski (in press) identified several diagnostic features that separated ankylosaurids from the Two Medicine Formation from *Dyoplosaurus*,

Euoplocephalus (including *Anodontosaurus*), and *Scolosaurus*: a proportionately small median nasal caputegulum not distinguished from surrounding caputegulae; keeled, trihedral squamosal horns with posteriorly-situated apices; quadratojugal horns with strong posterior curvature; nuchal crest not visible in lateral view; small occipital condyle; large orbit; basally excavated osteoderms with weakly ornamented surface texture; and steeply-pitched triangular caudal osteoderms.

Penkalski (in press) emphasized the small median nasal caputegulum of specimens from the Two Medicine Formation as an important difference between *Oohkotokia* and *Euoplocephalus*. In all specimens referred to *Oohkotokia*, the anterior portion of the rostrum is broken, and so the median nasal caputegulum is either absent or only partially preserved. Although FPDM V-31, NSM PV 20381, and TMP 2001.42.19 appear to have complete skulls, the anterior portion of the rostrum in each of these specimens is reconstructed. The morphology of the median nasal plate does not provide strong evidence for the separation of the Two Medicine Formation specimens from *Euoplocephalus*. However, the distinctive morphology of the squamosal horns of the Two Medicine Formation ankylosaurids noted by Penkalski (in press) differentiates the Two Medicine ankylosaurid from *Euoplocephalus*, and from *Anodontosaurus*. Skulls from the Two Medicine Formation share one feature that is not present in any other specimen referred to *Euoplocephalus* – a long, pointed, back-swept squamosal horn (Fig. 3.12M-P). As such, all of the skulls from this formation likely represent a single taxon. Although the squamosal horns of AMNH 5405, TMP 1991.127.1, and UALVP 31 are pointed (Fig. 3.12A-C), they are never as long as those in specimens from the Two Medicine Formation. No specimens from Alberta have the characteristic back-swept appearance in lateral view that is present in specimens from Montana. The Two Medicine ankylosaurid can be differentiated from *Dyoplosaurus* based on the morphology of the pedal unguals (U-shaped in dorsal view in TMP 2001.42.9, triangular in ROM 784).

Penkalski (in press) noted two main differences between MOR 433 and NHMUK R5161 (*Scolosaurus*). First, the transverse processes were proportionately longer relative to centrum width in MOR 433 compared to NHMUK R5161. Furthermore, NHMUK R5161 does not preserve any low-keeled oval osteoderms or steeply pitched triangular osteoderms, two morphologies that were found associated with the holotype skull of MOR 433 (see Penkalski (in press): Fig. 4D and F). In MPC 100/1305, a Mongolian ankylosaurid that preserves numerous *in situ* osteoderms, low-keeled oval osteoderms with off-centre keels are found only on the lateral sides of the trunk, and steeply pitched triangular osteoderms are found only on the lateral sides of the pelvis and tail. Low-keeled osteoderms are found only on the lateral sides of the pelvis and tail. Low-keeled osteoderms are found on the dorsal side of the trunk and tail (see Carpenter et al. 2011). Although NHMUK R5161 preserves most of the dorsal integument, it does not preserve osteoderms on the flanks or lateral sides of the tail, and so it is conceivable that the absence of the unique MOR 433 osteoderm morphologies in NHMUK R5161 is a preservational artifact. The length of the transverse processes relative to the width of the centrum varies along the caudal vertebral column in ankylosaurids, with transverse processes decreasing in size posteriorly. In order to demonstrate that the relatively longer transverse process in MOR 433 is a taxonomic difference and not a positional difference, the position of this caudal vertebra would need to be known so it could be compared to the equivalent position in NHMUK R5161.

Neither osteoderm morphology nor vertebral proportions provide compelling evidence to separate *Oohkotokia* from *Scolosaurus*. However, *Oohkotokia* and *Scolosaurus* share a cervical half ring morphology that differs markedly from those of *Anodontosaurus* and *Euoplocephalus*. TMP 2001.42.19, from the Two Medicine Formation of Montana, includes a partial first cervical half ring (Fig. 3.20Q, R) that is similar to the cervical half rings of NHMUK R5161 (Fig. 3.20P), and an isolated half ring from the Two Medicine Formation, USNM 7943 (Fig. 3.20S, T), shares this morphology. In both of the Two Medicine

specimens and *Scolosaurus*, the medial osteoderms are nearly flat and each has a low central prominence and a circular base. In contrast, the first cervical half rings of AMNH 5406, CMN 0210, UALVP 31, and all other referred *Euoplocephalus* half rings have medial osteoderms with longitudinal keels, even those in which the medial osteoderms are relatively low (e.g. AMNH 5404). (Gilmore 1917 also remarked on the differences in osteoderm morphology between USNM 7943 and the holotype of *E. tutus*, CMN 0210.) The first cervical half ring of *Anodontosaurus* has small interstitial osteoderms that are not present in any Two Medicine specimens. There are no features that differ significantly between the Two Medicine Formation specimens and *Scolosaurus*, and for this reason the Two Medicine ankylosaur is best referred to *Scolosaurus*.

TMP 2001.42.19 includes both a skull and tail club, which are both absent in the holotype of *Scolosaurus*. TMP 2001.42.19 provides insight into the growth of the tail club knob and variation of ankylosaurid knobs. The maximum width across the supraorbitals in TMP 2001.42.19 is 26 cm, and the maximum width of the knob is 31 cm. In contrast, the preserved portion of the skull of ROM 784 (*Dyoplosaurus*) has a maximum width across the supraorbitals of 33 cm, and the tail club knob maximum width is 16.6 cm. TMP 2001.42.1 is a smaller individual than ROM 784 yet has a larger tail club knob (Fig. 3.21M, O); the ratio of knob width to length also differs between the two specimens (1.07 in TMP 2001.42.1 vs. 0.68 in ROM 784). This suggests that the small knob and low width:length ratio of *Dyoplosaurus* may not be entirely due to ontogeny, as a larger knob is known in a smaller individual of *Scolosaurus*. An alternate explanation is that the timing of knob osteoderm growth occurred later in *Dyoplosaurus* relative to *Scolosaurus*. However, even if the knobs of both taxa eventually grew to equivalent sizes, the difference in the timing of growth is an interesting taxonomic difference.

3.4.1.4 Status of other specimens previously referred to *Euoplocephalus tutus*

Although numerous well-preserved skulls have been referred to *Euoplocephalus tutus*, none of the holotypes of the Dinosaur Park Formation ankylosaurids (*Euoplocephalus tutus*, *Dyoplosaurus acutosquameus*, and *Scolosaurus cutleri*) include good cranial material. This makes the referral of skulls to any given species difficult, and means that postcranial elements must be used to identify specimens to species level. However, non-overlapping postcranial material among the holotype specimens also makes this challenging. Each of the holotypes of *Anodontosaurus lambei*, *Euoplocephalus tutus* and *Scolosaurus cutleri* includes a first cervical half ring, but none is preserved in *Dyoplosaurus acutosquameus*. *Dyoplosaurus acutosquameus* and *Scolosaurus cutleri* both include pelvic and anterior caudal regions, but *Scolosaurus cutleri* does not preserve the tail club; the holotype of *Euoplocephalus tutus* preserves no postcrania other than the first cervical half ring. AMNH 5406 and UALVP 31 can be referred to *Euoplocephalus tutus* based on cervical half ring morphology, and UALVP 31 includes a good skull. The skull of TMP 1991.127.1 is nearly identical to that of UALVP 31 and so can also be confidently referred to *Euoplocephalus*; each skull even has a distinct shallow furrow on the posterior supraorbital (Fig. 3.10, 3.11).

The morphology of the pelvis can be used to differentiate *Dyoplosaurus acutosquameus* and *Scolosaurus cutleri*, and potentially *Euoplocephalus tutus* as well. The pelves of AMNH 5337 and AMNH 5409 differ from the pelvis of *Dyoplosaurus acutosquameus* in the orientation of the sacral transverse processes, which are anteroventrally directed in *Dyoplosaurus* but laterally directed in AMNH 5337 and AMNH 5409. AMNH 5337 and AMNH 5409 differ from NHMUK R5161 (*Scolosaurus*) in the relative length of the postacetabular process of the ilium. AMNH 5337 includes a skull that is generally similar to that of UALVP 31, but does have some notable differences. In particular, the squamosal horns of AMNH 5337 are much shorter and more rounded, and the

cranial caputegulae are less distinct, compared to those of UALVP 31 (Figs. 3.10, 3.11). Coombs (1978a) noted that smaller skulls had more prominent and pointed squamosal and quadratojugal horns compared to larger skulls. Penkalski (2001), in a morphometric analysis of referred *Euoplocephalus tutus* skulls, found that squamosal horn height decreased with increasing skull size. He also reported a positive correlation between skull size and rugosity of osteoderm sculpturing. If squamosal horn length and bluntness, and cranial caputegulum distinctness, are related to size, then they are probably a result of ontogenetic changes. Horner and Goodwin (2009), in a discussion of ontogeny in the pachycephalosaurids *Dracorex*, *Stygimoloch*, and *Pachycephalosaurus*, suggested that the pyramidal nodes on the nasals and the squamosal horns of these taxa decreased in size and became more rounded through ontogeny. Scannella and Horner (2010) also suggested that the epoccipitals of *Triceratops* become lower, and less distinct from the frill throughout ontogeny. It is possible that cranial ornamentation in *Euoplocephalus tutus* followed a similar trajectory as that observed for *Pachycephalosaurus* and *Triceratops*, with the squamosal horns being resorbed and the cranial sculpturing becoming less distinct. UALVP 31 appears to have resorption pits on the squamosal horns, which would support this hypothesis (Fig 3.10B). Penkalski and Blows (2013) state that none of the referred *Euoplocephalus* specimens, except for AMNH 5266 (herein considered *Anodontosaurus*) represented young juveniles. The ontogenetic stage of a dinosaur is best assessed using histological sections, and no studies have been published on histological sections of ankylosaur long bones for the purpose of determining ontogenetic stage. As such, it is not currently possible to confidently determine the relative ontogenetic stages of ankylosaurs, let alone specimens previously referred to *Euoplocephalus*. Histological sampling and analysis is required in order to test the hypothesis that changes in cranial ornamentation in *Euoplocephalus* are related to ontogeny.

Many of the diagnostic features of *Euoplocephalus tutus* proposed by Coombs (1978a) and Vickaryous and Russell (2003) have broader distributions among *Anodontosaurus*, *Dyoplosaurus*, and *Scolosaurus*. Ciliary osteoderms are also preserved in the holotype of *Dyoplosaurus* (Fig. 3.13G) and a shallow nasal vestibule, intranarial septum formed by a vertical process of the premaxilla, and medially convergent but anteriorly and posteriorly divergent maxillary tooth rows occur in *Anodontosaurus* and *Scolosaurus*. Premaxillae that are not covered by expanded nasals and that are equal or wider than the width between the most posterior maxillary teeth, slit-like nostrils, and a palate that does not taper anteriorly occur in both *Anodontosaurus* and *Scolosaurus* as well.

If the differences between the skulls of AMNH 5337 and UALVP 31 are not taxonomically significant, and because the pelvis of AMNH 5337 differs from those of *Dyoplosaurus acutosquameus* and *Scolosaurus cutleri* (but is consistent with what is preserved in UALVP 31), then AMNH 5337 is probably referable to *Euoplocephalus tutus*. In turn, the cervical half ring morphology of AMNH 5337 is similar to those of AMNH 5403, AMNH 5404, and AMNH 5405, all of which include skulls. Postcranially, AMNH 5337 and AMNH 5404 are large, robust individuals, whereas AMNH 5406, CMN 210, and UALVP 31 are relatively small, gracile individuals. Compared to other specimens, AMNH 5337 and AMNH 5404 have relatively larger deltopectoral and lateral supracondylar crests of the humeri and have muscle scars that are more prominent (Fig. 3.18D, E, I, J). The first cervical half rings of AMNH 5337, AMNH 5403, AMNH 5404, and AMNH 5405 are anteroposteriorly longer than those of AMNH 5406, CMN 0210, and UALVP 31 (Fig. 3.20). Penkalski (2001) suggested that the cervical half ring of AMNH 5406 was similar in size to other referred *Euoplocephalus tutus* specimens, which is true in terms of the mediolateral width, but not in terms of anteroposterior length.

Larger first cervical half rings are also found in specimens with lower, more rugose, and less distinct primary osteoderms (AMNH 5337, AMNH 5403,

AMNH 5404; Fig. 3.20J-L) compared to specimens with anteroposteriorly shorter cervical half rings (AMNH 5406, CMN 210, UALVP 31; Fig. 3.20A-H). As in the skulls, perhaps the cervical half ring osteoderms fused with the band but were resorbed during ontogeny. UALVP 31 has resorption pits on the apices of the medial osteoderms on the first cervical half ring (Fig. 3.20H). Larger cervical half rings with more rugose primary osteoderms that are completely fused to the cervical rings may belong to ontogenetically older individuals. Alternately, more robust individuals referred to *Euoplocephalus tutus* represent a distinct species; however, this seems unlikely given the continuum of morphologies observed in the referred specimens.

AMNH 5403 and AMNH 5405 include tail clubs with the round, semicircular morphology (e.g. Fig. 3.21H, J-L) that is distinct from the tail club knobs of *Anodontosaurus lambei* (AMNH 5245; Fig. 3.21A), and *Dyoplosaurus acutosquameus* (ROM 784, UALVP 47273; Fig. 3.21O, P); *Anodontosaurus* knobs are wider than long and have triangular major osteoderms, and *Dyoplosaurus* knobs are longer than wide. The tail club of TMP 2001.42.9 (Fig. 3.21M), here referred to *Scolosaurus cutleri*, has a similar round shape to those of AMNH 5403 and AMNH 5405. Because *Euoplocephalus* and *Scolosaurus* appear to overlap stratigraphically, and because their tail club morphology is similar, isolated round tail club knobs from the Dinosaur Park Formation can no longer be referred to *Euoplocephalus tutus*.

Penkalski (2001) suggested that ROM 1930 may be referable to *Scolosaurus cutleri*, although he did not formally resurrect that species. In particular, he indicated that radially ribbed, perforate, conical osteoderms only occur in ROM 1930 and NHMUK R5161 (Penkalski 2001:270). Later in the same paper, he stated that AMNH 5337 has perforate osteoderms (Penkalski 2001:287) and that most referred *Euoplocephalus tutus* osteoderms have some degree of ribbing or fluting (Penkalski 2001:289). Penkalski and Blows (2013) suggest that ROM 1930 might be referable to *Scolosaurus* (although do not list it as a

referred specimen), citing the lack of low-keeled osteoderms found in other *Euoplocephalus* specimens like AMNH 5406, and the presence of conical osteoderms similar to those in NHMUK R5161. ROM 1930 includes a skull (Figs. 3.10-3.12), three dorsal vertebrae, partial sacrum (Fig. 3.16A, B), caudal vertebrae (Fig. 3.16M), fragmentary right scapula, right humerus (Fig. 3.18C), and osteoderms (including *in situ* osteoderms on two blocks of articulated free caudal vertebrae). Field notes by G. F. Sternberg (1914; CMN) indicate that cervical half rings may also have been collected, but these are not yet prepared. The skull lacks postocular osteoderms and the squamosal horns do not have the long, backswept morphology of those from the Two Medicine Formation. If the referral of the Two Medicine ankylosaurid material to *Scolosaurus* is correct, then ROM 1930 is not referable to *Scolosaurus*.

ROM 813 is a remarkable but problematic specimen that preserves keratinous scale impressions as well as the underlying (deep) ossicles and osteoderms (Arbour et al. 2013). This specimen was referred to *Euoplocephalus tutus* by Penkalski (2001). However, there are few features that allow it to be confidently assigned to Ankylosauridae, let alone to a particular genus or species. The straight shaft of the broken ischium, and the rugose, thin-walled osteoderms suggest that ROM 813 is an ankylosaurid rather than a nodosaurid. ROM 813 has rectangular, keeled osteoderms, unlike those present in NHMUK R5161; and because NHMUK R5161 preserves nearly the entire dorsal integument it is unlikely that ROM 813 is referable to *Scolosaurus cutleri*. ROM 813 is from the lowest levels of the Dinosaur Park Formation and as such is unlikely to be referable to *Anodontosaurus lambei*. It does not have any triangular osteoderms such as those present on the tail of *Dyoplosaurus acutosquameus*, but it is unclear if any of the preserved integument in ROM 813 is from the tail. At present, it is impossible to determine if ROM 813 is referable to *Dyoplosaurus* or *Euoplocephalus*. This unsatisfactory result can only be resolved by finding additional specimens with *in situ* integument.

3.4.2 Systematic Paleontology

Dinosauria Owen, 1842

Ornithischia Seeley, 1887

Thyreophora Nopcsa, 1915

Ankylosauria Osborn, 1923

Ankylosauridae Brown, 1908

Ankylosaurinae Brown, 1908

3.4.2.1 *Anodontosaurus lambei* Sternberg, 1929

Holotype: CMN 8530, skull, lower jaws, caudal vertebra, ischium, pedal phalanx, and osteoderms (including first cervical half ring).

Referred Specimens: AMNH 5216 (tail club), AMNH 5223 (skull), AMNH 5245 (caudosacral and caudal vertebra, pelvis, tail club), NHMUK R4947 (skull), ROM 832 (fragmentary skull), TMP 1982.9.3 (two posterior dorsals with coossified ribs, partial pelvis, right femur, osteoderms including cervical half ring fragments), TMP 1994.168.1 (tail club), TMP 1996.75.01 (partial skull, cervical vertebra, partial ?first cervical half ring, ?second cervical half ring), TMP 1997.59.1 (skull), TMP 1997.132.01 (skull, three dorsal vertebrae, ribs, ?scapula, left humerus, ulna, radius, tibia, first and possibly second cervical half rings), USNM 10753 (tail club)

Holotype Locality: “90 feet above Red Deer river, in sec. 3, tp. 21, range 31, W. 4th prin. mer. This locality is about 8 miles southwest of Morrin, Alberta.”
(Sternberg 1929:28)

Distribution: Red Deer River, from Tolman Bridge to Drumheller, Alberta; Dinosaur Provincial Park, Alberta; South Saskatchewan River near Hilda, Alberta.

Formations: Horseshoe Canyon Formation; holotype probably from within the Horsethief Member, but referred specimens found throughout the Horsethief, Morrin, and Tolman members. Also present in the upper Dinosaur Park Formation, more than 30 meters above the Oldman-Dinosaur Park contact.

Revised Differential Diagnosis: Differs from *Euoplocephalus tutus* and *Scolosaurus cutleri* in having subcircular caputegulae at bases of quadratojugal and squamosal horns (postocular caputegulae), and interstitial osteoderms at bases of primary osteoderms on first cervical half ring; differs from *Euoplocephalus tutus* and *Dyoplosaurus acutosquameus* in having pointed, triangular major osteoderms on tail club knob and in having tail club knob width greater than length; differs from *Dyoplosaurus acutosquameus* in having laterally-directed sacral ribs, and U-shaped pedal unguals; differs from *Scolosaurus cutleri* in having a proportionately shorter postacetabular process of the ilium; differs from *Ankylosaurus magniventris* in having anteriorly-directed nares, and in lacking a continuous keel between the squamosal horn and supraorbitals.

3.4.2.2 *Dyoplosaurus acutosquameus* Parks, 1924

Holotype: ROM 784, fragmentary skull, complete caudal series of vertebrae including tail club, ribs, pelvis, hindlimb including pes, osteoderms *in situ*.

Referred Specimens: UALVP 47273 (partial tail club).

Holotype Locality: Dinosaur Provincial Park, Quarry Q002, 12U 5622422.480N, 466786.580 E.

Distribution: Dinosaur Provincial Park, Alberta.

Formation: Lower part of Dinosaur Park Formation.

Revised Differential Diagnosis: Differs from *Anodontosaurus lambei*, *Euoplocephalus tutus*, and *Scolosaurus cutleri* in having anterolaterally-directed sacral ribs, in having triangular unguals in dorsal view, and in having a tail club knob that is longer than wide; differs from *Scolosaurus cutleri* in having a proportionately shorter postacetabular process of the ilium, and in having triangular osteoderms on the lateral sides of the anterior portion of the tail; differs from *Ankylosaurus magniventris* in having anteriorly-directed nares, and in lacking a continuous keel between the squamosal horn and supraorbitals.

3.4.2.3 *Euoplocephalus tutus* Lambe, 1910

= *Stereocephalus tutus* Lambe, 1902

Holotype: CMN 210, fragmentary skull roof and partial first cervical half ring.

Referred Specimens: AMNH 5337 (skull, left mandible, one cervical vertebra, eleven dorsal vertebrae, humeri, scapulocoracoid, pelvis, osteoderms including first cervical half ring), AMNH 5403 (skull, both mandibles including prementary, four cervicals including axis, scapula, forelimbs, first and second cervical half rings, partial tail club knob), AMNH 5404 (skull, five caudals, ribs, right humerus, ischium, right femur, tibia, fibula, osteoderms, first cervical half ring), AMNH 5405 (skull, right mandible including prementary, handle vertebrae, humerus, ulna, osteoderms, first cervical half ring, tail club knob), AMNH 5406 (three dorsal vertebrae, ribs, scapulae, right humerus, ulna, radius, phalanges, osteoderms including first and second cervical half rings), CMN 842 (first cervical half ring), CMN 8876 (skull), ROM 1930 (skull, three dorsal vertebrae, two ?sacral vertebrae, twelve free caudals, transitional caudal, fragmentary right scapula, right humerus, osteoderms including *in situ* osteoderms and skin impressions on caudal vertebrae), TMP 1979.14.74 (partial skull), UALVP 31 (skull, right mandible, ribs, sacrum, scapula, humeri, right ilium, right ischium, right femur, tibia, pedal elements, osteoderms including first and second cervical half rings), UALVP 47977 (partial skull roof).

Holotype Locality: Dinosaur Provincial Park, exact locality unknown. Collected by L.M. Lambe in 1897 from the east side of the Red Deer River near the mouth of Berry Creek. This refers to the northwestern area of the park, near the old town of Steepleville.

Distribution: Dinosaur Provincial Park, Alberta; near Manyberries, Alberta.

Formation: Dinosaur Park Formation, found primarily in the lower 30 m of the formation.

Revised Differential Diagnosis: Differs from *Anodontosaurus lambei* and *Scolosaurus cutleri* in lacking subcircular caputegulae at the bases of the

quadratojugal and squamosal horns (postocular caputegulae); differs from *Anodontosaurus lambei* in lacking interstitial osteoderms at the bases of the primary osteoderms of the first cervical half ring, and in having semicircular major osteoderms in dorsal view on the tail club; differs from *Dyoplosaurus acutosquameus* in having laterally-directed sacral ribs; differs from *Scolosaurus cutleri* in having oval to subcircular-based keeled medial and lateral primary half ring osteoderms and in having a proportionately shorter postacetabular process of the ilium; differs from *Ankylosaurus magniventris* in having anteriorly-directed nares, and in lacking a continuous keel between the squamosal horn and supraorbitals.

3.4.2.4 *Scolosaurus cutleri* Nopcsa, 1928

= *Oohkotokia horneri* Penkalski, 2013

Holotype: NHMUK R5161, nearly complete skeleton with *in situ* osteoderms and skin impressions, lacking skull, distal half of tail, right forelimb, and right hindlimb.

Referred Specimens: MOR 433 (partial skull, both humeri, free caudal vertebra, and osteoderms), FPDM V-31 (partial skull and partial, reconstructed, mounted skeleton), NSM PV 20381 (skull, dorsal and caudal vertebrae, including damaged handle vertebrae, ribs, both scapulae, both ilia, partial ischia, and both femora, tibiae, and fibulae), TMP 2001.42.19 (skull, partial first cervical half ring, dorsals, sacrals, caudals including complete tail club, left humerus, left scapula, right femur, right and left tibiae, osteoderms), USNM 7943 (partial first cervical half ring).

Holotype Locality: Dinosaur Provincial Park, Quarry Q080, 12U, 5,622,321.978 N, 471,365.051 E; there is uncertainty over whether this is the correct quarry or whether it is from several hundred meters farther north.

Distribution: Dinosaur Provincial Park, Alberta; northwestern Montana.

Formations: Lower part of the Dinosaur Park Formation (or possibly Oldman Formation if mapped quarry position is wrong), and upper part of the Two Medicine Formation.

Revised Differential Diagnosis: Differs from *Anodontosaurus lambei* and *Euoplocephalus tutus* in the morphology of the squamosal horns, which are proportionately longer, backswept, and with distinct apices; differs from *Euoplocephalus tutus* in having small circular caputegulae at the bases of the squamosals and quadratojugals; differs from *Anodontosaurus lambei*, *Euoplocephalus tutus*, and *Dyoplosaurus acutosquameus* in having a proportionately longer postacetabular process of the ilium; differs from *Anodontosaurus lambei* and *Euoplocephalus tutus* in having proportionately large circular medial osteoderms with a low central prominences, and compressed, half-moon shaped lateral/distal osteoderms on the cervical half rings; differs from *Dyoplosaurus acutosquameus* in having laterally-directed sacral ribs; differs from *Dyoplosaurus acutosquameus* in having conical, osteoderms with centrally positioned apices on the lateral sides of the anterior portion of the tail; differs from *Anodontosaurus* and *Dyoplosaurus* in having a circular tail club knob in dorsal view, rather than a tail club knob that is wider than long (*Anodontosaurus*) or longer than wide (*Dyoplosaurus*); differs from *Ankylosaurus magniventris* in having anteriorly-directed nares, and in lacking a continuous keel between the squamosal horn and supraorbitals.

3.4.2.5 Indeterminate Ankylosauridae

Alberta

AMNH 5211 (tail club), AMNH 5266 (juvenile individual with vertebrae, ischium, right hindlimb with pes), CMN 125 (skull roof fragment), CMN 135 (tail club knob), CMN 268 (fragmentary first cervical ring), CMN 349 (tail club), CMN 2251 (partial tail club knob), CMN 2252 (partial tail club knob), CMN 2253 (partial tail

club knob), MACN Pv 12554 (tail club), NHMUK R8265 (left quadratojugal horn), NHMUK R36629 (?posterior supraorbital), NHMUK R36630 (quadratojugal horn), NHMUK R36631 (?squamosal horn), ROM 788 (tail club), ROM 813 (partial skeleton with *in situ* osteoderms, skin impressions), ROM 7761 (tail club knob), TMP 1967.13.2 (tail club knob fragment), TMP 1967.19.4 (left squamosal horn), TMP 1967.20.20 (right quadratojugal horn), TMP 1979.14.164 (partial skull), TMP 1980.8.284 (supraorbital), TMP 1980.16.1685 (fragmentary right mandible), TMP 1983.36.120 (tail club), TMP 1984.121.33 (partial tail club knob), TMP 1985.36.70 (free caudal vertebra), TMP 1985.36.330 (highly fragmentary skull in numerous pieces), TMP 1988.106.5 (left supraorbital), TMP 1991.36.321 (fragmentary first cervical ring), TMP 1991.36.743 (portion of frontonasal region), TMP 1992.36.334 (free caudal vertebra), TMP 1992.36.421 (right mandible), TMP 1993.36.79 (left squamosal), TMP 1993.36.421 (tail club), TMP 1998.83.1 (skull, cervical half ring: indeterminate because unprepared as of 2012), TMP 1993.66.13 (quadratojugal horn), TMP 1996.12.15 (portion of supraorbital region), TMP 1997.36.313 (right mandible), TMP 1998.93.55 (free caudal vertebra), TMP 1998.93.65 (free caudal vertebra), TMP 2000.57.3 (phalanges, tail club), TMP 2000.57.30 (portion of lacrimal/frontonasal region), TMP 2003.12.166 (fragmentary ?second cervical ring), TMP 2003.12.169 (first cervical ring distal osteoderm), TMP 2003.12.311 (skull, cervical half ring: indeterminate because unprepared as of 2012), TMP 2004.98.06 (mandible), TMP 2005.09.75 (free caudal), TMP 2005.12.43 (free caudal vertebra), TMP 2005.49.178 (portion of frontonasal region), TMP 2007.020.0063 (small quadratojugal horn), TMP 2007.20.80 (free caudal vertebra), TMP 2007.12.52 (second cervical half ring), TMP 2007.20.100 (free caudal vertebra), TMP 2012.005.2 (portion of lacrimal/frontonasal region), UALVP 16247 (tail club), UALVP 45931 (partial first and second cervical half rings), UALVP 47273 (tail club), UALVP 49314 (anterior supraorbital), UALVP 52875 (partial tail club knob), UALVP 54685 (posterior

supraorbital). Additionally, many isolated osteoderms and teeth from the Dinosaur Park Formation are in the TMP and UALVP collections.

Montana

AMNH 5470 (partial sacrum), AMNH 20870 (handle vertebrae), MOR 363 (braincase, both quadratojugal horns, and skull roof fragments), USNM 16747 (handle vertebrae).

3.4.3 Phylogenetic relationships of Campanian-Maastrichtian ankylosaurids from Alberta and Montana

The analysis retaining the character codings from Thompson et al. (2012), Matrix 1, produced two most parsimonious trees, with the best TBR score of 276 reached 150 times out of 192 (Fig. 3.23). The strict consensus tree has a consistency index (CI) of 0.62, and a retention index (RI) of 0.67. The Albertan ankylosaurids *Ankylosaurus*, *Anodontosaurus*, *Dyoplosaurus*, *Euoplocephalus*, and *Scolosaurus* did not form a clade, but instead formed a series of nested taxa leading towards a clade of Asian ankylosaurids (plus the North American *Nodocephalosaurus*). *Pinacosaurus grangeri* Gilmore, 1933 was more closely related to *Minotaurasaurus* than to *Pinacosaurus mephistocephalus*. Bootstrap and Bremer supports were low for all ankylosaurid interrelationships.

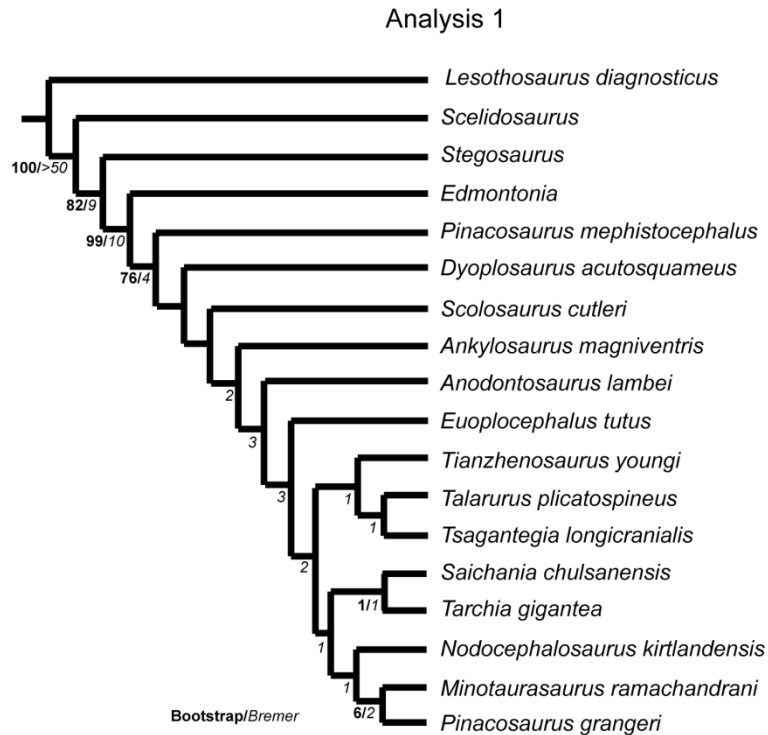


Figure 3.23. Results of phylogenetic analysis 1, retaining character state codings from Thompson et al. (2012). 50% majority rule tree shown, with bootstrap supports in bold and Bremer supports in italics.

The analysis with updated codings (Matrix 2) produced six most parsimonious trees of length 254, with the best score reached one time out of eleven (Fig. 3.24). The strict consensus tree had a CI of 0.63 and a RI of 0.66. Again, bootstrap and Bremer supports for ankylosaurid interrelationships were low. The Albertan ankylosaurids form a polytomy that is the sister group to a clade containing Asian ankylosaurids and *Nodocephalosaurus*. *Pinacosaurus grangeri* and *Pinacosaurus mephistocephalus* were recovered as sister taxa.

The final analysis incorporating new characters identified in this analysis (Matrix 3) resulted in 50 most parsimonious trees with the best TBR score of 269 reached five out of ten times (Fig. 3.25), with a CI of 0.65 and a RI of 0.69. Ankylosaurid interrelationships were completely unresolved in the strict consensus tree. A reduced consensus tree also had a completely unresolved

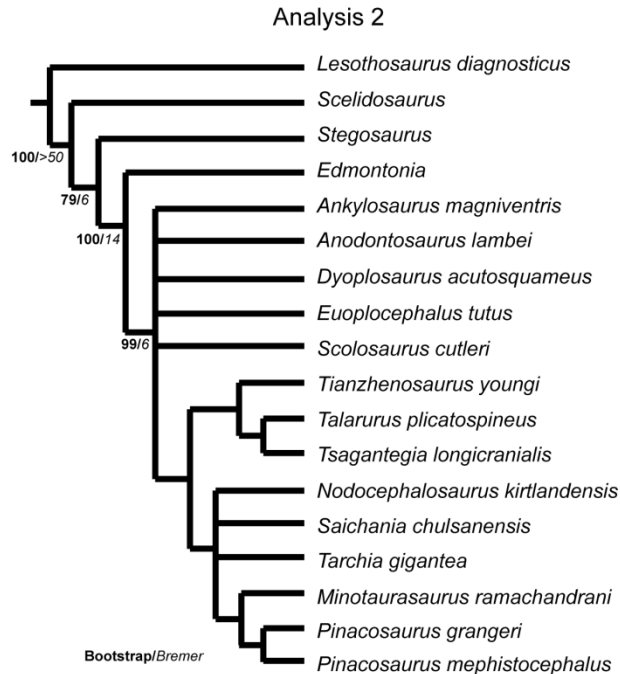


Figure 3.24. Results of phylogenetic analysis 2, modifying character state codings from Thompson et al. (2012). 50% majority-rule tree shown, with bootstrap supports in bold and Bremer supports in italics.

Ankylosauridae. Matrix 3 was analyzed in TAXEQ (Wilkinson 2001) to determine the amount of missing data, and to search for taxonomic equivalents.

Euoplocephalus, *Minotaurasaurus*, and *Pinacosaurus grangeri* had the least amount of missing data (each under 10%), and *Dyoplosaurus* and *Nodocephalosaurus* had the most missing data (each over 75%); overall, 36% of the character matrix was missing data. Six taxa were found to have potential taxonomic equivalents (*Dyoplosaurus*, *Minotaurasaurus*, *Nodocephalosaurus*, *Tarchia*, *Tianzhenosaurus*, and *Talarurus plicatospineus* Maleev, 1952), but in all cases the equivalency was asymmetric, and so no taxa could be safely removed from the analysis.

In the 50% majority rule tree, *Ankylosaurus*, *Anodontosaurus*, and *Euoplocephalus* formed a clade in 56% of all trees. *Pinacosaurus* was monophyletic in 72% of all trees. *Scolosaurus* was recovered as the most basal ankylosaurid, but *Dyoplosaurus* was recovered in a clade containing Asian

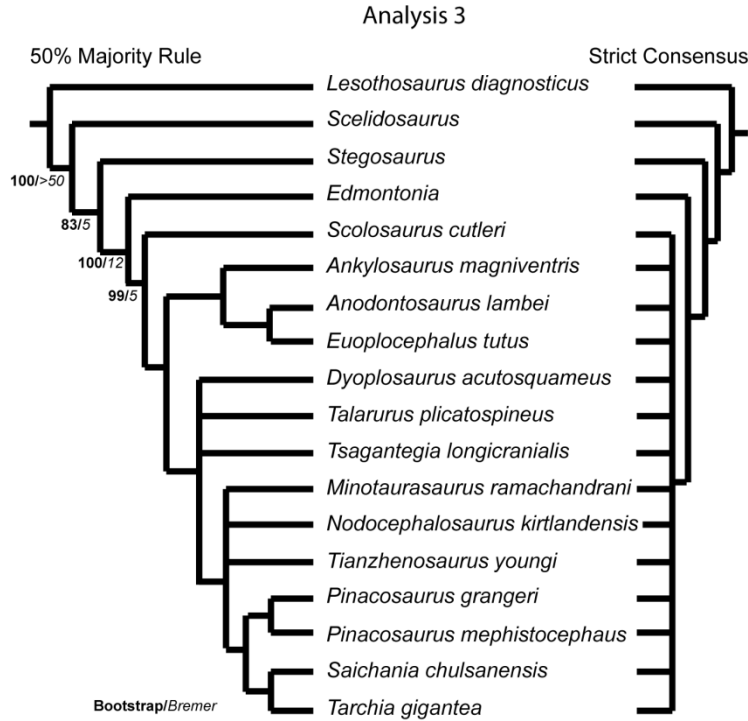


Figure 3.25. Results of phylogenetic analysis 3, with new characters added to modified character state codings from analysis 2.

ankylosaurids (plus *Nodocephalosaurus*). *Scolosaurus* has a relatively long postacetabular process (character state 142-0), a feature also present in nodosaurid ankylosaurs and basal thyreophorans, which may contribute to its relatively basal placement.

In all three analyses, the Asian ankylosaurids (plus *Nodocephalosaurus*) formed a monophyletic group in the strict consensus (Analyses 1 and 2) or majority-rule (Analysis 3) trees, but the North American ankylosaurids only partly formed a monophyletic group in Analysis 3. This indicates that, at present, it is best not to consider previous synonyms of *Euoplocephalus* as species of *Euoplocephalus*, but to treat them as distinct genera. The changing topology within the Ankylosauridae across these three analyses highlights the need for careful choice of characters and character codings and the identification of additional new characters.

3.4.4 Biogeographic and biostratigraphic implications

The results of this study indicate that ankylosaurid diversity in the Late Cretaceous of Alberta was higher than previously recognized (Fig. 3.26). Within the Dinosaur Park Formation, there are at least three ankylosaurid species: *Dyoplosaurus acutosquameus*, *Euoplocephalus tutus*, and *Scolosaurus cutleri*. A recent analysis of the biostratigraphy of megaherbivorous dinosaurs in the Dinosaur Park Formation by Mallon et al. (2012) found two main assemblage zones: Megaherbivore Assemblage Zone 1 (MAZ-1), from 0 to 28 meters (mostly corresponding to the *Centrosaurus-Corythosaurus* faunal zone *sensu* Ryan and Evans 2005), and MAZ-2, from 29 to 52 meters (mostly corresponding to the *Styracosaurus – Lambeosaurus* faunal zone *sensu* Ryan and Evans 2005). MAZ-2 may also extend into the Lethbridge Coal Zone, in the uppermost part of the Dinosaur Park Formation (Mallon et al. 2012), previously considered the pachyrhinosaur-*Lambeosaurus magnicristatus* faunal zone by Ryan and Evans (2005). *Scolosaurus* is currently represented by only a single specimen from either the Oldman Formation or the lower 10 m of the Dinosaur Park Formation (Fig. 3.1), in MAZ-1a (Mallon et al. 2012). Even with an additional specimen referred to *Dyoplosaurus*, this taxon is still only found in MAZ-1a as well. *Euoplocephalus* appears to primarily occur in MAZ-1, but two significant specimens—ROM 1930 and TMP 1997.132.1—have been recovered from the upper 30 meters of the formation. At present, ROM 1930 is best referred to *Euoplocephalus*. However, TMP 1997.132.1 shares several features with *Anodontosaurus lambei* from the Horseshoe Canyon Formation, and is here referred to that species. It is unusual for any Albertan dinosaur genus to be present in both the Dinosaur Park and Horseshoe Canyon formations, although cf. *Anchiceratops* and a *Pachyrhinosaurus*-like ceratopsid, both otherwise known only from the Horseshoe Canyon Formation, have been reported from the uppermost Dinosaur Park Formation (Brinkman et al. 1998; Mallon et al. 2012; Ryan et al. 2011). At present there are no morphological features that can

distinguish the upper Dinosaur Park Formation ankylosaurid from *Anodontosaurus lambei*. Future discoveries may yet provide evidence that the upper Dinosaur Park Formation ankylosaurid warrants taxonomic separation from *Anodontosaurus lambei*. Regardless, there appears to be little stratigraphic overlap between *Anodontosaurus lambei* and the lower Dinosaur Park Formation ankylosaurids *Dyoplosaurus acutosquameus*, *Euoplocephalus tutus*, and *Scolosaurus cutleri*.

In contrast to the high diversity in the lower Dinosaur Park Formation, ankylosaurid specimens in the Horseshoe Canyon Formation are referable only to *Anodontosaurus lambei* at present. *Anodontosaurus lambei* was present throughout the upper part of the formation (Fig. 3.26). Mallon et al. (2011), in an evaluation of variation within the Horseshoe Canyon Formation ceratopsid *Anchiceratops*, noted that this genus had a long stratigraphic range relative to other Albertan ceratopsids. *Anodontosaurus lambei* appears to have had a similarly long stratigraphic range.

The referral of ankylosaurid specimens from the Two Medicine Formation of Montana to *Scolosaurus cutleri*, previously known from only a single specimen from the Dinosaur Park Formation of Alberta, extends the geographic range of this taxon. For the Montanan specimens that had locality information, all were collected from the upper part of the Two Medicine Formation (Fig. 3.26). The uppermost part of the Two Medicine Formation (10 m below the top of the formation) was dated at 74 Ma (Rogers et al. 1993), whereas the top of the Dinosaur Park Formation was dated at 74.9 Ma (Eberth 2005), and the top of the Oldman Formation within Dinosaur Provincial Park was dated at 76.5 Ma (Eberth 2005); MOR 433 most likely occurred at a slightly younger time than most of the ankylosaurids from Dinosaur Provincial Park. Although there is uncertainty regarding the stratigraphic position of the holotype of *Scolosaurus*, it probably originated from at least the lowest part of the Dinosaur Park Formation, and it is possible it originated from the underlying Oldman Formation. This might suggest

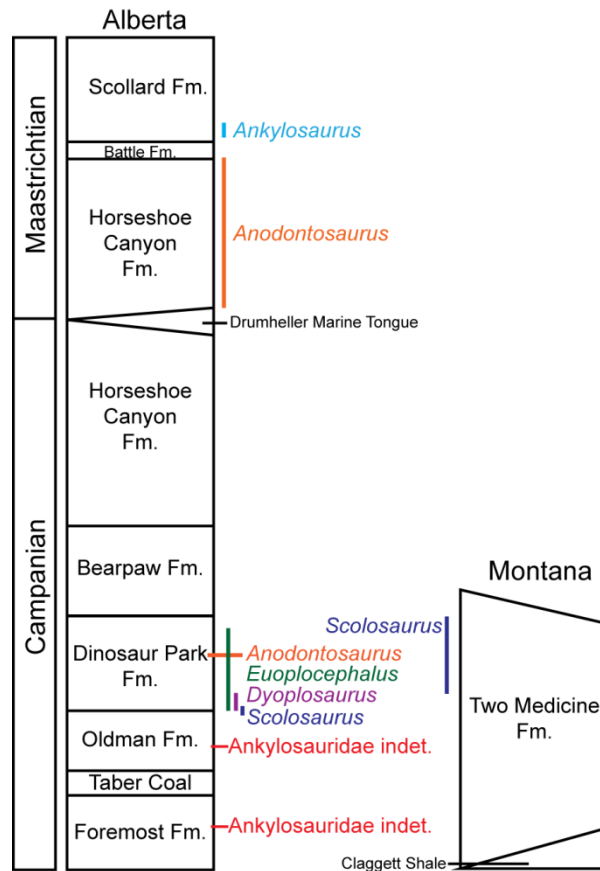


Figure 3.26. Stratigraphic distribution of Campanian-Maastrichtian ankylosaurid species in Alberta and northwest Montana. Indeterminate ankylosaurid material is known from the Foremost and Oldman formations in southern Alberta. The holotype of *Scolosaurus cutleri* may be from the Oldman Formation or the lower Dinosaur Park Formation; ankylosaurid specimens from the Upper Two Medicine Formation of Montana are referred to *Scolosaurus*. *Dyoplosaurus acutosquameus* is known from Megaherbivore Assemblage Zone 1 in the Dinosaur Park Formation. *Euoplocephalus tutus* has been identified from both Megaherbivore Assemblage Zone 1 and Megaherbivore Assemblage Zone 2 of the Dinosaur Park Formation, but is more common in Zone 1. *Anodontosaurus lambei* is rare in Megaherbivore Assemblage Zone 2 of the Dinosaur Park Formation, with most specimens identified from the Horsethief, Morrin, and Tolman members of the Horseshoe Canyon Formation. In Alberta, *Ankylosaurus magniventris* was present in the Scollard Formation.

that the referral of specimens from the Two Medicine Formation (*Oohkotokia*) to *Scolosaurus* is incorrect. However, it is possible that the occurrence of *Scolosaurus* in the Two Medicine Formation and (potentially) the Oldman

Formation is environmentally and ecologically related: the Oldman Formation represents the maximum regression of the Western Interior Seaway during the Campanian (Eberth 2005), and therefore a comparatively drier, more “upland” environment compared to the Dinosaur Park Formation. Although deposited during a transgressive phase, the Upper Two Medicine Formation represents a relatively dry environment, compared to the laterally equivalent Judith River Formation and the Dinosaur Park Formation (Trexler 2001). Cranial material associated with a *Scolosaurus* half ring from the Dinosaur Park Formation is needed to confirm the referral of the Two Medicine ankylosaurid material to *Scolosaurus* rather than *Oohkotokia*. Until then, *Oohkotokia* possesses no unique characters that separate it from *Scolosaurus*.

In Alberta, no Judithian ankylosaurid fossils have been recovered north of Dry Island Buffalo Jump Provincial Park, although ankylosaurid teeth have been collected from the Kleskun Hills locality near Grande Prairie (Miyashita and Fanti 2009). Although the teeth are the right size to be ankylosaurid teeth, the two teeth that were recovered are weathered and may represent teeth of juvenile nodosaurids. Nodosaurid fossils have been collected from as far north as the Matanuska Formation of Alaska (Gangloff 1995), but currently ankylosaurids appear to be restricted to more southern parts of Laramidia during the Late Cretaceous.

Nodocephalosaurus appears to have been related to the Asian ankylosaurids *Saichania* and *Tarchia*, a relationship first noted by Sullivan (1999). This is unusual, given that *Nodocephalosaurus* is currently known from the Campanian of New Mexico (southern Laramidia), and no northern Laramidian ankylosaurids have recently been hypothesized to have been closely related to any Asian species. It seems unusual that Asian ankylosaurid dinosaurs migrated into North America during the Late Cretaceous without leaving any close relatives in Alaska, Alberta, Montana, or Utah, through what is presumed to be the most likely dispersal route from Asia to New Mexico. The phylogenetic

analysis by Thompson et al. (2012), as well as Analysis 3 in this paper, recover the Albertan species *Dyoplosaurus acutosquameus* as having affinities with Asian ankylosaurids. Again, it is important to note that the position of *Dyoplosaurus acutosquameus* appears to be quite labile. There is a great deal of missing data in the character matrix for this taxon, and so a close relationship between *Dyoplosaurus acutosquameus* and Asian ankylosaurids should be regarded as tentative at best. However, if further study confirms this relationship, this could support the hypothesis of a dispersal of Asian ankylosaurids into North America during the Late Cretaceous.

3.5 Conclusions

Specimens that were once referred to a single genus, *Euoplocephalus*, are now shown to represent at least four distinct taxa, greatly increasing the diversity of Late Cretaceous North American ankylosaurids. Within Alberta, *Dyoplosaurus acutosquameus*, *Euoplocephalus tutus*, and *Scolosaurus cutleri* were restricted to the lower part of the Dinosaur Park Formation (although *Scolosaurus* may have occurred in the top of the Oldman Formation), and *Anodontosaurus lambei* was present in the upper part of the Dinosaur Park Formation and in the Horseshoe Canyon formation. *Oohkotokia horneri*, from the Two Medicine Formation of Montana, is morphologically indistinct from *Scolosaurus cutleri*. *Dyoplosaurus acutosquameus* has limited cranial material and is represented by only two specimens. In contrast, *Anodontosaurus lambei*, *Euoplocephalus tutus*, and *Scolosaurus cutleri* are known from numerous referred specimens, including both skulls and postcrania. The skeleton of *Anodontosaurus lambei* is not as completely known as that of *Euoplocephalus tutus*, for which nearly the entire skeleton is represented across numerous referred specimens. Although *Euoplocephalus tutus* still includes the most referred material, there is no specimen that includes *in situ* osteoderms, and so the arrangement of osteoderms in *Euoplocephalus tutus* is not known.

The recognition of several species within *Euoplocephalus tutus sensu lato* indicates that *Euoplocephalus tutus sensu stricto* was not as intraspecifically variable as previously suspected. Although cranial ornamentation can be variable, aspects of ankylosaurid cranial ornamentation are taxonomically informative, such as the overall shapes of the squamosal horns, the presence or absence of postocular caputegulae at the bases of the squamosal and quadratojugal horns, the morphology of the first cervical half ring, and the shape and proportions of the tail club knob. The morphology of the pelvis also appears to be taxonomically informative. Conversely, certain aspects of the cranial and postcranial skeleton, such as squamosal horn size and bluntness, cranial caputegulum distinctness, cervical half ring anteroposterior length, and robustness of limb elements (such as the size of the deltopectoral crest of the humerus) are more likely a result of ontogenetic variation. This information can be used to better interpret taxonomic versus intraspecific variation among other ankylosaurid taxa.

Appendix 3.1. Locality information for specimens referred to *Anodontosaurus lambei*, *Dyoplosaurus acutosquameus*, *Euoplocephalus tutus*, and *Scolosaurus cutleri*.

Specimen	Collector/ Year	Locality Information and Source
AMNH 5211	B. Brown, P. Kaisen, 1910	<p>“No. 11 Ankylosaurus caudal plate same locality + level as no. 12”; “No. 12 <i>Trachodon</i> left scapula 50 feet above river 1 ½ mile above Tolman’s”</p> <p>AMNH Collections Database; AMNH Vertebrate Paleontology Archives: Barnum Brown 1908-1911 Notebook</p>
AMNH 5216	B. Brown, P. Kaisen, 1911	<p>½ mile above Tolman Ferry, left bank; “No. 18 = Ankylosaur tail section with plate 30 ft above river Tolman Ferry”</p> <p>Part of AMNH traveling exhibit Dinosaurs: Ancient Fossils, New Discoveries as of 2013.</p> <p>AMNH Vertebrate Paleontology Archives: Barnum Brown 1908-1911 Notebook</p>
AMNH 5223	B. Brown, P. Kaisen	<p>2 mi. below Tolman Ferry, right bank</p> <p>AMNH Collections Database</p>
AMNH 5238	B. Brown, 1911	<p>Near mouth of Berry Creek</p> <p>This is probably near Steveville in Dinosaur Provincial Park.</p> <p>AMNH Collections Database; AMNH Vertebrate Paleontology Archives: Barnum Brown 1908-1911 Notebook</p>
AMNH 5266	B. Brown, P. Kaisen, Sternberg, Olsen, 1912	<p>10 mi. below Tolman Ferry, right bank 150 feet above the river; ?Section 32 T31 R21</p> <p>Specimen cards; AMNH Collections Database; AMNH Vertebrate Paleontology Archives: Barnum Brown 1908-1911 Notebook</p>
AMNH 5337	B. Brown, P. Kaisen, 1914	<p>Sand Creek, right bank 125 feet above river 12 mi. below Steveville Red Deer River</p> <p>Sand Creek is an alternate name for Little Sandhill Creek in Dinosaur Provincial Park. Pelvis on display at AMNH.</p> <p>AMNH Collections Database</p>
AMNH 5403	B. Brown, P. Kaisen, 1913	<p>Steveville 1 ½ mi. below, left bank 40 feet above river</p> <p>This is in Dinosaur Provincial Park.</p> <p>AMNH Collections Database</p>
AMNH 5404	B. Brown, P. Kaisen, 1913	<p>Steveville 12 mi. below, right bank 75 feet above river; Sternberg Map #60; UTM NAD83 E464501.570, N5623591.470</p> <p>AMNH 5404 has both field note data and GPS coordinates, but these do not agree. AMNH 5404 seems to be more like 6 mi</p>

		downstream of Steveville rather than 12 mi, using GPS data. Skull on display at AMNH.
		AMNH Collections Database; Currie and Koppelhus (2005) supplementary CD ROM; Sternberg 1950
AMNH 5405	B. Brown, P. Kaisen	Steveville 12 mi., right bank 75 feet above river This is in Dinosaur Provincial Park.
		AMNH Collections Database
AMNH 5406	B. Brown, P. Kaisen	Steveville 1 mi. below, left side 75 feet above river This is in Dinosaur Provincial Park.
		AMNH Collections Database
AMNH 5409	B. Brown, P. Kaisen	Steveville 1 ½ mi. below, left bank 20 feet above river; Sternberg Map #7; UTM NAD83 E457353.919, N5629594.606
		AMNH Collections Database; Currie and Koppelhus (2005) supplementary CD ROM; Sternberg 1950
AMNH 5470	B. Brown, P. Kaisen, Johnson	Two Medicine River, Montana, Glacier County, 16 mi SW of Cut Bank AMNH Collections Database
AMNH 20870		Two Medicine, Montana Specimen card
CMN 135	CM Sternberg 10 June 1919	"...southwest extremity of badlands near prairie level, south branch of Little Sandhill Creek." This is in Dinosaur Provincial Park.
		Specimen card; CH Sternberg field notes 1919
CMN 210	L.M. Lambe, 18 August 1897	East side of Red Deer River at mouth of Berry Creek Holotype of <i>Euoplocephalus tutus</i> . This is in Dinosaur Provincial Park.
		Data provided by M. Currie (CMN), 18 Jan 2012, from Lambe field notes
CMN 349	C.H. Sternberg; 13 June 1914	"... south side of Red Deer River, three miles above "Happy Jack Ferry" (Belly River Fm., Dead Lodge Canyon). This is in Dinosaur Provincial Park. Tail club on display at CMN.
		Data provided by M. Currie (CMN), 18 Jan 2012, from Sternberg field notes
CMN 2252	C.H. Sternberg; 1914	Sticker on specimen reads 1914-5; "Section of club...Sand Creek" This is in Dinosaur Provincial Park. CH Sternberg field notes 1914

CMN 8530	GF Sternberg, 9 September 1916	<p>"Armoured dinosaur. Found by G.F. Sternberg opposite Neil's ranch house on the river 8 miles southwest of Morrin, 90 feet above water...This specimen seems to be badly scattered in a bone bed, but there are so many plates I feel sure it is one individual." (G.F. Sternberg 1916); "It was collected by G.F. Sternberg in 1916, from the Edmonton formation, 90 feet above Red Deer river, in sec. 3, tp 21, range 31, W 4th prin. Mer. This locality is about 8 miles southwest of Morrin, Alberta, and the horizon is near the middle of the Edmonton beds. The specimen was preserved in a tenacious fine-grained sandstone which does not free well from some of the softer bones, particularly the under side of the skull and the roof of the mouth, thus making the preparation of this portion difficult." (Sternberg 1929:28); Garson's Badlands 90 feet above river (Eberth)</p> <p>Holotype of <i>Anodontosaurus lambei</i></p> <p>Specimen card; Sternberg (1929); GF Sternberg Field Notes 1916; D. Eberth pers. comm. 3 Oct 2012</p>
CMN 8876	H. Lowe, 22 June 1937	<p>"13. 5 miles a little east of south of Manyberries. In SW1/4 of Section 20, T. 3, R. 5, west of 4th meridian. In clay bed midway between two massive sandstone beds; below the middle of the section exposed at this spot."</p> <p>Data provided by M. Currie, 2011/2012, CMN</p>
FPDM V-31	Canada Fossils Ltd., 1997	<p>Private land, Blackfeet Indian Reservation, Montana; same property as NSM PV 20381 but different locality</p> <p>Originally nicknamed "Peggy". On display as mounted skeleton at FPDM.</p> <p>Pers. comm. A. Dzindic, 3 Dec 2010</p>
NHMUK R4947	Cutler	<p>Red Deer River</p> <p>Specimen card says "Purch WE Cutler July 1923", but it is unclear if this was also the year (or close to the year) it was collected.</p>
NHMUK R5161	WE Cutler, 1914	<p>"Professor Parks of Toronto informed F. A. Bather, the Keeper of the Natural History Museum in London, that according to information gained from Mr. Levi Sternberg ,,it seems that the specimen was found in the Belly River Series, Upper Cretaceous, about one half mile below <<Happy Jack>> ferry on the Red Deer River. This would make the location in Dead Lodge Canyon..." Nopcsa (1928:54); Sternberg Map #105; UTM NAD83 E471365.051, N5622321.978</p> <p>Holotype of <i>Scolosaurus cutleri</i>. C.H. Sternberg (1914) field notes indicate Cutler was on the south side of the river: "Drove out to camp at Happy Jack's and pitched our tents...Saw Mr. Cutlers camp across the river." On display as panel mount at NHMUK.</p> <p>Nopcsa (1928); CH Sternberg field notes 1914; Currie and Koppelhus (2005) supplementary CD ROM; Sternberg 1950</p>

NHMK R8265	CH Sternberg 1915	Red Deer River Specimen card
NHMK R36629- R36631	WE Cutler, 1914	Mexico Ranch, "Laehodon Pkg" Mexico Ranch is also known as Happy Jack's, or Happy Jack Ferry. This is surrounded by Dinosaur Provincial Park. Specimen cards
NSM PV 20381	Canada Fossils Ltd., 1996	Private land, Two Medicine Formation, Montana; same property as FPDM V-31 but different locality Originally nicknamed "Olive". On display as mounted skeleton at NSM. Pers. comm. A. Dzindic, 27 Sept 2011
MACN Pv 12554	L. Sternberg, 1926	"Specimen No 6 About four and a half feet of the tail and the tail club of a large armoured dinosaur. Found by L. Sternberg about a mile east of the River and a mile southeast of Steveville (100 feet above the river.) (Sent to Buenos Aires in an exchange.) Nodosauridae." This is in Dinosaur Provincial Park. Tail club on display at MACN. L. Sternberg Field Notes 1926 (ROM)
MOR 433	1986	Top Two Medicine Fm. Locality TM-034 Ank Landslide Butte, Glacier Co.
ROM 784	1919, L. Sternberg	Specimen card "1 mile south of river 2.5 miles up from Happy Jack Ferry."; UTM NAD83 E466,786.580 N5,622,422.480; Sternberg Map #93 Holotype of <i>Dyoplosaurus acutosquameus</i> L. Sternberg Field Notes 1919 (ROM); Currie and Koppelhus (2005) supplementary CD ROM; Sternberg 1950
ROM 788	L. Sternberg, 1921	"Specimen No 9 Large tail club with about 4 feet of tendons in place. This was found about 1/2 mile south of Nos 1 & 3. There are two sections, one with club and one with tendons. (Cat. No. 4973 ct old and 788 new number. Armoured, tail club, mounted in gallery.); Specimen # 1 is <i>Prosaurolophus maximus</i> : "on a branch of the main Sand Hill Creek about 2 miles from the mouth (where it empties into the river) and about one mile northwest of the crown and about 125 feet above the river (aneroid)."; Specimen # 2 is <i>Prosaurolophus</i> in same quarry as #1: "West branch, Sand Creek, 150 feet below prairie level, 125 feet up. ...Topographic map No. 79, Sec. 32, Tp. 20 R. 11 west of the fourth." This is in Dinosaur Provincial Park. Tail club on display at ROM. L. Sternberg Field Notes 1921 (ROM)

ROM 813	L. Sternberg 1919	<p>“This specimen is a plated fellow. Found about one-half mile north west of Jackson's Ranch, just below a large, sharp point or butte, 100 feet above the river level (aneroid)”; Sternberg Map #103; UTM NAD83 E470035.390, N5623289.679</p> <p>L. Sternberg Field Notes 1919 (ROM); Currie and Koppelhus (2005) supplementary CD ROM; Sternberg (1950)</p>
ROM 832	26 September 1916 GF Sternberg	<p>“Found by G.F. Sternberg, opposite Neal's ranch, sec. 10, T. 31, R. 21...Found 7 miles southwest of Morrin, about 75 feet above the water. This is the skull and first ring of plates. The ring of plates is complete and the back part of the skull is complete, but the front part is all broken up though I have all fragments...The top is preserved the best as it lay upside down.”</p> <p>Exchanged with ROM, March 1930</p> <p>G.F. Sternberg Field Notes 1916</p>
ROM 1930	GF Sternberg 1914	<p>“This specimen is about 60' below the coal seam and 250' above the river.” “Stegoasur Europlocephalus [sic] GHS. About 15 feet of body including head. Sacrum Pelvis arch limbs a few feet of the tail. Evidently the entire skeleton except tail ____? On south side river about 3 miles below “Happy Jack Ferry” Preserved in hard grey sand stone concretion covering a floor about 15 x 20 ft. and 35 ft. high at back end of quarry. The most difficult specimen we ever collected.”; Possibly the same as ROM 2162 in Currie and Koppelhus (2005): UTM NAD83 E474519.970, N5624073.730; Sternberg Map #112</p> <p>Originally collected for GSC/CMN, traded to ROM for <i>Styracosaurus</i> skeleton. Currie and Koppelhus (2005) include coordinates for a specimen called ROM 2162 (“scattered skeleton”), collected by CH Sternberg in 1914, however, there does not appear to be a specimen ROM 2162. The only ankylosaur collected by CH Sternberg in 1914 was ROM 1930, which was also a scattered skeleton. The GPS coordinates correspond well to an estimate made using only the field notes, and so it is highly likely that “ROM 2162” is actually ROM 1930. Skull on display at ROM.</p> <p>CH. Sternberg Field Notes 1914 (GSC/CMN); Currie and Koppelhus (2005) supplementary CD ROM; Sternberg (1950)</p>
ROM 7761	L Sternberg, 19 July 1954	<p>Could possibly be: “Levi drove over to another ranch for some prospecting, but won't say what he did. I found later that he got a small Ankylosaur tail club and saw a scattered skeleton, but no action was taken.”</p> <p>A.G. Edmund Field Notes 1954 (ROM)</p>
TMP 1979.14.164		<p>Dinosaur Provincial Park</p> <p>TMP Collections Database</p>

TMP 1982.9.3	TMP crew	“Fox Coulee; LSD 14-16-29-20W4; record says Midland Prov Pk, but location is Fox Coulee, east of tracks close to Fox Coulee BB” D. Eberth, pers. comm. 3 Oct 2012
TMP 1983.36.120	TMP crew	Dinosaur Provincial Park, S32 T020N R11W M04 On display at TMP Field Station, Dinosaur Provincial Park Visitor Centre TMP Collections Database
TMP 1984.121.33		Donation from Calgary Zoo, no locality data Specimen card, TMP Collections Database
TMP 1991.36.321	TMP crew	Dinosaur Provincial Park TMP Collections Database
TMP 1991.127.1	TMP crew	Stevenville Area, Dinosaur Provincial Park; 04 R12W T021N S33 TMP Collections Database
TMP 1993.36.421	TMP crew	Dinosaur Provincial Park TMP Collections Database
TMP 1994.168.1	Kurt Armbruster, TMP crew	Bleriot Ferry, Drumheller Valley; Horsethief Canyon, northern portion, along trail to TMP Day Digs bonebed excavation Specimen card; Pers. comm. D. Eberth October 2012
TMP 1996.75.01	TMP crew	Three Hills Locality, Three Hills Creek, S16 T020N R22W 04; UTM = 12: 359755; 5714550; Three Hills Creek, downstream from HWY 836 intersection with creek. Specimen card, TMP Collections Database; Pers. comm. B. Strilisky July 2012; pers. comm. D. Eberth 3 Oct 2012
TMP 1997.59.1	TMP crew	Rosebud Creek, S12 T027N R22W 04; UTM = 12; 362800; 5684000 TMP Collections Database, pers. comm. B. Strilisky July 2012
TMP 1997.132.01	TMP crew	Hilda; UTM = 12; 543367; 5596003 Collected from an iron-rich channel sandstone about 30m above the Oldman/Dinosaur Park contact; DPF in this area is about 60m thick; specimen’s stratigraphic position correlates roughly with middle of DPF at Dinosaur Provincial Park (pers. comm. D. Eberth, July 2011) TMP Collections Database; B. Strilisky pers. comm. July 2012
TMP 1998.83.1	D. Brinkman	UTM NAD83 E463074.172, N5624441.138 Currie and Koppelhus (2005), supplementary CD ROM
TMP 2000.57.30	D. Brinkman	Onefour, Sage Creek; 12 546114; 5432108 Specimen card, TMP Collections Database

TMP 2001.42.9	Canada Fossils Ltd, 1998	Blackfeet Indian Reservation, Montana Originally nicknamed "Uma". Pers. comm. A. Dzindic, 23 Feb. 2010
TMP2003.1 2.166	B. Bohdanowicz, 12 May 2003	Dinosaur Provincial Park, Iddesleigh; 12 474069; 5623906 Specimen card
TMP 2003.12.311	W Sloboda, 2003	UTM NAD83 E474080 N5623890 Currie and Koppelhus (2005), supplementary CD ROM
UALVP 31	GF Sternberg, 1921	¾ mile southeast of Steveville, 225 feet (aneroid) above the river (Gilmore 1923); GPS coordinates; Steveville #1; Sternberg Map #2; UTM NAD83 E458172.517, N5631004.186 Skull on display at UALVP. Gilmore 1923, UALVP catalogue; Sternberg (1950); Currie and Koppelhus (2005), supplementary CD ROM
UALVP 16247	LA Lindoe 1969	Dinosaur Provincial Park, Steveville #14 Tail club on display at UALVP.
UALVP 45931	L Lindoe	Specimen display card; UALVP catalogue; UALVP field notes Hilda #1; LSD 13, S8, T18, R3, W4 "...in the vicinity of Hilda 1 which is a micro site...The ankylosaur site would be higher than the micro site and on the main valley wall as opposed to out on the point where the micro site and the ceratopsian sites were." LA Lindoe, July 2012 UALVP catalogue, pers. comm. LA Lindoe July 2012
UALVP 47273	P. Bell, P. Currie, 15 July 2006	Dinosaur Provincial Park, Bonebed 91A UALVP catalogue
UALVP 47977	DW Krause, 1970	Dinosaur Provincial Park, "Happy Jack's" UALVP catalogue; UALVP field notes
USNM 7943	C.W. Gilmore	37N, 8W, Milk River, 1 mi. North of Blackfeet Indian Reservation, Two Medicine Specimen card
USNM 10753	GF Sternberg, T Hardy, 14 Sept 1916	"Found by Tomas Hardy, September 14, 7 miles west, 2 north of Morrin, Alta, sec. 28, T. 31, R. 21, on old Joe's place...East side of river about 50 feet above the water."; "2 miles up river from Starland Rec Area (east side)" (Eberth) Exchanged with the USNM in May 1922 Specimen card; GF Sternberg Field Notes 1916; D. Eberth pers. comm. 3 Oct 2012

USNM 11892 GF Sternberg, 26 May 1928 Glacier County, NW ¼, Sec 27, T37N, R8W, 0.5 mi S of Milk River; "collected by George F. Sternberg, May 26, 1928, from the Two Medicine formation, Upper Cretaceous, from the south side of Milk River, NW ¼ sec. 27, T. 37, N., R. 8 W., on the Blackfeet Indian Reservation, Glacier County, Mont." (Gilmore 1930:32)

Originally referred to *Dyoplosaurus* by Gilmore (1930)

Specimen card; Gilmore 1930

USNM 16747 C.W. Gilmore 1928 Glacier County, Montana, Sec 27, 37N, 8W Blackfeet Indian Reservation, Two Medicine

Specimen card

Appendix 3.2. Character statements and remarks. All character statements are the same as those in Thompson et al. (2012), but some character state codings have been altered for the ‘updated codings’ analysis (Matrix 2, Analysis 2). New characters for Matrix 3 and Analysis 3 appear last.

1. Antorbital fenestra: present (0); absent (1).
2. Lateral temporal fenestra, visible in lateral view: visible (0); hidden (1).
3. Supratemporal fenestra: open (0); closed (1).

Updated codings: *Dyoplosaurus* from ? to 1. This region of the skull is preserved in ROM 784.
4. Skull dimensions, including ornamentation: longer than wide (0); as wide, or wider than long (1).
5. Width of the posterior margin of the skull relative to the maximum width across the orbits: greater or equal (0); less (1).
6. Size of occiput: higher than wide (0); wider than high (1).

Updated codings: *Nodocephalosaurus* from ? to 1; *Talarurus* from ? to 1. Notes: The occiput is preserved in both *Nodocephalosaurus* and *Talarurus* and so the proportions of height vs. width can be coded.
7. External nares, opening faces: laterally (0); anterolaterally (1); anteriorly (2).
8. External nares, visible in dorsal view: visible (0); hidden (1).

Updated codings: *Pinacosaurus grangeri* from 1 to 0.
9. Near vertical narial septum separating the respiratory passage and lateral sinus: absent (0); present (1).
10. Near horizontal narial septum separating the respiratory passage and lateral sinus: absent (0); present (1).
11. Shape of respiratory passage: straight (0); sinuous (1).
12. Lateral sinuses: absent (0); present (1).
13. Orbits, angle of orbital axis: <40° (0); >40° (1).
14. Antorbital region of the dorsal skull surface: flat (0); domed (1).

Updated codings: *Nodocephalosaurus* from 0 to ?; *Minotaurasaurus* from 1 to 0. Notes: The holotype and only skull of *Nodocephalosaurus* is severely crushed and distorted, and so a dorsoventral dimension-based character coding for this taxon is dubious. As can be seen in lateral view, the skull of *Minotaurasaurus* is flat.

15. Development of the postocular shelf: not developed (0); completely separating orbit from temporal space (1).
16. Gap between palate and braincase: open (0); closed by a dorsal projection of the pterygoid (1).

Updated codings: *Tianzhenosaurus* from 1 to ?. Notes: This feature cannot be assessed using the figures or description in Pang and Cheng (1998), and the original specimen was not observed for this study.

17. Cranial sutures in adult specimens: visible (0); obliterated (1).

Updated codings: *Dyoplosaurus* from ? to 1; *Nodocephalosaurus* from ? to 1. Notes: Although fragmentary, the skull of *Dyoplosaurus* does not preserve open sutures, and so this character should be coded as “1” for this taxon. In *Nodocephalosaurus*, the cranial sutures are clearly obliterated.

18. Dimensions of premaxillary palate: longer than wide (0); wider than long (1).

Updated codings: *Minotaurasaurus* from ? to 1, *Tianzhenosaurus* from ? to 1.

19. Shape of the premaxillary palate: sub-triangular (0); sub-quadrate (1); sub-oval (2).
20. ‘V’ or ‘U’-shaped median indentation of the anterior margin of the premaxilla: absent (0); present (1).

Updated codings: *Ankylosaurus* from 1 to ?, *Minotaurasaurus* from 0 to ?. Notes: This region is broken in the holotype and only specimen of *Minotaurasaurus*, and in all specimens of *Ankylosaurus*.

21. Posteroventral extension of premaxillary tomium in lateral view: ends anterior to the maxillary teeth (0); obscures most anterior maxillary teeth (1).

22. Bone bordering anterior margin of internal nares: premaxilla (0); maxilla (1).

Updated codings: *Minotaurasaurus* from 0 to ?; *Pinacosaurus mephistocephalus* from 1 to ?, *Tianzhenosaurus* from 1 to ?. Notes: This region is obscured by sediment in the holotype and only skull of *Minotaurasaurus*. It is unclear from the figures in Godefroit et al. [8] of the holotype of *Pinacosaurus mephistocephalus* if the premaxilla or maxilla borders the

anterior margin of the internal nares, and so this character is modified from 1 to ?. This feature cannot be assessed using the figures or description in Pang and Cheng [6] of *Tianzhenosaurus*, and the original specimen was not observed for this study.

- 23.** Shape of the ventral margin of premaxillary tomium in lateral view: flat (0); convex (1); concave (2).

Updated codings: *Euoplocephalus* from 1 to 2; *Tianzhenosaurus* from 1 to ?. Notes: The holotype of *Tianzhenosaurus* is broken in this region.

- 24.** Shape of the maxillary tooth row: straight (0); medially convex (1).

Updated codings: *P. grangeri* from 0 to 1; *Tarchia* from 0 to 1; *Tsagantegia* from 0 to 1. Notes: In all of these taxa the maxillary tooth row is at least slightly medially convex.

- 25.** Maxillary tooth row position: lateral margin of skull (0); inset (1).

Updated codings: *Nodocephalosaurus* from ? to 1. Notes: The maxillary tooth row is clearly inset from the lateral margin of the skull in the holotype and only specimen of *Nodocephalosaurus*.

- 26.** Distance between most posterior extent of maxillary tooth rows relative to the width of the premaxillary beak: wider (0); narrower (1).

Updated codings: *Ankylosaurus magniventris* from 1 to 0. Notes: In AMNH 5214, the beak is narrower than the posterior width between the maxillary tooth rows; see Carpenter [9].

- 27.** Palpebral shape: rod (0); plate (1).

Updated codings: Changed all ankylosaurs to 1 where skull is known.

- 28.** Form of palpebral contact: mobile contact with prefrontal (0); extensive sutural contact with prefrontal, frontal and postorbital (1).

- 29.** Anterior and posterior supraorbitals (recognizable by distinct regions of ornamentation above the orbit): absent (0); present (1).

- 30.** Form of supraorbital ornamentation: boss-like, rounded laterally (0); sharp lateral rim, forming a ridge (1).

Updated codings: *Dyoplosaurus* from 1 to ?. Notes: The supraorbitals are poorly preserved in the holotype and only specimen of *Dyoplosaurus*.

- 31.** Form of the parietal surface: not domed (0); domed (1).

Updated codings: *Dyoplosaurus* from 1 to 0. Notes: Although the posterior region of the skull of *Dyoplosaurus* was described as 'domed' in Arbour et al. (2009), the domed region more likely represents the frontals, not the parietals.

- 32.** Proportions of jugal orbital ramus: depth greater than transverse breadth (0); transverse breadth greater than depth (1).

Updated codings: *Minotaurasaurus* from ? to 1. Notes: This feature is preserved in *Minotaurasaurus*.

- 33.** Shape of quadrate in lateral aspect: curved (anteriorly convex, posteriorly concave) (0); straight (1).

Updated codings: *Minotaurasaurus* from ? to 1; *Nodocephalosaurus* from ? to 1. Notes: This feature is preserved in both of these skulls and therefore can be coded.

- 34.** Inclination of quadrate in lateral aspect: near vertical (0); almost 45° anterolaterally (1).
35. Form of the anterior surface of the quadrate: transversely concave (0); not concave (1).

Updated codings: *Minotaurasaurus* from ? to 1. Notes: This feature is preserved in *Minotaurasaurus*.

- 36.** Ventral projection of the mandibular process of the quadrate in lateral view: projects beyond the quadratojugal ornamentation (0); hidden by quadratojugal ornamentation (1).

Updated codings: *Nodocephalosaurus* from ? to 1. Notes: This feature is preserved in *Nodocephalosaurus*. Although the specimen is distorted, it is apparent that the quadrate was obscured by the quadratojugal horn in lateral view.

- 37.** Form of quadrate mandibular extremity: symmetrical (0); medial condyle larger than lateral condyle (1).

Updated codings: *Nodocephalosaurus* from ? to 1. Notes: This feature is preserved in *Nodocephalosaurus*.

- 38.** Inclination of the articular surface of the quadrate condyle in posterior view: horizontal (0); ventromedially inclined at approximately 45° to horizontal (1).

Updated codings: *Minotaurasaurus* from 0 to 1.

- 39.** Lateral ramus of the quadrate: present (0); absent (1). (Serenó [2]: character 15)

- 40.** Dorsoventral depth of the pterygoid process of the quadrate: deep (0); shallow (1).

- 41.** Contact between paroccipital process and quadrate: sutural (0); fused (1).

42. Contact between pterygoids: pterygoids separate posteromedially, forming an interpterygoid vacuity (0); pterygoids joined medially forming a pterygoid shield (1).
43. Direction of the pterygoid flange: anterolateral (0); anterior/parasagittal (1).
44. Contact between basiptyergoid processes and pterygoid: sutural (0); fused (1).
45. Position of ventral margin of the pterygovomerine keel relative to alveolar ridge: dorsal (0); level (1).

Updated coding: *Minotaurasaurus* from 0 to ?, *Tianzhenosaurus* from 1 to ?. Notes: The pterygovomerine keel is broken in *Minotaurasaurus*, and so this character cannot be coded for this taxon. The extent and preservation of the vomer is unclear from the figures in Pang and Cheng [6].

46. Dorsal extent of median vomer lamina: does not meet skull roof (0); meets skull roof (1).
47. Pterygoid foramen: absent (0); present (1).

Updated coding: *Tarchia* from 0 to 1, *Tianzhenosaurus* from 0 to ?. Notes: This feature is present in the holotype and only known skull of *Tarchia*. It is unclear from the figures in Pang and Cheng (1998) if this feature is present in *Tianzhenosaurus*.

48. Position of posterior margin of pterygoid body relative to the anterior margin of the quadrate condyle: anteriorly positioned (0); in transverse alignment (1).

Updated codings: *Tianzhenosaurus* from 0 to 1.

49. Posteroventral secondary palate: absent (0); present (1).
50. Posterior palatal foramen: absent (0); present (1).

Updated codings: *Saichania* from 0 to 1, *Tsagantegia* from ? to 0, *Tianzhenosaurus* from 0 to ?.

51. Direction of paroccipital process extension: posterolateral (0); lateral (1).
52. Depth of the distal end of paroccipital processes: expanded (0); not expanded (1).

Updated codings: *Saichania* from 0 to 1; *Talarurus* from 0 to ?; *Tsagantegia* from ? to 0. Notes: The paroccipital processes are not noticeably expanded in *Saichania*, although the definition of 'expanded' versus 'not expanded' should probably be clarified. The paroccipital processes are broken in the holotype skull PIN 557 of *Talarurus* and in referred specimen PIN 3780/1. They are slightly expanded in *Tsagantegia*, although again this could be better described as being downturned distally.

53. Thickness of bone at the dorsal margin of the foramen magnum relative to surrounding bone: little difference (0); distinctly thickened (1).
Updated codings: *Euoplocephalus* from 0 to 1.
54. Bones forming the occipital condyle: basioccipital and exoccipital (0); basioccipital only (1).
Updated codings: *Ankylosaurus* from 0 to 1, *Euoplocephalus* from 0 to 1, *Minotaurasaurus* from ? to 1, *Nodocephalosaurus* from 0 to 1, *Saichania* from 0 to 1, *Tarchia* from 0 to 1, *Talarurus* from 0 to 1, *Tsagantegia* from 0 to 1, *Tianzhenosaurus* from 0 to ?.
55. Form of the ventral surface of basioccipital-basisphenoid region of the braincase: transversely convex (0); has a medial depression (1); has a medial longitudinal ridge (2).
56. Length of basisphenoid relative to the basioccipital: longer (0); shorter or equal (1).
Updated codings: *Minotaurasaurus* from ? to 1. Notes: The basisphenoid and basioccipital are preserved in *Minotaurasaurus*, and so this feature can be coded.
57. Form of basisphenoidal tuberosities: medially separated rounded rugose stubs (0); continuous transverse rugose ridge (1).
58. Size of basiptyergoid processes: twice as long as wide or over (0); less than twice as long as wide (1).
Updated codings: *Minotaurasaurus* from ? to 1, *Tsagantegia* from ? to 1. Notes: The basiptyergoid processes are preserved in *Minotaurasaurus* and *Tsagantegia*, and so this feature can be coded.
59. Form of the cranial nerve foramina IX-XII: separate foramina (0); single foramen shared with the jugular vein (1).
60. Degree of endocranial flexure: strong (0); weak (1).
61. Direction of occipital condyle: posterior (0); posteroventral (1).
Updated codings: *Tarchia* from 0 to 1.
62. Direction of the foramen magnum: posterior (0); posteroventral (1).
63. Premaxillary teeth: present (0); absent (1).
64. Cingula on maxillary and/or dentary teeth: absent (0); present (1).
Updated codings: *Tianzhenosaurus* from 1 to ?. It is unclear from the figures in Pang and Cheng [6] if this feature is present in *Tianzhenosaurus*.

65. Maxillary and/or dentary tooth crown shape: ≥ 13 denticles, tooth crown pointed (0); < 13 denticles, tooth crown rounded (1).

66. Number of dentary teeth: < 25 (0); ≥ 25 (1).

Updated codings: *Tsagantegia* from ? to 0; *Tianzhenosaurus* from 0 to ?. Notes: Pang and Cheng (1998:330) state that "...13 relatively complete teeth and three broken tooth bases are preserved", but it is unclear if this refers only to preserved teeth and partial teeth, or tooth alveoli. This also cannot be determined from the figures in Pang and Cheng (1998).

67. Position of mandible articulation relative to mandibular adductor fossa: posterior (0); posteromedial (1).

Updated codings: *Tianzhenosaurus* 1 to ?. Notes: The mandible is preserved but not figured.

68. Mandibular fenestra: present (0); absent (1).

Updated codings: *Tianzhenosaurus* 1 to ?. Notes: The mandible is preserved but not figured, and the presence or absence of the fenestra is not mentioned.

69. Depth of the dentary symphyseal ramus relative to half the maximum depth of the mandibular ramus in lateral view: deeper (0); shallower (1).

Updated codings: *Minotaurasaurus* from ? to 1, *Tianzhenosaurus* 1 to ?. Notes: Both dentaries are preserved in *Minotaurasaurus*, and so this feature can be coded. The mandible is preserved in *Tianzhenosaurus* but not figured, and this feature is not explicitly described.

70. Shape of dorsal margin of the dentary in lateral view: straight (0); sinuous (1).

Updated codings: *Tianzhenosaurus* 1 to ?. Notes: The dentary is preserved but not figured, and this feature is not explicitly described.

71. Shape of ventral margin of the dentary in lateral view: straight (0); sinuous (1).

Updated codings: *Euoplocephalus* from 1 to 0, *Tianzhenosaurus* 1 to ?. Notes: The dentary is preserved in *Tianzhenosaurus* but not figured, and this feature is not explicitly described.

72. Shape of the alveolar margin: weakly convex (0); strongly convex (1).

73. Development of the coronoid process: not developed (0); distinct (1).

74. Position of glenoid for quadrate relative to mandibular axis: medially offset (0); in line (1).

75. Size and projection of the retroarticular process: small with no dorsal projection (0); well developed with a dorsal projection (1).
76. Size of prementary ventral process: distinct, prong-shaped process (0); rudimentary eminence (1).
77. Ornamentation, defined as sculpturing of skull bones or addition of osteoderms (caputegulae): absent (0); present (1).
78. Cranial armour pattern: amorphous, rugose (0); pattern of polygons covering the skull roof (1).

Updated codings: *Tsagantegia* from 0 to 1; *Dyoplosaurus* from 0 to ?. Notes: Although the drawings of the holotype skull (MPC 700/17) of *Tsagantegia* in Tumanova [12] show amorphous cranial ornamentation, firsthand examination of the skull indicates that there are distinct low-relief polygons covering the skull roof. In the holotype of *Dyoplosaurus*, only the parietal region of the skull is preserved. Distinct polygons are generally not present in this region of the skull in *Euoplocephalus* and it is possible that *Dyoplosaurus* was similar in this regard. As such, this feature cannot be coded for *Dyoplosaurus*.

79. Distribution of polygons on skull roof: random (0); symmetrical (1).
80. A single large medial polygon of ornamentation in the parietal region: absent (0); present (1).

Updated codings: *Dyoplosaurus* from ? to 0. Notes: The parietal region of *Dyoplosaurus* is preserved, allowing this character to be coded.

81. A single medial polygon located posteriorly to the external nares: absent (0); present (1).
82. Surface of polygonal ornamentation on the dorsal surface of the skull: flat (0); domed (1).

Updated codings: *P. grangeri* from ? to 1; *Talarurus* from 0 to 1. Notes: Juvenile *P. grangeri* lack polygonal ornamentation on the dorsal surface of the skull, but the holotype skull AMNH 6523, of a larger, presumably adult individual, clearly preserves domed caputegulae on the skull surface. The holotype of *Talarurus* PIN 557 preserves distinctly domed cranial caputegulae.

83. Projection of postorbital/squamosal 'horns' relative to the posterior margin of the dorsal surface of the skull: horns end anteriorly (0); horns extend posteriorly beyond skull roof (1).

Updated codings: *Nodocephalosaurus* from ? to 1, *Tianzhenosaurus* from 0 to 1. Notes: Although the skull is crushed, the squamosal horns clearly project posteriorly beyond the nuchal shelf of *Nodocephalosaurus*.

- 84. Postorbital/squamosal 'horn': absent (0); present (1).
- 85. Shape of postorbital/squamosal 'horn': rounded (0); pyramidal (1).
- 86. Quadratojugal 'horn': absent (0); present (1).
- 87. Shape of quadratojugal 'horn': rounded (0); pyramidal (1).
- 88. Raised nuchal sculpturing, defined as a transversely expanded region of ornamentation at the posterior margin of the skull roof: absent (0); present (1).

Updated codings: *Minotaurasaurus* from 0 to 1; *Dyoplosaurus* from ? to 1. Notes: The nuchal shelf is preserved in both of these taxa, and both taxa have raised nuchal sculpturing.

- 89. Posterior projection of the nuchal shelf: does not obscure occiput in dorsal view (0); obscures occiput in dorsal view (1).
- 90. Length of mandibular osteoderm (caputegulum) with respect to the length of the mandible: less than or equal to half the length (0); over three quarters the length (1).
- 91. Mandibular osteoderm (caputegulum): absent (0); present (1).
- 92. Type of contact between the atlantal neural arch and intercentrum: open (0); fused in adult (1).

Updated codings: *Tianzhenosaurus* 1 to ?.

- 93. Type of contact between the atlantal neural arches: no median contact (0); median contact (1).

Updated codings: *Tianzhenosaurus* 1 to ?.

- 94. Contact between atlas and axis: articulated (0); fused (1).
- 95. Dimensions of cervical vertebrae centra: anteroposteriorly longer than transverse width (0); anteroposteriorly shorter than transverse width (1).

Updated codings: *Tianzhenosaurus* 1 to ?.

- 96. Ratio of maximum neural spine width to height in anterior cervicals: <0.25 (0); ≥0.25 (1).

Updated codings: *Tianzhenosaurus* 1 to ?.

- 97.** Alignment of anterior and posterior faces of cervical centra: aligned (0); anterior face dorsal to posterior face (1); anterior face ventral to posterior face (2).
- 98.** Ratio of anteroposterior (dorsal vertebra) centrum length to posterior centrum height: >1.1 (0); <1.1 (1).
Updated codings: *Tianzhenosaurus* 1 to ?.
- 99.** Longitudinal keel on ventral surface of dorsal centra: present (0); absent (1).
Updated codings: *P. grangeri* from ? to 1. Notes: a longitudinal keel is present on the ventral surface of dorsal centra in referred *P. grangeri* specimen PIN 614.
- 100.** Cross sectional shape of neural canal in posterior dorsals: circular (0) elliptical, with long axis running dorsoventrally (1).
Updated codings: *Saichania* from 0 to ?. Notes: Although a second specimen (MPC 100/1305) has been referred to *Saichania* by Carpenter et al. [16], it is currently unclear if there are shared diagnostic features between this specimen and the holotype (MPC 100/151). Additionally, although dorsal vertebrae are preserved in the holotype, they were not figured by Maryńska [17] and no reference is made to the shape of the neural canal. The postcrania of MPC 100/151 was not examined firsthand by VMA or PJC and so this character cannot be verified for *Saichania*.
- 101.** Shape of the proximal cross-section of the dorsal ribs: triangular (0); 'L'- or 'T'-shaped (1).
Updated codings: *Tianzhenosaurus* 1 to ?.
- 102.** Attachment of dorsal ribs to posterior dorsal vertebrae: articulated (0); fused (1).
Updated codings: *Tianzhenosaurus* 1 to ?.
- 103.** Contact between most posterior dorsal vertebrae: articulated (0); fused to form a presacral rod (1).
- 104.** Paravertebrae: absent (0); present (1).
- 105.** Longitudinal groove in ventral surface of the sacrum: absent (0); present (1).
Updated codings: *Tianzhenosaurus* 1 to ?.
- 106.** Number of sacral vertebrae: 5 (0); 4 (1); 3 (2).
- 107.** Ratio of maximum distal width to height of the neural spines of proximal caudals: ≤ 0.2 (0); > 0.2 (1).
Updated codings: *Tianzhenosaurus* 1 to ?.

- 108.** Direction of the transverse processes of proximal caudals: anterolaterally projecting (0); posterolaterally projecting (1); laterally projecting (2).
- Updated codings: *Ankylosaurus magniventris* from 2 to 0; *Edmontonia* 0 to 2, *Euoplocephalus* from 1 to 0; *Nodocephalosaurus* from 1 to 0. Notes: In *Ankylosaurus*, *Euoplocephalus*, and *Nodocephalosaurus*, the transverse processes of the free caudals project anterolaterally from the centrum. In *Edmontonia*, the transverse processes project laterally.
- 109.** Length of transverse processes relative to neural spine height in proximal caudals: sub-equal (0); approximately twice the length (1).
- Updated codings: *Euoplocephalus* from 1 to 0, *Tianzhenosaurus* 1 to ?. Notes: Although the proportions may change slightly along the vertebral column, the transverse processes are usually almost as long as the neural spine is high in *Euoplocephalus*.
- 110.** Persistence of transverse processes down the length of the caudal series: not present beyond the mid-length of the series (0); present beyond the mid-length of the series (1).
- 111.** Attachment of haemal arches to their respective centra: articulated (0); fused (1).
- Updated codings: *Nodocephalosaurus* from 0 to ?; *P. grangeri* from ? to 1, *Tianzhenosaurus* from 1 to ?. Notes: Caudal vertebrae have been referred to *Nodocephalosaurus* by Sullivan and Fowler (2006), but these were isolated elements unassociated with other, more diagnostic material, from the same formation as the holotype specimen. As such, it seems best to code this character as unknown for *Nodocephalosaurus* at present. Caudal centra with preserved haemal arches are present in *P. grangeri* referred specimen PIN 614.
- 112.** Shape of distal caudal postzygapophyses: short with a sub-triangular end (wedge-shaped) (0); long with a rounded end (tongue shaped) (1).
- Updated codings: *Dyoplosaurus* from ? to 1, *Pinacosaurus mephistocephalus* from ? to 1, *Saichania* from 1 to ?. A tail club is preserved in ROM 784 and has the typical handle vertebrae of other ankylosaurids. A tail club is also preserved in *Pinacosaurus mephistocephalus* and has modified distal caudal vertebrae. An isolated tail club has been referred to *Saichania*, but no tail club is preserved with the holotype material.
- 113.** Extent of pre- and postzygapophyses over their adjacent centra in posterior vertebrae: extend over less than half the length of the adjacent centrum (0); extend over more than half the length of the adjacent centrum (1).

Updated codings: *Saichania* from 1 to ?. Notes: An isolated tail club has been referred to *Saichania*, but no tail club is preserved with the holotype material.

- 114.** Shape of the posterior haemal arches: rounded haemal spine in lateral view with no contact between haemal arches (0); inverted 'T'-shaped haemal spine in lateral view, with contact between the ends of adjacent spines (1).

Updated codings: *Pinacosaurus mephistocephalus* from ? to 1, *Saichania* from 1 to ?, *Tianzhenosaurus* from 1 to ?. A tail club handle is preserved in *Pinacosaurus mephistocephalus*. An isolated tail club has been referred to *Saichania*, but no tail club is preserved with the holotype material. The tail club of *Tianzhenosaurus* was not figured or described.

- 115.** Ossified tendons in distal region of tail: absent (0); present (1).

Updated codings: *Saichania* from 1 to ?, *Tianzhenosaurus* from 1 to ?. An isolated tail club has been referred to *Saichania*, but no tail club is preserved with the holotype material.

- 116.** Dimensions of coracoid: longer than wide (0); wider than long or equal width and length (1).

- 117.** Form of the anterior margin of the coracoid: convex (0); straight (1).

- 118.** Anteroventral process of coracoid: absent (0); present (1).

- 119.** Size of coracoid glenoid relative to scapula glenoid: sub-equal (0); half the size (1).

Updated codings: *Pinacosaurus grangeri* from ? to 0.

- 120.** Contact between scapula and coracoid: articulated (0); fused (1).

- 121.** Scapula glenoid orientation: ventrolateral (0); ventral (1).

Updated codings: *Tianzhenosaurus* from 1 to ?.

- 122.** Ventral process of scapula at the posteroventral margin of glenoid: absent (0); present (1).

Updated codings: *Saichania* from ? to 1; *P. grangeri* from ? to 1. Notes: The scapula is preserved in the holotype specimen of *Saichania*, and a scapula is known in *P. grangeri* referred specimen PIN 614.

- 123.** Form of the scapula acromion process: not developed or ridge-like along the dorsal border of the scapula (0); flange-like and folded over towards the scapula glenoid (1); ridge terminating in a knob-like eminence (2).

Updated codings: *Tianzhenosaurus* from 1 to ?.

- 124.** Orientation of the acromion process of scapula: directed away from the glenoid (0); directed towards scapula glenoid (1).
Updated codings: *Tianzhenosaurus* from 1 to ?.
- 125.** Scapulocoracoid buttress: absent (0); present (1).
Updated codings: *Talarurus* from ? to 0. Notes: See PIN 557.
- 126.** Distal end of scapula shaft: narrow (0); expanded (1).
Updated codings: *Talarurus* from 1 to 0, *Tianzhenosaurus* from 1 to ?. Notes: In specimen PIN 557, the scapula is narrow distally.
- 127.** Contact between sternal plates: separate (0); fused (1).
- 128.** Separation of humeral head and deltopectoral crest in anterior view: continuous (0); separated by a distinct notch (1).
Updated codings: *Talarurus* from ? to 0. Notes: See PIN 557.
- 129.** Separation of humeral head and medial tubercle in anterior view: continuous (0); separated by a distinct notch (1).
Updated codings: *Talarurus* from ? to 0, *Euoplocephalus* from 1 to 0. Notes: See PIN 557 for *Talarurus*.
- 130.** Ratio of deltopectoral crest length to humeral length: ≤ 0.5 (0); > 0.5 (1).
Updated codings: *Tianzhenosaurus* from 1 to ?.
- 131.** Orientation of deltopectoral crest projection: lateral (0); anterolateral (1).
Updated codings: *Tianzhenosaurus* from 0 to ?.
- 132.** Shape of the radial condyle of humerus round / proximal end of radius in end-on view: non-circular (0); circular (1).
Updated codings: *Tianzhenosaurus* from 0 to ?.
- 133.** Ratio of the length of metacarpal V to metacarpal III: ≤ 0.5 (0); > 0.5 (1).
Updated codings: *Tianzhenosaurus* from 1 to ?.
- 134.** Manual digit number: 5 (0); 4 (1); 3 (2).
Updated codings: *Tarchia* from 1 to ?, *Tianzhenosaurus* from 1 to ?. Notes: The manus is unknown for *Tarchia*.

- 135.** Shape of manual and pedal ungual phalanges: claw shaped (0); hoof shaped (1).
Updated codings: *Dyoplosaurus* from ? to 1, *Edmontonia* from 0 to 1, *Tianzhenosaurus* from 1 to ?. Notes: The pedal unguals are preserved in ROM 784.
- 136.** Length of the preacetabular process of ilium as a percentage of total ilium length: $\leq 50\%$ (0); $> 50\%$.
Updated codings: *Dyoplosaurus* from 0 to ?, *Tianzhenosaurus* 1 to ?. Notes: The preacetabular process of the ilium of ROM 784 is broken, and so this character cannot be coded for *Dyoplosaurus*.
- 137.** Angle of lateral deflection of the preacetabular process of the ilium: 10° – 20° (0); 45° (1).
Updated codings: *Pinacosaurus mephistocephalus* from 0 to 1; *Dyoplosaurus* from 0 to 1, *Tianzhenosaurus* from 1 to ?.
- 138.** Orientation of the preacetabular portion of the ilium: near vertical (0); near horizontal (1).
Updated codings: *Tianzhenosaurus* from 1 to ?.
- 139.** Form of the preacetabular portion of the ilium: straight process (0); pronounced ventral curvature (1).
Updated codings: *Tianzhenosaurus* from 1 to ?.
- 140.** Lateral exposure of the acetabulum: exposed (0) acetabulum partially obscured as it is partially encircled by the distal margin of the ilium (1).
Updated codings: *Pinacosaurus mephistocephalus* from 0 to ?; *Tarchia* from 1 to ?; *Saichania* from 1 to ?, *Tianzhenosaurus* 1 to ?. Notes: The pelvis is not known for *Tarchia* or *Saichania*, and so this character cannot be coded. The pelvis is preserved in *Pinacosaurus mephistocephalus*, but it cannot be determined from the photographs in Godefroit et al. (1999) how this feature should be coded.
- 141.** Perforation of the acetabulum: present, open acetabulum (0); absent, closed acetabulum (1).
Updated codings: *Tianzhenosaurus* from 1 to ?.
- 142.** Postacetabular ilium length, relative to diameter of acetabulum: greater (0); smaller (1).
Updated codings: *Pinacosaurus grangeri* from ? to 1, *Tianzhenosaurus* from 1 to ?. Notes: The postacetabular process is shorter than the length of the acetabulum in specimen PIN 614 of *Pinacosaurus grangeri*.

- 143.** Pubis size: large (0); reduced (1).
Updated codings: *Euoplocephalus* from 1 to ?, *Tianzhenosaurus* from 1 to ?. Notes: A pubis is unknown for any specimen of *Euoplocephalus*.
- 144.** Prepubic process: present (0); absent (1).
Updated codings: *Euoplocephalus* from 1 to ?, *Tianzhenosaurus* from 1 to ?. Notes: A pubis is unknown for any specimen of *Euoplocephalus*.
- 145.** Structure and rotation of the body of the pubis: gracile without dorsolateral rotation (0); massive and dorsolaterally rotated (1).
Updated codings: *Euoplocephalus* from 1 to ?. Notes: A pubis is unknown for any specimen of *Euoplocephalus*.
- 146.** Size of pubic contribution to acetabulum: over 25 % (0); less than 25 % (1).
Updated codings: *Euoplocephalus*, *Saichania*, *Talarurus*, and *Tarchia*, from 1 to ?. Notes: A pubis is unknown in all of these taxa, and so this character cannot be coded.
- 147.** Shape of ischium: straight (0); ventrally flexed at mid-length (1).
Updated codings: *Dyoplosaurus* from ? to 0, *Tianzhenosaurus* from 0 to ?. Notes: Although the shafts are broken at the midlength of each ischium, the ischia of ROM 784 would have been straight.
- 148.** Shape of the dorsal margin of ischium: straight or concave (0); convex (1).
Updated codings: *Tianzhenosaurus* from 1 to ?.
- 149.** Angle between long axis of femoral head and long axis of shaft: <100° (0); 100° to 120° (1); >120° (2).
Updated codings: *Ankylosaurus* from 1 to 2, *Pinacosaurus grangeri* from 1 to 2, *Euoplocephalus* from 1 to 2. Notes: *Euoplocephalus* estimated from AMNH 5404. *Ankylosaurus* estimated from Carpenter (2004).
- 150.** Separation of femoral head from greater trochanter: continuous (0); separated by a distinct notch or change in slope (1).
Updated codings: *Tianzhenosaurus* from 1 to ?.
- 151.** Differentiation of the anterior trochanter of the femur: separated from femoral shaft by a deep groove laterally and dorsally (0); fused to femoral shaft (1).
Updated codings: *Tianzhenosaurus* from 1 to ?.

- 152.** Oblique ridge on lateral femoral shaft, distal to anterior trochanter: absent (0); present (1).
Updated codings: *Dyoplosaurus* from ? to 0. Notes: the femur is preserved in ROM 784, so this character can be coded.
- 153.** Form of the fourth trochanter: pendant (0); ridge-like (1).
Updated codings: *Dyoplosaurus* from ? to 1, *Tianzhenosaurus* from 1 to ?. Notes: the femur is preserved in ROM 784, so this character can be coded.
- 154.** Location of the fourth trochanter on the femoral shaft: proximal (0) distal, over half-way down the femoral shaft (1).
Updated codings: *Dyoplosaurus* from ? to 1, *Tianzhenosaurus* from 1 to ?. Notes: the femur is preserved in ROM 784, so this character can be coded.
- 155.** Maximum distal width of the tibia, compared to the maximum proximal width: narrower (0); wider (1).
Updated codings: *Dyoplosaurus* from ? to 1, *Tianzhenosaurus* from 1 to ?. Notes: the tibia is preserved in ROM 784, so this character can be coded.
- 156.** Contact between tibia and astragalus: articulated (0); fused, with suture obliterated (1).
Updated codings: *Tianzhenosaurus* from 1 to ?.
- 157.** Number of pedal digits: 5 (0); 4 (1); 3 (2).
Updated codings: *P. grangeri* from ? to 2, *Tianzhenosaurus* from 1 to ?. Notes: See description of *Pinacosaurus* manual and pedal elements in Currie et al. [21].
- 158.** Phalangeal number in pedal digit IV: 5 (0); ≤ 4 (1).
- 159.** Parasagittal row of keeled osteoderms situated on the dorsal aspect of the trunk: absent (0); present (1).
Updated codings: *Pinacosaurus mephistocephalus* from ? to 1; *Dyoplosaurus* from ? to 1. Notes: *in situ* osteoderms are preserved in the holotypes of both of these taxa (cervical half rings are osteodermal elements).
- 160.** Large, laterally compressed plates on the dorsal aspect of the trunk: absent (0); present (1).
- 161.** Lateral rows of osteoderms on the dorsal aspect of the trunk: absent (0); present (1).
- 162.** Number of distinct cervical pectoral bands: none (0); one (1); two (2).

Updated codings: changed all ankylosaurids to 2 where both cervical half rings are known. *Tarchia* from 1 to ?. Notes: No cervical half rings are preserved with diagnostic *Tarchia* material.

- 163.** Form of the cervical bands: separate at the midline, forming pairs of quarter rings (0); fused at the midline, forming half rings (1).

Updated codings: *Ankylosaurus magniventris* from 0 to 1. Notes: Firsthand examination of *Ankylosaurus magniventris* AMNH 5895 indicates that the two cervical ring fragments thought to go together by Carpenter [9] do not fit together. Instead, these represent fragments from the first and second cervical rings. Because they do not fit together, there is no reason to assume that *Ankylosaurus magniventris* had 'quarter rings', rather than the typical semicircular half rings found in all other ankylosaurids.

- 164.** Pectoral spikes: absent (0); present (1).

- 165.** Form of pectoral spikes: no grooves and a solid base (0); posterior groove with a hollow base (1).

- 166.** Sacral shield of fused osteoderms: absent (0); present (1).

Updated codings: *Euoplocephalus* from 0 to ?, *Dyoplosaurus* from 0 to ?, *Edmontonia* 1 to ?, *Saichania* from 0 to ?. Notes: There are no specimens that preserve *in situ* sacral osteoderms for *Euoplocephalus*, *Edmontonia*, or *Saichania*. *Dyoplosaurus* preserves osteoderms lateral to the ilia, but not on the dorsal surface.

- 167.** Form of ossicles in sacral armour: irregular ossicles (0); sub-hexagonal ossicles of similar sizes (1).

Updated codings: *Euoplocephalus* from 0 to ?. Notes: There are no specimens that preserve *in situ* sacral osteoderms for *Euoplocephalus*.

- 168.** Size of lateral trunk plates, sacral plates and caudal plates: small (0); large and hollow based (1).

Updated codings: *Euoplocephalus* from 1 to ?, *Tianzhenosaurus* from 1 to ?. Notes: There are no specimens that preserve *in situ* lateral trunk plates, sacral plates, and caudal plates for *Euoplocephalus*.

- 169.** Form of caudal plate: little dorsal projection (0); tall with thin dorsal extremity (1).

Updated codings: *Euoplocephalus* from 0 to ?, *Tianzhenosaurus* from 0 to ?. Notes: There are no specimens that preserve *in situ* caudal osteoderms for *Euoplocephalus*.

- 170.** Tail club: absent (0); present (1).
- 171.** New character (Analysis 3 only): Small (<2 cm diameter), circular caputegulae posterolateral to orbit, along ventral edge of squamosal horn and/or along dorsal edge of quadratojugal horns: absent (0); present (1)
- 172.** New character (Analysis 3 only): Cervical half rings: composed of osteoderms that are either tightly adjacent to one another or coossified at the edges, forming arc over the cervical region (0), composed of osteoderms and underlying bony band segments, osteoderms may or may not coossify to the band, forming arc over the cervical region (1).
- 173.** New character (Analysis 3 only): Composition of first cervical half ring: first cervical half ring has 4 to 6 primary osteoderms only (0), first cervical half ring has 4 to 6 primary osteoderms surrounded by small (<2 cm diameter) circular secondary osteoderms.
- 174.** New character (Analysis 3 only): Form of caudal osteoderms: dorsoventrally compressed, triangular in dorsal view (0), or low cones (1).
- 175.** New character (Analysis 3 only): Tail club knob shape: major knob osteoderms semicircular in dorsal view (1), triangular in dorsal view (2).
- 176.** New character (Analysis 3 only): Tail club knob proportions: tail club knob length > width (1), length = width (2), width > length (3).

Nodocephalosaurus kirtlandensis

111????????0?1????????11110????????????????0111????????????????11?0?1?
1111?????????????????1?0???
??

Pinacosaurus grangeri

111101110111111111110201111101111111100001110101100011101101110111101100111
????11111?101?01?21?1111001?01001111010?1?00?0100100101111011?10?10110101111?
110111000?101

Pinacosaurus mephistocephalus

11110?2001??11?????1??11??1111?0????????????????????1?1110?1?1000??1?????
111111011????????110?1??01?1?1????1111?0??10?10?10100????????????????121?
?0?0?1

Saichania chulsanensis

11110121011110111111121101111011111111000111010100011111?1111011111101111
100111111111111112??011?0?????0?1111?????1??00?0100100101????1?????1?????????????
0111000?101

Scolosaurus cutleri

1111012??111????1?????11?11110111111110?????????11100111?111?10????????????1110?
01111111?????????1??1002?0?01111100101010010?001????11110110????01????11012110?
210?1?101

Talarurus plicatospineus

11110?????1001?1?????????11110??1?????0?????????10?02101011????????????????1100??
011??11??????121?011100100?0111110?1010100?1???100101111011110?101101011111101
1100??101

Tarchia gigantea

1111011101110011111112011111011111111000011011111001111101110111110001111
1001111111111?????????????????011111?????????????10??11????1?????1?????????????
111?0??1?1

Tianzhenosaurus youngi

11110110??111011111?1110111111011111111?00?1?0010100011????11111011?1?????110
0110111111??11011?1?01010010?1011111?????1?00?1??100121111001?10?01?01?11112?1
01??00??101

Tsagantegia longicranialis

1110011010??001111111?011111101111111110001?001?1?0011??0?1111????????????1000
000111111??
??????

Pinacosaurus grangeri

11110110011111111111021112?1101111111110000111010110001110110111011101100111
???111111?101??01?2111111001?0101111101001?100?0100100101111011?10?10120101111?
110111000?101

Pinacosaurus mephistocephalus

11110?2001??111????????112?1111?0????????????????????????????1?1110?1?1000???1?????
111111011????????110?1???011111????1111?0???10?10?1110????????????????????1?121?
?0?0?1

Saichania chulsanensis

11110121011101111111121102?110111111111000111011110111111?11110111111101111
100111111111111112???11?0?????0?????????1?100?0100100101????????????????????1
011100??101

Scolosaurus cutleri

1111012???111??1?????11?1111011111110????????11100111?111?10????????????1110?
01111111????????1???1002?0?01111100101010010?001???11110110????01????11012110?
210?1?101

Talarurus plicatospineus

111101????1001?1????????2?110??1?????0????????1??12101011????????????1100?1
011??11?????121?011100100?0111110?101010000?0010010111101110?01201011111101
1100??101

Tarchia gigantea

11110111011100111111121112?11011111111100001111111011111111110111110001111
1001111111111111????????????????011111????????????10???1????????????????????101
?1?0??1?1

Tianzhenosaurus youngi

11110110??11101?111?1??0112?11011111111?00???01?100?11????111?1????????????1100
11?111111????0????0??1??1???0?11??101??
00????1

Tsagantegia longicranialis

1110011010??00?111111?1112?1101111111110001?0010100111?10?1111?0????????????110
0000111111??
???????

Dyoplosaurus acutosquameus

??1??????????1??????????0????????????????????????????????????1??????????1?????????
??1????????????????1000111?1????????????????0??1?11011?????01201?1111211??????0
?01???011

Euoplocephalus tutus

11110121101111111111121112?11011111111100001111111111110111110111101101111
0000011111111?011?11011100210001111011010100101001001?11110111???0120101111
211011100????1010112

Minotaurasaurus ramachandrani

1111011101?11011111?1??1112?1101101011110000?0101?10110111??1011101111101011110
00111111011??
??????1?????

Nodocephalosaurus kirtlandensis

111??1????????11??????1?2?110?1??11????????????????1111????????????????11?0?11
1111????????????????0??
??0?????

Pinacosaurus grangeri

11110110011111111111021112?11011111111100001110101100011101101110111101100111
???111111?101??01?2111111001?0101111101001?100?0100100101111011?10?10120101111?
110111000?101010012

Pinacosaurus mephistocephalus

11110?2001??111????????112?1111?0????????????????????????????1?1110?1?1000???1?????
1111111011????????110?1??011111????1111?0???10?10?1110????????????????1?121?
?0?0?1010???

Saichania chulsanensis

11110121011110111111121102?110111111111000111011110111111?111110111111101111
100111111111111112???11?0????0?????????1?100?0100100101????????????????1
011100??101011???

Scolosaurus cutleri

1111012???111??1?????11?11110111111110????????11100111?111?10????????????1110?
01111111????????1??1002?0?01????001????????001????11110110????0?????11012110?2
10?1?10?110112

Talarurus plicatospineus

111101????1001?1????????2?110??1?????0????????1??12101011????????????1100?1
011??11?????121?011100100?0111110?101010000?00100101111011110??012010111111101
1100??10101????

Tarchia gigantea

11110111011100111111121112?1101111111100001111111011111111110111110001111
10011111111111????????????????011111????????????10??1????????????????????101
?1?0??1?10??023

Tianzhenosaurus youngi

11110110??11101?111?1??0112?11011111111?00????01?100?11????111?1????????????1100
11?111111????0????0??1??1??0?11??101??
00????1??????

Tsagantegia longicranialis

1110011010??00?111111?1112?1101111111110001?0010100111?10?1111?0????????????110
0000111111??
????????0??????

4. OTHER ANKYLOSAURS FROM NORTH AMERICA

4.1 Introduction

This chapter reviews the taxonomic status of other ankylosaurids from North America (Fig. 4.1) not covered in the revision of *Euoplocephalus tutus* (Chapter 3). These include *Ahshislepelta minor* Burns and Sullivan, 2011, *Ankylosaurus magniventris*, and *Nodocephalosaurus kirtlandensis*, as well as a new ankylosaur from New Mexico. Ankylosaurs assigned to the Stegopeltinae are also reviewed here; the Stegopeltinae has been proposed as a clade of North American ankylosaurs of uncertain affinity united by the presence of a pelvic shield composed of coossified hexagonal osteoderms (Ford 2000). *Cedarpelta* from the Early Cretaceous of Utah, and *Nodocephalosaurus* from the Late Cretaceous of New Mexico seem to share affinities with Mongolian ankylosaurids (Carpenter 2001, Sullivan 1999).

4.2 The Stegopeltinae: *Aletopelta*, *Glyptodontopelta*, and *Stegopelta*

Stegopeltinae was erected by Ford (2000) as a subfamily of the Ankylosauridae. All of the diagnostic characters are based on the morphology of the osteoderms: 'stegopeltine' ankylosaurs have closely appressed hexagonal, pentagonal or quadrilateral dorsal pelvic osteoderms, the medial pectoral osteoderms have solid bases and ridged edges, and the cervical band is composed of three oval, ridged osteoderms. Ford (2000) included within the Stegopeltinae *Stegopelta*, the new genus *Glyptodontopelta*, and an unnamed Californian ankylosaur which would later become *Aletopelta coombsi* Ford and Kirkland, 2001. Ford (2000) suggested that the Stegopeltinae may have represented more basal members of the Ankylosauridae. Hexagonal, closely appressed pelvic osteoderms have a limited distribution within ankylosaurs. Besides *Aletopelta*, *Glyptodontopelta*, and *Stegopelta*, they are otherwise known



Figure 4.1. Map of Canada and the United States (excluding Alaska and the Canadian Arctic Archipelago) showing the locations of taxa discussed in this chapter. Abbreviations: Ahs, *Ahshislepelta minor*; Ale, *Aletopelta coombsi*; Ano, *Anodontosaurus lambei*; Ank, *Ankylosaurus magniventris*; Dyo, *Dyoplosaurus acutosquameus*; Euo, *Euoplocephalus tutus*; Gly, *Glyptodontopelta mimus*; Kai, undescribed Kaiparowits ankylosaurid; Nod, *Nodocephalosaurus kirtlandensis*; Sco, *Scolosaurus cutleri*; Ste, *Stegopelta landerensis*; Tat, *Tatankacephalus cooneyorum*; Zia, *Ziapelta sanjuanensis*.

only in *Antarctopelta oliveroi* Salgado and Gasparini, 2006 and *Nodosaurus textilis* Marsh, 1889, and one isolated cluster of similar osteoderms has been recovered from the Dinosaur Park Formation in Alberta (Arbour et al. 2011). The hypothesis that the presence of this form and arrangement of pelvic osteoderms is diagnostic of a clade of ankylosaurs, and that this clade is nested within the Ankylosauridae, will be tested in Chapter 10.

4.2.1 *Aletopelta coombsi* Ford and Kirkland, 2001

Holotype: SDNHM 33909, eight teeth, fragmentary scapulae, partial humerus, partial ulna, possible fragment of right ?radius, ulna, partial left and possibly right ischium, femora, tibiae, fibulae, four-five partial vertebrae, dorsal neural arch, neural arches of the sacrum, fragmentary ribs, osteoderms including pelvic shield and cervical half ring

Holotype locality and age: College Boulevard between El Camino Real and Palomar Airport Road, northwest of the Palomar-McClellan Airport, Carlsbad, California, SDNHM Locality 3392, 117°15'W, 33°9'N; Point Loma Formation, Upper Campanian.

Original diagnosis: Medium-sized ankylosaurid; teeth wider than tall; femur much longer than tibia and fibula; three metatarsals; pelvic shield of polygonal, low-peaked osteoderms; massive, short-pointed spike in shoulder region; hollow cap-like osteoderms across dorsum; hollow pup-tent-like osteoderms over neck and shoulders; triangular, dorsally compressed caudal osteoderms that are highly asymmetrical top to bottom; most osteoderms hollow and thin.

Discussion: SDNHM 33909 was originally described as an indeterminate nodosaurid that shared some similarities to *Edmontonia*, *Panoplosaurus*, and *Stegopelta*, by Coombs and Deméré (1996). Ford and Kirkland (2001) reassessed the specimen as an ankylosaurid ankylosaur, and, considering it taxonomically distinctive, named it *Aletopelta coombsi*. *Aletopelta* was considered a *nomen dubium* by Vickaryous et al. (2004). It was not included in the most recent comprehensive analysis of ankylosaurian interrelationships by Thompson et al. (2012).

Although the specimen includes elements from many regions of the body, assessing the taxonomic affinities of SDNHM 33909 is hampered by the taphonomic condition of most of the bones. The specimen was preserved in marine sediments, where the skeleton was scavenged by invertebrates and sharks, and acted as the substrate for encrusting pelecypods (Coombs and

Deméré 1996). The articular ends are missing from all of the limb elements, making comparisons with other species difficult. However, *Aletopelta* has hexagonal, closely appressed pelvic osteoderms forming a semi-continuous sheet over the pelvis (Fig. 4.2A, B), a feature found only in a few other North American ankylosaurids, including *Glyptodontopelta* and *Stegopelta*. *Aletopelta* can be differentiated from *Stegopelta* by the morphology of the cervical half ring (Fig. 4.2C). Although it is not clear if the first or second cervical half ring is represented in either *Aletopelta* or *Stegopelta*, the cervical half ring of *Stegopelta* appears to be composed of closely appressed adjacent osteoderms without an underlying band of bone, whereas the cervical half ring of *Aletopelta* is composed of osteoderms coossified to an underlying bony band. *Aletopelta* can be differentiated from *Glyptodontopelta* based on the surface texture of the osteoderms: in *Glyptodontopelta*, the pelvic osteoderms have a series of shallow furrows forming a dendritic pattern, whereas in *Aletopelta* the osteoderms have randomly distributed shallow pores and pits. The pelvic osteoderms of *Aletopelta* also vary more widely in size and shape compared to *Glyptodontopelta* and *Stegopelta*, and the osteoderms do not appear to be as tightly fused together compared to these taxa.

Ford and Kirkland (2001) considered SDNHM 33909 to share more similarities with ankylosaurids than with nodosaurids: the 4th trochanter is proximal to the femoral midlength as in ankylosaurids, the ischium does not appear to be bent as in nodosaurids, the deltopectoral crest expands more sharply than in nodosaurids, the proportions of the tibia and fibula were more similar to those of ankylosaurids, and there are some osteoderm morphologies that are present in ankylosaurids but not in nodosaurids. In the absence of a phylogenetic analysis, it is difficult to assign *Aletopelta* to either the Ankylosauridae or Nodosauridae, because the holotype has a mixture of features typically considered characteristic of both clades. Coombs (1978a) considered a proximally located 4th trochanter to be characteristic of nodosaurids, noting that

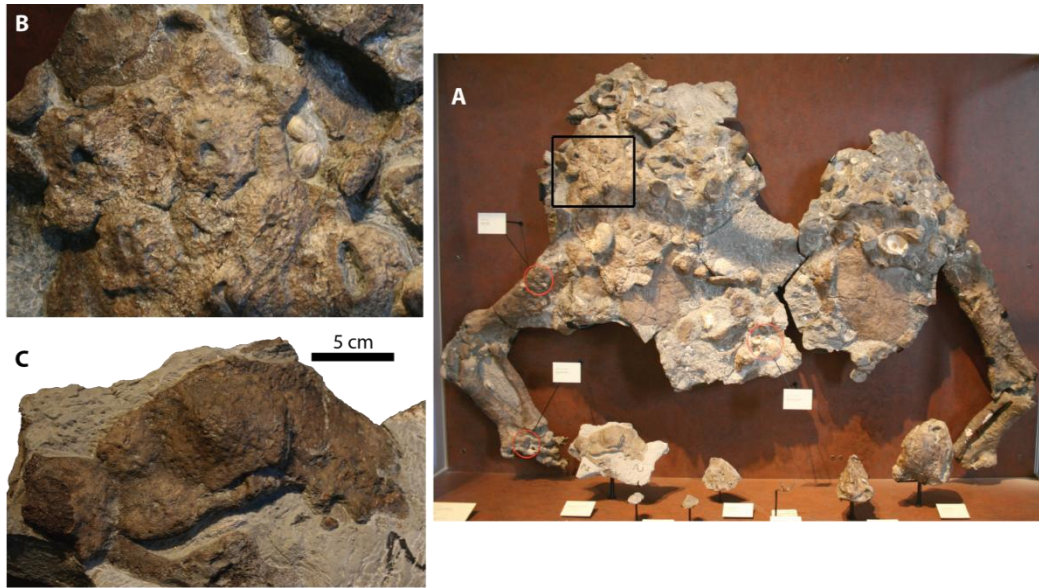


Figure 4.2. SDNHM 33909, holotype of *Aletopelta coombsi*. A) Articulated pelvis and hindlimbs on display, in dorsal view; osteoderms and teeth are mounted towards the bottom of the photograph. B) Closeup of the pelvic shield osteoderms in the box in A. C) Portion of a cervical half ring, external view.

the 4th trochanter of ankylosaurids was typically distal to the midlength of the femur. Therefore, the proximally located 4th trochanter of *Aletopelta* is more similar to the condition in nodosaurids, not ankylosaurids, although it should be noted that the position of the 4th trochanter in SDNHM 33909 is somewhat ambiguous because the proximal and distal ends of the femur are eroded and damaged. The large, spike-like osteoderm, if correctly identified as such, is unlike large osteoderms in other ankylosaurids, which tend to be more flattened and triangular, but is similar to the large, conical spikes of some nodosaurids. On the other hand, the cervical half ring includes an underlying bony band to which the overlying osteoderms are fused, which is more characteristic of ankylosaurids. The distal caudal osteoderms of SDNHM 33909 are not elongated and interlocking as in derived ankylosaurids, and *Aletopelta* most likely did not have a tail club. A revised skeletal reconstruction is presented in Figure 4.3 based on firsthand examination of SDNHM 33909, with the absence of a tail club being the most important difference between this reconstruction and that presented by

Ford and Kirkland (2001). The higher-level taxonomic assignment of *Aletopelta* will be assessed in the revised phylogenetic analysis in Chapter 10.

Status: Valid

Revised Diagnosis: Ankylosaur with hexagonal pelvic osteoderms forming semi-continuous sheet over the pelvis. Unlike *Glyptodontopelta*, pelvic osteoderms do not have dendritic surface texture. Unlike *Stegopelta*, first cervical half ring is composed of osteoderms fused to underlying bony band, not closely appressed adjacent osteoderms.

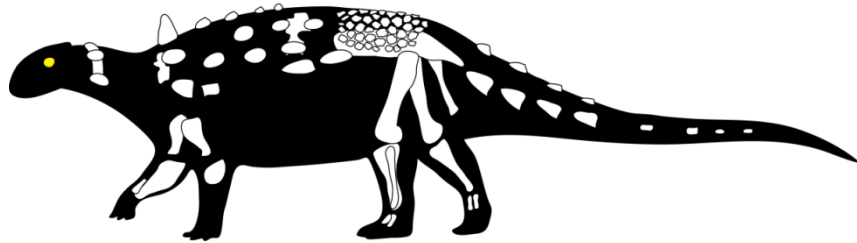


Figure 4.3. Preserved elements of SDNHM 33909, holotype of *Aletopelta coombsi*.

4.2.2 *Glyptodontopelta mimus* Ford, 2000

= *Edmontonia australis* Ford, 2000

Holotype: USNM 8610, coossified pelvic osteoderms (portion of pelvic shield), isolated thoracic and pelvic osteoderms, osteoderm fragments from cervical/pectoral rings.

Holotype locality and age: Barrel Springs Arroyo (De-na-zin Wash), 1.5 km southwest of Ojo Alamo Store, San Juan County, New Mexico, USA. Naashobito Member, Ojo Alamo Formation (early Maastrichtian, Late Cretaceous).

Referred specimens: NMMNH P-14266, two nearly complete lateral spines and numerous thoracic and cervical/pectoral osteoderm fragments; NMMNH P-25063, holotype of *E. australis*, pair of complete medial cervical osteoderms; NMMNH P-27420, complete right thoracic osteoderm; NMMNH P-27450, complete left medial cervical osteoderm; NMMNH P-27849, one fragmentary thoracic osteoderm and a fragmentary pelvic osteoderm; SMP VP-1147, complete

tertiary cervical/pectoral osteoderm; SMP VP-1319, incomplete lateral cervical/pectoral osteoderm; SMP VP-1580, 71 nearly complete osteoderms, numerous fragmentary osteoderms, and indeterminate postcranial fragments; SMP VP-1640, two incomplete osteoderms; SMP VP-1731, incomplete lateral osteoderm; SMP VP-1825, incomplete lateral thoracic osteoderm; SMP VP-1826, two osteoderm fragments; SMP VP-1831, one thoracic osteoderm; SMP VP-1832, one thoracic osteoderm; SMP VP-1863, one thoracic osteoderm; SMP VP-2026, osteoderm fragments; SMP VP-2067, one complete pelvic osteoderm with other osteoderm and indeterminate postcranial fragments; SMP VP-2077, incomplete rectangular, lateral cervical/pectoral osteoderm, complete pelvic osteoderm, and other osteoderm fragments; SMP VP-2109, one osteoderm fragment; USNM 8611, several osteoderm fragments (from Burns 2008).

Previous diagnoses: From Ford (2000): Large, asymmetric, irregularly hexagonal, pentagonal, or quadrilateral osteoderms with flat surfaces or low ridges, forming a solid shield over the pelvis. From Burns (2008): Nodosaurid ankylosaur with osteoderms with a distinctive dendritic pattern consisting of vascular furrows radially directed away from the keel, with randomly distributed small pits and pores; medial cervical osteoderms are rectangular with rounded edges and a medially-located keel.

Discussion: *Glyptodontopelta* is known almost exclusively from pelvic osteoderms (Fig. 4.4). Ford (2000) differentiated *Glyptodontopelta* from *Stegopelta* primarily on the basis of stratigraphy, as the two holotypes were separated in time by about 24 million years. This great a separation in time does support the hypothesis that *Glyptodontopelta* is distinct from *Stegopelta*, but stratigraphic position should not be used to diagnose species alone.

Glyptodontopelta was reassessed as a nodosaurid ankylosaur by Burns (2008) based on the presence of rectangular, articulating cervical/pectoral osteoderms, and the histology of the osteoderms; *Glyptodontopelta* osteoderms had nodosaurid-type internal structures consisting of a thick external layer of

compact bone with numerous structural fibers, and internal, basally situated trabecular bone. Burns (2008) also identified a unique characteristic of *Glyptodontopelta*, namely the dendritic surface texture of the osteoderms, which is unknown in other North American ankylosaurs. Although Burns (2008) did not directly compare *Glyptodontopelta* with *Aletopelta* and *Stegopelta*, the pelvic osteoderms of *Aletopelta* and *Stegopelta* do not appear to have the dendritic texture of *Glyptodontopelta*, supporting their non-synonymy. Isolated pelvic osteoderms with a similar overall morphology from the Dinosaur Park Formation of Alberta (NHMUK R4456, Arbour et al. 2011) do not have a dendritic surface texture, suggesting that the Dinosaur Park Formation specimen also does not represent *Glyptodontopelta*.

Status: Valid.

Revised Diagnosis: Ankylosaur with hexagonal, closely appressed pelvic osteoderms. Uniquely among ankylosaurs, osteoderms have distinctive dendritic pattern consisting of vascular furrows radially directed away from the keel, with randomly distributed small pits and pores.

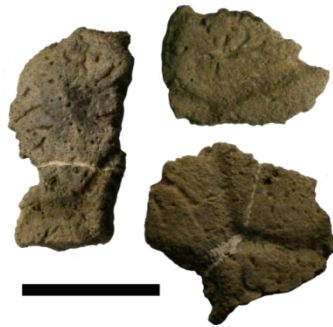


Figure 4.4. Pelvic shield osteoderms of USNM 8611, *Glyptodontopelta mimus*. Scale equals 2 cm.

4.2.3 *Stegopelta landerensis* Williston, 1905

Holotype: FMNH UR88, ?maxilla with 3 partial alveoli, ?indeterminate skull fragments, seven cervical vertebrae, two dorsal vertebrae, portions of the synsacrum, proximal caudal centrum, distal caudal centrum, parts of both scapulae, both humeral heads, proximal end of left ulna, proximal ends of both radii, parts of both ilia, distal end of tibia, metacarpal, metatarsal, possible

bifurcated pectoral osteoderm, half of a cervical half ring, post-cervical osteoderms.

Holotype locality and age: Near Conant Creek, T33N R93W r R94W, Fremont County, Wyoming. Frontier Formation, base of the Belle Fourche Member (about 97 Ma, or Cenomanian, according to Kirschbaum and Roberts 2005).

Previous diagnoses: From Carpenter and Kirkland (1998): Axis uniquely long, slender, strongly compressed laterally; mid- and posterior cervical centra with paired deep fossae separated by horizontal ridge for the capitulum of cervical (also present in *Texasetes pleurohalio* Coombs, 1995b); neural arch of dorsals flush with or overhanging anterior articular surface, unlike inset condition in other nodosaurids; dorsal centrum cylindrical as in *Struthiosaurus* and *Mymoorapelta*, but not strongly constricted as in *Sauropelta*, *Gastonia*, *Polacanthus*, or *Edmontonia*; acromion process centrally located high on scapular blade as in *Panoplosaurus* but unlike in *Sauropelta*; pelvic osteoderms hexagonal and closely appressed, but smaller than similar osteoderms of *Nodosaurus*.

Discussion: *Stegopelta* was named in a brief paper by Williston (1905), described in detail by Moodie (1910), and synonymized with *Nodosaurus* by Coombs (1978a). Carpenter and Kirkland argued that *Stegopelta* was distinct from *Nodosaurus*. *Stegopelta* shares with *Aletopelta* and *Glyptodontopelta* hexagonal pelvic osteoderms that form a sheet over the pelvis. Unlike *Glyptodontopelta*, the pelvic osteoderms of *Stegopelta* do not appear to have a dendritic surface texture, instead having a lightly pitted surface texture. *Stegopelta* can be differentiated from *Aletopelta*, which has a similar pelvic osteoderm morphology and texture, by the morphology of the cervical half ring. The partial cervical half ring preserved in *Stegopelta* has closely appressed adjacent osteoderms not fused to an underlying band of bone. In *Aletopelta*, the cervical half ring is composed of osteoderms coossified to an underlying bony band.

Status: Valid.

Revised Diagnosis: Ankylosaurian dinosaur with pelvic shield composed of hexagonal coossified osteoderms, and cervical half ring osteoderms not fused to an underlying band. Differs from *Glyptodontopelta* in the surface texture of the pelvic osteoderms, which lack the dendritic texture present in *Glyptodontopelta*.

4.3 Other ankylosaurids or putative ankylosaurids from North America

4.3.1 *Ahshislepelta minor* Burns and Sullivan, 2011

Holotype: SMP VP-1930, associated incomplete postcranial skeleton, including both scapulocoracoids, left humerus, proximal portion of left radius, vertebral fragments, osteoderms, and unidentifiable fragments.

Holotype locality and age: Ah-shi-sle-pah Wash, San Juan County, New Mexico, USA, southwest $\frac{1}{4}$ of S8, T22N, R10W (UTM coordinates on file at SMP). Kirtland Formation, Hunter Wash Member, San Juan Basin, New Mexico; Late Campanian, Late Cretaceous.

Diagnosis: Uniquely among ankylosaurs, dorsolateral overhang of scapular acromion process to 25% of the dorsoventral width of the scapula. Differs from other ankylosaurids except *Euoplocephalus tutus* in the superficial texture of the osteoderms, having uniformly distributed pitted rugosity with sparse distribution of reticular neurovascular grooves with neurovascular foramina extending perpendicularly to oblique into the bone (Burns and Sullivan 2011).

Discussion: *Ahshislepelta minor* can be distinguished from other North American ankylosaurs by its prominent, lateroventrally oriented acromion process that overhangs the scapular blade by 25% of the dorsoventral height of the scapula (Fig. 4.5). *Ankylosaurus* and *Euoplocephalus* have smaller, more ridge-like acromion processes. The acromion of *Ahshislepelta* bears some similarities to those of the Mongolian and Chinese ankylosaurids *Crichtonpelta*, *Pinacosaurus*,

and *Saichania*, which have prominent, tab-like acromion processes; in the Asian taxa, the acromion is laterally, not ventrolaterally, directed.

Status: Valid.

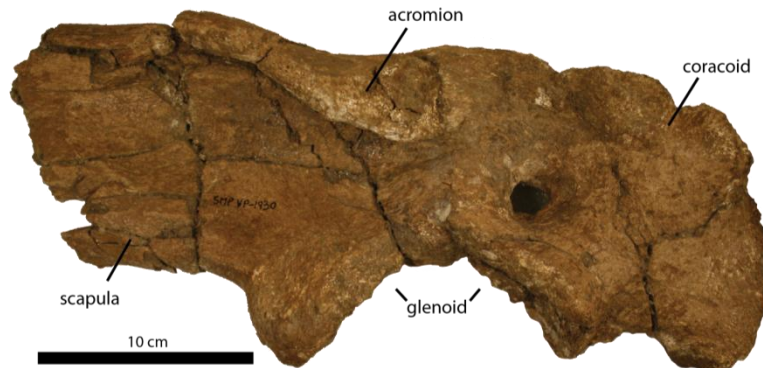


Figure 4.5. SMP VP-1930, holotype of *Ahshislepelta minor*. Right scapulocoracoid in lateral view, anterior is to the right.

4.3.2 *Ankylosaurus magniventris* Brown, 1908

Holotype: AMNH 5895, partial skull, two teeth, five cervical vertebrae, eleven dorsal vertebrae, three caudal vertebrae, right scapulocoracoid, ribs, osteoderms including portions of both cervical half rings

Holotype locality and age: Gilbert Creek, somewhere in S27 or 28, T22N, R40E, Garfield County, Montana, USA; Hell Creek Formation, 61-67 m below Cretaceous-Palaeogene boundary, late Maastrichtian (Carpenter 2004).

Referred specimens: AMNH 5214, complete skull, both mandibles, six ribs, seven caudal vertebrae including tail club, both humeri, left ischium, left femur, right fibula, osteoderms (left bank of Red Deer River, center of S26, T33, R22, Alberta, Canada; Scollard Formation, 45.4m below K-Pg boundary, Maastrichtian; Sternberg 1951, Carpenter 2004). AMNH 5866, more than 70 osteoderms (Seven Mile Creek drainage, S14-16, T40N, R63W, Niobrara County, Wyoming, USA; Lance Formation, Maastrichtian, Carpenter 2004). CCM V03, partial tail club handle (east side along Powder River drainage, somewhere in R1S, T53E, about 24 km south of Powderville, Powder River County, Montana, USA; upper Hell

Creek Formation; Maastrichtian; Carpenter 2004). CMN 8880, skull and left mandible (right bank of Red Deer River, SE ¼ S35, T33, R22, Alberta, Canada, 43.9 m below K-Pg boundary; Maastrichtian; Carpenter 2004). RSM P99.1 and RSM P99.4, osteoderms (coulee south of the village of Simmie, Saskatchewan; Frenchman Formation; Maastrichtian; Burns 2009).

Original diagnosis: From Brown (1908): Skull plates coossified in continuous sculptured shield; elements of braincase not distinguishable; parietal crest short, with bordering plates embossed; nostrils far forward; neural spines not greatly elevated above centra; parapophyses not rising above neural canal; anterior ribs with area for attachment of uncinat processes; posterior ribs coossified with vertebrae; scapula and coracoid coossified and curved. From Carpenter (2004): Largest known ankylosaur up to 6.25m; premaxillae expanded laterally by internal sinuses; external nares located laterally; maximum width of maxillary tooth rows same as width of premaxillary beak; external nares opposite 1st maxillary tooth; large, triangular osteoderm fused to postorbital and squamosal, directed posterodorsolaterally; large triangular osteoderm fused to jugal and quadratojugal, directed posteroventrolaterally; cranial ornamentation of large, flat polygons, including a large diamond-shaped internarial; sharp supraorbital osteoderms continuous with squamosal osteoderm; 34-35/35-36 cheek teeth; quadrate process of pterygoid directed laterally, not posterolaterally; cervical half ring of three keeled plates, outermost has a laterally projecting keel; post-cervical osteoderms smooth textured with sharp edge or lower keel along one margin.

Discussion: The cranial and postcranial morphology of *Ankylosaurus* was described in detail by Carpenter (2004), and so only new observations are included here. *Ankylosaurus magniventris* is the last and largest of the ankylosaurid dinosaurs. Similar to the ankylosaurids *Anodontosaurus*, *Euoplocephalus*, and *Scolosaurus*, from the Campanian of North America, *Ankylosaurus* has cranial sculpturing characterized by rectangular to hexagonal

frontonasal caputegulae, a large hexagonal median nasal caputegulum, a single loreal caputegulum, a single lacrimal caputegulum, and pyramidal squamosal and quadratojugal horns. Unlike *Anodontosaurus*, *Euoplocephalus*, and *Scolosaurus*, the keel on the anterior and posterior supraorbital osteoderms is continuous with the keel of the squamosal horn (Fig. 4.6). The squamosal horn is proportionately longer in *Ankylosaurus* compared to the squamosal horn of *Euoplocephalus* or *Anodontosaurus* (Fig. 4.6), and is not curved as in *Scolosaurus*.

The narial anatomy of *Ankylosaurus* is unique among ankylosaurids (Fig. 4.7), and differs greatly from that of *Anodontosaurus* and *Euoplocephalus* (a complete narial region is not preserved in any specimen referred to *Scolosaurus*). The narial region of ankylosaurids includes the external nares, nasal vestibules,

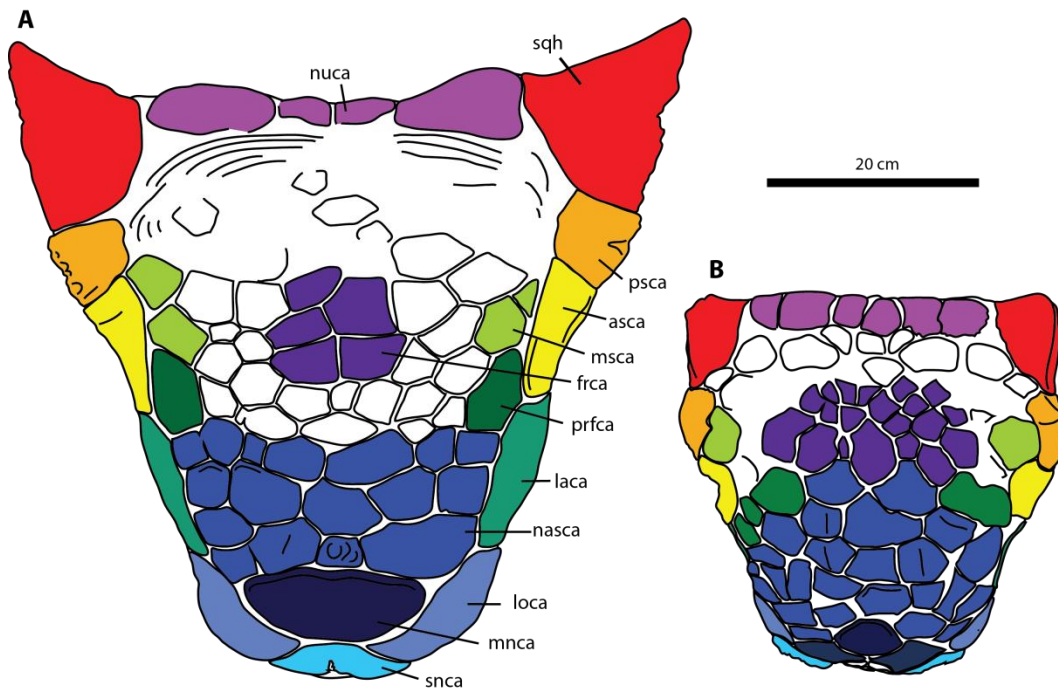


Figure 4.6. Skulls of *Ankylosaurus* and *Anodontosaurus* compared, dorsal view. A) AMNH 5214, *Ankylosaurus magniventris*. B) TMP 1997.59.1, *Anodontosaurus lambei*. Abbreviations: asca, anterior supraorbital caputegulum; frca, frontal caputegulum; laca, lacrimal caputegulum; loca, loreal caputegulum; mnca, median nasal caputegulum; msca, middle supraorbital caputegulum; nasca, nasal caputegulae; nuca, nuchal caputegulum; psca, posterior supraorbital caputegulum; prfca, prefrontal caputegulum; snca, supranarial caputegulum

and narial apertures. The border of the external naris in derived ankylosaurids is typically formed by a distinct edge on the premaxilla, and the external surface of the supranarial caputegulum. Posterior to the external naris is a concave region, roofed by the nasals, called the nasal vestibule. Within the nasal vestibule are the openings for the airway and sinuses, called the narial apertures.

Ankylosaurus and *Euoplocephalus* had a single, folded narial aperture. The external nares of *Anodontosaurus* and *Euoplocephalus* are anteriorly to slightly anterolaterally oriented. In *Ankylosaurus*, the external nares face laterally, and are not visible in anterior view. Small, rugose caputegulae anterior to the loreal and median nasal caputegulae are probably homologous to the supranarial caputegulae in other ankylosaurs, but these do not form the dorsal borders of the external nares in *Ankylosaurus*. Instead, the external nares are roofed by expanded, laterally bulbous loreal caputegulae (Fig. 4.7).

Some of the diagnostic characters for *Ankylosaurus* proposed by Carpenter (2004) are also present in the closely related species *Anodontosaurus* and *Euoplocephalus*. The quadrate process of the pterygoid is directed posterolaterally in *Ankylosaurus*, as in *Anodontosaurus* and *Euoplocephalus*. In *Ankylosaurus* and *Anodontosaurus* (e.g. TMP 1997.132.1), the maximum width of the maxillary tooth rows at their posteriormost extent relative to the width of the premaxillary beak is the same, although the width of the tooth rows may be smaller than the premaxillary beak width in some specimens of *Euoplocephalus* (e.g. ROM 1930).

A partial tail club and a few fragmentary caudal vertebrae are the only caudal elements known for *Ankylosaurus*. *Ankylosaurus* handle vertebrae are twice as wide as those of *Anodontosaurus* and *Euoplocephalus*, but are not longer (Fig. 4.8). As such, the tail of *Ankylosaurus* may have been shorter proportionate to body length compared to the tail of *Euoplocephalus*. The handle vertebrae of *Ankylosaurus* are unique among ankylosaurids, with U-shaped neural spines in dorsal view compared to the V-shaped neural spines in

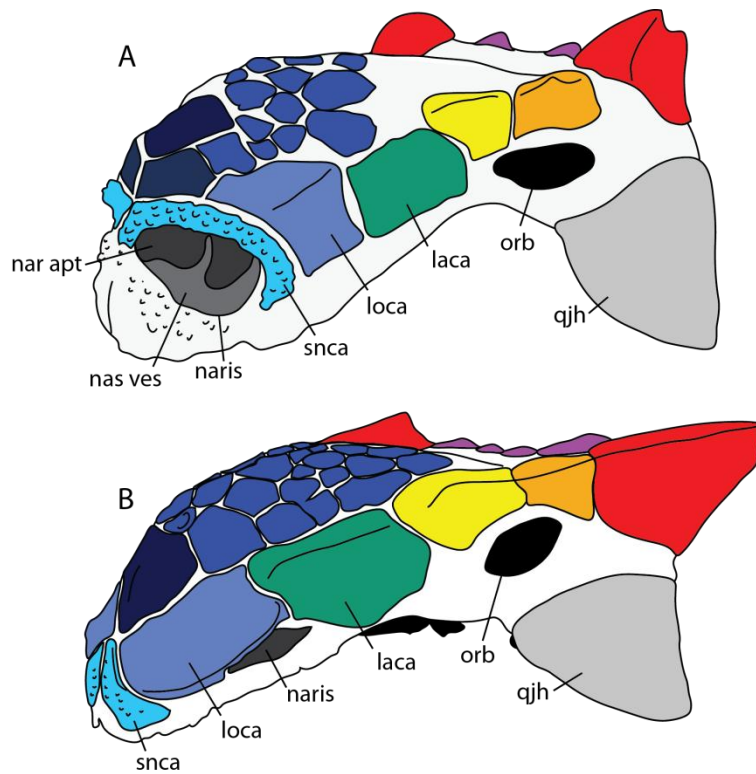


Figure 4.7. Narial regions of *Ankylosaurus* and *Euoplocephalus* compared, both skulls in oblique left anterolateral view and scaled to the same length. A) UALVP 31, *Euoplocephalus tutus*. B) AMNH 5214, *Ankylosaurus magniventris*. Abbreviations: laca, lacrimal caputegulum; loca, loreal caputegulum; naris, external naris; nar apt, narial aperture; nas ves, nasal vestibule; orb, orbit; qjh, quadratojugal horn; snca, supranarial caputegulum.

Anodontosaurus, *Euoplocephalus*, *Pinacosaurus*, and most other ankylosaurids (Fig. 4.8). Only a single tail club knob is known for *Ankylosaurus*, AMNH 5214. Although the skull of AMNH 5214 is more than twice as large in several dimensions compared to skulls belonging to *Anodontosaurus* or *Euoplocephalus*, the tail club knob, at about 45 cm wide (measured from Carpenter 2004 using ImageJ), is not larger than the largest tail club knobs from Horseshoe Canyon and Dinosaur Park Formation ankylosaurids (*Anodontosaurus* specimen AMNH 5425 is 59 cm wide, and an indeterminate tail club from Dinosaur Provincial Park, ROM 788, is 57 cm wide). If one were to extrapolate tail club size in *Ankylosaurus* using AMNH 5425 or ROM 788 as a guide, we might expect knob widths of 120 cm for *Ankylosaurus*. This seems exceptionally large and must surely exceed the

actual maximum width attained by individual *Ankylosaurus*, as there must be an upward limit of knob mass that the handle vertebrae can support. It is impossible to know whether or not AMNH 5214 represents a typical size for an *Ankylosaurus* tail club knob.

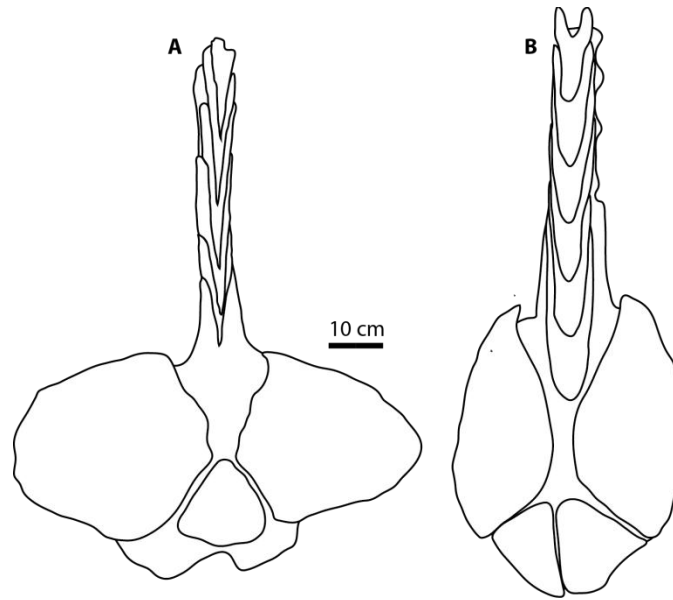


Figure 4.8. Tail clubs of *Ankylosaurus* and *Anodontosaurus* compared, dorsal view, posterior is towards the bottom. A) AMNH 5245, *Anodontosaurus lambei*. B) AMNH 5214, *Ankylosaurus magniventris*.

One final unusual feature of *Ankylosaurus* is the putative midline gap between paired halves of the cervical armour, rather than the cervical half ring of related species like *Anodontosaurus* and *Euoplocephalus*, described by Carpenter (2004). Firsthand examination of *Ankylosaurus magniventris* AMNH 5895 indicates that the two cervical ring fragments placed together by Carpenter (2004) do not fit together. The broken edges of the smaller and larger segments do not join together in any orientation, although weathering or breakage of the specimen could have removed the edges needed to fit the pieces back together snugly. In all other ankylosaurids for which a cervical armour is known, there is a complete half ring of bone with no midline gap. As such, it seems more likely that the two pieces represent fragments from the first and second cervical half rings.

When compared to cervical half rings from *Anodontosaurus* and *Euoplocephalus*, the best interpretation of the AMNH 5895 cervical half ring pieces is that the larger piece includes the ?left lateral and distal osteoderms (*sensu* Penkalski 2001) of the first cervical half ring, and the smaller piece represents the ?left distal osteoderm from the second cervical half ring. Carpenter (2004) also stated that there was no evidence for an underlying bony band as in *Saichania*, but the underlying band is clearly visible on both fragments, although it is easier to discern on the fragment of the second cervical half ring. In *Euoplocephalus* (CMN 0210), the distal osteoderm envelops the terminal edge of the cervical half ring, and the same morphology is observed in both fragments of half ring in AMNH 5895.

Status: Valid.

Revised Diagnosis: Ankylosaurid ankylosaur with pattern of flat, hexagonal frontonasal caputegulae. Uniquely among ankylosaurids, nasal vestibule roofed by loreal caputegulum and not supranarial caputegulum as in *Anodontosaurus*, *Euoplocephalus*, and *Scolosaurus*. External nares open laterally; narial opening not visible in anterior view. Loreal caputegulum laterally expanded and bulbous. Keel of anterior and posterior supraorbital caputegulae continuous with keel of squamosal horn. 34-35/35-36 maxillary teeth; greater number of maxillary teeth than in *Anodontosaurus* or *Euoplocephalus*. Neural spines of tail club handle vertebrae U-shaped in dorsal view (not V-shaped as in other ankylosaurids). Compared to *Anodontosaurus* and *Euoplocephalus* handle vertebrae of same length, neural arch of handle vertebrae in *Ankylosaurus* at least twice as wide as in *Anodontosaurus* or *Euoplocephalus*. Tail club knob approximately as wide as long (also present in *Euoplocephalus* and *Scolosaurus*), not wider than long as in *Anodontosaurus* or longer than wide as in *Dyoplosaurus*.

4.3.3 *Nodocephalosaurus kirtlandensis* Sullivan, 1999

Holotype: SMP VP-900, partial skull

Holotype locality and age: SMP locality 319, west of Willow Wash, SE ¼, NE ¼, NE ¼ of S3, T24N, R13W (Alamo Mesa East Quadrangle), San Juan County, New Mexico, USA; De-na-zin Member, Kirtland Formation, Upper Campanian.

Referred specimens: SMP VP-1957, fragment of skull roof with two caputegulae, possibly representing the frontal region (SMP locality 382, De-na-zin Member, Kirtland Formation).

Original diagnosis: Medium-sized ankylosaurid differing from *Euoplocephalus*, *Ankylosaurus*, *Pinacosaurus*, *Shamosaurus*, *Talarurus*, and *Tsagantegia* in having semi-inflated to bulbous polygonal osteoderms fused to nasal, frontal, and supraorbital regions of skulls; differs from all Asian and North American ankylosaurids in having prominent, anteroventrally directed quadratojugal horn, and in having a prominent post-maxillary/lacrimal ridge (osteoderm).

Discussion: *Nodocephalosaurus* was the first ankylosaurid recovered from North America with bulbous cranial caputegulae similar to those of the Campanian-Maastrichtian Asian ankylosaurids. SMP VP-900 is a partial, plastically deformed skull. The left side of the skull is relatively complete, including the squamosal horn, quadratojugal horn, supraorbitals, prefrontal, parietal, and frontonasal region (Fig. 4.9). Sullivan (1999) also identified portions of the anterior end of the rostrum. The plastic deformation of the skull is most apparent in ventral view, in which the braincase, base of the pterygoids, left quadrate, vomer, palatines, tooth row, palatal apertures, and maxilla are visible.

Sullivan (1999) reconstructed the quadratojugal horn and quadrate such that the apex of the quadratojugal horn pointed ventrally. A new interpretation rotates this element clockwise (Fig. 4.9C), nearly completing the ventral border of the orbit, but resulting in a gap between the quadratojugal and squamosal. This further emphasizes the anteriorly-directed apex of the quadratojugal horn, a feature considered diagnostic by Sullivan (1999). Even if the quadratojugal horn has been plastically deformed and pushed anteriorly in SMP VP-900, the apex of the horn is clearly anteriorly located, in contrast to the posteriorly-located apex

of some specimens of *Scolosaurus* (e.g. USNM 11892), and the U-shaped quadratojugal horn of some specimens of *Anodontosaurus* (e.g. CMN 8530, Arbour and Currie 2013a).

SMP VP-900 has a large, smooth osteoderm that extends from the lateral side of the rostrum onto the dorsal surface. In *Anodontosaurus*, *Euoplocephalus*, and *Scolosaurus*, the loreal osteoderm is present on the lateral side of the skull and nearly meets the median nasal caputegulum on the dorsal surface. If the large, smooth osteoderm in SMP VP-900 is the loreal osteoderm, then SMP VP-900 has a proportionately smaller lacrimal osteoderm compared to the lacrimal caputegulum of *Anodontosaurus*, *Euoplocephalus*, and *Scolosaurus*.

Sullivan (1999) noted that *Nodocephalosaurus* and the Mongolian species *Tarchia* (*sensu lato*) and *Saichania* all possessed bulbous cranial caputegulae. Although *Tarchia gigantea* is not a valid taxon (see Chapter 6), *Tarchia kielanae* (including *Minotaurasaurus ramachandrani*, see Chapter 6) does possess bulbous cranial caputegulae. In *Saichania* and *Tarchia*, the bulbous cranial caputegulae

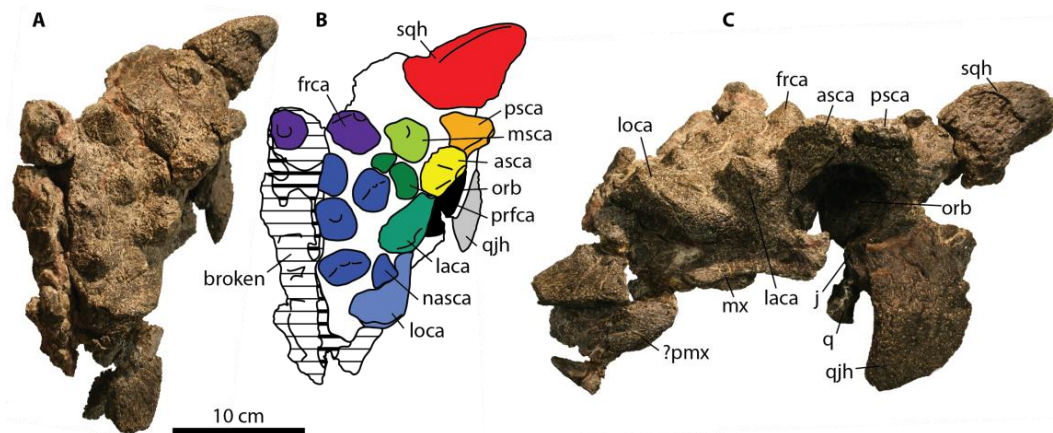


Figure 4.9. SMP VP-900, holotype of *Nodocephalosaurus kirtlandensis*. A) Skull in dorsal view. B) Interpretive diagram of skull in dorsal view. C) Skull in left lateral view. Abbreviations: asca, anterior supraorbital caputegulum; frca, frontal caputegulum; j, jugal; laca, lacrimal caputegulum; loca, loreal caputegulum; mnca, median nasal caputegulum; msca, middle supraorbital caputegulum; mx, maxilla; nasca, nasal caputegulae; nuca, nuchal caputegulum; orb, orbit; ?pmx, ?premaxilla; psca, posterior supraorbital caputegulum; prfca, prefrontal caputegulum; q, quadrate; qjh, quadratojugal horn; snca, supranarial caputegulum.

are pyramidal, with square, hexagonal, or rectangular bases, whereas in *Nodocephalosaurus* the cranial caputegulae are conical, with circular bases. In terms of cranial ornamentation, *Nodocephalosaurus* bears more similarities to the Mongolian taxon *Talarurus plicatospineus*, than it does to *Saichania* or *Tarchia*. PIN 557-3, the holotype skull of *Talarurus plicatospineus*, has faint but distinct caputegulae with circular bases in the frontonasal region. Although *Nodocephalosaurus* and *Talarurus* both possess conical caputegulae, the pattern differs in each: *Talarurus* does not have discernable middle supraorbital caputegulae, which are present in *Nodocephalosaurus*, and *Talarurus* has a raised, V-shaped area on the frontals that is absent in *Nodocephalosaurus*.

Nodocephalosaurus can be distinguished from *Ziapelta sanjuanensis* Arbour et al., in preparation, also from the De-na-zin Member of the Kirtland Formation, based on the form of the cranial ornamentation. Unlike the conical cranial caputegulae of *Nodocephalosaurus*, *Ziapelta* has mainly low-relief, hexagonal caputegulae similar to those of *Ankylosaurus*, *Anodontosaurus*, *Euoplocephalus*, and *Scolosaurus*.

Sullivan and Fowler (2006) and Burns and Sullivan (2011a) described additional ankylosaurid postcranial remains from the San Juan Basin and referred them to *Nodocephalosaurus* because, at the time, it was the only named ankylosaurid from the Kirtland Formation. With the discovery of *Ahshislepelta* in the Hunter Wash Member, and *Ziapelta* from the De-na-zin Member, isolated and nondiagnostic ankylosaurid remains can no longer be referred to *Nodocephalosaurus*. As such, SMP VP-1149 and SMP VP-1743 (caudal vertebrae), SMP VP-1870 (osteoderm), SMP VP-1632 (incomplete minor tail club osteoderm), SMP VP-1646 (incomplete tail club knob), and SMP VP-2074 (partial tail club knob), are referred to Ankylosauridae indet.

Status: Valid

Revised Diagnosis: Uniquely among ankylosaurids, has quadratojugal horn with anteriorly positioned apex. Unlike all ankylosaurids except *Talarurus*, has conical

frontonasal caputegulae with circular bases. Unlike *Talarurus*, lacks V-shaped upraised area of frontals. Lacrimal caputegulum smaller, more square than in *Ankylosaurus*, *Anodontosaurus*, *Euoplocephalus*. Loreal caputegulum more bulbous and ridge-like than in *Ankylosaurus*, *Anodontosaurus*, *Euoplocephalus*.

4.3.4 *Tatankacephalus cooneyorum* Parsons and Parsons, 2009

Holotype: MOR 1073, partial cranium including fragments of internasal septum, premaxillary fragments with three alveoli, maxillary-nasal fragment, orbital-postorbital-quadratojugal fragment, isolated tooth, large posterior fragment with parietal, squamosal, occiput, dorsal portion of left quadrate, braincase, right postorbital, right orbit, partial pterygoids, basisphenoid, partial basioccipital, parasphenoidal rostrum; rib fragments and two osteoderms.

Holotype locality and age: Middle Dome region, Harlowton, Wheatlan County, Montana, USA; Cloverly Formation, late Aptian to early Albian (Lower Cretaceous); Ostrom 1970

Original diagnosis: Unsegmented, enlarged nuchal crest; concave lateral process projecting from paroccipital process; keeled osteoderm on jugal process of quadratojugal dorsal to quadratojugal horn.

Discussion: Although originally described as a basal ankylosaurid by Parsons and Parsons (2009), a more recent phylogenetic analysis by Thompson et al. (2012) recovered *Tatankacephalus* as a nodosaurid. The phylogenetic relationships of *Tatankacephalus* will be assessed in the revised analysis in Chapter 10.

Status: Valid.

4.3.5 *Ziapelta sanjuanensis* Arbour, Burns, Sullivan, and Lucas in preparation

Holotype: NMMNH P-64484, nearly complete skull, left side of first cervical half ring, partial second cervical half ring, post-cervical osteoderms.

Holotype locality and age: L-8514, east branch of Hunter Wash, San Juan County, New Mexico, USA. De-na-zin Member, Kirtland Formation, Campanian, Upper Cretaceous.

Original diagnosis: Uniquely among ankylosaurine ankylosaurids, *Ziapelta* has a sub-triangular median nasal caputegulum; dorsoventrally deep squamosal horns curve anteriorly at the tips. Differs from other ankylosaurids in possessing a mixture of flat and weakly bulbous frontonasal caputegulae. Differs from *Nodocephalosaurus* in the irregular basal shape of the frontonasal caputegulae and in the manner in which the caputegulae are bulbous (conical in *Nodocephalosaurus*, irregularly convex in *Ziapelta*).

Discussion: *Ziapelta sanjuanensis* is one of three ankylosaurids currently known from the Kirtland Formation of New Mexico. Although it cannot be directly compared to *Ahshislepelta* because of a lack of overlapping elements, *Ahshislepelta* is from the stratigraphically lower Hunter Wash Member of the formation. *Ziapelta* can be differentiated from *Nodocephalosaurus* based on the form of the cranial ornamentation (Fig. 4.10). *Nodocephalosaurus* has distinct conical frontonasal caputegulae, whereas the caputegulum pattern of *Ziapelta* more closely resembles that of *Anodontosaurus* and *Euoplocephalus*, with square, hexagonal, or rectangular caputegulae. *Ziapelta* differs from *Ankylosaurus*, *Anodontosaurus*, *Euoplocephalus*, and *Scolosaurus* in the shape of the median nasal caputegulum, which is triangular in *Ziapelta* and hexagonal in the other taxa. *Ziapelta* has unique squamosal horns, which are more laterally projecting than in other North American ankylosaurids, and which are curved slightly ventrally.

Status: Valid.

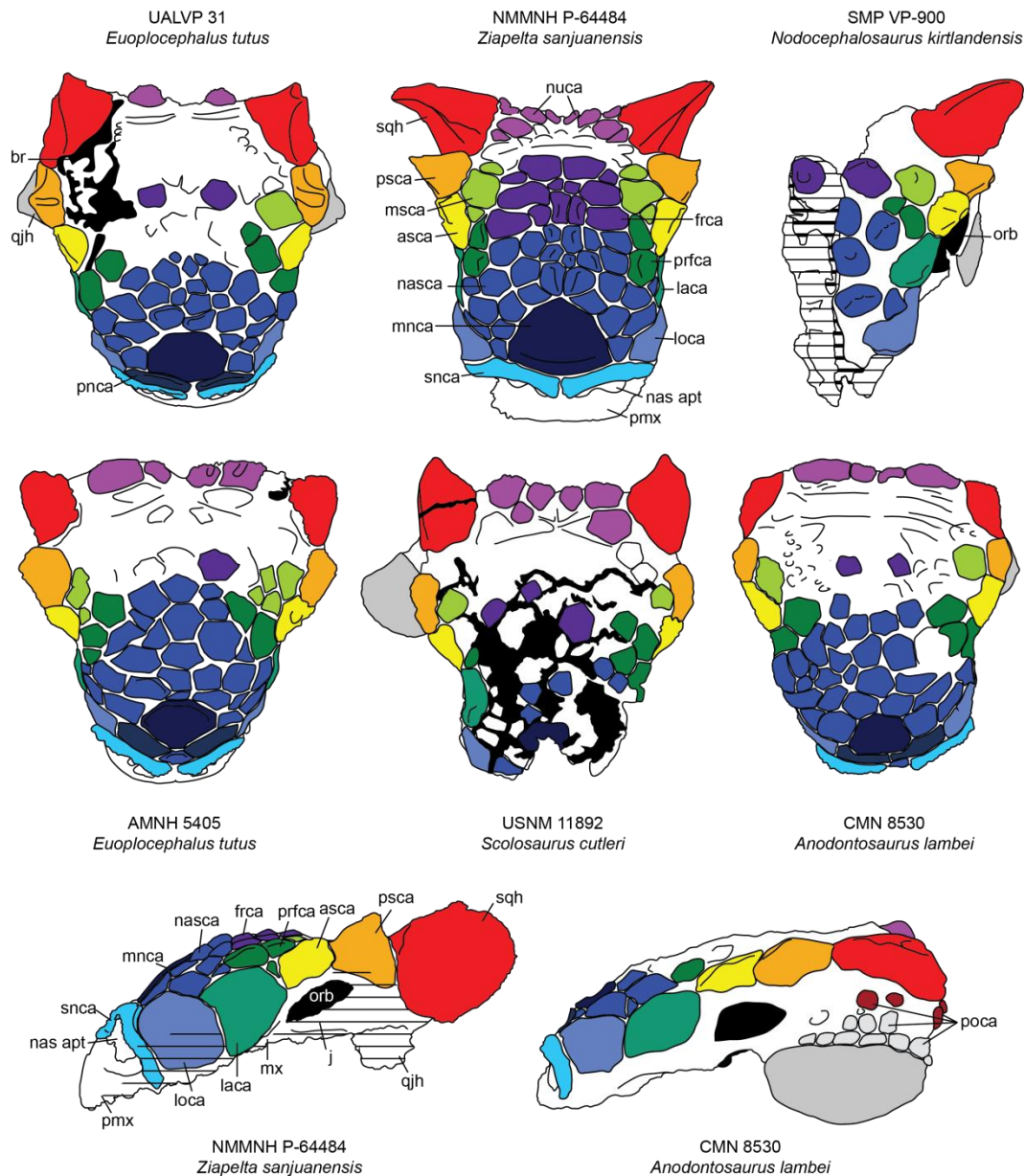


Figure 4.10. NMMNH P-64484, holotype of *Ziapelta sanjuanensis*, compared to other North American Campanian-Maastrichtian ankylosaurids, in dorsal and left lateral views. Abbreviations: asca, anterior supraorbital caputegulum; frca, frontal caputegulum; j, jugal; laca, lacrimal caputegulum; loca, loreal caputegulum; mnca, median nasal caputegulum; msca, middle supraorbital caputegulum; mx, maxilla; nasca, nasal caputegulae; nuca, nuchal caputegulum; orb, orbit; pnca, postnarial caputegulum; poca, postocular caputegulum; psca, posterior supraorbital caputegulum; prfca, prefrontal caputegulum; q, quadrate; qjh, quadratojugal horn; snca, supranarial caputegulum.

4.4 Other North American specimens

Kaiparowits Formation (76.5-74.7 Ma), Utah: UMNH VP 19473, right forelimb, left scapula and coracoid, one cervical vertebra, three caudal vertebrae, first cervical half ring, osteoderms; UMNH VP 19472, eight dorsal ribs, four proximal caudal vertebrae, tail club, osteoderms; UMNH VP 20202, complete skull, both dentaries, both cervical half rings, cervical vertebra, four dorsal vertebrae, six dorsal ribs, nearly complete sacrum, partial tail club handle, tail club knob, right coracoid, both scapulae, left humerus, left ilium, left tibia, left fibula, osteoderms (Loewen et al. 2013).

4.5 Discussion and conclusions

Whether or not the Stegopeltinae represents a valid clade of either nodosaurids or ankylosaurids will be assessed in the revised phylogenetic analysis in Chapter 10. All taxa previously assigned to Stegopeltinae (*Aletopelta*, *Stegopelta*, and *Glyptodontopelta*) are considered valid taxa, even though each is known from fragmentary remains.

Although typically considered the archetypal ankylosaur, *Ankylosaurus* has several highly unusual features in the skull and tail. The ventrally and posteriorly placed narial aperture, located underneath the loreal caputegulum, is unknown in any other ankylosaur. This represents a major rearrangement of the narial anatomy of *Ankylosaurus* from its closest relatives *Anodontosaurus* and *Euoplocephalus*, the functional implications of which are unknown. The tail club handle morphology of *Ankylosaurus* also differs from all other ankylosaurids, and *Ankylosaurus* would have had a proportionately shorter tail relative to overall body size compared to other ankylosaurids. The widened handle caudals may result from the increase in overall size in *Ankylosaurus*, and may represent a functional adaptation to presumed concomitant increases in tail club impact forces if the club were used in striking behaviour.

Sullivan (1999) considered *Nodocephalosaurus* to be closely related to the Mongolian ankylosaurids *Saichania* and *Tarchia*, although this was based only on the presence of bulbous caputegulae on the skull, and not the result of a rigorous phylogenetic analysis. The presence of an ankylosaurid closely related to Mongolian taxa in the late Campanian of New Mexico in turn suggested that there was some palaeogeographic connection between Asia and western North America at or somewhat before that time (Sullivan 1999). Although *Nodocephalosaurus* and *Ziapelta* occur in the same formation, *Ziapelta* seems to have more affinities to northern North American ankylosaurids than to *Nodocephalosaurus*. *Ziapelta* shares several features with *Ankylosaurus*, *Anodontosaurus*, *Euoplocephalus*, and *Scolosaurus*, such as the flat, square-to-hexagonal based cranial caputegulae. However, it also has some bulbous, convex cranial caputegulae, which are otherwise known only in *Nodocephalosaurus* and the derived Asian ankylosaurids. The phylogenetic relationships of *Nodocephalosaurus* and *Ziapelta*, and their biogeographic implications, will be discussed in Chapter 10.

Does the presence of *Ziapelta* in the southern portion of Laramidia support current hypotheses of distinct southern and northern North American dinosaur faunas (e.g., Lehman 2001; Sampson et al. 2010)? *Ziapelta* is not known from Montana or Alberta, and *Anodontosaurus*, *Euoplocephalus*, and *Scolosaurus* have not been recovered south of Montana. However, identifying northern and southern faunal provinces requires that the representative faunas occur at the same time; while this appears to be the case for the Kaiparowits Formation of Utah (Roberts et al. 2005), the upper Two Medicine Formation of Montana (Rogers et al. 1993), and the Dinosaur Park Formation of Alberta (Eberth and Hamblin 1993), the fauna of the Kirtland Formation occurs at a slightly younger time interval (Sullivan and Lucas 2006). The holotype of *Ziapelta* was collected from the De-na-zin Member of the Kirtland Formation, dated at 73.4 Ma (Sullivan, pers. comm. 2013). In Alberta, the equivalent time is represented by

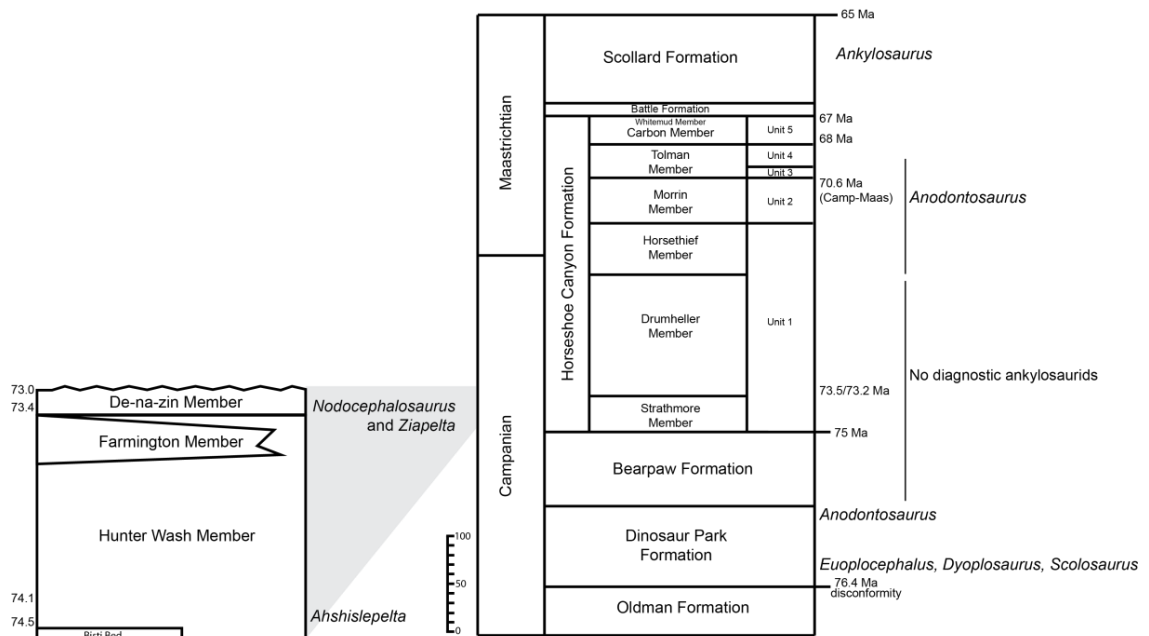


Figure 4.11. Stratigraphic distribution of Campanian-Maastrichtian ankylosaurids from North America. The left column represents strata in New Mexico, USA, and the right column represents strata in Alberta, Canada.

the base of the Drumheller Member of the Horseshoe Canyon Formation, and the Dorothy Tongue of the Bearpaw Formation (73.2-73.5 Ma, Eberth and Braman 2012). No identifiable ankylosaurids have been recovered from this part of the Horseshoe Canyon Formation (Fig. 4.11); *Anodontosaurus* is known from a few specimens in the upper part of the Dinosaur Park Formation (~75 Ma), and then from the Horsethief Member (71.5 Ma, Eberth and Braman 2012), Morrin Member, and Tolman Member of the Horseshoe Canyon Formation (Arbour and Currie 2013a). *Dyoplosaurus*, *Euoplocephalus*, and *Scolosaurus* occur in older sediments than *Ziapelta*, and *Ankylosaurus* is known from younger sediments. As a result, the presence of *Ziapelta* in the Kirtland Formation cannot be used to support hypotheses of dinosaur provincialism at this time; additional diagnostic ankylosaurid specimens from the Drumheller Member of the Horseshoe Canyon Formation, or other time-equivalent strata, are needed to clarify the paleobiogeography of Campanian ankylosaurids from Laramidia.

5. THE TAXONOMIC IDENTITY OF A NEARLY COMPLETE ANKYLOSAURID DINOSAUR SKELETON FROM THE GOBI DESERT OF MONGOLIA³

5.1 Introduction

The holotype of *Saichania chulsanensis* Maryańska, 1977 (MPC 100/151) is a well-preserved specimen that includes the skull and anterior portion of the skeleton (Fig. 5.1). The cervical half rings and postcervical osteoderms were preserved *in situ*, the skeleton was articulated, and the limbs were preserved under the body. A second articulated ankylosaurid skeleton with *in situ* osteoderms from the Baruungoyot Formation has been informally referred to *Saichania* in museum exhibits (Dinosaur Kingdom Nakasato, Japan; Mongolian Natural History Museum, Ulaanbaatar), and is often used as the basis for skeletal and life restorations of this species (e.g., Paul, 2010). MPC 100/1305 was formally referred to *Saichania* in a detailed descriptive monograph by Carpenter et al. (2011). This skeleton lacks the skull, first few cervical vertebrae, some manual and pedal phalanges, and both cervical half rings, but includes almost all of the postcranial skeleton, including abundant *in situ* osteoderms on the forelimbs, flanks, pelvic region, and tail (Fig. 5.1). As mounted, the skeleton includes a skull that Carpenter et al. (2011) identify as belonging to this specimen (MPC 100/1305). However, a cast of the holotype skull (MPC 100/151) was used to complete MPC 100/1305 in the skeletal mount. Carpenter et al. (2011) do not identify any postcranial features that support their referral of MPC 100/1305 to *Saichania*, and as such, their referral of MPC 100/1305 to *Saichania* appears to be based only on the skull. Because the skull in MPC 100/1305 is a cast of the holotype skull MPC 100/151, a reassessment of MPC 100/1305 is necessary. MPC

³ A version of this chapter is published: Arbour and Currie 2013. *Cretaceous Research* 46:24-30. P. Currie supervised the project and edited the manuscript.

100/1305 is an important specimen because it preserves one of the most complete suites of osteoderms of any ankylosaurid, and is the only ankylosaurid skeleton that preserves a nearly complete caudal osteoderm series. Information from this specimen can be used to assess the anatomical position of isolated ankylosaurid osteoderms from Mongolia, and to assess taxonomic variation of osteoderms among ankylosaurid taxa. It is therefore important to understand the taxonomic assignment of this specimen to understand the range of morphological variation in other ankylosaurs.

5.2 Materials and methods

Original specimens, or casts of original specimens, were examined firsthand where possible. The original material of MPC 100/151, the holotype of *Saichania chulsanensis*, was unavailable for study during the course of this project. A cast of MPC 100/151 with the bones in their *in situ* arrangement (prior to being fully prepared out of the matrix), on display at the Museum of Evolution in Warsaw, was examined, as was a cast of the skull. A mounted, high-quality cast of MPC 100/1305, on display at the Mongolian Museum of Natural History, was examined in lieu of the original material. PIN 614 is on display at the Orlov Museum of Paleontology (Russian Academy of Sciences) in Moscow, Russia, in a case that could not be opened. Measurements of specimens were taken with digital calipers and measuring tape, or are taken from the literature. Mongolian place name spellings follow those suggested by Benton (2000).

5.3 Stratigraphic provenance of MPC 100/1305

Carpenter et al. (2011) state that MPC 100/1305 was collected from the Baruungoyot Formation at Khulsan (Fig. 5.2), but did not indicate when or by which expedition the specimen was recovered. The catalogue records at the MPC indicate that MPC 100/1305 was collected by the Soviet-Mongolian Joint Paleontological Expedition in 1976. The catalogue record also indicates that

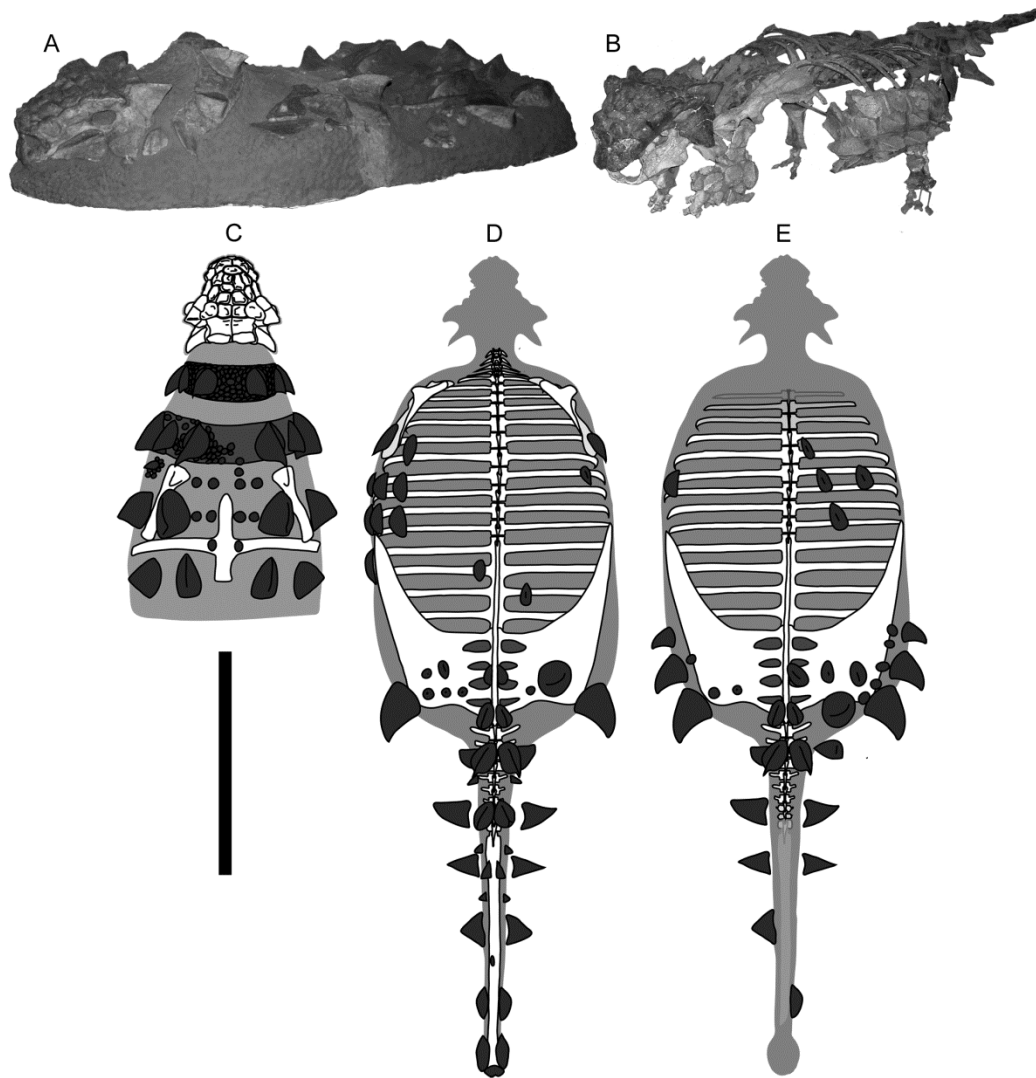


FIGURE 5.1. MPC 100/151 (holotype of *Saichania chulsanensis*) and MPC 100/1305 compared. Top left, cast of MPC 100/151 as it appeared *in situ*, left lateral view. Top right, mounted cast of MPC 100/1305 with cast MPC 100/151 skull, in oblique anterolateral view. Bottom row, diagrams of preserved elements in MPC 100/151, MPC 100/1305, and an uncollected AMNH specimen found at Ukhaa Tolgod, in dorsal view (scale bar equals 1 m and applies to MPC 100/151 and MPC 100/1305 only). The second cervical half ring of MPC 100/151 was slightly disarticulated, and is restored in this diagram; the cervical region is probably artificially long due to postmortem disarticulation, as the second cervical half ring in other articulated ankylosaurs covers the pectoral region. The diagram of the Ukhaa Tolgod specimen is based on a photograph published on the cover of *Geology* (1998), and is not shown to scale. This specimen has a similar pattern of pelvic and caudal osteoderms compared to MPC 100/1305.

the specimen was collected from Zamyn Khond (=Dzamyn Khond, Zamin Khond), not Khulsan. Barsbold (1981), Suzuki et al. (2000) and Watabe et al. (2010) consider the sediments at Zamyn Khond to represent the Djadokhta Formation.

A physical contact between the Baruungoyot and Djadokhta formations has not been identified (Gradzinski et al. 1977; Dingus et al. 2008), but it is generally recognized that the Djadokhta Formation is stratigraphically lower than the Baruungoyot Formation (Gradzinski et al. 1977, Jerzykiewicz and Russell 1991; Dashzeveg et al. 2005). The Djadokhta and Baruungoyot formations both represent semiarid environments with aeolian dunes, but the Baruungoyot Formation has more fluvial influences than the Djadokhta Formation (Jerzykiewicz 2000). Magnetostratigraphic results suggest that the Djadokhta Formation was deposited between about 71 to 75 Ma, during the late Campanian (Dashzeveg et al. 2005).

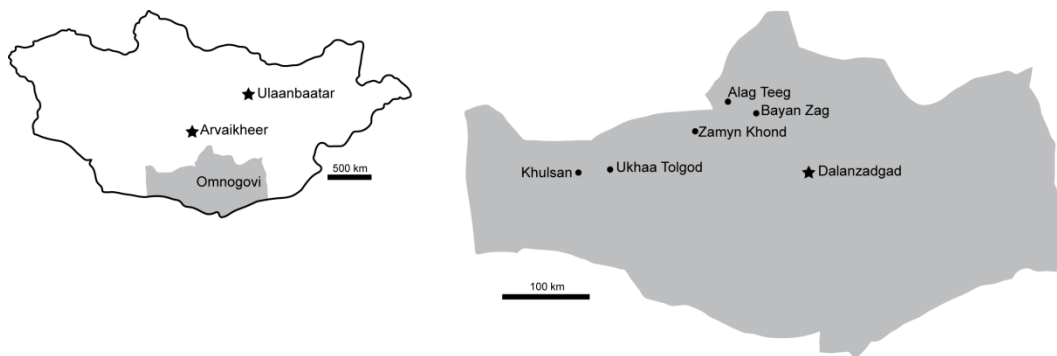


Figure 5.2. Maps of Mongolia and Omnogovi showing locations of Alag Teeg, Bayan Zag, Khulsan, Ukhaa Tolgod, and Zamyn Khond.

Pinacosaurus is the only ankylosaurid currently recognized from the Djadokhta Formation of Mongolia and correlative strata in China, and because MPC 100/1305 is also from the Djadokhta Formation, it is possible it may be referable to *Pinacosaurus*. The Japan-Mongolia Joint Paleontological Expeditions collected several ankylosaur specimens from Zamyn Khond, but these await full descriptions. At least one ankylosaurid skeleton from the Djadokhta Formation

at Ukhaa Tolgod bears a close resemblance to MPC 100/1305. Volume 26 of the journal *Geology* features a photograph on its cover (that accompanies Loope et al. 1998) of an articulated ankylosaurid with *in situ* osteoderms that are similar to those of MPC 100/1305. This specimen, also lacking a skull, was discovered by the AMNH expedition in 1993 (and photographed in 1997) at the Ankylosaur Flats sublocality of Ukhaa Tolgod; due to time constraints, it was not collected (L. Dingus and D. Loope, pers. comm. 2012). Dingus et al. (2008) note that articulated partial ankylosaurid skeletons were abundant at the Ukhaa Tolgod sublocality Ankylosaur Flats. This specimen represents a different individual than MPC 100/1305, because MPC 100/1305 had already been partially prepared and was figured on the frontispiece of Psihoyos and Knoebber (1994). The skeleton featured on the *Geology* cover has similar triangular osteoderms along the ilia (including prominent triangular osteoderms at the posterior corners) and caudal region (Fig. 5.1). Because this skeleton was not collected, it is not possible to refer it to any taxon. However, the ankylosaurid *Pinacosaurus grangeri* is known from a skull (MPC 100/1014) collected from Ukhaa Tolgod by the AMNH (Hill et al., 2003).

5.4 MPC 100/1305 compared to *Saichania chulsanensis*

The skull figured as belonging to MPC 100/1305 by Carpenter et al. (2011) is a cast of the holotype skull from *Saichania chulsanensis* (MPC 100/151; Maryańska, 1977); this can be verified by comparing various asymmetrical morphological features and taphonomic artifacts in the figures in Carpenter et al. (2011: Text-figs. 3, 5-8; Plates 1, 2) and Maryańska (1977: Plates 28-31). For example, in ventral view, both skulls have the same pattern of circular broken areas on the palate, and both have the same protuberance on the anterior edge of the left quadratojugal horn (Carpenter et al. 2011: Plate 1, Fig. 2; Maryańska 1977: Plate 28, Fig. 1b). In posterior view, both skulls have the same plaster-filled notch on the dorsal edge of the left nuchal osteoderm (Carpenter et al. 2011:

Plate 1, Fig. 6; Maryńska 1977: Plate 28, Fig. 1c). The pattern of cranial osteoderms is identical in both specimens, even though the osteoderm arrangements and shapes are bilaterally asymmetrical (Carpenter et al. 2011: Plate 1, Fig. 1; Maryńska 1977: Plate 28, Fig. 1a). Because the skull mounted with MPC 100/1305 does not belong to this specimen, postcranial features must be used to refer MPC 100/1305 to *Saichania*. Carpenter et al. (2011) do not identify any postcranial features that support their referral of MPC 100/1305 to *S. chulsanensis*. Fortunately, there are numerous overlapping elements between MPC 100/1305 and MPC 100/151 that could facilitate the referral of MPC 100/1305 to *S. chulsanensis*.

MPC 100/1305 preserves five partial cervical vertebrae, not four, as stated by Carpenter et al. (2011). These do not include the atlas and axis. Carpenter et al. (2011) describe the neural arches of MPC 100/1305 as X-shaped in dorsal view, and use this feature as a diagnostic character of *S. chulsanensis*. In MPC 100/1305, the cervical neural spines are broken, the prezygapophyses diverge anteriorly, and the postzygapophyses diverge posteriorly; this gives the combined prezygapophysis-postzygapophysis complex an X-shape in dorsal view (see Text-Fig. 12 in Carpenter et al. 2011). However, this is also true for *Euoplocephalus tutus* Lambe, 1902 (AMNH 5403) and *Ankylosaurus magniventris* Brown, 1908 (AMNH 5895, Carpenter 2004), and so this is not a diagnostic feature for *S. chulsanensis*. Carpenter et al. (2011) also suggest that the horizontal sheet of bone above the neural canal in MPC 100/151 is pathological in nature because it is not present in MPC 100/1305; however, a similar structure is also preserved in AMNH 5403 (*Euoplocephalus*; Arbour and Currie 2013a:Fig. 7), and so its absence in MPC 100/1305 is more likely a result of poor preservation, especially given that the cervicals in this specimen are broken.

Ten dorsal vertebrae are preserved in MPC 100/151, and ten dorsals are preserved in MPC 100/1305 (along with three dorsosacrals). The dorsal centra of MPC 100/1305 have shallow, indistinct depressions on the lateral surfaces

ventral to the transverse processes (Carpenter et al. 2011:Text-fig. 13). Carpenter et al. (2011) identify these as pleurofossae, a remarkable claim given that no other ornithischians possess unambiguous evidence for postcranial pneumaticity (Butler et al., 2012). O'Connor (2006) found that the presence of vertebral fossae alone cannot be used to support the inference of postcranial pneumaticity; to demonstrate pneumaticity, fossae or foramina must be directly connected to a large internal cavity in the vertebra. Fossae on the lateral sides of the centra of *Alligator* lumbar vertebrae are associated with fat deposits (O'Connor, 2006), and are similar to the lateral depressions on the dorsal vertebrae of MPC 100/1305. These depressions are not present in *Ankylosaurus* (AMNH 5895; Carpenter, 2004: Figs. 12-13), *Euoplocephalus* (AMNH 5337; Arbour and Currie 2013a:Fig. 8), *Pinacosaurus grangeri* Gilmore, 1933 (ZPAL MgD II/1), or *Talarurus plicatospineus* Maleev, 1952 (PIN 557-91). The dorsal vertebrae of MPC 100/151 were not figured by Maryańska (1977) and the original material was not available for study during the course of this project. Maryańska (1977) does not describe lateral depressions on the dorsal centra of MPC 100/151, so it is unclear if this is a feature unique to MPC 100/1305. Both MPC 100/151 and MPC 100/1305 preserve ossified sternal elements. The sternum of MPC 100/151 is not as well preserved than that of MPC 100/1305, but has the same trapezoidal shape.

Maryańska (1977) notes that the humerus of *S. chulsanensis* has an unusual proximal concavity lateral to the humeral head. As a result, the proximal edge of the deltopectoral crest has a spur-shaped process, unknown in other ankylosaurid humeri. The left humerus of MPC 100/1305 appears to have a similar proximal concavity, and as such strongly resembles the humerus of MPC 100/151. This feature is less prominent on the right humerus, leading Carpenter et al. (2011) to conclude that it was not of taxonomic significance, a conclusion that is supported in this paper. However, Carpenter et al. (2011) suggested that the humerus of MPC 100/1305 is less robust than that of MPC 100/151 and that

these proportional differences may represent sexual dimorphism in *S. chulsanensis*. Measurements of the humeri of MPC 100/1305 compared to those provided for MPC 100/151 by Maryńska (1977) do suggest that MPC 100/1305 is less robust than MPC 100/151. The maximum proximal width is 46% that of the total length of the humerus in MPC 100/1305, compared to 70% in MPC 100/151 (Table 5.1). However, it is equally plausible that this difference represents a taxonomic or ontogenetic difference rather than sexual dimorphism. When maximum humeral proximal width is plotted against humeral length across numerous ankylosaur specimens and taxa (based on data presented by Burns and Sullivan, 2011), MPC 100/1305 plots near the regression line for all specimens, but *S. chulsanensis* (MPC 100/151) plots well away from the line (Fig. 5.3). This suggests that the large deltopectoral crest of MPC 100/151 is not size-dependent, and is instead a unique feature of *S. chulsanensis*.

Table 5.1. Comparative measurements of MPC 100/151 (holotype of *Saichania chulsanensis*), PIN 614 (*Pinacosaurus grangeri*), and MPC 100/1305, in millimeters. New measurements for PIN 614 are marked by an asterisk; all other measurements for PIN 614 are from Maleev (1954). Measurements for MPC 100/151 from Maryńska (1977). Where elements from both the right and left sides are known, the right side measurement is given first.

	PIN 614	MPC 100/1305	MPC 100/151
Length from first cervical to distal end of tail	3660*	3270	
Scapula length	400	-, 245	400
Coracoid length	200	118, 120	
Humerus length	300	250, >265	300
Humerus greatest proximal width	135.5	107, 124	212
Humerus greatest distal width	132.5	-	163
Radius length	145.5	151, 142	182
Ulna length	225	-	210
Femur length	400	380, 370	-
Femur greatest width proximal end	102	109, 107	-
Tibia length	270	203, 215	-
Tail length	2100*	1610	
Tail club length	1160*	1040	-
Tail club knob length	110*	140	-

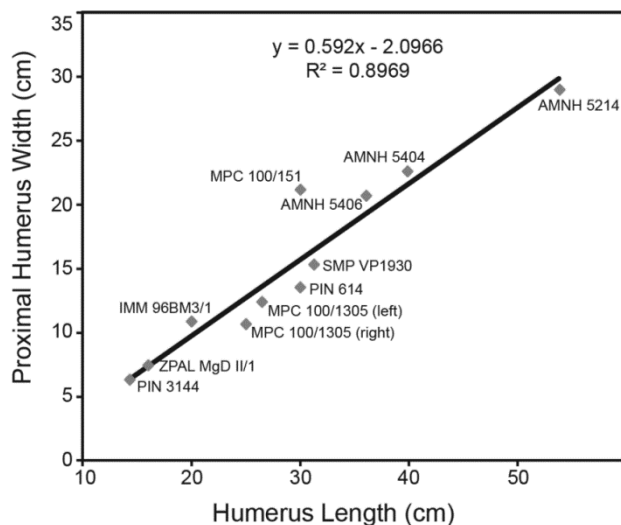


Figure 5.3. Maximum humeral width plotted against maximum humeral length for a variety of ankylosaurid species, including MPC 100/1305 (previously referred to *Saichania chulsanensis*), modified from Burns and Sullivan (2011). *Ahshislepelta minor* – SMP VP1930; *Ankylosaurus magniventris* – AMNH 5214; *Euoplocephalus tutus* – AMNH 5404, AMNH 5406; *Pinacosaurus grangeri* – PIN 614, ZPAL MgD II/1, PIN 3144; *Pinacosaurus mephistocephalus* – IMM 96BM3/1; *Saichania chulsanensis* – MPC 100/151.

Carpenter et al. (2011) noted that the outlines of the proximal ends of the metacarpals of MPC 100/1305 differed from those of MPC 100/151, and attributed this to intraspecific variation in *S. chulsanensis*. For the most part, the proximal ends of the metacarpals in both specimens are similar: metacarpal I is a rounded rectangle, metacarpal II is a rounded equilateral triangle, and metacarpal III is a right triangle. Metacarpals IV and V differ between the two specimens. In MPC 100/151, metacarpal IV wraps around metacarpal V, whereas in MPC 100/1305 metacarpal IV is less curved and more rectangular. In MPC 100/151, metacarpal V is a rounded equilateral triangle, and in MPC 100/1305, metacarpal V is a rounded rectangle. It is unclear if this represents a taxonomically significant difference between these specimens, as variation in metacarpal morphology has not been well documented for ankylosaurs. The pelvis, hindlimb, and tail of MPC 100/151 were not preserved, so no comparisons can be made for these elements with MPC 100/1305.

At present, MPC 100/1305 cannot be referred to *S. chulsanensis* because there are no diagnostic features of the postcrania shared between MPC 100/1305 and the holotype of *S. chulsanensis*. Carpenter et al. (2011) also observed that MPC 100/1305 differs from MPC 100/151 in several characters such as the robustness of the humerus, the outlines of the proximal ends of the metacarpals, and the parallel dorsal and ventral borders of the scapula (compared to divergent borders in MPC 100/151). These differences support referral of MPC 100/1305 to a different ankylosaurid genus or species.

5.5 Comparison with *Pinacosaurus*

There are two currently recognized species of *Pinacosaurus*. *Pinacosaurus grangeri* was first discovered at Bayan Zag (=Bayn Dzak, Shabarak Usu, the Flaming Cliffs). The holotype (AMNH 6523) is a crushed and distorted skull; it is the largest known skull for *Pinacosaurus* and probably represents either a subadult or adult individual. *P. grangeri* is also known from Alag Teeg and Ukhaa Tolgod in Mongolia, and Bayan Mandahu in Nei Mongol, China (Jerzykiewicz et al., 1993; Hill et al., 2003; Burns et al., 2011; Currie et al., 2011). Most of these specimens are from juveniles (ZPAL MgD II/1, IVPP 16853, IVPP 16854, MPC D100/1344), but a few specimens (PIN 614, MPC 100/1333) are from larger individuals. *Pinacosaurus mephistocephalus* Godefroit et al., 1999 is known from a single partial, articulated skeleton with skull and *in situ* osteoderms, from Bayan Mandahu in China. A third species, *Pinacosaurus ninghsiensis* Young, 1935, was referred to *Pinacosaurus* based on similarities in the teeth and jaws; Maryńska (1971) considered *P. ninghsiensis* a junior synonym of *P. grangeri*, a synonymy that has been upheld by subsequent authors (Vickaryous et al. 2004, Burns et al. 2011, Hill et al.). "*Syrmosaurus viminicaudus*" Maleev, 1952 was synonymized with *P. grangeri* by Maryńska (1971), based on the similarities in postcrania between PIN 614 and ZPAL MgD II/1. Buffetaut (1995) described

ankylosaur postcranial material from the Wangshi Group of Shandong, China, and referred these specimens to *Pinacosaurus* cf. *P. grangeri*.

Pinacosaurus grangeri is diagnosed by numerous cranial autapomorphies (Hill et al. 2001, Burns et al. 2011), but few diagnostic features of the postcrania have been identified. Maryańska (1977) included only a few postcranial characters in her revised diagnosis of *Pinacosaurus*, including a lightly built postcranial skeleton, slender limb bones, pentadactyl manus, and tetradactyl pes. Maryańska (1977) also described several unique features of *P. grangeri* that were not included in the diagnosis, such as the reduction of the neural spines in posterior cervical vertebrae, high dorsal neural arches relative to the heights of the centra, a relatively simpler sternal complex compared to *S. chulsanensis*, and a less-developed deltopectoral crest. Godefroit et al. (1999) emended the generic diagnosis for *Pinacosaurus* and included several more postcranial characters, including reduced neural arches on the posterior cervical vertebrae, strongly divergent preacetabular processes, two cervical half rings composed of three to four fused elements, and lightened osteoderms in two longitudinal series. According to Godefroit et al. (1999), diagnostic features for *P. mephistocephalus* included a scapular proximal width:length ratio of 0.36, a well-developed acromion process, a well-developed deltopectoral crest terminating distal to the midlength of the humerus, and a strongly expanded proximal end of the radius.

Unfortunately, many of the diagnostic postcranial characters for *Pinacosaurus* proposed by Maryańska (1977) and Godefroit et al. (1999) are either too vague to assess, or have wide distributions in the Ankylosauridae. Divergent preacetabular processes, a large deltopectoral crest, two cervical half rings, and 'lightened' osteoderms are present in all ankylosaurids. Cervical half rings composed of only three to four fused elements would be unique to *Pinacosaurus*, as most ankylosaurids have six segments in the cervical half rings. However, no complete cervical half rings referable to *Pinacosaurus* have only

three or four segments. Maryańska (1977) identified reduced neural arches on the posterior cervicals as a unique feature of *Pinacosaurus*, which was also reported for *P. mephistocephalus* by Godefroit et al. (1999). ZPAL MgD II/1 includes three cervical vertebrae, but the neural spines are broken in all three vertebrae. The cervical vertebrae are not figured in Godefroit et al. (1999) so this condition in *P. mephistocephalus* could not be assessed. Regardless, the cervical neural spines are damaged in MPC 100/1305, and so they cannot be used to refer this specimen to *Pinacosaurus*. Based on the figures in Godefroit et al. (1999), the acromion does not seem as prominent in *P. mephistocephalus* compared to that in MPC 100/1305. Finally, the proximal head of the radius in *Euoplocephalus tutus* is also expanded, so this is not a diagnostic character for *P. mephistocephalus*. The most recent systematic revision of *Pinacosaurus* by Burns et al. (2011) restricts the generic diagnosis to cranial characters.

Given the lack of diagnostic postcranial characters for both *P. grangeri* and *P. mephistocephalus*, it is challenging to compare MPC 100/1305 to these taxa. The largest *P. grangeri* skeleton, PIN 614 from Bayan Zag, lacks a skull but is about 3.66 m long from the first preserved cervical to the distal end of the tail club knob (Maleev, 1954, gives a length of 4.5 m), and is of a comparable size to MPC 100/1305, with a length of 3.27 m from the first preserved cervical to the distal end of the knob (2.8 m long, including the skull, in Carpenter et al., 2011).

Maleev (1954) noted the presence of 35–40 caudal vertebrae in PIN 614; personal observation of the specimen by VMA suggests that 30–35 caudal vertebrae may have been present, fifteen of which are free caudals. The exact number of caudal vertebrae in the tail club handle is difficult to determine because the vertebrae are obscured by numerous ossified tendons. MPC 100/1305 has 23–25 caudal vertebrae, ten of which are free caudals. *Dyoplosaurus acutosquameus* also has approximately 23 caudals (Arbour et al. 2009), and the referred *Tarchia gigantea* Maryańska, 1977 specimen ZPAL MgD I/113 has approximately 28 caudals (Arbour et al. 2013). PIN 614 has an

unusually high number of caudal vertebrae. ZPAL MgD II/9, also referred to *P. grangeri*, includes a tail club with at least 18 handle caudals. *P. grangeri* may have incorporated more distal caudal vertebrae into the tail club compared to other ankylosaurids, and if so, this may represent a taxonomic difference between PIN 614 and MPC 100/1305. However, in a review of the variability of tail length in dinosaurs, Hone (2012) noted intraspecific variation of caudal vertebral number in the ceratopsian *Leptoceratops* (first reported by Sternberg, 1951). Two specimens found adjacent to one another had caudal vertebral counts of 38 and 48.

The coracoid of MPC 100/1305 also differs from that of *Pinacosaurus*. Coracoids from the Alag Teeg *Pinacosaurus* bonebed (MPC 100/1322, MPC 100/1332) have round anterior edges, whereas the coracoids of MPC 100/1305 have flat anterior edges. The proportions of the humeri in MPC 100/1305 are more similar to those of PIN 614 than MPC 100/151; the maximum widths of the humeri in MPC 100/1305 are 47% and 43% those of the lengths of the right and left humeri, respectively, versus 45% in PIN 614 and 70% in MPC 100/151.

The morphology of the proximal ends of the metacarpals of MPC 100/1305 are consistent with those described for *P. grangeri* (Currie et al. 2011). In both *P. grangeri* and MPC 100/1305, metacarpal IV is approximately rectangular, and metacarpal V is a rounded rectangle, unlike the curved metacarpal IV and triangular metacarpal V of MPC 100/151. Carpenter et al. (2011) noted that MPC 100/1305 differed from *Pinacosaurus* in the pedal digit count, with MPC 100/1305 being tridactyl and *Pinacosaurus* being tetradactyl. Although Maryańska (1977) considered *P. grangeri* tetradactyl, recent work by Currie et al. (2011) using material from the Alag Teeg *Pinacosaurus* bonebed has demonstrated that the pes of *P. grangeri* was tridactyl. The pes of PIN 614 is tridactyl, which was also noted by Maleev (1954).

PIN 614 does not preserve any of the large triangular osteoderms at the posterior corners of the ilia, and the preserved caudal osteoderms do not include

some of the larger, osteoderms found in MPC 100/1305. However, Maleev (1954) noted that PIN 614 was preserved dorsal-side-up with the limbs tucked under the body, and that no osteoderms were preserved on the dorsal side of the body (they had presumably been lost prior to burial). The majority of the preserved osteoderms were found in the vicinity of the humerus and scapula, which may suggest that PIN 614 had forelimb osteoderms similar to MPC 100/1305.

5.6 What is MPC 100/1305?

MPC 100/1305, previously referred to *S. chulsanensis* by Carpenter et al. (2011), shares numerous overlapping elements with the holotype of *S. chulsanensis* but differs in the morphology of the humerus. MPC 100/151 has an unusually large deltopectoral crest for an ankylosaurid, whereas MPC 100/1305 has a deltopectoral crest of average size for an ankylosaurid. This suggests that MPC 100/1305 is not referable to *S. chulsanensis*. Additionally, MPC 100/1305 was collected from the Djadokhta Formation at Zamyn Khond, not the Baruungoyot Formation at Khulsan as reported by Carpenter et al. (2011). *P. grangeri* and *P. mephistocephalus* are the only two ankylosaurid species recognized from the Djadokhta Formation. There are a few differences between MPC 100/1305 and other specimens referred to *P. grangeri*, including the morphology of the anterior edge of the coracoid, and the number of caudal vertebrae. However, it is unclear if these differences are taxonomically significant, or if they represent ontogenetic or individual variation within *P. grangeri* or *P. mephistocephalus*. MPC 100/1305 does not share any species-level diagnostic characters with other Mongolian or Chinese ankylosaurs such as *Crichtonsaurus*, *Talarurus*, or *Tianzhenosaurus*, but does share some features that are present in some of these taxa, such as the proportions of the humerus and the morphology of the acromion process of the scapula. The caudal osteoderms of MPC 100/1305 differ from those of a specimen from the Nemegt

Formation referred to cf. *Tarchia gigantea* (ZPAL MgD I/113), which suggests these specimens do not represent the same species (Arbour et al. 2013). Given the abundance of *P. grangeri* in the Djadokhta Formation, and the similarity of MPC 100/1305 to an uncollected skeleton from a locality that has produced specimens definitively referable to *P. grangeri*, it seems most likely that MPC 100/1305 is a representative of *P. grangeri*. However, given the lack of diagnostic features that could refer this specimen to *Pinacosaurus*, at this time it is most prudent to consider MPC 100/1305 Ankylosauridae indet., or cf. *Pinacosaurus* at best.

6. THE ANKYLOSAURID DINOSAURS OF THE UPPER CRETACEOUS BARUUNGOYOT AND NEMEGT FORMATIONS OF MONGOLIA

6.1 Introduction

The Upper Cretaceous Baruungoyot and Nemegt formations of the Gobi Desert, Mongolia (Fig. 6.1), have produced several ankylosaurid specimens with distinctive bulbous, pyramidal cranial ornamentation. Three ankylosaurid taxa from the Baruungoyot and Nemegt formations were named during the 20th century: *Dyoplosaurus giganteus* Maleev, 1956, *Saichania chulsanensis* Maryańska, 1977, and *Tarchia kielanae* Maryańska, 1977. The holotype of a fourth taxon, *Minotaurasaurus ramachandrani* Miles and Miles, 2009, was purchased from the Tucson Gem, Mineral and Fossil Showcase (Arizona, USA) without provenance data, but it has been suggested that the skull was also collected in Mongolia (Dalton, 2009). *Dyoplosaurus giganteus* was reassigned to the genus *Tarchia* (as *Tarchia gigantea*) by Tumanova (1977). The holotype skull of *Tarchia kielanae*, ZPAL MgD I/111, is poorly preserved; therefore, most comparisons and phylogenetic analyses have used PIN 3142/250, a referred specimen, to represent *Tarchia gigantea* (Vickaryous et al. 2004; Miles and Miles 2009; Thompson et al., 2012). *Tarchia gigantea* and *Saichania chulsanensis* have been recovered as sister taxa in subsequent phylogenetic analyses (Carpenter, 2001; Vickaryous et al., 2004; Thompson et al., 2012).

The discovery of a new skull with some unusual features (MPC D100/1338) from the Baruungoyot Formation at Hermin Tsav prompted the following reassessment of the morphology and taxonomic assignments of previously described ankylosaurid specimens from Mongolia. New cranial characters are identified, and a revised phylogenetic analysis is conducted in order to determine the evolutionary relationships within derived ankylosaurids.

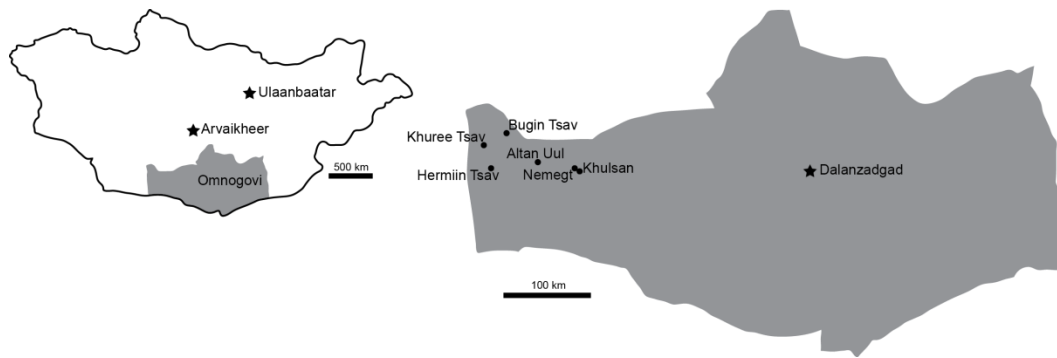


Figure 6.1. Maps of Mongolia and Omnogovi showing locations of specimen localities.

6.2 Materials and methods

Original specimens were examined, measured, and photographed where possible, supplemented by observation of casts and the literature.

Measurements were taken using digital calipers and a measuring tape.

Ankylosaur cranial ornamentation is useful for differentiating ankylosaur taxa, and in this paper the term 'caputegulum' (Latin: "skull tile"), originally coined by Blows (2001), is used to refer to the polygonal sculpturing on an ankylosaur skull. Although caputegulum originally referred only to flat cranial sculpturing (Blows 2001), it can also be applied to the bulbous, discrete cranial ornamentation found in some ankylosaurids. Arbour and Currie (2013a) use caputegulum with a location modifier (e.g. prefrontal caputegulum, supranarial caputegulum) to compare ornamentation patterns in specimens referred to *Euoplocephalus tutus* (Lambe, 1902) and these terms are used here and modified where necessary. Mongolian place names and stratigraphic units follow the spelling conventions outlined in Benton (2000).

The phylogenetic relationships of the Mongolian taxa within the Ankylosauridae were assessed using TNT v1.1 (Goloboff et al. 2008). The data matrix was assembled in Mesquite version 2.72 (Maddison and Maddison 2011) and included 160 characters for 20 species (character statements are given in Appendix 6.1, character matrix is in Appendix 6.2). Outgroup taxa included *Lesothosaurus diagnosticus* Galton, 1978 (a basal ornithischian), *Scelidosaurus*

harrisonii Owen, 1861(a basal thyreophoran), *Stegosaurus* (a stegosaur), the nodosaurid ankylosaurs *Panoplosaurus mirus* Lambe, 1919, and *Pawpawsaurus campbelli* Lee, 1996, and the basal ankylosaurid *Gastonia burgei* Kirkland, 1998. New ankylosaurid cranial characters have been identified and incorporated into a revised data matrix modified from Arbour and Currie (2013). Because several important specimens have been reassigned at the species level, character codings for *Tarchia* are significantly different than those in previous analyses. Characters were treated as unordered and of equal weight. The parsimony analysis conducted in T.N.T. used the Traditional Search option with one random seed and 1000 replicates of Wagner trees and the tree bisection reconnection (TBR) swapping algorithm.

6.3 Systematic Palaeontology

Dinosauria Owen, 1842

Ornithischia Seeley, 1887

Thyreophora Nopcsa, 1915

Ankylosauria Osborn, 1923

Ankylosauridae Brown, 1908

Ankylosaurinae Nopcsa, 1929

6.3.1 *Dyoplosaurus giganteus* Maleev, 1956

Holotype: PIN 551/29, series of caudal vertebrae, metatarsals, phalanges, osteoderms; also includes a partial tail club knob not described or figured by Maleev (1956) or subsequent authors.

Holotype locality and stratigraphy: Nemegt, Mongolia; Nemegt Formation (Upper Campanian – Lower Maastrichtian; Jerzykiewicz 2000)

Previous diagnoses: From Maleev (1956): Anterior caudal vertebrae short, high, amphicoelous; chevrons massive, fused to vertebra; distal caudal vertebrae long,

low; metatarsal bones short, wide; unguals thick, hoof-shaped; osteoderms sharp, thin-walled, with numerous pits and channels on the external surface.

Discussion: Maleev (1956) assigned PIN 551/29 (Fig. 6.2) to the genus *Dyoplosaurus* based on the similarity of the free caudal and handle caudal vertebrae to those of the North American taxon *Dyoplosaurus acutosquameus* Parks, 1924, but erected the new species *Dyoplosaurus giganteus* based on the greater size of PIN 551/29. PIN 551/29 is larger than ROM 784: the largest free caudal vertebra in ROM 784 is 63 mm high, whereas the largest preserved free caudal in PIN 551/29 is 126 mm high. However, because differences in size can result from ontogenetic or individual variation in addition to taxonomic variation, differentiating *Dyoplosaurus giganteus* from *Dyoplosaurus acutosquameus* based only on size differences is insufficient.

The preserved elements of PIN 551/29 do not differ significantly from any other Late Cretaceous ankylosaurine ankylosaurids, except for *Ankylosaurus magniventris* Brown, 1908, and one specimen also from the Nemegt Formation, ZPAL MgD I/113. In PIN 551/29, the handle caudal vertebrae have V-shaped neural spines in which the prezygapophyses diverge at an angle of about 22-26° (Fig. 6.2E). This is the typical condition for most ankylosaurids, including *Euoplocephalus tutus*, *Pinacosaurus grangeri* Gilmore, 1933, and *Talarurus plicatospineus* Maleev, 1952 (Arbour et al. 2009). *Ankylosaurus magniventris* has U-shaped neural spines in which the prezygapophyses diverge at an angle of about 60° (Arbour et al. 2009). ZPAL MgD I/113, a nearly complete tail from the Nemegt Formation, has handle vertebrae that have an intermediate morphology between V-shaped (e.g. *Euoplocephalus tutus*) and U-shaped (*Ankylosaurus magniventris*), with prezygapophyses diverging at an angle of about 37° (Arbour et al. 2009; Fig. 6.2F). Although the handle vertebrae of PIN 551/29 differ from those of ZPAL MgD I/113 and specimens referred to *Ankylosaurus magniventris*, they are indistinguishable from the handle vertebrae of all other ankylosaurines. Short, amphicoelous free caudal vertebrae, long handle vertebrae, fusion of

haemal arches to caudal vertebrae, robust metatarsals, hoof-shaped unguals, and pitted, thin-walled osteoderms are present in all ankylosaurines. PIN 551/29 has no autapomorphies, nor a unique combination of characters that differentiates this specimen from other ankylosaurines. As such, *Dyoplosaurus giganteus* must be regarded as a *nomen dubium*.

Status: *Nomen dubium*.

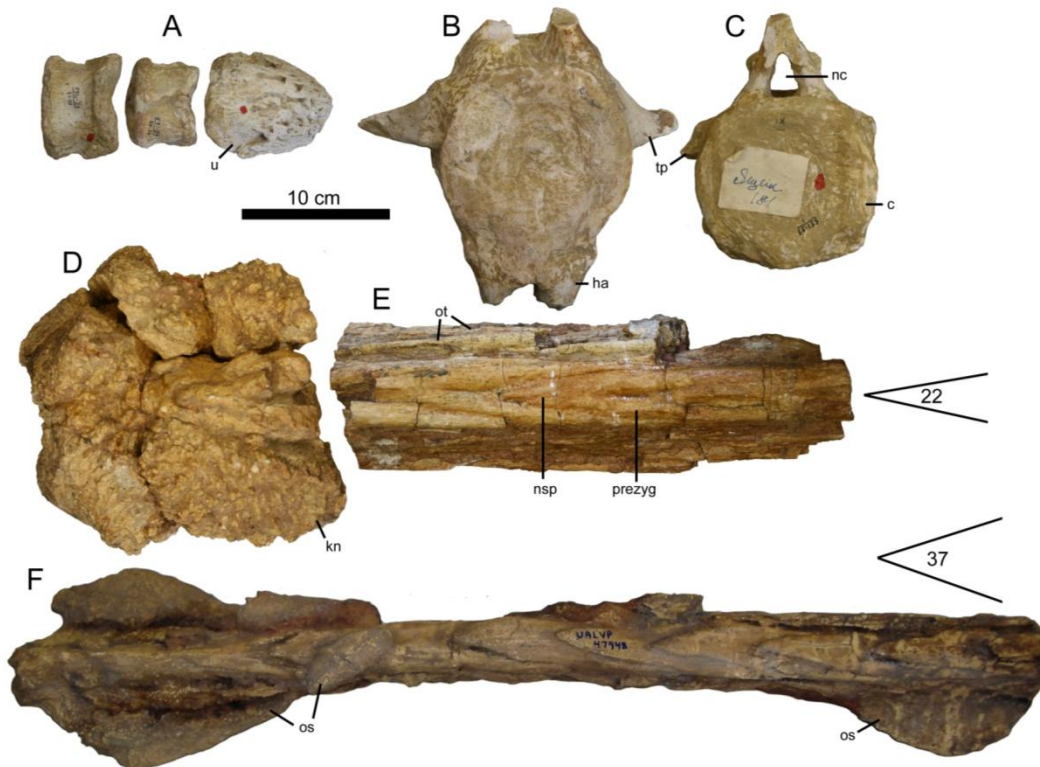


Figure 6.2. Ankylosaurid postcranial elements from the Nemegt Formation. A-E, selected elements of PIN 551-9, holotype of *Dyoplosaurus giganteus*: (A) pedal phalanges and ungual, (B) free caudal vertebra, (C) posterior free caudal vertebra, (D) tail club knob, and (E) distal portion of tail club handle. (F) Portion of tail club of ZPAL MgD I/113, previously referred to *Tarchia gigantea* (photograph of cast UALVP 47948). The morphology of the handle vertebrae of PIN 551-9 and ZPAL MgD I/113 differ, as the angle formed by the neural spine in dorsal view is considerably more acute in PIN 551-9 compared to ZPAL MgD I/113. Abbreviations: c, centrum; ha, haemal arch; kn, tail club knob; nc, neural canal; nsp, neural spine; os, osteoderm; ot, ossified tendon; prezyg, prezygapophysis; tp, transverse process; u, ungual.

6.3.2 *Tarchia kielanae* Maryńska, 1977

= *Minotaurasaurus ramachandrani* Miles and Miles, 2009

Holotype: ZPAL MgD I/111, posterior part of skull roof, braincase, and partial occiput.

Holotype locality and stratigraphy: Khulsan, Mongolia; Baruungoyot Formation (Mid-Upper Campanian, Jerzykiewicz, 2000)

Referred specimen: INBR21004, complete skull, mandibles, and predentary (holotype of *Minotaurasaurus ramachandrani*; provenance unknown)

Previous diagnoses: From Maryńska (1977), for *Tarchia kielanae*: Orbits not completely closed; exoccipital high and short, perpendicular to skull roof; occipital condyle directed posteroventrally; foramen magnum higher than wide; braincase tall; occipital condyle and occiput partly visible in dorsal view; one cranial nerve opening situated posterior to foramen ovale. From Miles and Miles (2009), for *Minotaurasaurus ramachandrani*: Large, horizontally elliptical external nares situated terminally; external nares rimmed laterally and posteriorly by well-developed osteoderm; anteriorly rimmed by thin, triangular osteoderm fused on premaxilla; foramina for premaxillary and maxillary sinuses housed within external nares; premaxillary part of snout broad; occipital condyle poorly developed (as in *Saichania chulsanensis*); occipital condyle directed ventrally; exoccipitals low and separated from skull roof by gap; dorsal part of exoccipitals near supraoccipital curved anterodorsally; quadrate nearly vertical; quadrate head not fused to paroccipital process; skull roof not overhanging occiput; maxillary shelf well-developed and wide to below middle of orbit; premaxilla forms anterior rim of palatal vacuity and separating maxillae from vomer (as in *Pinacosaurus*); premaxillary beak wider than distance between posterior maxillary tooth rows; pterygoid body horizontal (not vertical as in *Saichania chulsanensis*, *Tarchia*, most ankylosaurids); teeth similar to *Pinacosaurus* with weakly developed cingulum.

Discussion: Tumanova (1977), noting similarities between the newly-collected specimen PIN 3142/250, ZPAL MgD I/111 (holotype of *Tarchia kielanae*), and PIN 551/29 (holotype of *Dyoplosaurus giganteus*), reassigned *Dyoplosaurus giganteus* to *Tarchia* to form the new combination *Tarchia gigantea*; *Tarchia kielanae* was retained as a separate species. Although not explicitly stated, it is likely that *Tarchia* was favoured as the generic name over *Dyoplosaurus*, which has priority, because at the time *Dyoplosaurus acutosquameus* was considered a junior synonym of *Euoplocephalus tutus* (Coombs 1971, 1978a), and PIN 3142/150 was clearly not referable to *Euoplocephalus tutus*. In a comprehensive review of ankylosaurs from Mongolia, Tumanova (1987) retained *Tarchia kielanae* as a separate species, but noted that *Tarchia kielanae* and *Tarchia gigantea* could not be easily compared due to the fragmentary nature of ZPAL MgD I/111 (Fig. 6.3B); she suggested that *Tarchia kielanae* may be a synonym of *Tarchia gigantea*. *Tarchia kielanae* was later regarded as a junior synonym of *Tarchia gigantea* by Coombs and Maryńska (1990) and subsequent authors. Arbour et al. (2009) did not address the validity of *Dyoplosaurus giganteus* in their reappraisal of *Dyoplosaurus acutosquameus*. When *Tarchia* is discussed in the literature, comparisons are usually made with the more complete specimen PIN 3142/150 (Figs. 6.3A, 4E, 5A) rather than the holotype skull ZPAL MgD I/111. Although fragmentary, there are several important differences between the skulls of PIN 3142/150 and ZPAL MgD I/111, which indicate that these specimens do not represent the same taxon. As such, *Tarchia kielanae* is here regarded as a valid taxon, but PIN 3142/150 is not referable to *Tarchia kielanae*.

ZPAL MgD I/111 could not be located at ZPAL in October 2009, so the black and white photographs in Maryńska (1977) were used for comparisons. Much of the skull of ZPAL MgD I/111 is missing, and it is difficult to tell exactly which edges are broken, versus which edges are complete, in the figures in Maryńska (1977). Nevertheless, there are two notable features in the preserved part of ZPAL MgD I/111 that are unique: the occiput is visible in dorsal view, and

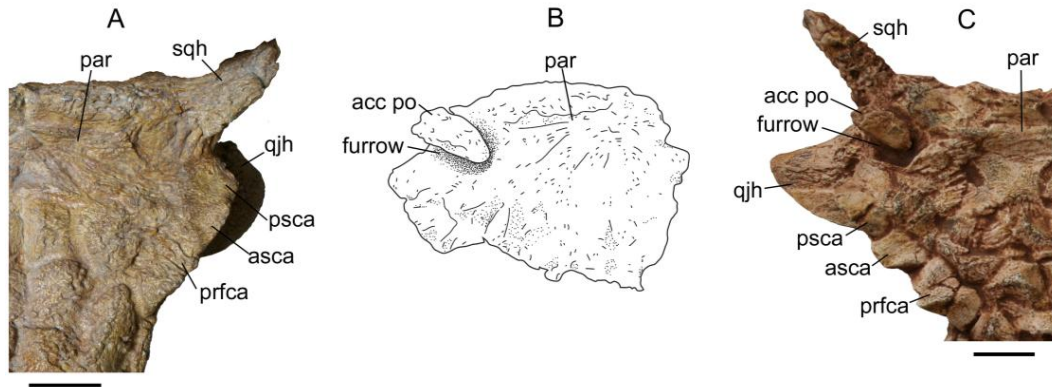


Figure 6.3. Comparison of the supraorbital, postorbital, and squamosal region of three Mongolian ankylosaurid specimens, in dorsal view. A) PIN 3142/250. B) ZPAL MgD I/111, holotype of *Tarchia kielanae* (modified from Maryańska 1977). C) INBR 21004, holotype of *Minotaurasaurus ramachandrani* (photograph of cast UALVP 49402). INBR 21004 has an unusual accessory postorbital ossification and postorbital furrow that is found in only one other specimen, ZPAL MgD I/111. As such, *Minotaurasaurus ramachandrani* should be considered a junior synonym of *Tarchia kielanae*. PIN 3142/250, previously referred to *Tarchia gigantea*, lacks an accessory postorbital ossification and postorbital furrow, and therefore is not referable to *Tarchia*; it is here referred to *Saichania chulsanensis*. Scales equal 5 cm. Abbreviations: acc po, accessory postorbital ossification; asca, anterior supraorbital caputegulum; furrow, furrow in postorbital; par, parietal; prfca, prefrontal caputegulum; psca, postorbital supraorbital caputegulum; sqh, squamosal horn.

the preserved portion of the 'squamosal' horn is surrounded anteriorly and laterally by a pronounced furrow (Fig. 6.3B). The furrow around the 'squamosal' horn is present in only one other known ankylosaur specimen, the holotype of *Minotaurasaurus ramachandrani*; comparison (Fig. 6.3C) shows that the furrow in ZPAL MgD I/111 corresponds to the unusual discrete postorbital ossification in INBR21004, rather than the squamosal horn proper. In contrast, no groove near the squamosal horn is present in PIN 3142/250 (Fig. 6.3A), there is no evidence dorsal view. *Minotaurasaurus ramachandrani* is here regarded as a junior synonym of *Tarchia kielanae*; differences between *Minotaurasaurus ramachandrani* and *Tarchia gigantea* noted by Miles and Miles (2009) almost certainly were between INBR21004 and PIN 3142/250, not INBR21004 and ZPAL MgD I/111. The supraoccipital does not appear to be coossified to the parietals

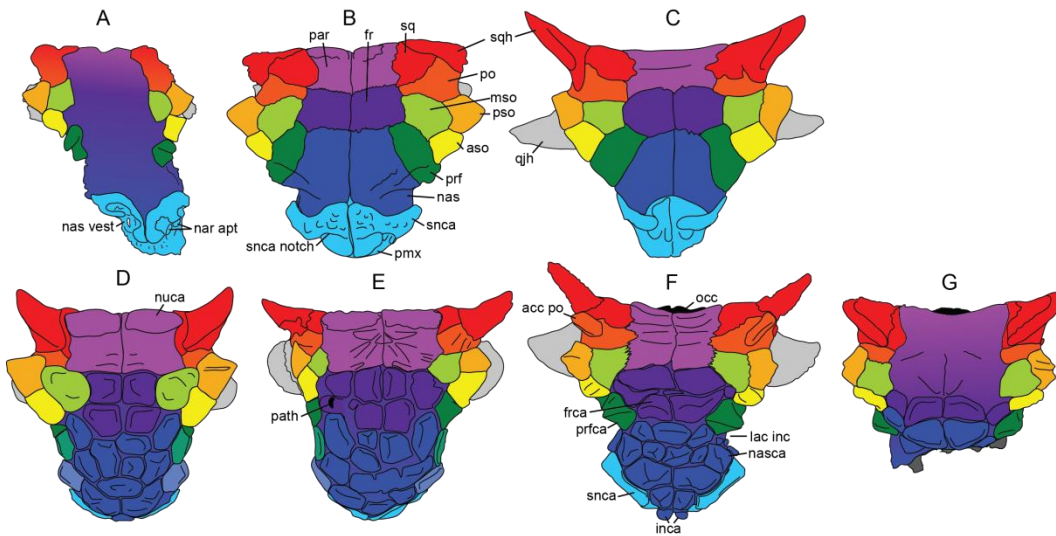


Figure 6.4. Ankylosaurid skulls in dorsal view, showing differences in cranial ornamentation patterns. (A) AMNH 6523, holotype of *Pinacosaurus grangeri*. (B) ZPAL MgD II/1, juvenile *Pinacosaurus grangeri*. (C) IMM 96BM3/1, holotype of *Pinacosaurus mephistocephalus* (drawn from Godefroit et al. 1999). (D) MPC 100/151, holotype of *Saichania chulsanensis*. (E) PIN 3142/250, *Saichania chulsanensis* referred specimen. (F) INBR21004, *Tarchia kielanae*. (G) MPC D100/1388, holotype of *Zaraapelta nomadis*, gen. et sp. nov. Skulls are all scaled to the same anteroposterior length from the anterior end of the skull to the posterior edge of the nuchal crest. Abbreviations: acc po, accessory postorbital ossification; asca, anterior supraorbital caputegulum; aso, anterior supraorbital; fr, frontal; frca, frontal caputegulum; inca, internarial caputegulum; lac, lacrimal; lac inc, lacrimal incisure; msca, middle supraorbital caputegulum; mso, middle supraorbital; nar, narial opening; nar apt, narial aperture; nas, nasal; nas vest, nasal vestibule; nasca, nasal caputegulum; nuca, nuchal caputegulum; occ, occiput; par, parietal; path, pathology; pmx, premaxilla; po, postorbital; prf, prefrontal; prfca, prefrontal caputegulum; psca, postorbital supraorbital caputegulum; pso, posterior supraorbital; qjh, quadratojugal horn; snca, supranarial caputegulum; sqh, squamosal horn.

for a distinct postorbital ossification, and the occipital condyle is not visible in INBR21004, but is in ZPAL MgD I/111. This may reflect an ontogenetic difference.

The referral of INBR21004 (holotype of *Minotaurasaurus ramachandrani*), but not PIN 3142/250, to *Tarchia kielanae* dramatically changes our understanding of the genus *Tarchia* and its diagnosis. *Tarchia kielanae* can be characterized by narrow-based, long squamosal horns (Fig. 6.4), a discrete accessory postorbital ossification (Fig. 6.4), a large and pointed prefrontal

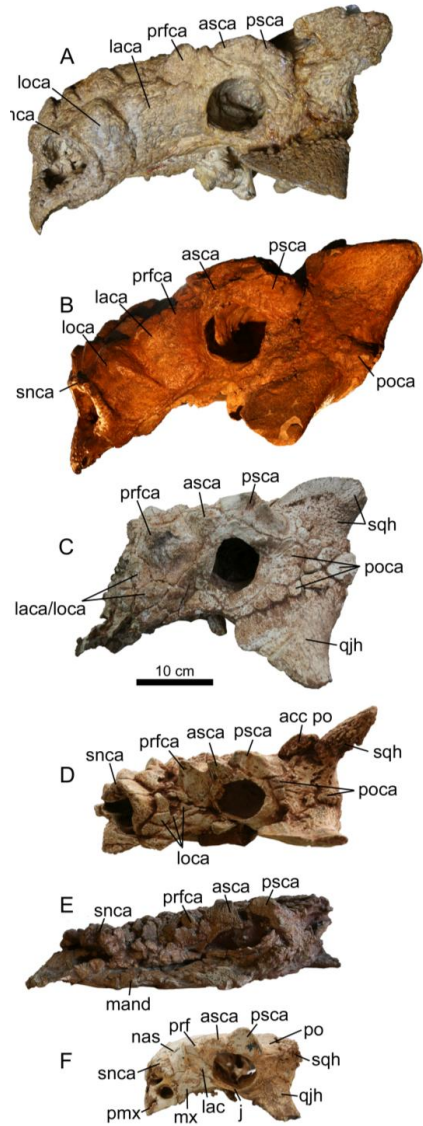


Figure 6.5. Mongolian ankylosaurid skulls in left lateral view. A) PIN 3142/250, referred specimen of *Saichania chulsanensis*. B) MPC 100/151, holotype of *Saichania chulsanensis* (photograph of cast mounted with MPC 100/1305, right side horizontally flipped). C) MPC D100/1388, holotype of *Zaraapelta nomadis*, gen. et sp. nov. D) INBR21004, *Tarchia kielanae* (photograph of cast UALVP 49402). E) AMNH 6523, holotype of *Pinacosaurus grangeri*. F) ZPAL MgD II/1, juvenile *Pinacosaurus grangeri*. Abbreviations: acc po, accessory postorbital ossification; asca, anterior supraorbital caputegulum; j, jugal; lac, lacrimal; laca, lacrimal caputegulum; loca, loreal caputegulum; mx, maxilla; nasca, nasal caputegulum; pmx, premaxilla; pmx orn, premaxillary ornamentation; po, postorbital; poca, postocular caputegulum; prf, prefrontal; prfca, prefrontal caputegulum; psca, postorbital supraorbital caputegulum; qjh, quadratojugal horn; snca, supranarial caputegulum; sq, squamosal; sqh, squamosal horn.

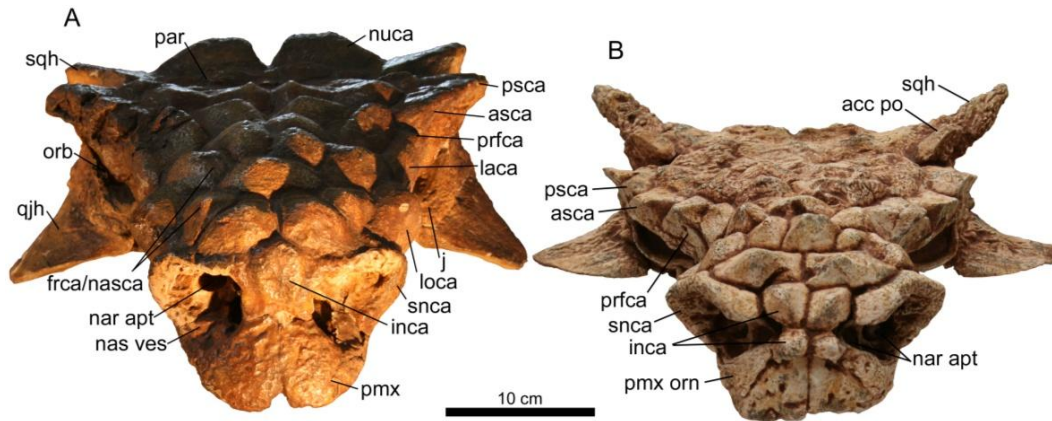


Figure 6.6. Crania of MPC 100/151, holotype of *Saichania chulsanensis* (A) and INBR21004, *Tarchia kielanae* (B) in anterior view. INBR21004 represented by cast specimen UALVP 49402. Abbreviations: acc po, accessory postorbital ossification; alv, alveolar ridge; ang, angular; asca, anterior supraorbital caputegulum; frca, frontal caputegulum; inca, internarial caputegulum; loca, loreal caputegulum; nar, narial opening; nar apt, narial aperture; nas ves, nasal vestibule; nasca, nasal caputegulum; nuca, nuchal caputegulum; orb, orbit; par, parietal; pmx, premaxilla; pmx orn, premaxillary ornamentation; prfca, prefrontal caputegulum; psca, postorbital supraorbital caputegulum; qjh, quadratojugal horn; snca, supranarial caputegulum; sqh, squamosal horn.

caputegulum (Fig. 6.4), numerous small caputegulae in the lacrimal and loreal positions (unlike the single lacrimal and single loreal caputegulae of *Saichania chulsanensis*; Fig. 6.5), a constriction in the snout anterior to the orbits ('lacrimal incisure' *sensu* Hill et al. 2003; Fig. 6.5), smooth-textured, broadly flaring supranarial caputegulae (Fig. 6.6), supranarial caputegulae separated at the midline by a pair of bulbous, square caputegulae (Fig. 6.6), premaxillary ornamentation with a sharp boundary (Fig. 6.6), and a long mandibular caputegulum (Fig. 6.7). Although numerous isolated postcranial specimens are known from the Baruungoyot Formation, at present none can be referred to *Tarchia kielanae* because of the lack of overlapping cranial material, and because *Tarchia kielanae* is not the only ankylosaurid known from this formation.

Status: Valid.

Revised Differential Diagnosis: Ankylosaurine ankylosaurid with bulbous frontonasal cranial ornamentation. Unique among ankylosaurines, has discrete

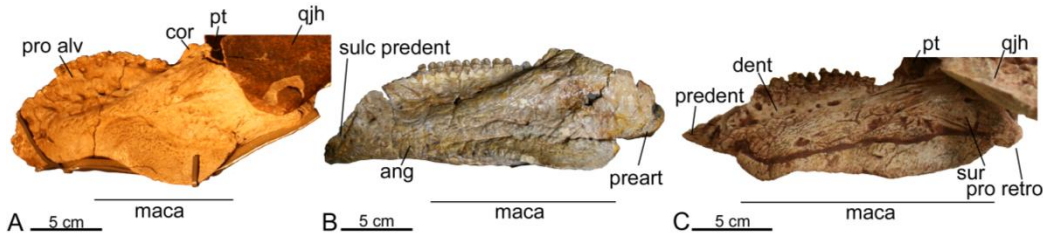


Figure 6.7. Mandibles of Mongolian ankylosaurids in lateral view. A) MPC 100/151, holotype of *Saichania chulsanensis* referred specimen, right mandible horizontally mirrored. B) INBR 21004, *Tarchia kielanae* left mandible. C) PIN 3140/250, *Saichania chulsanensis* referred specimen left mandible. Abbreviations: ang, angular; cor, coronoid; dent, dentary; maca, mandibular caputegulum; preart, prearticular; predent, predentary; pro alv, alveolar border; pro retro, retroarticular process; pt, pterygoid; qjh, quadratojugal horn; sulc predent, predentary sulcus; sur, surangular.

postorbital ossification separate from, but adjacent to, squamosal horn; smooth and widely flaring supranarial caputegulae; triangular region of rugose ornamentation with discrete edge on premaxilla ventral to nasal vestibule. Supranarial caputegulae separated by four bulbous internarial caputegulae (unlike *Saichania chulsanensis*, which has one flat internarial caputegulum). Numerous small lacrimal and loreal caputegulae, unlike *Saichania chulsanensis*. Ventral surface of frontal lacks scroll-like descending process found in *Euoplocephalus tutus*. Anterior and posterior supraorbitals each have distinct peak and separated by notch in dorsal view, unlike continuous-keeled supraorbitals in *Saichania chulsanensis*. Nuchal caputegulae less prominent than those in *Saichania chulsanensis*. Squamosal horns narrow cones, more slender than in *Saichania chulsanensis*. Pterygoid body oriented more horizontally than in *Saichania chulsanensis*. Occipital condyle and occiput partly visible in dorsal view, unlike in *Saichania chulsanensis*. Mandibular caputegulum extends nearly entire length of mandible, unlike *Saichania chulsanensis* in which caputegulum extends about half the length of mandible.

6.3.3 *Zaraapelta nomadis* gen. et sp. nov.

Holotype: MPC D100/1338, a partial skull missing the rostrum.

Etymology: *Zaraapelta nomadis*, *zapa* (Mongolian) hedgehog, in reference to the spiky appearance of the skull, and *pelta* (Latin), a small shield, in reference to the osteoderms found on all ankylosaurs; *nomadis*, from *nomas* (Latin), nomad, in reference to Mongolian travel company Nomadic Expeditions, which has facilitated many years of palaeontological fieldwork in the Gobi Desert.

Holotype Locality and Horizon: N43°28.345', E99°51.032' (WGS 84), Hermin Tsav, Gobi Desert, Mongolia; Baruungoyot Formation (Mid-Upper Campanian, Jerzykiewicz, 2000).

Differential Diagnosis: Ankylosaurine ankylosaurid with bulbous cranial ornamentation. Unlike other ankylosaurs, squamosal horn has unique smooth-textured keel offset from the rest of the squamosal horn by a distinct and abrupt change to a granular texture. Numerous small lacrimal and loreal caputegulae, as in *Tarchia kielanae* but unlike *Saichania chulsanensis*. Large, laterally projecting, pointed prefrontal caputegulum, but smaller than in *Tarchia kielanae*. Ventral surface of frontal has scroll-like descending process, similar to that in *Euoplocephalus* but unlike in *Tarchia kielanae*. Anterior and posterior supraorbitals each have distinct peak and are separated by notch in dorsal view, similar to *Tarchia kielanae* but unlike continuous-keeled supraorbitals in *Saichania chulsanensis*. Elaborate pattern of numerous postocular caputegulae present, with more postocular caputegulae than *Anodontosaurus lambei*, *Saichania chulsanensis* or *Tarchia kielanae*. Frontonasal caputegulae not present posterior to anterior edge of middle supraorbital, unlike *Saichania chulsanensis* and *Tarchia kielanae*, which have distinct frontonasal caputegulae extending to the posterior edge of the posterior supraorbital. Nuchal caputegulae less prominent than those in *Saichania chulsanensis*. Quadrate coossified to paroccipital process, as in *Saichania chulsanensis* but unlike *Tarchia kielanae*.

Occipital condyle and occiput partly visible in dorsal view, unlike in *Saichania chulsanensis* but similar to *Tarchia kielanae*.

Description: MPC D100/1338 (Figs. 6.4-5, 6.8-11) is a partial skull missing the portion of the rostrum anterior to the prefrontals. The left side is otherwise complete, but the right side of the skull is broken across the orbit and lacks the pterygoid, quadrate, quadratojugal, and jugal. No teeth are preserved *in situ*. The antorbital fenestra is absent and the laterotemporal fenestra is obscured in lateral view by the squamosal and quadratojugal. The skull bears the characteristic ankylosaurid cranial sculpturing on the dorsal surface, including prominent squamosal and quadratojugal horns. The description of this skull follows the regional terminology proposed by Vickaryous and Russell (2003) wherein the skull is subdivided into rostral, temporal, palatal, and occipital/basicranial regions.

Rostral Region – Both maxillae are badly damaged and missing their anterior ends. The tooth row is inset from the lateral side of the maxilla, and extends posteriorly almost to the pterygoid. At the posterior end of the maxilla, dorsal to the contact with the pterygoid flange, is a posteriorly-directed circular aperture for the maxillary artery (Fig. 6.10). The nasals are poorly preserved, and the posterior extents of the nasals are unknown. Ventrally, the nasals contribute to the median nasal septum. Anteriorly, the broken edge of the rostrum reveals three openings in each nasal. These openings lead to channels within the nasal that are confluent with a more posteriorly-placed, posteriorly-oriented opening on the ventral side of the skull roof (Fig. 6.11). These channels may represent parts of the nasal passages, which in *Euoplocephalus tutus* are complex and looping (Witmer and Ridgely, 2008).

The prefrontal caputegulum in *Zaraapelta nomadis* is a large, prominent triangle in dorsal view (Fig. 6.9), is slightly concave on its dorsal surface, and is most similar to that of *Tarchia kielanae*. It differs from the prefrontal caputegulae in *Saichania chulsanensis*, which are keeled and in dorsal view have

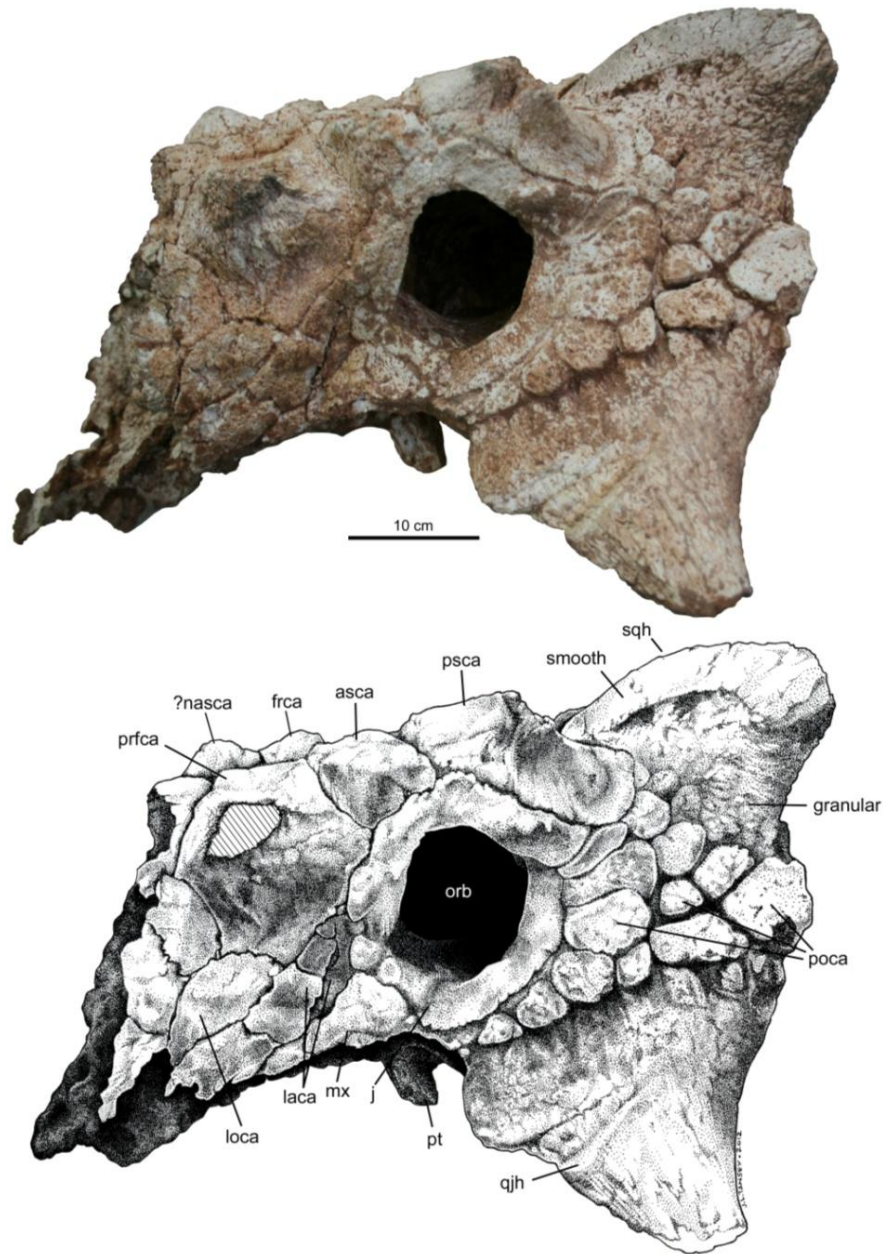


Figure 6.8. MPC D100/1338, holotype of *Zараpelta nomadis*, gen. et sp. nov., photograph and interpretive drawing in lateral view. Abbreviations: asca, anterior supraorbital caputegulum; frca, frontal caputegulum; j, jugal; laca, lacrimal caputegulum; loca, loreal caputegulum; mx, maxilla; nasca, nasal caputegulum; orb, orbit; poca, postocular caputegulum; prfca, prefrontal caputegulum; psca, postorbital supraorbital caputegulum; pt, pterygoid; qjh, quadratojugal horn; sqh, squamosal horn.

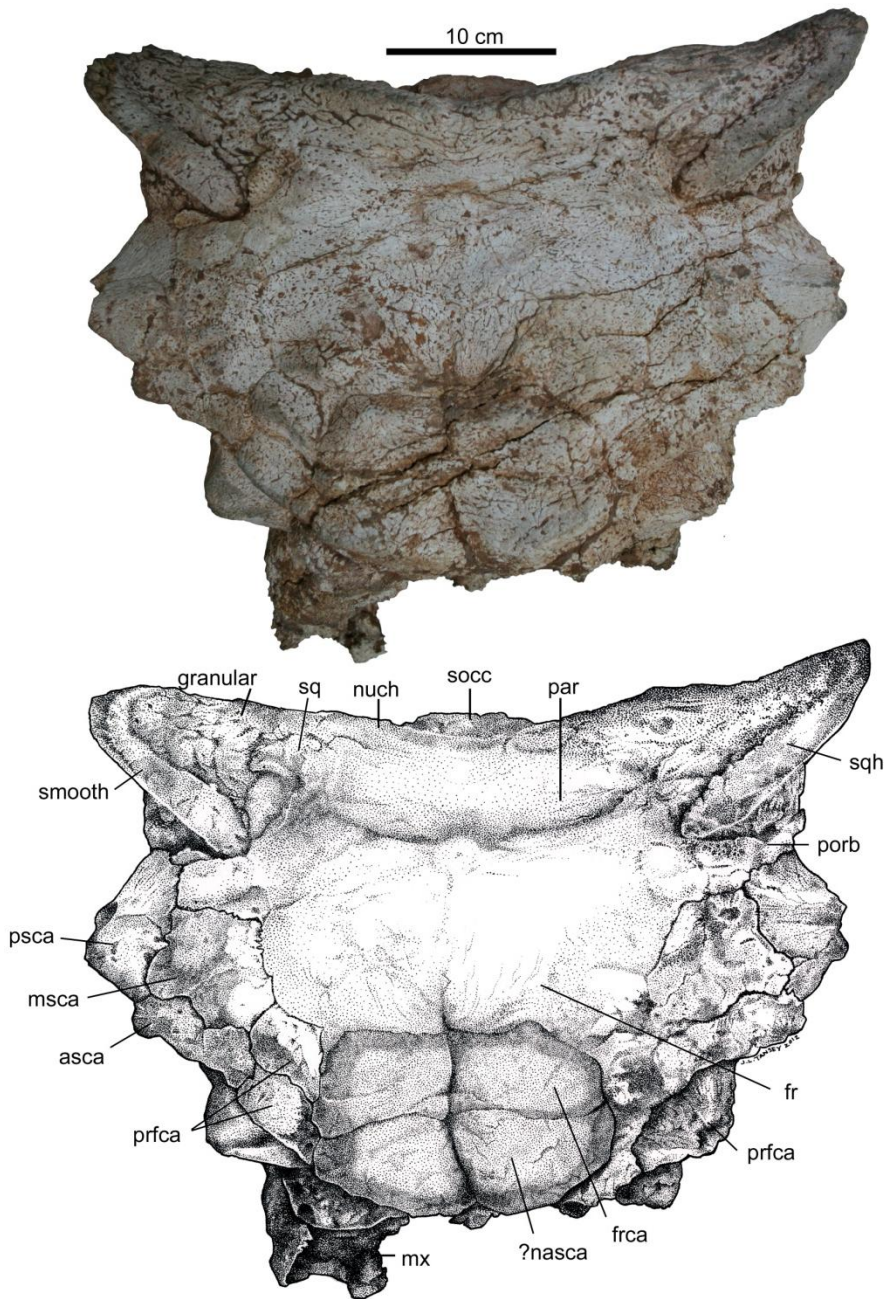


Figure 6.9. MPC D100/1338, holotype of *Zaraqapelta nomadis*, gen. et sp. nov., photograph and interpretive drawing in dorsal view. See list in text for an explanation of anatomical abbreviations. Abbreviations: asca, anterior supraorbital caputegulum; frca, frontal caputegulum; j, jugal; laca, lacrimal caputegulum; loca, loreal caputegulum; mx, maxilla; nasca, nasal caputegulum; nuch, nuchal crest; orb, orbit; poca, postocular caputegulum; porb, postorbital; prfca, prefrontal caputegulum; psca, postorbital supraorbital caputegulum; pt, pterygoid; qjh, quadratojugal horn; socc, supraoccipital; sq, squamosal; sqh, squamosal horn.

straight edges. In *Pinacosaurus grangeri*, the prefrontal caputegulum is prominent and sharply pointed. The boundaries of the lacrimal are not visible in MPC D100/1338, but in *Pinacosaurus grangeri* (ZPAL MgD II/1) this bone forms the anterior edge of the orbit.

The frontals are obscured by the frontonasal caputegulae, which are bulbous and pyramidal. In dorsal view, two pairs of transversely-oriented, rectangular to trapezoidal frontonasal caputegulae are present on each side of the midline of the skull (Fig. 6.8). Lateral to these are smaller, roughly square frontonasal caputegulae. The posterior region of the frontals does not have discrete ornamentation, but discrete frontonasal caputegulae are preserved anterior to the middle supraorbitals. Discrete caputegulae are present between the middle supraorbitals in *Saichania chulsanensis* and *Tarchia kielanae*, but are not present in this region in *Zaraapelta nomadis* (Fig. 6.4); instead, the most posterior discrete caputegulae in *Zaraapelta nomadis* are present anterior to the anterior edge of the middle supraorbital. Although the development of cranial ornamentation may proceed anteriorly to posteriorly (compare the *Pinacosaurus grangeri* juvenile specimen ZPAL MgD II/1 with the adult specimen AMNH 6523, Fig. 6.4), the absence of caputegulae in the posterior frontal region of *Zaraapelta nomadis* is probably not ontogenetically related, as the holotype of *Zaraapelta nomadis* is considerably larger than that of INBR21004. Ventrally, the frontal has a scroll-like, descending process (Figs. 6.10, 11), similar to that observed in some specimens of *Euoplocephalus tutus*; this may represent the posterior wall of the olfactory turbinate (Miyashita et al., 2011). Unlike in *Euoplocephalus tutus*, there is no groove associated with the descending process in the nasal cavity (Miyashita et al., 2011). In contrast, ZPAL MgD I/111 (*Tarchia kielanae*) does not appear to have a scroll-like, descending process on the frontal (Maryańska, 1977: Pl. 24, Fig. 6.2).

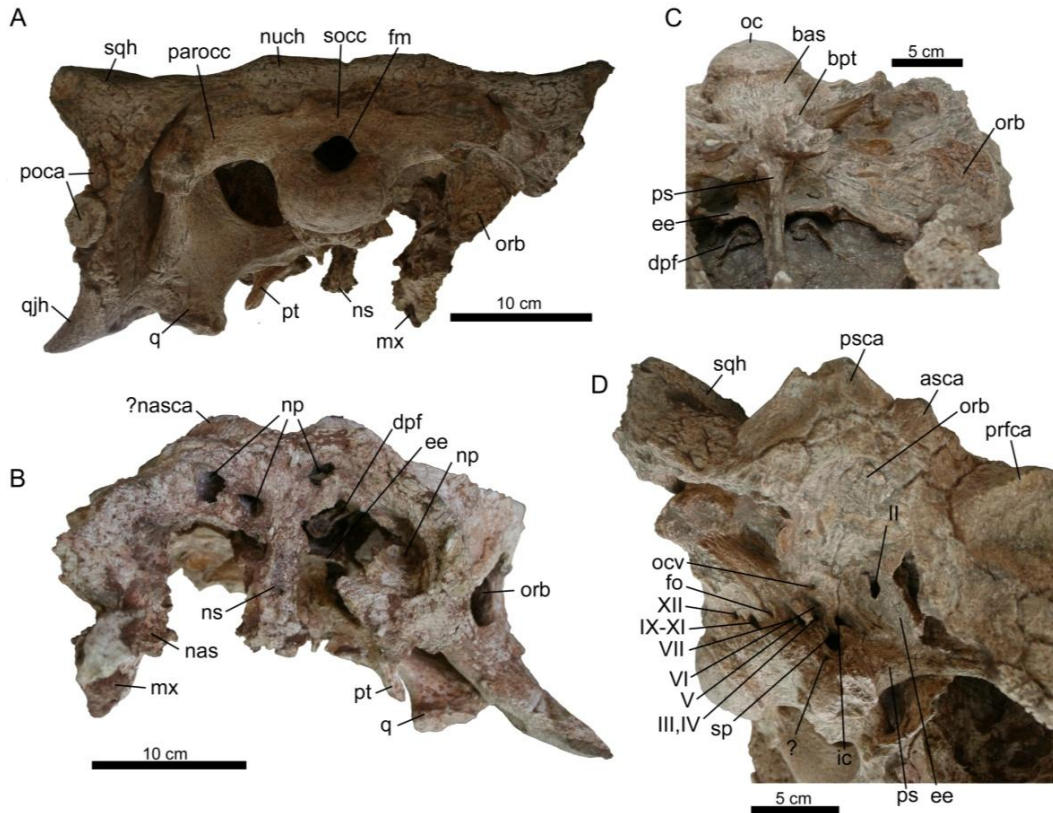


Figure 6.11. MPC D100/1338, holotype of *Zaraapelta nomadis*, gen. et sp. nov. A) Skull in posterior view. B) Skull in anterior view showing cross-section through rostrum. C) Detail of braincase, oblique anteroventral view. D) Detail of braincase, oblique anterolateral view. See list in text for an explanation of anatomical abbreviations. II, opening for optic nerve; III,IV, opening for oculomotor and trochlear nerves; V, opening for trigeminal nerve; VI, opening for abducens nerve; VII, opening for facial nerve; IX-XI, openings for glossopharyngeal, vagus, and accessory nerves; XII, opening for hypoglossal nerve; bas, basioccipital; bpt, basipterygoid process; bs, basisphenoid; dpf, descending process of frontal; ee, ectethmoid; fm, foramen magnum; fo, fenestra ovalis (fenestra vestibularis); ic, internal carotid artery; j, jugal; ls, laterosphenoid; ltf, laterotemporal fenestra; mx, maxilla; ns, nasal septum; np, nasal passage; oc, occipital condyle; ocv, orbitocerebral vein; orb, orbit; orbs, orbitosphenoid; parocc, paroccipital process; prfca, prefrontal caputegulum; ps, parasphenoid; psca, postorbital supraorbital caputegulum; pt, pterygoid; q, quadrate; qj, quadratojugal; qjh, quadratojugal horn; socc, supraoccipital; sp, sinus of pituitary; sqh, squamosal horn.

Temporal Region – Dorsal to the orbit are three supraorbital caputegulae: a smaller anterior supraorbital, a larger posterior supraorbital, and a middle supraorbital positioned more medially that does not reach the lateral edge of the skull (Fig. 6.9). The posterior supraorbital caputegulum, in dorsal view, is more triangular than the anterior supraorbital caputegulum, but the lateral edge is concave. In dorsal view, the lateral edges of the anterior and posterior supraorbitals form a continuous edge in *Saichania chulsanensis*; *Zaraapelta nomadis* is more similar to *Pinacosaurus grangeri* (but not *Pinacosaurus mephistocephalus*) and *Tarchia kielanae* in the morphologies of the supraorbitals, in which each supraorbital has a distinct apex in dorsal view (Fig. 6.4). No ciliary osteoderm (*sensu* Maidment and Porro, 2010) was preserved in MPC D100/1338. The boundaries of the postorbital cannot be distinguished, but in *Pinacosaurus grangeri* the postorbital contributes to the postocular shelf. The jugal forms the ventral border of the orbit; as in all ankylosaurs it is shallow, but it is proportionately deeper in *Zaraapelta nomadis* than the jugals in *Pinacosaurus grangeri* (IVPP V16853, ZPAL MgD II/1), *Pinacosaurus mephistocephalus* Godefroit, Pereda-Suberbiola, Li and Dong, 1999, and *Tarchia kielanae* (Fig. 6.5).

The parietals in MPC D100/1338 lack distinct caputegulae and are smooth with sparse pitting (Fig. 6.9). Posteriorly, the parietals form a nuchal shelf that nearly obscures the braincase in dorsal view; a small crescent of the supraoccipital is visible in dorsal view. This is similar to the condition in *Tarchia kielanae* but differs from *Pinacosaurus grangeri* and *Saichania chulsanensis*, in each of which the braincase is completely obscured by the nuchal shelf in dorsal view (Fig. 6.4). The nuchal shelf is fused to the supraoccipital and paroccipital processes. In *Saichania chulsanensis* and *Tarchia kielanae*, the nuchal shelf has two distinct caputegulae. In MPC D100/1338, there are two caputegulae, but the anterior border is weakly developed relative to those in *Saichania chulsanensis*

and *Tarchia kielanae*. In *Euoplocephalus tutus*, the nuchal shelf has four to six discrete caputegulae.

The squamosal forms the dorsal posterolateral corner of the skull, and is developed into the characteristically ankylosaurid pyramidal squamosal horn. The squamosal horn of MPC D100/1338 is unique among ankylosaurs. The dorsal keel is sharp and the immediately surrounding bone texture is smooth. A short distance from the keel, there is a distinct edge that demarcates a change in texture from smooth to granular (Figs. 6.8, 6.9). The squamosal horns of *Saichania chulsanensis* have uniform textures (Fig. 6.5). The squamosal horn in *Zaraapelta nomadis* is pyramidal, as in *Saichania chulsanensis*, not slender as in *Pinacosaurus mephistocephalus* or *Tarchia* (Fig. 6.4). The squamosal horns of *Tarchia kielanae* are narrow and project well beyond the posterior margin of the skull. *Tarchia kielanae* also uniquely has a set of accessory, elongate caputegulae (or possibly osteoderms) anterior to the squamosal horns, on top of the postorbitals. One potential explanation for the unusual bi-layered texture of *Zaraapelta nomadis* is that the postorbital osteoderm and squamosal horn of *Tarchia* fuse together during ontogeny, and that *Zaraapelta nomadis* represents a more mature specimen of *Tarchia*. INBR21004 still has visible supraorbital-frontal and squamosal-parietal sutures on the dorsal surface of the skull, unlike most other known ankylosaurid adults; this is similar to juvenile *Pinacosaurus grangeri*, which suggests that this specimen does not represent a fully mature individual (contra Carpenter et al. 2011). However, the squamosal horns of *Pinacosaurus grangeri* are anteroposteriorly short and blunt, in both juveniles (ZPAL MgD II/1) and adults (AMNH 6523; Fig. 6.4). The similarity of squamosal horn shape in juvenile and adult *Pinacosaurus grangeri* suggests that squamosal horn shape does not change dramatically throughout ontogeny. Additionally, the differences between the squamosal horns of *Tarchia kielanae* and *Zaraapelta nomadis* are well beyond the range of morphological variation observed in the

relatively large sample sizes of the North American genera *Anodontosaurus lambei*, *Euoplocephalus tutus*, and *Scolosaurus cutleri* (Arbour and Currie 2013a).

The quadratojugal forms the ventral posterolateral corner of the skull, and the quadratojugal horn is most likely an outgrowth of the quadratojugal (Vickaryous et al., 2001). In lateral view the quadratojugal horn is triangular, with a slightly concave posterior border (Fig. 6.8). In *Tarchia kielanae*, there is a distinct notch at the anterior and proximal edge of the quadratojugal horn, but in MPC D100/1338 the quadratojugal horn contacts the jugal in this region (Fig. 6.5). The quadratojugal horn has a smoother texture than the granular region of the squamosal horn, with a few shallow grooves radiating from the apex of the horn. The quadratojugal horn obscures the quadrate in lateral view.

Immediately posterior to the orbit are six caputegulae separated by shallow furrows; dorsally, these are long and rectangular, but they decrease in length ventrally (Fig. 6.8). Posterior to this set of caputegulae are seven smaller, square caputegulae separated by deep furrows, and which are more irregularly arranged. A large and particularly prominent triangular caputegulum is present at the posterior edge of the skull in lateral view. Three indistinct bumps are present at the very base of the squamosal horn. Some other ankylosaurids also have caputegulae in this region of the skull, such as *Anodontosaurus lambei* Sternberg, 1929, and *Tarchia kielanae*. However, in no other ankylosaurid are these smaller caputegulae as abundant or prominent.

Palatal Region – The vomers are badly damaged, but may have extended nearly to the level of the maxillary tooth rows (Fig. 6.10). The nasal passages were probably completely subdivided by the nasals and vomers. The palatines are not preserved. The right pterygoid is not preserved and the left pterygoid is damaged. The pterygoid body is transversely and vertically oriented. It is slightly concave ventrally, and a pterygoid foramen is present. The pterygoid body is fused to the basiptyergoid process, as in *Saichania chulsanensis*. The pterygoid flange projects anterolaterally; it is not tilted anteriorly as in *Tarchia kielanae*,

but has a horizontally flat ventral surface. Although the right pterygoid is not preserved, it appears that a substantial interpterygoid vacuity was present. The quadrate ramus projects posterolaterally and is fused to the quadrate (although the edges of the scarf joint are still slightly visible). The ectopterygoid cannot be distinguished.

Occipital/Basicranial Region – The supraoccipital is an unpaired median bone dorsal to the foramen magnum. It is fused to ventral surface of the parietals, and has a pair of low dorsal prominences (Fig. 6.11). The exoccipital and opisthotic are fused and form the paroccipital process. The exoccipital contributes to the lateral wall of the foramen magnum, and the opisthotic contributes to the lateral wall of the endocranial cavity. The exoccipitals contact the basioccipital ventromedially. The paroccipital process extends laterally from the foramen magnum, and the lateral terminus is fused with the quadrate. This is similar to the condition in *Saichania chulsanensis* but not in *Tarchia kielanae* where the paroccipital process and quadrate are not fused. The process does not fuse to the squamosal. In posterior view, the paroccipital process is somewhat downturned with a concave ventral surface. In dorsal view, the paroccipital processes are obscured by the nuchal crest. The basioccipital forms the posterior floor of the braincase. The occipital condyle is formed only by the basioccipital, and is the typical ankylosaurid reniform shape in posterior and ventral views. The occipital condyle is not offset from the rest of the basioccipital by a neck. The posterior edge of the occipital condyle is visible in dorsal view in *Zaraapelta nomadis*, unlike the conditions in almost all ankylosaurids, but similar to that of *Tarchia kielanae*. However, in *Tarchia kielanae* much more of the occiput is visible in dorsal view, including more of the occipital condyle and the paroccipital processes.

Anterior to the basioccipital is the unpaired basisphenoid. The contact between the basioccipital and basisphenoid is transversely through the basal tubera, which take the form of a rugose transverse ridge on the ventral surface

of the braincase (Fig. 6.10). Anteriorly, the basisphenoid bifurcates into stout, anterolaterally-directed basipterygoid processes. The basipterygoid process fuses to the posterior face of the pterygoid body. There are no sutural contacts that mark the boundaries of the prootic and opisthotic, but these bones form the lateral walls of the braincase.

The limits of the individual bones in the sphenoid region, as in many dinosaurs, are difficult to discern because of extensive fusion. The laterosphenoid is fused to the skull roof and contributes to the postocular shelf, which is weakly developed in MPC D100/1338 relative to other ankylosaurids like *Euoplocephalus tutus* (Miyashita et al., 2011). It is dorsoventrally shallow and extends approximately half the distance from the braincase to the lateral edge of the skull. The orbitosphenoid contributes to the lateral wall of the braincase and the medial wall of the orbit. The parasphenoid forms the anteroventral floor of the braincase and is indistinguishably fused to the basisphenoid. The parasphenoid tapers anteriorly into the long, triangular parasphenoid rostrum (cultriform process), which supports the interorbital septum. The mesethmoid and sphenethmoid are not visible in MPC D100/1338. The ectethmoid is a thin sheet of bone that separates the orbit from the olfactory region. It forms a horizontal shelf ventral to the scroll-like descending process of the frontal, which obscures the descending process in ventral view.

The quadrate is posterior to the pterygoid and anterior to the paroccipital process. It is fused to the paroccipital process, quadratojugal, and pterygoid. The quadratojugal overlaps the ventrolateral edge of the quadrate dorsal to the articular condyle. In ventral view, the articular condyle of the quadrate is roughly triangular, and is wider medially than laterally. In posterior view, the ventral surface of the articular condyle is weakly saddle-shaped.

6.3.4 *Saichania chulsanensis* Maryańska, 1977

Holotype: MPC 100/151, complete skull and both mandibles, seven cervical vertebrae (including fused atlas and axis), ten dorsal vertebrae, ribs, sternum, both scapulocoracoids, humerus, ulna, radius, manus, osteoderms including first and second cervical half rings; cast of specimen before individual elements were separated at ZPAL.

Holotype locality and stratigraphy: Khulsan, Mongolia; Baruungoyot Formation (Mid-Upper Campanian, Jerzykiewicz, 2000)

Referred specimens: PIN 3142/250, complete skull, both mandibles, and prementary (described by Tumanova 1977), undescribed cervical vertebrae, scapula, sacrum, ischia, femur, ribs, and osteoderms (some osteoderms on display at PIN), from Hermin Tsav I, Mongolia, Nemegt Formation, (Upper Campanian – Lower Maastrichtian, Jerzykiewicz, 2000).

Previous diagnoses: From Maryańska (1977): Large, oval external nostrils situated terminally, divided by horizontal septum; premaxillary sinus present; premaxillary portion of rostrum relatively narrow; premaxillae partly covered by well-developed ornamentation; occipital condyle weakly convex, ventrally directed; epipterygoid present; exoccipital low, perpendicular to skull roof, ventral part deflected anteriorly; quadrate oblique with condyle at level of middle part of orbit; orbits anteriorly and posteriorly closed by partly neomorphic bones; skull roof overhangs occipital region; palatal region with strongly developed anterior and posterior maxillary shelves; main body of maxilla surrounds palatal vacuities over small area laterally; one opening for nerves IX-XII; atlas and axis fused; strongly developed intercostal ossifications on trunk; limb bones very massive; forelimb strongly flexed; manus pentadactyl. From Carpenter et al. (2011): cranial ornamentation of large protuberances; squamosal horn large and triangular, contacts quadratojugal horn in occipital view; ridge-like, overhanging supraorbitals; external nares laterally flaring; deeply recessed nasal vestibule with multiple sinus foramina; orbit located at

mid-length of skull; paroccipital process L-shaped in vertical cross-section; tooth rows divergent posteriorly only; cervical neural arches X-shaped in dorsal view with low neural spines; dorsal centra long and low with pleurofossa; cervical armour with larger, posteriorly projecting, triangular osteoderms.

Discussion: The holotype specimen of *Saichania chulsanensis*, MPC 100/151, includes the articulated front half of the animal with skull and *in situ* osteoderms. A cast of the articulated specimen was made prior to final preparation. The skull was described in detail by Maryańska (1977) and Carpenter et al. (2011) and it shares (Figs. 6.4, 6.5) several features with PIN 3142/250, which was previously referred to *Tarchia gigantea*. Tumanova (1977) reassigned *Dyoplosaurus giganteus* to *Tarchia* (forming *Tarchia gigantea*) because the holotypes of both *Dyoplosaurus giganteus* and *Tarchia kielanae* were from coeval deposits from geographically close localities, and because of similarities in osteoderm shapes between ZPAL MgD I/111 (holotype of *Tarchia kielanae*) and the newly-collected PIN 3142/150 (although the osteoderms of PIN 3142/150 were not figured). Most discussions of the morphology and systematics of *Tarchia gigantea* focus on PIN 3142/250, and most character codings in phylogenetic analyses rely heavily on this specimen (Vickaryous et al., 2004; Thompson et al., 2011). The holotype of *Dyoplosaurus giganteus* lacks autapomorphies or a unique combination of characters and is a *nomen dubium*, and PIN 3124/250 differs in several respects from ZPAL MgD I/111 (Fig. 6.3). As such, PIN 3124/250 cannot be referred to *Tarchia kielanae* or *Tarchia gigantea*. Instead, PIN 3142/250 is here referred to the genus *Saichania chulsanensis*.

MPC 100/151 and PIN 3142/250 both have pyramidal squamosal horns, prominent nuchal caputegulae, a generally similar pattern of bulbous frontonasal caputegulae, large, flat, rectangular lacrimal caputegulae and large, flat, rectangular loreal caputegulae (Figs. 6.4, 6.5). The two skulls differ in some aspects of the cranial ornamentation. The internarial caputegulum is anteriorly forked and more rugose in PIN 3142/250 than in MPC 100/151, and the rugose

premaxillary ornamentation is limited to the most anterior parts of the premaxillae at the midline of the skull in PIN 3142/250. The supranarial caputegulae are anteroposteriorly narrower in PIN 3142/250 than in MPC 100/151. The skulls also differ in the relative sizes of the prefrontal caputegulum (smaller in MPC 100/151), middle supraorbital caputegulum (larger and rounder in MPC 100/151) and squamosal horn (deeper in MPC 100/151), and in the presence or absence of postocular caputegulae (present in MPC 100/151, absent in PIN 3142/250). The nuchal caputegulae are less prominent in PIN 3142/250 than in MPC 100/151. The quadrate and paroccipital process are coossified in MPC 100/151, but are not in PIN 3142. Finally, the rostrum of PIN 3142/250 is relatively longer than in MPC 100/151; the orbit is situated at about the midlength of the skull in MPC 100/151, but is more posterior in PIN 3142/250.

Although several differences between PIN 3124/250 and the holotype of *Saichania chulsanensis*, MPC 100/151 have been noted previously (Tumanova, 1987; Carpenter et al., 2011), some of these differences may result from intraspecific variation. This is difficult to assess with only two specimens, as any particular variation will, by default, represent the ends of a potential continuum of variation. Only a few ankylosaurids are known from enough specimens to assess intraspecific or ontogenetic variation: the North American ankylosaurids *Anodontosaurus lambei*, *Euoplocephalus tutus*, and *Scolosaurus cutleri* Nopcsa, 1928, and the Asian *Pinacosaurus grangeri*. A review of variation within *Anodontosaurus lambei*, *Euoplocephalus tutus* and *Scolosaurus cutleri* found that the overall pattern of frontonasal ornamentation, the depth of the squamosal horn, and the presence or absence of postocular caputegulae did not vary intraspecifically (Arbour and Currie 2013a). The exact shapes, sizes, and placements of individual frontonasal and frontoparietal caputegulae varied greatly among specimens, as did the prominence of the supranarial caputegulae. Squamosal horn length and bluntness varied within *Anodontosaurus lambei*, *Euoplocephalus tutus*, and *Scolosaurus cutleri*, although *Scolosaurus cutleri* had

longer and sharper squamosal horns relative to *Anodontosaurus lambei* and *Euoplocephalus tutus*. Taxonomically significant features of the skull included the presence or absence of postocular caputegulae, and the shapes of the squamosal horns (Arbour and Currie 2013a).

Based on variation within the North American taxa, the variation in the anteroposterior length of the supranarial caputegulae, and the size of the middle supraorbital caputegulae in PIN 3142/250 and MPC 100/151, may represent intraspecific variation. The presence or absence of postocular caputegulae was taxonomically significant for *Anodontosaurus lambei* and *Euoplocephalus tutus*, and so the presence of these caputegulae in MPC 100/151 and their absence in PIN 3142/250 may be important. Although squamosal horn length can vary within *Euoplocephalus tutus*, squamosal horn height at the base does not seem to vary greatly (Arbour and Currie 2013a), and so the difference in squamosal horn depths in MPC 100/151 and PIN 3142/250 may also be taxonomically significant.

In addition to variation in the cranial ornamentation, there are several differences in the morphology of the skull of MPC 100/151 and PIN 3142/250. Carpenter et al. (2011) noted that the orbit was positioned more anteriorly in the skull of MPC 100/151 compared to many other ankylosaurids. In lateral view, the orbit of MPC 100/151 is more anteriorly placed compared to that of PIN 3142/250 (Fig. 6.5). However, in *Anodontosaurus lambei* and *Euoplocephalus tutus*, the relative position of the orbit seems to be influenced in part by the length of the rostrum, which may result from taphonomic deformation in the dorsoventral plane 'lengthening' the snout as the arched rostrum is flattened (Arbour and Currie 2013: Fig. 6.5).

PIN 3142/250 has an unusual hole dorsal to the right orbit; remodeled bone along its rim indicates that this is pathological, not taphonomic, in nature (Fig. 6.4). The hole pierces directly into the orbital cavity. Gallagher et al. (1998) observed a zoned bony growth in the nasal passages between the internal nares

and right orbit using computed tomography scans. They suggested that the bony mass and hole may represent a healing puncture wound, possibly from a tyrannosaur bite. Further assessment of this unusual feature of PIN 3142/250 awaits a full description of the computed tomography scan results.

In MPC 100/151, the quadrates are coossified to the paroccipital processes. This has previously been interpreted as a taxonomically significant feature (Tumanova, 1987). However, fusion of skeletal elements can be related to ontogenetic state. Although most specimens of *Anodontosaurus lambei* and *Euoplocephalus tutus* do not show coossification of the quadrate and paroccipital process, at least one does (TMP 1997.132.1; see Arbour and Currie 2013a: Fig. 6).

The basiptyergoid processes in PIN 3142/250 are anteroposteriorly short, but distinct, nubs. In contrast, the basiptyergoid processes in MPC 100/151 are not distinctly separated, and this region is rugose. The morphologies of the basiptyergoid processes in *Anodontosaurus lambei* and *Euoplocephalus tutus* are similar among all referred specimens (Arbour and Currie 2013a), and so the difference in morphology between PIN 3142/250 and MPC 100/151 may be taxonomically significant.

Overall, MPC 100/151 and PIN 3142/250 share a large number of morphological features in common, and most differences between these specimens probably result from individual variation. These specimens represent at least the same ankylosaurid genus. However, a few differences between MPC 100/151 and PIN 3142/250 fall outside the range of variation observed in other better represented ankylosaurids: the presence or absence of postocular caputegulae, the depth of the squamosal horns, and the morphology of the basiptyergoid processes. Coossification of the quadrate and paroccipital process may also be taxonomically significant. Until additional specimens of potential *Saichania chulsanensis* skulls are described that may clarify some of these potential taxonomic differences, PIN 3142/250 will be referred to *Saichania chulsanensis*.

Saichania chulsanensis has some unique postcranial features. MPC 100/151 is the only ankylosaurid known to possess a fused atlas-axis complex. MPC 100/151 also has a particularly robust humerus, with a proximal width 70% of the humeral length; Arbour and Currie (2013b) suggest that this was unlikely to be size-related. The cervical half rings are the most elaborate of any known ankylosaurid. In addition to the typical six, keeled major osteoderms, the band is almost completely covered by coossified interstitial osteoderms (*sensu* Arbour and Currie 2013a). There is a proportionately larger conical osteoderm between the lateral and distal osteoderms of the second cervical half ring, which forms the centre of a rosette. Although some other ankylosaurids have interstitial osteoderms on the cervical half rings (*Anodontosaurus lambei*, *Scolosaurus cutleri*), these are usually found mostly at the bases of the major osteoderms, and do not form extensive sheets above the band.

Several specimens have been referred to *Saichania chulsanensis*, including MPC 100/1305, a nearly complete postcranial skeleton lacking a skull collected by a Russian-Mongolian expedition in 1976 (Arbour and Currie 2013b). The skull described for this specimen by Carpenter et al., (2011) is a cast of MPC 100/151; differences in humeral morphology between MPC 100/151 and MPC 100/1305, as well as stratigraphic position (MPC 100/151 was collected from the Baruungoyot Formation, whereas MPC 100/1305 was collected from the Djadokhta Formation), indicates that MPC 100/1305 should not be referred to *Saichania chulsanensis* (Arbour and Currie 2013b). Additionally, MPC 100/151 seems to have proportionately larger, taller osteoderms on the dorsum posterior to the second cervical half ring, relative to MPC 100/1305. ZPAL MgD I/114, a fragment of skull roof and osteoderms, was referred to *Saichania chulsanensis* by Maryńska (1977) but could not be located at the ZPAL collections during a visit by VMA in 2009. Because this specimen was not figured or described, it is not possible at present to assign it to any taxon. Tumanova (1987) referred PIN 3142/251, a nearly complete skeleton with skull, to *Saichania chulsanensis*, but

this specimen is undescribed (although the tail club is on display at the PIN) and so its taxonomic assignment cannot be verified.

At present, postcranial specimens from the Nemegt Formation previously referred to *Dyoplosaurus giganteus* cannot be referred to *Saichania chulsanensis*. This is unfortunate, because at least two tail club morphotypes are represented in the Nemegt Formation. PIN 551-29 (holotype of *Dyoplosaurus giganteus*), ZPAL MgD I/42 (free caudal vertebrae and tail club), and ZPAL MgD I/43 (the largest known tail club knob for any ankylosaur) have handle caudal vertebrae with V-shaped neural spines, in which the prezygapophyses diverge at an angle of about 22-26° (Fig. 6.2E), the typical condition for most ankylosaurines. ZPAL MgD I/113 has handle vertebrae in which the prezygapophyses diverge at an angle of about 37°, an intermediate morphology between the typical V-shaped morphology of taxa like *Euoplocephalus tutus* or *Pinacosaurus grangeri*, and the U-shaped morphology of *Ankylosaurus magniventris* (Arbour et al., 2009; Fig. 6.2F). This unusual morphology is unlikely to represent intraspecific variation, and so ZPAL MgD I/113 probably does not represent the same taxon as PIN 551-9, ZPAL MgD I/42, or ZPAL MgD I/43 (Arbour et al., 2013). Once the postcranium of PIN 3142/250 is described, it may be possible to refer either the V-shaped or intermediate morphology handle vertebrae to *Saichania chulsanensis*; but at present, the lack of overlapping material prevents assignment of either tail club morphotype to *Saichania chulsanensis*. However, tail clubs recovered from the Nemegt Formation indicate that at least two ankylosaurine species were present in this formation.

Status: Valid.

Revised Diagnosis: Ankylosaurine ankylosaurid with bulbous cranial ornamentation. Uniquely among ankylosaurines, has fused atlas and axis forming a syncervical; proximally wide humerus (proximal width 70% total humerus length); intercostal ossifications present (may also be present in MPC 100/1305); and cervical half rings composed of the underlying band, primary osteoderms,

and coossified interstitial osteoderms completely obscuring the band in external view. Supranarial caputegulae separated by one flat internarial caputegulum (unlike *Tarchia kielanae*, which has four bulbous internarial caputegulae), less broadly flaring than in *Tarchia kielanae*, and rugose (not smooth as in *Tarchia kielanae*). Single large loreal caputegulum and single large lacrimal caputegulum, unlike numerous small lacrimal and loreal caputegulae in *Tarchia kielanae* and *Zaraapelta nomadis*. Prefrontal caputegulum smaller, less laterally projecting than in *Tarchia kielanae* and *Zaraapelta nomadis*. Lateral edges of anterior and posterior supraorbitals continuous, not distinct peaks as in *Tarchia kielanae* and *Zaraapelta nomadis*. No accessory postorbital ossification as in *Tarchia kielanae*. Squamosal horns pyramidal, and larger and broader than in *Tarchia kielanae*. Squamosal horn has uniform texture, unlike bi-layered texture in *Zaraapelta nomadis*. Mandibular osteoderm about half the length of the mandible, anteroposteriorly shorter than in *Tarchia kielanae*.

6.3.5 Ankylosauridae gen. et sp. indet., from the Baruungoyot and Nemegt formations of Mongolia:

Baruungoyot Formation: PIN 3142/251, complete skeleton with skull, referred to *Saichania chulsanensis* by Tumanova (1987), tail club on display at PIN but rest of skeleton undescribed and unfigured (Hermin Tsav II); ZPAL MgD I/114, fragment of skull roof and osteoderms, referred to *Saichania chulsanensis* by Maryńska (1977) but not described or figured and could not be located during a visit in 2009 to ZPAL (Hermin Tsav II).

Nemegt Formation: PIN 551/29, caudal vertebrae, metatarsals, phalanges, osteoderms including partial tail club knob, holotype of *Dyoplosaurus giganteus* (Nemegt); PIN 5011/87, first cervical half ring, on display at PIN as *Tarchia*; MPC KID 233 – undescribed ankylosaurid skeleton (Hermin Tsav 1); MPC KID 329 – undescribed juvenile limb elements (Hermin Tsav 1); MPC KID 335 – caudal vertebra (Hermin Tsav 1); MPC KID 336 – undescribed juvenile material (Hermin

Tsav 1); MPC KID 373 – partial dentary (Hermin Tsav 1); MPC KID 399 – undescribed partial skeleton (partially excavated originally by Russian expedition in 1972; Hermin Tsav 1); MPC KID 515 – dorsal vertebrae, pedal phalanx, and osteoderms (Altan Uul II); MPC KID 538 – partial tail club handle (Altan Uul II); KID 586 – humerus (southwest of Bugeen Tsav); MPC KID 589 – cervical half ring fragment (Khuree Tsav); MPC KID 591 – free caudal vertebra and osteoderms (southwest of Bugeen Tsav); MPC KID 630 – humerus (southwest of Bugeen Tsav); MPC KID 636 – free caudals, handle caudal, osteoderms (southwest of Bugeen Tsav); MPC KID 637 – free caudal, osteoderms (southwest of Bugeen Tsav); numerous isolated osteoderms or clusters of osteoderms from MPC KID expeditions; ZPAL MgD I/42, tail club (Altan Uul IV); ZPAL MgD I/43, tail club, housed at MPC (Altan Uul IV); ZPAL MgD I/49, right humerus (Altan Uul IV); ZPAL MgD I/113, partial pelvis, nearly complete caudal series including free caudal vertebrae and handle but missing tail club knob, osteoderms, skin impressions (Altan Uul III).

6.4 Discussion

The phylogenetic analysis produced ten most parsimonious trees (Fig. 6.12), with the best TBR score of 253 reached one time out of fourteen. The strict consensus tree has a consistency index (CI) of 0.598, and a retention index (RI) of 0.673. The strict consensus tree has significantly better resolution of ankylosaurid interrelationships, better bootstrap support, and better Bremer support compared to the analyses in Arbour and Currie (2013). The strict consensus tree shows a close relationship between *Tarchia kielanae* and *Zaraapelta nomadis*. In 90% of the trees, *Saichania chulsanensis* is the sister taxon to *Tarchia kielanae* and *Zaraapelta nomadis*. These taxa all share pyramidal frontonasal caputegulae with sharp edges, and all except one specimen of *Saichania chulsanensis* (PIN 3142/250) have postocular caputegulae (also present in the North American taxa *Anodontosaurus lambei* and

Scolosaurus cutleri). *Tarchia kielanae* and *Zaraapelta nomadis* share supraorbital caputegulae with distinct apices (also present in *Pinacosaurus grangeri*), a pyramidal prefrontal caputegulum (also present in *Pinacosaurus grangeri*), and more than one caputegulum in the lacrimal and loreal regions.

Safe taxonomic reduction was performed with TAXEQ3, but no species could be safely removed without removing useful phylogenetic data. However, visual inspection of the trees showed that *Dyoplosaurus acutosquameus* was the most labile of the wildcard taxa, and so a second analysis with this taxon removed was performed. When *Dyoplosaurus* was removed, four most parsimonious trees were produced, with a best score of 251 reached 142 times out of 1000. The strict consensus tree had a CI of 0.612, and an RI of 0.693. The strict consensus tree has better resolution of ankylosaurine interrelationships, and slightly higher bootstrap and Bremer supports compared to the analysis that included *Dyoplosaurus acutosquameus*. In this analysis, *Tarchia kielanae* and *Zaraapelta nomadis* are always recovered as sister taxa, with *Saichania chulsanensis* forming the outgroup. These Mongolian ankylosaurids form a polytomy with a clade of primarily North American ankylosaurids (*Ankylosaurus magniventris*, *Anodontosaurus lambei*, *Euoplocephalus tutus*, and the Mongolian *Talarurus plicatospineus*), *Nodocephalosaurus kirtlandensis*, a monophyletic *Pinacosaurus*, and *Tianzhenosaurus youngi*. *Scolosaurus cutleri*, *Tsagantegia longicranialis*, and *Gastonia burgei* formed successive outgroups to this larger clade.

The results of this study provide strong support for a Baruungoyot Formation origin for INBR21004 (holotype of *Minotaurasaurus ramachandrani*, now referred to *Tarchia kielanae*). Miles and Miles (2009) state that the matrix around the specimen suggested an origin in the Gobi Desert of Mongolia or China. The referral of INBR21004 to *Tarchia kielanae*, the holotype of which was collected from the Baruungoyot Formation at Khulsan, strongly suggests that this

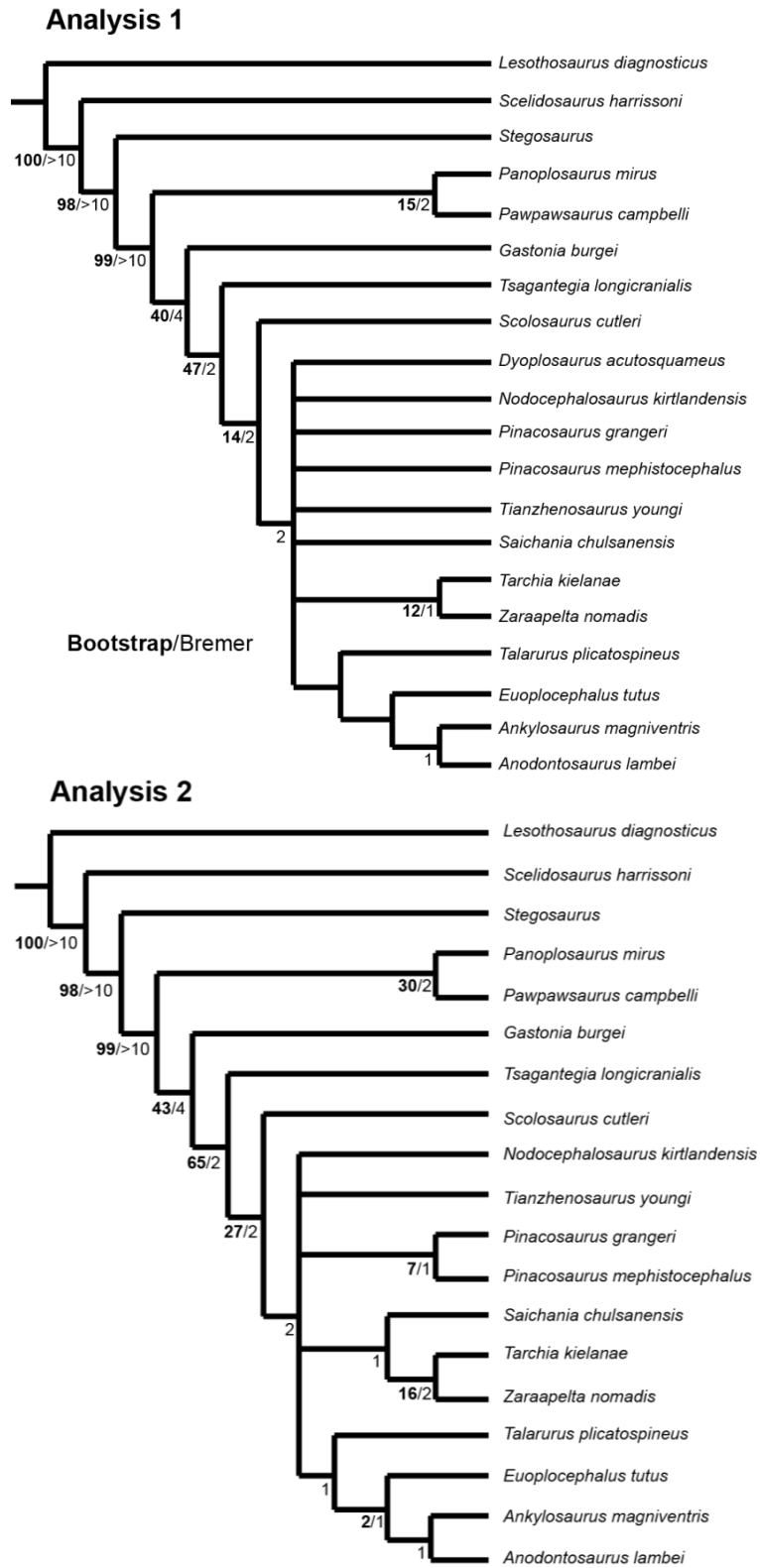


Figure 6.12. Strict consensus trees recovered from the cladistic analyses using the traditional search option in TNT, including bootstrap values (1000 replicates) and Bremer support values. Analysis 1 included all taxa, and Analysis 2 removed *Dyoplosaurus acutosquameus*.

specimen derives from the Baruungoyot Formation of the Mongolian Gobi. Additionally, the close relationship between *Tarchia kielanae* and *Zaraapelta nomadis* (also from the Baruungoyot Formation of the Mongolian Gobi) lends further support to the possible provenance of INBR21004 being Mongolia.

Three ankylosaurids have been identified from the Baruungoyot Formation (*Saichania chulsanensis*, *Tarchia kielanae*, and *Zaraapelta nomadis*), and at least two may have been present in the Nemegt Formation based on tail club morphotypes (tail club morphotype A and tail club morphotype B, one of which may belong to *Saichania chulsanensis*). Although the holotype of *Saichania chulsanensis* preserves some of the postcranium, *Tarchia kielanae* and *Zaraapelta nomadis* are at present only known from cranial material. As such, it is not possible to assign isolated ankylosaurid postcranial remains from the Baruungoyot Formation to any of the named species.

Many formations worldwide include more than one ankylosaur species, but only a few formations include three or more. The Aptian-Albian Mussentuchit Member of the Cedar Mountain Formation includes the nodosaurids *Animantarx ramaljonesi* Carpenter, Kirkland, Burge and Bird, 1999, and *Peloroplites cedrimontanus* Carpenter, Bartlett, Bird and Barrick, 2008, and the ankylosaurid *Cedarpelta bilbeyhallorum* Carpenter, Kirkland, Burge and Bird, 2001 (Carpenter et al., 2008); the Campanian Dinosaur Park Formation includes the nodosaurids *Edmontonia rugosidens* Gilmore, 1930 and *Panoplosaurus mirus* (Ryan and Evans, 2005) and the ankylosaurids *Dyoplosaurus acutosquameus*, *Euoplocephalus tutus*, and *Scolosaurus cutleri*, although *Scolosaurus cutleri* from Alberta may be derived from the Oldman Formation instead (Arbour and Currie 2013a). The Baruungoyot Formation includes the ankylosaurids *Saichania chulsanensis*, *Tarchia kielanae*, and *Zaraapelta nomadis*. If the single specimen of *Scolosaurus cutleri* from the Dinosaur Park Formation is instead from the underlying Oldman Formation, then the Baruungoyot Formation preserves the greatest diversity of ankylosaurid ankylosaurs in the world. In the Dinosaur Park

Formation, the beak shapes of nodosaurid ankylosaurs and ankylosaurid ankylosaurs may have reflected niche partitioning of food resources (Mallon, 2012). The beak morphology of *Zaraapelta nomadis* is unknown, but the beak morphologies of *Saichania chulsanensis* and *Tarchia kielanae* did not differ substantially, and dietary niche partitioning between ankylosaurids cannot alone explain the high diversity of ankylosaurids in the Baruungoyot Formation. Although an indeterminate sauropod is known from the Baruungoyot Formation (Weishampel et al. 2004), sauropods appear to have been rare components of the Baruungoyot ecosystem, and because of their ability to access forage at heights unavailable to ankylosaurs, it seems unlikely that sauropods and ankylosaurids would be in direct competition for food resources. Ankylosaurids can be considered the dominant megaherbivore in the Baruungoyot Formation, which was otherwise composed primarily of small herbivorous or omnivorous dinosaurs like the ceratopsian *Bagaceratops rozhdestvenskyi* Maryańska and Osmolska, 1975, the pachycephalosaurid *Tylocephale gilmorei* Maryańska and Osmolska, 1974, oviraptorids, alvarezsaurids, and avimimids, a small carnivorous velociraptorine (Weishampel et al. 2004; Longrich et al. 2010), and small birds, lizards, and mammals.

Alternately, ankylosaurid diversity in the Baruungoyot Formation may have been accomplished through sexual selection. *Saichania chulsanensis*, *Tarchia kielanae*, and *Zaraapelta nomadis* have some of the most elaborate cranial ornamentation of any ankylosaurids, with relatively more pronounced frontonasal, squamosal, and quadratojugal ornamentation compared to earlier ankylosaurids from Mongolia and China (e.g., *Pinacosaurus grangeri*, *Tsagantegia longicranialis* Tumanova, 1993) or contemporaneous ankylosaurids from North America (e.g., *Euoplocephalus tutus*, *Scolosaurus cutleri*). Somewhat surprisingly, a sexual display function for ankylosaurid cranial ornamentation has not previously been proposed, despite the fact that sexual display has been proposed as the function of far less elaborate structures in some theropods and

sauropods (see Hone et al. 2011 for a review). Knell et al. (2013) outline five characteristics that can be used to identify potential sexually selected traits in fossil animals: sexual dimorphism, ontogenetic changes, allometry, phylogenetic diversity and morphological disparity, and costliness. There are too few specimens to evaluate sexual dimorphism, ontogenetic changes, or allometry in the Baruungoyot and Nemegt formation ankylosaurids. However, there is no evidence for sexual dimorphism in the better represented North American genera *Anodontosaurus lambei*, *Euoplocephalus tutus*, and *Scolosaurus cutleri*. Although there is a relatively large sample of juvenile *Pinacosaurus grangeri*, few adult specimens are known, and so assessing ontogenetic or allometric changes in this genus is also difficult. The bone that forms ankylosaurid cranial ornamentation has a physiological cost, and would not seem to confer additional protection against predation; although this observation alone cannot be used to support a sexually-selected interpretation of elaborate ankylosaurid cranial ornamentation, it does provide support for the suggestion that ankylosaurid cranial ornamentation may have been at least partly sexually selected.

6.5 Conclusions

A systematic review of ankylosaurid material from the Baruungoyot and Nemegt formations of Mongolia shows that three species were present in the Baruungoyot Formation and two in the Nemegt Formation. "*Dyoplosaurus giganteus*" is a *nomen dubium* because the holotype lacks any diagnostic features at the level of genus or species. *Tarchia kielanae* is here recognized as a valid species based on the presence of a single autapomorphy, an accessory postorbital ossification surrounded by a distinct furrow. This feature is also present in the holotype of *Minotaurasaurus ramachandrani*. As such, *Minotaurasaurus ramachandrani* is considered a junior synonym of *Tarchia kielanae*, which in turn suggests that INBR 21004 may have been collected from the Baruungoyot Formation of Mongolia. A new genus and species, *Zaraapelta*

nomadis, is characterized by squamosal horns with a distinct bi-layered texture, and by extensive postocular ornamentation. PIN 3142/250, previously referred to *Tarchia gigantea*, is here referred to *Saichania chulsanensis*. At least two ankylosaurid species were present in the Nemegt Formation based on tail club morphotypes, but the lack of overlapping postcranial material precludes the referral of either morphotype to the one named species in the formation, *Saichania chulsanensis*. A revised phylogenetic analysis of the Ankylosauridae recovered *Tarchia kielanae* and *Zaraapelta nomadis* as sister taxa, and also showed a close relationship between these species and *Saichania chulsanensis*.

Appendix 6.1. Character statements.

General notes:

Codings for *Tarchia* are the same as those for *Minotaurasaurus* in Arbour and Currie (2013a), plus additional new characters in this analysis. Postcranial character codings from *Tarchia gigantea* were not transferred to *Tarchia kielanae* or *Saichania chulsanensis*, because no postcranial specimens can be definitely attributed to these species at this time.

Character addition and removal:

Characters 147-160 are new to this analysis. The following characters from Thompson et al. (2012) and Arbour and Currie (2013a) were removed from this analysis (see Chapter 10 for rationales):

Characters 9-12

Character 17

Characters 27-28

Character 31

Characters 52 and 53

Character 55

Character 60

Characters 71 and 72

Character 79

Character 85

Character 106

Character 109

Characters 143-146

Characters 160-161

Character 163

Characters 164-165

Character 167

Character 168

Character 169

Characters:

1. Antorbital fenestra: present (0); absent (1).

2. Modified: Lateral temporal fenestra, visible in lateral view: visible (0); not visible (1).
3. Supratemporal fenestra: open (0); closed (1).
4. Skull dimensions, including ornamentation: longer than wide (0); as wide, or wider than long (1).
5. Modified: Width of the posterior margin of the skull (including squamosal horns) relative to the maximum width across the orbits: greater or equal (0); less (1).
6. Size of occiput: higher than wide (0); wider than high (1).
7. Modified: External nares, defined as the outermost rim of the nasal vestibule, opening faces: laterally (0); anterolaterally (1); anteriorly (2).
8. External nares, visible in dorsal view: visible (0); hidden (1).
9. Orbits, angle of orbital axis: $<40^\circ$ (0); $>40^\circ$ (1).

Saichania from 1 to 0.

10. Antorbital region of the dorsal skull surface: flat (0); domed (1).
11. Development of the postocular shelf: not developed (0); completely separating orbit from temporal space (1).

Updated codings: *Tianzhenosaurus* from 1 to ?. Notes: Cannot be determined from Pang and Cheng (1998).

12. Gap between palate and braincase: open (0); closed by a dorsal projection of the pterygoid (1).
13. Dimensions of premaxillary palate: longer than wide (0); wider than long (1).
14. Shape of the premaxillary palate: sub-triangular (0); sub-quadrate (1); sub-oval (2).
15. 'V' or 'U'-shaped median indentation of the anterior margin of the premaxilla: absent (0); present (1).
16. Caudoventral extension of premaxillary tomium in lateral view: ends anteriorly to the maxillary teeth (0); obscures anteriormost maxillary teeth (1).
17. Bone bordering anterior margin of internal nares: premaxilla (0); maxilla (1).
18. Shape of the ventral margin of premaxillary tomium in lateral view: flat (0); convex (1); concave (2).
19. Shape of the maxillary tooth row: straight (0); medially convex (1).

20. Maxillary tooth row position: lateral margin of skull (0); inset (1).
21. Modified: Distance between posteriormost extent of maxillary tooth rows relative to the width of the premaxillary beak: wider (0); narrower (1). [The width of the premaxillary beak is measured where the lateral edges of the beak are most parallel, which is usually close to the posterior of the premaxilla.]
22. Anterior and posterior supraorbitals (recognisable by distinct regions of ornamentation above the orbit): absent (0); present (1).
23. Form of supraorbital ornamentation: boss-like, rounded laterally (0); sharp lateral rim, forming a ridge (1).
24. Proportions of jugal orbital ramus: depth greater than transverse breadth (0); transverse breadth greater than depth (1).
25. Shape of quadrate in lateral aspect: curved (anteriorly convex, posteriorly concave) (0); straight (1).
26. Inclination of quadrate in lateral aspect: near vertical (0); almost 45° anterolaterally (1).
27. Form of the anterior surface of the quadrate: transversely concave (0); not concave (1).
28. Ventral projection of the mandibular process of the quadrate in lateral view: projects beyond the quadratojugal ornamentation (0); hidden by quadratojugal ornamentation (1).
29. Form of quadrate mandibular extremity: symmetrical (0); medial condyle larger than lateral condyle (1).
30. Inclination of the articular surface of the quadrate condyle in posterior view: horizontal (0); ventromedially inclined at approximately 45° to horizontal (1).
31. Lateral ramus of the quadrate: present (0); absent (1).
32. Dorsoventral depth of the pterygoid process of the quadrate: deep (0); shallow (1).
33. Contact between paroccipital process and quadrate: sutural (0); fused (1).
34. Contact between pterygoids: pterygoids separate caudomedially, forming an interpterygoid vacuity (0); pterygoids joined medially forming a pterygoid shield (1).
35. Direction of the pterygoid flange: anterolateral (0); anterior/parasagittal (1).
36. Contact between basiptyergoid processes and pterygoid: sutural (0); fused (1).
37. Position of ventral margin of the pterygovomerine keel relative to alveolar ridge: dorsal (0); level (1).

38. Dorsal extent of median vomer lamina: does not meet skull roof (0); meets skull roof (1).
39. Pterygoid foramen: absent (0); present (1).
40. Position of posterior margin of pterygoid body relative to the anterior margin of the quadrate condyle: anteriorly positioned (0); in transverse alignment (1).
41. Caudoventral secondary palate: absent (0); present (1).
42. Posterior palatal foramen: absent (0); present (1).
43. Direction of paroccipital process extension: caudolateral (0); lateral (1).
44. Bones forming the occipital condyle: basioccipital and exoccipital (0); basioccipital only (1).
45. Length of basisphenoid relative to the basioccipital: longer (0); shorter or equal (1).
46. Form of basisphenoidal tuberosities: medially separated rounded rugose stubs (0); continuous transverse rugose ridge (1).
47. Size of basipterygoid processes: twice as long as wide or over (0); less than twice as long as wide (1).
48. Form of the cranial nerve foramina IX-XII: separate foramina (0); single foramen shared with the jugular vein (1).
49. Direction of occipital condyle: posterior (0); posteroventral (1).
50. Direction of the foramen magnum: posterior (0); posteroventral (1).
51. Premaxillary teeth: present (0); absent (1).
52. Cingula on maxillary and/or dentary teeth: absent (0); present (1).
53. Maxillary and/or dentary tooth crown shape: ≥ 13 denticles, tooth crown pointed (0); < 13 denticles, tooth crown rounded (1).
54. Number of dentary teeth: < 25 (0); ≥ 25 (1).
55. Position of mandible articulation relative to mandibular adductor fossa: posterior (0); posteromedial (1).
56. Mandibular fenestra: present (0); absent (1).
57. Depth of the dentary symphyseal ramus relative to half the maximum depth of the mandibular ramus in lateral view: deeper (0); shallower (1).
58. Shape of dorsal margin of the dentary in lateral view: straight (0); sinuous (1).

59. Development of the coronoid process: not developed (0); distinct (1).
60. Position of glenoid for quadrate relative to mandibular axis: medially offset (0); in line (1).
61. Size and projection of the retroarticular process: small with no dorsal projection (0); well developed with a dorsal projection (1).
62. Size of prementary ventral process: distinct, prong shaped process (0); rudimentary eminence (1).
63. Ornamentation, defined as sculpturing of skull bones or addition of osteoderms: absent (0); present (1).
64. Modified: Frontonasal and/or frontoparietal cranial ornamentation: rugose, not differentiated into discrete polygons (caputegulae) (0), differentiated into discrete polygons (caputegulae) (1).
65. A single large medial polygon of ornamentation in the parietal region: absent (0); present (1).
66. Modified: Median nasal caputegulum (located posterior to the supranarial ornamentation, on the midline of the skull): absent (0), present, hexagonal (1), present, triangular (1).
67. Modified: Frontonasal caputegulum relief: concave to flat (low relief) (0), bulbous (high relief) (1).
68. Modified: Projection of squamosal horns relative to the posterior margin of the dorsal surface of the skull: horns do not project past posterior margin of skull in dorsal view (0), horns project past posterior margin of skull in dorsal view (1).
69. Modified: Squamosal horn: absent (0); present (1).
70. Quadratojugal 'horn': absent (0); present (1).
71. Modified: Shape of quadratojugal horn in dorsal view: U-shaped, with round distal edge (0), triangular, with pointed distal edge (1).
72. Modified: nuchal ornamentation (at posterior margin of skull roof): absent (0); present (1).
73. Posterior projection of the nuchal shelf: does not obscure occiput in dorsal view (0); obscures occiput in dorsal view (1).
74. Modified: Length of mandibular caputegulum with respect to the length of the mandible: less than or equal to half the length (0); over three quarters the length (1).
75. Mandibular osteoderm: absent (0); present (1).

76. Type of contact between the atlantal neural arch and intercentrum: open (0); fused in adult (1).
77. Type of contact between the atlantal neural arches: no median contact (0); median contact (1).
78. Contact between atlas and axis: articulated (0); fused (1).
79. Dimensions of cervical vertebrae centra: anteroposteriorly longer than transverse width (0); anteroposteriorly shorter than transverse width (1).
80. Ratio of maximum neural spine width to height in anterior cervicals: <0.25 (0); ≥ 0.25 (1).
81. Alignment of anterior and posterior faces of cervical centra: aligned (0); anterior face dorsal to posterior face (1); anterior face ventral to posterior face (2).
82. Ratio of anteroposterior [dorsal] centrum length to posterior centrum height: >1.1 (0); <1.1 (1).
83. Longitudinal keel on ventral surface of dorsal centra: present (0); absent (1).
84. Cross sectional shape of neural canal in posterior dorsals: circular (0) elliptical, with long axis running dorsoventrally (1).
85. Shape of the proximal cross-section of the dorsal ribs: triangular (0); 'L'- or 'T'-shaped (1).
86. Attachment of dorsal ribs to posterior dorsal vertebrae: articulated (0); fused (1).
87. Contact between posteriormost dorsal vertebrae: articulated (0); fused to form a presacral rod (1).
88. Paravertebrae: absent (0); present (1).
89. Longitudinal groove in ventral surface of the sacrum: absent (0); present (1). (Parish 2005: 95).
90. Ratio of maximum distal width to height of the neural spines of proximal caudals: ≤ 0.2 (0); >0.2 (1).
91. Direction of the transverse processes of proximal caudals: craniolaterally projecting (0); caudolaterally projecting (1); laterally projecting (2).
92. Persistence of transverse processes down the length of the caudal series: not present beyond the mid-length of the series (0); present beyond the mid-length of the series (1).
93. Attachment of haemal arches to their respective centra: articulated (0); fused (1).

- 94.** Shape of distal caudal postzygapophyses: short with a sub-triangular end [wedge-shaped] (0); long with a rounded end [tongue shaped] (1).
- 95.** Extent of pre- and postzygapophyses over their adjacent centra in posterior vertebrae: extend over less than half the length of the adjacent centrum (0); extend over more than half the length of the adjacent centrum (1).
- 96.** Shape of the posterior haemal arches: rounded haemal spine in lateral view with no contact between haemal arches (0); inverted 'T'-shaped haemal spine in lateral view, with contact between the ends of adjacent spines (1).
- 97.** Ossified tendons in distal region of tail: absent (0); present (1).
- 98.** Dimensions of coracoid: longer than wide (0); wider than long or equal width and length (1).
- 99.** Form of the anterior margin of the coracoid: convex (0); straight (1).
- 100.** Cranioventral process of coracoid: absent (0); present (1).
- 101.** Size of coracoid glenoid relative to scapula glenoid: sub-equal (0); half the size (1).
- 102.** Contact between scapula and coracoid: articulated (0); fused (1).
- 103.** Scapula glenoid orientation: ventrolateral (0); ventral (1).
- 104.** Ventral process of scapula at the caudoventral margin of glenoid: absent (0); present (1).
- 105.** Form of the scapula acromion process: not developed or ridge-like along the dorsal border of the scapula (0) tab-like, perpendicular to scapular blade (1) flange-like and folded over towards the scapula glenoid (1) ridge terminating in a knob-like eminence (2).
- 106.** Orientation of the acromion process of scapula: directed away from the glenoid (0); directed towards scapula glenoid (1).
- 107.** Scapulocoracoid buttress: absent (0); present (1).
- 108.** Distal end of scapula shaft: narrow (0); expanded (1).
- 109.** Contact between sternal plates: separate (0); fused (1).
- 110.** Separation of humeral head and deltopectoral crest in anterior view: continuous (0); separated by a distinct notch (1).
- 111.** Separation of humeral head and medial tubercle in anterior view: continuous (0); separated by a distinct notch (1).

- 112.** Ratio of deltopectoral crest length to humeral length: ≤ 0.5 (0); > 0.5 (1).
- 113.** Orientation of deltopectoral crest projection: lateral (0); anterolateral (1).
- 114.** Shape of the radial condyle of humerus round / proximal end of radius in end-on view: non-circular (0); circular (1).
- 115.** Ratio of the length of metacarpal V to metacarpal III: ≤ 0.5 (0); > 0.5 (1).
- 116.** Manual digit number: 5 (0); 4 (1); 3 (2).
- 117.** Shape of manual and pedal ungual phalanges: claw shaped (0); hoof shaped (1).
- 118.** Length of the preacetabular process of ilium as a percentage of total ilium length: $\leq 50\%$ (0); $> 50\%$.
- 119.** Angle of lateral deflection of the preacetabular process of the ilium: 10° – 20° (0); 45° (1).
- 120.** Orientation of the preacetabular portion of the ilium: near vertical (0); near horizontal (1).
- 121.** Form of the preacetabular portion of the ilium: straight process (0); pronounced ventral curvature (1).
- 122.** Lateral exposure of the acetabulum: exposed (0) acetabulum partially obscured as it is partially encircled by the distal margin of the ilium (1).
- 123.** Perforation of the acetabulum: present, open acetabulum (0); absent, closed acetabulum (1).
- 124.** Postacetabular ilium length, relative to diameter of acetabulum: greater (0); smaller (1).
- 125.** Shape of ischium: straight (0); ventrally flexed at mid-length (1).
- 126.** Shape of the dorsal margin of ischium: straight or concave (0); convex (1).
- 127.** Angle between long axis of femoral head and long axis of shaft: $< 100^\circ$ (0); 100° to 120° (1); $> 120^\circ$ (2).
- 128.** Separation of femoral head from greater trochanter: continuous (0); separated by a distinct notch or change in slope (1).
- 129.** Differentiation of the anterior trochanter of the femur: separated from femoral shaft by a deep groove laterally and dorsally (0); fused to femoral shaft (1).
- 130.** Oblique ridge on lateral femoral shaft, distal to anterior trochanter: absent (0); present (1).
- 131.** Form of the fourth trochanter: pendant (0); ridge-like (1).

- 132.** Location of the fourth trochanter on the femoral shaft: proximal (0) distal, over half-way down the femoral shaft (1).
- 133.** Maximum distal width of the tibia, compared to the maximum proximal width: narrower (0); wider (1).
- 134.** Contact between tibia and astragalus: articulated (0); fused, with suture obliterated (1).
- 135.** Number of pedal digits: 5 (0); 4 (1); 3 (2).
- 136.** Phalangeal number in pedal digit IV: 5 (0); ≤ 4 (1).
- 137.** Parasagittal row of keeled osteoderms situated on the dorsal aspect of the trunk: absent (0); present (1).
- 138.** Number of distinct cervical pectoral bands: none (0); one (1); two (2).
- 139.** Sacral shield of fused osteoderms: absent (0); present (1).
- 140.** Form of sacral armour: rosettes 0, evenly-sized polygons 1
- 141.** Terminus of tail enveloped by >2 osteoderms, forming tail club knob: absent (0), present (1)
- 142.** Small (<2 cm diameter), circular osteoderms posterolateral to orbit, along ventral edge of squamosal horn and/or along dorsal edge of quadratojugal horns: absent (0); present (1)
- 143.** Cervical half rings: composed of osteoderms that are either tightly adjacent to one another or coossified at the edges, forming arc over the cervical region (0), composed of osteoderms and underlying bony band segments, osteoderms may or may not cossify to the band, forming arc over the cervical region (1).
- 144.** Composition of first cervical half ring: first cervical half ring has 4 to 6 primary osteoderms only (0), first cervical half ring has 4 to 6 primary osteoderms surrounded by small (<2 cm diameter) circular secondary osteoderms.
- 145.** Form of caudal osteoderms: dorsoventrally compressed, triangular in dorsal view (0), or low cones (1).
- 146.** Tail club knob shape: knob absent (0), major knob osteoderms semicircular in dorsal view (1), triangular in dorsal view (2).
- 147.** Tail club knob proportions: knob absent (0), tail club knob length $>$ width (1), length = width (2), width $>$ length (3)

- 148.** New character: Shape of respiratory passage: straight or arched (0), with anterior (rostral) and posterior (caudal) loops (*sensu* Witmer and Ridgely 2008). [Replaces characters 9-12 in Thompson et al. (2012) and Arbour and Currie (2013).]
- 149.** New character: Lacrimal incisure (Mediolateral constriction behind the narial osteoderms/at the prefrontals, giving the skull an hourglass-shaped outline in dorsal view): absent (0) present (1)
- 150.** New character: Domed caputegulae: rounded cones with circular bases (0) pyramidal with sharp edges (1)
- 151.** New character: Number of internarial caputegulae: none (0), 1 (1), more than 1 (2)
- 152.** New character: Supranarial caputegulae, notch dorsal to nasal vestibule absent (0), present (1).
- 153.** New character: Loreal caputegulum in lateral view: 1 caputegulum (0), more than 1 caputegulum (1)
- 154.** New character: Lacrimal caputegulum in lateral view: 1 caputegulum (0), more than 1 caputegulum (1)
- 155.** New character: Prefrontal osteoderm: flat with keel (0), sharply pointed and pyramidal (1).
- 156.** New character: Depth of jugal ramus relative to orbit height: jugal height is less than 15% orbit height (0), jugal height is more than 15% orbit height (1)
- 157.** New character: Supraorbital caputegulae, when viewed dorsally: combine to form continuous edge (0), have distinct apices (1)
- 158.** New character: Accessory postorbital ossification: absent (0), present (1)
- 159.** New character: Quadratojugal horn: lacks distinct neck at base (0), has distinct neck at base (1).
- 160.** New character: Squamosal horn: base has broad triangular cross-section and overall shape is pyramidal (0), base is oval in cross-section and overall shape is narrow, tapered cylinder (1)

7. OTHER ANKYLOSAURS FROM MONGOLIA AND UZBEKISTAN

7.1 The "Shamosaurinae": *Cedarpelta*, *Gobisaurus*, and *Shamosaurus*

Shamosaurinae was erected as a subfamily of Ankylosauridae by Tumanova (1983), who diagnosed it as follows: ankylosaurids with an anteriorly tapering rostrum; anterior wall of the pterygoid slopes gently posteriorly; pterygoids fused with basisphenoid; interpterygoidal cavity small; quadrates fused with lower edge of paroccipital processes; and occipital condyle circular rather than oval. At the time, the Shamosaurinae included *Shamosaurus scutatus* and *Saichania chulsanensis*. Although the name has not been used extensively by subsequent workers, Carpenter (2001) and Carpenter et al. (2008) have considered *Cedarpelta*, *Gobisaurus*, and *Shamosaurus* to be 'shamosaurine' ankylosaurids (but did not include *Saichania*). Whether or not the Shamosaurinae is a valid clade of ankylosaurids, or a grade of more basal ankylosaurids, will be tested in the revised phylogeny. Understanding the morphology and relationships of 'shamosaurine' or 'shamosaurine'-grade ankylosaurids may provide additional information on the evolution of several features present in the more derived ankylosaurine ankylosaurids, such as cranial ornamentation patterns and the tail club.

7.1.1 *Cedarpelta bilbeyhallorum* Carpenter, Kirkland, Burge, and Bird, 2001

Holotype: CEUM 12360, partial skull.

Paratypes: CEUM 10405, left premaxilla; CEUM 10410, left nasal fragment; CEUM 10421, right prefrontal; CEUM 10560, right lacrimal; CEUM 10352, right postorbital; CEUM 10598, jugal fragment; CEUM 10325, left frontal; CEUM 10332, parietal; CEUM 10345, right squamosal; CEUM 10417, left quadrate with attached quadrojugal; CEUM 10561, right quadratojugal; CEUM 10267, braincase; CEUM 10270, left surangular; CEUM 10529, left angular; CEUM 11288,

cervical centrum; CEUM 10258, CEUM 10409, CEUM 10442, CEUM 10360, dorsal centra; CEUM 12163, synsacrum of 2 dorsals, 4 sacrals, and 1 caudal; CEUM 10258, first? caudal; CEUM 10258, CEUM 10387, CEUM 10366, anterior caudals; CEUM 10255, CEUM 10257, CEUM 10260, CEUM 10261, CEUM 10262, CEUM 10349, CEUM 10400, CEUM 10412, mid-caudals; CEUM 10404, CEUM 10407, posterior caudals; CEUM 10258, right partial humerus; CEUM 10425, left ulna; CEUM 10266, left ischium; CEUM 10537, partial right ischium; CEUM10375, fragment of right ilium; CEUM 10248, CEUM 10445, cervical ribs; CEUM 10254, CEUM 10356, CEUM 10430, CEUM10449, CEUM 10984, metacarpals; CEUM 10247, CEUM 9970, phalanges; CEUM 9922, CEUM 10253, unguals; CEUM 10526, CEUM 10359, CEUM 10394, CEUM 10431, CEUM 10459, CEUM 10248, keeled osteoderms; CEUM 10359, CEUM 9960, CEUM 9962, CEUM 10548, CEUM 10414, CEUM 10441, compressed conical osteoderms; CEUM 10338, flat osteoderm.

Holotype and paratype locality and age: Price River 1 (PR-1) locality (CEM site), CEUM 42EM352U, CEU90-2, Carbon County, Utah, USA. Cedar Mountain Formation, base of the Mussentuchit Member, Albian-Cenomanian (Carpenter et al. 2008).

Referred Specimens: CEUM 10396, cervical; CEUM 10412, CEUM 10404, caudals; CEUM 10371, coracoid; CEUM 10256, CEUM 11629, humeri; CEUM 10266, ischium; CEUM 11334, femur; CEUM 11640, tibia; referred specimens were collected from the Price River II Quarry, locality number EM 372, about 24.5 km southeast of Price, Emery County, Utah, USA; Cedar Mountain Formation, base of Mussentuchit Member (Carpenter et al. 2008).

Previous diagnoses: From Carpenter et al. (2001): Premaxilla with short rostrum anterior to nasal process; paired premaxillae parallel-sided, not divergent posterolaterally as in other ankylosaurids; cutting edge of beak confined to anteriormost portion of premaxillae; six alveoli in premaxilla; quadrate sloped posteriorly; quadrate head not coossified with paroccipital process as in

Shamosaurus; occipital condyle on a long neck as in nodosaurids and projecting horizontally, not obliquely downward as in all other known ankylosaurids and nodosaurids; basitubera as a very large, ventral projecting wedge; pterygoids anteroposteriorly elongated and vaulted in nodosaurid fashion; well-developed trochlearlike process along the lateral edge of pterygoid; large oval process for adductor tendon on medial side of coronoid process; ischium with large knob on medial side near pubic peduncle.

Discussion: CEUM 12360 was briefly described by Carpenter and Kirkland (1998) as an indeterminate shamosaurine ankylosaurid, and named as the new taxon *Cedarpelta* by Carpenter et al. (2001). Carpenter et al. (2001) noted similarities between *Cedarpelta*, *Shamosaurus*, and an (at the time) unnamed third taxon that would eventually become *Gobisaurus*. In 2008, Carpenter et al. described new postcranial material for *Cedarpelta*, and considered *Cedarpelta* to represent an ankylosaurid based on the morphology of the postcrania. A detailed review of the cranial and postcranial material of *Cedarpelta* was outside the scope of this study, although a representative sample (including the original skull material) was examined, in coding the character matrix.

Status: Valid.

**7.1.2 *Gobisaurus domoculus* Vickaryous, Russell, Currie, and Zhao, 2001
= *Zhongyuansaurus luoyangensis* Xu, Lu, Xhang, Jia, Hu, Zhang, Wu, And Ji,
2007**

Holotype: IVPP V12563, skull and unknown postcranial material. Photographs and field records show that most of an articulated skeleton was collected, but the whereabouts of the unprepared postcranial skeleton has been unknown since the 1980s. The holotype was not available for study at the IVPP in August 2010. A cast of the holotype skull is in the TMP collection, TMP 1990.000.4.

Holotype locality and age: Believed to have been collected from the same locality as *Shaochilong maortuensis* (= "*Chilantaisaurus*" *maortuensis*), from the

Maortu region of the Alashan Desert of China, from the Ulansuhai Formation. When *Gobisaurus* was first described, the age of the Ulansuhai Formation (from which *Shaochilong* was collected, see Brusatte et al. 2009) was thought to be Aptian-?Albian (Vickaryous et al. 2001). However, the Ulansuhai Formation is at least younger than 92 Ma (Turonian, early Late Cretaceous; Kobayashi and Lu 2003).

Referred specimens: HGM 41HIII-0002 (holotype of *Zhongyuansaurus luoyangensis*), nearly complete skull, fragmentary lower jaw, one cervical neural spine, one complete and five partial dorsal vertebrae, seven proximal caudal vertebrae, three posterior caudal centra, seven fused distal caudals, ribs, left humerus, both ischia, pubis, osteoderms; Henan Province, Ruyang County, Liu Dianxiang; Mangchuan Formation, Sichuan group, ?early Late Cretaceous, no older than Barremian (Jiang et al. 2011).

Previous diagnoses: From Vickaryous et al. (2001), for *Gobisaurus*: Orbits 20% of cranial length, external nares 23% of cranial length; premaxillary processes of vomers elongate, visible in palatal view; basipterygoid processes robust, not fused to pterygoid body; differing from *Shamosaurus* by: cranium longer than wide; lacking cranial sculpturing in antorbital region; premaxillary rostrum width greater than distance between posteriormost maxillary teeth; maxillary tooth row length relatively shorter compared to overall skull length; reduced supraorbital bosses; anterior surface of pterygoid vertically oriented. From Xu et al (2007), for *Zhongyuansaurus*: Skull length greater than width (ratio 1.4); no osteoderms fused to skull surface; no premaxillary teeth; straight maxillary tooth row with 18 teeth; parietals flat; posterior margin of skull straight; semicircular occipital condyle; proximal and distal humeral widths nearly equal; concave scars for M. latissimus dorsi and M. teres major; ischium shaft straight.

Discussion: *Gobisaurus* shares many similarities with the Mongolian taxon *Shamosaurus scutatus* (Fig. 7.1). Both of these taxa have long, triangular skulls with small squamosal horns and supraorbitals that are less prominent than in

other ankylosaurids. Some of the features used to differentiate *Gobisaurus* from *Shamosaurus* by Vickaryous et al. (2001) do not differ between the two species: large orbits relative to skull size (20% skull length) were considered diagnostic of *Gobisaurus*, but the orbits are approximately 20% the length of the skull in *Shamosaurus*, the skull is longer than wide in *Shamosaurus* as in *Gobisaurus*, and the supraorbital bosses are not prominent in either *Gobisaurus* or *Shamosaurus*. Vickaryous et al. (2001) considered sculpturing in the antorbital region absent in *Gobisaurus* (although they describe it as having a rugose, pockmarked texture), but it is present and similar to that in *Shamosaurus*. A premaxillary rostrum width greater than the distance between the posterior maxillary teeth was also thought to differentiate *Gobisaurus* from *Shamosaurus* (Vickaryous et al. 2001), but this is not the condition in *Gobisaurus* or in *Shamosaurus*, where the premaxillary rostrum width is smaller than the width between the posterior maxillary teeth. A few characters are difficult to assess in *Shamosaurus*, including whether or not the basiptyergoid processes are fused or not fused to the pterygoid body, and the extent of the premaxillary processes of the vomers, because these regions are damaged in the holotype skull. Two characters that differentiate *Gobisaurus* from *Shamosaurus* include the relatively long tooth row of *Shamosaurus* (approximately 40% of skull length, versus 26.7% in *Gobisaurus*), and the orientation of the anterior surface of the pterygoid (vertical in *Gobisaurus*, anteroventral in *Shamosaurus*, although the skull of *Shamosaurus* is slightly taphonomically deformed).

Zhongyuansaurus is indistinguishable from *Gobisaurus* in all of these features, except those which cannot be assessed because of damage (Fig. 7.1C, D). In particular, in *Zhongyuansaurus* the vomers appear to have elongate premaxillary processes similar to those in *Gobisaurus*. For this reason, *Zhongyuansaurus* is here regarded as a junior synonym of *Gobisaurus*. Both *Gobisaurus* and *Zhongyuansaurus* lack well-constrained geologic dates, but both

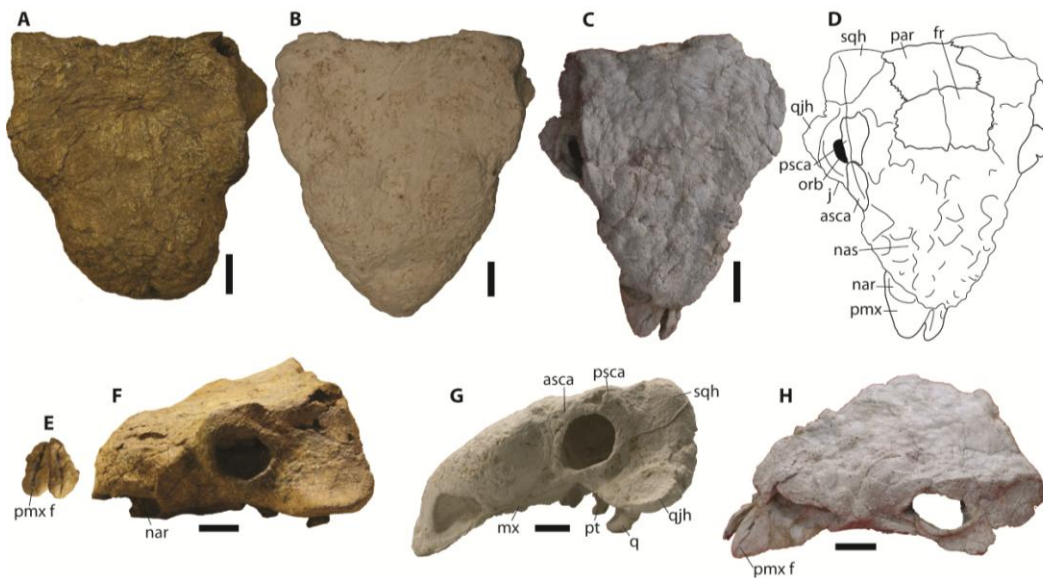


Figure 7.1. Skulls of shamosaurine ankylosaurids compared. A) PIN 3779/2, holotype of *Shamosaurus scutatatus*, dorsal view (premaxillae are separately mounted). B) TMP 1990.000.4, cast of IVPP V12563, holotype of *Gobisaurus domoculus*, dorsal view. C) HGM 41HIII-0002, holotype of *Zhongyuansaurus luoyangensis*, dorsal view. D) Interpretive diagram of HGM 41HIII-0002. E) Premaxillae of PIN 3779/2, *Shamosaurus*, in anterior view. F) PIN 3779/2, oblique left lateral view. G) TMP 1990.000.4, *Gobisaurus*, left lateral view. H) HGM 41HIII-002, *Zhongyuansaurus*, oblique right lateral view (mirrored to facilitate comparisons). Scale bar in all specimens is 10 cm. Abbreviations: asca, anterior supraorbital caputegulum; fr, frontal; j, jugal; mx, maxilla; nas, nasal; nar, naris; orb, orbit; par, parietals; pmx, premaxilla; pmx f, furrow on premaxilla; psca, posterior supraorbital caputegulum; pt, pterygoid; q, quadrate; qjh, quadratojugal horn; sqh, squamosal horn.

are probably from the late Early Cretaceous or early Late Cretaceous; HGM 41HIII-0002 is no older than Barremian (Jiang et al. 2011).

HGM 41HIII-0002 (the holotype of *Zhongyuansaurus*) provides additional morphological information for *Gobisaurus* not present in IVPP V12563. Cranial sutures are uncommonly encountered in ankylosaurs, but the frontal-nasal, frontal-supraorbital, frontal-parietal, parietal-postorbital, postorbital-squamosal, and parietal-squamosal sutures are clearly visible in HGM 41HIII-0002 (Fig. 7.1C). These sutural boundaries are similar to those present in juvenile *Pinacosaurus grangeri* (ZPAL MgD II/1), and *Tarchia* (INBR21004; see Chapter 6). As in IVPP

V12563 (*Gobisaurus*) and PIN 3779/2 (*Shamosaurus*), HGM 41HIII-0002 has irregular, roughly textured skull ornamentation, rather than discrete caputegulae as in taxa like *Ankylosaurus* or *Saichania*; the ornamentation is present on the nasals, prefrontals, and partly on the frontals. *Pinacosaurus grangeri* has similar rough, irregular texturing at the borders of the nares.

Xu et al. (2007) assigned HGM 41HIII-0002 to the Nodosauridae based on its skull proportions (longer than wide), and the absence of a tail club, and so much of their comparison and discussion was with other nodosaurid taxa. Longer-than-wide skulls should be considered plesiomorphic for Ankylosauria and not a derived condition of nodosaurids, as the basal thyreophoran *Scelidosaurus* has a skull that is longer than wide, as does the basal ankylosaur *Gargoyleosaurus* and the ankylosaurid *Shamosaurus*.

Most notably, HGM 41HIII-0002 clearly preserves the handle of a tail club (contra Xu et al. 2007 and Carpenter et al. 2008), even though knob osteoderms are not present (Fig. 7.2A, B). No nodosaurid is known to have elongated, tightly interlocking and fused distal caudal vertebrae; as such, HGM 41HIII-0002 can immediately be referred to the Ankylosauridae. The tail club of HGM 41HIII-0002 appears to preserve the distalmost caudal vertebra; the last three vertebrae in the handle abruptly shorten, and the terminal vertebra is rounded at the distal end, similar to what was observed in CT scans (Fig. 7.2C, D) of an Albertan tail club (UALVP 16247, Arbour 2009). The tail club of HGM 41HIII-0002 is unusual compared to other ankylosaurid tail clubs because it preserves no evidence for the large terminal knob osteoderms. No known ankylosaurid specimen preserves the distal end of the handle without at least some of the knob preserved, because the knob osteoderms envelop and are tightly appressed to the vertebrae. This suggests that either a large terminal knob was not present in HGM 41HIII-0002, or that the knob osteoderms were smaller or more loosely associated with the handle vertebrae.

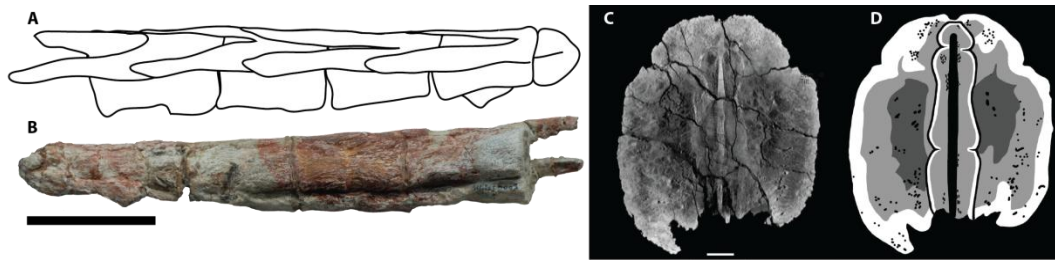


Figure 7.2. HGM 41HIII-0002, the holotype of *Zhongyuansaurus luoyangensis*, includes a tail club handle. A) Handle in left dorsolateral view, drawn from Xu et al. (2007). B) Handle in right ventrolateral view; the deep groove along the bottom is the haemal canal. The terminal vertebra appears to be present: in X-ray images of the ankylosaurid tail club knob UALVP 16247 (X-ray in C, interpretive drawing in D; posterior is up), the terminal vertebra is a small nub compared to the long distal caudals of the handle.

Carpenter et al. (2008) also recognized the close relationships between *Zhongyuansaurus* and *Shamosaurus*, referring *Zhongyuansaurus* to the Shamosaurinae. They noted the presence of typically ankylosaurid features, such as the obscured laterotemporal fenestra and straight ischium. However, a few features described as typically ankylosaurid and present in *Zhongyuansaurus*, but more commonly associated with nodosaurid ankylosaurs, included a narrow premaxillary beak and posterolaterally-directed paroccipital processes.

Status: Valid.

Revised Diagnosis: Ankylosaurian dinosaur with low-relief frontonasal ornamentation not subdivided into distinct caputegulae, as in *Crichtonpelta* and *Shamosaurus*; squamosal horns shorter and more rounded than in *Crichtonpelta*; quadratojugal horn has centrally-located apex, unlike *Crichtonpelta*; no prominences on nuchal crest, unlike *Crichtonpelta*; tooth row shorter relative to over all skull length than in *Shamosaurus* (26.7% in *Gobisaurus*, 40% in *Shamosaurus*); anterior surface of pterygoid is vertical, whereas it slopes anteroventrally in *Shamosaurus*.

7.1.3 *Shamosaurus scutatus* Tumanova, 1983

Holotype: PIN 3779/2, skull and partial postcranial skeleton; the skull and two cervical half rings of the holotype are on display at PIN. Skull and lower jaws figured by Tumanova (1987), scapula and two dorsal vertebrae figured by Tumanova (2000), but remainder of skeleton undescribed and unfigured.

Holotype locality and age: Khamryn-Us (=Khamareen Us), southeastern Gobi, Mongolia; Zuunbayan (=Dzun Bayn, Dzunbayn, Dzunbain) Formation (roughly equivalent to the Khukhtyk/Huhteg Svita), Aptian-Albian (Tumanova 1987, Jerzykiewicz and Russell 1991,)

Referred Specimens: PIN 3779/1, portion of skull, (Khamryn-Us; Dzun Bayn Formation). PIN 3101, fragmentary mandible (Khovboor, Aptian-Albian)

Original diagnosis: Skull completely covered with small osteoderms; postorbital osteoderms do not coalesce into spines; osteoderms do not close the quadrate condyle region laterally; orbits located at middle of skull, directed almost entirely laterally; upper region of premaxillae covered with osteoderms; anterior region of snout is a narrow oval shape, narrower than the distance between the posterior maxillary teeth; posterior maxillary shelf well developed; ventral surface of palatal bones slope laterally; jaw articulation far behind posterior edge of orbit; occipital condyle oriented ventrally; ventral surface of basioccipital bone narrow and circular.

Discussion: As discussed for *Gobisaurus*, *Shamosaurus* and *Gobisaurus* share numerous cranial features (Fig. 7.1). *Shamosaurus* can be differentiated from *Gobisaurus* (including *Zhonyuansaurus*) by the length of the tooth row (40% of skull length in *Shamosaurus* vs. 26.7% in *Gobisaurus*), and the orientation of the anterior surface of the pterygoid (vertical in *Gobisaurus*, anteroventral in *Shamosaurus*). *Shamosaurus* shares with the holotype of *Zhongyuansaurus* (HGM 41HIII-0002) a deep, pronounced longitudinal furrow on the premaxillary beak, which is shallower in the holotype of *Gobisaurus* (IVPP V12563). The deep longitudinal furrow on the premaxilla is not known in other ankylosaurids.

The cervical half rings of PIN 3779/2 are complete, and each includes six osteoderms coossified to an underlying band of bone (Fig. 7.3). The medial osteoderms are low with an indistinct keel directed away from the midline posteriorly. The lateral osteoderms have taller keels than the medial osteoderms, and the keels point laterally. The distal osteoderms are the largest on each cervical half ring. The apex of the keel is anteriorly positioned and laterally directed. The apex of the keel on the distal osteoderm is located anterior to the anterior edge of the half ring band. The second cervical half ring is similar in morphology to the first cervical half ring, but is about twice as long anteroposteriorly, and about one third wider mediolaterally than the first cervical half ring.

Status: Valid.

Revised Diagnosis: Ankylosaurian dinosaur with low-relief frontonasal ornamentation not subdivided into distinct caputegulae, as in *Crichtonpelta* and *Gobisaurus*; squamosal horns shorter and more rounded than in *Crichtonpelta*; quadratojugal horn has centrally-located apex, unlike *Crichtonpelta*; no prominences on nuchal crest, unlike *Crichtonpelta*; tooth row longer relative to overall skull length than in *Gobisaurus* (26.7% in *Gobisaurus*, 40% in *Shamosaurus*); anterior surface of pterygoid slopes anteroventrally, unlike vertical surface in *Gobisaurus*.



Figure 7.3. First and second cervical half rings of PIN 3779/2, holotype of *Shamosaurus scutatus*, anterior view.

7.2 Other ankylosaurids from Mongolia

7.2.1 *Amtosaurus magnus* Kurzanov and Tumanova, 1978

Holotype: PIN 3780/2, an isolated braincase

Holotype locality and age: Amtgay, Bayanshiree Formation

Previous diagnoses: From Kurzanov and Tumanova (1978): occiput and braincase high; occipital condyle with narrow oval outline; longitudinal ridges extend between occipital condyle and basal tubera; floor of anterior portion of braincase slightly inflected; dorsum sellae with small triangular process that extends into pituitary fossa; fenestra ovalis situated considerably dorsal to jugular foramen; two foramina for cranial nerve XII positioned at same level. From Tumanova (1987): All previous characters, plus posteroventrally inclined occipital condyle and fenestra ovalis that is not confluent with jugular foramen.

Status: Indeterminate ornithischian, as per Parish and Barrett (2004).

7.2.2 *Maleevus disparoserratus* (Maleev, 1952)

= *Syrmosaurus disparoserratus* Maleev, 1952

Holotype: PIN 554/1, two fragments of the left and right maxillae

Holotype locality and age: Shireegin Gashoon, Bayanshiree Formation.

Jerzykiewicz (2000) considered the Baynshiree Formation Late Cenomanian-Coniacian to ?Early Santonian in age. A magnetostratigraphic and palynological analysis of the sediments at Bayn Shiree were deposited during the Cretaceous Long Normal interval (chron 34 normal), from the Cenomanian to no later than the latest Santonian (Hicks et al. 1999).

Referred specimen: PIN N 554/2-1, partial braincase, from holotype locality.

Original diagnosis: From Maleev (1952): Lower jaw short and narrow, with symphyseal edge turned outward and alveolar edge elevated; teeth with low lamellar crown and rugose sculpture, 3-5 serrations on each side of apical serration. From Tumanova (1987): Occipital condyle almost round and ventrally

oriented; basioccipital with two small projections ventrally that diverge forwards; depression located in middle more pronounced towards occipital condyle; floor of endocranium almost straight; maxillary shelves poorly developed; upper maxillary teeth with cingulum separated from crown by W-shaped swelling on external side.

Discussion: The holotype of *Maleevus* is represented only by fragments of the maxillae. Teeth with W-shaped cingula are present in *Pinacosaurus grangeri*, and so this feature cannot be considered diagnostic for *Maleevus*. There is no overlapping material between the holotype maxillae and the referred braincase, and so the diagnostic characters of the braincase cannot be applied to *Maleevus*. Additionally, the described diagnostic features of the braincase are present in many other ankylosaurids. *Maleevus disparoserratus* must be considered a *nomen dubium*.

Status: *Nomen dubium*.

7.2.3 *Talarurus plicatospineus* Maleev 1952

Holotype: PIN 557, partial skull (PIN 557-3) and postcranial skeleton

Holotype locality and age: Bayn Shiree, Gobi Desert, Mongolia. Jerzykiewicz (2000) considered the Baynshiree Formation Late Cenomanian-Coniacian to ?Early Santonian in age. A magnetostratigraphic and palynological analysis of the sediments at Bayn Shiree were deposited during the Cretaceous Long Normal interval (chron 34 normal), from the Cenomanian to no later than the latest Santonian (Hicks et al. 1999).

Referred specimen: Fragments of six individuals from the same location as the holotype in PIN collection, portions of which make up a mounted skeleton on display at the PIN (Tumanova 1987). PIN 3780/1, skull roof with occipital section and braincase (Baynshin Tsav, =Bayshin Tsav, Baishin Tsav, Baynshiree Formation). Undescribed material collected by the Korea-Mongolia Joint International Dinosaur Project, from Bayn Shiree, includes: MPC KID 154 (dorsal

vertebra neural arch), MPC KID 167 (dorsal vertebra, partial cervical half ring), MPC KID 185 (partial coracoid), MPC KID 186 (quadrate, quadratojugal horn), MPC KID 187 (free caudal centrum with fused haemal arch, cervical half ring fragments, possible tail club knob fragments), MPC KID 166 (skull). Undescribed material collected by the Korea-Mongolia Joint International Dinosaur Project, from Shine Us Khudag, includes: MPC KID 151 (braincase), KID MPC 155 (seven dorsals, three caudal vertebrae, ribs, ilia and sacrum, both ischia, osteoderms, ossified tendons), MPC KID 162 (bonebed collection - skull roof fragments, quadrate, unidentified cranial fragments, dentary fragment, two caudal vertebrae, pathological rib, tibia with coossified astragalus, distal fibula with coossified calcaneum and distal tarsal, phalanges, cervical ring fragments, osteoderm, indeterminate fragments; some non-ankylosaurian material as well). Putative *Talarurus* specimens have also been collected by Mongolia and Japan Joint Paleontological Expedition (JMJPE), at Bayn Shiree (Matsumoto et al. 2010).

Previous diagnoses: From Maleev (1952): Skull trapezoidal, covered with numerous osteoderms; cervical vertebrae short and tall; dorsal vertebrae long with tall centra and flat articular surfaces; posterior ribs coossified to vertebrae; ilia long, trough-like, and strongly widened and thickened near the acetabulum; sacrum composed of nine vertebrae (four true sacrals, four dorsosacrals, and one caudosacral); tail long; anterior caudals short with tall centra; posterior caudals long, low, with strongly developed neural and haemal arches joined into tail-club; forelimb shorter than hindlimb; unguals hoof-like; osteoderms present. From Tumanova (1987): Distinct pyramidal osteoderms above and behind orbits; skull roof covered with small tubercular osteoderms; occipital plan perpendicular to skull roof; paroccipital processes inclined somewhat posterolaterally; occipital condyle narrow oval, posterolaterally inclined; quadrate not attached to paroccipital processes; basioccipital with medial protuberance, depressions on sides of protuberance; floor of skull cavity straight; fenestra ovalis does not merge with jugular foramen.

Discussion: The holotype skull of *Talarurus* is poorly preserved, and includes only the roof of the posterior portion of the cranium. Nearly all parts of the skeleton are represented by portions of at least six individuals from the same locality as the holotype skull (Tumanova 1987), which have been used to create a composite mounted skeleton on display at the Orlov Museum of Paleontology in Moscow. As mounted, the skeleton has four digits in the pes, which is unlikely given that other closely related ankylosaurids, such as *Pinacosaurus* and *Euoplocephalus*, only had three digits in the pes (Currie et al. 2011). Another unusual aspect of the mounted skeleton is that portions of cervical half rings have been arranged in transverse rows along the entire body (Fig. 7.3), rather than only in the cervical and pectoral regions as in other ankylosaurids.

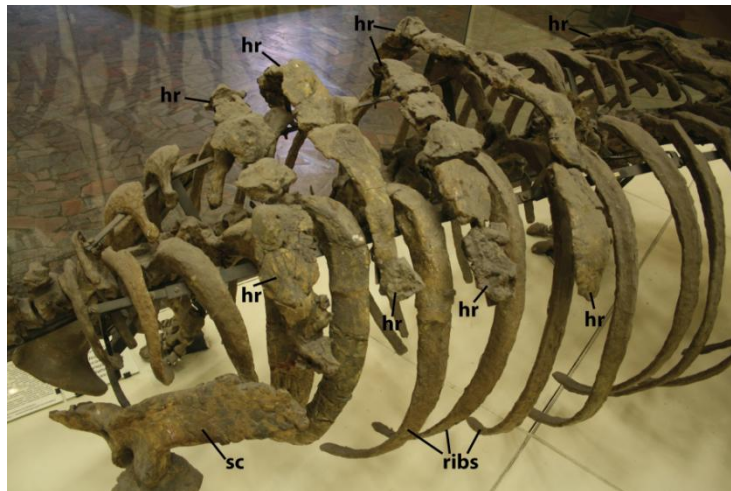


Figure 7.4. Mounted skeleton of PIN 557, *Talarurus plicatospineus*, showing the numerous cervical half ring fragments that have been arranged down the body; oblique left dorsolateral view.

The diagnoses for *Talarurus* presented by Maleev (1952) and Tumanova (1987) mostly include features that are broadly distributed among ankylosaur and ankylosaurid taxa. However, *Talarurus* has distinctive cranial ornamentation that differentiates it from other ankylosaurids from North America and Asia (Fig. 7.5). Maleev (1956) described the cranial ornamentation of PIN 557-3 as consisting of tetragonal, pentagonal, and hexagonal polygons with pitted

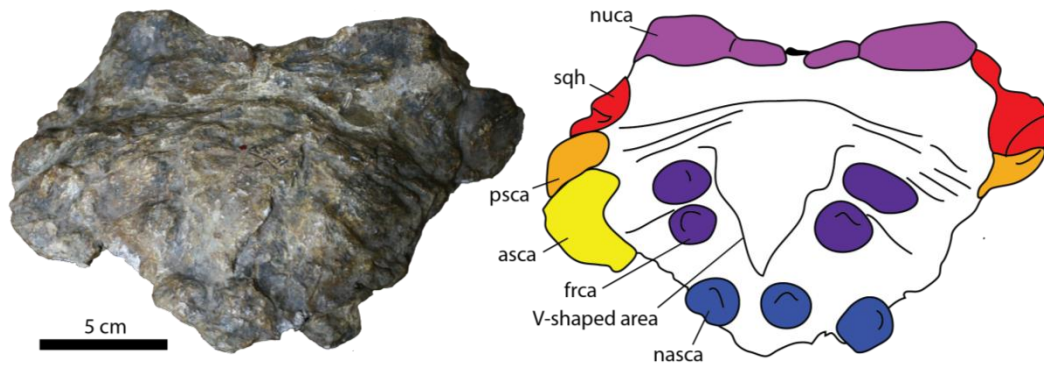


Figure 7.5. PIN 557-3, holotype skull of *Talarurus plicatospineus*, in dorsal view and with interpretive diagram. Abbreviations: asca, anterior supraorbital caputegulum (broken on left side); frca, frontal caputegulum; nasca, nasal caputegulum; nuca, nuchal caputegulum; psca, posterior supraorbital caputegulum; sqh, squamosal horn (broken on both sides).

external surfaces. However, the morphology appears to have been captured more accurately by Tumanova (1987) who noted the presence of small tubercular osteoderms on the skull roof. PIN 557 has symmetrically arranged, low conical frontonasal and fronto-prefrontal caputegulae. There is also a raised, V-shaped area without caputegulae on the frontals (Fig. 7.5). Overall, the cranial ornamentation of PIN 557 is most similar to that of *Nodocephalosaurus*, which also has conical frontonasal caputegulae. *Nodocephalosaurus* lacks the V-shaped raised area on the frontals present in *Talarurus*. The referred skull (3780/1), which is more complete, also appears to have some weakly bulbous caputegulae. However, the overall pattern seems to include more caputegulae compared to PIN 557. The number of caputegulae in *Anodontosaurus* and *Euoplocephalus* can vary somewhat, especially the number of caputegulae in the frontoparietal region, so it is unclear if the difference between PIN 557 and PIN 3780/1 is taxonomically significant.

Status: Valid

Revised Diagnosis: Unlike all other ankylosaurids except *Nodocephalosaurus*, has conical frontonasal caputegulae with circular bases. Unlike *Nodocephalosaurus*, has V-shaped upraised area of frontals.

7.2.4 *Tsagantegia longicranialis* Tumanova, 1993

Holotype: MPC 700/17

Holotype locality and age: Tsagan-Teg, southeastern Gobi, Mongolia; Upper Cretaceous

Original diagnosis: Skull roof covered with numerous small osteoderms indistinctly manifested in relief; upper postorbital spines not developed; osteoderms not overhanging occiput; orbits behind level of middle of skull length; osteodermal ring around orbits separated from surrounding osteoderms by distinct groove, ring decreasing size of orbits; premaxillary rostrum trapezoidal; anterior and posterior maxillary shelves weakly developed; medial part of anterior wall of pterygoids inclined posteriorly; contact of basisphenoid with pterygoids sutural; plane of occiput perpendicular to plan of skull roof; lower margin of paroccipital processes bending slightly inward, distal ends curved slightly ventrally; prootic, opisthotic and exoccipital bones fused but with distinct boundaries; occipital condyle a wide oval, oriented posteroventrally; quadrate bones fused with paroccipital processes; jaw articulation to level of posterior margin of orbit of behind it; ventral surface of basioccipital bone with central depression, separated by gentle crests from lateral depressions; cingulum and lingulum of maxillary teeth dissected by vertical groove.

Discussion: Several characters from the original diagnosis for *Tsagantegia* are present in many ankylosaurids: the sutural contact of the basiptyergoids with the pterygoids; distal curvature to the paroccipital processes; fused prootic, opisthotic, and exoccipital; and oval occipital condyle. The relatively long rostrum, and small squamosal horns, of *Tsagantegia* is reminiscent of *Shamosaurus* and other more basal ankylosaurs (Fig. 7.6). However, several features suggest that *Tsagantegia* is more derived relative to *Gobisaurus* and *Shamosaurus*. *Tsagantegia* has a more rounded, U-shaped premaxillary beak in dorsal and ventral view compared to *Shamosaurus*, which is more similar to the condition in taxa like *Euoplocephalus* or *Saichania* (Fig. 7.6). *Tsagantegia* also has

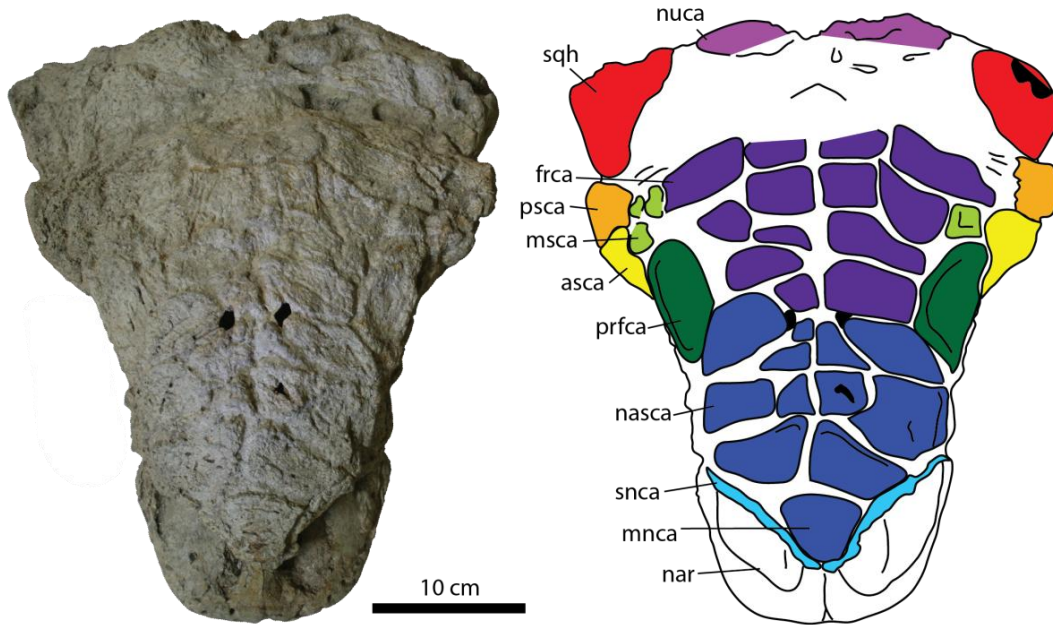


Figure 7.6. MPC 700/17, holotype of *Tsagantegia longicranialis*, dorsal view. Abbreviations: asca, anterior supraorbital caputegulum (broken on left side); frca, frontal caputegulum; mnca, median nasal caputegulum; msca, middle supraorbital caputegulum; nar, naris; nasca, nasal caputegulum; nuca, nuchal caputegulum; prfca, prefrontal caputegulum; psca, posterior supraorbital caputegulum; snca, supranarial caputegulum; sqh, squamosal horn (broken on both sides).

distinct cranial caputegulae (Fig. 7.6), unlike the rugose, amorphous ornamentation of *Gobisaurus* and *Shamosaurus*. Previously published line drawings of MPC 700/17 (Tumanova 1993) suggested that the cranial ornamentation was relatively indistinct, and similar in form to ankylosaurids such as *Shamosaurus*. However, firsthand examination of the skull shows that the ornamentation is divided into discrete, flat caputegulae with a strongly symmetric pattern. The caputegulae are typically rectangular or square, unlike the predominantly hexagonal caputegulae of derived North American ankylosaurids such as *Ankylosaurus* or *Euoplocephalus*. Tumanova (1993) considered the distinct furrow around the orbit to be a diagnostic feature of *Tsagantegia*. However, a ring-like furrow around the orbit is variably developed

in *Euoplocephalus* (it is partially present in AMNH 5405), and so this may not be a taxonomically significant feature of the cranial ornamentation.

Status: Valid

Revised Diagnosis: Uniquely among ankylosaurids, cranial caputegulae predominantly rhomboidal and trapezoidal. Cranial caputegulae present, unlike irregular ornamentation of *Gobisaurus* and *Shamosaurus*, and flat, unlike bulbous caputegulae of *Saichania* and *Tarchia*. Skull longer than wide, unlike proportions of *Saichania* and *Tarchia*. Premaxillary beak wider and more U-shaped in palatal view than narrow, triangular beak of *Gobisaurus* and *Shamosaurus*.

7.3 Other Ankylosaurids from Central Asia

7.3.1 *Bissektipelta archibaldi* (Averianov, 2002)

= *Amtosaurus archibaldi* Averianov, 2002

Holotype: ZIN PH 1/16, partial braincase and skull roof

Holotype locality and age: Dzharakuduk, central Kyzylkum Desert, Uzbekistan; Bissekty Formation, upper Turonian-Coniacian.

Original diagnosis: From Parish and Barrett (2004): Single autapomorphy of distinctive pattern of grooves on the dorsal skull roof forming a truncated Y shape that separates three flat polygonal areas of remodelled bone; three separate exits for hypoglossal nerve (restricted distribution within Ankylosauria).

Discussion: *Bissektipelta* is an enigmatic and fragmentary ankylosaurid from a region in which ankylosaurid fossils are otherwise unknown. The pattern of cranial ornamentation described by Parish and Barrett (2004) is unique among ankylosaurids, with three large, flat caputegulae in the frontal and parietal regions. The grooves separating the caputegulae form a distinctive Y shape. Distinct caputegulae are not common in the posterior frontal or parietal regions

of many ankylosaurid skulls, and when present these are typically smaller than what is preserved in ZIN PH 1/16.

Status: Valid.

Ankylosaur remains have also been reported by Efremov (1944), Nessov (1995), and Averianov et al. (2012) from localities in Uzbekistan, Kazakhstan, and Tadjikistan, but were not described in detail or figured. Most of these specimens are represented only by teeth and osteoderms. Tumanova et al. (2003) described a single tooth and osteoderm from the Arkhara region of Amur Oblast, Russia. Carpenter (2012) referred to this specimen as a nodosaurid, possibly because the silhouette accompanying the Russian article shows an ankylosaur without a tail club; however, the morphology of the tooth and osteoderm appear to be more consistent with those of ankylosaurid ankylosaurs.

8. ANKYLOSAURS FROM CHINA

8.1 Introduction

At least two major clades within the Ankylosauria are well supported by numerous phylogenetic studies. The Ankylosauridae were present primarily in Asia and North America, and derived members of this clade are characterized by shortened skulls, pyramidal squamosal horns, and tail clubs, among other features. The Nodosauridae were present primarily in Europe and North America, and derived members of this clade have a kinked ischium, more massive osteoderms, and lack a tail club. In recent years, several putative nodosaurid ankylosaurs have been identified from Japan and China. However, many of the putative nodosaurid features identified in these species represent plesiomorphic character states in Ankylosauria, such as the presence of a long rostrum, or the absence of a tail club. A comprehensive review of ankylosaurs from China (Fig. 8.1) and Japan is undertaken here to determine which species are valid, and to help identify new characters for use in the revised phylogenetic analysis in Chapter 10.

8.2 Systematic Palaeontology

8.2.1 *Bienosaurus lufengensis* Dong, 2001

Holotype: IVPP V15311 (originally IVPP V9612, but this was also the specimen number for *Sinornithoides youngi*), partial right lower mandible, fragmentary frontal, other cranial fragments

Holotype locality and age: Dark Red Beds, Lower Lufeng Formation (=Zhangjiawa Member, Lufeng Formation, *sensu* Fang et al. 2000), Lower Jurassic (?Hettangian, Luo and Wu 1994); Lufeng Basin, Yunnan Province, China

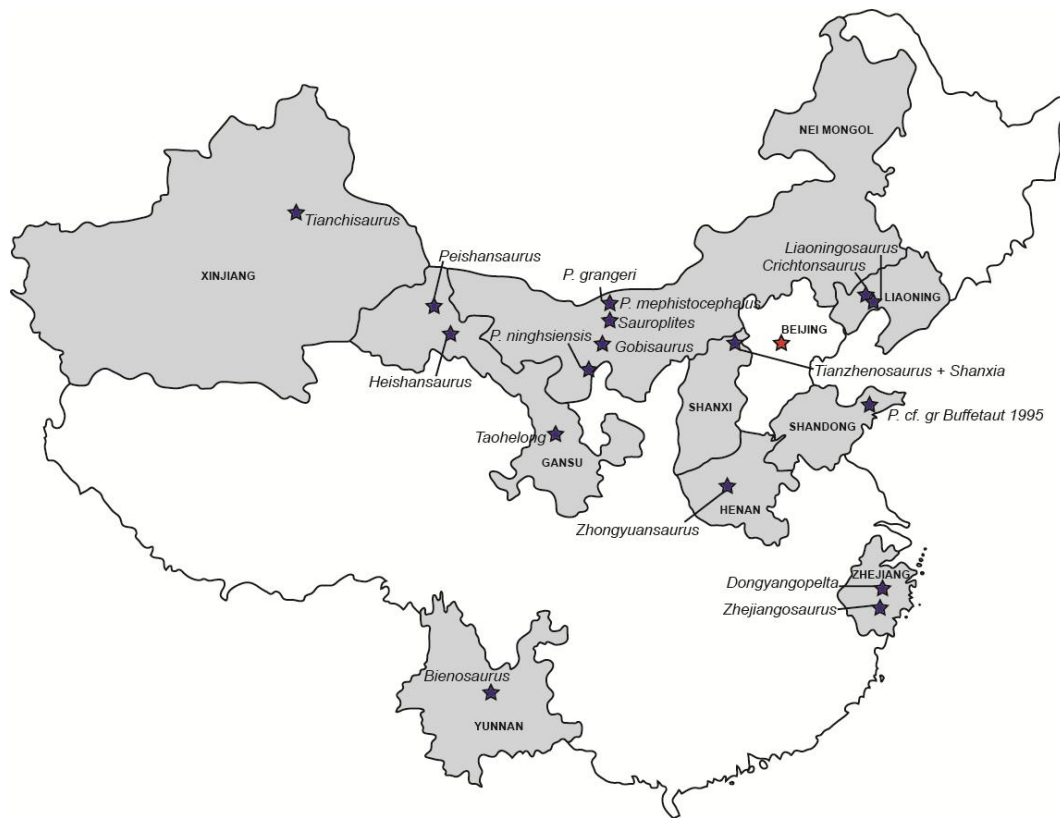


Figure 8.1. Geographic locations of Chinese ankylosaurs discussed in this chapter.

Original diagnosis: predentary short and wide; frontal thick with small osteoderms fused to surface; teeth small, leaf-shaped, with symmetrical crown and developed cingulum

Discussion: All of the diagnostic characters in Dong (2001) are widely distributed among ankylosaurs. Dong (2001) considered the absence of osteoderms preserved with IVPP V9612 to indicate that it was neither an ankylosaur nor a stegosaur, but a more basal thyreophoran. Osteoderms are found in all thyreophorans, and the absence of osteoderms in this highly fragmentary specimen does not indicate osteoderms were absent in life. *Bienosaurus* includes no diagnostic characters and is thus regarded as a *nomen dubium*.

Status: *Nomen dubium*; Thyreophora indet.

8.2.2 *Crichtonsaurus bohlini* Dong, 2002

Holotype: IVPP V12745, a partial left mandible with three teeth

Holotype Locality and Age: Cenomanian-Turonian Sunjiawan Formation;

?holotype locality is 120° 42' 49 longitude, 41° 42' 40 latitude, Beipiao Basin, Liaoning, China

Referred specimens: IVPP V12746 (two cervical vertebrae and a dorsal vertebra) and LPM 101 (four sacral vertebrae, seven caudal vertebrae, a scapula, coracoid, humerus, femur, pedal elements, and osteoderms). Referred specimens were collected from a single quarry, but not from the same quarry as the holotype.

Note: The Liaoning Paleontological Museum of China (located in Shenyang), which uses the abbreviation LPMC, opened many years after LPM 101 was described; it seems most likely that the "Paleontology Museum of Liaoning" refers to the Sihetun Fossil Museum in Shangyuan, which displays many specimens with LPM numbers.

Previous diagnoses: From Dong, 2002: Mandible without lateral osteoderm; teeth small with symmetrical crown and underdeveloped cingulum; 8-10 denticles per tooth; short cervical vertebrae; amphicoelus dorsal vertebrae with tall neural arch and broad neural spine lacking distal swelling; transverse processes of dorsal vertebrae project dorsolaterally; sacral rod with four sacrals, four to five dorosacrals; tail club knob present; scapula and coracoid not fused; osteoderm morphologies include spines, small nodules, and cervical half ring (modified from Chinese text in Dong 2002). From Lu et al. (2007): Ratio of humerus to femur 0.7; ratio of femur to tibia 1.1; ratio of deltopectoral crest length to humeral length 0.44.

Discussion: The IVPP specimens could not be located in August 2010 (VMA). Many of the proposed diagnostic characters of *Crichtonsaurus bohlini* have a broad distribution within Ankylosauria (small teeth, short cervical vertebrae, amphicoelus dorsal vertebrae with a tall neural arch and spine and dorsolaterally projecting transverse processes, tail club, osteoderms, and cervical half ring). As

the holotype specimen is only a fragment of a lower jaw, and none of the referred specimens include overlapping cranial material, the diagnosis should be restricted to features preserved in the holotype. Of these, *Pinacosaurus grangeri* (ZPAL MgD II/1) has dentary teeth with 8-10 denticles arranged symmetrically on the crown and a weakly developed cingulum; the teeth in ZPAL MgD II/1 are similar to those in IVPP V12745. The holotype was not available for study at the IVPP in August 2010, and only the medial surface was figured by Dong (2002); as such, the presence or absence of a mandibular osteoderm cannot be assessed. However, the mandibular osteoderm in ZPAL MgD II/1 is restricted to the posterior corner of the angular, and so its absence in the fragmentary holotype of *Crichtonsaurus bohlini* does not necessarily mean it was absent in the complete jaw. There are no diagnostic characters in the holotype of *Crichtonsaurus bohlini*, and so this species must be considered a *nomen dubium*.

Status: *Nomen dubium*

8.2.3 *Crichtonpelta* gen. nov.

***Crichtonpelta benxiensis* (Lü, Ji, Gao, And Li, 2007), comb. nov.**

= *Crichtonsaurus benxiensis* Lü, Ji, Gao, and Li, 2007

Etymology: After Michael Crichton, author of Jurassic Park, and *pelta* (Latin), a small shield, in reference to the osteoderms found on all ankylosaurs.

Holotype: BXGMV0012, nearly complete skull

Holotype Locality and Age: Sunjiawan Formation; considered Cenomanian-Turonian in age in Dong (2002) but late Albian by Jiang and Sha (2006); Beipiao, Liaoning Province

Referred specimens: BXGMV0012-1, an incomplete skeleton without skull, found in the same quarry as the holotype. Mounted skeleton (as "*Crichtonsaurus bohlini*") with original but undescribed skull on display at Sihetun Fossil Museum (alternately, Sihetun Visitor Facility or Beipiao City Palaeontological Museum)

near Beipiao, China (cast of same skull and skeleton on display at Fukui Prefectural Dinosaur Museum, Japan).

Previous diagnosis: From Lü et al. (2007): Width of skull 84.6% length; deep depression medial to notch between orbit and squamosal horn; small opening on ventral surface of [basi]occipital; paroccipital processes fused to quadrates; three sinuses on each side of snout. Angle between dorsal vertebra transverse processes and neural spine 50°; scapula and coracoid fused; large foramen for supracoracoid nerve enters coracoid and exits scapula; oblique articular surface of ulna embraces 70% length of ulna; humerus proximal width to length is 0.65; humerus proximal width to distal width 1.43.

Emended diagnosis: Uniquely among ankylosaurines, apex of quadratojugal horn directed dorsally. Low-relief frontonasal ornamentation not subdivided into distinct caputegulae, as in *Gobisaurus*, *Pinacosaurus*, and *Shamosaurus*; jugal is dorsoventrally deeper than in *Pinacosaurus grangeri* or *P. mephistocephalus*; lacks lacrimal incisure (*sensu* Hill et al. 2003) present in *Pinacosaurus grangeri*; squamosal horns shorter than in *Pinacosaurus mephistocephalus*; squamosal horns longer, more pointed than in *Gobisaurus* or *Shamosaurus*; quadratojugal horn has posteriorly offset apex, unlike centrally-located apex in *Gobisaurus* and *Shamosaurus*; nuchal crest with two distinct prominences, unlike *Gobisaurus* and *Shamosaurus* which lack nuchal prominences.

Redescription and Discussion: The holotype species of *Crichtonsaurus*, *C. bohlini*, lacks diagnostic characters and is here considered a *nomen dubium*. However, *Crichtonsaurus benxiensis* includes a well-preserved skull that can be differentiated from other ankylosaur species (Fig. 8.2A-C). The new combination *Crichtonpelta benxiensis* is proposed here to receive the diagnostic material of “*Crichtonsaurus*” *benxiensis*.

Lü et al. (2007) referred *C. benxiensis* to *Crichtonsaurus* based on the ratio of the humerus length to femur length, the morphology of the humerus and femur, and the morphology of the anterior caudal vertebrae. The proportions of

the humerus and femur of both *C. benxiensis* and *C. bohlini* do not differ substantially from other ankylosaurs, nor does the morphology of the anterior caudal vertebrae. The anterior caudal vertebrae are similar to those of many ankylosaurids and so cannot be used to refer *C. benxiensis* to *Crichtonsaurus*. In fact, the referred humeri of *C. benxiensis* differ markedly from those of the referred *C. bohlini*: the deltopectoral crest does not extend as far down the shaft in *C. benxiensis* as in *C. bohlini* (based on the line drawing of LPM 101-7 in Dong 2002: fig. 6). The deltopectoral crest extends somewhat less than half the length of the humerus in *C. benxiensis* (45.7%, based on measurements in Lu et al. 2007). This is lower than the range reported for *Pinacosaurus grangeri* from the Alag Teeg bonebed, although Burns and Tumanova (in preparation) noted difficulty in accurately measuring the length of the deltopectoral crest, and recommend against using this feature as a diagnostic character for ankylosaurs.

Lü et al. (2007) differentiated *C. benxiensis* from *C. bohlini* based on its overall larger size, fusion of the scapula and coracoids into a scapulocoracoid, and the straight shape of the lateral margin of the deltopectoral crest. As *C. benxiensis* and *C. bohlini* are found in the same formation, differentiating these taxa based on two size-related characters is unwise, as these differences may be related to ontogenetic changes. The remaining character, the shape of the lateral margin of the deltopectoral crest, may represent intraspecific variation, as this is a subtle difference between both species. Scapulocoracoid fusion is likely influenced by ontogenetic stage, and Lü et al. (2007) point out that the scapulocoracoid is fused in the larger *C. benxiensis* and unfused in the smaller *C. bohlini*. The scapula of BXGMV0012-1 also differs markedly from that of LPM 101-5 (*C. bohlini*). The scapula of BXGMV0012-1 bears a distinctive laterally-projecting, tab-like acromion, which is also present in the Mongolian ankylosaurid MPC 100/1305 but which appears to be absent in LPM 101-5. BXGMV0012 is a partial skull missing the anterior portion of the rostrum (the premaxillae, maxillae, and part of the nasals), the palate, the left squamosal

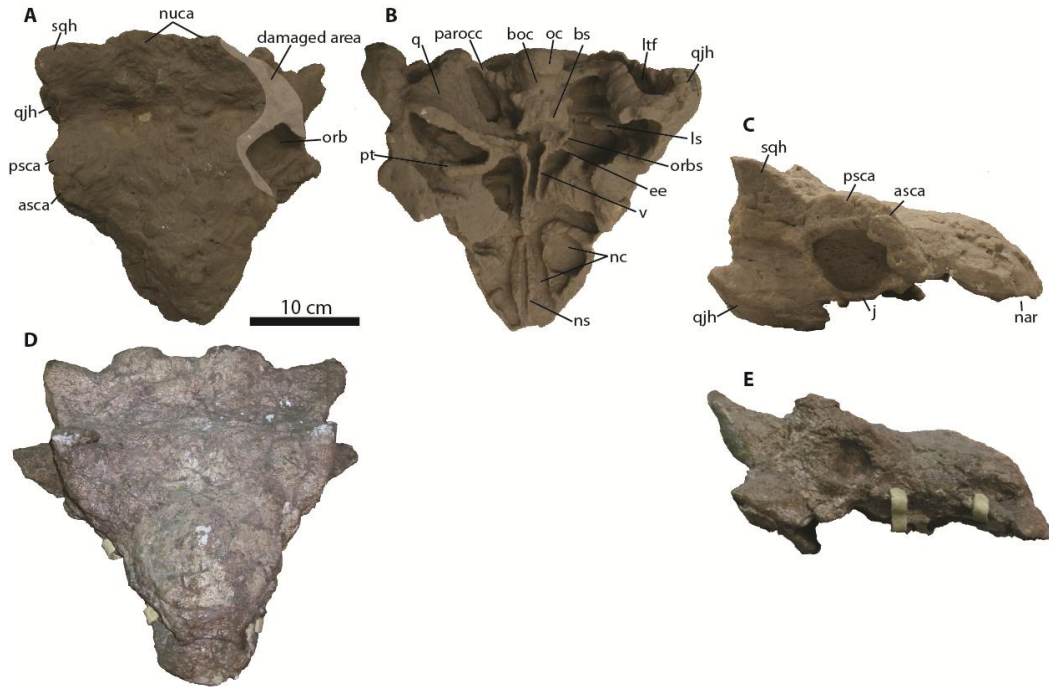


Figure 8.2. Holotype specimen of *Crichtonpelta benxiensis*, BXGMV0012 (photos of cast specimen UALVP 52015), and possible referable specimen on display in Liaoning. BXGMV0012 in A) dorsal view, B) ventral view, and C) right lateral view. Skull of a specimen on display at the Sihetun Fossil Museum in D) dorsal view and E) right lateral view. Abbreviations: asca, anterior supraorbital caputegulum; boc, basioccipital; bs, basisphenoid; ee, ectethmoid; j, jugal; ls, laterosphenoid; ltf, laterotemporal fenestra; nar, external naris; nc, nasal canal (respiratory passage); ns, nasal septum; nuca, nuchal caputegulum; oc, occipital condyle; orb, orbit; orbs, orbitosphenoid; parocc, paroccipital process; psca, posterior supraorbital caputegulum; pt, pterygoid; q, quadrate; qjh, quadratojugal horn, sqh, squamosal horn; v, vomer.

horn, and the left supraorbitals; the left supraorbital region was damaged during preparation (Lü et al. 2007). An undescribed skull and partial skeleton from the Sunjiawan Formation and on display at the Sihetun Fossil Museum (as "*Crichtonsaurus" bohlini*) corroborates features described for BXGMV0012, but is not itself described in this paper (Fig. 8.2D,E).

Overall, BXGMV0012 has a blocky, triangular outline in dorsal view. Lü et al. (2007) considered the proportions of the skull to be diagnostic (skull width 84.6% of the skull length), but because the anterior portion of the rostrum is missing, this cannot be used as a diagnostic character. Lü et al. (2007) also

considered the posterior margin of the skull to be 'expanded', and that this differed from the condition in other ankylosaurids. The posterior margin of the skull does not appear to be significantly expanded relative to the rostrum, or relative to other ankylosaurids. Cranial sutures are not visible, and the cranial ornamentation is not divided into discrete caputegulae (except for the squamosal and quadratojugal horns and the supraorbital caputegulae) but is instead rugose and irregular. This is similar to the condition in *Gobisaurus*, *Pinacosaurus*, and *Shamosaurus*.

The premaxillae, maxillae, and anterior portions of the nasals are broken in BXGMV0012. The tooth rows are not preserved. No sutures are visible on the dorsal skull surface, and so the posterior extent of the nasals, as well as the boundaries of the prefrontals, frontals, parietals, postorbitals, and squamosals cannot be determined. Lü et al. (2007) reported that the external nares face anteriorly rather than laterally or anterolaterally, and that a premaxillary sinus was preserved on the ventral surface. However, the external nares are poorly preserved, but what is present suggests that the nares faced laterally (Fig. 8.2C). The premaxillary sinus is located anterior to the nasal vestibule in *Pinacosaurus* (Hill et al. 2003) and INBR21004 (*Tarchia*), and so the structure identified by Lü et al. (2007) is unlikely to represent the premaxillary sinus. The palate is not preserved, and therefore the ventral surfaces of the nasals are visible (Fig. 8.2B). There is a gap along the median nasal septum (formed by the nasals). Sinuses in each nasal represent the complex looping nasal passages (Witmer and Ridgely 2008).

Lü et al. (2007) coded BXGMV0012 as possessing bulbous polygonal cranial ornamentation in the rostral region, when in fact this specimen possesses flat, indistinct cranial sculpturing. Lü et al. (2007) also coded BXGMV0012 as lacking ornamentation on the premaxilla, but little, if any, of the premaxilla is preserved and it is not possible to code this character for BXGMV0012.

Ankylosaurids have three supraorbital bones above the orbit. The anterior and posterior supraorbitals form the lateral edge of the skull above the orbit in dorsal view, and the middle supraorbital is more medially located. In BXGMV0012, the middle supraorbital cannot be discerned, but the boundaries of the anterior and posterior supraorbitals are visible. The lateral edges of the anterior and posterior supraorbitals are continuous in dorsal view, and overall each supraorbital has a rounded, bulbous appearance. The jugal forms the ventral border of the orbit. The frontals cannot be distinguished in dorsal view and it is unclear if they possessed a scroll-like descending process as in *Euoplocephalus* (Miyashita et al. 2011) and *Zaraapelta*.

The parietals of BXGMV0012 form a posterior nuchal shelf that obscures the occiput in dorsal view, as in most ankylosaurids except *Tarchia* and *Zaraapelta*, and some specimens referred to *Pinacosaurus grangeri* (Hill et al. 2003). The nuchal shelf has two distinct, transversely long prominences. The surface texturing on the parietals is similar to the rest of the dorsal skull surface. There are two shallow depressions posterior and medial to the orbits; in many ankylosaurids (e.g. *Euoplocephalus* and *Saichania*) the parietals form a shallow, continuous transverse depression posterior to the orbits.

Dorsally, the squamosals form the posterior corners of the skull (Fig. 8.2A). The squamosal horn is pyramidal, similar to those of *Ankylosaurus* and *Saichania*, but proportionately smaller relative to skull size. Ventrally, the quadratojugals form the posterior corners of the skull. The quadratojugal horn is deltaic, relatively short mediolaterally compared to species like *Saichania* or *Tarchia*, and the apex is offset posteriorly. The apex of each quadratojugal horn is slightly dorsally upturned, which appears to be a unique feature of *Crichtonpelta* unrelated to taphonomic distortion, as it is present in the holotype (Fig. 8.2C) and the undescribed skull on display at the Sihetun Visitor Centre (Fig. 8.2E). No postocular caputegulae are present on the lateral surface of the skull between the squamosal and quadratojugal horns.

Much of the palatal region of BXGMV0012 is broken, including the palatines, vomers, and palatal surface of the premaxillae and maxillae. The right pterygoid is missing, and the left pterygoid is distorted. It is not clear if the pterygoid body was fused to the basiptyergoid process. The quadrate ramus of the pterygoid overlaps the quadrate, and the suture is faint but visible. The preserved part of the vomers shows that they were thin and delicate, as in other ankylosaurids.

The supraoccipital is fused to the ventral surface of the parietals and forms the dorsal border of the foramen magnum. Ventrally, it has a pair of low prominences at the dorsolateral edges of the foramen magnum. The exoccipital contributes to the lateral wall of the foramen magnum, and the opisthotic contributes to the lateral wall of the endocranial cavity; together these are fused to form the paroccipital processes. The lateral terminus of the paroccipital process is fused to the quadrate, as in *Saichania* and *Zaraapelta*. Dorsal to the paroccipital process, there is a distinct ridge where the paroccipital is fused to the parietal.

The reniform occipital condyle is formed entirely from the basioccipital, which also forms the posterior floor of the braincase. The basisphenoid contributes to the anterior floor of the braincase and has a small, sharply demarcated, circular depression (Lü et al. 2007 stated that this depression was on the “occipital”). A similar depression is present in the holotype of *Saichania*. The contact between the basioccipital and basisphenoid is somewhat eroded, but appears to have been a rugose transverse ridge. The basiptyergoid processes are poorly preserved, but do not appear to have fused to the posterior faces of the pterygoid bodies. The prootic and opisthotic form the lateral walls of the braincase, but cannot be distinguished from each other.

The laterosphenoid contributes to the postocular shelf, which appears to have been strongly-developed as in *Euoplocephalus* (Miyashita et al. 2011); this is unlike the condition in *Zaraapelta*. The orbitosphenoid and parasphenoid are

difficult to discern, but the orbitosphenoid likely contributed to the lateral wall of the braincase and medial wall of the orbit, and the parasphenoid contributed to the anteroventral wall of the braincase and to the interorbital septum, as in other ankylosaurs like *Euoplocephalus* (Miyashita et al. 2011). The ectethmoid contributes to the anterior wall of the orbit, and separates the orbit from the olfactory region.

The quadrate is fused to the paroccipital process, quadratojugal, and pterygoid, and is anteroventrally oriented. The quadratojugal does not overlap the quadrate as extensively in BXGMV0012 as in *Zaraapelta*. The articular condyles of both quadrates are broken, but may have been somewhat narrower than in other ankylosaurids.

The lack of discrete cranial caputegulae in BXGMV0012 is similar to the conditions in *Gobisaurus*, *Pinacosaurus*, and *Shamosaurus*. *Crichtonpelta* lacks the distinctive lacrimal incisure that gives the skull of *Pinacosaurus grangeri* an hourglass-shaped outline in dorsal view, and the squamosal horns are not as long as those of *P. mephistocephalus*. *Crichtonpelta* differs from *Gobisaurus* and *Shamosaurus* by having a larger, more triangular, pointed squamosal horn in both dorsal and lateral views. The quadratojugal horn has a posteriorly offset apex in *Crichtonpelta*, but a centrally located apex in *Gobisaurus* and *Shamosaurus*. The nuchal crest of *Gobisaurus* and *Shamosaurus* lack prominences or discrete caputegulae as in many other ankylosaurids, but in *Crichtonpelta* there are two distinct prominences similar to those of *Saichania*. One autapomorphy is present in *Crichtonpelta*: the dorsally upturned apex of the quadratojugal horn is not present in any other known ankylosaurid.

8.2.4 *Dongyangopelta yangyanensis* Chen, Zheng, Azuma, Shibata, Lou, Jin, and Jin, 2013

Holotype: DYM F0136, dorsosacral vertebrae, sacral vertebrae, dorsal ribs, partial right ilium, right femur, three pedal phalanges, osteoderms, and ossified tendons.

Holotype Locality and Age: Pinglinggang Hill, Yangyan Village, Mazhai Town, Dongyang City, Zhejiang Province, China. Chaochuan Formation (Albian-Cenomanian).

Original diagnosis: Anterior surface of first dorsosacral centrum strongly inflated laterally, curves posteriorly; pelvic shield composed of large pebble-shaped bosses surrounded by either smaller tubercles or flat expanses of bone; osteoderms have rough notches and grooves; domed triradiate osteoderm present; iliac blade convex dorsally above acetabulum, lateral to acetabulum the blade is steeply downturned, and recurves almost horizontally at the lateral edge; anterior end of preacetabular process curves lateroventrally; preacetabular process has shallow groove laterally at anterior end; femur maximum distal width to total length ratio of 0.41.

Discussion: *Dongyangopelta yangyanensis* is notable for being one of only a few ankylosaur species from China known to have possessed a pelvic shield of fused osteoderms (Fig. 8.3A). In some ankylosaurs, such as *Gastonia*, *Polacanthus* (Fig. 8.3D) and *Sauroplices* (Fig. 8.3B) the pelvic shield is composed of osteoderm rosettes in which the large, central osteoderms are surrounded by smaller osteoderms (Category 2 shields of Arbour et al. 2011). In others, like *Aletopelta* and *Stegopelta*, the pelvic shield is composed of roughly equal-sized, hexagonal osteoderms (Category 3 shields of Arbour et al. 2011). The pelvic shield of *Dongyangopelta* is unique among ankylosaurs for having larger osteoderms incompletely ringed by smaller osteoderms.

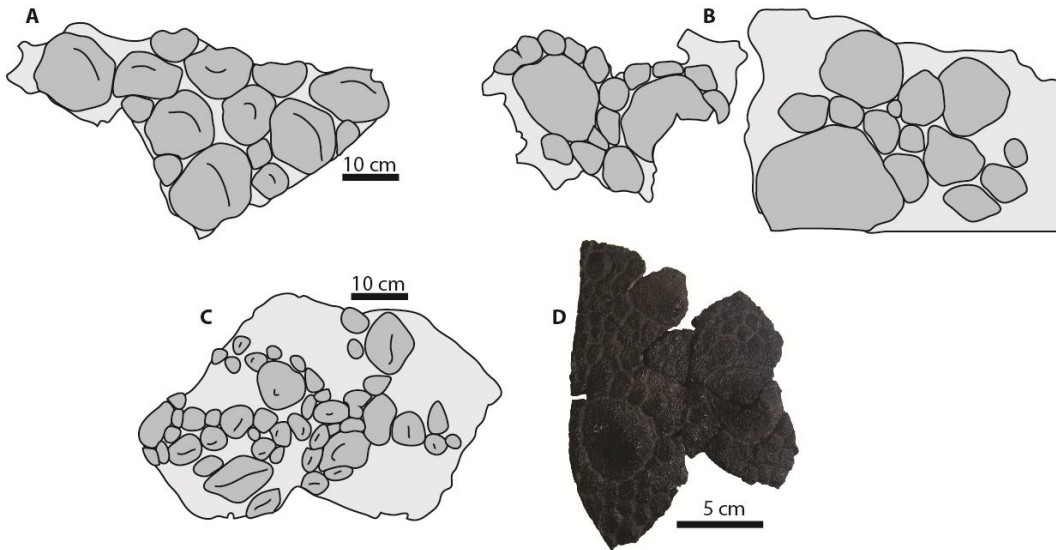


Figure 8.3. Pelvic shields of ankylosaurs from China and Europe. A) DYM F0136, holotype of *Dongyangopelta yangyanensis*, drawn from Chen et al. (2013). B) *Sauroplites scutigera*, drawn from Bohlin (1953). C) GSDM 00021, holotype of *Taohelong jinchengensis*, drawn from Yang et al. (2013). D) NHMUK R9293, *Polacanthus* sp.

The holotype of *Dongyangopelta yangyanensis* derives from the same formation as that of *Zhejiangosaurus lishuiensis*. Chen et al. (2013) differentiated *Dongyangopelta* from *Zhejiangosaurus* based on differences in the morphology of the dorsosacral vertebrae and the dorsal surface of the ilium, the prominence and orientation of the femoral head, the proportions of the femur, and the position of the fourth trochanter and scar for the M. gastrocnemius. The anterior faces of the first dorsosacral vertebrae in both *Dongyangopelta* and *Zhejiangosaurus* are strongly expanded laterally. Although the anterior face is flat in *Dongyangopelta* and slightly concave in *Zhejiangosaurus*, slight differences in the degree of concavity of the articular faces is present even in single individuals of many ankylosaurs. The lateral edge of the ilium in some ankylosaurs (e.g. *Euoplocephalus* AMNH 5409) is more flat and horizontal compared to the convex surface directly over the acetabulum, which creates a sigmoid appearance. More complete ilia are required to determine whether or not the sigmoid appearance of the dorsal surface of the ilium of *Dongyangopelta*

is an autapomorphic feature. Differences noted in the femur are all minor, and difficult to assess without a larger sample size; the fourth trochanter is not located more proximally in *Dongyangopelta* compared to *Zhejiangosaurus*. No major differences are apparent between the holotypes of *Dongyangopelta* and *Zhejiangosaurus*, but because the holotype of *Zhejiangosaurus* preserves no diagnostic features, and the holotype of *Dongyangopelta* does, *Dongyangopelta* is here considered a valid species, and not a junior synonym of *Zhejiangosaurus*.

Status: Valid

Revised diagnosis: Ankylosaurian dinosaur with pelvic shield formed of loosely spaced osteoderm rosettes, with the central osteoderm not completely ringed by smaller osteoderms.

8.2.5 *Heishansaurus pachycephalus* Bohlin, 1953

Holotype: No specimen number given, fragmentary skull, cervical, dorsal, sacral, and caudal vertebrae, ribs, osteoderms; reportedly lost (Sullivan 2006); casts (AMNH 2062) of some of the material available.

Holotype locality and age: northwest of Chia-yü-kuan, China; Minhe Formation, Campanian-Maastrichtian (Weishampel et al. 2004)

Original diagnosis: None provided.

Discussion: Maryańska (1977) regarded *Heishansaurus* as a *nomen dubium* and indeterminate ankylosaur, and Maryańska et al. (2004) referred it to the Pachycephalosauria as a *nomen dubium*. Sullivan (2006) reassessed the status of *Heishansaurus* as a pachycephalosaurid and concluded that this taxon represents an indeterminate ankylosaurid, a conclusion that is supported in this paper.

Status: *Nomen dubium*, Ankylosauria indet.

8.2.6 *Liaoningosaurus paradoxus* Xu, Wang, and You, 2001

Holotype: IVPP V12560, nearly complete, articulated skeleton preserved with the ventral surface exposed on a limestone slab

Holotype locality and age: Baicaigou locality (Wangjiagou in Xu et al 2001), Dawangzhangzi Beds of Yixian Formation, about 122 Ma (Xu and Norell 2006)

Referred specimens: CYGYB 208 (nearly complete skeleton preserved on slab with dorsal surface exposed), CYGYB 237 (nearly complete skeleton preserved on slab with ventral surface exposed).

Previous diagnosis: From Xu et al. (2001): Differs from all other ankylosaurs by the presence of shell-like ventral armour, a trapezoidal sternum with a slender, distally pointed posterolateral process and a short medial articular margin, and a pes greater than twice as long as the manus.

Discussion: IVPP V12560 is one of the smallest known ankylosaur skeletons (Fig. 8.4). Numerous features indicate that IVPP V12560 is an ankylosaur, such as the presence of osteoderms in the cervical region, and the closed acetabulum and divergent ilia of the pelvis. Unfused neural arches, small size, and the absence of osteoderms posterior to the cervical/pectoral region (as in juvenile *Pinacosaurus grangeri*) suggest that IVPP V12560 is a juvenile individual.

Xu et al. (2001) identified a tubercled, bony plate covering much of the ventral side of the abdomen in IVPP V12560, and noted that a 'shell-like' ventral bony plate is not present in any other ankylosaur. Arbour et al. (in press) suggest instead that this region represents skin impressions (Fig. 8.5), with the 'tubercles' being epidermal scales. The edges of the tubercled region do not show a bony internal texture, and the pattern of tubercles is consistent with the basement scale pattern (*sensu* Bell 2012) commonly preserved in hadrosaur skin impressions.

The morphology of the sternum (Fig. 8.6), and the proportions of the manus and pes, were also considered diagnostic for *Liaoningosaurus* by Xu et al. (2001). Whether or not a sternum is preserved is unclear. The element identified by Xu et al. (2001) as the left sternum is adjacent to several other elements and the boundaries of the sternum are unclear (Fig. 8.4). The posterolateral process as identified by Xu et al. (2001) is pointing anteriorly, although it is possible that

the sternum was displaced postmortem. This element is dissimilar from other ankylosaur sterna. In nodosaurids, the sternal elements are paddle-like, with

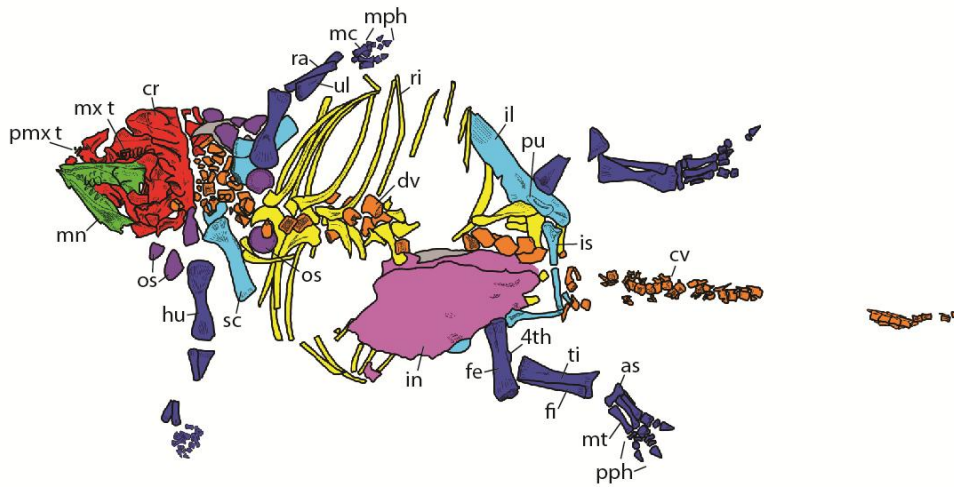


Figure 8.4. IVPP V12560, holotype of *Liaoningosaurus paradoxus*, overview of specimen.

Abbreviations: 4th, 4th trochanter; as, astragalus; cr, cranium; cv, caudal vertebrae dv, dorsal vertebrae; fe, femur; fi, fibula; hu, humerus; il, ilium; in, integument; is, ischium; mc, metacarpals; mn, mandible; mph, manual phalanges; mt, metatarsals; mx t, maxillary teeth; os, osteoderm; pmx t, premaxillary teeth; pph, pedal phalanges; pu, pubis; ra, radius; ri, ribs; sc, scapula; ti, tibia; ul, ulna.



Figure 8.5. Closeup of preserved integument in IVPP V12560, *Liaoningosaurus paradoxus*. Scale bar at bottom of image is in millimetres.

ovoid medial ends that narrow posterolaterally (Vickaryous et al. 2004). In ankylosaurids, the sternal elements fuse at the midline to form a median diamond shape, with narrower posterolaterally directed processes. In IVPP V12560, if the sternal element as figured by Xu et al. (2001) is duplicated and reflected to create a complete sternum, the resulting outline is butterfly-shaped, with the maximum anterior length present on the lateral side of the sternum, not at the midline (Fig. 8.6). If this element is one of the sternal plates, then *Liaoningosaurus* had a sternum unlike that known for any ankylosaur. However, this element occurs in a complex and difficult to interpret region of the skeleton. It is not entirely clear, from firsthand observation of the specimen, that the putative sternal represents a single element. As such, this element should not be used to diagnose *Liaoningosaurus*.

Xu et al. (2001) considered the proportions of the manus and pes (with the pes more than twice the length of the manus) to be diagnostic. This is difficult to evaluate, because few ankylosaurs preserve both a manus and pes, and no other ankylosaur specimen preserves a complete manus and a complete

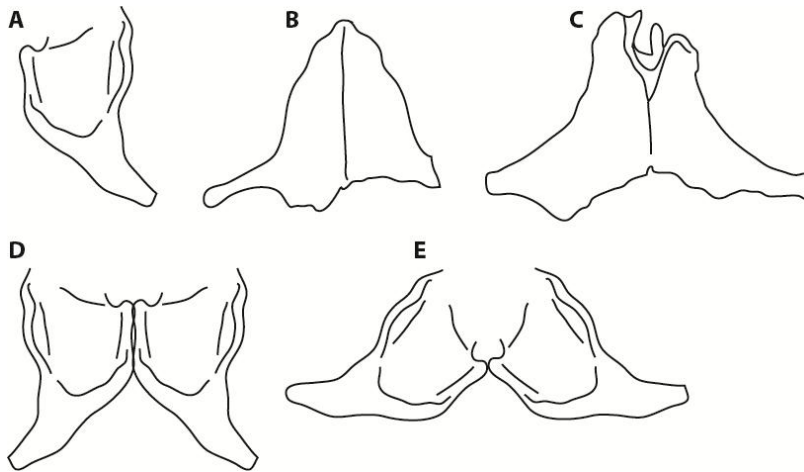


Figure 8.6. Sternal elements of ankylosaurids from Asia, anterior is up, scaled to the same length. A) Putative sternal element of IVPP V12560, *Liaoningosaurus paradoxus*. B) Sternals of PIN 614, *Pinacosaurus grangeri*, drawn from Maleev (1954). C) Sternals of MPC 100/1305, indeterminate ankylosaurid from Mongolia, drawn from Carpenter et al. (2011). Alternate arrangements of the single sternal element of *Liaoningosaurus* (D and E) do not result in a sternal morphology found in other ankylosaurids.

pes, from which measurements can be taken. MPC 100/1305 includes a complete pes and a partial manus; the pes is slightly more than twice as long as the preserved part of the manus.

No autapomorphies can be identified in *Liaoningosaurus*. However, triangular unguals that lack a proximal mediolateral constriction are known in only one other ankylosaur, the derived ankylosaurine *Dyoplosaurus acutosquameus* from the Campanian of Alberta. *Liaoningosaurus* is unlikely to represent the same species as *Dyoplosaurus*. Although the premaxilla is not preserved in *Dyoplosaurus*, the premaxilla of a derived ankylosaurine is edentulous, whereas premaxillary teeth are present in *Liaoningosaurus*. Premaxillary teeth are present in only a few ankylosaur species: the Jurassic-aged *Gargoylesaurus*, and the Albian-Cenomanian species *Cedarpelta*, *Pawpawsaurus campbelli*, and *Silvisaurus condrayi* Eaton, 1960. The unique combination of characters present in *Liaoningosaurus* allows this species to be

differentiated from other ankylosaurs, and so it is here regarded as a valid taxon that lacks autapomorphies.

Status: Valid.

Revised Diagnosis: Differs from all ankylosaurs except *Dyoplosaurus* in having triangular rather than U-shaped unguals. Differs from derived ankylosaurines in possessing premaxillary teeth.

8.2.7 *Peishansaurus philemys* Bohlin, 1953

Holotype: No specimen number provided; fragment of right lower mandible

Holotype locality and age: Ehr-Chia-Wu-Tung, Gansu Province, China; Minhe Formation, Campanian-Maastrichtian (Weishampel et al. 2004).

Original diagnosis: None provided.

Discussion: *Peishansaurus* is illustrated by two line drawings and a photograph in Bohlin (1953). It is impossible to determine if this material is ankylosaurian from the figures.

Status: *Nomen dubium*; ?Thyreophora indet.

8.2.8 *Pinacosaurus* Gilmore, 1930

Type species: *Pinacosaurus grangeri*

Previous diagnoses: From Gilmore (1930): Skull covered with numerous small osteoderms; large quadratojugal horn; skull longer than wide; rounded beak lacking osteoderms; small external nares open laterally; posteriorly-placed orbits; palate divided longitudinally by vertical median bony plate; small, dentate teeth. From Hill et al. (2001): Skull longer than wide in adult; premaxillary beak edge not covered by secondary dermal ossifications; large, anteriorly-facing nares roofed by osteoderms; premaxillary struts define at least two additional openings in narial region leading to extensive premaxillary sinus; prominent supraorbitals; lacrimal incisure (pinching of snout in lacrimal region), beak only slightly wider than distance between posteriormost maxillary teeth; quadrate

and paroccipital process not coossified; quadrate head lying directly below posterior margin of orbit. From Burns et al. (2011) – posterior embayment of supranarial ornamentation dorsal to nares and apertures creating shallow nasal vestibule; paranasal apertures not enclosed by external nares; weakly-developed cranial ornamentation; differing from other ankylosaurines in interpterygoid vacuity between palate and braincase; secondary palate flat; occipital condyle composed of multiple elements; differing from Asian ankylosaurines in having a hemispherical occipital condyle; differing from North American ankylosaurines in having flat cranial roof anterior to the orbits in lateral profile; anteriorly excavated quadrate; cingula present on teeth; posterior margin of pterygoid anterior to ventral margin of pterygoid process of quadrate; fused basiptyergoid process-ptyergoid contact.

Revised diagnosis: Ankylosaurian dinosaur with frontonasal cranial ornamentation not subdivided into discrete caputegulae. Skull longer than wide in adult specimens, unlike *Ankylosaurus*, *Euoplocephalus*, *Saichania*, or *Tarchia*, but similar to *Gobisaurus* and *Shamosaurus*. Differs from *Gobisaurus* and *Shamosaurus* in presence of paranasal apertures, and pointed, protruding prefrontal caputegulum. Unlike *Crichtonpelta*, lacks prominent nuchal ornamentation, and quadratojugal horn apex is not directed dorsally.

Discussion: *Pinacosaurus* is represented by more specimens than any other Asian ankylosaur. Aggregations of articulated skeletons are known from Bayan Mandahu in China and Ukhaa Tolgod in Mongolia, a bonebed of associated and disarticulated elements is known from Alag Teeg in Mongolia, and isolated individuals have been collected from numerous localities in both Mongolia and China. Cranial anatomy for *Pinacosaurus* has been documented in detail by Maryńska (1971, 1977), Hill et al. (2001), and Burns et al. (2011). Unusually for ankylosaurs, *Pinacosaurus* is known almost entirely from juvenile individuals.

Most of the autapomorphies proposed for *Pinacosaurus* describe features of the narial region (Fig. 8.7). The narial region of ankylosaurs includes

the external naris, nasal vestibule, and narial apertures. The border of the external nares is formed by a distinct edge on the premaxilla, and the external surface of the supranarial caputegulum. Posterior to the external naris is a concave region, topped by the supranarial caputegulae, called the nasal vestibule. Within the nasal vestibule are the openings for the airway and sinuses, called the narial apertures. In *Euoplocephalus*, aperture A opens into an initially sagittally-oriented passage that becomes complexly folded posteriorly (Witmer and Ridgely 2008). In *Pinacosaurus*, aperture A is posteriorly and medially located relative to the other apertures (Hill et al. 2001). Most specimens referred to *Pinacosaurus* differ from ankylosaurs like *Saichania* and *Tarchia* in that aperture A is visible in dorsal view, due to a notch-like embayment of the supranarial caputegulum (Fig. 8.7). This embayment was considered diagnostic for *Pinacosaurus* by Burns et al. (2011). However, IMM 96BM3/1, the holotype of *Pinacosaurus mephistocephalus*, lacks this embayment. An embayment-like morphology is present in IMM 96BM3/1 on the right side, but represents breakage of the premaxilla and nasal. The left side of the skull shows that the supranarial caputegulum was transversely oriented across the nasal vestibule, and contacted the internarial septum without an embayment. As such, Aperture A is not visible in dorsal view in this specimen (although the single pair of C apertures are visible).

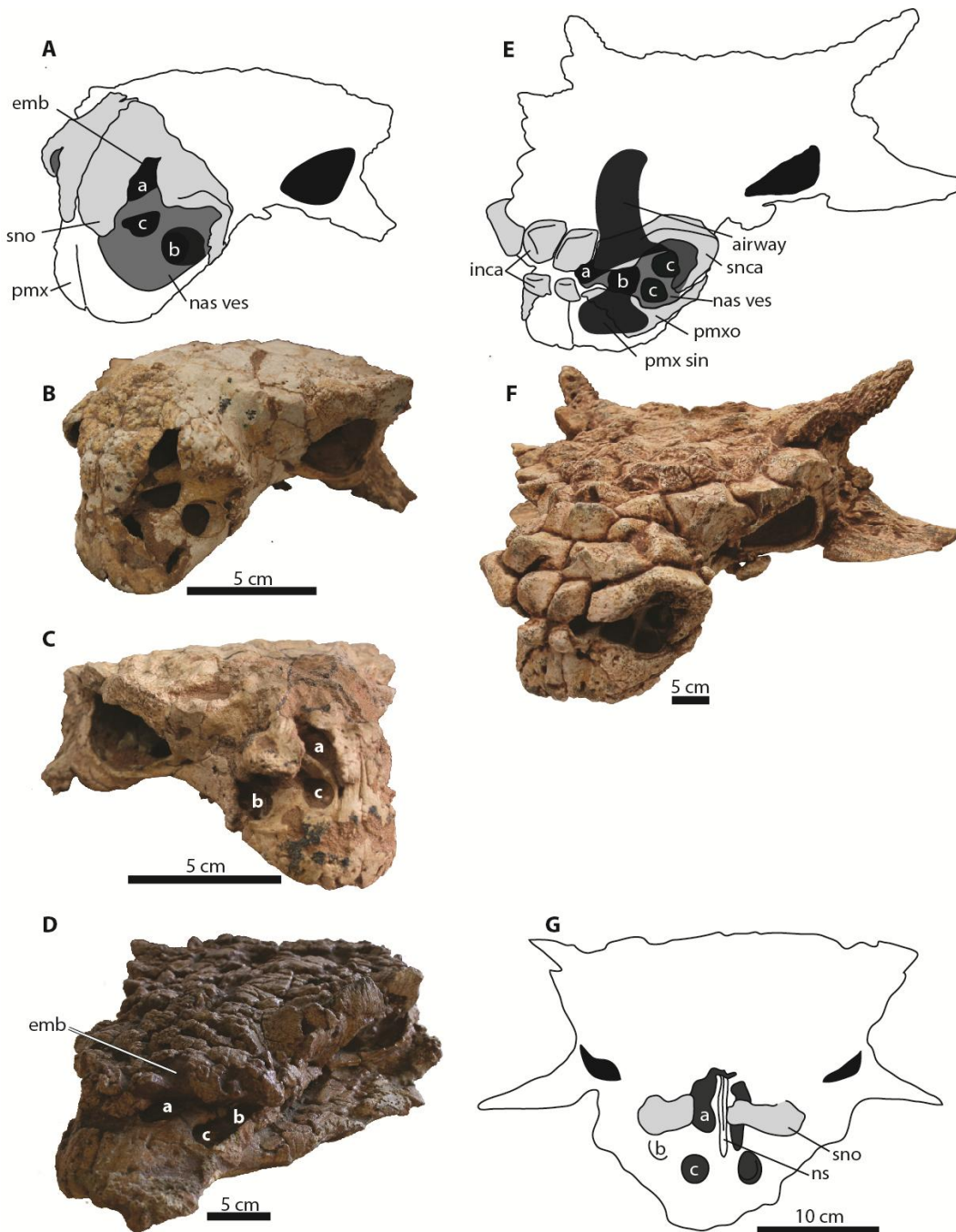
Hill et al. (2001), based on the morphology of IMM 96BM3/1, suggested that Aperture B may not be a foramen, but rather a thin-walled fossa that has broken in ZPAL MgD II/1; evidence from CT scans, while not conclusive, indicated a thin wall of bone may have been present in this region in MPC 100/1014. Skulls referred to *Pinacosaurus* have a variable number of "C" apertures, which open into true sinuses in the premaxilla that are not confluent with the airway (Hill et al. 2001, Witmer and Ridgely 2008). In INBR21004, aperture B is a paranasal aperture (not a fossa) that opens into the premaxillary sinus, and aperture C3 is a fossa with a thin bony floor. The C apertures/fossae in *Saichania* and *Tarchia* are

obscured in dorsal view by the supranarial ornamentation, but are at least partly visible in dorsal view in *Pinacosaurus*.

The smooth premaxillae of *Pinacosaurus* differentiate this taxon from *Saichania* and *Tarchia*, both of which have ornamentation on at least parts of the premaxillae. The premaxillae of *Gobisaurus* and *Shamosaurus* also lack ornamentation (longitudinal furrows are present, but not the rugosity characteristic of *Saichania* or *Tarchia*). As in *Gobisaurus* and *Shamosaurus*, the frontonasal ornamentation of *Pinacosaurus* is not subdivided into the discrete caputegulae present in ankylosaurids like *Euoplocephalus* or *Saichania*.

The marked 'pinching' anterior to the orbits and posterior to the narial region (the lacrimal incisure, *sensu* Hill et al. 2001) is present in many specimens referred to *Pinacosaurus*, but not in IMM 96BM3/1. The lacrimal incisure is also present in INBR21004 (*Tarchia*), and so while it is not an autapomorphy of *Pinacosaurus*, it is a feature with a relatively limited distribution within ankylosaurids.

The parietal region of *P. mephistocephalus* obscures the occiput in dorsal view; in at least some skulls referred to *P. grangeri* (e.g. MPC 100/1014) the occiput is visible in dorsal view. Hill et al. (2003) note that it is unclear if this is exaggerated due to taphonomic distortion of their specimen. Vickaryous et al. (2004) found only a single autapomorphy for *P. mephistocephalus*, a domed cranial roof posterior to the orbits. The domed cranial roof was upheld as an autapomorphy for *P. mephistocephalus* by Burns et al. (2011). The term 'dome' suggests that there is a hemispherical prominence in the parietal region of *P. mephistocephalus*. The parietal region of several nodosaurids (*Edmontonia*, *Panoplosaurus*, *Pawpawsaurus*) are dome-shaped, but the parietals of most ankylosaurids are anteriorly-sloping, resulting in a transversely-oriented trough-like depression posterior to the supraorbitals and anterior to the nuchal shelf. The parietals of *P. mephistocephalus* do not appear 'domed', but instead slope anteriorly as in other ankylosaurids. In some ankylosaurids (e.g. *Saichania*) the



posterior margin of the coossified parietals (the nuchal shelf) can bear large nuchal caputegulae. The posterior margin of the paired parietals may be proportionately taller in *P. mephistocephalus* compared to *P. grangeri*, although the absence of a lateral view photograph of the specimen in Godefroit et al. (1999) makes it difficult to assess this feature.

The squamosal horns of *Pinacosaurus grangeri* are pyramidal, such as those of *Euoplocephalus* and *Saichania*, but relatively small compared to those taxa (including in the adult-size holotype AMNH 6523). The apex of the squamosal horn does not extend past the posterior margin of the skull roof in dorsal view. Additionally, in *Pinacosaurus grangeri* the greatest width of the skull is across the supraorbitals, not the squamosals, unlike the condition in *Saichania* or *Tarchia*, but similar to the condition in *Gobisaurus* and *Shamosaurus*. The squamosal horns of IMM 96BM3/1, the holotype of *Pinacosaurus mephistocephalus*, differ markedly from those in specimens of *P. grangeri*. The squamosal horns of *P. mephistocephalus* are long and narrow, extending far beyond the posterior margin of the skull roof in dorsal view. The greatest width of the skull is across the squamosal horns, not the supraorbitals, in *P. mephistocephalus*. The quadratojugal horns are also proportionately longer in IMM 96BM3/1 than in any *P. grangeri* skull.

P. grangeri and *P. mephistocephalus* share several features, including rugose frontonasal ornamentation not differentiated into caputegulae, premaxillae with no ornamentation, and paranasal apertures visible in dorsal view. Numerous differences indicate that these are distinct species, including the

Figure 8.7. Narial anatomy of the Mongolian ankylosaurids *Pinacosaurus grangeri*, *Pinacosaurus mephistocephalus*, and *Tarchia kielanae*. A) Interpretive drawing of major aspects of the narial anatomy of ZPAL MgD II/1, juvenile *Pinacosaurus grangeri*. B) ZPAL MgD II/1 skull in oblique left anterolateral view. C) IVPP V16853, juvenile *Pinacosaurus grangeri* skull in oblique right anterolateral view. D) AMNH 6523, holotype skull of *Pinacosaurus grangeri*, adult or subadult, in oblique left anterolateral view. E) Interpretive drawing of major aspects of the narial anatomy of INBR21004, *Tarchia kielanae*. F) INBR21004 skull in oblique left anterolateral view. G) Interpretive drawing of major aspects of the narial anatomy of IMM 96BM3/1, holotype of *Pinacosaurus mephistocephalus*, in anterior view (drawn from Godefroit et al. 1999). Abbreviations: a-c, narial apertures/fossae; emb, embayment of the supranarial ornamentation; inca, intranarial caputegulae; nas ves, nasal vestibule; ns, nasal septum; pmx, premaxilla; pmxo, premaxillary ornamentation; pmx sin, premaxillary sinus; snca, supranarial caputegulae; sno, supranarial ornamentation.

morphology of the squamosal horns, the absence of a lacrimal incisure in *P. mephistocephalus*, and the absence of an embayment in the supranarial ornamentation. The embayment in the supranarial ornamentation was considered an autapomorphy for *Pinacosaurus* by Burns et al. (2011). Its absence in *P. mephistocephalus* indicates either 1) that *P. mephistocephalus* is not referable to *Pinacosaurus*, or 2) the embayment is an autapomorphy of *P. grangeri* rather than *Pinacosaurus*.

***Pinacosaurus grangeri* Gilmore, 1930**

= ***Pinacosaurus ninghsiensis* Young, 1935**

= ***Syrmosaurus viminicaudus* Maleev, 1952**

= ***Syrmosaurus viminicaudus* Maleev, 1954 (emended spelling)**

Holotype: AMNH 6523, skull and mandibles

Holotype locality and age: Bayan Zag (=Bayn Dzak, Shabarakh Usu, the Flaming Cliffs)

Referred specimens: ZPAL MgD II/1 (skull, mandibles, prementary, cervicals, dorsal, caudals, ribs, scapula, coracoids, humerus, radius, ulna, ilium, both femora, tibia, fibula, cervical half ring fragments), ZPAL MgD II/9 (caudals, tail club handle, pelvis, manus, femur, tibia, pes), ZPAL MgD II/31 (tail club handle); PIN 614, nearly complete skeleton without skull (holotype of *Syrmosaurus viminicaudus*), PIN 3780/3, skull; IVPP no catalogue number, fragment of upper jaw, partial right mandible, 23 vertebrae, right scapula (misidentified as an ilium by Young (1935)), right humerus, partial ischia, right femur, both tibiae, two metatarsals, radius or ulna, fibula, ilium ('indeterminate' by Young 1935), fragments of cervical half ring, osteoderms (holotype of *Pinacosaurus ninghsiensis*, Ningxia, Inner Mongolia, China). MPC 100/1305, a nearly complete skeleton with *in situ* osteoderms but lacking a skull, may also be referable to *Pinacosaurus grangeri* (see Chapter 5; Arbour and Currie 2013b).

From the Alag Teeg Bonebed: MPC 100/1307, pedal elements; MPC 100/1308 tibiae, pedal elements; MPC 100/1309, pedal elements; MPC 100/1310, left forelimb; MPC 100/1311, hindlimb and pedal elements; MPC 100/1312, pedal elements; MPC 100/1313, pedal elements; MPC 100/1315, manual elements from two individuals; MPC 100/1316, tibiae, fibulae, pedal elements; MPC 100/1317, manual elements; MPC 100/1318, manual elements; MPC 100/1319, left pes; MPC 100/1320, tibia, fibula, right pes; MPC 100/1321, skull and postcranial elements; MPC 100/1322, quadrates, coracoid, ulna, ischium, three femora of two individuals; MPC 100/1323, right ulna, manus, both pedes; MPC 100/1324, vertebrae, coracoid, osteoderms; MPC 100/1325, right manus; MPC 100/1326, forelimb, manus, associated caudal vertebrae; MPC 100/1327, left tibia and pes; MPC 100/1328, left pes; MPC 100/1329, vertebrae, manual and pedal elements; MPC 100/1330, cervical half ring fragments, vertebrae, manus; MPC 100/1331, complete right pes; MPC 100/1332, scapula, coracoid, ribs; MPC 100/1333, ilia, humeri, radius, ulna, both manus, pes (large individual); MPC 100/1334, tibia, fibula, pedal elements; MPC 100/1335, skull, forelimbs, hindlimb; MPC 100/1335, osteoderms; MPC 100/1337, right manus; MPC 100/1338, manual elements; MPC 100/1339, right ulna, radius, manus, tibiae, fibulae, both pedes; MPC 100/1340, radius, ulna, manus; MPC 100/1341, radius, ulna, manus; MPC 100/1342, tibia, fibula, pes; MPC 100/1343, hindlimb, both pedes; MPC 100/1344, skull, cervical vertebrae, cervical half ring, articulated dorsal vertebrae, scapula, humerus, both femora, tail; MPC 100/1345, cervical half ring, rib; MPC 100/1346, coracoid, humerus; MPC 100/1347, frontal. Additional undescribed Alag Teeg material in the Hayashibara Museum collections, and at the PIN.

From Bayan Mandahu: IVPP V16853, skull and cervical half rings (Bayan Mandahu, locality 100); IVPP V16283, partial skull (Bayan Mandahu, locality 100), IVPP V16854, nearly complete skeleton with skull (Bayan Mandahu, locality 101);

IVPP V16346, partial skull (Bayan Mandahu, locality 106); IVPP V16855, skull and skeleton (Bayan Mandahu, unknown locality).

Status: Valid.

Revised diagnosis: Ankylosaurid with undifferentiated frontonasal ornamentation, and with paranasal apertures/fossae. Uniquely among ankylosaurids, has an embayment in supranarial ornamentation dorsal to the narial opening. Differs from *Pinacosaurus mephistocephalus* in having short squamosal horns that do not extend far past posterior margin of skull; width across squamosal horns is not greater than width across supraorbitals; and has lacrimal incisure.

***Pinacosaurus mephistocephalus* Godefroit, Pereda Suberbiola, Li, and Dong
1999**

Holotype: IMM 96BM3/1, skull and articulated postcrania with *in situ* cervical half rings

Holotype locality and age: Quarry SBDE 96BM3 (41°47.269' N 106°43.573'E, 1239 m elevation), Bayan Mandahu, Inner Mongolia, China. Bayan Mandahu Formation

Previous diagnoses: From Godefroit et al. (1999): Two pairs of premaxillary foramina leading to premaxillary sinuses; 'gland' opening facing anteriorly; lower and upper premaxillary foramina smaller than 'gland' opening; external nares only visible in dorsal view; orbits circular and laterally oriented; no posterodorsal premaxillary process protruding between maxilla and nasal; square-shaped lacrimal; parietal much shorter than frontal; wide frontoparietal process of postorbital; deep frontoparietal depression; scapula relatively short and robust (proximal width:length = 0.36); well-developed acromial process; well-developed deltopectoral crest that terminates distal to midlength; proximal articular surface of radius strongly expanded anteroposteriorly and mediolaterally.

Status: Valid.

Revised diagnosis: Ankylosaurid with undifferentiated frontonasal ornamentation, and with paranasal apertures/fossae. Differs from *Pinacosaurus grangeri* in absence of embayment in supranarial ornamentation; squamosal horns are long and slender, and extend well past posterior margin of skull, and width across squamosal horns is greater than width across supraorbitals; differs from *Pinacosaurus grangeri* and *Tarchia* in absence of lacrimal incisure.

8.2.9 *Saichania chulsanensis* Maryańska, 1977

= *Shanxia tianzhenensis* Barrett, You, Upchurch and Burton, 1998

= *Tianzhenosaurus youngi* Pang and Cheng, 1998

Holotype: MPC 100/151, complete skull and both mandibles, seven cervical vertebrae (including fused atlas and axis), ten dorsal vertebrae, ribs, sternum, both scapulocoracoids, humerus, ulna, radius, manus, osteoderms including first and second cervical half rings; cast of specimen before individual elements were separated at ZPAL.

Holotype locality and stratigraphy: Khulsan, Mongolia (43°30.419' N, 101°07.646' E); Baruungoyot Formation (Mid-Upper Campanian, Jerzykiewicz 2000)

Referred specimens: HBV-10001 (holotype of *Tianzhenosaurus youngi*), nearly complete skull, HBV-10002 (*Tianzhenosaurus youngi* paratype), incomplete right mandible, and HBV-10003 (*Tianzhenosaurus youngi* paratype), nearly complete postcranial skeleton, all from Kangdailiang near Zhaojiagou Village, Tianzhen County, Shanxi Province; Upper Cretaceous Huiquanpu Formation. IVPP V11276 (holotype of *Shanxia tianzhenensis*), fragmentary skull (skull roof, ?quadratojugal, braincase, occiput), axis, five additional cervicals, three dorsals, four caudals, right humerus, fragment of ?ilium, complete right femur, distal portion of left femur, one osteoderm; Wu Valley, Tian Zhen County, Shanxi Province, China, about 270 km northwest of Beijing; Huiquanpu Formation, Upper Cretaceous. PIN 3142/250, complete skull, both mandibles, and predermaty (described by Tumanova 1977), undescribed cervical vertebrae,

scapula, sacrum, ischia, femur, ribs, and osteoderms (some osteoderms on display at PIN), from Hermin Tsav I, Mongolia, Nemegt Formation, (Upper Campanian – Lower Maastrichtian, Jerzykiewicz, 2000).

Previous diagnoses: From Maryńska (1977): Large, oval external nostrils situated terminally, divided by horizontal septum; premaxillary sinus present; premaxillary portion of rostrum relatively narrow; premaxillae partly covered by well-developed ornamentation; occipital condyle weakly convex, ventrally directed; epipterygoid present; exoccipital low, perpendicular to skull roof, ventral part deflected anteriorly; quadrate oblique with condyle at level of middle part of orbit; orbits anteriorly and posteriorly closed by partly neomorphic bones; skull roof overhangs occipital region; palatal region with strongly developed anterior and posterior maxillary shelves; main body of maxilla surrounds palatal vacuities over small area laterally; one opening for nerves IX-XII; atlas and axis fused; strongly developed intercostal ossifications on trunk; limb bones very massive; forelimb strongly flexed; manus pentadactyl. From Carpenter et al. (2011): cranial ornamentation of large protuberances; squamosal horn large and triangular, contacts quadratojugal horn in occipital view; ridge-like, overhanging supraorbitals; external nares laterally flaring; deeply recessed nasal vestibule with multiple sinus foramina; orbit located at mid-length of skull; paroccipital process L-shaped in vertical cross-section; tooth rows divergent posteriorly only; cervical neural arches X-shaped in dorsal view with low neural spines; dorsal centra long and low with pleurofossa; cervical armour with larger, posteriorly projecting, triangular osteoderms. From Pang and Cheng (1998), for *Tianzhenosaurus youngi*: Skull low, flat, medium-sized, isosceles triangle shape; skull roof covered with irregular bony tubercles; premaxilla relatively long; orbit small, surrounded by bony ring; narial opening horizontally elongate; septomaxilla does not separate narial openings; maxillary tooth rows slightly convergent posteriorly; basicranium short; maxilloturbinal located laterally in middle part of palatal vault; occipital region vertical; occipital

condyle narrow, high; occipital condyle not visible in dorsal view; opisthotic extends lateroventrally as curved process; mandible deep with convex ventral border; no mandibular ornamentation; tooth crowns have cingula on labial sides, swollen bases, and middle ridge on lingual sides; cervical centrum short, amphicoelous; dorsal centrum long, amphiplatyan; eight fused vertebrae in sacrum, including three dorsosacrals, four sacrals, one caudosacral; anterior caudals short, thick; posterior caudals narrow, elongate; tail club present; scapula rectangular, plate-like; proximal and distal ends of humerus moderately expanded, not twisted; femur thick, lacking fourth trochanter; tarsometatarsal and digits typical for ankylosaurs. From Barrett et al. (1998), for *Shanxia tianzhenensis*: Differs from all other ankylosaurids in the shape of the squamosal horns – squamosal horns are slender, elongate, posterolaterally inclined at angle of 145° to transverse axis of skull, have narrow junction with skull roof in occipital view, and shaped like isosceles triangles in dorsal view.

Discussion: *Shanxia tianzhenensis* and *Tianzhenosaurus youngi* were both described in June 1998 based on ankylosaurid material from the Huquanpu Formation of China. Sullivan (1999) suggested that *Shanxia* was a *nomen dubium* because the sole autapomorphy (the shape of the squamosal horn) was known to be variable in *Euoplocephalus*. Sullivan (1999) noted that the holotypes of *Tianzhenosaurus* and *Saichania* differed in the arrangement of cranial ornamentation, but considered *Tianzhenosaurus* a junior synonym of *Saichania* because the two skulls were similar in overall morphology. Upchurch and Barrett (2000) concurred that *Tianzhenosaurus* may be synonymous with *Saichania*, but rejected the suggestion by Sullivan (1999) that *Shanxia* was a junior synonym of *Tianzhenosaurus*, citing the morphology of the squamosal horn and absence of large nuchal osteoderms as distinguishing characteristics of *Shanxia*. *Shanxia tianzhenensis* and *Tianzhenosaurus youngi* are here considered subjective junior synonyms of *Saichania chulsanensis*, extending the geographic range of this taxon.

Sullivan (1999) suggested that squamosal horn shape was not a reliable feature for distinguishing ankylosaurid taxa, because of the high variability of squamosal horn shape in *Euoplocephalus*. A review of specimens referred to *Euoplocephalus* (Chapter 3, Arbour and Currie 2013a) showed that at least four species were represented by *Euoplocephalus tutus sensu lato*: *Anodontosaurus lambei*, *Dyoplosaurus acutosquameus*, *Euoplocephalus tutus sensu stricto*, and *Scolosaurus cutleri* (including *Oohkotokia horneri*). Squamosal horn bluntness did vary within *Euoplocephalus*. However, specimens from the Two Medicine Formation (*Scolosaurus cutleri*) always had proportionately longer, more pointed, squamosal horns with a distinctive backswept appearance. The squamosal horns of *Anodontosaurus* were also typically smaller and blunter than those of *Euoplocephalus*. Overall, the sharpness of ankylosaurid squamosal horns may vary within a population, but the overall shape and angle of projection from the skull (provided little plastic deformation has occurred, see Chapter 2 and Arbour and Currie 2012) are useful for distinguishing among ankylosaurid species. The squamosal horns of *Tarchia* are elongate rods, the horns of *Saichania* are deep with a dorsolateral keel, and the squamosal horns of *Zaraapelta* have a unique two-layered appearance (Chapter 6). The squamosal horns of *Shanxia* and *Tianzhenosaurus*, in dorsal view, are dorsally flat, isosceles triangles. The holotype skull of *Tianzhenosaurus* is plastically deformed, but the right squamosal horn projects from the skull at approximately the same angle as the preserved squamosal horn in *Shanxia*.

Upchurch and Barrett (2000) argued that *Shanxia* differed from *Tianzhenosaurus* because *Shanxia* lacked large nuchal caputegulae, which are present in the holotype of *Tianzhenosaurus*. The posterior margin of the skull roof in the holotype of *Shanxia* appears to be broken medial to the right squamosal horn and dorsal to the right paroccipital process (Barrett et al. 1998:Fig. 2). Dorsal to the left side of the foramen magnum, the parietals extend farther posteriorly, obscuring the occipital condyle in dorsal view. The

supraoccipital and medial end of the paroccipital processes are visibly broken in figure 2C in Barrett et al. (1998). In posterior view, the left side of the parietals bears a distinct nuchal prominence, as would be expected in this region in most ankylosaurids. It is possible that the nuchal caputegulae are not as obvious in the holotype of *Shanxia* due to breaks in this region. The preserved nuchal caputegulum on the posterior edge of the left parietal appears slightly smaller than that of the holotype of *Tianzhenosaurus*. There is some variability in the proportions of the nuchal caputegulae within *Anodontosaurus* and *Euoplocephalus* (Fig. 3.10-12; Arbour and Currie 2013a). It is possible that this difference represents either taphonomic or individual variation.

Thompson et al. (2012) recovered *Shanxia* in a basal position to *Tianzhenosaurus*, and noted three characters that differentiated the two taxa: the posterior projection of the squamosal horns, the form of the cranial ornamentation, and the attachment of the haemal arches to the caudal centra. One of the squamosal horns in the holotype of *Tianzhenosaurus* projects at the same angle as that in *Shanxia*, and the cranial ornamentation is similar in the overlapping regions of the two skulls. The haemal arches are described as unfused in *Shanxia* (Barrett et al. 1998), but the figured caudals appear highly weathered, and it seems possible that the haemal arches have simply broken off. Fusion of the haemal arches to their respective centra may also depend on size and ontogenetic stage.

There are no features that can distinguish *Shanxia* from *Tianzhenosaurus*, and because the squamosal horns are similar and because they come from the same formation, these probably represent the same species. Of these two species, the holotype of *Tianzhenosaurus youngi* provides the most complete anatomical information, but also demonstrates that *Tianzhenosaurus* (and *Shanxia*) cannot be differentiated from the Mongolian ankylosaurid *Saichania chulsanensis* (Fig. 6.3-6.6). The skulls of HBV-10001 (holotype of *Tianzhenosaurus youngi*) and MPC 100/151 (holotype of *Saichania chulsanensis*) both have

bulbous frontonasal ornamentation, a single internarial caputegulum (unlike *Tarchia kielanae*, which has several internarial caputegulae), and broad, pyramidal squamosal horns (unlike the narrow, rod-like squamosal horns of *Tarchia kielanae*). The quadrate and paroccipital process are fused in HBV-10001, as they are in MPC 100/151. One notable difference between HBV-10001 and MPC 100/151 is the presence of a distinct rim of ornamentation encircling the orbit in HBV-10001, which is absent in MPC 100/151. However, this feature is variably developed in specimens referred to *Euoplocephalus* (see Arbour and Currie 2013a: fig. 5), and so this difference most likely represents individual variation between HBV-10001 and MPC 100/151. There are no taxonomically significant differences between the skulls of HBV-10001 and MPC 100/151, and for this reason *Tianzhenosaurus youngi* is considered a junior synonym of *Saichania chulsanensis*.

The postcranial skeleton of *Tianzhenosaurus* was described briefly in Pang and Cheng (1998) but no elements were figured. *Saichania chulsanensis* has a uniquely large deltopectoral crest on the humerus, and a unique first cervical half ring. If the humerus of *Tianzhenosaurus* is later shown to differ from that of *Saichania*, then *Tianzhenosaurus* could be reinstated as a distinct taxon. In that case, *Tianzhenosaurus youngi* would still have priority over *Shanxia tianzhenensis*. Both taxa were named in the same month of the same year, which makes determining which has priority somewhat difficult. Article 21 of the ICZN (Determination of date) states: "21.3 Date incompletely specified. If the day of publication is not specified in a work, the earliest day on which the work is demonstrated to be in existence as a published work is to be adopted as the date of publication, but in the absence of such evidence the date to be adopted is 21.3.1 the last day of the month, when month and year, but not day, are specified or demonstrated." Upchurch and Barret (2000:216) noted that "Both names were published in June 1998: Barrett et al.'s publication appeared on the 15th June, whereas Pang and Cheng's work appeared in a journal which lacked a

specific date in June. Under ICZN rules, Pang and Cheng's name, *Tianzhenosaurus*, is deemed to have appeared at the end of June 1998." Sullivan (2000:218) countered, "Regarding their claim of taxonomic priority, I checked with Ms. Gladys Calix-Ferguson (Marketing Executive-Journals, Taylor & Francis Ltd., London; the company that distributes "Progress in Natural Science") who stated that the journal was in their office at the end of May 1998. I can only conclude that the publication date was no later than June 1st." Because Sullivan (2000) demonstrated that Pang and Cheng (1998) was in existence by June 1st, and because Barrett et al. (1998) was published explicitly on June 15, then *Tianzhenosaurus* would have priority over *Shanxia*.

Status: Valid.

Revised Diagnosis: Ankylosaurine ankylosaurid with bulbous cranial ornamentation. Uniquely among ankylosaurines, has fused atlas and axis forming a syncervical; proximally wide humerus (proximal width 70% total humerus length); intercostal ossifications present (may also be present in MPC 100/1305); and cervical half rings composed of the underlying band, primary osteoderms, and coossified interstitial osteoderms completely obscuring the band in external view. Supranarial caputegulae separated by one flat internarial caputegulum (unlike *Tarchia kielanae*, which has four bulbous internarial caputegulae), less broadly flaring than in *Tarchia kielanae*, and rugose (not smooth as in *Tarchia kielanae*). Single large loreal caputegulum and single large lacrimal caputegulum, unlike numerous small lacrimal and loreal caputegulae in *Tarchia kielanae* and *Zaraapelta nomadis*. Prefrontal caputegulum smaller, less laterally projecting than in *Tarchia kielanae* and *Zaraapelta nomadis*. Lateral edges of anterior and posterior supraorbitals continuous, not distinct peaks as in *Tarchia kielanae* and *Zaraapelta nomadis*. No accessory postorbital ossification as in *Tarchia kielanae*. Squamosal horns pyramidal, and larger and broader than in *Tarchia kielanae*. Squamosal horn has uniform texture, unlike bi-layered texture in *Zaraapelta*

nomadis. Mandibular osteoderm about half the length of the mandible, anteroposteriorly shorter than in *Tarchia kielanae*.

8.2.10 *Sauroplices scutigera* Bohlin, 1953

Holotype: No specimen number provided; ribs, ?ischium, osteoderms. Casts (AMNH 2074) of some of the material are available.

Holotype locality and age: Tebch (41°30'N, 106°59'E), 11 km north of the town of Uradi Houqi, Inner Mongolia, China, Barremian-Aptian (Eberth et al. 1993).

Original diagnosis: None provided.

Discussion: *Sauroplices* is represented primarily by osteoderms that were apparently preserved in life position (Bohlin 1953), with much of the postcranial skeleton weathered away. Maryańska (1977) considered *Sauroplices* a valid taxon based on the grooved ornamentation on the osteoderms; Coombs (1978a) also retained it as a distinct taxon of ankylosaur. *Sauroplices* was considered a *nomen dubium* by Coombs and Maryańska (1990) and Vickaryous et al. (2004). *Sauroplices* includes parts of a Category 2 pelvic shield (Arbour et al. 2011), with coossified osteoderm rosettes, a feature that is otherwise known with certainty from two other ankylosaurs from Asia (*Dongyangopelta* and *Taohelong*; Fig. 8.3). The preserved portions of the pelvic shield in *Sauroplices* are slightly different from other ankylosaurs with Category 2 pelvic shields. In *Sauroplices*, the large central osteoderms in each rosette are separated from each other by only one ring of smaller osteoderms (Fig. 8.3B). In contrast, in ankylosaurs such as *Gastonia* (Kirkland 1998), *Mymoorapelta* (Kirkland and Carpenter 1994), and *Polacanthus* (Blows 1987), the large central osteoderms in each rosette are separated by several smaller osteoderms. Although extremely fragmentary and poorly understood, the morphology of the pelvic shield of *Sauroplices* can be differentiated from other ankylosaurs, and so *Sauroplices scutigera* is here considered a valid taxon.

Status: Valid

Revised diagnosis: Ankylosaurian dinosaur with pelvic shield composed of coossified osteoderm rosettes, in which the large central osteoderms of each rosette are separated by only a single ring of smaller osteoderms.

8.2.11 *Taohelong jinchengensis* Yang, You, Li, and Hong, 2013

Holotype: GSDM 00021, caudal vertebra, three dorsal ribs, left ilium, osteoderms including portion of pelvic shield.

Holotype locality and age: Lanzhou-Minhe Basin near border of Yongjing and Lintao counties in Gansu Province; Hekou Group, Lower Cretaceous

Original diagnosis: Neural canal of caudal vertebra an inverted trapezium; lateral edge of preacetabular process an inverted S-shape; pelvic shield composed of irregularly arranged osteoderms of various sizes.

Discussion: The morphology of the neural canal in *Taohelong* is not unique, but the other diagnostic characters proposed by Yang et al. (2013) have relatively limited distributions within the Ankylosauria. The ilium in the majority of ankylosaurs has a straight or gently convex lateral edge in dorsal view. In contrast, the lateral edge of the holotype of *Taohelong* is strongly sigmoidal, a condition only present in a few other ankylosaurs, including *Sauropelta edwardsi* (Coombs 1978a), *Struthiosaurus languedocensis* and *Struthiosaurus* sp. from the Iberian peninsula (Garcia and Pereda Suberbiola 2003). Besides *Taohelong*, ankylosaurs with a sigmoidal lateral edge to the ilium are present only in the Late Cretaceous. Additionally, no other ankylosaurs with this ilium morphology are known to have possessed a Category 2 pelvic shield (*sensu* Arbour et al. 2011) of coossified osteoderm rosettes. The pelvic shield of *Taohelong* differs from those preserved in *Dongyangopelta* and *Sauropelites* (Fig. 8.3). In *Dongyangopelta*, the central osteoderm of the rosette is not always completely ringed by smaller osteoderms. In *Sauropelites*, it appears the central osteoderm of one rosette was only separated from the central osteoderm of another rosette by a single smaller osteoderm, rather than several as in *Taohelong*. The combination of an ilium

with a sigmoidal lateral edge, and a pelvic shield of coossified osteoderm rosettes, is unique to *Taohelong jinchengensis*.

Status: Valid.

Revised diagnosis: Ankylosaurian dinosaur with unique combination of ilium with sigmoidal lateral edge in lateral view, and pelvic shield composed of osteoderm rosettes in which the central osteoderms are separated by several smaller osteoderms.

8.2.12 *Tianchiasaurus nedegoapeferima* Dong, 1993

= *Jurassosaurus nedegoapeferkimoruma* Dong vide Holden, 1992

= *Tianchiasaurus nedegoapeferima* Dong, 1993; emended Dong, 1994

Nomenclatural note: *Tianchiasaurus* is referred to as both *Tianchiasaurus* and *Tianchisaurus* by Dong (1993). ICZN Article 32.2.1 states that if a name is spelled more than one way in the establishing paper, then the correct original spelling is that chosen by the first reviser. In this case, Dong (1994) is the first reviser and *Tianchiasaurus* is the correct spelling.

Holotype: IVPP V10614, fragments of skull, five cervicals, six dorsals, seven sacrals, three caudals, limb fragments, osteoderms.

Holotype Locality and Age: Sangonghe Valley (Fukang County, Xinjiang, China), on north slope of Bogda Feng, 35 km northwest of Urumqi; upper part of the Toutunhe Formation, Middle Jurassic (Dong 1993; Maisch et al. 2003).

Original diagnosis: Numerous osteoderms in pectoral region and thorax; skull heavy and wider than that of *Scelidosaurus*; mandible thinner than in other ankylosaurs, similar to those in stegosaurs; atlas intercentrum and neural arch not coossified with ribs; dorsal vertebrae amphiplatyan; dorsal centra and ribs not coossified; sacrum with seven vertebrae; small, flat tail club knob; long, prominent fourth trochanter of femur; metatarsals primitive.

Discussion: IVPP V10614 could not be located at the IVPP in August 2010.

Although photographs of IVPP V10614 in Dong (1993) are clear, the fragmentary

nature of many of the elements makes it difficult to assess the validity of *Tianchisaurus*. All of the described diagnostic characters are widely distributed with the Ankylosauria, except potentially the relatively thin mandible. However, the mandible as figured does not appear substantially thinner than in other ankylosaurs. A long, prominent fourth trochanter would be unusual in an ankylosaur, but this feature is later described as a ridge, consistent with the condition in other ankylosaurs.

The "tail club" of IVPP V10614 may not represent a tail club knob, although it is difficult to assess from the photos alone. The putative knob appears subdivided by deep grooves into three sections, with two larger sections flanking a small triangular area. In most ankylosaurid knobs, the major osteoderms are clearly separated at the midline in dorsal and ventral view, and the terminal end of the knob is made up of more than one osteoderm (e.g. Arbour and Currie 2013a: Fig. 14). It is unclear what the putative knob of IVPP V10614 represents, but it is unlikely that it is a true tail club knob. A partial cervical half ring is present in IVPP V10614. Dong (1993) considered the cervical half ring to be composed of osteoderms coossified to each other. Based on the figured image, the half ring appears to be composed of osteoderms atop a band, a feature more typically found in ankylosaurids than nodosaurids. Unfortunately, *Tianchisaurus* lacks diagnostic characters to distinguish it from other Jurassic ankylosaurs like *Gargoyleosaurus* and *Mymoorapelta*, and as such it must be considered a *nomen dubium*.

Status: *Nomen dubium*, Ankylosauria indet.

8.2.13 *Zhejiangosaurus lishuiensis* Lü, Jin, Sheng, Li, Wang, and Azuma, 2007

Holotype: ZMNH M8718, sacrum with eight vertebrae, fourteen caudal vertebrae, right ilium, partial left ilium, partial ischium, pubis, both femora, both tibiae, both fibulae, both pedes.

Holotype Locality and Age: Liancheng, Lishui of Zhejiang Province. Chaochuan Formation (Cenomanian). 28°28'35.4"N, 119°51'54.3"E

Original diagnosis: Sacrum with three sacrals and five dorsosacrals; preacetabular process of ilium long and slender; sacral ribs oriented dorsolaterally and slightly posteriorly; fourth trochanter located at midlength of femur; fibula more slender than tibia; ratio of tibia to femur length 0.46.

Discussion: Three sacral vertebrae and numerous coossified dorsosacral vertebrae are present in many ankylosaurs, and the fourth trochanter is located near the midlength of the femur in most ankylosaurids. The fibula is always more slender than the tibia in all dinosaurs, and the taxonomic utility of limb proportions in ankylosaurs is currently unknown. As such, there are no autapomorphies for *Zhejiangosaurus* in the original description of this taxon. ZMNH M8718 does have some unusual features that have a relatively limited distribution within ankylosaurs. The distal ends of the sacral and dorsosacral neural spines are greatly expanded, and in dorsal view form successive teardrop-shapes (Lu et al. 2007 incorrectly described this feature as the fusion of osteoderms to the sacral neural spines). Although this morphology was also described for several ankylosaurids from Alberta (ROM 1930, TMP 1982.9.3, Arbour and Currie 2013a), the expansion of the neural spines in *Zhejiangosaurus* is far greater than in other taxa. Longitudinal ridges are present on the lateral sides of the caudal vertebrae; these are not present in most ankylosaurids, but are known for *Sauropelta edwardsi* (Ostrom 1970). It is unclear if these ridges may be a result of the dorsoventral compression that seems to have affected some of the caudal vertebrae in ZMNH M8718. Unfortunately, ZMNH M8718 preserves no autapomorphies, nor does it preserve a unique combination of characters, and so *Zhejiangosaurus* must be regarded as a *nomen dubium*. *Dongyangopelta* (here considered a valid taxon) and "*Zhejiangosaurus*" are derived from the same formation in southeast China; if these two species are

shown to represent the same taxon, then *Zhejiangosaurus* has priority over *Dongyangopelta*.

Lu et al. (2007) referred ZMNH M8718 to the Nodosauridae based on the morphology of the synsacrum, caudal vertebrae, ilium, and femur. Lu et al. (2007) suggest that the longitudinal ridges on the lateral surfaces of the caudal vertebrae were similar to those from ankylosaurs without tail clubs (although they did not list any specific taxa as examples). The fourth trochanter is described as proximal to the midlength of the femur, a trait more associated with nodosaurids (Lu et al. 2007). However, no measurements are provided, and the figures provided in Lu et al. (2007) show a fourth trochanter that is nearly at the midlength of the femur, and not noticeably proximal or distal to the midlength. The claim that the tail of ZMNH M8718 is short relative to other ankylosaurs, and that ZMNH M8718 and other nodosaurids had no active function for the tail, is a misinterpretation of the conclusions of Coombs 1979. ZMNH M8718 appears to have had a typically proportioned ankylosaurid tail, based on the preserved elements. Lu et al. (2007) compare the synsacrum of ZMNH M8718 with those of *Edmontonia* and *Silvisaurus*, but do not explain how it is characteristic of nodosaurids rather than ankylosaurids. Finally, Lu et al. (2007) note that the convex lateral margin of the ilium of ZMNH M8718 differs from the curved lateral margin of *Struthiosaurus* and the straight lateral margin of *Euoplocephalus*, but do not explain how this is a typically nodosaurid feature. In fact, the ilium of ZMNH M8718, although broken, bears more similarity to that of *Euoplocephalus* than that of *Struthiosaurus*; as figured by Lu et al. (2007) the preacetabular process is more divergent in ZMNH M8718 and *Euoplocephalus* compared to *Struthiosaurus*. As such, ZMNH M8718 appears to have more affinities with ankylosaurids than with nodosaurids, but at the very least it cannot be confidently referred to Nodosauridae.

Status: *Nomen dubium*, Ankylosauria indet.

8.2.14 Other ankylosaurian remains from China

Qiupa Formation, Luanchuan, Henan, China: tooth, partial dorsal vertebra, ?ischium (Jia et al. 2010)

Lower Red Unit, Xinminbao Group, Mazongshan, Gansu (Late Barremian to Aptian, or possibly Albian): undescribed ankylosaurid elements (Tang et al. 2001)

8.2.15 Japanese ankylosaur

Specimen: MCM A522, Left rear half of the skull, with associated teeth, and atlas articulated with occipital condyle.

Locality and Age: Omakisawa River (tributary of Shuparo River), Oyubari region, Hokkaido, Japan. The specimen was collected as an eroded block that must have eroded out upstream; the strata in this area mostly represent the Middle Yezo Group (Maruyama, Hikagenosawa, and Takinosawa formations), and Hawakaya et al. (2005) considered the specimen to derive from the upper part of the Hikagenosawa Formation and to be Cenomanian in age.

Discussion: Hawakaya et al. (2005) referred MCM A522 to the Nodosauridae based on the presence of a laterotemporal fenestra, a hemispherical occipital condyle on a relatively long neck, and teeth with relatively few denticles. The specimen does have a visible laterotemporal fenestra in lateral view; however, the lateral edge of the skull is broken and so it is unclear if this is a taphonomic artefact – ankylosaurids still retain laterotemporal fenestrae, but they are obscured by the quadratojugals and squamosals in lateral view. The occipital condyle is still articulated with the atlas vertebra, so it is unclear how the hemispherical morphology of this element was determined. A low denticle count has been shown to be characteristic of nodosaurids (Coombs 1990), and so this feature provides the best support for MCM A522 being referable to the Nodosauridae.

8.3 Discussion and conclusions

This review of ankylosaurian diversity in China has found support for many previously named taxa, but several taxa are shown to be *nomina dubia* or junior synonyms. Valid ankylosaurs from China include *Dongyangopelta*, *Gobisaurus* (discussed in Chapter 7 along with *Zhongyuansaurus*), *Liaoningosaurus*, *Pinacosaurus grangeri*, *Pinacosaurus mephistocephalus*, *Saichania chulsanensis*, *Sauroplices scutiger*, and *Taohelong*. *Bienosaurus*, *Crichtonsaurus bohlini*, *Heishansaurus*, *Peishansaurus*, *Tianchisaurus*, and *Zhejiangosaurus* lack diagnostic characters and therefore represent *nomina dubia*. A new generic name is proposed for "*Crichtonsaurus*" *benxiensis*, *Crichtonpelta benxiensis*. *Shanxia* and *Tianzhenosaurus* are both junior synonyms of *Saichania chulsanensis*, making *Saichania* one of the most widely distributed ankylosaurids from Asia.

"*Zhejiangosaurus*" was originally described as a nodosaurid, but does not share any synapomorphies with that clade, and the morphology of the ilium is more consistent with that of ankylosaurids. *Dongyangopelta* and *Taohelong* both have pelvic shields of fused osteoderms, a feature more associated with basal ankylosaurs and nodosaurids, and the lateral edge of the ilium in *Taohelong* is sigmoidal like that in nodosaurids. *Taohelong* was recovered as a polacanthine nodosaurid in a phylogenetic analysis (Yang et al. 2013), and represents the best evidence yet for a nodosaurid presence in Asia. The tooth morphology of the fragmentary ankylosaur specimen from Japan is also more similar to the teeth of nodosaurids than the teeth of ankylosaurids. Overall, some ankylosaurs from China and Japan do seem to have nodosaurid affinities, and these relationships will be tested in the revised phylogenetic analysis in Chapter 10.

9. ANKYLOSAURIAN DINOSAURS FROM GONDWANA

9.1 Introduction

The vast majority of ankylosaur fossils are known from Laurasia, with ankylosaurid ankylosaurs present in North America and Asia, and nodosaurid ankylosaurs present in North America and Europe. However, a handful of ankylosaur fossils are known from Gondwana. These include *Minmi paravertebra* from the Albian of Australia, highly fragmentary indeterminate ankylosaur remains from the Campanian of New Zealand, *Antarctopelta oliveroi* from the Campanian of Antarctica, and an indeterminate ankylosaur from the Campanian-Maastrichtian of Argentina. The phylogenetic relationships of these ankylosaurs are uncertain, and as such, their palaeobiogeographic significance is not well understood. *Minmi* has variously been recovered as the most basal ankylosaur, as the basalmost ankylosaurid, and as a basal (but not most basal) ankylosaurid. *Antarctopelta* was recently recovered as the most basal nodosaurid, but has also been considered to possess both nodosaurid and ankylosaurid features. Finally, the Argentinian ankylosaur material, although fragmentary, has nodosaurid features. Are Gondwanan ankylosaurs more closely related to each other than to Laurasian ankylosaurs, thus representing a unique radiation of southern ankylosaurs? Or, are some Late Cretaceous Gondwanan ankylosaurs more closely related to Laurasian taxa, thus representing faunal interchange between Gondwana and Laurasia? The phylogenetic relationships of the Gondwanan ankylosaurs will be tested in Chapter 10, in order to investigate the biogeographic significance of Gondwanan ankylosaurs.

9.2 Systematic Palaeontology

9.2.1 *Minmi paravertebra* Molnar, 1980

Holotype: QM F10329, eleven dorsal vertebrae and associated rib bases, five incomplete ribs, partial pes, ventral osteoderms, two unidentified elements

Holotype locality and age: on Injune Road, 1km south of Mack Gulley, north of Roma, Queensland; Minmi Member, Bungil Formation, Aptian-Neocomian

Referred specimen: QM F1801, as *Minmi* sp. in Molnar (1996), nearly complete skeleton including skull, axial skeleton to proximal part of tail, left shoulder girdle, left humerus, radius, and ulna, left ilium, both ischia, both pubes, both femora, *in situ* dorsal osteoderms; south of Flinders River on Marathon Station, east of Richmond, Queensland, Allaru Mudstone, Albian. QM F33286 (partial thoracic region with articulated pelvis and osteoderms), QM F35259 (ribs with osteoderms), QM F119849 (vertebrae, ribs, osteoderms), QM F33565 (partial femur), and QM F33566 (distal tibia) from the Barremian-Albian of Queensland were referred to *Minmi* by Leahey and Salisbury (2013).

Original diagnosis: Paravertebral elements present; pavement of small osteoderms ventrally; dorsal vertebrae amphiplatyan without notochordal prominences; transverse processes slender and triangular in cross-section; neural canal broad; posterior intervertebral notch shallow.

Discussion: Ossicles (osteoderms of about less than 5mm in diameter) are present in several specimens of North American ankylosaurids (Arbour et al. in press), and so their presence cannot be considered diagnostic of *Minmi paravertebra*. Amphiplatyan dorsal vertebrae are ubiquitous throughout Ankylosauria, and the presence or absence of notochordal prominences can vary within a single individual. The morphology of the neural canal and intervertebral notch are consistent with those of other ankylosaurs, as is the morphology of the transverse processes. This leaves only the presence of paravertebral elements as a potential diagnostic character for *Minmi paravertebra*.

Molnar (1980) noted the presence of bony rods alongside the dorsal vertebrae in QM F10329, but suggested that these only superficially resembled ossified tendons, because two of the elements were coossified in one location. He proposed the term 'paravertebrae' to refer to these elements. Molnar and Frey (1987) further described the paravertebral elements of QM F10329. Somewhat confusingly, the paravertebral elements are described as being both homologous and not homologous with the ossified tendons of other ornithischians. Molnar and Frey (1987) note that the paravertebral elements represent different tendons of the epaxial musculature, and identify the three classes of paravertebrae as representing the ossified tendons of the *M. articulospinalis* (class 1 paravertebra), *M. spinoarticularis* (class 2 paravertebra), and *M. neurospinalis* (class 3 paravertebra). However, the 'paravertebrae' of *Minmi* were instead stated to represent sesamoids, rather than ossified tendons; additionally, Molnar and Frey (1987) stated that no bony structures similar to paravertebrae had ever been described, but also that the paravertebrae of *Minmi* were homologous with the ossified tendons of other ankylosaurs. Ossified tendons of the dorsal musculature are widespread among Ornithischia, and are present in several ankylosaurs, such as *Ankylosaurus magniventris* (AMNH 5895; Carpenter 2004) and *Nodosaurus textilis* (YPM 1815; Lull 1921). The only other similar structures in ornithischians are the ossified myorhabdoi (intermuscular bones located superficially within the myosepta) unique to pachycephalosaurs (Brown and Russell 2012); however, these bear no resemblance to the 'paravertebrae' described for *Minmi*. It is unclear why the term 'paravertebra' is necessary if the paravertebrae of QM F10329 represent the ossified tendons of the dorsal epaxial musculature. For this reason, the term 'paravertebra' should be abandoned, as it is redundant with 'ossified tendon'. This has important implications for the diagnosis of *Minmi*, and also removes a character used in recent ankylosaur phylogenetic analyses (Thompson et al. 2012, Vickaryous et al. 2004).

One aspect of the ossified tendon complex of QM F10329 that is unique is the sheet-like ossification at the anterior end of the M. articularis tendon. Molnar and Frey (1987) interpreted this as an ossified aponeurosis. Reports of ossified aponeuroses are uncommon; in humans, a few rare diseases cause ossification of the aponeuroses and other connective tissues. In non-human tetrapods, extant male *Tragulus* (chevrotains, or mouse deer) show remarkable sheath-like ossifications in the soft tissues covering the pelvis and dorsal vertebrae (Rothschild et al. 2010). Although far more extensive than that preserved in QM F10329, the ossified aponeuroses of *Minmi* may have been similar. If the ossified aponeuroses of the M. articularis tendons are not pathological in origin for QM F10329, then these may be autapomorphic for *Minmi*, as similar structures have not been observed in other ankylosaurs. For this reason, *Minmi paravertebra* is retained as a valid species.

QM F18101 was referred to *Minmi* because it possesses 'paravertebrae', including ossified aponeuroses and ossified tendons (Molnar 1996). Ossified tendons are visible along the dorsal vertebrae in a cast of QM F18101 (USNM 508490) and in the figures in Molnar (1996) and Molnar (2001), but ossified aponeuroses are not clearly discernable in the cast or figures. The referral of QM F18101 to *Minmi* will be retained here pending a complete description of the fully prepared skeleton.

Status: Valid

Revised diagnosis: Ankylosaur with sheet-like ossification at the anterior end of the M. articularis tendon.

9.2.2 *Antarctopelta oliveroi* Salgado and Gasparini, 2006

Holotype: MLP 86-X-28-1, cranial fragments, left dentary fragment with *in situ* tooth, three isolated teeth, two cervical vertebrae and latex cast prepared from natural mould of three articulated vertebrae, fragments of dorsal ribs, two dorsosacral centra, three coossified sacral centra, eight caudals, glenoid portion

of left scapula, fragment of right ilium, distal portion of left femur, five metapodials, two phalanges, osteoderms

Holotype locality and age: Santa Marta Cove, North James Ross Island, Antarctica, locality D6-1; lower part of the Gamma Member, Santa Marta Formation, Marambio Group (upper Campanian)

Original diagnosis: Cervical centra short (centrum length 70% centrum height), anterior articular faces higher than posterior faces; anterior caudal vertebrae with slender transverse processes; centra of most posterior caudals dorsoventrally depressed, with articular faces anteriorly inclined and laterally expanded; transverse processes of posterior caudals well developed (length 40% centrum width), dorsoventrally depressed, positioned within anterior half of centrum; at least six morphotypes of osteoderms, including narrow and spine-shaped, ovoid plates with rugose surface textures, plates with smooth surface textures, polygonal with rugose texture, shield-shaped with dorsal keel, and small button-like osteoderms.

Discussion: *Antarctopelta* is the second most complete ankylosaur known from Gondwana, after *Minmi*. Although many parts of the skeleton are represented, many of the bones are fragmentary or damaged, and few cranial elements have been identified. Some characters in the original diagnosis are present in other ankylosaurs. The cervical centra were described as anteroposteriorly short, with the length 70% of the centrum height. However, a cervical vertebra from *Euoplocephalus* (AMNH 5403) also has a cervical centrum in which the length is about 70% of the height (Arbour and Currie 2013a), so the cervicals of *Antarctopelta* are not notably short. None of the osteoderms preserved in the holotype have a unique morphology.

Several of the diagnostic features described for *Antarctopelta* relate to the morphology of the postcervical vertebrae, which are highly unusual for ankylosaurs. The anterior of the two coossified vertebrae considered part of the sacral rod in MLP 86-X-28-1 (Salgado and Gasparini 2006) has, in ventral view, an

articular face with a distinct rim, which is not typically present in ankylosaurs. The centrum is dorsoventrally lower compared to the dorsosacral vertebrae of most ankylosaurs. Finally, the ribs are not coossified to the vertebra, which is highly unusual for an ankylosaur; dorsosacrals and posterior dorsals have coossified ribs in *Ankylosaurus* (Carpenter 2004), *Edmontonia* (Gilmore 1930), *Euoplocephalus* (Arbour and Currie 2013a), *Hungarosaurus tormai* Ósi, 2005, *Talarurus* (Maleev 1952), and many other ankylosaurs.

The proximal caudal vertebra identified by Salgado and Gasparini (2006), although fragmentary, has a triangular outline in anterior or posterior view (Fig. 9.1C), with a nearly flat ventral surface in anterior view and a ventrally located transverse process/caudal rib. This morphology is inconsistent with proximal caudal morphology in all other ankylosaurs, in each of which the centrum is circular or slightly heart-shaped in anterior or posterior view, and in which the transverse process/caudal rib is located at about the midheight on the centrum. The proximal caudal identified by Salgado and Gasparini (2006) probably does not belong to an ankylosaur, but the morphology is consistent with the proximal caudal or pygal vertebrae of mosasaurs. It compares well with the caudals of *Hainosaurus* and *Tylosaurus* (Lindgren 2004: fig. 4), *Plioplatecarpus* (Mulder 2001: fig. 4A; Fernandez et al. 2008: fig. 7F), and *Taniwhasaurus* (Fernandez and Martin 2009: Fig. 6H), all of which have centra with roughly triangular faces, and transverse processes positioned at nearly the ventral edge of the centrum.

The distal caudal vertebra identified by Salgado and Gasparini (2006) shares with ankylosaurid handle caudals a centrum with 'binocular'-shaped articular faces. However, ankylosaurid handle vertebrae rarely have transverse processes/caudal ribs, and when present, these are low, rounded nubs, unlike the anteroposteriorly long and dorsoventrally flat transverse processes present in MLP 86-X-28-1. Nodosaurid distal caudal vertebrae also lack such anteroposteriorly long transverse processes. This also suggests that these vertebrae may not belong to an ankylosaur. The distal caudal vertebrae referred

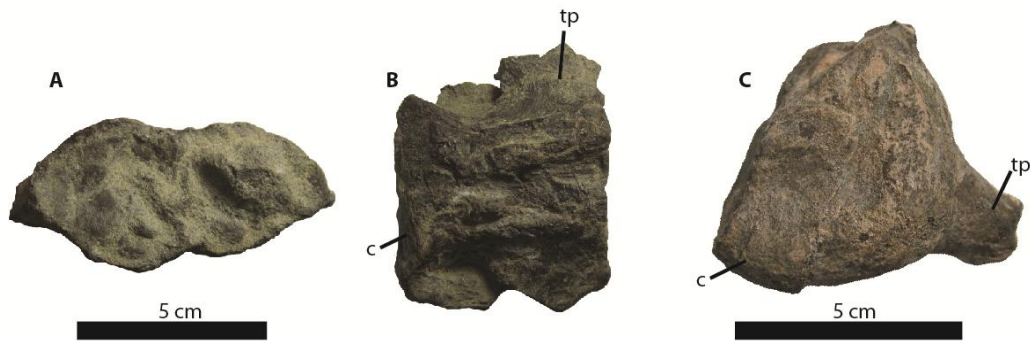


Figure 9.1. Non-ankylosaurian elements of MLP 86-X-28-1, holotype of *Antarctopelta oliveroi*. A 'distal caudal vertebra' identified by Salgado and Gasparini (2006) in anterior (A) and dorsal (B) views is more likely an elasmosaurid plesiosaur cervical vertebra. C) A proximal caudal vertebra identified by Salgado and Gasparini (2006) is probably not ankylosaurian, and is more likely a pygal vertebra from a mosasaur.

to *Antarctopelta* may instead be referable to a plesiosaur (Fig. 9.1A, B).

Elasmosaurid cervicals characteristically have well-defined articular margins, anteroposteriorly long articulations for the cervical ribs, and centra with binocular-shaped articular faces (O'Keefe and Street 2009). The 'distal caudals' of MLP 86-X-28-1 share some similarities with the cervicals of *Mauisaurus* (Hiller et al. 2005: Fig. 11).

The bones attributed to *Antarctopelta* were collected from a 2 x 3m area, leading previous authors to interpret the material as belonging to a single individual. However, Olivero et al. (1991) suggested that the presence of large numbers of nautilid phragmocones associated with the skeleton indicated that this represented a strandline on a beach. MLP 86-X-28-1 was found associated with fish vertebrae, bivalves, gastropods, nautilid cephalopods, and a condrichthyan tooth (Olivero et al. 1991, Gasparini 1996, Salgado and Gasparini 2006). Plesiosaur and mosasaur remains have been collected from other horizons and localities in the Gamma Member (Olivero et al. 1991). The presence of plesiosaur and mosasaur elements associated with the ankylosaur elements of MLP 86-X-28-1 is therefore not unlikely, given the abundance of other marine vertebrate and invertebrate remains associated with the specimen.

The elements of MLP 86-X-28-1 that are definitely ankylosaurian include a fragment of the mandible, ribs, and osteoderms (including portions of a pelvic shield); the cranial fragments most likely also belong to an ankylosaur. The scapula and coracoid are fragmentary, but consistent with those of ankylosaurs. Some of the diagnostic characters proposed by Salgado and Gasparini (2006) are more broadly distributed among ankylosaurs (cervical vertebra proportions, osteoderm morphologies). The remaining characters are derived from elements that are probably not ankylosaurian. At present, no autapomorphies at the genus or species level can be identified from the elements that are definitely ankylosaurian, and so *Antarctopelta* is a *nomen dubium*. Nevertheless, several interesting features suggest that MLP 86-X-28-1 has affinities with the nodosaurid ankylosaurs. MLP 86-X-28-1 includes portions of a Category 3 pelvic shield (Arbour et al. 2011), which are formed of coossified polygons of uniform size. The osteoderms are typically roughly hexagonal. *Aletopelta*, *Glyptodontopelta*, *Nodosaurus*, and *Stegopelta* have pelvic shields similar to those of MLP 86-X-28-1. *Aletopelta* and *Glyptodontopelta* were not included in the most recent analysis of ankylosaurian relationships by Thompson et al. (2012), but *Nodosaurus* and *Stegopelta* were recovered as nodosaurids, as was *Antarctopelta*.

Status: *Nomen dubium*.

9.2.3 Argentinian ankylosaur

Specimens: MPCA-Pv 77, tooth; MPCA-Pv 68/69/70, three posterior dorsal vertebrae; MPCA-Pv 71, caudal vertebrae; MPCA-Pv 72/73, two caudal centra; MPCA-SM 1, right femur; MPCA-Pv 78, partial cervical half ring; MPCA-Pv 41-43, 74-76, osteoderms

Locality and age: Salitral Moreno, 40 km south of General Roca, Río Negro Province, Argentina; Sandy Member, Allen Formation (Campanian-Maastrichtian)

Discussion: The specimens described by Coria and Salgado (2001) all belong to a fairly small-bodied ankylosaur (or ankylosaurs, if multiple individuals are represented). The material was collected from a small area of 50 m², but as it was associated with hadrosaur and titanosaur bones in a channel deposit, it cannot be demonstrated that all of these ankylosaur elements represent the same individual.

Several osteoderms were recovered. Two fragments of coossified osteoderms appear to be fragments of the cervical half rings, based on their arched morphology (Fig. 9.2C-E). One of these fragments is smaller than the other, but both fragments preserve at least two osteoderms. The osteoderms do not appear to be coossified to an underlying band as in ankylosaurids like *Ankylosaurus* (AMNH 5895), *Euoplocephalus* (CMN 0210, UALVP 31), *Saichania* (MPC 100/151) or *Shamosaurus* (PIN 3779/2). Instead, the cervical half rings are formed only of osteoderms coossified at their edges, similar to the nodosaurids *Edmontonia* (AMNH 5665) or *Panoplosaurus* (CMN 2759) (Carpenter 1990) although the sutures are largely obscured in the Argentinian specimens. The osteoderms of the cervical half rings differ significantly from those of other ankylosaurs, because the osteoderms are dorsoventrally tall, but mediolaterally narrow. In most ankylosaurs, the osteoderms of the cervical half rings are not taller than they are wide, even those with relatively tall keels such as *Euoplocephalus*. Additionally, the keels of the two osteoderms on the larger fragment are not aligned perpendicular to the half ring as a whole, but instead are diagonally oriented (but parallel to each other). Two more osteoderms may also belong to the larger cervical half ring, because they have a similar tall and narrow morphology and compare well with the preserved cervical half ring fragment. The morphology of the coossified osteoderms, representing cervical half ring fragments, are so unlike those recorded for other ankylosaurs, that they may indicate that the Argentinian ankylosaur represents a distinct genus or species.

The femur (MPCA-SM 1) is 25.24 cm long, compared to 53.5 cm (AMNH 5404) and 51.5 cm (UALVP 31) in *Euoplocephalus* (Arbour and Currie 2013a) and 67 cm in *Ankylosaurus* (Carpenter 2004). MPCA-SM 1 is similar in size to a juvenile *Anodontosaurus* (AMNH 5266), which is 25.5 cm long (Arbour and Currie 2013a). The femur has a distinct, hemispherical head, similar to the condition in *Dongyangopelta* (Chen et al. 2013), *Hoplitosaurus* (USNM 4752), and *Nodosaurus* (Lull 1921). Two scars are visible in anterior view, with one scar more medially located and one more laterally located; the scars are approximately parallel dorsally (Fig. 9.2A). The dorsal edge of the medial scar is located at the ventrolateral edge of the femoral head, and the ventral edge of the medial scar is merges with the ridge-like fourth trochanter on the medial side of the femoral shaft. The dorsal end of the lateral scar is located towards the medial edge of the greater trochanter, is roughly parallel to the medial scar for about half of the length of the femur, and then curves laterally towards the lateral condyle where it becomes indistinct. The lesser trochanter (fused medially to the greater trochanter) also bears a sharply defined rugose ridge on its lateral edge. Based on the locations of the scars, the medial scar most likely represents the linea intermuscularis cranialis, which in non-maniraptoran theropods originates proximally on the anterior side of the femur and inserts distally on the anteromedial surface of the femoral shaft (Hutchinson 2001). The lateral scar most likely represents the linea intermuscularis caudalis, which connects the base of the greater trochanter to the proximal posterior tip of the lateral condyle (Hutchinson 2001). Between these intermuscular lines would have originated the M. femorotibialis externus (Romer 1927, Hutchinson 2001). The intermuscular lines are more prominent in MPCA-SM 1 than in any other ankylosaur. Faint intermuscular lines in the same positions as in MPCA-SM 1 are present in *Hoplitosaurus* (USNM 4752; Fig. 9.2B) and *Nodosaurus* (Lull 1921: Pl. IV). The prominent intermuscular lines may also be diagnostic of a new genus or species represented by the Argentinian material.

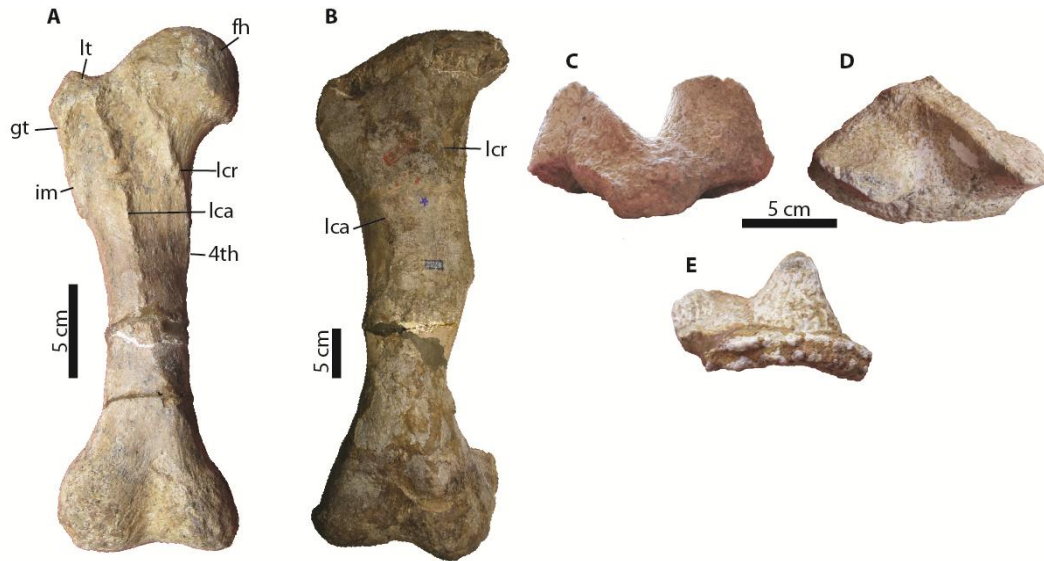


Figure 9.2. Femur and osteoderms of an Argentinian ankylosaur. A) MPCA-SM 1, right femur in anterior view, compared to B) right femur of USNM 4752, holotype of *Hoplitosaurus marshi*. Portion of the ?second cervical half ring, MPCA-Pv 78 in C) ?anterolateral view and D) dorsal/external view. E) Portion of the ?first cervical half ring, unnumbered but one of MPCA-Pv 41-43, or 74-76. Abbreviations: 4th, 4th trochanter; fh, femoral head; gt, greater trochanter; im, intermuscular line; lca, linea muscularis caudalis; lcr, linea muscularis cranialis; lt, lesser trochanter.

9.2.4 Other Gondwanan ankylosaurs

Australia: Teeth (NMV P186435, NMV P186463, NMV P198953, NMV P199128, NMV P199198, NMV P208229, NMV P209963, NMV P210093, NMV P212808, NMV P216508, NMV P221060, NMV P221105; rib: NMV P208085), osteoderms (NMV P199100, NMV P221200, NMV P221201, NMV P221213), dorsal vertebra (NMV P186391), and an isolated rib (NMV P199988), from the 'Wonthaggi formation' of the Strzelecki Group (latest Hauterivian–Albian), at the Bunurong Marine Park, Victoria, (Barrett et al. 2010); dorsal vertebra (NMV P216739) from the Eumeralla Formation, Otway Group (Albian-Aptian) at Lake Copco, Dinosaur Cove, Victoria (Barrett et al. 2010); teeth (QM F44324 - QM F44326,) from the Winton Formation (Albian-Cenomanian) at Belmont Station, central western Queensland (Leahey and Salisbury 2013).

New Zealand: Partial rib (CD 545), and two partial caudal vertebrae (CD 546) from the Maungataniwha Member, Tahora Formation (Late Cretaceous), at Mangahouanga Stream, North Island, New Zealand (Molnar and Wiffen 1994).

India: Several putative ankylosaur fossils from India have later been attributed to other dinosaurian taxa. A huge osteoderm (AMNH 1959) collected from Bara Simla (Jubalpur) was originally thought to derive from a stegosaur (Huene and Matley 1933) or an ankylosaur (?*Lametasaurus*, Coombs 1978a), but is instead a titanosaurid (possibly *Jainosaurus* or *Isisaurus*) osteoderm (Chatterjee and Rudra 1996). *Lametasaurus* is now considered a theropod (Carrano et al. 2010). Chatterjee and Rudra (1996) noted that ankylosaur remains (including vertebrae, a scapulocoracoid, humerus, femur, and osteoderms) had been collected from the Lameta Group near Raiholi village in Gujarat. However, these remains have not been described further.

Madagascar: Two teeth described from the Cenomanian-Turonian of Madagascar by Piveteau (1926) have been variously referred to *Stegosaurus madagascariensis*, nodosaurid ankylosaurs (Russell et al. 1976), and the crocodyliform *Simosuchus clarki* (Naish and Martill 2001). Maidment (2010) suggested that these teeth differed from those of *Simosuchus* and stegosaurs, and belonged to an indeterminate ankylosaur.

9.3 Discussion and conclusions

The holotype of "*Antarctopelta*" represents a mixture of material from an ankylosaur, plesiosaur (cervical vertebrae), and possibly a mosasaur (pygal vertebra). None of the ankylosaur material preserves diagnostic features, rendering "*Antarctopelta*" a *nomen dubium*. Nevertheless, "*Antarctopelta*" is a significant specimen because of its provenance and because the morphology of

the pelvic osteoderms is similar to those of 'stegopeltine' ankylosaurs from North America.

The 'paravertebrae' of *Minmi paravertebra* are not significantly different from the ossified tendon complex in the dorsal region of other ankylosaurs (and ornithischians more broadly), with the exception of ossified aponeuroses on some of the tendons. *Minmi paravertebra* is tentatively retained as a valid species based on the presence of ossified aponeuroses. However, the more complete specimen of *Minmi* (*Minmi* sp.) may or may not preserve ossified aponeuroses, although ossified tendons are present in the dorsal region.

The only ankylosaur material from South America has previously been considered an indeterminate ankylosaur, possibly referable to the Nodosauridae, but may warrant a new genus or species name. The morphology of the cervical half ring is unique, and the femur has intermuscular lines which are much more prominent compared to those in other ankylosaurs.

Part 4. Phylogenetic analysis

10. PHYLOGENETIC ANALYSIS OF THE ANKYLOSAURIDAE

10.1 Introduction

Using the revised taxonomic descriptions and assessments in this dissertation, a new phylogenetic analysis was performed in order to better understand the phylogenetic relationships within the Ankylosauridae, and the evolution of traits such as the tail club. The following questions will be addressed using the results of the revised phylogenetic tree:

1. Is there any evidence for nodosaurid ankylosaurs in Asia?

Several recently described Chinese and Japanese ankylosaurs have been referred to the Nodosauridae, but only two of these descriptions (Chen et al. 2013 for *Dongyangopelta*, and Yang et al. 2013 for *Taohelong*) include phylogenetic analyses to support these referrals. A revised phylogenetic analysis incorporating new characters may support the identification of some Asian taxa as nodosaurids, or may suggest that some Asian 'nodosaurids' are instead ankylosaurids.

2. Is the Shamosaurinae a valid clade?

Shamosaurus and *Gobisaurus* are sometimes recovered as sister-taxa in phylogenetic analyses (Vickaryous et al. 2004), whereas Thompson et al. (2012) found them to be successive outgroups to more derived ankylosaurids. Carpenter (2001) and Carpenter et al. (2008) have suggested that *Cedarpelta* may be a shamosaurine ankylosaur; Thompson et al. (2012) recovered *Cedarpelta* as a basal ankylosaurid.

3. Is the Stegopeltinae a valid clade?

Ford (2000) hypothesized that *Stegopelta*, *Glyptodontopelta*, and *Aletopelta* may form a clade within the Ankylosauridae based on the presence of

a pelvic shield composed of coossified hexagonal osteoderms. "*Antarctopelta*" also has a pelvic shield with this morphology. Only *Stegopelta* has been included in previous phylogenetic analyses.

4. At what point does the tail club first appear, and are there any trends in tail club evolution?

Thompson et al. (2012) considered the tail club only to be present in ankylosaurine ankylosaurids, not in shamosaurine or shamosaurine-grade ankylosaurids. This is potentially based on a misunderstanding of the term 'tail club', and ignores the important role of the handle vertebrae in identifying the tail club in ankylosaurids. Coombs (1995a) noted that the ankylosaurid tail club is composed of two morphological features: modified, interlocking distal caudal vertebrae (the handle), and enlarged terminal osteoderms (the knob). The term 'tail club' thus does not refer solely to the large terminal osteoderms, but to the entire distal structure of the ankylosaurid tail.

Both the knob and handle are functionally important for tail club impacts (Arbour and Snively 2009), and so this leads to the question: which came first, the knob or the handle (or both)? Did modifications to the handle vertebrae evolve in order to support the increasing weight of the knob osteoderms and to provide strength for knob impacts, after enlargements to the terminal osteoderms had already occurred? Or did the rigid handle evolve first, as a bat-like structure that would have functioned efficiently in tail strikes even without an enlarged knob? Or did both structures evolve at about the same time, as a single functional unit? Predictions for the anatomy represented by these three scenarios are as follows (Fig. 10.1):

1. Knob-first hypothesis: Basal ankylosaurids should have tapered tail vertebrae similar to nodosaurids, but the terminal osteoderms should fully envelop the terminal caudal vertebrae. Complete knobs

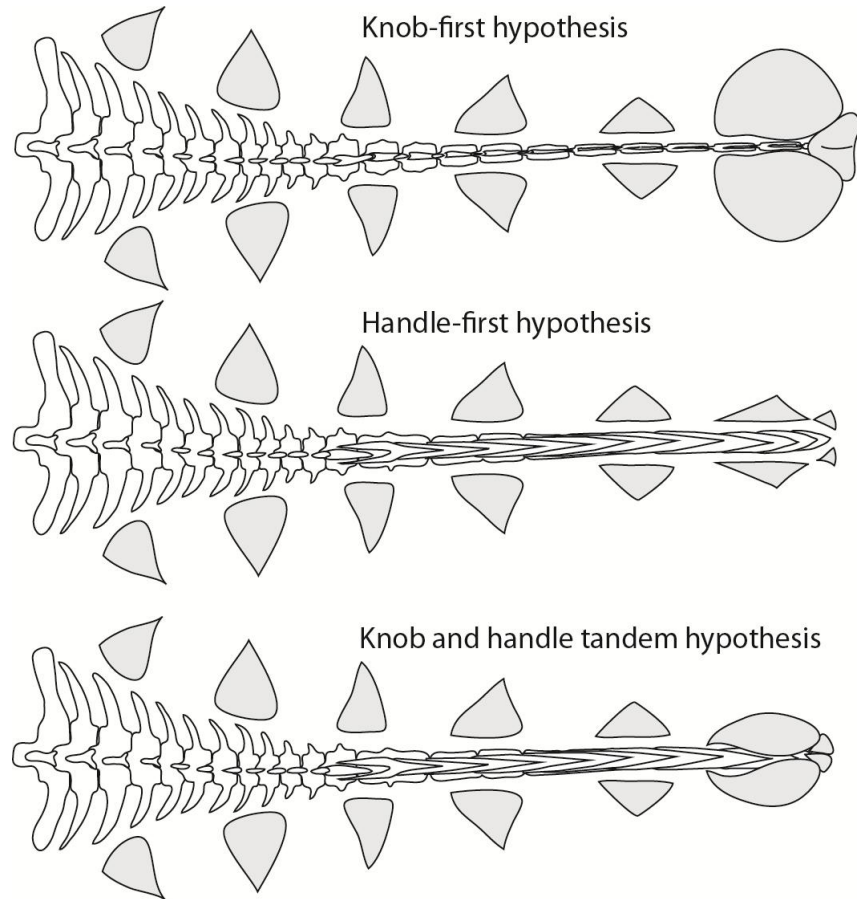


Figure 10.1. Three hypotheses for the evolution of the ankylosaurid tail club.

should be preserved at least as isolated structures, and may or may not be large. This morphology would have functioned more like a flail than a club or an axe, because the distal half of the tail would have remained flexible. Modifications to the distal caudal vertebrae would have evolved later, perhaps to support greater knob weights, or for increased strength during impacts.

2. Handle-first hypothesis: Basal ankylosaurids should have recognizable handle vertebrae, but the knob will not be preserved around terminal caudals. The distal portion of the tail may still preserve osteoderms, but these will not be as closely associated with the terminal caudal vertebrae as in more derived species. This morphology would have functioned similarly to derived ankylosaurid tail clubs in impacts, but the tail may

have been more like a bat than an axe. Knob osteoderms may have eventually enveloped the tail tip as a more rigid structure in order to stabilize their positions; as elements of the dermis, they may have been easily displaced in a strike.

3. Tandem knob and handle evolution hypothesis: Basal ankylosaurids should possess at least a rudimentary handle and knob. Recognizable handle vertebrae and knob osteoderms should appear at the same time in the fossil record. The knob may be small, but will envelop terminal caudal vertebrae; handle vertebrae may not be as robust as later species but will still have the characteristic rigidly interlocking appearance. Increasing use of the tail for impacts may have resulted in concurrent evolution of the knob and handle, and their functions may be closely interrelated, with the evolution of one impossible without the presence of the other.

5. Are there any biogeographic patterns within the Ankylosauridae?

Do ankylosaurids originate in Mongolia or North America? Is *Nodocephalosaurus*, from the Late Cretaceous of North America, more closely related to Mongolian ankylosaurids than other North American ankylosaurids? Are any ankylosaurids present in Gondwana?

10.1.1 Previous phylogenetic analyses

Although pre-cladistic in nature, Coombs' (1978a) revision of the Ankylosauria is a benchmark study in the systematics of ankylosaurs, and his bipartite division of the ankylosaurs into the Ankylosauridae and Nodosauridae has been largely upheld by subsequent phylogenetic analyses (Fig. 10.2). Many of the anatomical features described by Coombs (1978a) were modified into characters in the earliest phylogenetic analyses of the group, and have been

retained since. Maryńska (1977) also provided important perspectives on the evolution and possible biogeographic relationships of the Asian ankylosaurids.

Sereno (1984, 1986) was the first to examine the relationships of the Ornithischia using cladistic philosophies (but not numerical analyses). Lists of synapomorphies were provided for distinct ankylosaurid and nodosaurid clades. Sereno (1998) formally defined the Ankylosauridae as all ankylosaurs more closely related to *Ankylosaurus* than to *Panoplosaurus*, and also defined the Ankylosaurinae as all ankylosaurids more closely related to *Ankylosaurus* than to *Shamosaurus* or *Minmi*.

Discoveries of relatively complete Jurassic and Early Cretaceous ankylosaurs from western North America (Lee 1996, Carpenter et al. 1998, Kirkland 1998) resulted in the first numerical phylogenetic analyses of the interrelationships of ankylosaurs. Lee (1996) included Ankylosauridae as an operational taxonomic unit (OTU) for investigating the relationships of *Pawpawsaurus* within the Nodosauridae. The relationships of *Gargoyleosaurus* were assessed by Carpenter et al. (1998), but both Nodosauridae and Ankylosauridae were treated as OTUs; Wilkinson et al. (1998) had numerous criticisms of this analysis, including issues with both taxon and character sampling. Kirkland (1998) found support for a third clade of ankylosaurs, resurrecting the Polacanthinae as the sister group to the Ankylosaurinae (Fig. 10.2). This analysis incorporated substantially more characters related to the osteoderms compared to previous analyses. The phylogenetic analysis by Kirkland (1998) remains the only analysis of the ankylosaurs to recover a monophyletic Polacanthinae (or Polacanthidae).

Hill et al. (2003) and Vickaryous et al. (2004) presented results from larger analyses with more characters and greater taxonomic sampling. Vickaryous et al. (2004) conducted an analysis on 21 of the 'best known' ankylosaurs, with *Lesothosaurus* and *Huayangosaurus* as the outgroups (Fig. 10.2). *Gargoyleosaurus*, *Gastonia*, and *Minmi* were recovered as basal ankylosaurids,

along with *Gobisaurus*, *Shamosaurus*, and ankylosaurines from Mongolia, China, and North America. *Cedarpelta* was recovered as a basal nodosaurid. Only taxa with cranial material were included in the analysis, so the relationships of *Crichtonpelta* (as *Crichtonsaurus*), *Liaoningosaurus* (for which the skull is small, crushed, and difficult to interpret or code), and *Stegopelta* could not be assessed. The Ankylosaurinae included *Tsagantegia* as the most basal member of the clade, followed by *Tarchia*. A derived clade of ankylosaurines included two sister groups, one composed of Asian ankylosaurids (*Pinacosaurus*, *Saichania*, *Talarurus*, and *Tianzhenosaurus*) and one composed of *Ankylosaurus*+*Euoplocephalus*. Subsequent descriptions of new ankylosaurs (e.g., Lü et al 2007; Parsons and Parsons 2009) have generally used this data matrix, with modifications for new taxa and the inclusion of perhaps a few new characters.

The most recent comprehensive analysis of the Ankylosauria was undertaken by Thompson et al. (2012), drawn largely from the unpublished PhD dissertation of Parish (2005). This analysis included almost all known valid ankylosaurs and multiple outgroup taxa (for a total of 51 taxa), a thorough description of the methods used, characters representing cranial, postcranial, and osteodermal anatomy, and a detailed list of synapomorphies (both ambiguous and unambiguous) for each recovered clade. There is much to commend in this analysis, but numerous problematic character codings were noted in Chapter 3 (and Arbour and Currie 2013a), and a more detailed assessment of the validity of each taxon would have been desirable. Thompson et al. (2012) recovered two major clades within the Ankylosauria, representing the Nodosauridae and Ankylosauridae (Fig. 10.2). Putative polacanthid/polacanthine ankylosaurs were all recovered as basal nodosaurids, but these did not form a clade within the Nodosauridae. *Gargoyleosaurus* and *Gastonia* were recovered as basal nodosaurids, and *Cedarpelta* and *Liaoningosaurus* were recovered as basal ankylosaurids.

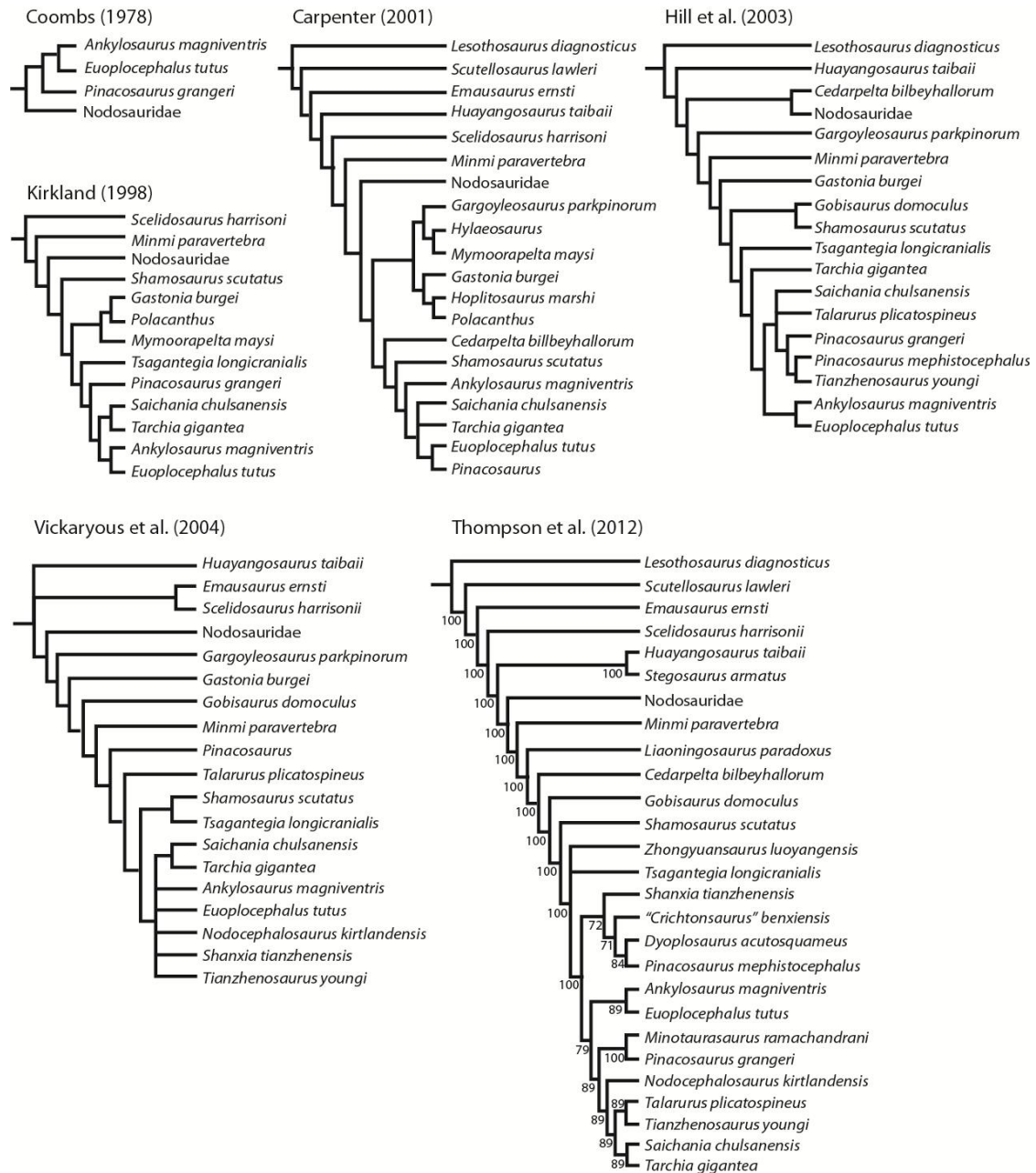


Figure 10.2. Previous phylogenetic analyses of the Ankylosauria and Ankylosauridae. The tree shown for Thompson et al. (2012) is the 50% majority rule tree before taxa were removed.

10.1.2 Carpenter (2001) and compartmentalization

Carpenter (2001) conducted a large phylogenetic analysis of the Ankylosauria, but used an unorthodox 'compartmentalization' approach that has important ramifications for the conclusions presented in his study. All ankylosaurs were assigned to one of three 'nodes' prior to the actual analysis.

Ankylosaurs were assigned to the Ankylosauridae, for example, if they were known to have possessed a tail club. However, some ankylosaurs were also assigned to this node even though the presence or absence of a tail club was unknown (*Cedarapelta*, *Shamosaurus*), with no rationale provided – *Cedarapelta* and *Shamosaurus* were simply identified as 'primitive ankylosaurids'. Four sets of character matrices were analyzed separately: a matrix for the Ankylosauromorpha (Ankylosauria+Scelidosaurus), with Ankylosauridae, Nodosauridae, and Polacanthidae coded as operational taxonomic units, and then individual matrices for each of Ankylosauridae, Nodosauridae, and Polacanthidae. Individual nodes were then analyzed separately, and the resulting trees pasted onto the "Ankylosauromorpha" analysis to create a summary analysis.

Carpenter (2001) argued that the 'nodes' should be relatively stable because taxa are assigned based on synapomorphies that will not change: "the tail club with [sic] always be a synapomorphy for the Ankylosauridae" (Carpenter 2001:461). This kind of assumption is unacceptable when investigating the ingroup relationships of the taxa under study, because it does not allow for the possibility (however unlikely) that the tail club is plesiomorphic for Ankylosauria and secondarily lost in nodosaurids. The compartmentalization approach assumes that the synapomorphies of a clade under study are well-established *before* the analysis occurs.

Compartmentalization is, in a sense, used in all phylogenetic studies, unless one is attempting to reconstruct a phylogenetic tree for all life on Earth. Any given phylogenetic study is attempting to reconstruct only part of the entire tree of life. As such, compartmentalization can be thought of as broadly equivalent to the process of taxon selection (that is, which taxa to include in the ingroup in an analysis). Including supraspecific operational taxonomic units is also common practice in large analyses, especially where the clade is well-supported by previous, more detailed studies; for example, Butler et al. (2008)

conducted a large phylogeny of the Ornithischia and included Ankylosauria as an OTU. Indeed, even species are a form of compartmentalization, as they represent a set of individuals that are *a priori* assumed to represent a single operational taxonomic unit. Compartmentalization only becomes a problem when it interferes with the hypotheses being tested. Carpenter (2001) concluded that the results of his study support the presence of three ankylosaur clades, the Ankylosauridae, Nodosauridae, and Polacanthidae; however, the phylogenetic analysis could not test for the monophyly of the Polacanthidae because taxa were assigned to that node *a priori*.

There are other issues with the analysis of Carpenter (2001). Several of the characters in the Ankylosauromorpha analysis include character states for absent, present, and secondarily absent. It is unwise to *a priori* code a character as secondarily absent, because ideally a phylogenetic analysis will help elucidate whether or not a given character state is plesiomorphic, synapomorphic, or reversed. Additionally, the character matrix shows *Nodosaurus* represented by 100% missing data.

10.2 Methods

10.2.1 Taxon Selection

All species described and revised in this dissertation were included in the revised phylogenetic analysis. In total, forty-three taxa are included in the original character matrix (Table 10.1), although some are eventually removed through safe and 'unsafe' taxonomic reduction. *Lesothosaurus*, *Scelidosaurus*, and *Stegosaurus* serve as outgroups for the Ankylosauria. The character matrix includes 14 taxa that have previously been considered ankylosaurids by most workers: *Ankylosaurus*, *Anodontosaurus*, *Crichtonpelta*, *Dyoplosaurus*, *Euoplocephalus*, *Gobisaurus*, *Nodocephalosaurus*, *Pinacosaurus*, *Saichania*,

Table 10.1. Status of taxa discussed in this thesis and/or included in the phylogenetic analysis.

Outgroup Taxa	
<i>Gargoyleosaurus parkpinorum</i>	Valid
<i>Gastonia burgei</i>	Valid
<i>Lesothosaurus diagnosticus</i>	Valid
<i>Mymoorapelta maysi</i>	Valid
<i>Panoplosaurus mirus</i>	Valid; conceptually restricted to the holotype specimen only
<i>Sauropelta edwardsi</i>	Valid
<i>Scelidosaurus harrisoni</i>	Valid
<i>Stegosaurus spp.</i>	Valid
Ingroup Taxa	
<i>Ahshislepelta minor</i>	Valid
<i>Aletopelta coombsi</i>	Valid
<i>Amtosaurus magnus</i>	<i>Nomen dubium</i> ; indeterminate ornithischian
<i>Ankylosaurus magniventris</i>	Valid
<i>Anodontosaurus lambei</i>	Valid, previously synonymous with <i>Euoplocephalus tutus</i>
<i>Antarctopelta oliveroi</i>	<i>Nomen dubium</i>
<i>Argentine ankylosaur</i>	New taxon
<i>Bienosaurus lufengensis</i>	<i>Nomen dubium</i>
<i>Bissektipelta archibaldi</i>	Valid
<i>Cedarpelta bilbeyhallorum</i>	Valid
<i>Crichtonsaurus benxiensis</i>	New combination <i>Crichtonpelta benxiensis</i>
<i>Crichtonsaurus bohlini</i>	<i>Nomen dubium</i>
<i>Dongyangopelta yangyanensis</i>	Valid
<i>Dyoplosaurus acutosquameus</i>	Valid, previously synonymous with <i>Euoplocephalus tutus</i>
<i>Dyoplosaurus giganteus</i>	<i>Nomen dubium</i>
<i>Euoplocephalus tutus</i>	Valid
<i>Glyptodontopelta mimus</i>	Valid
<i>Gobisaurus domoculus</i>	Valid
<i>Heishansaurus pachycephalus</i>	<i>Nomen dubium</i>
<i>Liaoningosaurus paradoxus</i>	Valid
<i>Maleevus disparoserratus</i>	<i>Nomen dubium</i>
<i>Minmi paravertebra</i>	Tentatively valid
<i>Minotaurasaurus ramachandrani</i>	Junior synonym of <i>Tarchia kielanae</i>
<i>Nodocephalosaurus kirtlandensis</i>	Valid
<i>Oohkohtokia horneri</i>	Junior synonym of <i>Scolosaurus cutleri</i>
<i>Pinacosaurus grangeri</i>	Valid
<i>Pinacosaurus mephistocephalus</i>	Valid
<i>Pinacosaurus ninghsiensis</i>	Junior synonym of <i>Pinacosaurus grangeri</i>
<i>Saichania chulsanensis</i>	Valid
<i>Sauroplices scutigera</i>	Valid
<i>Scolosaurus cutleri</i>	Valid, previously synonymous with <i>Euoplocephalus tutus</i>
<i>Shamosaurus scutatus</i>	Valid
<i>Shanxia tianzhenensis</i>	Junior synonym of <i>Saichania chulsanensis</i>
<i>Stegopelta landerensis</i>	Valid
<i>Talarurus plicatospineus</i>	Valid
<i>Taohelong jinchengensis</i>	Valid

Ingroup Taxa, continued	
<i>Tarchia gigantea</i>	Redundant combination; note that PIN 3142/250 is here referred to <i>Saichania chulsanensis</i>
<i>Tarchia kielanae</i>	Valid
<i>Tatankacephalus cooneyorum</i>	Valid
<i>Tianchisaurus nedegoapeferima</i>	<i>Nomen dubium</i>
<i>Tianzhenosaurus youngi</i>	Junior synonym of <i>Saichania chulsanensis</i>
<i>Tsagantegia longicranialis</i>	Valid
<i>Zaraapelta nomadis</i>	New taxon (Nomen nudum)
<i>Zhejiangosaurus lishuiensis</i>	<i>Nomen dubium</i>
<i>Zhongyuansaurus luoyangensis</i>	Junior synonym of <i>Gobisaurus domoculus</i>
<i>Ziapelta sanjuanensis</i>	New taxon (Nomen nudum)

Scolosaurus, *Shamosaurus*, *Talarurus*, *Tarchia*, and *Tsagantegia*. Two new, currently unpublished taxa (*Zaraapelta* and *Ziapelta*) are also included. Other previously named taxa that have not been included in previous phylogenetic analyses include *Ahshislepelta*, *Aletopelta*, *Bissektipelta*, *Glyptodontopelta*, and *Sauroplices*.

Several of the taxa included in this analysis have had uncertain taxonomic affiliations or have been referred to both the Ankylosauridae and the Nodosauridae (*Aletopelta*, "*Antarctopelta*", *Cedarpelta*, *Dongyangopelta*, *Liaoningosaurus*, *Minmi*, *Sauroplices*, *Taohelong Tatankacephalus*, *Tianchisaurus*, and "*Zhejiangosaurus*"). In order to assess whether or not these taxa represented ankylosaurids, nodosaurids, or more basal ankylosaurs, several nodosaurids and basal ankylosaurs were also included in the analysis. These included *Gargoyleosaurus*, *Gastonia*, *Mymoorapelta*, *Panoplosaurus*, *Pawpawsaurus*, and *Sauropelta*. Given current uncertainty regarding the assignment of various specimens to *Panoplosaurus mirus*, *Edmontonia longiceps*, and *Edmontonia rugosidens* (Burns and Currie 2012), character codings for *Panoplosaurus* were restricted to those features present in the holotype specimen CMN 2759, and do not include information from the commonly-referred specimen ROM 1215. As discussed in Chapter 9, it is not clear if QM F1801 (*Minmi* sp.) is referable to *Minmi paravertebra*, and so these are treated as separate taxa in this analysis. The phylogenetic relationships of the Gondwanan ankylosaurs were tested by also including the unnamed Argentinian

ankylosaur material, with the assumption that this represents a single individual. In order to test the validity of the Stegopeltinae, *Stegopelta* and *Glyptodontopelta* were also included in the analysis.

10.2.2 Character revision and new characters

The character matrix presented here is modified from the most recent comprehensive analysis of the Ankylosauria by Thompson et al. (2012). In the revision of specimens referred to *Euoplocephalus* (Chapter 3; Arbour and Currie 2013a), numerous characters were identified as having been coded incorrectly, and changes to characters were noted in that chapter. Character state differences between Thompson et al. (2012) and this dissertation are summarized in this chapter. Thirty-eight new characters representing aspects of the skull, postcrania, and osteoderms have been identified and incorporated into the revised character matrix.

Pairs of characters in Thompson et al. (2012), such as 'Mandibular osteoderm absent/present' followed by 'length of mandibular osteoderm' were consolidated into single, multistate characters such as 'mandibular osteoderm: absent, short, long', based on recommendations by Maddison (1998). Forming the characters in this way avoids unnecessary missing data that can create unrealistic tree topologies. Maddison (1998) described a hypothetical situation in which the morphology of tailed and tailless lizards was treated as two separate characters: tails present or absent, and tails red or blue. In this scenario, tailless lizards would be coded as missing data for the colour character. However, tail colour evolution does not occur separately from the evolution of tails, and so it is more desirable to have a character that recognizes the presence or absence of tails in addition to their colour. In particular, missing data of this sort can cause problems if two clades are separated by taxa for which the character is inapplicable.

One problem with this philosophy of character construction is that it duplicates the counting of gains or losses of a character if there are multiple morphologies of a given character represented. Whereas Maddison (1998) recommended constructing multistate characters that included the absence of the feature as a character state, Brazeau (2011) argued against this approach. Instead, Brazeau (2011) suggests that the 'absence' state should only occur once in a matrix for any given feature, and that characters should be scored as missing data where there is no logical interpretation of the character for that taxon. This issue of inapplicable characters could influence the phylogenetic analysis of ankylosaurs presented here, because there are numerous osteoderm characters but *Lesothosaurus*, the most basal outgroup taxon, lacks osteoderms completely, and *Stegosaurus* lacks all osteoderms except for the paired midline plates and tail spikes.

There appears to have been a general reluctance to use features of the cranial ornamentation and osteoderms to create new characters for ankylosaur phylogenetic analyses (Vickaryous et al. 2004, Thompson et al. 2012). This may stem from concerns about high variability of cranial ornamentation in *Euoplocephalus*, which was partly the result of the mixing of multiple species in the genus. However, aspects of the cranial ornamentation provided a wealth of new characters for the revised phylogenetic analysis (Fig. 10.3). Chapter 3 details the aspects of cranial ornamentation that are more or less variable in *Anodontosaurus*, *Euoplocephalus*, and *Scolosaurus*. In these taxa, the overall shape of the squamosal horn (pyramidal or backswept) remains the same, but the sharpness and length varies. The frontonasal caputegulae pattern is relatively constant, but the exact size and shape of individual caputegulae can vary. The number of discrete frontonasal and frontoparietal caputegulae is also more consistent between specimens than might be expected, with all specimens (excluding those with severe damage) having around 30 caputegulae. The sharpness of the supraorbital caputegulae varies. All specimens have a single pair

of loreal caputegulae, a single pair of lacrimal caputegulae, and a single hexagonal median nasal caputegulum (which can vary somewhat in size). All specimens have more than two nuchal caputegulae, with most having four. The presence or absence of postocular caputegulae is taxonomically significant between these taxa, with postocular caputegulae absent in *Euoplocephalus*, and present in *Anodontosaurus* and *Scolosaurus* (although *Scolosaurus* has fewer postocular caputegulae compared to *Anodontosaurus*). Using the information gained from the relatively large sample size of *Anodontosaurus*, *Euoplocephalus*, and *Scolosaurus*, many new characters related to the cranial ornamentation of North American and Asian ankylosaurs have been created and incorporated into this revised analysis.

Other cranial characters have been identified from studies of the anatomy of various ankylosaurid taxa (Fig. 10.3). The presence or absence of paranasal apertures or fossae, the presence or absence of a premaxillary sinus, and the presence or absence of a lacrimal incisure arise from a review of the cranial anatomy of *Pinacosaurus* in Chapter 8. Examination of skulls from Mongolia and China also shows that the depth of the jugal relative to the orbit may also be phylogenetically useful. The presence or absence of deep longitudinal grooves on the premaxilla stems from the review of 'shamosaurine' ankylosaurids. Results from a study on the internal cranial anatomy of *Euoplocephalus* (Miyashita et al. 2011) were used to identify two more cranial characters: the presence or absence of vascular impressions in the nasal passages, and the presence or absence of a scroll-shaped descending process of the frontal.

In the postcranial skeleton, osteoderms provide a wealth of potentially useful characters. Although osteoderms are some of the most commonly recovered ankylosaur fossils, the wide variety of shapes in a single individual means that it can be difficult to assess the taxonomic significance of variation in morphology and texture. Only a few ankylosaur specimens preserve nearly

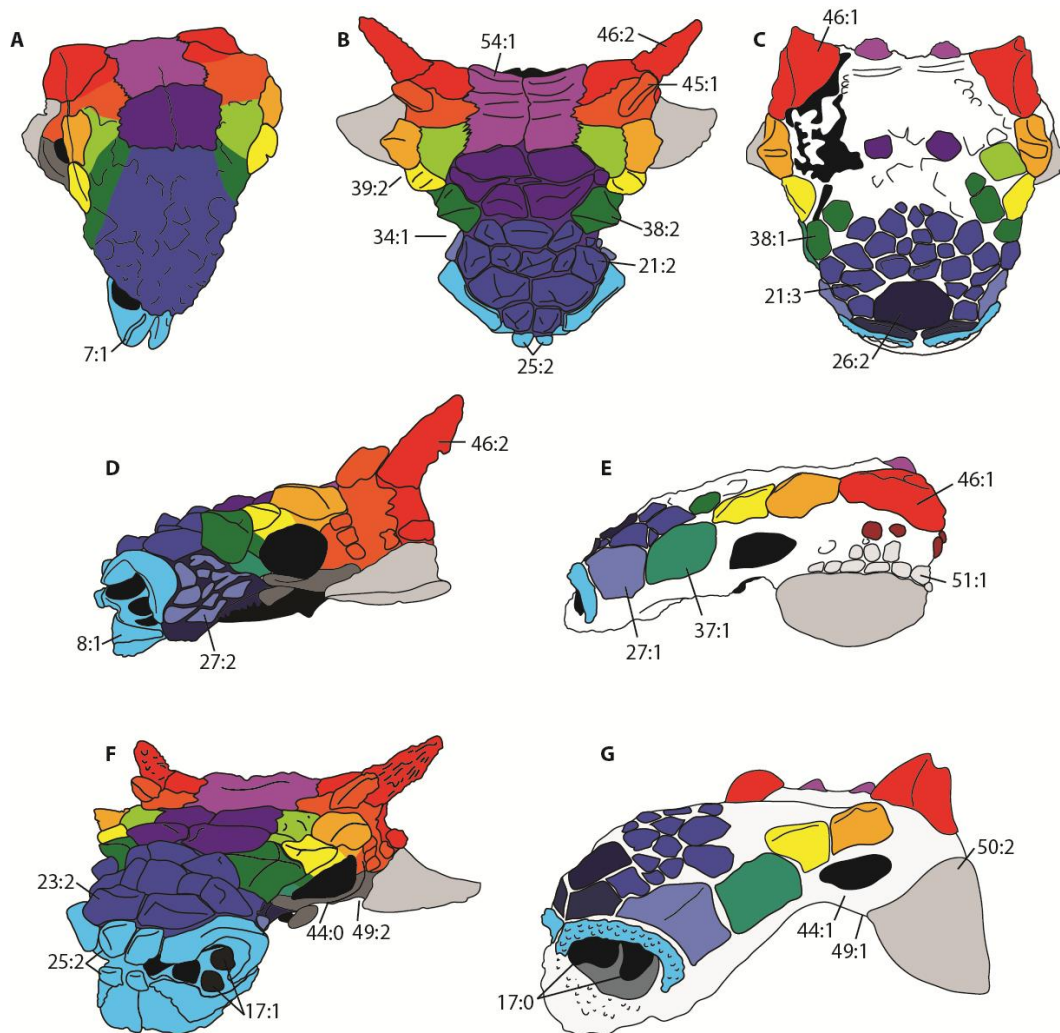


Figure 10.3. Summary of new cranial characters presented in this dissertation. Labeled features show the character number followed by the character state. *Gobisaurus domoculus* specimen 41HIII-0002 in A) dorsal view (drawn from Xu et al. 2007). *Tarchia kielanae* specimen INBR 21004 in B) dorsal, D) left lateral, and F) oblique anterolateral views. *Euoplocephalus tutus* specimen UALVP 31 in C) dorsal and G) oblique anterolateral views. *Anodontosaurus lambei* holotype CMN 8530 in E) left lateral view.

complete suites of *in situ* osteoderms, and sometimes these specimens (like MPC 100/1305, see Chapter 5) lack diagnostic features that allow their referral to known taxa. Nevertheless, recent work on the systematic value of ankylosaur osteoderms (Burns 2008; Burns and Currie, in press) has resulted in several new characters based on osteoderm gross morphology, surface texture, internal

histology, and arrangement on the body. These previously identified characters are supplemented by several new osteoderm characters identified in this dissertation. This analysis includes the largest suite of characters related to osteoderms of any analysis to date, including the revised characters proposed by Burns and Currie (in press), with 28 characters based on osteoderms. The review of specimens previously referred to *Euoplocephalus* (Chapter 3, Arbour and Currie 2013a) provided several new characters related to the cervical osteoderms and tail club knob. A review of pelvic shield morphology in ankylosaurs (Arbour et al. 2011) resulted in a new character about the arrangement of osteoderms in the pelvic region, and a review of skin impressions in ankylosaurs (Arbour et al. In press) resulted in a new character about the presence or absence of millimeter-sized ossicles. Revision of the ankylosaurs from China (Chapter 8) resulted in a new character noting the presence or absence of prominent furrows on deeply excavated triangular osteoderms, and revision of the ankylosaurs from Gondwana (Chapter 9) resulted in a new character noting the fusion of osteoderms on the dorsal ribs.

Few new characters from the postcranial endoskeleton could be identified, partly because postcrania associated with diagnostic cranial material are relatively uncommon, and partly because the existing characters covered most of the taxonomically variable features.

10.2.2.1 Characters removed from the character list in Thompson et al. (2012):

Forty-one characters from Thompson et al. (2012) have been removed from this character matrix because the characters were difficult to code consistently, because new anatomical interpretations make them redundant, or because they represented compound characters (Table 10.2 summarizes changes to the numbers of characters added, modified, or removed for different regions of the body). Several characters have been revised to reflect new anatomical interpretations. For example, the 'paranasal' sinuses of at least *Euoplocephalus*

Table 10.2: Summary of character revisions and additions.

	Total Characters	New characters	Extensively modified characters	Deleted characters
Cranium	78	26	2	20
Mandibles	9	0	0	3
Teeth	5	0	1	0
Axial Skeleton	21	2	0	5
Pectoral Girdle	12	0	0	0
Pelvic Girdle	11	1	1	3
Appendicular Skeleton	18	0	1	0
Osteoderms and Integument	28	9	1	10
Total	182	38	6	41

and ROM 1215 (*Edmontonia* or *Panoplosaurus*) are now known to represent portions of the looping nasal airway (Witmer and Ridgely 2008). Other characters have been modified to reflect new terminology, such as the terminology surrounding cranial ornamentation (caputegulae vs. osteoderms, see Arbour and Currie 2013a, Chapter 3). Modifications to existing characters are noted in the list of character statements. Efforts have also been made to split compound characters (*sensu* Brazeau 2011) into non-compound characters. For example, character 65 had tooth crown shape and denticles linked (≥ 13 denticles and tooth crown pointed, and < 13 denticles, tooth crown rounded) but was revised as one character describing the number of denticles, and one character describing the shape of the tooth crown.

The characters that have been removed from Thompson et al. (2012), along with the rationale, are as follows:

Characters 9-12. 9, near vertical narial septum separating the respiratory passage and lateral sinus absent/present. 10, near horizontal narial septum separating the respiratory passage and lateral sinus absent/present. 11, shape of

respiratory passage straight/sinuuous. 12, lateral sinuses absent/present. Witmer and Ridgely (2008) have shown that the respiratory passage and lateral sinus in *Euoplocephalus* both represent a complex looping airway. These characters have been replaced by the new character 18.

Character 17, cranial sutures in adult specimens. It is not always possible to determine which specimens represent adult individuals, and so it is not possible to assess whether or not fusion of cranial elements represents ontogenetic vs. taxonomic differences.

Character 23, shape of the ventral margin of premaxillary tomium in lateral view, flat/convex/concave. This feature is broken in many specimens and difficult to assess.

Characters 27 and 28. 27, palpebral shape rod/plate. 28, form of palpebral articulation mobile/sutural. These characters concern the palpebral, which is not present in ankylosaurs (see Maidment and Porro 2010).

Character 29, anterior and posterior supraorbitals (recognizable by distinct regions of ornamentation above the orbit), absent/present. The supraorbitals are described by other characters, making an absent/present character redundant.

Characters 52 and 53. 52, depth of the distal end of paroccipital processes, expanded/not expanded. 53, thickness of bone at the dorsal margin of the foramen magnum relative to surrounding bone, little difference/distinctly thickened. The relative depth of the distal ends of the paroccipital processes, and the relative thickness of bone at the dorsal margin of the foramen magnum, are difficult to quantify and code consistently.

Character 55, form of the ventral surface of basioccipital-basisphenoid region of the braincase, transversely convex/medial depression/medial longitudinal ridge. This character needs to be reassessed, as it is not immediately clear how states 0 (transversely convex) and 1 (medial depression) differ.

Characters 61 and 62. 61, direction of occipital condyle, posterior/posteroventral. 62, direction of the foramen magnum, posterior, posteroventral). It is unclear which orientation the skull needs to be in initially in order to interpret this character, and tilting the skull in the horizontal plane changes the orientation of the occipital condyle and foramen magnum.

Characters 71 and 72. 71, shape of ventral margin of the dentary in lateral view, straight/sinuuous. 72, shape of the alveolar margin, weakly convex/strongly convex. The ventral margin of the dentary is straight in all ankylosaurids where it is preserved. Character 72 could not be assessed because it was not clear in which view the character referred.

Character 79, distribution of polygons on skull roof, random/symmetrical. No ankylosaurids have completely random distributions of cranial caputegulae, but there is always some amount of asymmetry. This character did not provide a cut-off for what constitutes random vs. symmetrical.

Character 84, postorbital/squamosal 'horn', absent/present. The squamosal horns are described by other characters, making an absent/present character redundant.

Character 85, shape of postorbital/squamosal 'horn', rounded/pyramidal. This character described the shape of the squamosal horn, which is replaced by a new set of characters.

Character 86, quadratojugal 'horn', absent/present. The quadratojugal horns are described by other characters, making an absent/present character redundant.

Character 88, nuchal ornamentation (at posterior margin of skull roof), absent/present. The nuchal ornamentation is described by other characters, making an absent/present character redundant.

Character 77, ornamentation, defined as sculpturing of skull bones or addition of osteoderms, absent/present. This has been replaced by an expanded set of ornamentation characters.

Character 91, mandibular caputegulum, absent/present. The mandibular caputegulum is described by other characters, making an absent/present character redundant.

Character 97, alignment of anterior and posterior faces of cervical centra, aligned/ anterior face dorsal to posterior face/ anterior face ventral to posterior face. The alignment of the anterior and posterior faces of the cervicals varies along the vertebral column.

Character 104, paravertebrae, absent/ present. As discussed in Chapter 9, paravertebrae are equivalent to ossified tendons in the dorsal region, which are present in all ornithischians.

Character 106, number of sacral vertebrae, 5/4/3. This character described the number of sacral vertebrae. Because ankylosaurs incorporate numerous dorsal and caudal vertebrae into the sacral rod, it is unclear if this character referred

only to 'true' sacral vertebrae, or all dorsosacrals, sacrals, and caudosacrals. It is also not clear how this number is affected by ontogeny or size.

Character 109, length of transverse processes relative to neural spine height in proximal caudals, sub-equal/approximately twice the length. The length of the transverse processes varies along the vertebral column, and although this character referred to the proximal caudals, it was not clear just how proximal they had to be in order to be included.

Character 112, shape of distal caudal postzygapophyses, wedge-shaped/ tongue shaped. This character was difficult to interpret, although it was obviously meant to represent the presence of handle vertebrae in the tail club. It has been replaced by two new characters.

Characters 144-146. 144, prepubic process, present/absent. 145, structure and rotation of the body of the pubis, gracile without dorsolateral rotation/massive and dorsolaterally rotated. 146, size of pubic contribution to acetabulum, > 25%/ <25%. These characters describe features of the pubis, which is markedly reduced or potentially absent in most ankylosaurids, and preserved in very few specimens. Character 145 is also a compound character.

Characters 160-161. 160, large, laterally compressed plates on the dorsal aspect of the trunk, absent/present. 161, lateral rows of osteoderms on the dorsal aspect of the trunk, absent/present. Both characters describe osteoderm morphology, and have been replaced by an expanded set of osteoderm characters. Additionally, character 161 (lateral rows of osteoderms on dorsal aspect of trunk) was redundant with character 159 (parasagittal rows of keeled osteoderms on dorsal aspect of trunk).

Character 163, form of the cervical bands, quarter rings/half rings. The presence of 'quarter rings' in ankylosaurids is based on a misinterpretation of the cervical half rings in *Ankylosaurus*. No ankylosaurids have quarter rings – the rings always form a semi-circle over the cervical vertebrae. The cervical osteoderms of *Scelidosaurus* may or may not form a complete band above the neck, but this morphology is better represented by revised cervical armour characters.

Characters 164-165. 164, pectoral spikes absent/present. 165, form of pectoral spikes, no grooves and a solid base/posterior groove with a hollow base. These characters are replaced by an expanded set of osteoderm characters. Additionally, character 165 was a compound character.

Character 166, pelvic shield of fused osteoderms, absent/present. The pelvic shield is described by other characters, making an absent/present character redundant.

Character 167, form of ossicles in sacral armour, irregular ossicles/sub-hexagonal ossicles of similar sizes. "Ossicles" are not well defined, and this character is replaced by an expanded set of osteoderm characters.

Character 168, size of lateral trunk plates, sacral plates and caudal plates, small/large and hollow based. 'Large' and 'small' were undefined, and 'large' was also associated with 'hollow', making it a compound character.

Character 169, form of caudal plates, little dorsal projection/ tall with thin dorsal extremity. It is unclear which ankylosaurs would have the first character state, and the second most likely refers to 'splates' (*sensu* Blows 2001). The wording is unclear, and the second character state is a compound character.

Character 170, tail club, absent/present; Revised in Arbour and Currie 2013a as Terminus of tail enveloped by >2 osteoderms, forming tail club knob, absent/present. The tail club knob is described by other characters, making an absent/present character redundant.

10.2.3 Characters

Changes to the character state codings from Thompson et al. (2012) are provided in the character statements. Codings for *Tarchia* include changes to codings for *Minotaurasaurus* as outlined in Chapter 3 (Arbour and Currie 2013a). Postcranial character codings from *Tarchia gigantea* were not transferred to *Tarchia kielanae* or *Saichania chulsanensis*, because no postcranial specimens can be definitely attributed to these species at this time. For *Antarctopelta*, character codings were removed for material that was not definitively ankylosaurian.

Cranium

1. Antorbital fenestra: present (0), absent (1). (Serenó 1999: 8, Thompson et al. 2012: 1).
2. Modified: Lateral temporal fenestra, visible in lateral view: visible (0), not visible (1). (Carpenter et al. 1998 : 6 Thompson et al. 2012: 2).
3. Supratemporal fenestra: open (0), closed (1). (Lee 1996: 2, Thompson et al. 2012:).

Updated codings: Chapter 3 (Arbour and Currie 2013a) - *Dyoplosaurus* from ? to 1, as this region of the skull is preserved in ROM 784.

4. Skull dimensions, including ornamentation: longer than wide (0), as wide, or wider than long (1). (Carpenter et al. 1998: 1, Thompson et al. 2012: 4).
5. Modified: Width of the posterior margin of the skull (including squamosal horns where applicable) relative to the maximum width across the orbits:

- greater or equal (0), less (1). (Vickaryous et al. 2004: 6, Thompson et al. 2012: 5).
6. Modified: Antorbital region of the dorsal skull surface: flat (0), arched (1). (Sereno 1999: 99, Thompson et al. 2012: 14).
- Updated codings: *Cedarpetta* 1 to ?; the skull is taphonomically distorted.
Minmi sp. from 1 to 0.
- Chapter 3 (Arbour and Currie 2013a) - *Nodocephalosaurus* from 0 to ?.
- The holotype and only skull of *Nodocephalosaurus* is severely crushed and distorted, and so a dorsoventral dimension-based character coding for this taxon is dubious.
7. New character: Deep longitudinal furrow on premaxilla: absent (0), present (1)
8. New character: Ornamentation on premaxillary beak: absent (0), present (1)
9. New character: Premaxillary sinus: absent (0), present (1)
10. Dimensions of premaxillary palate: longer than wide (0), wider than long (1). (Vickaryous et al. 2001: 13, Thompson et al. 2012: 18).
11. Shape of the premaxillary palate: sub-triangular (0), sub-quadrangle (1), sub-oval (2). (Sereno 1999: 80, Thompson et al. 2012: 19).
- Updated codings: *Gobisaurus* and *Shamosaurus* from 1 to 2.
12. 'V' or 'U'-shaped median indentation of the anterior margin of the premaxilla: absent (0), present (1). (Sereno 1999: 91, Thompson et al. 2012: 20).
- Updated codings: *Pawpawsaurus* from 0 to ?; this region is broken in the only known specimen.
- Chapter 3 (Arbour and Currie 2013a) - *Ankylosaurus* from 1 to ?, because this region is broken in all specimens of *Ankylosaurus*.
13. Caudoventral extension of premaxillary tomium in lateral view: ends anteriorly to the maxillary teeth (0), obscures anteriormost maxillary teeth (1). (Sereno 1999: 100, Thompson et al. 2012: 21).

Updated codings: *Cedarpelta* from 0 to ?; this region is damaged. *Minmi* sp. from 0 to ?; the premaxilla is poorly preserved in this specimen.

14. Bone bordering anterior margin of internal nares: premaxilla (0), maxilla (1). (Thompson et al. 2012: 22).

Updated codings: Chapter 3 (Arbour and Currie 2013a) - *Pinacosaurus mephistocephalus* from 1 to ?, because it is unclear from the figures in Godefroit et al. (1999) of the holotype of *Pinacosaurus mephistocephalus* if the premaxilla or maxilla borders the anterior margin of the internal nares.

15. Modified: External nares, defined as the outermost rim of the nasal vestibule, opening faces: laterally to anterolaterally (0) anteriorly (1) ventrolaterally (2). (Carpenter et al. 1998: 10, Thompson et al. 2012: 7).
16. External nares, visible in dorsal view: visible (0), hidden (1). (Thompson et al. 2012: 8)
17. New character: Paranasal apertures/fossae: no fossae or apertures present besides primary opening for nasal airway (0), paranasal apertures/fossae present (1)
18. New character: Shape of respiratory passage: straight or arched (0), with anterior (rostral) and posterior (caudal) loops (*sensu* Witmer and Ridgely 2008).
19. New character: Vascular impressions on dorsal surface of posterior nasal passage (airway): absent (0) present (1)
20. Modified: Frontonasal and/or frontoparietal cranial ornamentation: absent (0) rugose, not differentiated into discrete polygons (caputegulae) (1), differentiated into discrete polygons (caputegulae) (2). (after Carpenter et al. 1999, Thompson et al. 2012: 77).

Updated codings: *Minmi* sp. ? to 1, as the specimen has grooves along the cranial surface that demarcate discrete polygons. *Mymoorapelta* from 1 to ?, as although additional cranial elements for *Mymoorapelta* were

noted in an abstract by Kirkland et al. (2010), this material has yet to be described. *Tatankacephalus* from 0 to 2, according to Parsons and Parsons (2009). *Shamosaurus* from 1 to 0.

Chapter 3 (Arbour and Currie 2013a) - *Dyoplosaurus* from 0 to ?; in the holotype of *Dyoplosaurus*, only the parietal region of the skull is preserved. Distinct polygons are generally not present in this region of the skull in *Euoplocephalus* and it is possible that *Dyoplosaurus* was similar in this regard. As such, this feature cannot be coded for *Dyoplosaurus*. *Tsagantegia* from 0 to 1; although the drawings of the holotype skull (MPC 700/17) of *Tsagantegia* in Tumanova (1993) show amorphous cranial ornamentation, firsthand examination of the skull indicates that there are distinct low-relief polygons covering the skull roof.

21. New character: Number of caputegulae in frontonasal and prefrontal region: no caputegulae (0), 10 or fewer (1), 11 to 30 (2) more than 30 (3)
22. Modified: Majority of frontonasal and/or frontoparietal caputegulum relief: caputegulae absent (0), caputegulae concave or flat (1), caputegulae strongly bulbous (2). (After Sullivan 1999 , Thompson et al. 2012: 82).
Updated codings: *Minmi* sp. from ? to 1; *Pawpawsaurus* from 1 to 2.
Chapter 3 (Arbour and Currie 2013a) - *Talarurus* from 0 to 2. The holotype of *Talarurus*, PIN 557, preserves distinctly domed cranial caputegulae.
23. New character: Domed frontonasal caputegulae: domed caputegulae absent (0), rounded cones with circular bases (1) pyramidal with sharp edges (2)
24. New character: Supranarial caputegulae, notch or embayment dorsal to nasal vestibule: no supranarial caputegulae (0), notch absent (1), notch present (2).
25. New character: Number of internarial caputegulae: none (0), 1 (1), more than 1 (2).

26. New character: Median nasal caputegulum (located posterior to the supranarial ornamentation, on the midline of the skull): absent (0), present, hexagonal (1), present, triangular (2). (Vickaryous et al. 2004: 9).
27. New character: Loreal caputegulum in lateral view: no caputegulum (0) 1 caputegulum (1), more than 1 caputegulum (2)
28. Shape of the maxillary tooth row: straight (0), medially convex (1). (Vickaryous et al. 2001: 18, Thompson et al. 2012: 24).

Updated codings: *Cedarpetta* from 0 to ?; this is not preserved.

Gobisaurus from 0 to 1, *Shamosaurus* from 0 to 1.

Chapter 3 (Arbour and Currie 2013a) - *P. grangeri* from 0 to 1; *Saichania* from 0 to 1; *Tsagantegia* from 0 to 1. In all of these taxa the maxillary tooth row is at least slightly medially convex.

29. Maxillary tooth row position: lateral margin of skull (0), inset (1). (Lee 1996: 4, Thompson et al. 2012: 25).

Updated codings: Chapter 3 (Arbour and Currie 2013a) -

Nodocephalosaurus from ? to 1. The maxillary tooth row is clearly inset from the lateral margin of the skull in the holotype of

Nodocephalosaurus.

30. Modified: Distance between posteriormost extent of maxillary tooth rows relative to the width of the premaxillary beak: wider (0), narrower (1). [The width of the premaxillary beak is measured where the lateral edges of the beak are most parallel, which is usually close to the posterior of the premaxilla.] (Serenio 1999: 102, Thompson et al. 2012: 26).

Updated codings: *Tatankacephalus* from 1 to ?, as this region is not completely preserved in the only known specimen.

Chapter 3 (Arbour and Currie 2013a) - *Ankylosaurus magniventris* from 1 to 0. Notes: In AMNH 5214, the beak is narrower than the posterior width between the maxillary tooth rows; see Carpenter [9].

31. Caudoventral secondary palate: absent (0), present (1) (Thompson et al. 2012: 49).
32. Posterior palatal foramen: absent (0), present (1). (Lee 1996: 17, Thompson et al. 2012: 50).
Updated codings: Chapter 3 (Arbour and Currie 2013a) - *Saichania* from 0 to 1, *Tsagantegia* from ? to 0.
33. Gap between palate and braincase: open (0), closed by a dorsal projection of the pterygoid (1). (Serenio 1999: 61, Thompson et al. 2012: 16).
34. New character: Lacrimal incisure (mediolateral constriction behind the nares/at the prefrontals, giving the skull an hourglass-shaped outline in dorsal view): absent (0) present (1)
35. New character: Lacrimal caputegulum in lateral view: no caputegulum (0) 1 caputegulum (1), more than 1 caputegulum (2)
36. New character: Prefrontal caputegulum: no caputegulum (0) flat (1), sharply pointed and pyramidal (2).
37. New character: Scroll-like descending process of the frontal: absent (0) present (1)
38. Modified: Form of supraorbitals (including ornamentation): absent (0), boss-like, rounded laterally (1), sharp lateral rim, forming a ridge (2). (Vickaryous et al. 2001: 5, Thompson et al. 2012: 30). *Tatanka* ? to 2; Updated codings: *Antarctopelta* to ?, as it is not certain that the described element is a supraorbital. *Pawpawsaurus* from 2 to 1.
Chapter 3 (Arbour and Currie 2013a) - *Dyoplosaurus* from 1 to ?. The supraorbitals are poorly preserved in the holotype and only specimen of *Dyoplosaurus*.
39. New character: Supraorbitals, when viewed dorsally: no supraorbitals (0), combine to form continuous edge (1), have distinct apices (2).
Updated codings: *Gastonia* from ? to 1, *Talarurus* from ? to 1.
40. Orbits, angle of orbital axis: <40° (0), >40° (1). (Thompson et al. 2012: 13).

Updated codings: *Saichania* from 1 to 0.

- 41. New character: Ciliary osteoderm (eyelid ossification): absent (0) present (1)
- 42. Development of the postocular shelf: not developed (0), completely separating orbit from temporal space (1). (Sereno 1999: 104, Thompson et al. 2012: 15).
- 43. Proportions of jugal orbital ramus: depth greater than transverse breadth (0), transverse breadth greater than depth (1). (Sereno 1999: 1, Thompson et al. 2012: 32).

Updated codings: *Shamosaurus* from ? to 1.

- 44. New character: Depth of jugal ramus relative to orbit height: jugal height is less than 15% orbit height (0), jugal height is more than 15% orbit height (1)
- 45. New character: Accessory postorbital ossification: absent (0), present (1)
- 46. New character: Squamosal/postorbital horn: no horn (0) base has broad triangular cross-section and overall shape is pyramidal (1), base is oval in cross-section and overall shape is narrow, tapered cylinder (2)
- 47. Modified: Projection of squamosal/postorbital horns relative to the posterior margin of the dorsal surface of the skull: horns absent (0), horns do not project past posterior margin of skull in dorsal view (1), horns project past posterior margin of skull in dorsal view (2) (Thompson et al. 2012: 83).

Updated codings: *Minmi* sp. from ? to 0.

Chapter 3 (Arbour and Currie 2013a) - *Nodocephalosaurus* from ? to 1.

Although the skull is crushed, the squamosal horns clearly project posteriorly beyond the nuchal shelf of *Nodocephalosaurus*.

- 48. Modified: Shape of jugal/quadratojugal horn in dorsal view: quadratojugal horn absent (0), horn U-shaped, with round distal edge (1), horn triangular, with pointed distal edge (2) (Thompson et al. 2012: 82). Updated codings: *Pawpawsaurus* from 1 to 0. *Mymoorapelta* from 1 to ?. Although additional cranial elements for *Mymoorapelta* were noted in an abstract by Kirkland et al. (2010), these have yet to be described.

49. New character: Jugal/quadratojugal horn: no horn (0) lacks distinct neck at base (1), has distinct neck at base (2).
50. New character: Jugal or quadratojugal horn size relative to orbit size: no horn (0), length of base of jugal/quadratojugal horn equal to or less than the length of the orbit (1), length of base of jugal/quadratojugal horn is 110% or greater length of orbit (2).
51. New character: Small (<2 cm diameter), circular caputegulae posterolateral to orbit (postocular caputegulae), along ventral edge of squamosal horn and/or along dorsal edge of quadratojugal horns: absent (0), present (1)
52. New character: [This character is inverted from character 31 from Thompson et al. 2012] Form of the parietal surface: parietals flat to slightly convex (0), parietals concave, forming a trough-like surface posterior to the supraorbitals and anterior to the posterior edge of the skull (1).
53. A single large medial polygon of ornamentation in the parietal region: absent (0), present (1) (Thompson et al. 2012: 80).
- Updated: *Lesothosaurus*, *Scelidosaurus*, and *Stegosaurus* from ? to 0, as these taxa lack this feature. *Minmi* sp. ? to 1. *Tatankacephalus* from 0 to ? because the preserved portions do not demonstrate that a caputegulum was present in this region.
54. New character: Number of discrete nuchal caputegulae: none (0), 2 (1), greater than 2(2)
55. Posterior projection of the nuchal shelf: does not obscure occiput in dorsal view (0), obscures occiput in dorsal view (1). (Vickaryous et al. 2004: 12, Thompson et al. 2012: 89).
56. Shape of quadrate in lateral aspect: curved (anteriorly convex, posteriorly concave) (0), straight (1). (Vickaryous et al. 2001: 38, Thompson et al. 2012: 33).

Updated codings: *Pawpawsaurus* from 0 to 1.

Chapter 3 (Arbour and Currie 2013a) - *Nodocephalosaurus* from ? to 1.

57. Inclination of quadrate in lateral aspect: near vertical (0), almost 45° anterolaterally (1). (Lee 1996: 10, Thompson et al. 2012: 34).
58. Form of the anterior surface of the quadrate: transversely concave (0), not concave (1). (Lee 1996: 12, Thompson et al. 2012: 35).
Updated codings: *Pawpawsaurus* from 1 to 0.
59. Ventral projection of the mandibular process of the quadrate in lateral view: projects beyond the quadratojugal ornamentation (0), hidden by quadratojugal ornamentation (1). (Vickaryous et al. 2004 : 40, Thompson et al. 2012: 36).
Updated codings: *Cedarpetta* from 0 to ?; the skull is reconstructed and taphonomically distorted. *Minmi* sp. from 0 to 1; the quadrate is not visible in lateral view in the published figures or in the cast.
Chapter 3 (Arbour and Currie 2013a) - *Nodocephalosaurus* from ? to 1.
Notes: This feature is preserved in *Nodocephalosaurus*. Although the specimen is distorted, it is apparent that the quadrate was obscured by the quadratojugal horn in lateral view.
60. Form of quadrate mandibular extremity: symmetrical (0), medial condyle larger than lateral condyle (1). (Serenio 1999: 10, Thompson et al. 2012: 37).
Updated codings: Chapter 3 (Arbour and Currie 2013a) - *Nodocephalosaurus* from ? to 1. Notes: This feature is preserved in *Nodocephalosaurus*.
61. Inclination of the articular surface of the quadrate condyle in posterior view: horizontal (0), ventromedially inclined at approximately 45° to horizontal (1). (Serenio 1999: 14, Thompson et al. 2012: 38).
62. Lateral ramus of the quadrate: present (0), absent (1). (Serenio 1999: 15, Thompson et al. 2012: 39).
63. Dorsoventral depth of the pterygoid process of the quadrate: deep (0), shallow (1). (Lee 1996: 7, Serenio 1999: 60, Thompson et al. 2012: 40).

64. Contact between paroccipital process and quadrate: sutural (0), fused (1).
(Carpenter et al. 1998: 13, Thompson et al. 2012: 41).
65. Contact between pterygoids: pterygoids separate caudomedially, forming an interpterygoid vacuity (0), pterygoids joined medially forming a pterygoid shield (1). (Thompson et al. 2012: 42).
Updated codings: *Cedarpelta* to ?; not preserved.
66. Direction of the pterygoid flange: anterolateral (0), anterior/parasagittal (1).
(Vickaryous et al. 2001: 29, Thompson et al. 2012: 43).
67. Contact between basipterygoid processes and pterygoid: sutural (0), fused (1). (Vickaryous et al. 2001: 30, Thompson et al. 2012: 44).
68. Position of ventral margin of the pterygovomerine keel relative to alveolar ridge: dorsal (0), level (1). (Serenio 1999: 59, Thompson et al. 2012: 45).
69. Dorsal extent of median vomer lamina: does not meet skull roof (0), meets skull roof (1). (Lee 1996: 14, Thompson et al. 2012: 46).
Updated codings: *Cedarpelta* from 0 to ?; not preserved.
70. Pterygoid foramen: absent (0), present (1). (Hill et al. 2003: 21, Thompson et al. 2012: 47).
71. Position of posterior margin of pterygoid body relative to the anterior margin of the quadrate condyle: anteriorly positioned (0), in transverse alignment (1). (Vickaryous et al. 2004: 28, Thompson et al. 2012: 48).
Updated codings: *Cedarpelta* from ? to 0.
72. Size of occiput: higher than wide (0), wider than high (1). (Lee 1996: 1, Thompson et al. 2012: 6).
73. Direction of paroccipital process extension: caudolateral (0), lateral (1).
(Carpenter et al. 1998: 11, Vickaryous et al. 2004: 33, Thompson et al. 2012: 51).
Updated codings: *Shamosaurus* from 0 to 1.

74. Bones forming the occipital condyle: basioccipital and exoccipital (0), basioccipital only (1). (Lee 1996: 9, Thompson et al. 2012: 54). Mym 0 to ?, undescribed
- Updated codings: *Mymoorapelta* from 0 to ?, as the material is undescribed. *Shamosaurus* from 0 to 1.
- Chapter 3 (Arbour and Currie 2013a) - *Ankylosaurus* from 0 to 1, *Euoplocephalus* from 0 to 1, *Minotaurasaurus* from ? to 1, *Nodocephalosaurus* from 0 to 1, *Saichania* from 0 to 1, *Talarurus* from 0 to 1, *Tsagantegia* from 0 to 1.
75. Length of basisphenoid relative to the basioccipital: longer (0), shorter or equal (1). (Serenó 1999: 12, Thompson et al. 2012: 56).
- Updated codings: *Mymoorapelta* from 1 to ?, as the cranial material is undescribed.
76. Form of basisphenoidal tuberosities: medially separated rounded rugose stubs (0), continuous transverse rugose ridge (1). (Vickaryous et al. 2001: 32, Thompson et al. 2012: 57).
- Updated codings: *Mymoorapelta* from 0 to ?, as the cranial material is undescribed.
77. Size of basiptyergoid processes: twice as long as wide or over (0), less than twice as long as wide (1). (Thompson et al. 2012: 58).
- Updated codings: *Mymoorapelta* from 1 to ?, as the cranial material is undescribed.
- Chapter 3 (Arbour and Currie 2013a) - *Tsagantegia* from ? to 1.
78. Form of the cranial nerve foramina IX-XII: separate foramina (0), single foramen shared with the jugular vein (1). (Thompson et al. 2012: 59).
- Updated codings: *Mymoorapelta* from 0 to ?, as the cranial material is undescribed.

Mandibles

79. Position of mandible articulation relative to mandibular adductor fossa: posterior (0), posteromedial (1). (Serenio 1999: 64, Thompson et al. 2012: 67).
Updated codings: *Minmi* sp. 1 to ?, as this region is not preserved in the specimen.
80. Mandibular fenestra: present (0), absent (1). (Thompson et al. 2012: 68).
81. Depth of the dentary symphyseal ramus relative to half the maximum depth of the mandibular ramus in lateral view: deeper (0), shallower (1). (Serenio 1999: 17, Thompson et al. 2012: 69).
82. Shape of dorsal margin of the dentary in lateral view: straight (0), sinuous (1). (Serenio 1999: 4, Thompson et al. 2012: 70).
83. Development of the coronoid process: not developed (0), distinct (1). (Serenio 1999: 108, Thompson et al. 2012: 73).
84. Position of glenoid for quadrate relative to mandibular axis: medially offset (0), in line (1). (after Carpenter et al. 1999, Thompson et al. 2012: 74).
85. Size and projection of the retroarticular process: small with no dorsal projection (0), well developed with a dorsal projection (1). (Thompson et al. 2012: 75).
86. Size of prementary ventral process: distinct, prong shaped process (0), rudimentary eminence (1). (Serenio 1999: 66, Thompson et al. 2012: 76).
87. Modified: Length of mandibular caputegulum with respect to the length of the mandible: less than or equal to half the length (0), over three quarters the length (1). (after Carpenter et al. 1999, Thompson et al. 2012: 90).

Teeth

88. Premaxillary teeth: present (0), absent (1). (Serenio 1999: 18, Thompson et al. 2012: 63).

89. Cingula on maxillary and/or dentary teeth: absent (0), present (1). (Carpenter et al. 1998: 21, Thompson et al. 2012: 64).

Updated codings: *Mymoorapelta* from 0 to ?, as the material is undescribed. *Stegopelta* ? to 1. *Tatankacephalus* 0 to 1; the tooth is weathered but a cingulum appears to be present in the figure by Parsons and Parsons (2009).

90. Modified: Maxillary and/or dentary tooth crown shape (Thompson et al. 2012: 65, in part): pointed (0), rounded (1)

Updated codings: *Ankylosaurus* from 0 to 1.

91. Modified: Maxillary and/or dentary tooth denticles: < 13 denticles (0), ≥13 denticles (1) (Thompson et al. 2012: 65, in part).

Ankylosaurus from 0 to 1.

92. Number of dentary teeth: <25 (0), ≥25 (1). (Thompson et al. 2012: 66).

Updated codings: Chapter 3 (Arbour and Currie 2013a) - *Tsagantegia* from ? to 0.

Axial Skeleton

93. Type of articulation between the atlantal neural arch and intercentrum: open (0), fused in adult (1). (Serenio 1999: 19, Thompson et al. 2012: 92).

94. Type of contact between the atlantal neural arches: no median contact (0), median contact (1). (Serenio 1999: 68, Thompson et al. 2012: 93).

95. Contact between atlas and axis: articulated (0), fused (1). (Vickaryous et al. 2004: 46, Thompson et al. 2012: 94).

96. Dimensions of cervical vertebrae centra: anteroposteriorly longer than transverse width (0), anteroposteriorly shorter than transverse width (1). (after Kirkland et al. 1998, Thompson et al. 2012: 95).

Updated codings: *Stegopelta* from 0 to 1. *Mymoorapelta* from from 1 to 0, *Sauropelta* from ? to 1,.

97. Ratio of maximum neural spine width to height in anterior cervicals: <0.25 (0), ≥0.25 (1). (after Carpenter et al. 1999, Thompson et al. 2012: 96)*.

Updated codings: *Mymoorapelta* from 1 to 0.

98. Ratio of anteroposterior dorsal centrum length to posterior centrum height: >1.1 (0), <1.1 (1). (Thompson et al. 2012: 98).

Updated codings: *Minmi* sp. 1 to ?; this feature is not described in the paper or visible in the cast, and it is unclear if this was coded based on the holotype of *Minmi* paravertebræ or the referred specimen.

Mymoorapelta from 1 to 0.

99. Longitudinal keel on ventral surface of dorsal centra: present (0), absent (1). (Thompson et al. 2012: 99).

Updated codings: *Minmi* sp. 1 to ?; this feature is not described in the paper or visible in the cast, and it is unclear if this was coded based on the holotype of *Minmi* paravertebræ or the referred specimen.

Chapter 3 (Arbour and Currie 2013a) - *P. grangeri* from ? to 1. A longitudinal keel is present on the ventral surface of dorsal centra in referred *P. grangeri* specimen PIN 614.

100. Cross sectional shape of neural canal in posterior dorsals: circular (0) elliptical, with long axis running dorsoventrally (1). (after Carpenter 1990, Thompson et al. 2012: 100).

Updated codings: *Euoplocephalus* from 0 to 1, *Stegopelta* from 0 to 1. *Minmi* sp. 1 to ?; this feature is not described in the paper or visible in the cast, and it is unclear if this was coded based on the holotype of *Minmi* paravertebræ or the referred specimen. *Antarctopelta* 1 to ?, not preserved.

Chapter 3 (Arbour and Currie 2013a) - *Saichania* from 0 to ?, because MPC 100/1305 is not referable to *Saichania*. Although dorsal vertebrae are preserved in the holotype, they were not figured by Maryańska [17] and no reference is made to the shape of the neural canal. The postcrania

of MPC 100/151 was not examined firsthand by VMA or PJC and so this character cannot be verified for *Saichania*.

101. Shape of the proximal cross-section of the dorsal ribs: triangular (0), 'L'- or 'T'-shaped (1). (Thompson et al. 2012: 101).

102. Attachment of dorsal ribs to posterior dorsal vertebrae: articulated (0), fused (1). (Thompson et al. 2012: 102).

Updated codings: *Minmi* sp. 1 to ?; this feature is not described in the paper or visible in the cast, and it is unclear if this was coded based on the holotype of *Minmi* paravertebra or the referred specimen. *Mymoorapelta* from 0 to 1, as the dorsal rib is fused to the vertebra in MWC 1801.

Stegopelta 0 to ?, as only one dorsal is preserved and it is unclear if it is an anterior or posterior dorsal.

103. Contact between posteriormost dorsal vertebrae: articulated (0), fused to form a presacral rod (1). (Thompson et al. 2012: 103).

104. Longitudinal groove in ventral surface of the sacrum: absent (0), present (1). (Thompson et al. 2012: 105).

Updated codings: *Minmi* sp. to ?; not described in paper or visible in cast.

105. New character: Longitudinal ridge at approximate mid-height of centrum of mid and distal caudals: absent (0) present (1)

106. Ratio of maximum distal width to height of the neural spines of proximal caudals: ≤ 0.2 (0), > 0.2 (1). (after Carpenter 2001, Thompson et al. 2012: 107).

107. Direction of the transverse processes of proximal caudals: craniolaterally projecting (0), caudolaterally projecting (1), laterally projecting (2). (after Carpenter 2001, Thompson et al. 2012: 108).

Updated codings: *Mymoorapelta* 0 to 2, *Gargoyleosaurus* to 2.

Chapter 3 (Arbour and Currie 2013a) - *Ankylosaurus magniventris* from 2 to 0; *Euoplocephalus* from 1 to 0; *Nodocephalosaurus* from 1 to 0. In

Ankylosaurus, *Euoplocephalus*, and *Nodocephalosaurus*, the transverse processes of the free caudals project anterolaterally from the centrum.

108. Persistence of transverse processes down the length of the caudal series: not present beyond the mid-length of the series (0), present beyond the mid-length of the series (1). (Thompson et al. 2012: 110).

Updated codings: *Antarctopelta* 1 to ?, as no caudals are preserved.

109. Attachment of haemal arches to their respective centra: articulated (0), fused (1). (Thompson et al. 2012: 111).

Updated codings: *Minmi* sp. 1 to ?; not described or visible in cast.

Chapter 3 (Arbour and Currie 2013a) - *Nodocephalosaurus* from 0 to ?; *P. grangeri* from ? to 1, Notes: Caudal vertebrae have been referred to *Nodocephalosaurus* by Sullivan and Fowler (2006), but these were isolated elements unassociated with other, more diagnostic material, from the same formation as the holotype specimen. As such, it seems best to code this character as unknown for *Nodocephalosaurus* at present. Caudal centra with preserved haemal arches are present in *P. grangeri* referred specimen PIN 614.

110. Extent of pre- and postzygapophyses over their adjacent centra in posterior vertebrae: extend over less than half the length of the adjacent centrum (0), extend over more than half the length of the adjacent centrum (1). (Serenio 1999: 109, Thompson et al. 2012: 113).

Updated codings: Chapter 3 (Arbour and Currie 2013a) - *Saichania* from 1 to ?. Notes: An isolated tail club has been referred to *Saichania*, but no tail club is preserved with the holotype material.

111. New character: In tail club handle vertebrae, shape of each interlocking neural arch in dorsal view: distal caudal vertebrae do not form handle (0), V-shaped, angle of divergence about 22-26° (1), V-shaped, angle of divergence about 35-37° (2), U-shaped, angle of divergence greater than 60° (3)

112. Shape of the posterior haemal arches: rounded haemal spine in lateral view with no contact between haemal arches (0), inverted 'T'-shaped haemal spine in lateral view, with contact between the ends of adjacent spines (1). (Sereno 1999: 71, Thompson et al. 2012: 114).

Updated codings: Chapter 3 (Arbour and Currie 2013a) - *Pinacosaurus mephistocephalus* from ? to 1, *Saichania* from 1 to ?. A tail club handle is preserved in *Pinacosaurus mephistocephalus*. An isolated tail club has been referred to *Saichania*, but no tail club is preserved with the holotype material.

113. Ossified tendons in distal region of tail: absent (0), present (1). (Sereno 1999: 97, Thompson et al. 2012: 115). Scolio from ? to 1

Updated codings: Chapter 3 (Arbour and Currie 2013a) - *Saichania* from 1 to ?. An isolated tail club has been referred to *Saichania*, but no tail club is preserved with the holotype material.

Pectoral Girdle

114. Dimensions of coracoid: longer than wide (0), wider than long or equal width and length (1). (Thompson et al. 2012: 116).

Updated codings: *Minmi* sp. 0 to ?; not described or visible in cast.

115. Form of the anterior margin of the coracoid: convex (0), straight (1). (Thompson et al. 2012: 117).

Updated codings: *Minmi* sp. 0 to ?; not described or visible in cast.

116. Cranioventral process of coracoid: absent (0), present (1). (Thompson et al. 2012: 118).

Updated codings: *Minmi* sp. 0 to ?; not described or visible in cast.

117. Size of coracoid glenoid relative to scapula glenoid: sub-equal (0), half the size (1). (Sereno 1999: 89, Thompson et al. 2012: 119).

Updated codings: *Minmi* sp. 0 to ?; not described or visible in cast.

Chapter 3 (Arbour and Currie 2013a) - *Pinacosaurus grangeri* from ? to 0.

118. Contact between scapula and coracoid: articulated (0), fused (1). (Thompson et al. 2012: 120).

119. Scapula glenoid orientation: ventrolateral (0), ventral (1). (Sereno 1999: 87, Thompson et al. 2012: 121).

Updated codings: *Minmi* sp. 0 to ?; not described or visible in cast.

120. Ventral process of scapula at the caudoventral margin of glenoid: absent (0), present (1). (Thompson et al. 2012: 122). Scaled from ? to 1

Updated codings: Updated codings: *Minmi* sp. 0 to ?; not described or visible in cast.

Chapter 3 (Arbour and Currie 2013a) - *Saichania* from ? to 1; *P. grangeri* from ? to 1. The scapula is preserved in the holotype specimen of *Saichania*, and a scapula is known in *P. grangeri* referred specimen PIN 614.

121. Form of the scapula acromion process: not developed or ridge-like along the dorsal border of the scapula (0) flange-like and folded over towards the scapula glenoid (1) ridge terminating in a knob-like eminence (2).

(Vickaryous et al. 2004: 52, Thompson et al. 2012: 123)

Updated codings: *Minmi* sp. 0 to ?; not described or visible in cast.

122. Orientation of the acromion process of scapula: directed away from the glenoid (0), directed towards scapula glenoid (1). (after Kirkland 1998, Thompson et al. 2012: 124).

Updated codings: *Minmi* sp. 0 to ?; not described or visible in cast.

123. Scapulocoracoid buttress: absent (0), present (1). (Parish 2005: 116).

Updated codings: Chapter 3 (Arbour and Currie 2013a) - *Talarurus* from ? to 0; present in PIN 557.

Updated codings: *Minmi* sp. 0 to ?; not described or visible in cast.

124. Distal end of scapula shaft: narrow (0), expanded (1). (Sereno 1999: 20, Thompson et al. 2012: 125).

Updated codings: Updated codings: *Minmi* sp. 0 to ?; not described or visible in cast.

Chapter 3 (Arbour and Currie 2013a) - *Talarurus* from 1 to 0. In specimen PIN 557, the scapula is narrow distally.

125. Contact between sternal plates: separate (0), fused (1). (Sereno 1999: 112, Vickaryous et al. 2004: 60, Thompson et al. 2012: 126).

Pelvic Girdle

126. Length of the preacetabular process of ilium as a percentage of total ilium length: $\leq 50\%$ (0), $> 50\%$. (Thompson et al. 2012: 136).

Updated codings: *Minmi* from 1 to 0.

Chapter 3 (Arbour and Currie 2013a) - *Dyoplosaurus* from 0 to ?, *Tianzhenosaurus* 1 to ?. Notes: The preacetabular process of the ilium of ROM 784 is broken, and so this character cannot be coded for *Dyoplosaurus*.

127. Angle of lateral deflection of the preacetabular process of the ilium: 10° – 20° (0), 45° (1). (Sereno 1999: 21, Thompson et al. 2012: 137).

Updated codings: Chapter 3 (Arbour and Currie 2013a) - *Pinacosaurus mephistocephalus* from 0 to 1; *Dyoplosaurus* from 0 to 1.

128. Orientation of the preacetabular portion of the ilium: near vertical (0), near horizontal (1). (Kirkland 1998: 45, Thompson et al. 2012: 138).

129. Form of the preacetabular portion of the ilium: straight process (0), pronounced ventral curvature (1). (Thompson et al. 2012: 139).

130. New character: Lateral edge of ilium in dorsal view: straight (0), sinuous (1)

131. Lateral exposure of the acetabulum: exposed (0) acetabulum partially obscured as it is partially encircled by the distal margin of the ilium (1). (Thompson et al. 2012: 140)

Updated codings: Chapter 3 (Arbour and Currie 2013a) - *Pinacosaurus mephistocephalus* from 0 to ?; *Saichania* from 1 to ?. Notes: The pelvis is

not known for *Saichania*, and so this character cannot be coded. The pelvis is preserved in *Pinacosaurus mephistocephalus*, but it cannot be determined from the photographs in Godefroit et al. (1999) how this feature should be coded.

132. Perforation of the acetabulum: present, open acetabulum (0), absent, closed acetabulum (1). (Sereno 1999: 74, Thompson et al. 2012: 141).

Updated codings: *Minmi* sp. from 0 to ?. Molnar (1996) includes a drawing that reconstructs the pelvis with an open acetabulum, but no rationale for this interpretation is given, and it is not clear from the papers or cast that this would be the case.

133. Postacetabular ilium length, relative to diameter of acetabulum: greater (0), smaller (1). (Sereno 1999: 114, Thompson et al. 2012: 142).

Updated codings: Chapter 3 (Arbour and Currie 2013a) - *Pinacosaurus grangeri* from ? to 1. The postacetabular process is shorter than the length of the acetabulum in specimen PIN 614 of *Pinacosaurus grangeri*.

134. Modified: Pubis: present (0), indistinct from ilium (1) (Kirkland 1998: 46, Thompson et al. 2012: 143)

135. Shape of ischium: straight (0), ventrally flexed at mid-length (1). (Kirkland 1998: 37, Thompson et al. 2012: 147).

Updated codings: *Mymoorapelta* from ? to 1, as reported by Kirkland et al. 2010.

Chapter 3 (Arbour and Currie 2013a) - *Dyoplosaurus* from ? to 0. Although the shafts are broken at the midlength of each ischium, the ischia of ROM 784 would have been straight.

136. Shape of the dorsal margin of ischium: straight or concave (0), convex (1). (Sereno 1999: 115, Thompson et al. 2012: 148).

Limbs

137. Separation of humeral head and deltopectoral crest in anterior view: continuous (0), separated by a distinct notch (1). (Thompson et al. 2012: 128).
Updated codings: *Mymoorapelta* from ? to 0.
Chapter 3 (Arbour and Currie 2013a) - *Talarurus* from ? to 0. Notes: See PIN 557.
138. Separation of humeral head and medial tubercle in anterior view: continuous (0), separated by a distinct notch (1) (Thompson et al. 2012: 129).
Updated codings: *Mymoorapelta* from ? to 0.
Chapter 3 (Arbour and Currie 2013a) - *Talarurus* from ? to 0, *Euoplocephalus* from 1 to 0.
139. Ratio of deltopectoral crest length to humeral length: ≤ 0.5 (0), > 0.5 (1). (Thompson et al. 2012: 130).
140. Orientation of deltopectoral crest projection: lateral (0), anterolateral (1). (Serenio 1999: 113, Thompson et al. 2012: 131).
141. Shape of the radial condyle of humerus round / proximal end of radius in end-on view: non-circular (0), circular (1). (Thompson et al. 2012: 132).
Updated codings: *Minmi* sp. 0 to ?; not described or visible in cast.
142. Ratio of the length of metacarpal V to metacarpal III: ≤ 0.5 (0), > 0.5 (1). (Serenio 1999: 6, Thompson et al. 2012: 133).
Updated codings: *Minmi* sp. 0 to ?; not preserved in the specimen.
143. Manual digit number: 5 (0), 4 (1), 3 (2). (Thompson et al. 2012: 134).
Updated codings: *Minmi* sp. 0 to ?; not preserved in the specimen.
144. Modified: Shape of manual and pedal ungual phalanges: narrow, claw-shaped (0) wide, hoof-shaped, U-shaped in dorsal view (1), wide, hoof-shaped, triangular in dorsal view (2) (Serenio 1999: 7, Thompson et al. 2012: 135).

- Updated codings: *Minmi* sp. to ?; not preserved in the specimen.
145. Angle between long axis of femoral head and long axis of shaft: <100° (0), 100° to 120° (1), >120° (2). (Thompson et al. 2012: 149).
- Updated codings: *Minmi* sp. 0 to ?; not preserved in the specimen.
- Chapter 3 (Arbour and Currie 2013a) - *Ankylosaurus* from 1 to 2, *Pinacosaurus grangeri* from 1 to 2, *Euoplocephalus* from 1 to 2. Notes: *Euoplocephalus* estimated from AMNH 5404. *Ankylosaurus* estimated from Carpenter (2004).
146. Separation of femoral head from greater trochanter: continuous (0), separated by a distinct notch or change in slope (1). (Thompson et al. 2012: 150).
- Updated codings: *Antarctopelta* from 1 to ?, as this feature is not preserved in the specimen. *Minmi* sp. 0 to ?; not preserved in the specimen.
147. Differentiation of the anterior trochanter of the femur: separated from femoral shaft by a deep groove laterally and dorsally (0), fused to femoral shaft (1). (Kirkland 1998: 36, Thompson et al. 2012: 151).
- Updated codings: *Minmi* sp. 0 to ?; not clear in the specimen.
148. Oblique ridge on lateral femoral shaft, distal to anterior trochanter: absent (0), present (1). (Thompson et al. 2012: 152).
- Updated codings: *Minmi* sp. 0 to ?; not described or visible in cast.
- Chapter 3 (Arbour and Currie 2013a) - *Dyoplosaurus* from ? to 0.
149. Form of the fourth trochanter: pendant (0), ridge-like (1). (Sereno 1999: 24, Thompson et al. 2012: 153).
- Updated codings: *Minmi* sp. 0 to ?; not described or visible in cast.
- Chapter 3 (Arbour and Currie 2013a) - *Dyoplosaurus* from ? to 1.
150. Location of the fourth trochanter on the femoral shaft: proximal (0) distal, over half-way down the femoral shaft (1). (Thompson et al. 2012: 154).
- Updated codings: *Minmi* sp. 0 to ?; not described or visible in cast.

Chapter 3 (Arbour and Currie 2013a) - *Dyoplosaurus* from ? to 1.

151. Maximum distal width of the tibia, compared to the maximum proximal width: narrower (0), wider (1). (Sereno 1999: 188, Thompson et al. 2012: 155).

Updated codings: *Minmi* sp. 0 to ?; not described or visible in cast.

Chapter 3 (Arbour and Currie 2013a) - *Dyoplosaurus* from ? to 1.

152. Contact between tibia and astragalus: articulated (0), fused, with suture obliterated (1). (Thompson et al. 2012: 156).

Updated codings: *Minmi* sp. 0 to ?; not described or visible in cast.

Ankylosaurus from 1 to ?, as a tibia is unknown for this species.

Anodontosaurus from ? to 1.

153. Number of pedal digits: 5 (0), 4 (1), 3 (2). (Thompson et al. 2012: 157).

Updated codings: *Talarurus* from 1 to ?; the mounted skeleton is a composite of many individuals.

Chapter 3 (Arbour and Currie 2013a) - *P. grangeri* from ? to 2, See description of *Pinacosaurus* manual and pedal elements in Currie et al. (2011).

154. Phalangeal number in pedal digit IV: 5 (0), ≤ 4 (1). (Sereno 1999: 26, Thompson et al. 2012: 158).

Updated codings: *Talarurus* from 1 to ?; the mounted skeleton is a composite of many individuals.

Postcranial osteoderms and integument

155. Maximum number of contiguous osteoderms per transverse row (excluding basement ossicles): no osteoderms (0) two (1), four (2), six (3), eight (4), ten or more (5). (Brochu 1997: 37, Hill 2005: 313, Burns and Currie, in press: 69)

Updated codings: *Saichania* 3 to ?, as MPC 100/1305 is no longer included in *Saichania*. *Minmi* sp. from ? to 5.

156. Dimensions of largest osteoderm: no osteoderms (0) smaller than a dorsal centrum (1), equal to or larger than a dorsal centrum (2). (Lee 1997: 125, Hill 2005: 309, Burns and Currie, in press: 68)
157. Keel height: no osteoderms (0) shorter than width of osteoderm (1), taller than width of osteoderm (2). (Hill 2005: 320; Burns and Currie, in press 71)
158. Basal surface of osteoderms: no osteoderms (0) flat or gently concave (1), deeply excavated (2), strongly convex (3). (Carpenter 2001:34, Hill 2005:331, Burns and Currie, in press:72).
159. Margin of osteoderms: no osteoderms (0), tapering or rounded (1), crenulated (2), squared-off with sutural boundary (3). (Hill 2005:340; Burns and Currie, in press: 74)
160. External neurovascular grooves on osteoderms: no osteoderms (0) absent or faint (1), present and random (2), present and parallel or radiate (3). (Hill 2005:316; Burns and Currie, in press:70)
161. External rugosity profile of skeletally mature osteoderms: no osteoderms (0) hummocky (1), pitted (2), smooth (3), projecting (4). (Burns and Currie, in press: 83)
162. External cortical histology of skeletally mature osteoderms: no osteoderms (0) lamellar bone (1), ISFB (2). (Burns and Currie, in press: 80)
Updated codings: *Pinacosaurus grangeri* and *P. mephistocephalus*, *Saichania* changed to ?, as the taxonomic assignment of isolated osteoderms used in previous studies cannot be verified.
163. Haversian bone in osteoderms: no osteoderms (0) absent in core of skeletally mature osteoderms (1), may be present in in core of skeletally mature osteoderms (2). (Burns and Currie, in press: 81)
Updated codings: *Pinacosaurus grangeri* and *P. mephistocephalus*, *Saichania* changed to ?, as the taxonomic assignment of isolated osteoderms used in previous studies cannot be verified.

164. Basal cortex of skeletally mature osteoderms: no osteoderms (0) present (1), absent or poorly developed (2). (Burns and Currie, in press: 82)
Updated codings: *Pinacosaurus grangeri* and *P. mephistocephalus*, *Saichania* changed to ?, as the taxonomic assignment of isolated osteoderms used in previous studies cannot be verified.
165. Structural fiber arrangement in osteoderms: no osteoderms (0) structural fibres absent (1), reaches orthogonal arrangement near osteoderm surfaces (2), diffuse throughout (3), highly ordered sets of orthogonally arranged fibers in the superficial cortex (4). (Burns and Currie, in press: 91)
Updated codings: *Pinacosaurus grangeri* and *P. mephistocephalus*, *Saichania* changed to ?, as the taxonomic assignment of isolated osteoderms used in previous studies cannot be verified.
166. Gular osteoderms: absent (0), present (1). (Hill 2005:305; Burns and Currie, in press: 65)
167. Number of distinct cervical pectoral bands: none (0), one (1), two (2). (Kirkland 1998: 38, Thompson et al. 2012:162)
Updated codings: *Shamosaurus* from 1 to 2; two are present in the holotype. *Stegopelta* to ?, as only one is preserved. *Gargoyleosaurus* from 1 to 2, as two are preserved in the holotype.
168. New character: Form of cervical half rings: cervical half rings absent (0), composed of osteoderms that are either tightly adjacent to one another or coossified at the edges, forming arc over the cervical region (1), composed of osteoderms and underlying bony band segments, osteoderms may or may not coossify to the band, forming arc over the cervical region (2).
169. New character: Composition of first cervical half ring with band: no cervical half ring with band (0), first cervical half ring has 4 to 6 primary osteoderms only (1), first cervical half ring has 4 to 6 primary osteoderms surrounded by small (<2 cm diameter) circular secondary osteoderms (2).

170. Distal spines on cervical half ring: absent (0), present, projecting dorsoposteriorly (1), present, projecting anteriorly (2). (Carpenter 2001: 83, Burns and Currie, in press: 85)
171. Osteoderms on proximal limb segments: absent (0), present (1). (deBraga and Rieppel 1997:167, Lee 1997: 127, Heckert and Lucas 1999:60, Hill 2005: 306, Burns and Currie, in press: 66)
172. New character: Millimeter-sized ossicles abundant in spaces between osteoderms in thoracic or caudal regions (excluding pelvic region), absent (0), present (1)
173. New character: Deeply excavated, dorsoventrally flattened triangular osteoderms: absent (0), right or obtuse-angled triangles (1), right or obtuse-angled triangles that abruptly narrow distally into a spike ('splates' of Blows 2001) (2)
174. New character: On deeply excavated triangular osteoderms, furrows perpendicular to basal edge: no deeply excavated triangular osteoderms (0), furrows absent (1), furrows present (2)
175. Modified: Lateralmost osteoderms in thoracic region: absent (0), ovoid or sub-ovoid with a longitudinal keel (1) triangular, dorsoventrally flattened elements (2), solid, conical spikes (3). (Carpenter 2001:36, Hill 2005: 336, Burns and Currie, in press: 73)
176. New character: Thoracic osteoderms coossified to dorsal ribs: no osteoderms coossified to ribs (0), at least some osteoderms coossified to ribs (1)
177. New character: Form of pelvic osteoderms: no osteoderms (0) unfused (1), coossified osteoderm rosettes (2), coossified evenly-sized polygons (3).
178. Caudal osteoderms: absent (0), present on dorsal or dorsolateral surfaces of tail only (1), completely surrounding tail (2). (Hill 2005:307, Burns and Currie, in press: 67)

- 179.Modified: Morphology of proximal, lateral caudal osteoderms: osteoderms absent (0), triangular with round/blunt apex (1) triangular with pointed apex (2). (Hill 2005:342, Burns and Currie, in press: 75)
- 180.Modified: Keel height of caudal osteoderms relative to thoracic osteoderms: osteoderms absent (0), keels equal in external-basal height (1), keels taller in caudal osteoderms (2). (Hill 2005: 343, Burns and Currie, in press: 76)
- 181.New character: Tail club knob shape: knob absent (0), major knob osteoderms semicircular in dorsal view (1), triangular in dorsal view (2).
- 182.New character: Tail club knob proportions: knob absent (0), tail club knob length > width (1), length = width (2), width > length (3)

10.2.4 Analytical methods and software

The character matrix was assembled in Mesquite version 2.72 (Maddison and Maddison, 2011) and analyzed in TNT v1.1 (Goloboff et al. 2008). Characters were treated as unordered and of equal weight. The parsimony analysis conducted in TNT used the Traditional Search option with one random seed and 1000 replicates of Wagner trees and the tree bisection reconnection (TBR) swapping algorithm. The data were then subjected to a bootstrap analysis that was resampled with 1000 replicates using a heuristic search with the TBR swapping algorithm. Bremer supports were calculated in TNT, and the consistency and retention indices were calculated in Mesquite. TAXEQ3 (Wilkinson 2001) was used to identify taxonomic equivalents for wildcard taxa that could then be safely deleted ("Safe Taxonomic Reduction", Wilkinson 2001, 2003). A list of synapomorphies was produced in TNT, and accelerated transformations (ACCTRAN) and delayed transformations (DELTRAN) optimizations were investigated in MacClade v4.08.

Biogeographic reconstructions were performed using the S-DIVA function (Statistical Dispersal-Vicariance Analysis) in RASP 2.1 beta (Reconstruct Ancestral State in Phylogenies, Yu et al. 2010). Biogeographic assignments were divided

into Africa, Asia, Europe, Gondwana, northern North America, and southern North America. North America was subdivided into two biogeographic regions based on current hypotheses of dinosaur provinciality; northern North America includes Alberta, Alaska, and Montana, and southern North America includes California, New Mexico, Utah, and other American states south of Montana. Antarctica, Australia, and South America were grouped into a single region, Gondwana.

The stratigraphic consistency index (SCI) was calculated for the consensus trees produced in the third iteration of the character matrix. The SCI is a relatively simple metric that divides the number of stratigraphically consistent nodes by the total number of nodes on a tree (Huelsenbeck 1994). A node is stratigraphically consistent when the oldest first occurrence above the node is equal to or younger than the oldest first occurrence of the node's sister taxon. The ingroup relationships of the Nodosauridae were not included in the SCI calculation, as the taxon sampling for this clade is incomplete.

10.3 RESULTS

10.3.1 First iteration: All taxa included

The best score of 463 was hit 263 times out of 1000, and 2620 most parsimonious trees were retained. The strict consensus tree recovered all eurypodans (stegosaurs+ankylosaurs) as an unresolved polytomy (Fig. 10.4). *Lesothosaurus* was the most basal taxon in the analysis, and *Scelidosaurus* was the sister taxon to the Eurypoda. The 50% majority rule tree had substantially better resolution, with many clades found in more than 80% of the most parsimonious trees. This suggests that a few species are acting as wildcard taxa, most likely because of large amounts of missing data.

In the majority-rule tree (Fig. 10.4), Ankylosauria, *Antarctopelta*, and *Stegosaurus* formed a polytomy. The basal placement of *Antarctopelta* is almost

certainly incorrect given that the holotype specimen is known from the Campanian and has pelvic osteoderms similar to those of other Cretaceous ankylosaurs. Instead, the basal position of *Antarctopelta* more likely represents missing data, given the fragmentary nature of the only specimen. Two clades within the Ankylosauria are recognized, and represent the Ankylosauridae and Nodosauridae. *Ahshislepelta*, *Minmi* sp., and *Mymoorapelta* were recovered as stem-ankylosaurs; *Ahshislepelta* is probably present in this position because of missing data, given that the only specimen is from Campanian-aged sediments. Although the focus of this dissertation is not on the ingroup relationships of the Nodosauridae, several taxa of interest were recovered as nodosaurids in this analysis. *Tatankacephalus*, originally identified as an ankylosaurid but recovered as a nodosaurid by Thompson et al. (2012), was recovered as a basal nodosaurid in this analysis. The Argentinian ankylosaur was recovered in an unresolved polytomy of derived nodosaurids, including *Panoplosaurus*, *Pawpawsaurus*, and *Sauropelta*. *Glyptodontopelta* and *Stegopelta* were recovered in this clade, as was the Jurassic Chinese taxon *Tianchisaurus*. The placement of the Jurassic-aged *Tianchisaurus* in a relatively derived position within the Nodosauridae is unexpected, and may be influenced by the large amount of missing data for this taxon. *Taohelong* and *Sauroplices* are sister-taxa in this analysis, and together are the sister group to the primarily North American nodosaurids just described. *Dongyangopelta* is found outside of this clade. The results of this analysis present convincing evidence for Asian nodosaurids, with *Dongyangopelta*, *Sauroplices*, and *Taohelong* all present in the Cretaceous of China. Even if a more comprehensive analysis shows that these taxa are part of a 'polacanthine' grade or clade, the nodosaurid (rather than ankylosaurid) affinities of these taxa are clear.

On the other side of the tree, *Gastonia* and *Minmi paravertebra* are recovered as the most basal ankylosaurids. *Aletopelta*, *Cedarpelta*, *Crichtonpelta*,

Liaoningosaurus, and *Gobisaurus*+*Shamosaurus* form an unresolved polytomy

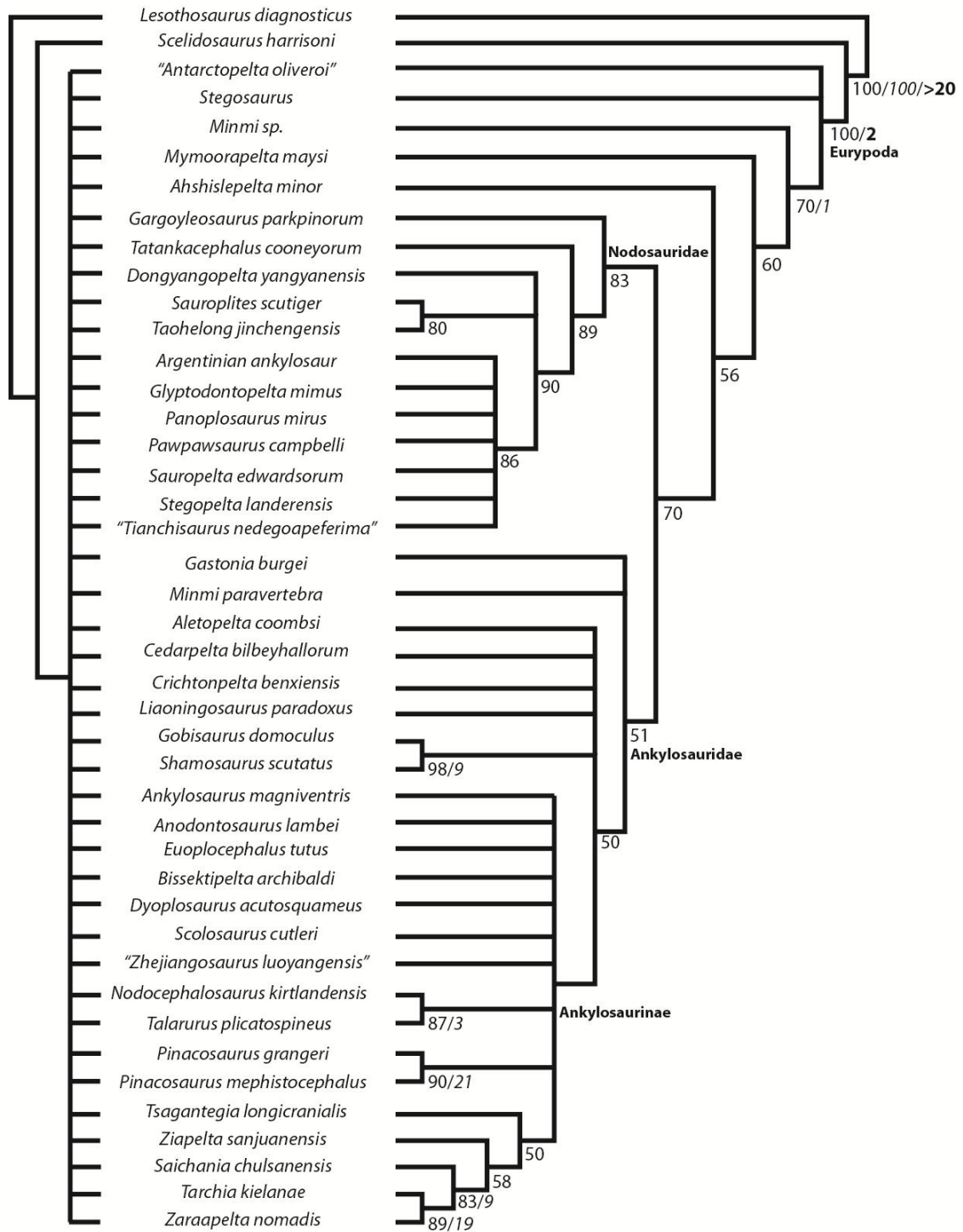


Figure 10.4. Results of the phylogenetic analysis, first iteration, with all taxa included. The strict consensus tree is on the left, and the 50% majority rule tree is on the right. Frequencies (normal font), bootstrap values (italic font), and Bremer supports (bold font) are indicated on the 50% majority rule tree.

with the remaining ankylosaurids. Within the more derived clade of ankylosaurids, *Tarchia* and *Zaraapelta* are sister taxa, with *Saichania*, *Tsagantegia* and *Ziapelta* forming successive outgroups, *Pinacosaurus* is monophyletic, and *Talarurus* and *Nodocephalosaurus* are sister taxa; these clades, and the remainder of the taxa (*Ankylosaurus*, *Anodontosaurus*, *Bissektipelta*, *Dyoplosaurus*, *Euoplocephalus*, *Scolosaurus*, and "*Zhejiangosaurus*"), form an unresolved polytomy. Relationships within this tree are poorly supported; only two steps are required to collapse Euryptoda into an unresolved polytomy. Bootstrap supports for relationships within the Ankylosauria were low, except for *Pinacosaurus grangeri*+*Pinacosaurus mephistocephalus* and *Tarchia*+*Zaraapelta*.

10.3.2 Second iteration: safe taxonomic reduction

Safe taxonomic reduction was performed using TAXEQ3, which identified *Bissektipelta* (95.05% missing data), and *Minmi paravertebra* (97.25% missing data) as safe to remove from the character matrix without removing phylogenetically important information. A new analysis of the revised matrix resulted in 3720 most parsimonious trees, with a best score of 463 hit 474 times out of 1000. Removing *Bissektipelta* and *Minmi paravertebra* from the matrix substantially improved resolution in the strict consensus tree (Fig. 10.5). Distinct nodosaurid and ankylosaurid clades were recovered in 100% of the trees. Within the Ankylosauridae, there was increased resolution within the clade of derived ankylosaurids. Bremer support has increased compared to the first iteration of the analysis, but most clades can be collapsed with only one additional step. Bootstrap values have also increased, but are still low for most clades.

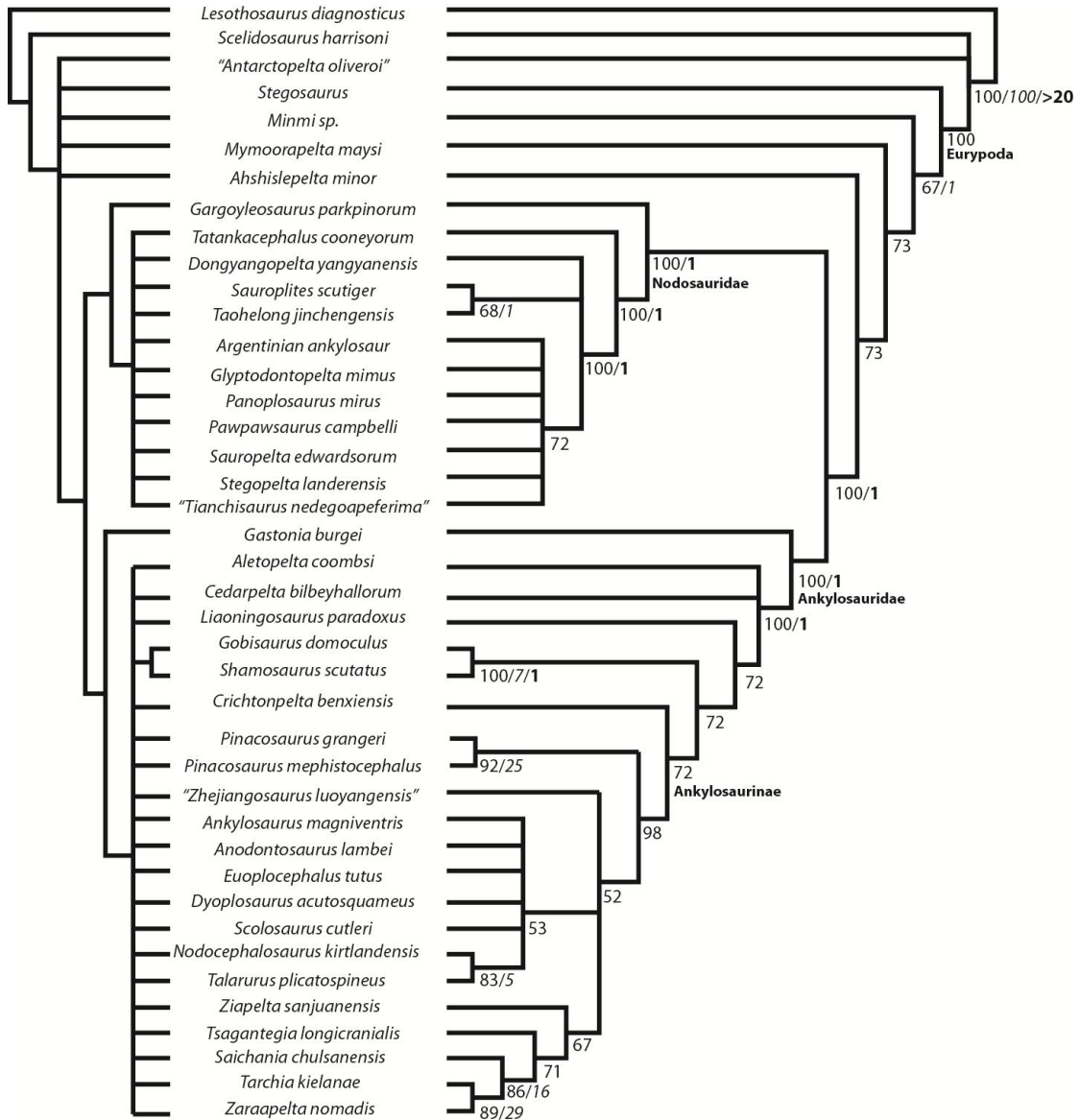


Figure 10.5. Results of the phylogenetic analysis, second iteration, with *Bissektipelta* and *Minmi paravertebra* removed. The strict consensus tree is on the left, and the 50% majority rule tree is on the right. Frequencies (normal font), bootstrap values (italic font), and Bremer supports (bold font) are indicated on the 50% majority rule tree.

10.3.3 Third iteration: additional taxonomic reduction

In the third iteration, additional problematic taxa were removed from the dataset without having been marked as 'safe' to remove by TAXEQ3. In the previous analyses, *Ahshislepelta* (87.36% missing data), *Antarctopelta* (88.46%

missing data), and *Tianchisaurus* (86.81% missing data) were recovered in phylogenetic positions inconsistent with their stratigraphic provenance, and so these taxa were removed from the dataset. In previously published analyses (Thompson et al. 2012, Arbour and Currie 2013a), *Dyoplosaurus* (68.68% missing data) has proven to be particularly labile and to cause instability within derived ankylosaurids (Thompson et al. 2012; Arbour and Currie 2013a), and so it was removed. "*Zhejiangosaurus*" (78.57% missing data) lacks cranial remains and so may also be contributing to instability within the Ankylosauridae, as the remaining taxa with the exception of *Liaoningosaurus* can be coded for most cranial characters. Removing these taxa potentially removes phylogenetically important data, but may also help improve resolution in the trees.

The analysis produced 1600 most parsimonious trees with a best score of 447 hit 446 times out of 1000. The strict consensus trees (Fig. 10.6) shows a topology similar to that of the strict consensus tree in the second iteration, but with a more fully-resolved Ankylosauridae. The majority-rule tree demonstrates that most clades are found in all of the most parsimonious trees. A clade of primarily North American ankylosaurids (*Ankylosaurus*, *Anodontosaurus*, *Euoplocephalus*, *Scolosaurus*, and *Nodocephalosaurus*+*Talarurus*), a clade of primarily Mongolian taxa (*Saichania*, *Tsagantegia*, *Ziapelta*, and *Tarchia*+*Zaraapelta*), *Gobisaurus*+*Shamosaurus*, and a monophyletic *Pinacosaurus* were present in all trees. Bremer supports were highest for this analysis, but again many clades only require one additional step to collapse.

In the strict consensus tree of this analysis, the Ankylosauridae includes *Aletopelta*, *Ankylosaurus*, *Anodontosaurus*, *Cedarpelta*, *Crichtonpelta*, *Euoplocephalus*, *Gastonia*, *Gobisaurus*, *Liaoningosaurus*, *Nodocephalosaurus*, *Pinacosaurus*, *Saichania*, *Scolosaurus*, *Shamosaurus*, *Talarurus*, *Tarchia*, *Tsagantegia*, *Zaraapelta*, and *Ziapelta*. Taxa that were removed from the first analysis, but that were also recovered in this clade in the majority rule tree for

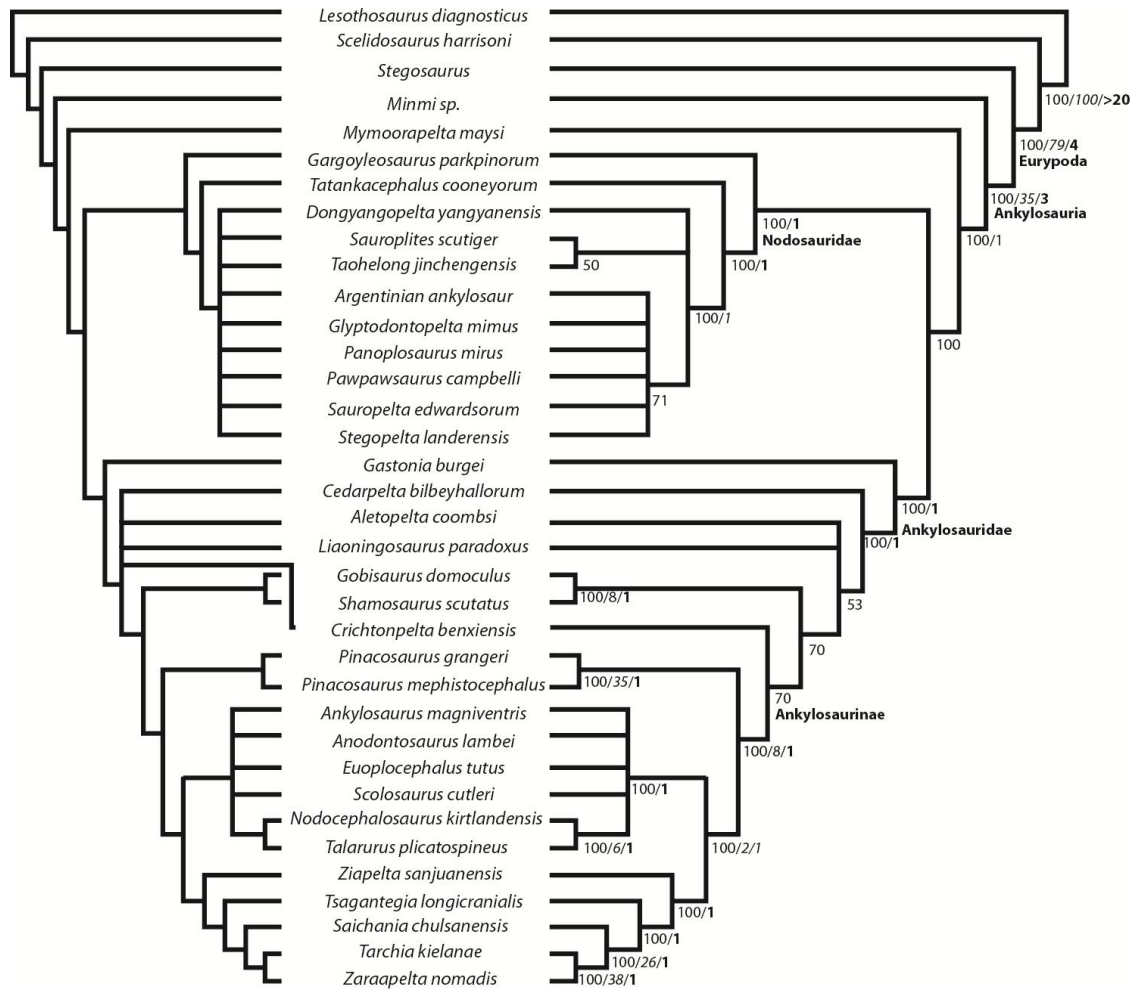


Figure 10.6. Results of the phylogenetic analysis, third iteration, with *Ahshislepelta*, "*Antarctopelta*", *Dyoplosaurus*, "*Tianchisaurus*", and "*Zhejiangosaurus*" removed. The strict consensus tree is on the left, and the 50% majority rule tree is on the right. Frequencies (normal font), bootstrap values (italic font), and Bremer supports (bold font) are indicated on the 50% majority rule tree.

the first iteration include *Bissektipelta*, *Dyoplosaurus*, *Minmi paravertebra*, and "*Zhejiangosaurus*". The Ankylosauridae is characterized by the following characters:

- arched antorbital region (Character 6); reversed to flat in *Talarurus*, and the clade of Mongolian ankylosaurines; also present in *Panoplosaurus*

- maxilla bordering the anterior margin of the internal nares (Character 14); except in *Pinacosaurus grangeri*, where the premaxilla borders the internal nares
- respiratory passage with anterior and posterior loops (Character 18), ACCTRAN
- rugose cranial ornamentation (Character 20); present only in basal members of the clade
- laterally-directed paroccipital processes (Character 73)
- prezygapophyses and neural spines overlap more than half the length of the adjacent vertebra (Character 110), ACCTRAN
- coracoid longer than wide (Character 114), ACCTRAN; reversed from the basal condition in ankylosaurs
- coracoid with straight anterior margin (Character 115), ACCTRAN
- coracoid with anteroventral process (Character 116), ACCTRAN
- acromion process of the scapula flange-like (Character 121), ACCTRAN
- scapulocoracoid buttress (Character 123), ACCTRAN
- fused sternal plates (Character 125), ACCTRAN
- distal width of tibia greater than proximal width (Character 151), ACCTRAN
- crenulated osteoderm margins (Character 159); rounded in *Ziapelta*
- no gular osteoderms (Character 166)
- cervical half rings with an underlying bony band (Character 168)

Ankylosaurids more derived than *Gastonia* share the following synapomorphies:

- lateral temporal fenestra not visible in lateral view (Character 2)
- V or U shaped indentation on midline of premaxillary beak (Character 12), ACCTRAN; also in *Gargoyleosaurus*
- trough-like parietals (Character 52), ACCTRAN

- occiput obscured by the nuchal shelf (Character 55), ACCTTRAN; reversed in *Tarchia* and *Zaraapelta* where occipital condyle is visible
- occipital condyle composed of basioccipital alone (Character 74), ACCTTRAN; reversed in *Gobisaurus*, *Pinacosaurus*, and *Shamosaurus*, where the exoccipital contributes to the occipital condyle as well
- basisphenoidal tuberosities are a transverse rugose ridge (Character 76); reversed in *Gobisaurus* and *Talarurus*
- teeth have rounded crowns with 13 or more denticles (Character 91)
- proximal caudal vertebra neural spine width:height less than 0.2 (Character 106), ACCTTRAN
- prezygapophyses and neural spines overlap more than half the length of the adjacent vertebra (Character 110), DELTRAN
- ossified tendons in the distal part of the tail (Character 113), ACCTTRAN; also present in *Minmi*
- coracoid has cranioventral process (Character 116), DELTRAN
- scapula has a ventral process at the glenoid (Character 120), ACCTTRAN
- scapular blade is narrow distally (Character 124), ACCTTRAN
- postacetabular ilium length smaller than the diameter of the acetabulum (Character 126)
- acetabulum obscured laterally (Character 131), ACCTTRAN
- pubis reduced and indistinct from ilium (Character 134), ACCTTRAN
- straight ischia (Character 135) with convex dorsal margins (Character 136)
- 4th trochanter located midway down the femur (Character 150); also present in *Gargoyleosaurus*
- distal width of tibia greater than proximal width (Character 151), DELTRAN

A derived clade containing most of the Asian and North American taxa represents most taxa typically considered 'ankylosaurine' ankylosaurids by

previous workers. The Ankylosaurinae was named by Nopcsa (1918) but formally defined by Sereno (1998) as all ankylosaurids more closely related to *Ankylosaurus* than to *Minmi* or *Shamosaurus*, and was revised by Vickaryous et al. (2004) as all ankylosaurids more closely related to *Ankylosaurus* than to *Shamosaurus*. In this study, the Ankylosaurinae includes *Ankylosaurus*, *Anodontosaurus*, *Euoplocephalus*, *Nodocephalosaurus*, *Pinacosaurus*, *Saichania*, *Scolosaurus*, *Talarurus*, *Tarchia*, *Tsagantegia*, *Zaraapelta*, and *Ziapelta*. In 73% of the most parsimonious trees in the third iteration, *Crichtonpelta* was the most basal ankylosaurine. Taxa that were removed from the first analysis, but that were also recovered in this clade in the majority rule tree for the first iteration include *Bissektipelta*, *Dyoplosaurus*, and "*Zhejiangosaurus*". The Ankylosaurinae is supported by numerous synapomorphies, including:

- skull as wide or wider than long (Character 4), ACCTAN; reversed in *Tsagantegia*
- premaxillary palate longer than wide (Character 11), ACCTAN
- premaxillary tomium obscures anteriormost maxillary teeth (Character 13); also present in *Gastonia*
- opening of external naris faces anteriorly (Character 15), ACCTAN; except for *Ankylosaurus*, where the narial opening faces ventrolaterally
- respiratory passage with anterior and posterior loops (Character 18), DELTRAN
- loreal caputegulum (Character 27), ACCTAN
- maxillary tooth row medially convex (Character 28); also present in *Minmi* sp. and derived nodosaurids
- width between posteriormost extent of maxillary tooth rows narrower than width of premaxillary beak (Character 30); except in *Ankylosaurus* and *Saichania*, where width is greater
- lacrimal caputegulum (Character 35)
- prefrontal caputegulum (Character 36)

- supraorbitals form a sharp edge above orbit (Character 38)
- squamosal horns project past posterior margin of skull in dorsal view (Character 47), ACCTRAN; except in *Anodontosaurus*, *Euoplocephalus*, *Talarurus*, and *Tsagantegia*
- two or more nuchal caputegulae (Character 54), ACCTRAN
- occiput obscured by the nuchal shelf (Character 55), DELTRAN; reversed in *Tarchia* and *Zaraapelta* where occipital condyle is visible
- quadrate obscured by quadratougal horn (Character 59), ACCTRAN; not obscured in *Tarchia*
- median vomer lamina meets skull roof (Character 69), DELTRAN; reversed in *Tarchia*
- pterygoid foramen present (Character 70)
- cervical neural spine width:height ratio is greater than 0.25 (Character 97), DELTRAN
- ossified tendons in the distal part of the tail (Character 113), DELTRAN; also present in *Minmi*
- coracoid with straight anterior margin (Character 115), DELTRAN
- scapula has a ventral process at the glenoid (Character 120), DELTRAN
- scapulocoracoid buttress (Character 123), DELTRAN
- fused sternal plates (Character 125), DELTRAN
- acetabulum obscured laterally (Character 131), DELTRAN
- pubis reduced and indistinct from ilium (Character 134), DELTRAN
- deltopectoral crest greater than 50% length of humerus (Character 139), ACCTRAN
- >120° angle between long axis of femoral head and long axis of shaft (Character 145), DELTRAN; also present in *Gargoyleosaurus*
- tibia and astragalus fused (Character 152), DELTRAN; also present in *Aletopelta* and some nodosaurids
- three pedal digits (Character 153), DELTRAN

- tail club knob osteoderms present, semicircular in dorsal view (Character 181), with length approximately equal to width (Character 182), ACCTRAN

Gobisaurus and *Shamosaurus* are the sister-group to the Ankylosaurinae (i.e. the Shamosaurinae) and are united by the following synapomorphies:

- deep longitudinal furrow on premaxilla (Character 7)
- external nares hidden in dorsal view (Character 16); also present in derived ankylosaurines
- quadratojugal horn basal length greater than 110% orbit length (Character 50); also present in derived ankylosaurines

The basalmost ankylosaurines are *Pinacosaurus grangeri* and *Pinacosaurus mephistocephalus*, and possibly *Crichtonpelta*. The two species of *Pinacosaurus* are united by the presence of paranasal apertures or fossae (also present in *Saichania*, *Tarchia*, and *Zaraapelta*) and a jugal orbital ramus height less than 15% the height of the orbit (also present in *Tarchia*). These form the outgroup to an unnamed clade of derived ankylosaurines, characterized by:

- frontonasal ornamentation differentiated into flat caputegulae (Character 20); also present in derived nodosaurids
- supranarial caputegulae (Character 24)
- hexagonal median nasal caputegulum (Character 26), ACCTRAN; triangular in *Ziapelta*, absent in *Saichania*, *Tarchia*, and *Zaraapelta*
- one loreal caputegulum (Character 27), DELTRAN; also present in *Panoplosaurus*
- more than 30 caputegulae in the frontonasal and prefrontal regions (Character 31)

- posterior palatal foramen (Character 32), ACCTRAN; absent in *Tsagantegia*
- frontal has scroll-like descending process (Character 37)
- quadratojugal horn basal length greater than 110% orbit length (Character 50); also present in *Gobisaurus* and *Shamosaurus*
- more than two nuchal caputegulae (Character 54), DELTRAN
- occipital condyle formed by basioccipital alone (Character 74), DELTRAN; also present in *Cedarpelta*, *Crichtonpelta*, and many nodosaurids
- retroarticular process with dorsal projection (Character 85)
- mandibular caputegulum over three quarters length of mandible (Character 87)
- lateralmost osteoderms in thoracic region are ovoid with a longitudinal keel (Character 175); also present in *Scelidosaurus*

A clade of primarily North American ankylosaurids includes *Ankylosaurus*, *Anodontosaurus*, *Euoplocephalus*, *Nodocephalosaurus*, *Scolosaurus*, and *Talarurus* (Mongolian). *Nodocephalosaurus* and *Talarurus* are united to the exclusion of all other taxa in this clade by the presence of domed caputegulae that are rounded cones. This North American clade is characterized by the following features:

- vascular impressions on dorsal surface of posterior respiratory passage (Character 19); absent in *Talarurus*
- single hexagonal median nasal caputegulum (Character 26), DELTRAN; also present in *Tsagantegia*, and a single triangular median nasal caputegulum is present in *Ziapelta*
- posterior palatal foramen (Character 32), DELTRAN; also present in *Saichania*
- ciliary osteoderm (Character 41), ACCTRAN

- posterior margin of pterygoid body in transverse alignment with anterior margin of quadrate condyle (Character 71); also present in *Gastonia*, nodosaurids more derived than *Tatankacephalus*
- proximal caudal vertebra neural spine width:height less than 0.2 (Character 106), DELTRAN; also present in *Cedarpelta*
- acromion process ridge-like along dorsal border of scapula (Character 121)
- osteoderm neurovascular groove pattern random (Character 160)
- millimeter-sized ossicles abundant in spaces between osteoderms in thoracic or caudal regions (excluding pelvic region) (Character 171); also present in *Minmi*

The sister-group to this North American clade is a clade of primarily Mongolian ankylosaurines, including *Saichania*, *Tarchia*, *Tsagantegia*, *Zaraapelta*, and *Ziapelta* (North American). Only a few characters support this clade:

- atlas and axis coossified (Character 93), ACCTAN; also present in *Panoplosaurus*
- cervical half ring with interstitial osteoderms surrounding the primary osteoderms (Character 169); also present in *Anodontosaurus*

Within this clade, *Saichania*, *Tarchia*, *Tsagantegia* and *Zaraapelta* are united by:

- flat antorbital region (Character 6); also present in basal ankylosaurs and most nodosaurids
- 11 to 30 caputegulae in the frontonasal and prefrontal region (Character 21)
- internarial caputegulae (Character 25)
- two nuchal caputegulae (Character 54); also present in *Shamosaurus*

- paroccipital process and quadrate coossified (Character 64); unfused in *Tarchia*

A deeply nested clade contains *Saichania*, *Tarchia*, and *Zaraapelta*. These taxa are united by numerous features:

- ornamentation on premaxillary beak (Character 8)
- external nares hidden in dorsal view (Character 16); also present in North American clade of ankylosaurines and *Gobisaurus*+*Shamosaurus*
- paranasal apertures or fossae (Character 17); also present in *Pinacosaurus*
- frontonasal caputegulae bulbous and pyramidal (Character 22)
- no hexagonal median nasal caputegulum (Character 26), ACCTRAN
- postocular caputegulae (Character 51); also present in *Anodontosaurus* and *Scolosaurus*
- single opening for cranial nerves IX-XII (Character 78), ACCTRAN; separate openings in *Zaraapelta*

Finally, *Tarchia* and *Zaraapelta* are united by the following features:

- multiple lacrimal caputegulae (Character 35)
- sharply pointed, pyramidal prefrontal caputegulum (Character 36)
- supraorbitals have distinct apices (Character 39), ACCTRAN; also present in *Nodocephalosaurus*, *Pinacosaurus grangeri*
- occiput not obscured in dorsal view (Character 55)

10.3.4 Results of the biogeographic analysis

The results of the biogeographic analysis in RASP are presented in Figure 10.7. SDIVA cannot accept polytomies, so tree 1 from the third iteration of the dataset was used for this analysis. The results indicate a southern North American origin for the Ankylosauridae, and an Asian origin for all ankylosaurids more derived than *Liaoningosaurus*.

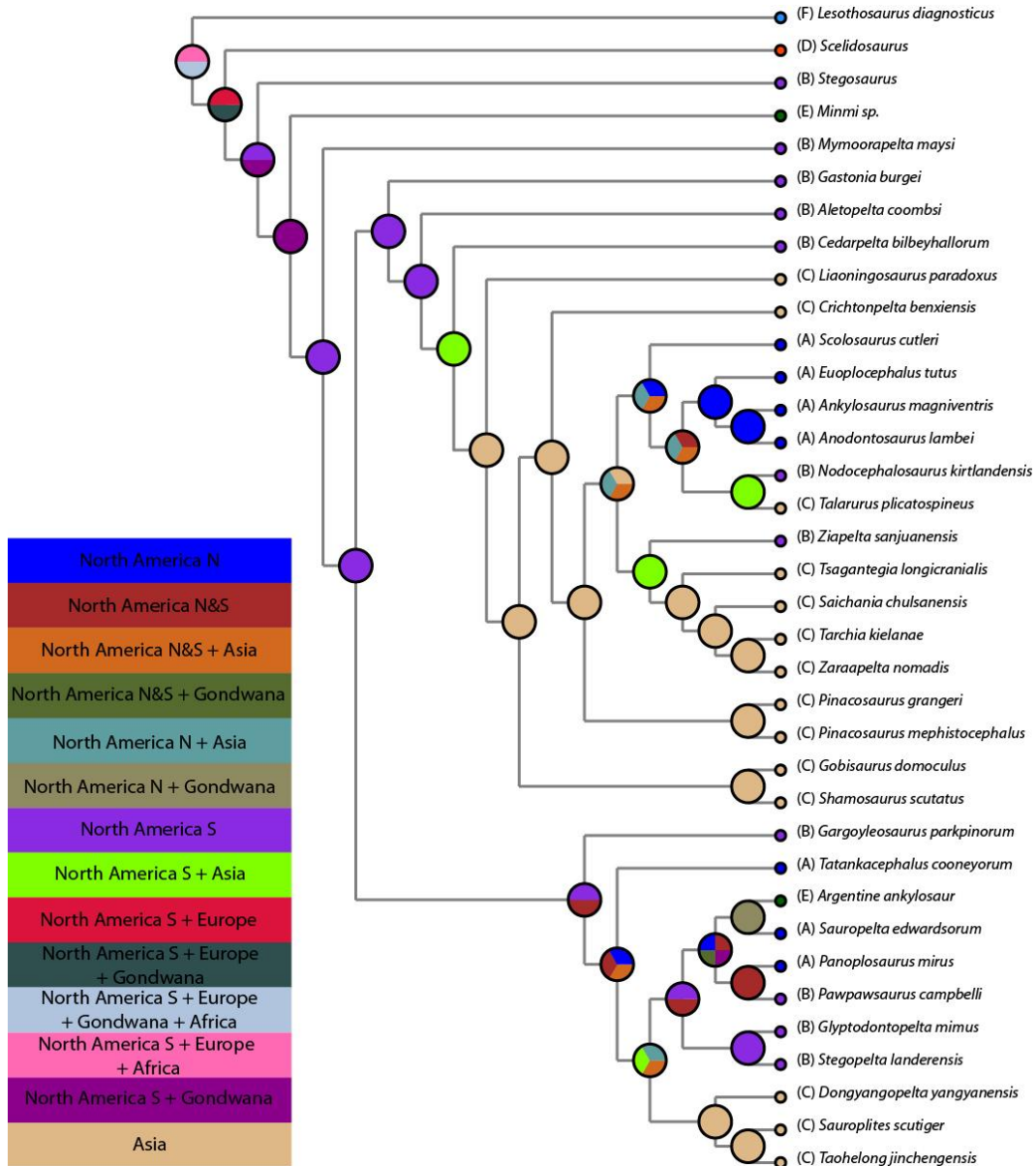


Figure 10.7. Results of the biogeographic analysis using S-DIVA. North America - South includes American states south of Montana, and North America - North includes Alberta, Canada and Montana, USA.

10.4 Discussion

The preferred tree in this dissertation is the strict consensus tree of the third iteration of the dataset (Fig. 10.8), with one modification: *Crichtonpelta* was recovered as more derived than *Shamosaurus*+*Gobisaurus* in 70% of the most parsimonious trees, and is shown in this position in all figures from this point onwards. The remainder of this discussion will use this tree as the basis for comments about the relationships and evolution of the ankylosaurids.

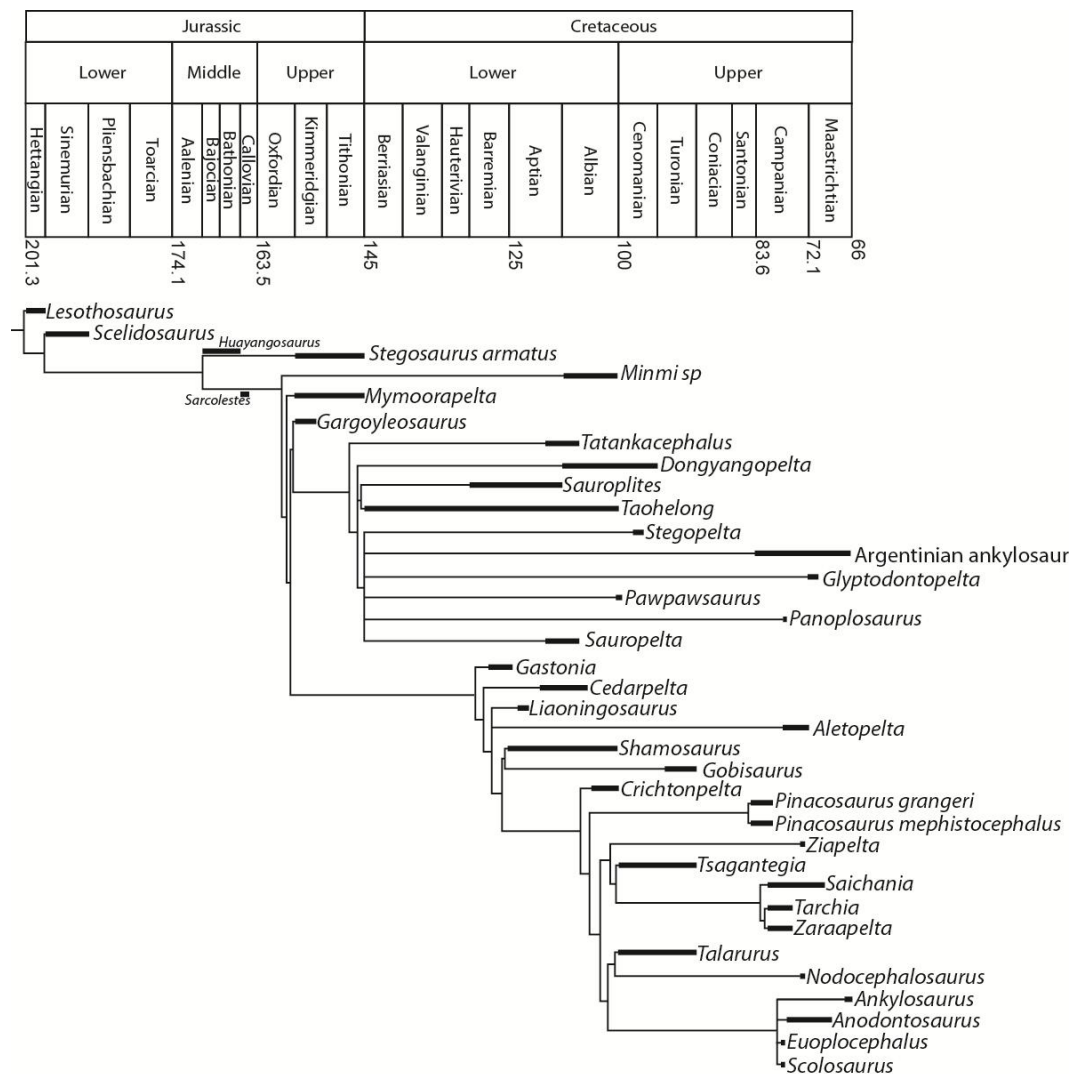


Figure 10.8. Time-calibrated phylogeny of the Ankylosauridae and selected nodosaurids and other thyreophorans, based on the strict consensus tree of the third iteration of the character matrix.

10.4.1 Nodosaurid ankylosaurs were present in Asia

Some authors (Chen et al. 2013, Hawakaya et al. 2005, Lu et al. 2007, Xu et al. 2007, Yang et al. 2013), have argued for the presence of nodosaurids in Asia, but these arguments have sometimes been based on incorrect interpretations of plesiomorphic ankylosaur features as representative of the nodosaurid condition. For example, *Zhongyuansaurus* (considered a junior synonym of *Gobisaurus* here) was considered a nodosaurid by Xu et al. (2007) because its skull was longer than wide. Anteroposteriorly short skulls are a derived feature of some ankylosaurids, and so the presence of a long snout cannot be used to refer an ankylosaur to the Nodosauridae. However, several ankylosaurs from China (*Dongyangopelta*, *Sauroplices*, and *Taohelong*) were recovered as relatively derived nodosaurids in the revised phylogenetic analysis presented here. *Taohelong* was recovered as the sister taxon to *Polacanthus* by Yang et al. (2013), but *Polacanthus* was not included in the dataset for this dissertation. Additional taxon sampling (for example, including *Hoplitosaurus*, *Hylaeosaurus*, and *Polacanthus*) in future analyses may recover a polacanthid or polacanthine clade that includes *Dongyangopelta*, *Sauroplices*, and *Taohelong*.

Other Asian ankylosaurs previously considered to represent nodosaurids included *Zhejiangosaurus* and a specimen from Japan. *Zhejiangosaurus* was recovered as an ankylosaurid in this analysis. The Japanese ankylosaur material was not included in the revised phylogenetic analysis. However, the morphology of the teeth is more consistent with that of nodosaurid ankylosaurs.

10.4.2 Shamosaurinae is monophyletic but unnecessary

Gastonia, *Cedarpelta*, *Liaoningosaurus*, and *Gobisaurus*+*Shamosaurus* formed successive outgroups to a clade of more derived ankylosaurids. *Liaoningosaurus* may occupy this basal position because of missing data, or because it is a juvenile; juvenile individuals are sometimes recovered in more basal positions than adults of the same species when coded separately in

phylogenetic analyses (Campione et al. 2013). On the other hand, a relatively basal position in Ankylosauridae is consistent with the Lower Cretaceous provenance of *Liaoningosaurus*, and *Liaoningosaurus* retains premaxillary teeth, which are lost in more derived ankylosaurines. Regardless, *Gobisaurus* and *Shamosaurus* are so similar in anatomy that it would not be ill conceived to subsume *Gobisaurus domoculus* as a second species of *Shamosaurus*; an entire subfamily for these two species seems unwarranted. Instead, *Cedarpelta*, *Gastonia*, *Gobisaurus*, *Liaoningosaurus*, and *Shamosaurus* should simply be considered stem or basal ankylosaurids.

10.4.3 Stegopeltinae is not monophyletic

This analysis finds no support for the Stegopeltinae, although it should be noted that all putative 'stegopeltines' are fragmentary. *Glyptodontopelta* and *Stegopelta* were both recovered as derived nodosaurids, but were never recovered as sister-taxa. *Antarctopelta* consistently fell outside of the Euryopoda until it was removed, and *Aletopelta* is recovered as a relatively derived ankylosaurid. *In situ* pelvic osteoderms are unknown for many nodosaurids, and future discoveries may show that pelvic shields with coossified hexagonal osteoderms are more widely distributed among nodosaurids than currently recognized; fragments of this pelvic shield morphology from the Dinosaur Park Formation (Arbour et al. 2011), from which *Edmontonia* and *Panoplosaurus* are known but no potential 'stegopeltines' have been recovered, lends support to this hypothesis. It should also be noted, however, that the pelvic osteoderms of *Aletopelta* vary more widely in size, and are not as sharply hexagonal, compared to those in *Antarctopelta* and *Glyptodontopelta*. The pelvic osteoderm morphology in *Aletopelta* may not be homologous to that of the other 'stegopeltine' ankylosaurs. More complete taxonomic sampling of the Nodosauridae is probably needed to resolve whether or not the Stegopeltinae is a valid clade of ankylosaurs.

10.4.4 *Ahshislepelta*, *Tatankacephalus*, and most 'polacanthids' are nodosaurids

Ahshislepelta and *Tatankacephalus* have previously been described as ankylosaurid ankylosaurs, although Thompson et al. (2012) recovered *Tatankacephalus* as a nodosaurid. The results of this analysis suggest that both *Ahshislepelta* and *Tatankacephalus* are nodosaurids.

Although the validity of the proposed Polacanthidae or Polacanthinae was not the main focus of this review, some comments are warranted. Coossified pelvic osteoderms forming a continuous sheet across the pelvis (a pelvic or sacral shield) have been considered by many authors to be a synapomorphy of this clade (Kirkland 1998, Carpenter 2001). However, coossified pelvic osteoderms are present in most of the stratigraphically lowest ankylosaurs, such as *Gastonia*, *Gargoyleosaurus*, and *Mymoorapelta*, which were recovered as basal members of the Ankylosauria, Nodosauridae, and Ankylosauridae, respectively. Coossified pelvic osteoderms are also present in stratigraphically higher ankylosaurs, such as *Glyptodontopelta* and *Stegopelta* (here recovered as derived nodosaurids) and *Aletopelta* (here recovered as a basal ankylosaurid). The presence of a pelvic shield in numerous basal ankylosaurs, as well as in more derived members of both the Nodosauridae and Ankylosauridae, suggests that fused pelvic osteoderms are plesiomorphic for ankylosaurs, and not a synapomorphy of a polacanthid or polacanthine clade. Another feature commonly ascribed to a polacanthid clade is the presence of flattened, triangular osteoderms, but these are also present in derived ankylosaurids from the Upper Cretaceous of Mongolia. Additional taxon sampling is required to fully resolve the validity of the Polacanthidae or Polacanthidae, but the results of this analysis suggest that polacanthine or polacanthid taxa are basal ankylosaurs.

10.4.5 Gondwanan ankylosaurs are not monophyletic

In all analyses, the Early Cretaceous *Minmi* sp. was recovered as a basal ankylosaur, in a more basal position than Jurassic ankylosaurs from North America. The absence of more derived ankylosaurs in Australia can mostly be attributed to the scarcity of Upper Cretaceous dinosaur-bearing localities and discoveries. Although "*Antarctopelta*" was recovered as a basal eurypodan, this most likely reflects the large amount of missing data for this specimen. The presence of a pelvic shield composed of coossified hexagonal osteoderms in this taxon suggests that *Antarctopelta* has affinities to Late Cretaceous nodosaurids from North America, like *Glyptodontopelta*. The Argentinian ankylosaur was nested deep within the sampled nodosaurids in this analysis, and most likely represents a southern migration of North American nodosaurids into South America during the Late Cretaceous, as suggested by Coria and Salgado (2001). At present, there is no evidence for a unique Gondwanan radiation of ankylosaurs; the Antarctic and South American ankylosaurs more likely represent a southward migration of nodosaurids from North America during the Late Cretaceous. However, ankylosaurs are unknown from the Upper Cretaceous of Australia, so future discoveries may demonstrate a unique Australian radiation of ankylosaurs.

10.4.6 Cranial caputegulae evolved independently in ankylosaurids and nodosaurids

Cranial ornamentation has been underutilized in ankylosaur phylogenetic analyses, but the results of this analysis show that carefully selected features can help resolve ankylosaurid interrelationships. Similar approaches may yield productive results for nodosaurids, which were poorly resolved in the analysis by Thompson et al. (2012).

Discrete caputegulae appear to have evolved independently in nodosaurids and ankylosaurids. The basalmost members of both clades have

rugose, amorphous cranial ornamentation. In ankylosaurids, caputegulae only appear in the ankylosaurines. North American ankylosaurines typically had more numerous frontonasal caputegulae than Asian ankylosaurines, and generally had flat caputegulae (with the exception of *Nodocephalosaurus*, and to a certain extent *Ziapelta*). In contrast, Mongolian ankylosaurines had fewer frontonasal caputegulae, which were typically bulbous (with the exception of *Tsagantegia*).

10.4.7 The tail club handle appears before the knob in the fossil record

The oldest specimen to possess either of the two modifications present in derived ankylosaurid tail clubs (distal caudal vertebrae modified to form a handle, or terminal osteoderms enlarged and enveloping the tail terminus) is the holotype (41HIII-0002; Fig. 7.2) of *Zhongyuansaurus* (here synonymized with *Gobisaurus*). Thompson et al. (2012) considered *Zhongyuansaurus* to be the first known ankylosaurid in which the tail club was definitively absent. However, 41HIII-0002 clearly preserves the distal section of the tail, and the distal caudal vertebrae have the characteristic morphology of handle vertebrae from more derived ankylosaurids. 41HIII-0002 was collected from no earlier than the Barremian of China, and so the tail club handle had evolved at least by that point. However, in 73% of the most parsimonious trees from the third iteration of the character matrix, *Crichtonpelta* was recovered as more derived than *Gobisaurus*, and *Crichtonpelta* occurs in the late Albian of China. The mounted skeleton on display at the Sihetun Fossil Museum is presented as having a tail club, but it is unclear if this has been sculpted or if it represents real fossil material, and the tail vertebrae have not yet been described or figured. *Crichtonpelta* may have also possessed handle vertebrae.

At the base of the Ankylosauridae, *Gastonia* most likely did not have either a tail club handle or knob. Bonebed material of *Gastonia* at the DMNH includes hundreds of caudal vertebrae of many sizes and positions within the vertebral series, and none have the distinctive morphology of handle vertebrae.

Additionally, no knob-like osteoderms are present in this collection, either. Caudal material for *Cedarpetta* is more fragmentary, and distal caudal vertebrae are currently unknown. *Liaoningosaurus*, from the early Aptian of China, does not possess a tail club knob. However, osteoderms are only preserved in the pectoral region (Fig. 8.4), as in juvenile *Pinacosaurus*, and so it is possible that the full complement of osteoderms had not yet developed in the holotype specimen IVPP V12560. One intriguing observation is the apparent rigidity of the distal tail in IVPP V12560, a feature also present in other *Liaoningosaurus* specimens on display in China (CYGYB 208, CYGYB 237). The neural arches of distal tail vertebrae interlock in all of these specimens, and the prezygapophyses overlap the adjacent vertebra by at least 50% of the centrum length, a feature not present in more basal ankylosaurids where the overlap is only about 25% of the centrum length (e.g. *Mymoorapelta* MWC 5819; Fig. 10.9), but which is present in ankylosaurid handle vertebrae. Based on the available specimens, *Liaoningosaurus* may have had a tail club handle, pushing the origin of the ankylosaurid tail club back to the early Aptian.

41HIII-0002 preserves a tail club handle that includes the terminal caudal vertebra, but no traces of the knob osteoderms are present. Knob osteoderms may have been present and simply disarticulated from the handle after death. However, in isolated tail club knobs from more derived ankylosaurids, there are almost always some fragments of the distal caudal vertebrae associated with the knob or knob osteoderms, most likely because of the close association between these elements in the living animal. *Gobisaurus* is the most basal ankylosaurid to preserve evidence for a tail club. This suggests that the handle-first hypothesis may best explain the evolution of the ankylosaurid tail club. However, hypothesis 3, the tandem handle and tail club evolution hypothesis, cannot be ruled out. More basal taxa like *Gargoyleosaurus* and *Scelidosaurus* had spiky lateral tail osteoderms that would certainly have been effective weapons if the tails were swung from side to side, even if they were not being used to deliver forceful



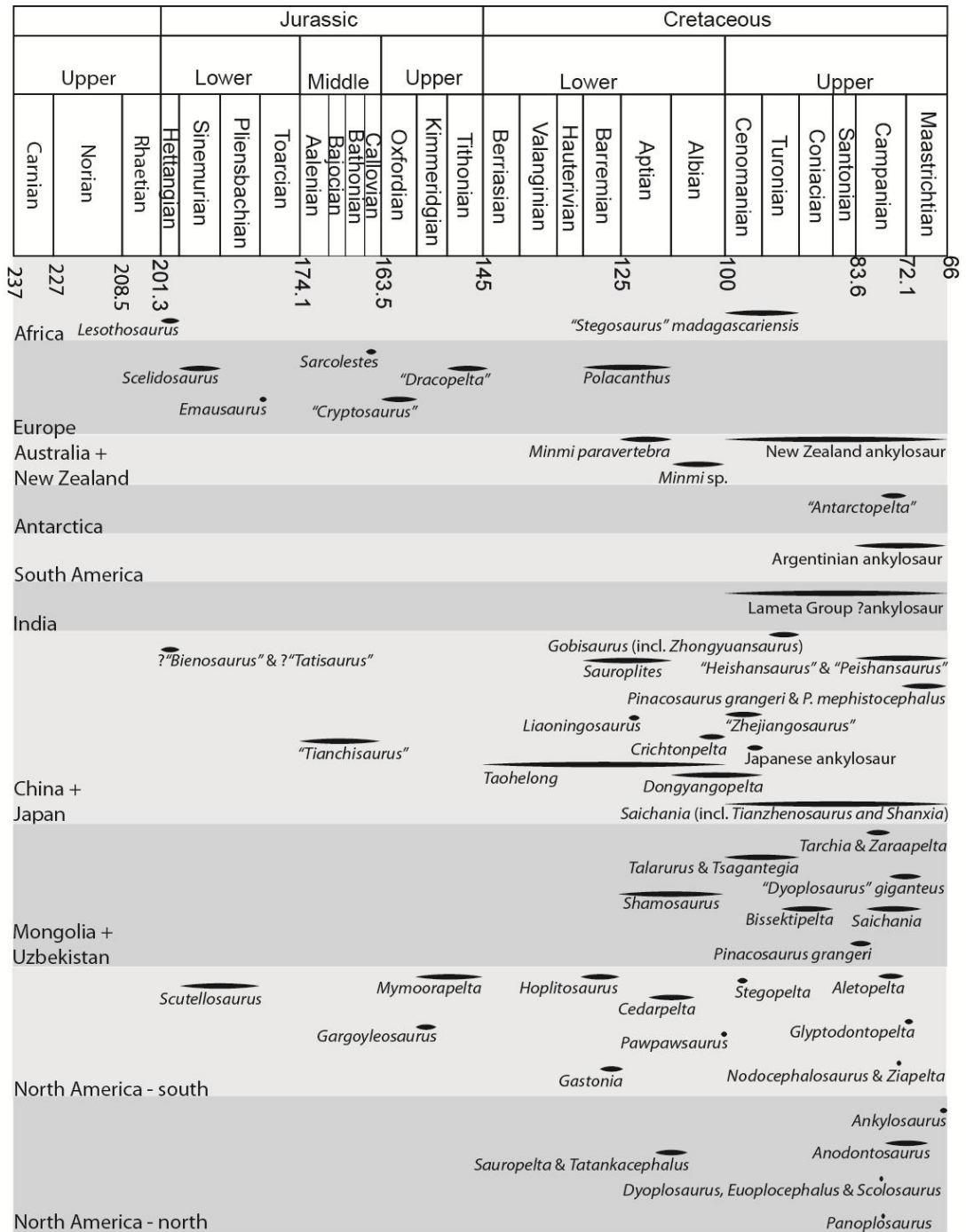
Figure 10.9. Distal caudal vertebrae of *Liaoningosaurus* and *Mymoorapelta* compared. A) MWC 5819, two distal caudal vertebrae of *Mymoorapelta maysi*, anterior is to the right. B) IVPP V12560, holotype of *Liaoningosaurus paradoxus*, distal caudal vertebrae, anterior is to the left.

impacts. The knob-first hypothesis can probably be rejected. A tail club knob is unknown in any taxon (or in any of the strata these taxa are recovered from) that lacks handle vertebrae; the putative knob of *Tianchisaurus* is dissimilar to the knobs of derived ankylosaurids, and most likely does not represent a true knob (see Chapter 8). Biomechanically speaking, a large knob of dermal bone at the end of a flexible tail should more easily result in trauma to the bones and connective tissues in the distal tail, making the knob-first scenario unlikely.

10.4.8 Ankylosaurines replace nodosaurids in Asia during the late Early Cretaceous, and migrate into North America during the mid Late Cretaceous

The stratigraphic record (Fig. 10.10) of Ankylosauria begins in the Middle Jurassic with enigmatic and rare taxa like *Cryptosaurus* and *Sarcolestes*. In this analysis, *Gargoyleosaurus* was recovered as a basal nodosaurid, meaning that the divergence of the Nodosauridae from the Ankylosauridae must have occurred by the Kimmeridgian. If future analyses recover *Gargoyleosaurus* as a more basal taxon outside the ankylosaurid-nodosaurid split, then the two clades must have at least diverged by the mid Early Cretaceous, based on the basal ankylosaurids *Cedarpelta* (Aptian-Albian), *Gastonia* (Aptian), and *Liaoningosaurus* (Aptian). Ankylosaurine ankylosaurids had evolved by the Cenomanian-Turonian, or by the Albian if *Crichtonpelta* is an ankylosaurine.

Excluding the ingroup relationships of the Nodosauridae in this study, the 50% majority rule tree of iteration three (in which *Crichtonpelta* is an ankylosaurine) has a stratigraphic consistency index of 0.71. *Aletopelta*, *Cedarpelta*, *Minmi* sp., and *Ziapelta* occur in the 'wrong' positions on the tree based on their stratigraphic provenance, although *Cedarpelta* is only somewhat out of place. Stratigraphically and biogeographically, *Ziapelta* would be expected to occur in the clade of North American ankylosaurines, but instead it was recovered as the basalmost member of a clade of Mongolian ankylosaurines, for reasons that are unclear at present. *Aletopelta* may occur in a relatively basal position within the Ankylosauridae because of missing data, and the biogeographic and evolutionary relationships of this taxon remain enigmatic. *Minmi* sp. is often recovered as a basal ankylosaur but occurs in the Albian, well after the nodosaurid-ankylosaurid split in the Late Jurassic or Early Cretaceous. Perhaps *Minmi* sp. represents a clade of Australian ankylosaurs that diverged from the ankylosaurid-nodosaurid lineage, but additional specimens and taxa from Australia are required in order to demonstrate a unique Australian clade of ankylosaurs.



The presence of nodosaurid ankylosaurs (including 'polacanthine' taxa) in the Early Cretaceous of Asia, North America, and Europe indicates that nodosaurids must have achieved a Laurasian distribution early in their evolution.

It is unlikely that the absence of Late Cretaceous nodosaurids in Asia is a result of insufficient sampling, as Late Cretaceous sediments in Mongolia have been intensively sampled for nine decades. Their absence in the Late Cretaceous of Asia therefore represents the extinction of this lineage in that region. Why nodosaurids went extinct in Asia but continued to thrive in North America and Europe is unknown. However, it is interesting that the Asian nodosaurids seem to have disappeared as the Asian ankylosaurids began to diversify. Better stratigraphic resolution of many of the Lower and middle Cretaceous Asian ankylosaurs is needed in order to investigate this pattern further.

Results from the biogeographic analysis demonstrate that ankylosaurine ankylosaurids originated in Asia, and later migrated into North America. This analysis also suggests that ankylosaurids had a southern North American origin, but the absence of diagnostic Jurassic ankylosaurs from Asia that could be included in the phylogenetic analysis must influence this result. Based on their stratigraphic distribution, ankylosaurines must have migrated into North America no later than the Campanian, but more likely between the Albian and Turonian.

Figure 10.10 [previous page]. Stratigraphic distributions of ankylosaurs and early thyreophorans discussed in this dissertation. *Lesothosaurus* is a basal ornithischian or basal ankylosaur, and "*Bienosaurus*", *Emausaurus*, *Scelidosaurus*, *Scutellosaurus*, and "*Tatisaurus*" are basal thyreophorans. Ankylosaurs of uncertain affinity include "*Antarctopelta*", "*Cryptosaurus*", "*Dracopelta*", *Minmi paravertebra*, *Sarcolestes*, "*Stegosaurus*" *madagascariensis*, "*Tianchisaurus*", and specimens from India, Japan, and New Zealand. *Minmi* sp. and *Mymoorapelta* are the most basal ankylosaurs. Nodosaurid ankylosaurs include *Ahshislepelta*, *Dongyangopelta*, *Gargoyleosaurus*, *Glyptodontopelta*, *Hoplitosaurus*, *Panoplosaurus*, *Pawpawsaurus*, *Polacanthus*, *Sauropelta*, *Sauroplices*, *Stegopelta*, *Taohelong*, *Tatankacephalus*, and the Argentinian ankylosaur. Ankylosaurid ankylosaurs include *Aletopelta*, *Ankylosaurus*, *Anodontosaurus*, *Bissektipelta*, *Cedaropelta*, *Crichtonopelta*, *Dyoplosaurus*, *Euoplocephalus*, *Gastonia*, *Gobisaurus*, *Liaoningosaurus*, *Nodocephalosaurus*, *Pinacosaurus*, *Saichania*, *Scolosaurus*, *Shamosaurus*, *Talarurus*, *Tarchia*, *Tsagantegia*, *Zaraapelta*, "*Zhejiangosaurus*", *Ziapelta*.

Ambiguity in the timing of the Asian-North American dispersal results from imprecision in the age of two key taxa, *Talarurus* and *Tsagantegia*. Both taxa are from the same formation in Mongolia, but *Tsagantegia* is recovered as a member of a primarily Asian clade of ankylosaurines, and *Talarurus* is recovered as a member of a primarily North American clade of ankylosaurines. The age range of these specimens is anywhere from Cenomanian to Turonian. Additional stratigraphic work on the Bayanshiree Formation is required in order to further investigate the timing of ankylosaurine dispersals into North America from Asia.

At present, the biogeographic distribution of ankylosaurids in North America cannot be used to support or reject hypotheses of dinosaur provinciality in Laramidia, because the southern species (*Nodocephalosaurus* and *Ziapelta*) occur at a time where ankylosaurids are unknown in northern Laramidia (see Chapter 4). In eastern North America (Appalachia), dinosaur remains are much less common, but fragmentary ankylosaur remains have been discovered. *Priconodon crassus* Marsh, 1888 (considered a valid taxon by Coombs 1978a, Carpenter and Kirkland 1998, and West and Tibert 2004, but a *nomen dubium* by Vickaryous et al. 2004) is known only from teeth from the Aptian-Albian Arundel Formation of Maryland, although Carpenter and Kirkland (1998) also referred an isolated tibia to this genus. All previous workers have considered *Priconodon* to represent a nodosaurid ankylosaur. More recently, an impression of a small ankylosaur from the early Aptian Patuxent Formation of Maryland was named *Propanoplosaurus marylandicus* Standford, Weishampel, and DeLeon, 2011, and was considered a nodosaurid ankylosaur. To date, no ankylosaurid remains are known from Appalachia. Given that the Western Interior Seaway would have been a barrier to west-east dinosaur migration during the Late Cretaceous, and given that ankylosaurine ankylosaurids migrated into western North America from Asia, it is possible that ankylosaurines may never have dispersed into Appalachia.

Ankylosaurids do not appear to have dispersed into Europe or Gondwana. *Minmi* sp. is recovered by most analyses (Vickaryous et al. 2004, Thompson et al. 2012), including this one, as a basal ankylosaur. The Argentinian ankylosaur appears to be related to Late Cretaceous North American nodosaurids, and most likely represents a dispersal from North America into South America during the Campanian (as suggested by Coria and Salgado 2001, but without support from a phylogenetic analysis). This is consistent with the biogeographic pattern for hadrosaurids noted by Prieto-Marquez (2010b). "*Antarctopelta*", from the Campanian of James Ross Island in Antarctica, was recovered as a basal nodosaurid by Thompson et al. (2012), but this result is based on the inclusion of material in the character codings that may or may not belong to an ankylosaur. In the first iteration of the phylogenetic analysis in this dissertation, "*Antarctopelta*" was recovered as a stem eurypodan, which is inconsistent with the available material and is most likely the result of the huge amount of missing data. The presence of fused hexagonal pelvic osteoderms in *Antarctopelta*, which are otherwise only found in North American species, suggests that *Antarctopelta* may also represent part of the North American nodosaurid dispersal into South America. The absence of diagnostic ankylosaur material from other regions of Gondwana, including Africa and India, most likely represents undersampling, rather than a true absence of material.

Anodontosaurus lambei 29.12%

11110100?11111110?123101011111111011121011110112121102111111111000011111111110
1111001?21111????????1110?00?11111????????1110011?101001?????01011112??2?22
2??????220????????23

"*Antarctopelta oliveroi*" 88.46%

??
???100????11??1????????????????0??11111??????
??????13?????

Argentinian ankylosaur 88.46%

??
????????????01111?1012?0??11110??????1221??????1
???????????????

Bissektipelta archibaldi 95.05%

?1??????????????2?1????????????????????????????????????10????????????????111??0?????
??
???????????????

Cedarpelta bilbeyhallorum 59.34%

11100?00?0100?0???10000?00?100?1000?1?0?1?0?1???000??101?11110??0???01?1111011
??1????00??????1?????1100??0?0??11????????????????011010????10101????????????
???????????????????

Crichtonpelta benxiensis 46.15%

111001??????10?1?10000?????1010?0?201?11?001201010011110?1111000?100111111??
????????????110111110010?0???00101111010?11110?1?1??0000????20101110????????
???????????????????

Dongyangopelta yangyanensis 91.76%

??
????????????11110??1??????????212313????????
??11??2?????

Dyoplosaurus acutosquameus 68.68%

??1??????????????2?10??????????????11?1??0?????1021?????????????????????????
?????11?????????????0100111?1?????????????110011?101????0??2201?111121?21&22221??
????????1111??10211

Euoplocephalus tutus 5.49%

11110100?111111101123101011111110111211111011212010211111111000011111111110
11111011211110??011111111000001111101101110010111100111101001001?12010111121?2
1&22223&4211202210?11????10?12

Gargoyleosaurus parkpinorum 36.81%

10100000?111000000?221011000101??001?210??110112110000012?0111100?010?010010101
111110??000010101????1??0?0?????????????????????????????????????211001?????21&221
13221??2100??10202?2???

Gastonia burgei 25.27%

10100101?11?11000??10000000011101000?110?111011211000001110011100001?011101000
1????????1000?????????1111010?0001?????11010?1?11100010010100?0??201010?????21&
21&221321120?2?0??10202?2100

Glyptodontopelta mimus 96.15%

??
??11333?????1??
??????3?????

Gobisaurus domoculus 53.85%

11100110?01101010??100000000101?1000?100?1110112120100111?011110000??00110100?1
????????1??????????11????????11?????????????????????1????0?0000??1????????????????
????????0?????????00

Liaoningosaurus paradoxus 77.47%

??
?0111?????????0?0?0??01010??0?0?00?111000110010000?102?00?111000????????????
???????????????????

Pinacosaurus mephistocephalus 55.49%

11110100?????101???0?010???11???0?1?211?11002222101??1?0?????????????????????1?1
0???1111101???????11????011111????1111?0?11100???????10?10?????????????2122?3??
?022100???????????

Saichania chulsanensis 29.12%

11110001?11111111??22221101110111011121101110122121101111111111100011101111111
11111011211110111111?11?????????????1??1?110?01??????????10100101??????????21&2
221?????0222000???0???????

Sauropelta edwardsorum 19.78%

101010??????????0???0?????0?10???110?11101111100?00011011111??11??1011?10111
1110?2?100111010110101111000001010011112101011101010010100111001110100111521&2
1222212312101000110110200

Sauroplices scutigera 93.96%

??
?????????????????1??1231&33?????
?????12?2??????

Scolosaurus cutleri 39.01%

11110?????????1?1?23101?1111????010?211??110122121102111111110?????????111111??
?????????111?????????1??100?0011111001?1110?0?1110011010?001?????1????11?12152?222?
?????2210110?10110212

Shamosaurus scutatus 52.75%

11100110?011?1010??100000000101?1000?110?111011212010111010111110011?0011011??1
111000?11??1&2??1
3?????2210??????????????

Stegopelta landerensis 91.21%

??
???10????00?1?1?????????????????????20?1?????????????????1?????????????????1??2??????10
??????13??????

Talarurus plicatospineus 46.70%

111100????????102?21????????0?1?210?1?10112??01021?1?????0??????1111010????
????????????11?011100000111101101110000?111001111010010010120101111???21?23??
?????2?0?????0??????

Taohelong jinchengensis 90.11%

??
????????????????1????10????????????????????1?1?1?101????????????????????21?31&33????
????????2??2?????

Tarchia kielanae 53.85%

11110001111?1?111??22212021111?1122?221?1101222211010101011110000?0101111111
11111011211110??
????????????????????

Tatankacephalus cooneyorum 77.47%

?0101??0????1?????2?10??01?0?????21??1??011??00?00?1?????1?01?1?0?010010????
?????01??12113????
????????????????

"*Tianchisaurus nedegoapeferima*" 86.81%

??
????????????????11??1?????211?21??????
????????????????

Tsagantegia longicranialis 59.89%

11100000?11111100??2210111111101011?210?11101121?01011111111110001?001111?10?
????????11?0??
????????????????

Zaraapelta nomadis 71.43%

111?00??????????02?22??2?1??1?221220?110122121100011111111001?1??1111110??
??
????????????????

Part 5. Conclusions

5. Conclusions and Future Work

This dissertation presents a significant rearrangement of the taxonomy of many ankylosaurid genera. Referred specimens of *Euoplocephalus tutus* represented four distinct taxa - *Anodontosaurus lambei*, *Dyoplosaurus acutosquameus*, *Scolosaurus cutleri*, and *Euoplocephalus tutus* – greatly increasing the diversity of ankylosaurids in the Campanian-Maastrichtian of North America. In contrast, the Chinese and Mongolian ankylosaurids *Saichania chulsanensis*, *Shanxia tianzhenensis*, and *Tianzhenosaurus youngi*, and specimens referred to *Tarchia "gigantea"* probably represent a single genus, *Saichania*. One recurring theme during the course of this project has been the importance of referring to the holotype specimens when searching for apomorphies, and not relying on "proxy holotypes" (Parker 2012). This was particularly important for the cases of *Euoplocephalus*, *Tarchia*, and *Minmi*. Each of these genera are based on highly fragmentary holotypes, and more complete specimens have largely supplanted the holotypes to form 'proxy holotypes' when these taxa are discussed in the literature. When *Tarchia gigantea* is discussed in the literature, the specimen being referenced is usually PIN 3142/250, not the holotype of *Tarchia*. However, PIN 3142/250 differs markedly from the holotype of *Tarchia*, which in turn has a unique feature present only in one other specimen, the holotype of *Minotaurasaurus*. As another example, the nearly complete skeleton MPC 100/151 has been referred to *Saichania*, but a close comparison of this skeleton to that of the holotype of *Saichania* shows several potentially important differences, and no shared derived features. Referred specimens are often critical sources of anatomical information in phylogenetic analyses, filling in data points that may be absent in the holotype of a given taxon. The correct identification and referral of specimens to known taxa is vitally important in order to avoid the creation of chimeric taxa in phylogenetic analyses. The results of a phylogenetic analysis are only as good as the anatomical data entered into the character matrix.

It is also important to revisit 'neglected' taxa or specimens, or taxa considered *nomina dubia*, as new discoveries may help put these taxa into context. For example, *Sauroplices* has generally been overlooked for the last few decades because it is represented only by osteoderms. However, the holotype preserves a portion of a feature with a limited distribution in ankylosaurs – a pelvic shield – and the pelvic shield has a distinctive morphology not present in other ankylosaurs. *Sauroplices* is considered a valid taxon in this dissertation, but even if other authors consider it a *nomen dubium*, it can be included in phylogenetic analyses; this specimen also provides additional support for the presence of nodosaurid ankylosaurs in Asia.

In addition to referring back to holotypes, two other factors have proven to be important in untangling the taxonomy and systematics of the ankylosaurids: 1) understanding the role of not just biological sources of variation, but also of taphonomy, in morphological variability, and 2) understanding the stratigraphic distribution of specimens. The relatively large sample size of specimens referred to *Euoplocephalus sensu lato* showed that taphonomic distortion can influence aspects of the morphology previously hypothesized to represent potential taxonomic variation. However, the stratigraphic data available for this large sample size also helped elucidate true taxonomic differences in cranial ornamentation patterns. The cranial ornamentation of ankylosaurs can be useful for distinguishing species and genera and should not be discounted as being too intraspecifically variable. The overall shape, size, and pattern of the frontonasal caputegulae, the number and shapes of the caputegulae that rim the skull in dorsal view (the nuchal, supraorbital, lacrimal, loreal, and supranarial caputegulae), and the general shapes of the squamosal and quadratojugal horns are all taxonomically important features.

The results of the revised phylogenetic analysis presented here show a monophyletic Ankylosauridae consisting of *Aletopelta*, *Gastonia*, *Gobisaurus*,

Liaoningosaurus, *Shamosaurus*, and a suite of derived ankylosaurids (ankylosaurines). There is convincing evidence for the presence of nodosaurids in Asia during the Early Cretaceous, with *Dongyangopelta*, *Sauropilites*, and *Taohelong* all recovered as nodosaurid ankylosaurs. In the mid Cretaceous, Asian nodosaurids appear to have been replaced by ankylosaurine ankylosaurids. Modifications to the ankylosaurid tail occurred at this time, with distinct handle vertebrae appearing potentially as early as the Albian, with *Liaoningosaurus*. The large osteodermal knob would not appear until the Late Cretaceous. Ankylosaurines migrated into North America from Asia by the Campanian, and probably between the Albian and Turonian, where they diversified into a clade of ankylosaurines characterized by arched snouts and numerous flat caputegulae. There is no evidence for any ankylosaurids in Gondwana; the Ankylosauridae appears to be completely restricted to Asia and North America.

The results of this revised phylogeny introduce new questions for future studies. Why do Asian nodosaurids appear to go extinct at about the same time that ankylosaurines begin to diversify? What were the selective pressures for evolving a stiff, bat-like tail? When, more precisely, did ankylosaurines migrate into North America? And finally, do ankylosaurines show the same latitudinal provinciality in North America that has been observed for other ornithischians? Future research could investigate the stratigraphy and age of the Baynshiree Formation of Mongolia and the relationships of *Talarurus* and *Tsagantegia*, which seem to be important for understanding the biogeography of Late Cretaceous ankylosaurines. In North America, further sampling in Utah and the southern USA may reveal new ankylosaurine species. Future phylogenetic analyses including more nodosaurid ankylosaurs may help clarify the relationships of the 'polacanthid/polacanthine' ankylosaurs, the Asian nodosaurids, the 'stegopeltines', and the Gondwanan ankylosaurs.

Literature Cited

- Alberta Geological Survey. 2012. Alberta Township System (ATS) and Universal Transverse Mercator (UTM) map conversion tools. Available at http://www.ags.gov.ab.ca/gis/map_converters/conversion_tools.html. Accessed September 2010-June 2012.
- American Museum of Natural History. 2012. Division of Paleontology Collections Database. Available at <http://research.amnh.org/paleontology/search.php>. Accessed September 2010-June 2012.
- American Museum of Natural History. 2012. Division of Paleontology, Vertebrate Paleontology Archives. Available at <http://research.amnh.org/paleontology/collections/vertebrate-paleontology-archives>. Accessed September 2010-June 2012.
- Arbour VM. 2009. Estimating impact forces of tail club strikes by ankylosaurid dinosaurs. *PLOS ONE* 4:e6738.
- Arbour VM, Snively E. 2009. Finite element analyses of ankylosaurid dinosaur tail club impacts. *Anat Rec* 292: 1412–1426.
- Arbour VM, Currie PJ. 2012. Analyzing taphonomic deformation of ankylosaur skulls using retrodeformation and finite element analysis. *PLOS ONE* 7:e39323.
- Arbour VM, Currie PJ. 2013a. *Euoplocephalus tutus* and the diversity of ankylosaurid dinosaurs in the Late Cretaceous of Alberta, Canada, and Montana, USA. *PLOS ONE* 8:e62421.
- Arbour VM, Currie PJ. 2013b. The taxonomic identity of a nearly complete ankylosaurid dinosaur skeleton from the Gobi Desert of Mongolia. *Cretaceous Research* 46:24-30.
- Arbour VM, Burns ME, Currie PJ. 2011. A review of pelvic shield morphology in ankylosaurs (Dinosauria: Ornithischia). *Journal of Paleontology* 85:298-302.

- Arbour, V.M., Burns, M.E., Sissons, R.L. 2009. A redescription of the ankylosaurid dinosaur *Dyoplosaurus acutosquameus* Parks, 1924 (Ornithischia: Ankylosauria) and a revision of the genus. *Journal of Vertebrate Paleontology* 29:1117-1135.
- Arbour VM, Burns ME, Bell PR, Currie PJ. In press. Epidermal and dermal integumentary structures of ankylosaurian dinosaurs. *Journal of Morphology*.
- Arbour VM, Lech-Hernes NL, Guldberg TE, Hurum JH, Currie PJ. 2013. An ankylosaurid dinosaur from Mongolia with *in situ* armour and keratinous scale impressions. *Acta Palaeontologica Polonica* 58:55-64.
- Averianov AO, Sues H-D, Tleuberdina PA. 2012. The forgotten dinosaurs of Zhetysu (eastern Kazakhstan; Late Cretaceous). *Proceedings of the Zoological Institute RAS* 316:139-147.
- Barrett PM, You H, Upchurch P, Burton A. 1998. A new ankylosaurian dinosaur (Ornithischia: Ankylosauria) from the Upper Cretaceous of Shanxi Province, People's Republic of China. *Journal of Vertebrate Paleontology* 18:376-384.
- Barrett PM, Rich TH, Vickers-Rich P, Tumanova TA, Inglis M, Pickering D, Kool L, Kear BP. 2010. Ankylosaurian dinosaur remains from the Lower Cretaceous of southeastern Australia. *Alcheringa* 34:205-217.
- Barsbold R. 1981. [Edentulous carnivorous dinosaurs of Mongolia]. [Transactions of the Joint Soviet-Mongolian Paleontological Expedition] 15, 28-39. [Russian, English translation by C. Siskron and S.P. Welles]
- Baszio S. 1997. Systematic palaeontology of isolated dinosaur teeth from the Latest Cretaceous of south Alberta, Canada. *Courier Forschungsinstitut Senckenberg* 196:33-77.
- Bell PR. 2012. Standardized terminology and potential taxonomic utility for hadrosaurid skin impressions: a case study for *Saurolophus* from Canada and Mongolia. *PLOS ONE* 7:e31295.

- Benton MJ. 2000. Conventions in Russian and Mongolian palaeontological literature. In: Benton MJ, Shishkin MA, Unwin DM, Kurochkin EN (eds.) *The Age of Dinosaurs in Russia and Mongolia*. Cambridge: Cambridge University Press, xvi-xxxix.
- Blows WT. 1987. The armoured dinosaur *Polacanthus foxi* from the Lower Cretaceous of the Isle of Wight. *Palaeontology* 30:557-580.
- Blows WT. 2001. Dermal armor of the polacanthine dinosaurs. In: Carpenter K (ed.) *The Armored Dinosaurs*. Bloomington: Indiana University Press, pp. 363-385.
- Bohlin B. 1953. Fossil reptiles from Mongolia and Kansu. *Sino-Swedish Expedition Publication* 37:1-113.
- Boyd AA, Motani R. 2008. Three-dimensional re-evaluation of the deformation removal technique based on "jigsaw puzzling". *Palaeontologica Electronica* 11(7A):7p.
- DeBraga M, Rieppel O. 1997. Reptile phylogeny and the interrelationships of turtles. *Zoological Journal of the Linnean Society* 120: 281–354.
- Brazeau MD. 2011. Problematic character coding methods in morphology and their effects. *Biological Journal of the Linnean Society* 104:489-498.
- Brinkman DB, Ryan MJ, Eberth DA. 1998. The paleogeographic and stratigraphic distribution of ceratopsids (Ornithischia) in the Upper Judith River Group of western Canada. *Palaios* 13:160-169.
- Brochu CA. 1997. Morphology, fossils, divergence timing, and the phylogenetic relationships of *Gavialis*. *Systematic Biology* 46: 479–522.
- Brown B. 1908. The Ankylosauridae, a new family of armored dinosaurs from the Upper Cretaceous. *Bulletin of the American Museum of Natural History* 24:187-201.
- Brown CM, Russell AP. 2012. Homology and architecture of the caudal basket of Pachycephalosauria (Dinosauria: Ornithischia): the first occurrence of myorhabdoi in Tetrapoda. *PLOS ONE* 7:e30212.

- Brusatte SL, Benson RBJ, Chure DJ, Xu X, Sullivan C, Hone DWE. 2009. The first definitive carcharodontosaurid (Dinosauria: Theropoda) from Asia and the delayed ascent of tyrannosaurids. *Naturwissenschaften* 96:1051-1058.
- Buffetaut, E. 1995. An ankylosaurid dinosaur from the Upper Cretaceous of Shandong (China). *Geological Magazine* 132:683-692.
- Burns ME. 2008. Taxonomic utility of ankylosaur (Dinosauria, Ornithischia) osteoderms: *Glyptodontopelta mimus* Ford, 2000: a test case. *Journal of Vertebrate Paleontology* 28:1102-1109.
- Burns ME. 2009. An armoured dinosaur of the Frenchman Formation: using osteoderms to study ankylosaur geographic and stratigraphic distribution. Frenchman Formation Terrestrial Ecosystems Conference, June 2009.
- Burns ME, Currie PJ. In press. External and internal structure of ankylosaur (Dinosauria, Ornithischia) osteoderms and their systematic relevance. *Journal of Vertebrate Paleontology*.
- Burns ME, Currie PJ. 2012. Quantitative analyses of cranial characters in *Panoplosaurus* and *Edmontonia* (Ankylosauria: Nodosauridae) and their taxonomic implications for the clade. *Journal of Vertebrate Paleontology, Program and Abstracts*, 2012, p. 72.
- Burns ME, Sullivan RM. 2011. A new ankylosaurid from the Upper Cretaceous Kirtland Formation, San Juan Basin, with comments on the diversity of ankylosaurids in New Mexico. *New Mexico Museum of Natural History and Science Bulletin* 53:169-178.
- Burns ME, Sullivan RM. 2011a. The tail club of *Nodocephalosaurus kirtlandensis* (Dinosauria: Ankylosauridae), with a review of ankylosaurid tail club morphology and homology. *New Mexico Museum of Natural History and Science Bulletin* 53:179–186.
- Burns ME, Currie PJ, Sissons RL, Arbour VM. 2011. Juvenile specimens of *Pinacosaurus grangeri* Gilmore, 1933 (Ornithischia: Ankylosauria) from the

- Late Cretaceous of China, with comments on the specific taxonomy of *Pinacosaurus*. *Cretaceous Research* 32: 174-186.
- Butler RJ, Upchurch P, Norman DB. 2008. The phylogeny of the ornithischian dinosaurs. *Journal of Systematic Palaeontology* 6:1-40.
- Butler RJ, Barrett PM, Gower DJ. 2012. Reassessment of the evidence for postcranial skeletal pneumaticity in Triassic archosaurs, and the early evolution of the avian respiratory system. *PLoS ONE* 7: e34094.
- Campione NE, Brink KS, Freedman EA, McGarrity CT, Evans DC. 2013. '*Glishades ericksoni*', an indeterminate juvenile hadrosaurid from the Two Medicine Formation of Montana: implications for hadrosauroid diversity in the latest Cretaceous (Campanian-Maastrichtian) of western North America. *Palaeobiodiversity and Palaeoenvironments* 93:65-75.
- Carpenter K. 1982. Skeletal and dermal armor reconstruction of *Euoplocephalus tutus* (Ornithischia: Ankylosauria) from the Late Cretaceous Oldman Formation of Alberta. *Canadian Journal of Earth Sciences* 19:689–697.
- Carpenter K. 1990. Ankylosaur systematics: example using *Panoplosaurus* and *Edmontonia* (Ankylosauria: Nodosauridae). In: Carpenter K, Currie PJ (eds.) *Dinosaur Systematics: Approaches and Perspectives*. Cambridge: Cambridge University Press, pp281-298.
- Carpenter K. 2001. Phylogenetic analysis of the Ankylosauria. In: Carpenter K (ed.) *The Armored Dinosaurs*. Bloomington: Indiana University Press, 455-483.
- Carpenter K. 2004. Redescription of *Ankylosaurus magniventris* Brown 1908 (Ankylosauridae) from the Upper Cretaceous of the Western Interior of North America. *Canadian Journal of Earth Sciences* 41:961-986.
- Carpenter K. 2012. Ankylosaurs. In: Brett-Surman MK, Holtz TR, Farlow JO (eds.) *The Complete Dinosaur*, 2nd Edition. Bloomington: Indiana University Press, pp. 505-252

- Carpenter K, Kirkland JI. 1998. Review of Lower and middle Cretaceous ankylosaurs from North America. *New Mexico Museum of Natural History and Science Bulletin* 14:249-270.
- Carpenter K, Miles C, Cloward K. 1998. Skull of a Jurassic ankylosaur (Dinosauria). *Nature* 393:782-783.
- Carpenter K, Kirkland JI, Burge D, Bird J. 1999. Ankylosaurs (Dinosauria: Ornithischia) of the Cedar Mountain Formation, Utah, and their stratigraphic distribution. *Utah Geological Survey Miscellaneous Publication* 99-1:243-251.
- Carpenter K, Kirkland JI, Burge DL, Bird J. 2001. Disarticulated skull of a new primitive ankylosaurid from the Lower Cretaceous of eastern Utah. In: Carpenter K (ed.) *The Armored Dinosaurs*. Bloomington: Indiana University Press, 211-238.
- Carpenter K, Bartlett J, Bird J, Barrick R. 2008. Ankylosaurs from the Price River Quarries, Cedar Mountain Formation (Lower Cretaceous), east-central Utah. *Journal of Vertebrate Paleontology* 28:1089-1101.
- Carpenter K, Hayashi S, Kobayashi Y, Maryańska T, Barsbold R, et al. (2011) *Saichania chulsanensis* (Ornithischia, Ankylosauridae) from the Upper Cretaceous of Mongolia. *Palaeontographica Abteilung A* 293:1-61.
- Carrano MT, Wilson JA, Barrett PM. 2010. The history of dinosaur collecting in central India, 1828-1947. *Geological Society, London, Special Publications* 343:161-173.
- Chatterjee S, Rudra DK. 1996. KT events in India: impact, rifting, volcanism and dinosaur extinction. *Memoirs of the Queensland Museum* 39:489-532.
- Chen R, Zheng W, Azuma Y, Shibata M, Lou T, Jin Q, Jin X. 2013. A new nodosaurid ankylosaur from the Chaochuan Formation of Dongyang, Zhejiang Province, China. *Acta Geologica Sinica (English Edition)* 87: 801-840.

- Colbert EH. 1981. A primitive ornithischian dinosaur from the Kayenta Formation of Arizona. *Museum of Northern Arizona Bulletin* 53:1-61.
- Coombs WP, Jr. 1971. The Ankylosauria. PhD dissertation, Columbia University, New York, 487 p.
- Coombs WP, Jr. 1972. The bony eyelid of *Euoplocephalus* (Reptilia, Ornithischia). *Journal of Paleontology* 46:637-650.
- Coombs WP, Jr. 1978a. The families of the ornithischian dinosaur Order Ankylosauria. *Palaeontology* 21:143-170.
- Coombs WP, Jr. 1978b. An endocranial cast of *Euoplocephalus* (Reptilia, Ornithischia). *Palaeontographica Abteilung A* 161:176-182.
- Coombs WP, Jr. 1978c. Forelimb muscles of the Ankylosauria (Reptilia: Ornithischia). *Journal of Paleontology* 52:642-658.
- Coombs WP, Jr. 1979. Osteology and myology of the hindlimb in the Ankylosauria (Reptilia, Ornithischia). *Journal of Paleontology* 53:666-684.
- Coombs WP, Jr. 1986. A juvenile ankylosaur referable to the genus *Euoplocephalus* (Reptilia, Ornithischia). *Journal of Vertebrate Paleontology* 6:162-173.
- Coombs WP, Jr. 1995a. Ankylosaurian tail clubs of middle Campanian to early Maastrichtian age from western North America, with description of a tiny club from Alberta and discussion of tail orientation and tail club function. *Canadian Journal of Earth Sciences* 32:902-912.
- Coombs WP, Jr. 1995b. A new nodosaurid ankylosaur (Dinosauria: Ornithischia) from the Lower Cretaceous of Texas. *Journal of Vertebrate Paleontology* 15:298-312.
- Coombs WP, Jr, Deméré TA. 1996. A Late Cretaceous nodosaurid ankylosaur (Dinosauria: Ornithischia) from marine sediments of coastal California. *Journal of Paleontology* 70: 311-326.
- Currie PJ, Russell DA. 2005. The geographic and stratigraphic distribution of articulated and associated dinosaur remains. In: Currie PJ, Koppelhus EB

- (eds.) Dinosaur Provincial Park: A spectacular ancient ecosystem revealed. Bloomington: Indiana University Press, pp. 537-570.
- Currie PJ, Badamgarav D, Koppelhus EB, Sissons R, Vickaryous MK. 2011. Hands, feet, and behaviour in *Pinacosaurus* (Dinosauria: Ankylosauridae). *Acta Palaeontologica Polonica* 56:489-504.
- Dalton R. 2009. Paper sparks fossil fury: paleontologists criticize publication of specimen with questionable origin. *Nature News* doi:10.1038/news.2009.60.
- Dashzeveg D, Dingus L, Loope DB, Swisher CC, III, Dulam T, Sweeney M. 2005. New stratigraphic subdivision, depositional environment, and age estimate for the Upper Cretaceous Djadokhta Formation, southern Ulan Nur Basin, Mongolia. *American Museum Novitates* 3498:1-31.
- Degrange FJ, Tambussi CP, Moreno K, Witmer LM, Wroe S (2010) Mechanical analysis of feeding behavior in the extinct "terror bird" *Andalgalornis steulleti* (Gruiformes: Phorusrhacidae). *PLoS ONE* 5:e11856.
- Dingus L, Loope DB, Dashzeveg D, Swisher CC, Chuluun M, Novacek MJ, Norell MA. 2008. The geology of Ukhaa Tolgod (Djadokhta Formation, Upper Cretaceous, Nemegt Basin, Mongolia). *American Museum Novitates* 3616, 1-40.
- Dixon JR (2000) Amphibians and reptiles of Texas: With keys, taxonomic synopses, bibliography, and distribution maps, 2nd ed. College Station: Texas A&M University Press, 425 p.
- Dong Z. 1993. An ankylosaur (ornithischian dinosaur) from the Middle Jurassic of the Junggar Basin, China. *Vertebrata Palasiatica* 31:257-266.
- Dong Z-M. 1994. Erratum. *Vertebrata Palasiatica* 32:142.
- Dong Z-M. 2002. A new armored dinosaur (Ankylosauria) from Beipiao Basin, Liaoning Province, northeastern China. *Vertebrata Palasiatica* 10:276-285.
- Eaton TH, Jr. 1960. A new armored dinosaur from the Cretaceous of Kansas. *The University of Kansas Paleontological Contributions: Vertebrata* 8:1-24.

- Eberth DA. 2005. The geology. In: Currie PJ, Koppelhus EB (eds.) *Dinosaur Provincial Park: A spectacular ancient ecosystem revealed*. Bloomington: Indiana University Press, pp. 54-82.
- Eberth DA, Hamblin AP. 1993. Tectonic, stratigraphic, and sedimentologic significance of a regional discontinuity in the upper Judith River Group (Belly River wedge) of southern Alberta, Saskatchewan, and northern Montana. *Canadian Journal of Earth Sciences* 30:174-200.
- Eberth DA, Braman DR. 2012. A revised stratigraphy and depositional history for the Horseshoe Canyon Formation (Upper Cretaceous), southern Alberta plains. *Canadian Journal of Earth Sciences* 49:1053-1086.
- Eberth DA, Russell DA, Braman DR, Deino AL. 1993. The age of the dinosaur-bearing sediments at Tebch, Inner Mongolia, People's Republic of China. *Canadian Journal of Earth Sciences* 30:2101-2106.
- Efremov IA. 1944. [Dinosaur horizon of Middle Asia and some questions of stratigraphy]. *Izvestiya Akademii Nauk SSSR, Seriya Geologicheskaya* 3: 40–58. [In Russian]
- Evans DC. 2007. Ontogeny and evolution of lambeosaurine dinosaurs (Ornithischia: Hadrosauridae). PhD dissertation, University of Toronto, Ontario, Canada, 530 pp.
- Fang X, Long Q, Lu L, Zhang Z, Pan S, Wang Y, Li X, Cheng Z. 2000. Lower, Middle, and Upper Jurassic subdivision in the Lufeng region, Yunnan Province. In: *Proceedings of the Third National Stratigraphical Congress of China*. pp.208-214; Geological Publishing House, Beijing. [In Chinese; translation by Will Downs, 2002]
- Fernández M, Martín J, Casadío S. 2008. Mosasaurs (Reptilia) from the late Maastrichtian (Late Cretaceous) of northern Patagonia (Río Negro, Argentina). *Journal of South American Earth Sciences* 25:176-186.

- Fernández M, Martin JE. 2009. Description and phylogenetic relationships of *Taniwhasaurus antarcticus* (Mosasauridae, Tylosaurinae) from the upper Campanian (Cretaceous) of Antarctica. *Cretaceous Research* 30:717-726.
- Ford TL. 2000. A review of ankylosaur osteoderms from New Mexico and a preliminary review of ankylosaur armor. *New Mexico Museum of Natural History and Science Bulletin* 17:157-176.
- Ford TL, Kirkland JI. 2001. Carlsbad ankylosaur: an ankylosaurid and not a nodosaurid. In: Carpenter K (ed.) *The Armored Dinosaurs*. Bloomington: Indiana University Press, pp. 239-260.
- Fox W. 1866. On a new Wealden saurian named *Polacanthus*. Report of the British Association for the Advancement of Science, Birmingham 1865:56.
- García G, Pereda Suberbiola X. 2003. A new species of *Struthiosaurus* (Dinosauria: Ankylosauria) from the Upper Cretaceous of Villeveyrac (Southern France). *Journal of Vertebrate Paleontology* 23:156-165.
- Gallagher WB, Tumanova TA, Dodson P, Axel L. 1998. CT scanning Asian ankylosaurs: paleopathology in a *Tarchia* skull. *Journal of Vertebrate Paleontology* 18:44A-45A.
- Galton PM. 1978. Fabrosauridae, the basal family of ornithischian dinosaurs (Reptilia: Ornithischia). *Paläontologische Zeitschrift* 52:138-159.
- Galton PM. 1980. Partial skeleton of *Dracopelta zbyzskii* n. gen. and n. sp., an ankylosaurian dinosaur from the Upper Jurassic of Portugal. *Géobios* 13:451-457.
- Gangloff RA. 1995. *Edmontonia* sp., the first record of an ankylosaur from Alaska. *Journal of Vertebrate Paleontology* 15:195-200.
- Gasparini Z, Pereda-Suberbiola X, Molnar RE. 1996. New data on the ankylosaurian dinosaur from the Late Cretaceous of the Antarctic Peninsula. *Memoirs of the Queensland Museum* 39:583-594.
- Geomagic, Inc. (2008) Geomagic Studio. North Carolina, USA.

- Gilmore CW. 1914. Osteology of the armored Dinosauria in the United States National Museum, with special reference to the genus *Stegosaurus*. United States National Museum Bulletin 89:1-136.
- Gilmore CW. 1917. *Brachyceratops*: a ceratopsian dinosaur from the Two Medicine Formation of Montana, with notes on associated fossil reptiles. Prof Pap US Geol Surv 103:1-45.
- Gilmore CW. 1923. A new species of *Corythosaurus*, with notes on other Belly River Dinosauria. Canadian Field-Naturalist 37:46-52.
- Gilmore CW. 1930. On dinosaurian reptiles from the Two Medicine Formation of Montana. Proceedings of the United States National Museum 77:1-39.
- Gilmore CW. 1933. Two new dinosaurian reptiles from Mongolia with notes on some fragmentary specimens. American Museum Novitates 679:1-20.
- Godefroit P, Pereda-Suberbiola X, Li H, Dong Z. 1999. A new species of the ankylosaurid dinosaur *Pinacosaurus* from the Late Cretaceous of Inner Mongolia (P.R. China). Bulletin de l'Institut Royal des Sciences Naturelles de Belgique, Sciences de la Terre 69(suppl.):17-366.
- Goloboff P, Farris S, Nixon K. 2008. TNT (Tree analysis using New Technology) ver. 1.1. Published by the authors, Tucumán, Argentina.
- Government of Alberta. 2012. HeRMIS – Heritage Resources Management Information System, Royal Tyrrell Museum. Available at <https://hermis.alberta.ca/rtmp/>. Accessed September 2010-June 2012.
- Gradziński R, Kielan-Jawaorowska Z, Maryńska T. 1977. Upper Cretaceous Djadokhta, Barun Goyot, and Nemegt Formations of Mongolia, including remarks on previous subdivisions. Acta Geologica Polonica 27:281-318.
- Haas G. 1969. On the jaw muscles of ankylosaurs. American Museum Novitates 2399:1-11.
- Haubold H. 1990. Ein neuer Dinosaurier (Ornithischia, Thyreophora) aus dem Unteren Jura des nördlichen Mitteleuropa. Revue de Paleobiologie 9:149-177. [In German]

- Heckert AB, Lucas SG. 1999. A new aetosaur (Reptilia: Archosauria) from the Upper Triassic of Texas and the phylogeny of aetosaurs. *Journal of Vertebrate Paleontology* 19: 50–68.
- Hicks JF, Brinkman DL, Nichols DJ, Watabe M. 1999. Paleomagnetic and palynologic analyses of Albian to Santonian strata at Bayn Shireh, Burkhan, and Khuren Dukh, eastern Gobi Desert, Mongolia. *Cretaceous Research* 20:829-850.
- Hill RV. 2005. Integrative morphological data sets for phylogenetic analysis of Amniota: the importance of integumentary characters and increased taxonomic sampling. *Systematic Biology* 54:530–547.
- Hill RV, Witmer LW, Norell MA. 2003. A new specimen of *Pinacosaurus grangeri* (Dinosauria: Ornithischia) from the Late Cretaceous of Mongolia: ontogeny and phylogeny of ankylosaurs. *American Museum Novitates* 3395:1-29.
- Hiller N, Mannering AA, Jones CM, Cruickshank ARI. 2005. The nature of *Mauisaurus haasti* Hector, 1874 (Reptilia: Plesiosauria). *Journal of Vertebrate Paleontology* 25:588-601.
- Hone DWE. 2012. Variation in the tail length of non-avian dinosaurs. *Journal of Vertebrate Paleontology* 32: 1082-1089.
- Hone DWE, Naish D, Cuthill IC. 2011. Does mutual sexual selection explain the evolution of head crests in pterosaurs and dinosaurs? *Lethaia* 45:139-156.
- Horner JR, Goodwin MB. 2009. Extreme cranial ontogeny in the Upper Cretaceous dinosaur *Pachycephalosaurus*. *PLOS ONE* 4:e7626.
- Huelsenbeck JP. 1994. Comparing the stratigraphic record to estimates of phylogeny. *Paleobiology* 20:470-483.
- Holden C. 1993. Paleontology's "Jurassic" windfall. *Science* 258:1879.
- Huene F, Matley CA. 1933. The Cretaceous Saurischia and Ornithischia of the Central Provinces of India. *Palaeontologica Indica (New Series), Memoirs of the Geological Survey of India* 21:1-74.

- Hughes NC. 1999. Statistical and imaging methods applied to deformed fossils. In: Harper DAT, editor. Numerical Palaeobiology: Computer-Based Modelling and Analysis of Fossils and their Distributions. New York: John Wiley & Sons, pp. 157–180.
- Hutchinson JR. 2001. The evolution of femoral osteology and soft tissues on the line to extant birds (Neornithes). *Zoological Journal of the Linnean Society* 131:169-197.
- Jia SH, Lü JC, Xu L, Hu WY, Li JH, Zhang JM. 2010. Discovery and significance of ankylosaur specimens from the Late Cretaceous Qiupa Formation in Luanchuan, Henan, China. *Geological Bulletin of China* 29:483-487. [In Chinese with English abstract]
- Jiang XJ, Liu YQ, Ji SA, Zhang XL, Xu L, Jia SH, Lü JC, Yuan CX, Li M. 2011. Dinosaur-bearing strata and K/T boundary in the Luanchuan-Tantou Basin of western Henan Province, China. *Science China Earth Sciences* 54:1149-1155.
- Jiang B, Sha J. 2006. Late Mesozoic stratigraphy in western Liaoning, China: a review. *Journal of Asian Earth Sciences* 28:205-217.
- Jerzykiewicz T. 2000. Lithostratigraphy and sedimentary settings of the Cretaceous dinosaur beds of Mongolia. In: Benton MJ, Shishkin MA, Unwin DM, Kurochkin EN, eds. *The Age of Dinosaurs in Russia and Mongolia*. Cambridge: Cambridge University Press, 279-296.
- Jerzykiewicz T, Russell DA. 1991. Late Mesozoic stratigraphy and vertebrates of the Gobi Basin. *Cretaceous Research* 12:345-377.
- Jerzykiewicz T, Currie PJ, Eberth DA, Johnston PA, Koster EH, Zheng JJ. 1993. Djadokhta Formation correlative strata in Chinese Inner Mongolia: an overview of the stratigraphy, sedimentary geology, and the paleontology and comparisons with the type locality in the pre-Altai Gobi. *Canadian Journal of Earth Sciences* 30: 2180-2195.

- Kirkland JI. 1998. A polacanthine ankylosaur (Ornithischia: Dinosauria) from the Early Cretaceous (Barremian) of eastern Utah. *New Mexico Museum of Natural History and Science Bulletin* 14:271-281.
- Kirkland JI, Carpenter K. 1994. North America's first pre-Cretaceous ankylosaur (Dinosauria) from the Upper Jurassic Morrison Formation of western Colorado. *BYU Geology Studies* 40: 25-42.
- Kobayashi Y, Lü J-C. 2003. A new ornithomimid dinosaur with gregarious habits from the Late Cretaceous of China. *Acta Palaeontologica Polonica* 48:235-259.
- Kirkland JI. 1998. A polacanthine ankylosaur (Ornithischia: Dinosauria) from the Early Cretaceous (Barremian) of eastern Utah. *New Mexico Museum of Natural History and Science Bulletin* 14:271-281.
- Kirkland JI, Carpenter K, Hunt AP, Scheetz RD (1998) Ankylosaur (Dinosauria) specimens from the Upper Jurassic Morrison Formation. *Modern Geology* 23:145-177.
- Kirkland J, Hunt-Foster R, Foster J, Loewen M. 2010. Newly recovered skeletal elements of the Late Jurassic dinosaur *Mymoorapelta* from its type locality in the Morrison Formation permits reevaluation of ankylosaur phylogeny. *Journal of Vertebrate Paleontology* 28 (3, suppl):116A.
- Kirschbaum MA, Roberts LNR. 2005. Stratigraphic framework of the Cretaceous Mowry Shale, Frontier Formation and adjacent units, southwestern Wyoming Province, Wyoming, Colorado, and Utah. In: USGS Southwestern Wyoming Province Assessment Team (eds.) *Petroleum systems and geologic assessment of oil and gas in the southwestern Wyoming Province, Wyoming, Colorado, and Utah*, U.S. Geological Survey Digital Data Series DDS-69-D. U.S. Geological Survey, Denver, Colorado, pp. 1-31.
- Knell RJ, Naish D, Tomkins JL, Hone DWE. 2013. Sexual selection in prehistoric animals: detection and implications. *Trends in Ecology and Evolution* 28:38-47.

- Knoll F. 2002. Nearly complete skull of *Lesothosaurus* (Dinosauria: Ornithischia) from the Upper Elliot Formation (Lower Jurassic: Hettangian) of Lesotho. *Journal of Vertebrate Paleontology* 22:238-243
- Kurzanov SM, Tumanova TA. 1978. The structure of the endocranium in some Mongolian ankylosaurs. *Palaeontological Journal* 1978:90-96.
- Lambe LM. 1902. New genera and species from the Belly River Series (mid-Cretaceous). *Geological Survey of Canada Contributions to Canadian Palaeontology* 3:25-81.
- Lambe LM. 1910. Note on the parietal crest of *Centrosaurus apertus* and a proposed new generic name for *Stereocephalus tutus*. *Ottawa Naturalist* 14:149–151.
- Lambe LM. 1919. Description of a new genus and species (*Panoplosaurus mirus*) of an armoured dinosaur from the Belly River Beds of Alberta. *Transactions of the Royal Society of Canada, series 3* 13:39-50.
- de Lapparent AF, Zbyszewski G. 1957. Les dinosauriens du Portugal. *Mémoires des Services Géologiques du Portugal, nouvelle série*, 2:1-63. [In French; translation by Matthew Carrano, 2002]
- Larson DW. 2010. The occurrences of vertebrate fossils in the Deadhorse Coulee Member of the Milk River Formation and their implications for provincialism and evolution in the Santonian (Late Cretaceous) of North America. Unpublished MSc thesis, University of Alberta, Edmonton, Alberta, Canada, 280 p.
- Leahey LG, Salisbury SW. 2013. First evidence of ankylosaurian dinosaurs (Ornithischia: Thyreophora) from the mid-Cretaceous (late Albian-Cenomanian) Winton Formation of Queensland, Australia. *Alcheringa* 37:249-257.
- Lee Y-N. 1996. A new nodosaurid ankylosaur (Dinosauria: Ornithischia) from the Paw Paw Formation (late Albian) of Texas. *Journal of Vertebrate Paleontology* 16:232-245.

- Lee MSY. 1997. Pareiasaur phylogeny and the origin of turtles. *Zoological Journal of the Linnean Society* 120: 197–280.
- Lindgren J. 2005. The first record of *Hainosaurus* (Reptilia: Mosasauridae) from Sweden. *Journal of Palaeontology* 79:1157-1165.
- Lehman TM. 2001. Late Cretaceous dinosaur provinciality. In: Tanke DH, Carpenter K (eds.) *Mesozoic Vertebrate Life*. Bloomington: Indiana University Press, pp. 310-328.
- Loewen, MA, Burns ME, Getty MA, Kirkland JI, Vickaryous MK. 2013. A review of the Late Cretaceous ankylosaurian dinosaurs from the Grand Staircase of southern Utah; in Titus, AL (ed.), *The Late Cretaceous in Utah*, Indiana University Press, pp. 445-462.
- Longrich NR, Currie PJ, Dong Z-H. 2010. A new oviraptorid (Dinosauria: Theropoda) from the Upper Cretaceous of Bayan Mandahu, Inner Mongolia. *Palaeontology* 53:945-960.
- Loope DB, Dingus L, Swisher CC, Minjin C. 1998. Life and death in a Late Cretaceous dune field, Nemegt basin, Mongolia. *Geology* 26, 27-30.
- Lü J, Ji Q, Gao Y, Li Z. 2007. A new species of the ankylosaurid dinosaur *Crichtonsaurus* (Ankylosauridae : Ankylosauria) from the Cretaceous of Liaoning Province, China. *Acta Geologica Sinica* 81:883-897.
- Lü J, Jin X, Sheng Y, Li Y, Wang G, Azuma Y. 2007. New nodosaurid dinosaur from the Late Cretaceous of Lishui, Zhejiang Province, China. *Acta Geologica Sinica* 81:344-350.
- Lucas FA. 1901. A new dinosaur, *Stegosaurus marshi*, from the Lower Cretaceous of South Dakota. *Proceedings of the United States National Museum* 23:591-592.
- Lucas SG. 1996. The thyreophoran dinosaur *Scelidosaurus* from the Lower Jurassic Lufeng Formation, Yunnan, China. In: Morales M (ed.) *The Continental Jurassic*. Flagstaff: Museum of Northern Arizona Bulletin 60:81-85.

- Lucas S. 2001. Chinese Fossil Vertebrates. New York: Columbia University Press.
- Luo Z-X, Wu X-C. 1994. The small tetrapods of the Lower Lufeng Formation, Yunnan, China. In: Fraser NC, Sues H-D (eds.) In the shadow of dinosaurs: early Mesozoic tetrapods. New York: Cambridge University Press, pp. 251-270.
- Lull RS. 1921. The Cretaceous armored dinosaur, *Nodosaurus textilis* Marsh. American Journal of Science, Fifth Series 1:97-126.
- Lydekker R. 1893. On the jaw of a new carnivorous dinosaur from the Oxford Clay of Peterborough. Quarterly Journal of the Geological Society 49:284-287.
- Lydekker R. 1889. On the remains and affinities of five genera of Mesozoic Reptiles. Quarterly Journal of the Geological Society 45:41-59.
- Maddison WP. 1993. Missing data versus missing characters in phylogenetic analysis. Systematic Biology 42:576-581.
- Maddison DR, Maddison WP. 2000. MacClade 4: Analysis of phylogeny and character evolution. Version 4.0. Sinauer Associates, Sunderland, Massachusetts. [version 4.08 copyright 2005]
- Maddison WP, Maddison DR. 2011. Mesquite: a modular system for evolutionary analysis, ver. 2.72. <http://mesquiteproject.org>.
- Maidment SCR. 2010. Stegosauria: a historical review of the body fossil record and phylogenetic relationships. Swiss Journal of Geosciences 103:199-210.
- Maidment SCR, Porro LB. 2010. Homology of the palpebral and origin of the supraorbital ossifications in ornithischian dinosaurs. Lethaia 43:95-111.
- Maidment SCR, Norman DB, Barrett PM, Upchurch P. 2008. Systematics and phylogeny of Stegosauria (Dinosauria: Ornithischia). Journal of Systematic Palaeontology 6:367-407.
- Maisch MW, Matzke T. 2003. Theropods (Dinosauria, Saurischia) from the Middle Jurassic Toutunhe Formation of the southern Junggar Basin, NW China. Palaeontologische Zeitschrift 77:281-292.

- Maleev EA. 1952. [A new ankylosaur from the Upper Cretaceous of Mongolia.]
Doklady Akademii Nauk, SSSR 87:273-276. [In Russian; translation by T. and
F. Jeletsky, 1956]
- Maleev EA. 1954. [The armored dinosaurs of the Cretaceous period in Mongolia
(Family Syrmosauridae)]. Doklady Akademii Nauk, SSSR 48, 142-170. [In
Russian; translation by Robert Welch]
- Maleev EA. 1956. [Armored dinosaurs of the Upper Cretaceous of Mongolia,
Family Ankylosauridae]. Trudy Paleontol. Inst. Akademiia nauk SSSR 62:51-
91. [In Russian; translation by R. Welch]
- Mallon JC. 2012. Evolutionary palaeoecology of the megaherbivorous dinosaurs
from the Dinosaur Park Formation (Upper Campanian) of Alberta, Canada.
Unpublished Ph.D. Dissertation, University of Calgary.
- Mallon JC, Evans DC, Ryan MJ, Anderson JS (2012) Megaherbivorous dinosaur
turnover in the Dinosaur Park Formation (upper Campanian) of Alberta,
Canada. *Palaeogeography Palaeoclimatology Palaeoecology* 350-352:124-
138.
- Mallon JC, Holmes R, Eberth DA, Ryan MJ, Anderson JS (2011) Variation in the
skull of *Anchiceratops* (Dinosauria, Ceratopsidae) from the Horseshoe
Canyon Formation (Upper Cretaceous) of Alberta. *Journal of Vertebrate
Paleontology* 31:1047-1071.
- Marsh OC. 1888. Notice of a new genus of Sauropoda and other new dinosaurs
from the Potomac Formation. *American Journal of Science* 135:89-94.
- Marsh OC. 1889. Notice of gigantic horned Dinosauria from the Cretaceous.
American Journal of Science 38:173-175.
- Maryańska T. 1971. New data on the skull of *Pinacosaurus grangeri*
(Ankylosauria). *Palaeontologia Polonica* 25:45-53.
- Maryańska T, Osmolska H. 1974. Pachycephalosauria, a new suborder of
ornithischian dinosaurs. *Palaeontologia Polonica* 30:45-102.

- Maryańska T, Osmolska H. 1975. Protoceratopsidae (Dinosauria) of Asia. *Palaeontologica Polonica* 33:133-181.
- Maryańska T. 1977. Ankylosauridae (Dinosauria) from Mongolia. *Palaeontologia Polonica* 37:85-151.
- Maryańska T, Chapman RE, Weishampel DB. 2004. Pachycephalosauria. In: *The Dinosauria* 2nd Ed. 464-477.
- Miles CA, Miles CJ. 2009. Skull of *Minotaurasaurus ramachandrani*, a new Cretaceous ankylosaur from the Gobi Desert. *Current Science* 96:65-70.
- Miyashita T, Fanti F. 2009. A high latitude vertebrate fossil assemblage from the Late Cretaceous of west-central Alberta, Canada: evidence for dinosaur nesting and vertebrate latitudinal gradient. *Palaeogeography, Palaeoclimatology, Palaeoecology* 275:37-53.
- Miyashita T, Arbour VM, Witmer LM, Currie PJ. 2011. The internal cranial morphology of an armoured dinosaur *Euoplocephalus* corroborated by X-ray computed tomographic reconstruction. *Journal of Anatomy* 219:661-675.
- Molnar RE. 1980. An ankylosaur (Ornithischia: Reptilia) from the Lower Cretaceous of southern Queensland. *Memoirs of the Queensland Museum* 20:77-87.
- Molnar RE. 1996. Preliminary report on a new ankylosaur from the Early Cretaceous of Queensland, Australia. *Memoirs of the Queensland Museum* 39:653-668.
- Molnar RE. 2001. Armor of the small ankylosaur *Minmi*. In: Carpenter K (ed.) *The Armored Dinosaurs*. Bloomington: Indiana University Press, pp. 341-362.
- Molnar RE, Frey E. 1987. The paravertebral elements of the Australian ankylosaur *Minmi* (Reptilia: Ornithischia, Cretaceous). *Neues Jahrbuch für Geologie und Paläontologie* 175:19-37.
- Molnar RE, Wiffen J. 1994. A Late Cretaceous polar dinosaur fauna from New Zealand. *Cretaceous Research* 15:689-706.

- Motani R. 1997. New technique for retrodeforming tectonically deformed fossils, with an example for ichthyosaurian specimens. *Lethaia* 30:221–228.
- Mulder EWA. 2001. Co-ossified vertebrae of mosasaurs and cetaceans: implications for the mode of locomotion of extinct marine reptiles. *Paleobiology* 27:724-734.
- Naish D, Martill D. 2001. Armoured dinosaurs: thyreophorans. In: Martill D, Naish D (eds) *The dinosaurs of the Isle of Wight*. London: The Palaeontological Association, pp. 147-184.
- Naish D, Martill DM. 2008. Dinosaurs of Great Britain and the role of the Geological Society of London in their discovery: Ornithischia. *Journal of the Geological Society* 165:613-623
- Nessov LA. 1995. [Dinosaurs of Northern Eurasia: new data about assemblages, ecology and paleobiogeography]. Saint Petersburg, Izdatelstvo Sankt-Peterburgskogo Universiteta, 156 p. [In Russian; translation by T. Platanova and H.-D. Sues]
- Nopcsa F. 1915. Die dinosaurier der Siebenbürgischen Landesteile Ungarns [The dinosaurs of the Transylvanian province in Hungary]. *Mitteilungen Jahrbuch Ungarische Geologische Reichsanstalt* 23:1-26. [In German; translation by DB Weishampel]
- Nopcsa F. 1928. Palaeontological notes on reptiles. *Geologica Hungarica, Series Palaeontologica* 1:1-84.
- Nopcsa F. 1929. Dinosaurier reste aus Siebenbürgen. V. *Geologica Hungarica Series Palaeontologica* 4:1-76.
- Norman DB. 1984. A systematic reappraisal of the reptile order Ornithischia. In: Reif W-E, Westphal F (eds.) 3rd Symposium on Mesozoic Terrestrial Ecosystems, Short Papers. Tübingen, Germany: Attempto Verlag, 157-162.
- Norman D. 2001. *Scelidosaurus*, the earliest complete dinosaur. In: Carpenter K (ed.) *The Armored Dinosaurs*. Bloomington: Indiana University Press, pp.3-24.

- Norman DB, Butler RJ, Maidment CR. 2007. Reconsidering the status and affinities of the ornithischian dinosaur *Tatisaurus oehleri* Simmons, 1965. *Zoological Journal of the Linnean Society* 150:865-874.
- Nowak RM. 1999. *Walker's Mammals of the World, Sixth Edition*. Baltimore: The Johns Hopkins University Press, 1936 p.
- O'Connor PM. 2006. Postcranial pneumaticity: an evaluation of soft-tissue influences on the postcranial skeleton and the reconstruction of pulmonary anatomy in archosaurs. *Journal of Morphology* 267: 1199-1226.
- O'Keefe FR, Street HP. 2009. Osteology of the cryptocleidoid plesiosaur *Tatenectes laramienseis*, with comments on the taxonomic status of the Cimoliasauridae. *Journal of Vertebrate Paleontology* 29:48-57.
- Osborn HF. 1923. Two Lower Cretaceous dinosaurs from Mongolia. *American Museum Novitates* 95:1-10.
- Ostrom JH. 1970. Stratigraphy and Paleontology of the Cloverly Formation (Lower Cretaceous) of the Bighorn Basin Area, Wyoming and Montana. Peabody Museum of Natural History, Yale University, Bulletin 35, 234p.
- Oliver J. 1951. Ontogenetic changes in osteodermal ornamentation in skinks. *Copeia* 1951:127-130.
- Olivero E, Gasparini Z, Rinaldi C, Scasso R. 1991. First record of dinosaurs in Antarctica (Upper Cretaceous, James Ross Island): paleogeographic implications. In: Thomson MRA, Crame JA, Thomson JW (eds). *Geological Evolution of Antarctica*. Cambridge University Press, Cambridge, 617-622.
- Ósi A. 2005. *Hungarosaurus tormai*, a new ankylosaur (Dinosauria) from the Upper Cretaceous of Hungary. *Journal of Vertebrate Paleontology* 25:370-383.
- Owen R. 1842. Report on British fossil reptiles. *Reports of the British Association for the Advancement of Science* 11:60-204.

- Owen R. 1861. A monograph of a fossil dinosaur (*Scelidosaurus harrisonii*, Owen) of the Lower Lias, part I. Monographs on the British Fossil Reptilia from the Oolitic Formations 1:1-14.
- Pang Q, Cheng Z. 1998. A new ankylosaur of Late Cretaceous from Tianzhen, Shanxi. Progress in Natural Science 8:326-334.
- Parish JC, Barrett PM. 2004. A reappraisal of the ornithischian dinosaur *Amtosaurus magnus* Kurzanov and Tumanova 1978, with comments on the status of *A. archibaldi* Averianov 2002. Canadian Journal of Earth Sciences 41:299-306.
- Parker WG. 2012. Redescription and taxonomic status of specimens of *Episcoposaurus* and *Tyothorax*, the earliest known aetosaurs (Archosauria: Suchia) from the Upper Triassic of western North America, and the problem of proxy "holotypes". Earth and Environmental Science Transactions of the Royal Society of Edinburgh 103:313-338.
- Parks WA. 1924. *Dyoplosaurus acutosquameus*, a new genus and species of armored dinosaur, and notes on a skeleton of *Prosaurolophus maximus*. University of Toronto Studies Geological Series 18:1-35.
- Parsons WL, Parsons KM. 2009. A new ankylosaur (Dinosauria: Ankylosauria) from the Lower Cretaceous Cloverly Formation of central Montana. Canadian Journal of Earth Sciences 46:721-738.
- Paul GS. 2010. The Princeton Field Guide to Dinosaurs. Princeton University Press, New Jersey.
- Penkalski P. In press. A new ankylosaurid from the late Cretaceous Two Medicine Formation of Montana, USA. Acta Palaeontologica Polonica.
- Penkalski P. 2001. Variation in specimens referred to *Euoplocephalus tutus*. In: Carpenter K (ed.) The armored dinosaurs. Bloomington: Indiana University Press, pp. 363–385.

- Penkalski P, Blows WT. 2013. *Scolosaurus cutleri* from the Dinosaur Park Formation of Alberta, Canada. Canadian Journal of Earth Sciences 50:171-182.
- Pereda Suberbiola X, Dantas P, Galton PM, Luis Sanz J. 2005. Autopodium of the holotype of *Dracopelta zbyzewskii* (Dinosauria, Ankylosauria) and its type horizon and locality (Upper Jurassic: Tithonian, western Portugal). Neues Jahrbuch für Geologie und Paläontologie 235:175-196.
- Piveteau J. 1926. Contribution à l'étude des formations lagunaires du nord-ouest de Madagascar. Bulletin de la Société Géologique de France 5:33-38.
- Ponce de León MS. 2002. Computerized paleoanthropology and Neanderthals: the case of Le Moustier 1. Evolutionary Anthropology Suppl. 1:68-72.
- Porro LB, Holliday CM, Anapol F, Ontiveros LC, Ontiveros LT, Ross CF. 2011. Free body analysis, beam mechanics, and finite element modeling of the mandible of *Alligator mississippiensis*. Journal of Morphology 272:910–937.
- Prieto-Márquez A. 2010. Global phylogeny of Hadrosauridae (Dinosauria: Ornithopoda) using parsimony and Bayesian methods. Zoological Journal of the Linnean Society 159:435–502.
- Prieto-Márquez A. 2010b. Global historical biogeography of hadrosaurid dinosaurs. Zoological Journal of the Linnean Society 159:503-525.
- Psihoyos L, Knoebber J. 1994. Hunting Dinosaurs. Random House, New York.
- Rasband WS. 2012. ImageJ. Bethesda, Maryland, USA.
- Retallack GJ. 2007. Growth, decay and burial compaction of *Dickinsonia*, an iconic Ediacaran fossil. Alcheringa 31:215–240.
- Roberts EM, Deino AL, Chan MA. 2005. $^{40}\text{Ar}/^{39}\text{Ar}$ age of the Kaiparowits Formation, southern Utah, and correlation of contemporaneous Campanian strata and vertebrate faunas along the margin of the Western Interior Basin. Cretaceous Research 26:307-318.

- Rogers RD, Swisher CC, Horner JR. 1993. $^{40}\text{Ar}/^{39}\text{Ar}$ age and correlation of the nonmarine Two Medicine Formation (Upper Cretaceous), northwestern Montana, U.S.A. *Canadian Journal of Earth Sciences* 30:1066-1075.
- Romer AS. 1927. The pelvic musculature of ornithischian dinosaurs. *Acta Zoologica* 8:225-275.
- Rosenbaum JN, Padian K. 2000. New material of the basal thyreophoran *Scutellosaurus lawleri* from the Kayenta Formation (Lower Jurassic) of Arizona. *PaleoBios* 20:13-23.
- Ross FD, Mayer GC (1983) On the dorsal armor of the Crocodylia. In: Rhodin AGJ, Miyata K, (eds.) *Advances in herpetology and evolutionary biology: essays in honor of Ernest E. Williams*. Cambridge, Massachusetts: Museum of Comparative Zoology, pp. 305-331.
- Rothschild BM, Martin LD, Timm RM. 2010. A new spontaneous model of fibrodysplasia ossificans progressiva. *Brazilian Geographical Journal: Geosciences and Humanities Research Medium* 1:228-237.
- Ryan MJ, Evans DC. 2005. Ornithischian dinosaurs. In: Currie PJ, Koppelhus EB (eds.) *Dinosaur Provincial Park: a spectacular ancient ecosystem revealed*. Bloomington: Indiana University Press, pp. 312-348.
- Ryan MJ. 2003. Taxonomy, systematics and evolution of centrosaurine ceratopsids of the Campanian Western Interior Basin of North America. PhD dissertation, University of Calgary, Alberta, Canada, 578 pp.
- Ryan MJ, Russell AP. 2001. Dinosaurs of Alberta (exclusive of Aves). In: Tanke DH, Carpenter K, (eds.) *Mesozoic vertebrate life*. Bloomington: Indiana University Press, pp. 279-297.
- Ryan MJ, Eberth DA, Brinkman DB, Currie PJ, Tanke DH. 2011. A new *Pachyrhinosaurus*-like ceratopsid from the Upper Dinosaur Park Formation (Late Campanian) of southern Alberta, Canada. In: Ryan MJ, Chinnery-Allgeier BJ, Eberth DA (eds.) *New perspectives on horned dinosaurs: The*

- Royal Tyrrell Museum Ceratopsian Symposium. Bloomington: Indiana University Press, pp. 141-155.
- Rybczynski N, Vickaryous MK. 2001. Evidence of complex jaw movement in the Late Cretaceous ankylosaurid *Euoplocephalus tutus* (Dinosauria: Thyreophora). In: Carpenter K (ed.) The armored dinosaurs. Bloomington: Indiana University Press pp. 299-317.
- Russell D, Russell D, Taquet P, Thomas H. 1976. New collections of vertebrates in the Upper Cretaceous continental terrains of the Majunga region (Madagascar). *Comptes Rendus de la Société Géologique de France* 5:205-208.
- Salgado L, Gasparini Z. 2006. Reappraisal of an ankylosaurian dinosaur from the Upper Cretaceous of James Ross Island (Antarctica). *Geodiversitas* 28:119-135.
- Sampson SD, Loewen MA, Farke AA, Roberts EM, Forster CA, Smith JA, Titus AL. 2010. New horned dinosaurs from Utah provide evidence for intracontinental dinosaur endemism. *PLOS ONE* 5:e12292.
- Scannella J, Horner JR. 2010. *Torosaurus* Marsh, 1891, is *Triceratops* Marsh, 1889 (Ceratopsidae: Chasmosaurinae): synonymy through ontogeny. *Journal of Vertebrate Paleontology* 30:1157-1168.
- Seeley HG. 1887. On the classification of the fossil animals commonly named Dinosauria. *Proceedings of the Royal Society of London* 43:165-171.
- Sereno PC. 1999. The evolution of dinosaurs. *Science* 284:2137-2147.
- Simmons DJ. 1965. The non-therapsid reptiles of the Lufeng Basin, Yunnan, China. *Field Geology* 15:1-93.
- Srivastava DC, Shah J. 2006. Digital method for strain estimation and retrodeformation of bilaterally symmetric fossils. *Geology* 34:593-596.
- Stanford R, Weishampel DB, DeLeon VB. 2011. The first hatchling dinosaur reported from the eastern United States: *Propanoplosaurus marylandicus*

- (Dinosauria: Ankylosauria) from the Early Cretaceous of Maryland, U.S.A. *Journal of Paleontology* 85:916-924.
- Strand7 Pty Ltd. 2008. Strand7. Sydney, Australia.
- Sternberg CM. 1929. A toothless armoured dinosaur from the Upper Cretaceous of Alberta. Canada Department of Mines Geological Survey Bulletin (Geological Series) 54:28-33.
- Sternberg CM. 1950. Steveville—West of the Fourth Meridian, Alberta. Geological Survey of Canada Topographic Map 969A.1/31 680 scale (1 inch to ½ mile).
- Sternberg CM. 1951. Complete skeleton of *Leptoceratops gracilis* Brown from the Upper Edmonton Member on the Red Deer River, Alberta. Bulletin of the National Museum of Canada 123:225-255.
- Sullivan RM. 1999. *Nodocephalosaurus kirtlandensis*, gen. et sp nov., a new ankylosaurid dinosaur (Ornithischia: Ankylosauria) from the Upper Cretaceous Kirtland Formation (Upper Campanian), San Juan Basin, New Mexico. *Journal of Vertebrate Paleontology* 19:126-139.
- Sullivan RM. 2000. Reply to Upchurch and Barrett. *Journal of Vertebrate Paleontology* 20:218-219.
- Sullivan RM. 2006. A taxonomic review of the Pachycephalosauridae (Dinosauria: Ornithischia). *New Mexico Museum of Natural History and Science Bulletin* 35:347-365.
- Sullivan RM, Lucas SG. 2006. The Kirtlandian land-vertebrate “age”—faunal composition, temporal position and biostratigraphic correlation in the nonmarine Upper Cretaceous of western North America. *New Mexico Museum of Natural History and Science Bulletin* 35:7–29.
- Sullivan RM, Fowler DW. 2006. New specimens of the rare ankylosaurid dinosaur *Nodocephalosaurus kirtlandensis* (Ornithischia: Ankylosauridae) from the Upper Cretaceous Kirtland Formation (De-na-zin Member), San Juan Basin,

- New Mexico. New Mexico Museum of Natural History and Science Bulletin 35:259-261.
- Suzuki S, Watabe M. 2000. Report on the Japan-Mongolia Joint Paleontological Expedition to the Gobi desert, 1998. Hayashibara Museum of Natural Sciences Research Bulletin 1:83-98.
- Tang F, Luo Z-X, Zhoe Z-H, You H-L, Georgi JA, Tang Z-L, Wang X-Z. 2001. Biostratigraphy and palaeoenvironment of the dinosaur-bearing sediments in Lower Cretaceous of Mazongshan area, Gansu Province, China. Cretaceous Research 22:115-129.
- Tanke DH. 2005. Identifying lost quarries. In: Currie PJ, Koppelhus EB (eds.) Dinosaur Provincial Park: A spectacular ancient ecosystem revealed. Bloomington: Indiana University Press, pp. 34-53.
- Tanke DH. 2010. Lost in plain sight: rediscovery of William E. Cutler's missing *Eoceratops*. In: Ryan MJ, Chinnery-Allgeier BJ, Eberth DA, editors. New perspectives on horned dinosaurs: The Royal Tyrrell Museum Ceratopsian Symposium. Bloomington: Indiana University Press, pp. 541-550.
- Thompson RS, Parish JC, Maidment SCR, Barrett PM. 2012. Phylogeny of the ankylosaurian dinosaurs (Ornithischia: Thyreophora). Journal of Systematic Palaeontology 10:301-312.
- Trexler D. 2001. Two Medicine Formation, Montana: Geology and Fauna. In: Tanke DH, Carpenter K (eds.) Mesozoic vertebrate life. Bloomington: Indiana University Press, pp. 298-309.
- Tseng ZJ, Binder WJ. 2010. Mandibular biomechanics of *Crocota crocuta*, *Canis lupus*, and the late Miocene *Dinocrocota gigantea* (Carnivora, Mammalia). Zoological Journal of the Linnean Society 158:683–696.
- Tumanova TA. 1977. New data on the ankylosaur *Tarchia gigantea*. Paleontological Zhurnal 4:92-100.

- Tumanova TA. 1983. [The first ankylosaur from the Lower Cretaceous of Mongolia.] Trudy Sovmestnoi Sovetskoi-Mongol'skoi Paleontologicheskoi Ekspeditsii 24:110-120. [In Russian, translation by R. Welch]
- Tumanova TA. 1993. [A new armored dinosaur from south-eastern Gobi]. Paleontologicheskii Zhurnal 27:92-98. [In Russian]
- Tumanova TA, Alifanov VR, Bolotsky YL. 2003. [The first findings of ankylosaurs in Russia.] Priroda 3:69-70. [In Russian]
- Twiss RJ, Moores EM. 1992. Structural Geology. New York: W.H. Freeman and Company, 532 p.
- Upchurch P, Barrett PM. 2000. The taxonomic status of *Shanxia tianzhenensis* (Ornithischia, Ankylosauridae); a response to Sullivan (1999). Journal of Vertebrate Paleontology 20:216-217.
- Sullivan RM. 2000. Reply to Upchurch and Barrett. Journal of Vertebrate Paleontology 20:218-219.
- Vickaryous MK, Russell AP. 2003. A redescription of the skull of *Euoplocephalus tutus* (Archosauria: Ornithischia): a foundation for comparative and systematic studies of ankylosaurian dinosaurs. Zoological Journal of the Linnean Society 137:157–186.
- Vickaryous MK, Russell AP, Currie PJ. 2001a. Cranial ornamentation of ankylosaurs (Ornithischia: Thyreophora): reappraisal of developmental hypotheses. In: Carpenter K, (ed.) The Armored Dinosaurs. Bloomington: Indiana University Press, 318-340.
- Vickaryous MK, Russell AP, Currie PJ, Zhao X-J. 2001b. A new ankylosaurid (Dinosauria: Ankylosauria) from the Lower Cretaceous of China, with comments on ankylosaurian relationships. Canadian Journal of Earth Sciences 38:1767-1780.
- Vickaryous MK, Maryańska T, Weishampel DB. 2004. Ankylosauria. In: Weishampel DB, Dodson P, Osmolska H (eds.) The Dinosauria, 2nd Edition. Berkeley: University of California Press, pp. 363-392.

- Watabe M, Tsogtbaatar K, Suzuki S, Saneyoshi M. 2010. Geology of dinosaur-fossil-bearing localities (Jurassic and Cretaceous: Mesozoic) in the Gobi Desert: Results of the HMNS-MPC Joint Paleontological Expedition. Hayashibara Museum of Natural Sciences Research Bulletin 3:41-118.
- Weishampel DB, Barrett PM, Coria RA, Loeuff JL, Xu X, Zhao X, Sahni A, Gomani EMP, Noto CR. 2004. Dinosaur Distribution. In: Weishampel DB, Dodson P, Osmolska H (eds.) *The Dinosauria*, 2nd Edition. Berkeley: University of California Press, 517-606.
- West A, Tibert N. 2004. Quantitative analyses for the type material of *Priconodon crassus*: a distinct taxon from the Arunel [sic] Formation in southern Maryland. Geological Society of America Abstracts with Programs 36:423.
- White T. 2003. Early hominids – diversity or distortion? *Science* 299:1994–1997.
- Wilkinson M. 1995. Coping with abundant missing entries in phylogenetic inference using parsimony. *Systematic Biology* 44:501-514.
- Wilkinson M, Upchurch P, Barrett PM, Gower DJ, Benton MJ. 1998. Robust dinosaur phylogeny? *Nature* 396:423-424.
- Wilkinson M. 2001. TAXEQ3: software and documentation. Department of Zoology, The Natural History Museum, London.
- Wilkinson M. 2003. Missing entries and multiple trees: instability, relationships, and support in parsimony analysis. *Journal of Vertebrate Paleontology* 23:311-323.
- Witmer LM, Ridgely RC. 2008. The paranasal air sinuses of predatory and armored dinosaurs (Archosauria: Theropoda and Ankylosauria) and their contribution to cephalic structure. *Anatomical Record* 291:1362-1388.
- Xu X, Wang X-L, You H-L. 2001. A juvenile ankylosaur from China. *Naturwissenschaften* 88:297-300.
- Xu L, Lü J, Zhang X, Jia S, Hu W, Zhang J, Wu Y, Ji Q. 2007. A new nodosaurid dinosaur fossil from the Cretaceous Period of Ruyang, Henan. *Acta Geologica Sinica* 81:433-438.

- Xu X, Norell MA. 2006. Non-avian dinosaur fossils from the Lower Cretaceous Jehol Group of western Liaoning, China. *Geological Journal* 41:419-437.
- Yang J-T, You H-L, Li D-Q, Kong D-L. 2013. First discovery of polacanthine ankylosaur dinosaur in Asia. *Vertebrata Palasiatica* 7:17-30. [In Chinese, with English abstract]
- Yu Y, Harris AJ, He XJ. 2012. RASP (Reconstruct Ancestral State in Phylogenies) 2.1b. Available at <http://mnh.scu.edu.cn/soft/blog/RASP>.
- Yu Y, Harris AJ, He XJ. 2010. S-DIVA (statistical dispersal-vicariance analysis): a tool for inferring biogeographic histories. *Molecular Phylogenetics and Evolution* 56:848-850.
- Zollikofer CPE, Ponce de León MS, Lieberman DE, Guy F, Pilbeam D, et al. (2005) Virtual cranial reconstruction of *Sahelanthropus tchadensis*. *Nature* 434:755–759.